ECOLOGY OF METAL-MICROBE INTERACTIONS IN FERROMANGANESE CRUSTS OF THE AFANASIY-NIKITIN SEAMOUNT

Thesis submitted to Goa University for the Award of the Degree of

DOCTOR OF PHILOSOPHY

in

MARINE SCIENCE

By

SUJITH P.P.

Research Guide

Dr. Maria-Judith B.D. Gonsalves

National Institute of Oceanography

(Council of Scientific and Industrial Research)

Dona Paula, Goa – 403 004, India

GOA UNIVERSITY

Taleigao, Goa

December, 2013

Certificate

This is to certify that the thesis entitled ***"Ecology of metal-microbe interactions in ferromanganese crusts of the Afanasiy-Nikitin Seamount"*** submitted by **Sujith P.P.** for the award of the degree of **Doctor of Philosophy** in **Marine Science** is based on his original studies carried out by him under my supervision. The thesis or any part thereof has not been previously submitted for any degree or diploma in any University or Institution.

Place: Dona Paula

Date: 25/06/2014

Judith

Dr. Maria-Judith B.D. Gonsalves
Research Guide,
National Institute of Oceanography,
Dona Paula, Goa-403 004, India.

All the corrections suggested by the examiners are incorporated.

25/06/2014

Declaration

As required under the University ordinance 0.19.8 (vi), I state that the present thesis entitled ***"Ecology of metal-microbe interactions in ferromanganese crusts of the Afanasiy-Nikitin Seamount"*** is my original contribution and the same has not been submitted on any previous occasion. To the best of my knowledge, the present study is the first comprehensive work of its kind from the area mentioned. The literature related to the problem investigated has been cited. Due acknowledgements have been made whenever facilities and suggestions have been availed of.

Sujith P.P.

Acknowledgements

I take this opportunity to thank all who have helped me in successfully completing this thesis work. First and foremost I thank my advisor, Dr. Maria-Judith, for her mentorship, guidance and for the freedom to pursue my interests. Her contributions were significant which helped me to make this thesis practically possible in the present form. The present Director Dr. S.W.A. Naqvi, National Institute of Oceanography and former Director Dr. Satish R. Shetye are acknowledged for providing an excellent research environment. Financial assistance in the form of Senior Research Fellowship provided by the Council of Scientific and Industrial Research helped me in accomplishing the major part of the research work.

Many thanks to Dr. Savita Kerkar for being an informal co-guide and a helpful faculty research council member. I also feel fortunate to have had extremely helpful research committee members: Dr. G.N. Nayak, Dr. H.B. Menon and Dr. Savita Kerkar. They were very generous in lending their time for the assessment and evaluation of my progress reports. I am thankful to Prof G. N. Nayak, the Head, Department of Marine Sciences, Goa University for words of encouragement and support. I owe my sincere thanks to all my teachers who introduced me to different facets of science. My sincere thanks to supervisor, Dr. P.A. LokaBharathi, who taught me the basics of metal-microbe interactions, and I am grateful for her patience and skills as a teacher and advisor over the years. It helped me in broadening my views and appreciation for interdisciplinary research in geomicrobiology. I would also like to thank Dr. Shanta Achuthankutty for constructive criticisms that have strengthened my arguments which made the work seem all the more worthwhile. Dr. S.S. Mamatha and Dr. S. Krishnamurthi are thanked for being supportive.

I feel indebted to Dr. V.K. Banakar for giving me an opportunity to work under the Ministry of Earth Science funded project on Co-crust and for allowing me to participate in one of the cruises to the CIOB. Words of encouragement and constant support from him always helped me in progressing further. I owe my many thanks to the captain and crew aboard the Akademik Boris Petrov and JOIDES resolution for the samples. I also thank Dr. Rahul K. Sharma, project leader of PMN-EIA for accommodating me under the project at the end of my CSIR-SRF. Due respect and thanks is extended to Dr. K.A.

Kamesh Raju for the support and help in acquiring of funds to attend the meeting at Mauritius. InterRidge is also thanked for financial assistance.

Special thanks to Dr. V.P. Rao for invaluable assistance with XRD analysis. I express my gratitude to Prof. David L. Kirchman, University of Delaware for teaching the basics of 'R' a statistical tool for the analysis of 454 data. Dr. M.P. Tapaswi is thanked for continuous support with required literature for reference. I also thank Mr. V.D. Khedekar and G.A. Prabhu who were instrumental in analysis of samples for microscopy and X-ray characterization. Mrs. Chanda Panwar is acknowledged for being generous in lending her time and expertise in helping with the TEM analysis at AIIMS, New Delhi. I express my thanks to Mr. V. Subramanian for keeping the different analytical equipments functional within the laboratory. Administrative support provided by the staff Mr. Yashwant of Marine Science Department, Goa University and Mr. Talkatnal of NIO are greatly acknowledged. Administration department and HRM, National Institute of Oceanography are thanked for their cooperation and help as and when required. Many thanks to the past and present colleagues of the marine microbiology laboratory with whom I have interacted namely Sheryl, Christabelle, Anindita, Sunita, Shashikant, Runa, Shanti, Shagufta, Sneha, Varatharajan, Sonali, Samita, Dhillan, Siju, Cejoice, Anu, Vijitha, Subina, Geeta, Sree, Divya, Feby, Christy, Mithila, Mahima, Sushanta, Elaine, Sam, Swatantar, Miriam, Marilyn, Reena, Amruta, Tresa, Tanya, Nausim and Ashish for making the entire work more enjoyable.

Thanks to my friends at NIO: Manoj, Vineesh, Sijin, Sudhir, Subha, Kuldeep, Rajesh, Ravi, Sanitha, Linshy, Vidya and Ankita for the help and support. I would like to thank all other members of the NIO family who directly or indirectly helped me with this research work. I am grateful to my parents, who provided the foundation and inspiration that makes me who I am, and thank them for their unbelievable love and support. Finally, I thank my wife, Deepa, and son, Jeeva, for their love, support and patience, at which I am constantly amazed.

Sujith Puzhambatty Premkumar

Dedicated to

My Beloved

Parents,

Wife and Son

TABLE OF CONTENTS

List of Figures

values indicate immobilization (mbsf: meters below seafloor, G^+: media with added glucose and G^-: media without added glucose).

Figure 8.7. Plots show the significant difference ($p \leq 0.001$) in the biotic versus abiotic cycling of Mn in subsurface sediments of the Andaman Sea under oxic versus suboxic incubation conditions in the presence (G^+) and absence (G^-) of added glucose (0.001%). The corresponding symbol with vertical bar under each category indicates the least squares means and the standard error at 0.95 confidence intervals.

List of Tables

Appendix tables

List of Plates

ABBREVIATIONS

ABP	Akademic Boris Petrov
ANME	Anaerobic methanotrophic archaea
ANOVA	Analysis of variance
ANS	Afanasiy-Nikitin Seamount
AOM	Anaerobic oxidation of methane
ATP	Adenosine tri phosphate
BC	Box core
BDL	Below detection level
CCD	Carbonate compensation depth
CFU	Colony forming units
CIOB	Central Indian Ocean Basin
CMC	Carboxymethyl cellulose
CR	Carlsberg Ridge
CRM	Certified reference materials
CTAB	Cetyltrimethyl ammonium bromide
CTD	Conductivity temperature and depth
DO	Dissolved Oxygen
EDS	Energy dispersive spectrum
EIO	Equatorial Indian Ocean
EMBL	European molecular biology laboratory
EPS	Extracellular polysaccharides
Fe-Mn	Ferromanganese
G	Glucose
H'	Shannon eveness index
HEPES	N-2-hydroxyethylpiperazine-N'-2-ethanesulfonic acid
IR	Infrared
J'	Simpson eveness index
MOF	Marine oxidation fermentation medium
MPa	Megapascal
MPN	Most probable number
NAD	Nicotinamine adenine dinucleotide

NDL	Non-detectable levels
NGHP	National gas hydrate program
NMS	Nitrate-mineral salt medium
NO_2^-	Nitrite
NO_3^-	Nitrate
OD	Optical density
OMZ	Oxygen minimum zone
ORP	Oxidation reduction potential
OTU's	Operational taxonomic units
PCA	Principal component analysis
PO_4^{3-}	Phosphate
REE's	Rare earth elements
SDS-PAGE	Sodium dodecyl sulphate paraacrylamide gel electrophoresis
SEM	Scanning electron microscopy
SiO_3^{2-}	Silicate
SNK	Students Newman-Keuls test
TBC	Total bacterial counts
tDNA	Total DNA
TEM	Transmisson electron microscopy
TEMED	Tetramethylethylenediamine
TIC	Total inorganic carbon
TOC	Total organic carbon
VAMPS	Visualization and analysis of microbial population structures
XCB	Extended core barrel
XRD	X-ray diffraction analysis
ZMA	ZoBell marine agar

CHAPTER 1

Introduction

1.1. Seamounts as an ecological niche

Seamounts are underwater elevations rising from the ocean floor many hundreds of meters or more and which does not break the sea surface to become an island (Consalvey *et al.,* 2010; Lavelle and Mohn, 2010). They are often conical in shape and erode to become less regular over geological time. They are generally volcanic in origin and serve as potential sites for ferromanganese (Fe-Mn) deposition and are locations for current-topographic interactions and biophysical coupling (Clark *et al.,* 2010) and form an ecological niche. Ecological research studies ranges from individuals to the biosphere. This study mainly deals with community ecology which is about interacting species within a particular area like the seamount. The seamount support a high number of planktonic and consumer biomass than the surrounding seawater which is mostly oligotrophic. One of the important processes proposed to support the larger biomass of seamount consumers is trophic subsidy (Genin, 2004). This mechanism may be a key to the pathway that supports the biological community of oligotrophic systems and consequently the benthic seamount communities where *in-situ* primary production on its own would be inadequate (Genin and Dower, 2007; Consalvey *et al.,* 2010). This occurs because 1) the summit and flanks of the seamount trap the fall of vertically migrating planktonic organisms and 2) the flow of water interrupt with seamount topographies and the resulting accelerated currents sequentially intensify the horizontal food supply to seamount communities (Clark *et al.,* 2010).

This work aims at filling in the lacunae, as the study of microbiology of seamounts is still in its infancy though there are considerable efforts in understanding the seamount topographies and its effect on the surrounding water column (Emerson and Moyer, 2010). The present study was conducted despite logistic issues like difficulty in regular sampling over rocky habitat, strong currents and highly variable hard substratum and also a number of other general issues related to oceanographic fieldwork (Rogers, 1994; Emerson and Moyer, 2010, McClain *et al.,* 2010) (Plates 1.1 &1.2). Hence till date, only few hundred seamounts have been sampled biologically out of the estimated 100,000 or more thought to be present in the global ocean (Wessel *et al.,* 2010). Most data have come from environmental observations, but experiments are

specific hypotheses (Clark et al., 2010) about microbial participation in the accretion process of crust-environmental coupling. There are also some potentially important environmental agents that have received less attention to date, such as 1) discrete pulses of organic matter/debris to the seafloor which could have direct influence on the seamount biome and the associated metal accretion process and 2) the effect of organic and inorganic ligands on the interactions between microbes and metals in the hydrogenetic crusts. In view of scanty information on the above aspects, experimental studies on the ecology of hydrogenetic crusts has been carried out with glucose as a model compound for organic carbon, ascorbate as a model compound for an organic reductant and EDTA as a model compound for an inorganic ligand.

1.2. Metal rich mineral deposits and their formation

Seamounts are also one of the marine environments where the migration of Fe and Mn from less oxidizing to more oxidizing conditions contributes to the formation of Fe, Mn and Fe-Mn mineral deposits (Glasby, 2006). These deposits occur in almost all geomorphologic and tectonic environments of the ocean basins in the form of nodules, crusts, cements, mounds and sediment-hosted strata-bound layers. They are formed by one or more of four processes namely (1) hydrogenetic precipitation from cold ambient seawater, (2) precipitation from hydrothermal fluids, (3) precipitation from sediment pore waters by diagenetic reactions and (4) replacement of rocks and sediments (Hein *et al.*,1997). The three major prerequisites that underpin the formation of Fe-Mn crusts are sediment free hard and exposed surfaces, availability of large pool of dissolved Mn and Fe and oxygenated ambient seawater (Banakar *et al.*, 1997). Depending on the type of reactions or the combination of the said processes, they vary in their mineralogy, Fe/Mn ratio, trace metal contents, rare-earth element patterns and growth rates. The hydrogenetic crusts are normally formed by a continuous process on tectonically stable and geologically old seamounts and exhibit Fe/Mn ratio near unity (1±0.3). Whereas, hydrothermal deposits are episodic, have distinctly different composition from hydrogenetic type of crusts and vary highly in Fe/Mn ratio from 24000 to 0.001 (Hein *et al.*, 1997). On the other hand, the precipitation of metal ions from sediment pore waters by diagenetic reactions lead to the formation of Fe-Mn concretions/nodules (Reyss *et al.*, 1982). They differ from hydrogenetic nodules and crusts in their Mn/Fe ratio ($\geq$ 2.5). Because of the high enrichment of Co, Pt and Au in hydrogenetic crusts,

attention has been drawn to the crusts as potential economic resources (Manheim, 1986).

1.3. Afanasiy-Nikitin seamount: a potential site for hydrogenetic Fe-Mn crust

The Afansiy-Nikitin seamount (ANS) in the Northern Central Indian Ocean is one of the low productive environments characterized by seasonal thermohaline alteration, voluminous precipitation, and fresh water inflow (Sardessai *et al.*, 2010). This seamount is situated at 3°S latitude and 83 °E longitude in the northern part of the Central Indian Ocean, and is located 1000 km southeast of Sri Lanka (Rajani *et al.*, 2005). It extends ~300 km in the north south direction and ~200 km in the east west direction (Paul *et al.*, 1990; Parthiban and Banakar, 1999). It was formed during the Late-Cretaceous (Sborshchikov *et al.*, 1995) and evolved as a part of the 85 °E ridge (Borisova *et al.*, 2001). It was discovered by the Russians during the R.V. Vityaz cruise of 1959 (Bogorov and Bezrukov, 1961). The emplacement of the seamount was at ~75 Ma (Cande and Kent, 1992; Karner and Weissel, 1990) and the age of the crusts was estimated to be ~5-20 Ma old (Rajani *et al.*, 2005). The ANS covers a total area of 50,000 km^2 above the carbonate compensation depth (CCD), of which 5000 km^2 falls in the intermediate oxygen minimum zone (OMZ) (< 2ml/l O). The ANS is a potential site for the formation of Co enriched Fe-Mn crusts. Approximate resource evaluation states 0.9 million tonnes of Co metal for 180 million tonnes of Fe-Mn crust assuming an average crust thickness of 2 cm and Co content of 0.5% covering the whole 5000 km^2 area. The significance of the ANS is not only because of its tectonic history but also due to the presence of potentially economically important Co-enriched Fe-Mn crusts (Parthiban and Banakar, 1999). These crusts are also highly enriched with elements like Ce (maximum: 0.37%, average: ~0.22%) and Pt (maximum: 1ppm, average: ~0.5ppm) (Banakar *et al.*, 2007; Banakar, 2010) apart from Mn and Fe which constitute the major (oxy)hydroxide mineral phases of the Fe-Mn crust. The substrate of the crust is composed of fresh-water phreatic calcite cement, terebratulinae casts, rounded and ferruginised basalt clasts and weathered coralline algal fragments (Banakar *et al.*, 1997). The Fe-Mn deposition on the ANS is formed by hydrogenetic process and contains promising source of Co (0.5-1%), Ni (~0.26%) and other rare earth elements. The mineral phases are composed of poorly crystalline vernadite (δMnO_2) (Parthiban and Banakar, 1999) resembling the amorphous mineral oxide phases of Mn produced by bacteria. Here the bacterial production accounts for the overall production of the

region whereas primary production by phytoplankton is very low. The region exhibits sub-surface maxima for chlorophyll 'a' over seasons (Fernandes *et al.,* 2008). The summit of the seamount protrudes above the CCD at 1550m (Rudenko, 1994) and lies at a shallower depth beneath the intermediate OMZ (Banakar *et al.,* 1997). This is a most suitable conditions for the colloidal precipitation of Fe-Mn (oxy)hydroxides and an ideal environment that suits the biological processes.

1.4. Interactions between microorganisms and metals

Metals are an essential part of all ecosystems and occur in both elemental and ore forms in nature (Tripathi and Srivastava, 2007). The microorganisms adapted to such metal rich deep-sea environments however show activity for metal immobilization and mobilization because organic food supplies are restricted in the open-ocean. These chemically based ecosystems present surprising diversity and show multiple abilities in organisms to tolerate metals. Different mechanisms for the uptake and release of metal ions from their surrounding environment could therefore operate in these organisms. The biogenic oxides of Mn for example produced by one organism with the potential to degrade humic substances to simpler compounds feed the growth of several other organisms with the required substrates (Sunda and Kieber, 1994). In the absence of carbon or energy, the storage of the metal serves as a respiratory substrate and energy for growth through the oxidation of reduced Mn (Tebo *et al.,* 1997). Besides, bacterial cells couple the oxidation of organic matter to the dissimilatory reduction of the metal oxides (Lovley and Philips, 1988; Nealson *et al.,* 1988). The dissolution of the oxides could occur by one of the two processes wherein direct contact between the cell surface and the oxide leads to solubilization or indirectly through microbially mediated changes in the reducing conditions (Baglin *et al.,* 1992; Sand *et al.,* 2001). In some cases, metal may be reduced to fulfill a nutritional need for soluble ions (de Vrind *et al.,* 1986) or to scavenge excess reducing power as in the case of nitrate and iron reduction (Robertson *et al.,* 1988; Lovley, 1991). The microorganisms that are associated with the metal-rich deep sea habitats belong to divergent phylogenetic lineages such as *Firmicutes*, *Proteobacteria*, *Actinobacteria* and *Bacteroidetes*. This broad phylogenetic diversity mirrors their physiological diversity (Tebo *et al.,* 2005).

The elements like Mn, Co and Ni are essential micronutrients required for most, if not all, living organisms as constituent of many metalloenzymes and proteins involved

in electron transport, redox, and other important reactions (Ford *et al.*, 1995). The primitive size and larger surface area to volume ratio permit microbial cells to interact with metal ions at different rates (Ledin, 2000). It is interesting that only prokaryotes have the ability to oxidize metals and conserve energy in those reactions. Inevitably, certain microbes (eubacteria and archaea) use some metals or metalloids as electron donors or acceptors in their energy metabolism (Ehrlich, 2002). Certain organisms have the ability to bind metal ions at the cell surface or to transport them into the cell for various intracellular functions (Ehrlich, 1997). The bacterial adaptation to heavy metal rich environments shows activities for biosorption, bioprecipitation, extracellular sequestration, transport mechanisms and/or chelation (Haferburg and Kothe, 2007). Although the requirements of metal ions for growth are generally small, the heavy metal uptake systems would operate at higher concentrations. It thereby influences the toxicity of metal ions to microorganisms at the individual and community level. The different strategies that bacteria engage in order to tolerate excess metal concentrations includes a) the production of stable precipitates or chelates with essential metabolites, b) catalyzing the decomposition of essential metabolites and thereby making the metabolites unavailable to the cells, c) acting as antimetabolites, d) replacing structurally or electrochemically important elements and thereby interfering with enzymatic or cellular function (Ehrlich, 1978). The metal uptake by bacteria involves a) the nonspecific binding of the metal cations to cell surfaces, slime layers, extracellular matrices, etc and b) metabolism-dependent intracellular uptake (Gadd, 1990). The heavy metal on uptake intracellularly may precipitate or compartmentalize to a more innocuous form such as phosphide, sulphide, carbide or hydroxide deposits (Ehrlich, 1997). The interactions however when deadly exerts morphological changes, altered cell metabolism, bacteriostasis or lethality in bacteria (Ehrlich, 1978). Interactions between bacteria and metal ions would also lead to the formation of biogenic minerals. The interactions of bacteria with metals may have several implications on the environment, as metals have an essential role in the biogeochemical cycling of carbon, nitrogen, phosphorous and several associated elements in the seamount ecosystem. Besides, they could also serve as suitable candidates for cleaning up or remediating metal-contaminated environments.

Substantial studies have determined the bacterial diversity of hydrothermally active seamounts of Pacific and Atlantic Oceans (Emerson and Moyer, 2010; Clark *et al.*,

2010) but very little evidence exists on the bacterial ecology of hydrogenetic seamount Fe-Mn crusts and the associated sediments (Kato and Yamagishi, 2011). Studies related to hydrothermal systems report the dominance of ζ- and ε-*Proteobacteria* (Emerson and Moyer, 2010) and one study from the Takuyo-Daigo Seamount, northwest Pacific report γ- and α-*Proteobacteria* in the hydrogenetic crusts (Nitahara *et al.*, 2011). The bacterial diversity of the mid-ocean ridge systems are composed of known, non-photosynthetic lineages of organisms like the *Firmicutes*, *Verrucomicrobia*, *Thermales* and the *Cytophaga–Flexibacter–Bacteroides* groups (Takai *et al.*, 2006). On the other hand, Mn and S oxidizing bacterial communities belonging to class α-*Proteobacteria*, β-*Proteobacteria*, γ-*Proteobacteria*, *Actinobacteria* and *Bacilli* dominate the deep-sea low-temperature influenced oceanic crust basalts and sediments along the ridge axis (Rathsack *et al.*, 2009).

The hydrogenetic Fe-Mn crusts are potential ore-deposits because of their widespread occurrence and high concentrations of valuable trace and rare earth elements present in it (Pulyaeva and Hein, 2010). Yet, investigations of hydrogenetic crusts are far less numerous than those of hydrothermal crusts and equivalent insights have not been made. Several studies addressed the capacity of bacteria in forming minerals by induced and controlled mechanisms however their direct role in the process has only been accepted for manganese nodules where bacteria with surface S-layers arranged on biofilm like structures initiate the deposition of Mn. It has been found that the enrichment of trace and rare earth elements in diagenetic deposits could occur by abiogenic or biogenic routes that progress and proceeds in close association with organic molecules and matrices (Lowenstam and Weiner, 1989). Studies have also identified manganese-mineralized and silicified textures resembling fossil biofilms and microbialites in Mn oxide and barite deposits (Ivarsson *et al.*, 2010; Kilias, 2011). Such interactions between microorganisms and metals were found to yield oxides and hydroxides of low crystallinity (Hein *et al.*, 2000). However, the origin of cobalt-enriched Fe-Mn crusts is thought to be purely of abiogenic reaction even though coccolithophores are reported to act as bio-seeds for initial Mn deposition in crusts (Wang and Muller, 2010). In spite of the recognized importance of microbial participation in mineral formation (Ferris *et al.*, 1987), studies on cobalt-enriched Fe-Mn crusts are scanty. As in diagenetic deposits where there is bacterial involvement, it is hypothesized that the hydrogenetic crust formation may also be triggered or

accelerated by bacterial activity. An understanding of the different ecological types of bacteria around crust deposits would throw light on the predominant groups participating in these processes. It was therefore one of the primary objectives of the present study to understand the role of bacteria in the accretion or dissolution of the Fe-Mn crust containing high concentrations of Co and Ni. The study also compares and contrasts the culturability and *in vitro* metal immobilizing/mobilizing activity of bacteria under simulated deep-sea temperature and/or pressure conditions in microcosm and/or with bacterial isolates for samples from the Carlsberg Ridge (CR), Central Indian Ocean Basin (CIOB) and the Andaman Sea to understand the difference in the cycling of Mn, Co and Ni from one ecosystem to the other (Figure 1.1, Table 1.1). Understanding of the microbe-metal interactions provides insight into the potential influence of micro-organisms to alter oxidation states of heavy metals, and to influence their behavior in the environment (Nedelkova *et al.,* 2007). The findings of the present study would aid in exploration studies for removal and/or recovery of economically important metals like Co and Ni from valuable ores by bioleaching/precipitation. To address the above hypothesis the following objectives are proposed.

1.5. Objectives

- To elucidate the distribution of cobalt and nickel tolerant bacteria in unique marine ecosystems.
- To delineate the phylogeny of culturable and non-culturable bacterial community.
- To provide experimental evidence for the immobilization and mobilization of metal ions by bacterial communities/isolates from different marine environments.

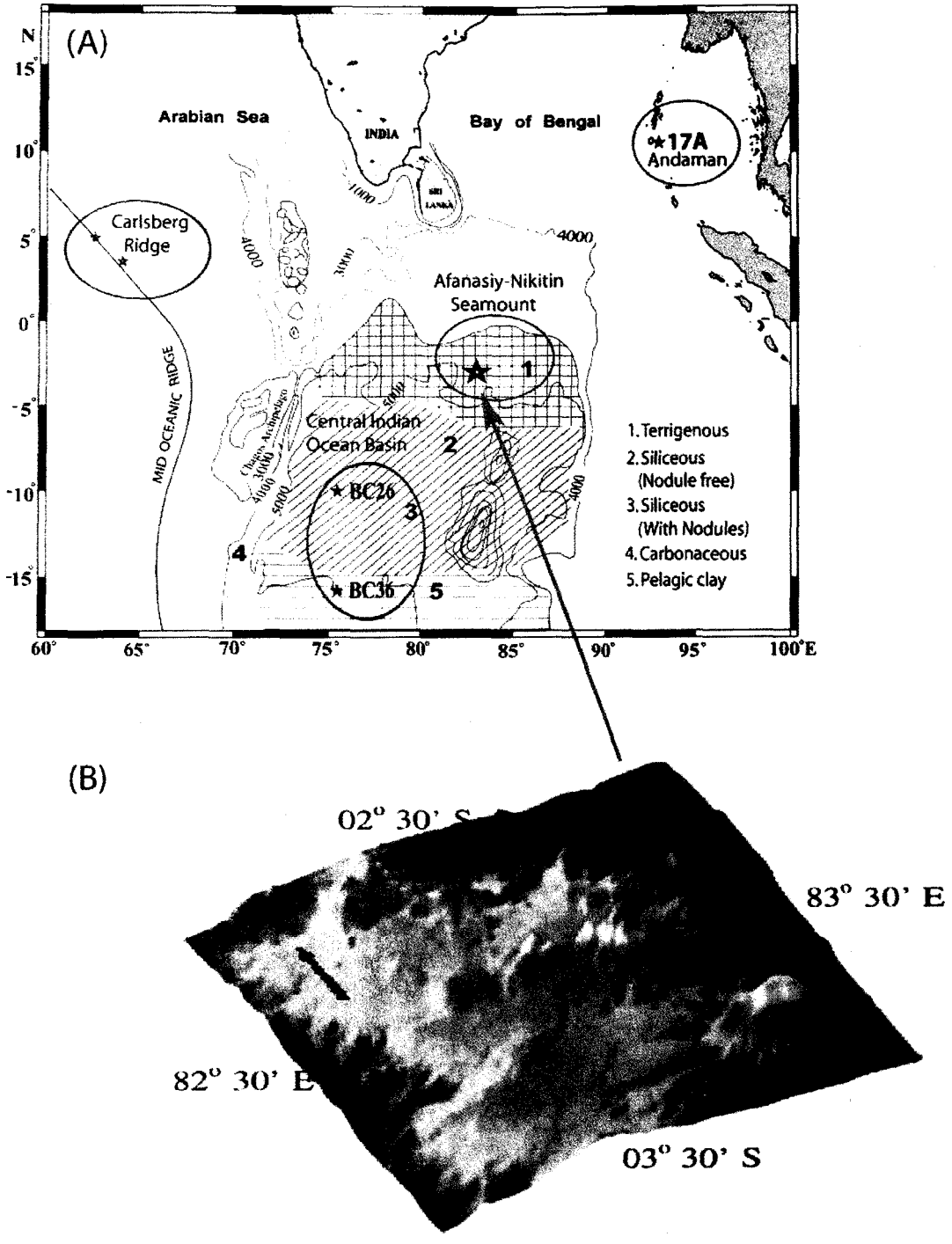

Figure 1.1. A) Map showing different sampling locations indicated by the symbol star modified from Mascarenhas-Pereira *et al.* (2006) and B) bathymetry image of the Afanasiy-Nikitin Seamount (Banakar *et al.*, 2007).

late 1.1. A) Onboard Akademik Boris Petrov cruise to CIOB, B) CTD rossette for water sampling,

) Field data collection, D) Dredging of Fe-Mn crusts, E) Box coring of sediments , F) Lowering of CTD.

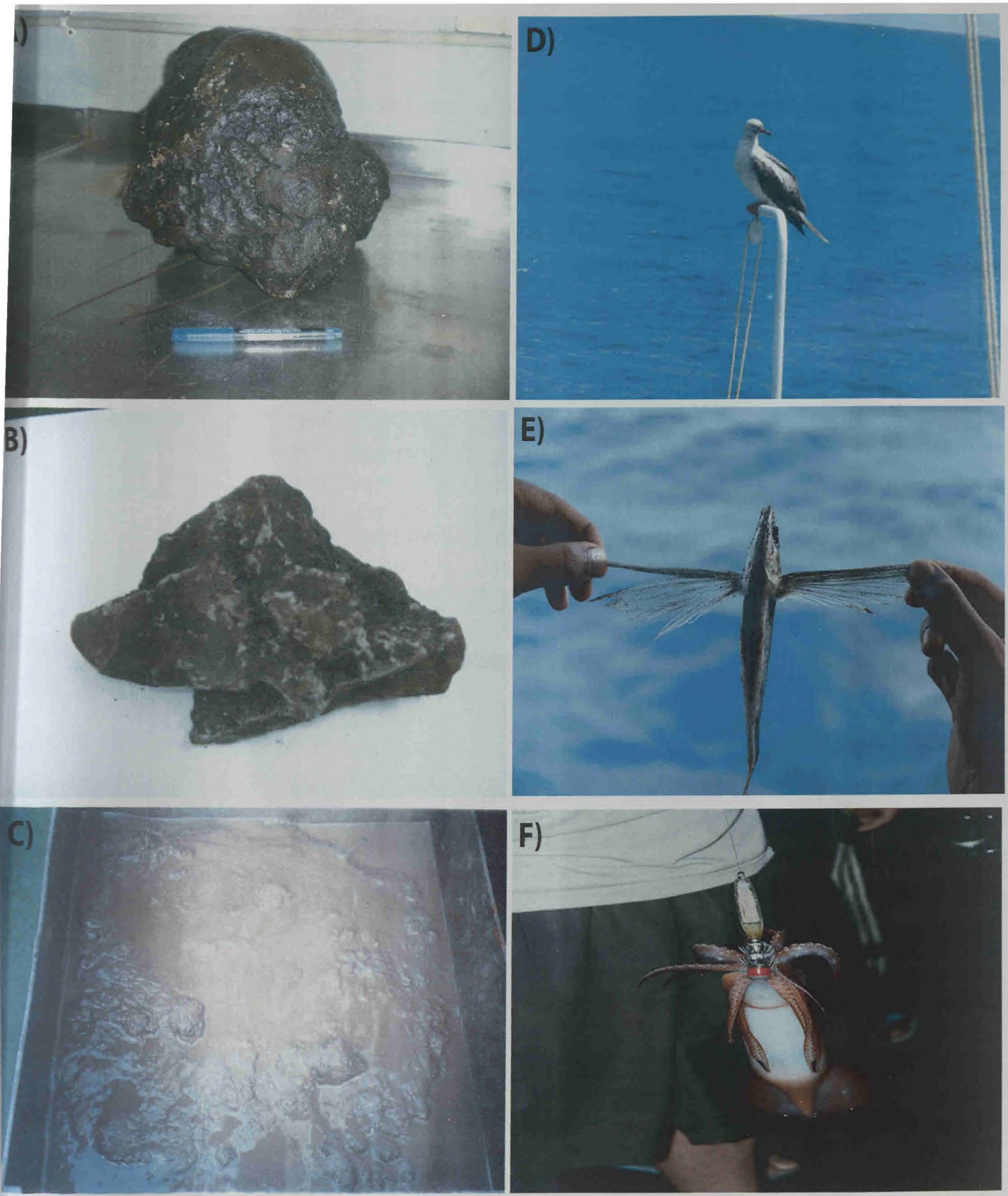

Plate 1.2. Left panel-samples onboard Akademic Boris Petrov and right panel- the ANS environment. A) Cobalt rich Fe-Mn crust, B) Rock sample from Carlsberg Ridge, C) Box corer holding sediments with nodules, D, E and F different life forms observed in the ANS region.

Table 1.1. Details of samples used in the present study collected from different geographical location of the Indian Ocean region.

Area	Lat/Long	Depth (m)	Sample code	Sample type
ANS	0°59'N/82°59'E	4310	ABP37/CTD1	Water
	3°00'S/82°59'E	2704	ABP37/CTD5	Water
	4°29'S/82°40'E	3422	ABP37/DRG04	Crust
	3°30'S/82°36'E	3561	ABP37/DRG07	Crust
	3°17'S/83°12'E	2100	ABP37/DRG10	Crust
	3°20'S/83°15'E	2204	ABP37/DRG10A	Crust
	2°43'S/82°47'E	3304	ABP37/DRG11A	Crust
	2°51'S/82°52'E	3309	ABP37/DRG14	Crust
	3°22'S/83°12'E	3325	CC2/ADR04	Crust
	3°01'S/83°01'E	2415	CC2/ADR11	Crust
	3°01'S/83°03'E	1987	CC2/ADR12	Crust
	3°00'S/83°08'E	2815	CC2/ADR18	Crust
	2°58'S/82°51'E	3345	CC2/ADR24	Crust
	2°59'S/82°54'E	2357	CC2/ADR27	Crust
CR	3°40'N/63°50'E	2924	ABP36/DRG22	Basalt with Mn-oxide coating
	3°39'N/63°49'E	2312	ABP36/DRG23	Basalt with Mn-oxide coating
CIOB	9°59'S/75°30'E	5339	ABP26/BC26	Sediment & Nodule
	16°01'S/75°28'E	5042	ABP26/BC36	Sediment & Nodule
Andaman	10°45'N/93°06'E	1344	NGHP-17A	Sediment

1.6. References

Baglin EG, Noble EG, Lampshire DL, Eisele JA. 1992. Solubilization of manganese from ores by heterotrophic micro-organisms. Hydrometallurgy 29: 131-144.

Banakar VK, Hein JR, Rajani RP, Chodankar AR. 2007. Platinum group elements and gold in ferromanganese crusts from Afanasiy–Nikitin seamount, equatorial Indian Ocean: Sources and fractionation. J Earth Syst Sci 116: 3-13.

Banakar VK, Pattan JN, Mudholkar AV. 1997. Palaeoceanographic conditions during the formation of ferromanganese crust from the Afanasiy Nikitin seamount, north central Indian Ocean-geochemical evidence. Mar Geol 136: 299-315.

Banakar VK. 2010. Deep-sea ferromanganese deposits and their resource potential for India. J Indian Inst Sci 90: 535-541.

Bogorov VG, Bezrukov PL.1961. Vityaz in the Indian Ocean. Prioda 10: 12-35 (in Russian).

Borisova AY, Portnyagin MV, Sushchevskaya NM, Tsekhonya TI, Kononkova NN. 2001. Olivine basalts of the Afanasiy-Nikitin Rise, Indian Ocean: Petrology and deuteric alteration. Geochem Internat 35: 346-358.

Cande SC, Kent DV. 1992. A new geomagnetic polarity time scale for the late Cretaceous and Cenozoic. J Geophys Res 97: 13917-13951.

Clark MR, Rowden AA, Schlacher T, Williams A, Consalvey M, Stocks KI, Rogers AD, O'Hara TD, White M, Shank TM, Hall-Spencer JM. 2010. The Ecology of Seamounts: Structure, Function, and Human Impacts. Ann Rev Mar Sci 2: 375-400.

Consalvey M, Clark MR, Rowden AA, Stocks KI. 2010. Life on seamounts. In: Life in the world oceans: diversity, distribution, and abundance. McIntyre AD (ed) Blackwell publishing Ltd., USA, pp. 123-138.

de Vrind JPM, Boogerd FC, De Vrind-De Jong EW. 1986. Manganese Reduction by a marine *Bacillus* species. J Bacteriol 167: 30-34.

Ehrlich HL. 1978. How microbes cope with heavy metals, Arsenic and Antimony in their environment. In: Microbial life in extreme environments. Kushner DJ (ed) Academic Press, London, pp. 381-408.

Ehrlich HL. 1997. Microbes and metals. Appl Microbiol Biotechnol 48: 687-692.

Ehrlich HL. 2002. Geomicrobiology, Marcel Dekker Inc., New York, USA.

Emerson D, Moyer CL. 2010. Microbiology of seamounts: Common patterns observed in community structure. Oceanography 23: 148-163.

Fernandes V, Rodrigues V, Ramaiah N, Paul JT. 2008. Relevance of bacterioplankton abundance and production in the oligotrophic equatorial Indian Ocean. Aquat Ecol 42: 511-519.

Ferris FG, Fyfe WS, Beveridge TJ. 1987. Bacteria as nucleation sites for authigenic minerals in a metal-contaminated lake sediment. Chem Geol 63: 225-232.

Ford T, Maki J, Mitchell R. 1995. Metal-microbe interactions. In: Bioextraction and biodeterioration of metals. Gaylarde CC, Videla HA (eds) Cambridge University Press, Cambridge, pp. 1-23.

Gadd GM. 1990. Heavy metal accumulation by bacteria and other microorganisms. Experientia 46: 834-840.

Genin A, Dower JF. 2007. Seamount plankton dynamics. In: Seamounts: Ecology, Fisheries & Conservation. Pitcher TJ, Morato T, Hart PJB, Clark MR, Haggan N, Santos RS (eds) Blackwell Publishing Ltd, Oxford, UK, pp. 86-100.

Genin A. 2004. Bio-physical coupling in the formation of zooplankton and fish aggregations over abrupt topographies. J Mar Syst 50: 3-20.

Glasby GP. 2006. Manganese: Predominant Role of Nodules and Crusts. In: Marine Geochemistry. Schulz HD, Zabel M (eds) Springer, Berlin-Heidelberg, pp. 371-427.

Haferburg G, Kothe E. 2007. Microbes and metals: interactions in the environment. J Basic Microbiol 47: 453-467.

Hein JR, Koschinsky A, Bau M, Manheim FT, Kang JK, Roberts L. 2000. Cobalt rich ferromanganese crusts in the Pacific. In: Handbook of Mineral Deposits. Cronan DS (ed) CRC, Boca Raton, pp. 239-279.

Hein JR, Koschinsky A, Halbach P, Manheim FT, Bau M, Kang J-K, Lubick N. 1997. Iron and manganese oxide mineralization in the Pacific. Geol Soc London Spl Pub 119: 123-138.

Ivarsson M, Kilias S.P, Broman C, Naden J, Detsi K. 2010. Fossilized microorganisms preserved as fluid inclusions in epithermal veins, Vani Mn-Ba deposit, Milos Island, Greece. Thessaloniki 100: 297-307.

Kato S, Yamagishi A. 2011. Microbial biodiversity and biogeography on the deep seafloor. In: Changing Diversity in Changing Environment. Grillo O, Venora G (eds) InTech, pp. 357-374.

Kilias SP. 2011. Microbial mat–related structures in the quaternary cape Vani manganese-oxide (-barite) deposit, NW Milos island, Greece. SEPM Spl Pub 101: 97-110.

Lavelle JW, Mohn C. 2010. Mountains in the Sea: motion, commotion, and biophysical connections at deep ocean seamounts. Oceanography 23: 90-103.

Ledin M. 2000. Accumulation of metals by microorganisms-processes and importance for soil systems. Earth-Sci Rev 51: 1-31.

Lovley DR, Phillips EJP. 1988. Novel mode of microbial energy metabolism: Organic carbon oxidation coupled to dissimilatory reduction of iron or manganese. Appl Environ Microbiol 54: 1472-1480.

Lovley DR. 1991. Dissimilatory Fe(III) and Mn(IV) reduction. Microbiol Rev 55: 259-287.

Lowenstam HA, Weiner S. 1989. On Biomineralization. Oxford University Press, New York.

Manheim FT. 1986. Marine cobalt resources. Science 232: 600-608.

Mascarenhas-Pereira MBL, Nath BN, Borole DV, Gupta SM. 2006. Nature, source and composition of volcanic ash in sediments from a fracture zone trace of Rodriguez Triple Junction in the Central Indian Basin. Mar Geol 229: 79-90.

Nealson KH, Tebo BM, Rosson RA. 1988. Occurrence and mechanisms of microbial oxidation of manganese. Adv Appl Microbiol 33: 279-318.

Nedelkova M, Merroun ML, Rossberg A, Hennig C, Selenska-Pobell S. 2007. *Microbacterium* isolates from the vicinity of a radioactive waste depository and their interactions with uranium. FEMS Microbiol Ecol 59: 694-705.

Nitahara S, Kato S, Urabe T, Usui A, Yamagishi A. 2011. Molecular characterization of the microbial community in hydrogenetic ferromanganese crusts of the Takuyo-Daigo Seamount, northwest Pacific. FEMS Microbiol Lett 321: 121-129.

Parthiban G, Banakar VK. 1999. Chemistry and possible resource potential of cobalt-rich ferromanganese crusts from Afanasiy-Nikitin Seamount in the Indian Ocean. Indian Mineralogist 33: 125-132.

Paul J, Singh RN, Subrahmanyam C, Drolia RK. 1990. Emplacement of Afanasiy-Nikitin seamount based on transfer function analyses of gravity and bathymetry data. Earth Planet Sci Lett 96: 419-426.

Pulyaeva IA, Hein JR. 2010. Paleoceanographic conditions during the formation of Fe-Mn crusts from the Pacific Ocean: Biostratigraphic and compositional evidence. In: Toward the Sustainable Development of Marine Minerals: Geological, Technological, and Economic Aspects UMI 2010, 39th Underwater Mining Institute, Gelendzhik, Russia. pp. 1-11.

Rajani RP, Banakar VK, Parthiban G, Mudholkar AV, Chodankar AR. 2005. Compositional variation and genesis of ferromanganese crusts of the Afanasiy-Nikitin Seamount, Equatorial Indian Ocean. J Earth Syst Sci 114: 51-61.

Rathsack K, Stackebrandt E, Reitner J, Schumann G. 2009. Microorganisms isolated from deep sea low-temperature influenced oceanic crust basalts and sediment samples collected along the Mid-Atlantic Ridge. Geomicrobiol J 26: 264-274.

Reyss JL, Marchig V, Ku TL. 1982. Rapid growth of a deep-sea manganese nodule. Nature 295: 401- 403.

Robertson LA, Van Niel EWJ, Torremans RAM, Kuenen GJ. 1988. Simultaneous nitrification and denitrification in aerobic chemostat cultures of *Thiosphaera pantotropha*. Appl Environ Microbiol 54: 2821-2818.

Rudenko MV. 1994. Morphostructure of the Afanasiy-Nikitin seamount. Oceanol 33: 525-530.

Sand W, Gehrke T, Jozsa P, Schippers A. 2001. (Bio)chemistry of bacterial leaching-direct vs. indirect bioleaching. Hydrometallurgy 59: 159-175.

Sardessai S, Shetye S, Maya MV, Mangala KR, Prasanna Kumar S. 2010. Nutrient characteristics of the water masses and their seasonal variability in the eastern equatorial Indian Ocean. Mar Environ Res 70: 272-282.

Sborshchikov IM, Murdmaa IO, Matveenkov VV, Kash-intsev GL, Golmshtock GI, Al'mukhamedov AI. 1995. Afanasiy-Nikitin Seamount within the intraplate deformation zone, Indian Ocean. Mar Geol 128:115-126.

Sunda WG, Kieber DJ. 1994. Oxidation of humic substances by manganese oxides yields low-molecular-weight organic substrates. Nature 367: 62-64.

Takai K, Nakagawa S, Reysenbach AL, Hoek J. 2006. Microbial ecology of Mid-Ocean Ridges and Back-Arc Basins. In: Back-Arc spreading systems: geological, biological, chemical and physical interactions. Christie DM, Fisher CR, Lee SM, Givens S (eds) Geophysical Monograph Series, American Geophysical Union, pp.185-213.

Tebo BM, Ghiorse WC, van Waasbergen LG, Siering PL, Caspi R. 1997. Bacterially mediated mineral formation: insights into manganese(II) oxidation from molecular genetic and biochemical studies. In: Geomicrobiology: interactions between microbes and minerals. Banfield JF, Nealson KH (eds) Mineralogical Society of America, Washington, DC, pp. 225-266.

Tebo BM, Johnson HA, McCarthy JK, Templeton AS. 2005. Geomicrobiology of manganese(II)oxidation. Trends Microbiol 13: 421-428.

Tripathi P, Srivastava S. 2007. Mechanism to combat cobalt toxicity in cobalt resistant mutants of *Aspergillus nidulans*. Indian J Microbiol 47: 336-344.

Wang X, Muller WEG. 2010. Are Polymetallic Nodules, Crusts and Vents Biominerals? J Sci Hal Aquat 2: 5-20.

CHAPTER 2

Review of literature

2.1. Seamount and its characteristics

Seamounts are described as active or extinct seafloor volcanoes with heights exceeding ~100 m. They are geographically isolated topographic features on the seafloor whose summit regions may temporarily emerge above sea level. They do not include features located on the continental shelves or form a part of other major landmasses (Staudigel *et al.,* 2010). They are ubiquitous in distribution, occur in clusters or groups, and vary in size and number. The environmental characteristics of seamounts are similar to that of any other marine habitats having similar physical attributes and similar biotic assemblages (Woodward, 2003). They are mostly aphotic, have basalts as the substrate, and are encircled by consistently cold and highly saline waters. The biota of the seamount mostly depends on the overlying water body for their food (Etnoyer *et al.,* 2010). Seamounts support ecologically important communities, determine habitats for fish, and act as obstacles to currents. Consequently, they enhance tidal energy dissipation and ocean mixing. Seamounts have metal resource potential which can be related to their volcanic and hydrothermal activity or their prolonged history of exposure to seawater (Staudigel and Clague, 2010; Hein *et al.,* 2010). The colloidal precipitation of metal ions from seawater leads to the formation of hydrogenetic Fe-Mn crusts on seamounts which are a potential ore with reference to the enrichment of "high-tech metals" that are used in solar cells, computer chips, and hydrogen fuel cells (Hein *et al.,* 2010). The different economically important metals that are enriched in the hydrogenetic Fe-Mn crusts on the ANS include Co (maximum: 0.9%, average: ~ 0.5%), Ce (maximum: 0.37%, average: ~0.22%) and Pt (maximum: 1 ppm, average: ~ 0.5 ppm) (Banakar *et al.,* 2007; Banakar, 2010).

2.2. Studies on seamounts

Seamounts are important for researchers from different disciplines like geology, oceanography, biology and economics as it gives information about basic planetary and oceanic processes, ecology and fisheries, and hazards and metal resources (Wessel *et al.,* 2010). The studies on seamounts have mostly been dealt with survey and bathymetry, plate tectonics, mineralogy, geochemistry and paleooceanography (Calvert and Cronan, 1978; Goddard *et al.,* 1987; Banakar *et al.,* 1997; Usui and Someya, 1997;

Krishna, 2003; Allain *et al.*, 2008; Krishna *et al.*, 2009; Pulyaeva and Hein, 2010; Sardessai *et al.*, 2010; Wessel *et al.*, 2010; Mendonca *et al.*, 2012; Kamesh Raju *et al.*, 2012). Comprehensive studies on seamount biology in general have been related to higher groups of organisms like fishes, crustaceans, corals, decapods, gastropods and others (Wilson and Kaufmann, 1987; Verlaan, 1992; de Forges *et al.*, 2000; Brewin *et al.*, 2009; Iyer, 2009; Clark *et al.*, 2010; Sautya *et al.*, 2011; Iyer *et al.*, 2012b). Studies related to lower groups of organisms like bacteria and fungi of seamounts and mid-oceanic ridges are mostly hydrothermal based (Moyer *et al.*, 1995; Emerson and Moyer, 2002; Sunamura *et al.*, 2004; Nakagawa *et al.*, 2005; Takai *et al.*, 2005; Templeton *et al.*, 2005; Emerson, 2009; Sudek *et al.*, 2009; Connell *et al.*, 2009; Glazer and Rouxel, 2009; Rassa *et al.*, 2009; Huber *et al.*, 2010; Emerson and Moyer, 2010; Clark *et al.*, 2010; Mohandass *et al.*, 2012). In addition, works have also been carried out on the microbial ecology of Fe-Mn concretions/nodules of soils and deep-ocean floor sediments (Cahyani *et al.*, 2007; He *et al.*, 2008; Wang *et al.*, 2010; Tully and Heidelberg, 2013). Several detailed interdisciplinary research related to seamounts have been carried out on the Pacific and Atlantic oceans, but similar studies are sparse in the Indian Ocean and more so in the Arabian Sea and the Bay of Bengal (Iyer *et al.*, 2012a). Only scanty evidence exists for the microbial ecology of hydrogenetic seamount Fe-Mn crusts and the associated sediments (Nitahara *et al.*, 2011; Liao *et al.*, 2011). These crusts are a potential source of high-tech metals (Gonzalez *et al.*, 2010; Hein *et al.*, 2010). It is therefore important to understand the bacterial ecology of the hydrogenetic crusts and the role of bacteria in the enrichment process of economically important metals. The increasing demand for elements like tellurium, bismuth, cobalt, zirconium, niobium, tungsten, molybdenum, platinum, titanium, and thorium enriched in these crust may direct our attention to Fe-Mn crust mining in future.

The Afanasiy-Nikitin seamount (ANS) located in the northern part of the Central Indian Ocean was discovered by the Russians during the R.V. Vityaz cruise of 1959 (Bogorov and Bezrukov, 1961). The occurrence of Fe-Mn crust in the ANS was discovered later on by Banakar *et al.* (1997). The Fe-Mn crust deposition on the ANS is by hydrogenetic process and contains promising source of Co (0.5 to 1%) and other rare earth elements. The substrate of the crust is composed of fresh-water phreatic calcite cement, terebratulinae casts, rounded and ferruginised basalt clasts and weathered coralline algal fragments (Banakar *et al.*, 1997). The mineral phases are composed of

poorly crystalline δMnO_2 (Parthiban and Banakar, 1999) that resembles the amorphous oxide phases of Mn produced by bacteria. Also, the internal features of the crust and nodules show features that resemble that of biological entity (Iyer, 1991; Banakar and Tarkian, 1991; Wang *et al.,* 2009). Therefore, it is of utmost importance to understand the contribution of microorganisms to the accretion and dissolution processes of Fe-Mn crust as they could have a major role in the crust accretion process. Studies that have been so far carried out in the ANS are preliminary and deal with the tolerance of bacterial isolates to cobalt and its immobilization (Krishnan *et al.,* 2006). Therefore the detailed outlook of the microbial interactions of the ANS helps in understanding the system better. This would help in harnessing the potential of microbes in the recovery of metals from ores by precipitation and bioleaching.

2.3. Formation of metal rich mineral deposits

2.3.1. Abiogenic mineralization

Abiogenic mineralization describes processes which involves only inorganic reactions. It involves the chemical and physical forces driving accumulation of new inorganic material (eg. Hydrothermal vents) from solution (Wang and Muller, 2010). The process is controlled by the initial mineral growth rate, the magnitude of supersaturation of the inorganic precursors as well as the temperature (Persson *et al.,* 1995). The diagenetic mineralization occurs by the relatively sudden change in the oxidizing conditions in the sedimentary environments. The reduced elements like Fe, Mn and particulate organic carbon in sediment pore water undergo oxidation at the redox fronts by oxidants (molecular oxygen and nitrate) diffusing from the overlying water column (Wilson *et al.,* 1986).

2.3.2. Biogenic mineralization

Deep sea minerals like crusts and polymetallic nodules are not only formed by abiogenic (mineralization) routes such as hydrogenetic, hydrothermal and diagenetic processes but also by biogenic (biomineralization) mineralization involving microorganisms (Wang and Muller, 2009). Biogenic mineralization develops and proceeds in close association with organic molecules and matrices (Lowenstam and Weiner, 1989). These mineralization processes occur widely and involves the participation of both prokaryotic (bacteria) and eukaryotic (plants, protozoa and metazoa) organisms (Gilbert *et al.,* 2005). The interaction of bacteria with metal ions

can lead to the formation of minerals. It occurs as an induced (Frankel and Bazylinski, 2003) or a controlled (Bazylinski and Frankel, 2003) process. In the induced mechanism, reactions occur at the interface between organic membranes and their inorganic environment (eg. nodules and crusts). The organic matrix functions as the nucleation platform for the deposition of the mineral followed by physical or chemical processes (Wang and Muller, 2009; Chu *et al.,* 2012). In the controlled mechanism, the precipitation of metals occurs on the existing bio-seeds and organic matrices. It is purely a biological process in which the biomolecules such as proteins, polysaccharides or glycoproteins control the initiation and growth of the mineral (Konhauser, 2007; Wang and Muller, 2009). The controlled process occurs both extracellularly like in *Bacillus subtilis* (Urrutia and Beveridge, 1994) and intracellularly like in *Ramlibacter tataouinensis* and magnetotactic bacteria (Benzerara *et al.,* 2004; Edwards and Bazylinski, 2008; Baumgartner and Faivre, 2011). Within the nodules, bacteria with surface S-layers are arranged on biofilm like structures, around which Mn deposition starts. In crusts coccolithophores represent the dominant organisms that act as bio-seeds for initial Mn deposition (Wang and Muller, 2010).

2.4. Ecology of metal microbe interactions

The involvement of microorganisms in the formation of Fe-Mn mineral deposits was under controversy for a long period among geochemists (Harris and Troup, 1970). While some geochemists agreed that microorganisms could create microenvironments suitable for mineral formation (Dean and Ghosh, 1981), others agreed that enzyme catalysis could mediate oxidation-reduction reactions (Callender and Bowser, 1976). Yet, it was difficult to accept microbial participation in Fe-Mn mineral formation in environments where purely physico-chemical mechanisms apply (Callender and Bowser, 1976). This problem was difficult to resolve as literature for direct evidence of bacterial participation (eg. Sterile control experiments) was lacking (Ghiorse, 1984). Nevertheless, microbiologists with assortment of powerful microscopic techniques, specific metabolic inhibitors, and other tools available for probing microbial presence and activity in microhabitats proceeded to understand the mechanism (Rosswall, 1973). This was followed by many reports, concerning Fe and Mn encrusted microorganisms associated directly with natural samples. There were many clear demonstrations of intimate associations of microorganisms with minerals in fresh and saltwater Fe-Mn concretions (Ghiorse and Hirsch, 1982), bog ore and iron spring deposits (Crearar *et al.,*

1979), rock varnish (Dorn and Oberlander 1981), detrital particles in lakes and ponds (Gregory and Staley, 1982), water distribution systems (Ridgway and Olson, 1981), fjords (Emerson *et al.,* 1982), and surface films of swamps and shallow ponds (Ghiorse and Hirsch, 1982). Recognizing the deficiencies of relying on only microscopic techniques, radiotracer methods in conjunction with metabolic poisons and electron microscopic observations were employed to study the biogeochemical role of metal cations in the natural environment (Emerson *et al.,* 1982). Further, several studies addressed the metal-microbe interactions at the cellular and molecular level (Beveridge *et al.,* 1997; Holden and Adams, 2003; Edwards *et al.,* 2005; Haferburg and Kothe, 2007; Ehrlich and Newman, 2009; Tebo *et al.,* 2010; Dong, 2010). The bacterial participation in nodule growth has been considered positively (Riemann, 1983; Ehrlich, 1975; Banerjee and Iyer, 1991; Wang and Muller, 2009; Nayak *et al.,* 2013). However, the microbial involvement in hydrogenetic Fe-Mn crust formation is under debate among researches as it is thought to be formed purely by physicochemical processes.

However different bacterial groups have been encountered in allied systems. The bacterial diversity of the mid-ocean ridge systems are composed of known, non-photosynthetic lineages of organisms like the *Firmicutes*, *Verrucomicrobia*, *Thermales* and the *Cytophaga–Flexibacter–Bacteroides* groups (Takai *et al.,* 2006). On the other hand, Mn and S oxidizing bacterial communities belonging to class α-*Proteobacteria*, β-*Proteobacteria*, γ-*Proteobacteria*, *Actinobacteria* and *Bacilli* dominate the deep-sea low-temperature influenced oceanic crust basalts and sediments along the ridge axis (Rathsack *et al.,* 2009). Studies related to hydrothermal systems reported the dominance of ζ- and ε-*Proteobacteria* (Emerson and Moyer, 2010) and one study from the Takuyo-Daigo Seamount, northwest Pacific reported γ- and α-*Proteobacteria* in the hydrogenetic crusts (Nitahara *et al.,* 2011). Many experimental studies in general with bacterial isolates have also proved their capability in biological weathering of rock substrates (Thorseth *et al.,* 1995; Daughney *et al.,* 2004) and in Fe and Mn oxidation (Konhauser, 1998; Sujith and Loka Bharathi, 2011). The different bacterial groups known to reduce Mn oxides includes *Bacillus*, *Deferribacter*, *Thermoanaerobacter*, *Fervidobacterium*, *Desulfovibrio*, *Shewanella*, *Achromobacter*, *Enterobacter* and *Salmonella* sp (Ehrlich, 1980; Pak *et al.,* 2002; Das *et al.,* 2011). Other than metal oxidation, studies have also been carried out on the reductive solubilization of the metal oxides to understand interactions.

2.4.1. Types of interactions

The interactions of microorganisms with metal ions could be one of several processes involving assimilatory or dissimilatory reactions. In the assimilatory reactions the metal that is oxidized or reduced is incorporated into the cellular material as a cofactor in enzymes (e.g. in oxidoreductases). While in the dissimilatory reactions, the metal ion may be used as an electron donor or acceptor for respiration and are typically not incorporated into the cell (Holden and Adams, 2003). The succeeding paragraphs explain the different types of interactions that bacteria have with metal ions.

2.4.1.1. Extracellular interactions

Among the different mechanisms that bacteria follow in reducing heavy metal toxicity, extracellular interactions play a major role (Figure 2.1). The extracellular interactions function through the elaboration of detoxifying agents which then reacts with the metals outside the cell, rendering them harmless. In other words, the extracellular material acts as a resistant barrier for the metal entering into the cell. Such interactions may be important, especially in slime-producing organisms or those organisms that grow in an extracellular matrix (Dugan *et al.,* 1970; Kurek *et al.,* 1991). It permits the organisms to grow and survive in the presence of high metal concentrations which gets adsorbed and precipitated within the extracellular matrix (Ford and Ryan, 1995). Further, they could also help bind metal ions and serve as nucleation sites (Dong, 2010). Apart from these functions extracellular polysaccharides (EPS) and other surface appendages help the bacterial cells in attaching to the surfaces, serve as anchors to solid surfaces and participate in the dissolution of solid mineral phases (Welch and Vandevivere, 1994; Welch *et al.,* 1999). The interactions vary from the ability to leach metals by the production of acidic metabolites to the formation of colloidal-sized EPS metal complexes. This occurs as a direct consequence of negatively charged functional groups like pyruvyl, phosphoryl, hydroxyl, succinyl, and uronyl groups on the exopolymer (Ford and Ryan, 1995).

2.4.1.2. Cell-surface interactions

The uptake and accumulation of metal ions by the bacterial cells from any environment are primarily adsorbed on the cell walls or other components located outside the protoplast. Such an uptake of the metal may or may not have an essential cell function. The different components encountered at the cell surface which may be

involved in such adsorption phenomena consists of slime layers, capsules, sheaths, stalks, flagella and fimbriae (Kaltwasser and Frings, 1980). The binding of metal ions on cell surfaces govern the distribution of metals in natural waters (Schultze-Lam *et al.*, 1996). When Gram-negative bacteria are considered for metal binding it is the phosphoryl group that serves as the most abundant electronegative site in their cell walls (Ferris, 1989; Schultze-Lam *et al.*, 1996). Whereas, in Gram-positive bacteria it is the carboxyl and phosphoryl group that act as potential sites for metal binding (Doyle, 1989). Such interactions lead to the nucleation and the formation of fine-grained minerals during which anions from the external milieu serve as counter-ions for additional metal complexation (Schultze-Lam *et al.*, 1996). Therefore, metal binding to cell-surface functional groups is considered to be an important step prior to intracellular accumulation and utilization in different cellular functions.

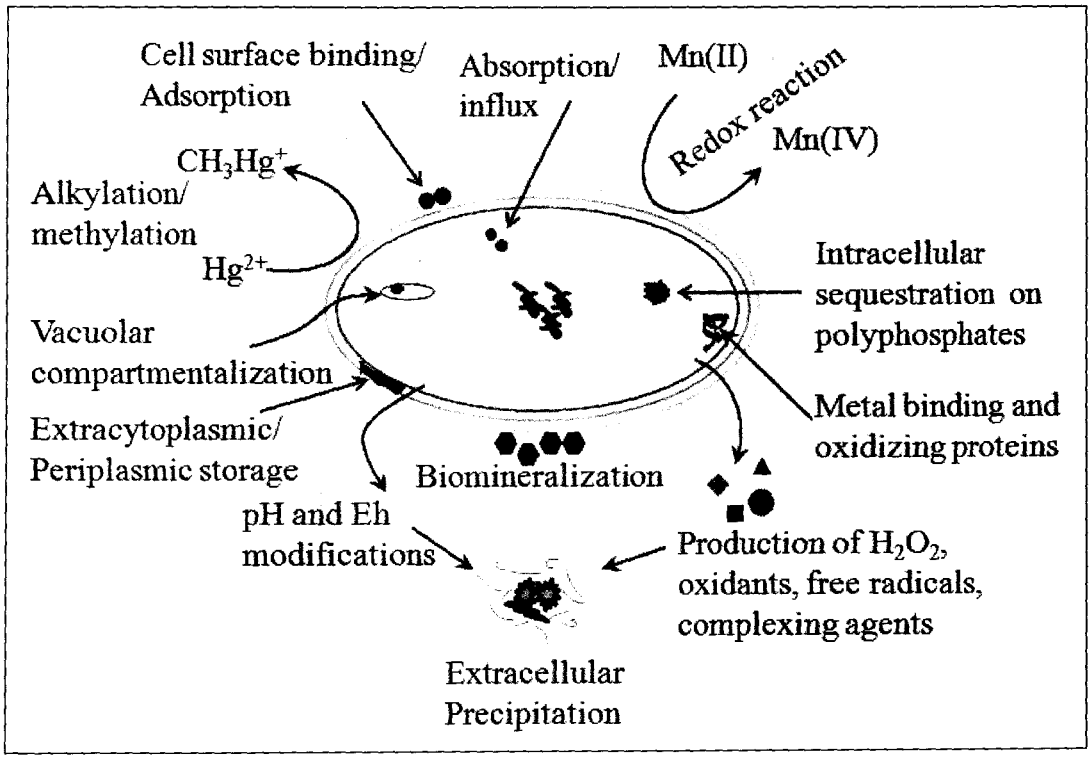

Figure 2.1. Different mechanisms involved in the interaction of bacteria with the metal ions.

2.4.1.3. Intracellular interactions

The uptake of metal ions in excess exerts toxic effect on bacterial cells (Nies, 1999). The toxicity is overcome through trafficking systems that comprise uptake

systems, efflux systems, metallochaperones and metal-storage proteins (Komeda *et al.*, 1997; Eitinger *et al.*, 2005). Also, bacteria counterbalance the intracellular concentration of toxic metals by a concerted increase in inorganic sulfide and Pi contents (Aiking *et al.*, 1984). Nevertheless, in some instances bacteria concentrate metals intracellularly in substantial amounts (Sar *et al.*, 2001; Glasauer *et al.*, 2004). This occurs as an adaptive strategy wherein bacterial cells avoid heavy metal toxicity through vacuolar compartmentalization and by sequestration in polyphosphate bodies (Keasling, 1997; Gonzalez and Jensen, 1998). This helps the bacterial cells in regulating the cytosolic metal ion concentration. The metal ions which get bound to polyphosphates undergo hydrolysis at the expense of adenosine triphosphate (ATP). The inorganic metal phosphates so released are transported outside the bacterial cell through inorganic phosphate transport system.

2.5. Major forms of marine mineral deposits

The mineralization process whether abiogenic or biogenic leads to the formation of mineral deposits on seamounts. These mineral deposits comprise of six different types namely the 1) hydrogenetic Fe-Mn crusts, 2) hydrothermal iron oxides 3) hydrothermal manganese oxides 4) hydrothermal sulfide, sulfate and sulfur deposits, 5) Phosphorite deposits and 6) hydrogenetic Fe-Mn nodules on sediment-covered seamount surfaces (Hein *et al.*, 2010). Apart from the six types of mineral deposits on seamounts the other major forms widely distributed in the ocean are the polymetallic nodules formed by the precipitation of metal ions from sediment pore water (diagenesis). Here, the three major mineral deposits namely the hydrogenetic Fe-Mn crusts, hydrothermal manganese oxides and diagenetic Fe-Mn oxides are described with special emphasis on the deposits in the ANS, CR and the CIOB sediments respectively.

2.5.1. Hydrogenetic deposits

Mineral deposits formed on the summit and slopes of the seamount by hydrogenetic processes have Fe and Mn as the major oxide sink with relatively high concentrations of Co (Hein *et al.*, 1992). The hydrogenetic precipitation is basically an inorganic colloidal-chemical and surface-chemical mechanism (Usui *et al.*, 1989; Halbach *et al.*, 2008; Glasby *et al.*, 2010). The colloidal precipitation entails the inorganic speciation and the partitioning of hydrated dissolved elements from seawater between Mn oxide and Fe oxyhydroxide phases based on the surface charge. Cations

bind strongly to negatively charged MnO_2 surfaces by coulombic electrostatic interactions. Anions and those ions with neutral and those with low charge density interact with FeOOH phase by forming specific covalent bonds (Koschinsky and Hein, 2003). The primary balance between electrostatic interaction forces (attractive or repulsive, depending on surface charge) and attractive van der Waals forces acting upon colloid–colloid and colloid–surface collisions respectively controls the rates of colloid aggregation and deposition (Kretzschmar and Schäfer, 2005). The chemical composition of crusts in general is characterized by four elemental associations representing a hydrogenetic group (Mn, Co, Ni), a biogenetic or hydrothermal group (Ba, Zn,Cu), a detrital group (Si, Al) and a carbonate fluorapatite group (P, Ca) (Wen *et al.,* 1997, Koschinsky and Hein, 2003). These hydrogenetic manganese deposits occur in topographic heights where the supply of terrigenous, volcanogenic and biogenic components is very low (Usui and Someya, 1997). They are present in the mixing layer between the upper OMZ and the lower oxygen rich bottom zone (Hein *et al.,* 2000). They occur at water depths of 400-4000m and the thickest deposits are at 800-2500m water depth (Hein *et al.,* 2000). They principally contain the minerals vernadite (δMnO_2) and todorokite [$(Na, Ca, Mn)_2 Mn_5O_{12}. 3H_2O$] apart from birnessite ($Na_4Mn_{14}O_{27}.9H_2O$) (Cronan, 1975; Nath, 2007). Ni and Cu are more enriched in deep-water deposits like todorokite whereas Co is more in encrustations on exposed rock surfaces in elevated areas rich in δMnO_2 (Cronan, 1975). The Co enriched crusts are also found where water masses are most isolated from continental-coastal and hydrothermal sources of metals (Manheim and Lane-Bostwick, 1988). The hydrogenous crusts are characterized by very high porosity (60%), extremely high specific surface area (300 m^2/g) and extremely slow growth rate (1-6 mm/Ma) (Cowen *et al.,* 1993; Koschinsky and Hein, 2003). They occur on most seamounts in the ocean basins and have a mean Fe/Mn ratio of 0.7 for open-ocean seamount crusts and 1.2 for continental margin seamount crusts (Hein *et al.,* 1997). The concentration of elements in the crusts are governed by the metal concentration in seawater, colloid surface charge, degree of oxidation, types of complexing agents, physical properties and growth rates (Li, 1981).

2.5.2. Hydrothermal deposits

Hydrothermal crusts are mineral deposits with high Mn and/or Fe content with sparse enrichment of trace metals. They are formed under conditions of high

temperature, depleted salinity, reducing pH and elevated Mn and Fe concentrations (Juniper and Tebo, 1995; Murton *et al.,* 2006). The massive release of hydrothermal fluid associated with venting along the ridge axis may have major implications for chemical flux into the ocean and for enhanced biological activity (Cann and Strens, 1987). The hydothermal activity is accompanied by event plumes producing tens of cubic kilometers of warm and turbid water (Baker *et al.,* 1987). The metal ions derived from these active submarine volcanoes precipitate chemically to form hydrothermal deposits (Koschinsky and Hein, 2003). Such deposits occur in areas with high heat flow such as mid-ocean ridges, back-arc basins and hotspot volcanoes (Glasby, 2006). They commonly occur on submarine volcanoes along the modern active oceanic arcs and less frequently in backarc rifts as well as on inactive ridges and spreading centers (Shterenberg *et al.,* 1990) on basaltic and ultramafic rock substrates (Wiseman, 1936). The growth rate of hydrothermal manganese deposits occur probably three orders of magnitude or more higher than that of hydrogenetic deposits (Usui *et al.,* 1989). They are characterized by high to extremely high growth rates (>1000 mm Ma^{-1}) and depleted levels of Cu, Ni, Zn, Co, Pb and silicate minerals (Glasby, 2006). They show the characteristic feature of very high Mn/Fe ratio of 10 to 4670 (Glasby, 2006) and low concentrations of metallic elements such as Cu, Ni, Co, Pb, Zn, V, Y, U, Th and rare earth elements (REE's) (Usui *et al.,* 1989). The dominant minerals observed near hydrothermal vents are Fe-oxides (rich in Si and Mn) and Fe-sulfides, along with some sulfates, silicates, and carbonates (Juniper and Tebo, 1995; Glasby, 2006). The mineral phases are composed of pyrolusite, braunite, bementite, hematite, chlorite, smectite, quartz, anhydrite and todorokite minerals (Mottl, 1983; Jones, 1985). They occur in all types of active oceanic environments such as at active mid-ocean spreading centers in the depth range of 250-5440m, in back-arc basins in the depth range of 50-3900m, in island arcs in the depth range of 200-2800m (Eckhardt *et al.,* 1997), in mid-plate submarine rift zones in the depth range of 1500-2200m (Hein *et al.,* 1996) and at hot spot volcanoes in the depth range of 638-1260m (Eckhardt *et al.,* 1997).

2.5.3. Diagenetic deposits

The Fe-Mn concretions/nodules formed on the ocean floor by diagenetic process have relatively higher enrichment of Ni than that of Co present in the hydrogenetic crusts. Nodules are predominantly present in areas of oxygen-rich waters and low sedimentation and differ from that of hydrogenetic crusts in their Mn/Fe ratio.

Diagenetic nodules have Mn/Fe ratio of ≥ 2.5 and hydrogenetic nodules have Mn/Fe ratio of ≤ 2.5. Co is known to positively correlate with Fe in diagenetic nodules and with Mn in hydrogenetic nodules. Also, hydrogenetic nodules and crusts contain higher Co content than diagenetic nodules (Halbach *et al.,* 1983). The Co-enrichment in nodules inversely relates to the growth rate: slower the growth rates higher the Co concentration. The diagenetic nodules sometimes grow at extreme rate of 168mm Myr^{-1} which is two orders of magnitude higher than the usual growth rate, sources of metals being sediment pore water (Reyss *et al.,* 1982). While the hydrogenetic nodules grow at a rate of 1-5mm Myr^{-1} with the source of metals being bottom seawater (Krishnaswami *et al.,* 1982). Diagenetic nodules are porous, light and have an average specific gravity of about 2.4. Their colour varies from earthy black to brown depending upon the relative Mn and Fe content. On an average, nodules contain 32% Mn-dioxide, 22% Fe-oxides, 19% silicon dioxide and 14% water by weight while other elements like aluminum oxides, calcium and magnesium carbonates, metals like Ni, Co, Cu, Zn and Mo are present in smaller quantities (Mero, 1960). Nodules from the Pacific, Indian and Atlantic Oceans contain 1.5, 0.91 and 0.56% Co respectively (Hamilton, 1994). The dominant mineral phases in nodules are todorokite, vernadite and hydrous iron (Thijssen *et al.,* 1985). In diagenetically formed nodules Ni is enriched unlike the hydrogenetic crust where Co is highly enriched and the hydrothermal crust where Mn is enriched.

2.6. Cobalt an essential nutrient and a trace metal

2.6.1. Geochemistry of cobalt

The hydrogenetic crusts are important because of the high concentration of Co. The name cobalt refers to the German word *kobold,* meaning *'goblin'* or *'evil sprite'* (Lindsay and Kerr, 2011). It is the 30th most abundant element (Kim *et al.,* 2006; Lindsay and Kerr, 2011) and exists in the oxidation states of Co^{1+} to Co^{4+}. Co(II) the dissolved species of Co occurs in a number of different solid phases such as carbonate and sulfide minerals, whereas Co(III) occurs as hydroxides or oxyhydroxide phases and is often associated with Fe-Mn crusts and manganese nodules (Ahrland, 1975; Manheim, 1986). It is a less siderophilic element compared to Ni and has higher affinity for sulfur (Zajic, 1969). The Co^{2+} has an ionic radius of 0.72Å and an atomic radius of 1.32Å (Young, 1957; Hamilton, 1994). Being a powerful oxidizing agent, Co on oxidation of water liberates oxygen (Kim *et al.,* 2006). Greater part of the Earth's

cobalt is bound to the iron core and only small quantities are concentrated in the silicate rocks. It is naturally distributed in 3 different mineral forms namely sulphides, arsenides and oxides. The oxidized form of the mineral includes asbolite ($CoO.2MnO_2.4H_2O$), heterogenite ($CoO.2Co_2O_3.6H_2O$), sphaerocobaltite ($CoCO_3$) and erythrite ($3CoO.\ A_{S2}O_5.8H_2O$) (Young, 1957). It occurs in the Earth's crust at a concentration of 20 ppm and in seawater at a concentration of 4×10^{-4} ppm (Okamoto and Eltis, 2011). The concentration of Co in surface water and ground water are below 1 $\mu g\ l^{-1}$ in pristine areas and 1 to 10 $\mu g\ l^{-1}$ in populated areas. Mean concentration of Co in seawater is >1 $\mu g\ l^{-1}$ and in rain water is 0.3 to 1.7 $\mu g\ l^{-1}$ (Young, 1957). However, its concentration in seawater varies from continental margins to the open ocean. In the continental margin its concentration is about 0.1 $\mu g\ l^{-1}$ and decreases to 7 $ng\ l^{-1}$ in the offshore surface water and 2 $ng\ l^{-1}$ at deeper depths (Knauer *et al.*, 1982, Coughtrey and Thorne, 1983). It occurs at an average concentration of 0.001% in soils and 98% of it are bound to the sediments and suspended particulate matter in the shallow waters (Robertson *et al.*, 1973). Dissolved Co concentrations decreases with increasing depth and is precipitated in the adsorbed state with oxides of Fe and Mn and crystalline sediments such as aluminosilicate and goethite (Blust, 2012).

2.6.2. Sources and uses of cobalt

Sources of environmental Co are both natural and anthropogenic (Barceloux, 1999). Natural sources include erosion (wind-blown continental dusts), weathering of rocks and soil, seawater spray, volcanoes, forest fires and continental and marine biogenic emissions. The major anthropogenic sources of environmental Co include mining and processing of cobalt-bearing ores, (Smith and Carson, 1981). Significant resources of cobalt are present in the deep-sea nodules and crusts. They are estimated to contain anywhere from 2.5 to 10 million tonnes of Co. Certain encrustation deposits ("cobalt-rich crusts") in shallow waters constitute an important potential source of Co with concentration up to 2.5% (Kim *et al.*, 2006). Co is economically and environmentally important as it forms dense and strong alloys with certain metals and metalloids. It is an important component in superalloys, permanent magnets and other products (Tebo and Lee, 1993).

2.6.3. Bacterial requirement of cobalt

Co is typically found in association with Ni in nature and it is in low abundance with respect to Fe. Still, Co is an essential element in prokaryotes and is generally required in higher concentrations by anaerobes than by aerobes (Santander *et al.,* 1997). The largest groups of enzymes that require Co are the B_{12} enzymes; however, several different types of Co-containing enzymes have been identified (Kobayashi and Shimizu, 1999). In addition, Co sometimes has a role as an enzymatic super acid and, in this regard, has proven useful as an experimental substitute for zinc as a probe of the metal coordination environment (Maret and Vallee, 1993). Eight non-corrin Co containing enzymes have been isolated and characterized. They include methionine aminopeptidase, prolidase, nitrile hydratase, glucose isomerase, methylmalonyl-CoA carboxytransferase, aldehyde decarbonlyase, lysine-2,3-aminomutase and bromoperoxidase (Kobayashi and Shimizu, 1999). The main role of Co is as an intrinsic part of vitamin B_{12} or cobalamin synthesis (Blust, 2012; Eitinger, 2013a). Co is required by ruminal microorganisms for the synthesis of vitamin B_{12} (McDowell, 2000) and is essential for phytoplankton productivity apart from Mn, Fe, Ni, Cu, and Zn. Co could substitute for zinc in enzymes required for phytoplankton productivity and forms an essential part of primary production (Price and Morel, 1990; Intwala *et al.,* 2008). Growth of the microbial community and Vitamin B_{12} production are limited by low Co levels (Taylor and Sullivan, 2008). It is also an essential element required for organisms growing with nitrate as the sole source of nitrogen as it acts as an inducer of nitrate reductase enzyme (Nicholas *et al.,* 1962). It plays an important role in the metabolism of *Rhizobia* and its symbiotic relationship with leguminous host (Lowe and Evans, 1962). The predominance of bacteria tolerant to Co and their ability to exploit bioavailable Co required for enzyme synthesis from Fe-Mn crust could help them colonize the metal hydroxide surfaces and become more enriched with metal cations over long periods.

2.6.4. Bacterial oxidation and reduction of cobalt

The enrichment of Co occurs by adsorption of Co(II) to the vacant sites of the Mn oxides (Murray and Dillard, 1979; Hem *et al.,* 1985). Subsequent to adsorption, the fixation of Co takes place through oxidation of Co(II) by Mn(IV). The Co(III) replaces the displaced Mn in the surface of marine manganates (Burns, 1976). Since Mn oxides catalyze the oxidation of Co(II) through chemical reaction, Mn oxidizing

microorganisms are also expected to do the indirect oxidation of Co(II) through biogenic Mn oxide formation (Murray *et al.,* 2007). Apart from that, Mn oxidizing organisms could also catalyze the direct oxidation of Co(II) because the redox potential of Co is rather similar to Mn (Tebo and Lee, 1993; Lee and Tebo, 1994). This has been examined in detail and the environmental cycling of Co has been shown to be microbially mediated (Tebo *et al.,* 1984; Lee and Fischer, 1993; Moffett and Ho, 1996; Taillefert *et al.,* 2002). On the other hand, several prokaryotes have been shown to couple the oxidation of organic and inorganic molecules to the reduction of Co(III) to Co(II) (Witschel *et al.,* 1999; Blessing *et al.,* 2001; Liu *et al.,* 2002; Roh *et al.,* 2002). The bacterial reduction of $Co^{III}EDTA^-$ has been proposed to couple with the chemical oxidation of $Co^{II}EDTA^{2-}$ by the Mn(IV) oxide mineral pyrolusite resulting in biotic-abiotic cycling between $Co^{II}EDTA^{2-}$ and $Co^{III}EDTA^-$ (Gorby *et al.,* 1998). Since bacteria could use EDTA as a sole source of carbon, nitrogen and energy (Witschel *et al.,* 1999) they play an important role in the biodegradation of EDTA-metal complexes in the natural environment (Thomas *et al.,* 1998; Satroutdinov *et al.,* 2003). Now it is also clear that $Co^{III}EDTA^-$ could serve as terminal electron acceptor for anaerobic respiration in *Shewanella alga* strain BrY and in dissimilatory Fe(III)-reducing bacterium *Geobacter sulfurreducens* (Caccavo *et al.,* 1994; Gorby *et al.,* 1998). The *Shewanella alga* strain BrY could reduce $Co^{III}EDTA^-$ to $Co^{II}EDTA^{2-}$ enzymatically with a 1:1 stoichiometry (Gorby *et al.,* 1998). The redox potential for $Co^{III}EDTA^-$ /$Co^{II}EDTA^{2-}$ ($E^{0'}$ = 129mV) is stated to be great enough to provide energy to support microbial growth with acetate, lactate or H_2 as an electron donor. It is also suggested that soluble CoEDTA complexes could serve as electron shuttles between metal reducing bacteria and Mn(IV) minerals (Gorby *et al.,* 1998). This would diminish the requirement of direct cell contact with the mineral surface in dissimilatory metal reducing bacteria that grows with Mn(IV) oxide as a terminal electron acceptor. Studies have shown that pure cultures of bacteria that are capable of degrading EDTA includes the genus *Agrobacterium* that degrades Fe(III)-EDTA complex (Lauff *et al.,* 1990), strain BNC-1a gram negative bacterium that degrade Mg-EDTA, Ca-EDTA, Mn-EDTA and Zn-EDTA (Nortemann, 1992; Henneken *et al.,* 1995), and the third a gram negative *Proteobacteria* DSM 9103 from which the enzyme complex EDTA monooxygenase that catalyzes the primary degradation of EDTA has been isolated and purified (Witschel *et al.,* 1997).

2.7. Nickel an essential element for few important reactions

2.7.1. Geochemistry of nickel

Ni is closely related to Co in its chemical and biochemical properties. It is the Earth's 22nd most abundant element and the 7th most abundant transition metal. It is depleted in surface ocean waters and enriched at depth (Twining *et al.,* 2012). It typically exists in the Ni(0) and Ni(II) oxidation states although the +I and +III oxidation states can exist under certain conditions. The ionic radius of Ni(II) is 0.69Å and atomic radius is 1.39Å. Ni concentrations vary widely in different environmental niches, ranging from 0.1 ng g^{-1} to 0.1 mg g^{-1} levels in many aquatic systems, 10-40 ppm in most soils, and several hundred ppm in serpentine soils (Macomber and Hausinger, 2011). Natural background levels of Ni in open ocean water is 0.2–0.7 μg l^{-1}, and in fresh water systems is generally less than 2 μg l^{-1} (Chau and Kulikovsky-Cordeiro, 1995). Average Ni concentrations in lakes are 0.38 μg l^{-1} and in stream waters 0.52 μg l^{-1}. Ni occurs as Ni(II) throughout the pH and Eh ranges in most natural waters. However, Ni is capable of forming strong complexes with organic ligands. When present in anoxic sediments with high sulfate reducing activity it occurs as NiS and in fertilized agricultural soils as $Ni_3(PO_4)_2$. In alkaline/calcareous waters it exists in the stable form of $NiHCO^{3+}$, $NiCO_3^0$ and $Ni(OH)_2^0$. In most soils Ni is bound to ion exchange sites or is coprecipitated with aluminium and Fe (oxy)hydroxides (Nieminen *et al.,* 2007). It's abundance in the Earth's crust is about 80 μg g^{-1} (Adriano, 2001). It is least enriched in sedimentary rocks (≤ 70 μg g^{-1}), basalts (150 μg g^{-1}) and granitic rocks (≤ 15 μg g^{-1}) and is highly enriched in ultramafic rocks such as peridotite and serpentine (2000 μg g^{-1}) (Turekian and Wedepohl, 1961). Under oxic conditions, Ni exists primarily as the free aquo species and the hydrous oxides of Fe and Mn control speciation. Hydrous Mn oxides (i.e. Mn (oxy)hydroxides) are far more important with regard to Ni speciation than Fe (oxy)hydroxides [such as $Fe(OH)_3$] because the former are not affected by pH whereas the latter are (Richter and Theis, 1980; Green-Pedersen *et al.,* 1997). Ni tends to adsorb to Fe (oxy)hydroxides more strongly at higher pH values owing to increased electrostatic attraction between the negatively charged oxide surfaces and positively charged Ni cations (Green-Pedersen *et al.,* 1997). At lower pH, competition between Ni^{2+} and H^+ causes Ni dissociation from hydrous oxides. Under hypoxic or anoxic conditions, sulfides control Ni speciation through the formation of insoluble Ni sulfides.

2.7.2. Sources and uses of nickel

Natural geological activities such as weathering and volcanoes, forest fires and vegetation, and wind-blown dust lead to Ni distribution in natural environments at modest levels (Iyaka, 2011; Schaumloffel, 2012). Elevated Ni concentrations in surface waters may result from a variety of anthropogenic sources which include mining, smelting and refining, metal plating and manufacturing, Ni-cadmium battery disposal, and fossil fuel refining and combustion (Stokes, 1981; Nriagu and Pacyna, 1988; Doig and Liber, 2007). Nickel's economic importance lies in its unique physicochemical characteristics, the most important of which include its strength, high temperature stability, corrosion resistance, malleability, ductility, heat and electrical conductive properties and aesthetic properties (Mukherjee, 1998; Reck *et al.*, 2008; Pyle and Couture, 2012). Metallic nickel and nickel compounds are used in manifold industrial and commercial applications such as stainless steel, corrosion-resistant industrial equipment, building materials, medical equipment (including cardiac stents), food and beverage storage containers, catalysts for hydrogenating vegetable oils, electromagnetic shielding, electroplating, battery production, jewellery and coinage, electronic storage media, catalysts, inks and dyes, ceramics, foundries, pigments and strong magnets (Nieminen *et al.*, 2007; Reck *et al.*, 2008; Schaumloffel, 2012; Pyle and Couture, 2012). Besides, its applications include chemicals and allied products, petroleum refining, metal products, aerospace applications, machinery and transportation, marine applications, building construction, electrical equipment, automobile production, ship building and many others (Mukherjee, 1998). Economically exploitable ore deposits for Ni are the laterites and sulfides containing 1-3% Ni (Mukherjee, 1998).

2.7.3. Bacterial requirement of nickel

Ni is an important trace element required for many prokaryotic microorganisms, in the domains of bacteria and archaea (Sawers, 2012). It is also a trace nutrient for certain fungi, algae and plants (Eitinger, 2013b). Ni represents an essential cofactor of a group of unrelated metalloenzymes catalyzing central reactions in energy and nitrogen metabolism, in detoxification processes, and in a side reaction of the methionine salvage pathway (Eitinger, 2013b). It plays an important role in at least four biological processes: hydrolysis of urea, uptake and production of hydrogen, methanogenesis, and acetogenesis (Hausinger, 1987). The Ni(II) is generally the metal species that is specifically transported by microorganisms. Ni is associated with enzymes as a

component of mononuclear, dinuclear or multinuclear prosthetic groups and these are essential for catalytic function (Sawers, 2013). Seven microbial enzymes that contain Ni have been characterized in detail. They include urease, [NiFe] hydrogenase, Ni-superoxide dismutase, carbon monoxide dehydrogenase, acetyl CoA synthase/decarbonylase, acireductone dioxygenase and methyl coenzyme M reductase, as well as some forms of glyoxalase I (Macomber and Hausinger, 2011). There are also other proteins specifically involved in Ni metabolism. These are either required for transport of Ni or for its insertion into the prosthetic groups of Ni enzymes (Sawers, 2013).

2.7.4. Bacterial oxidation and reduction of nickel

Biological oxidation of Ni(II) to Ni(III) has not been documented. This has been mainly because of the unstable nature of Ni(III) in aqueous medium (Nies, 1999). However, bacteria are found to immobilize soluble Ni [Ni(II)] by intracellular accumulation and precipitation. Adsorption (Hitchcock *et al.,* 2009) and immobilization of Ni occurred with bacterial cells (Sujith *et al.,* 2010; 2011). The intracellular sequestration and its compartmentalization at high concentration also occurred with Ni in selected bacterial strains (Sar *et al.,* 2001; Tripathi and Srivastava, 2006). Subsequent to uptake and accumulation of Ni in the cell envelope by bacteria, Ni(II) was precipitated as nickel phosphide and nickel carbide crystals in *Pseudomonas aeruginosa* (Sar *et al.,* 2001). A Mn oxidizing bacterial isolate belonging to *Halomonas* sp also immobilized Ni as nickel phosphide and nickel sulphide (Sujith *et al.,* 2010). Further, studies carried out with *Escherichia coli* expressing an alkaline phosphatase enzyme revealed that nickel is immobilizied as a complex with hydrogen uranyl phosphate (Basnakova *et al.,* 1998). Ni forms strong complexes with organic matter and Fe (oxy)hydroxides (Nimmo *et al.,* 1989; Donat *et al.,* 1994; Nieminen *et al.,* 2007; Doig and Liber, 2007) and therefore the bioavailability of Ni may be limited in the natural environment. Studies on the interactions between bacteria and Ni have mostly dealt with the inhibition of microbial activities by divalent nickel ions and the nickel-dependent stimulation of growth and metabolism in microbes (Kaltwasser and Frings, 1980). Nevertheless, it has been shown recently that bacterial genera belonging to *Pseudomonas* are capable of reducing Ni(II) to elemental Ni under aerobic conditions (Zhan *et al.,* 2012). The bacterium utilized several substrates as electron donors during the bioreduction of divalent Ni. In this organism, Ni(II) has been proposed to serve as

an electron acceptor (Zhan *et al.*, 2012). In general the heterotrophic bacteria and others belonging to *Thiobacillus* group of organisms are also known to participate in the reductive leaching of Ni from nickeliferous lateritic ore, natural pentlandite and nickel bearing-pyrrhotite (Sukla and Panchanadikar, 1993; Cwalina *et al.*, 2000; Ke and Li, 2006).

2.8. Manganese a redox sensitive element with highest number of oxidation states

2.8.1. Geochemistry of manganese

Mn is the fifth most abundant transition metal in the Earth's crust (Tebo *et al.*, 2007) and is the second most common trace metal after iron (Tebo *et al.*, 1997). It exist in seven different oxidation states ranging from 0 to +7 and in nature it occurs in +II, +III and +IV oxidation states (Tebo *et al.*, 1997; 2004). The name manganese is derived from the Greek word mangania, meaning magic (Horsburgh *et al.*, 2002). It occupies the 25^{th} position in the periodic table and belongs to group VII transition elements (Cellier, 2002). The geochemistry of Mn is a complex pattern of mutually exclusive chemical reactions of oxidation and reduction (Kirchner and Grabowski, 1972). The geochemical behavior of Mn differs in environment which shows gradation in oxygen profile (Roitz *et al.*, 2002). It occurs as highly soluble Mn(II) in oxygen-deficient settings and as insoluble oxyhydroxides under well-oxygenated conditions (Calvert and Pedersen, 1996). The concentration of soluble Mn in the environments varies with change in redox condition and the group of microorganisms present. The oxidation of Mn by microorganisms result in decrease in the dissolved Mn(II) concentration of metal and increase in the particulate/higher oxidation states (Mn(III) and Mn(IV)) of Mn (Ehrlich, 1976; 1978). Redox transitions between soluble Mn(II) ions and insoluble Mn(III) and Mn(IV) oxides form the backbone of aquatic biogeochemistry of Mn (Sunda and Huntsman, 1990). Mn(III) being a strong oxidant and a reductant, it has been largely ignored due to its property to disproportionate to Mn(II) and MnO_2 (Johnson, 2006). However, recent improvements in the understanding of Mn chemistry indicate that dissolved Mn exist mostly as Mn^{3+} in sub-oxic regions (Trouwborst *et al.*, 2006). Mn being one of the strongest oxidant in the natural environment, eventually participates in redox reactions and due to its sorptive characteristics, controls the distributions and bioavailability of several toxic and essential trace elements (Tebo *et al.*, 2004).

2.8.2. Sources and uses of manganese

Mn enrichment occurs as a result of both artificial and natural processes. The sources of Mn in the ocean are atmospheric input, intense scavenging at mid-depth and fluxes from reducing shelf and slope sediments and emanations from submarine hydrothermal vents (Saager *et al.*, 1989). It occurs at a concentration of 100-1000 ppm in river, 1-10 ppm in ground water (Nealson, 1983) and averages 8 μg kg^{-1} in freshwater and 0.2 μg kg^{-1} in seawater (Bowen, 1979; Ehrlich, 2002). The concentration of dissolved Mn (Mn^{2+}) in the open ocean ranges from 0.2 to 3 nmol kg^{-1} of seawater (Glasby, 2006). Further details about its distribution and abundance can be seen in Figure 2.2. Mn is principally used in steel industry as a hardening agent, also in the production of Mn alloys, in colouring glass, ceramics, dyes, pigments, soil and food supplements and medicine. It is also used in tissue specific contrasting agents in nuclear magnetic resonance tomography (Pearson and Greenway, 2005).

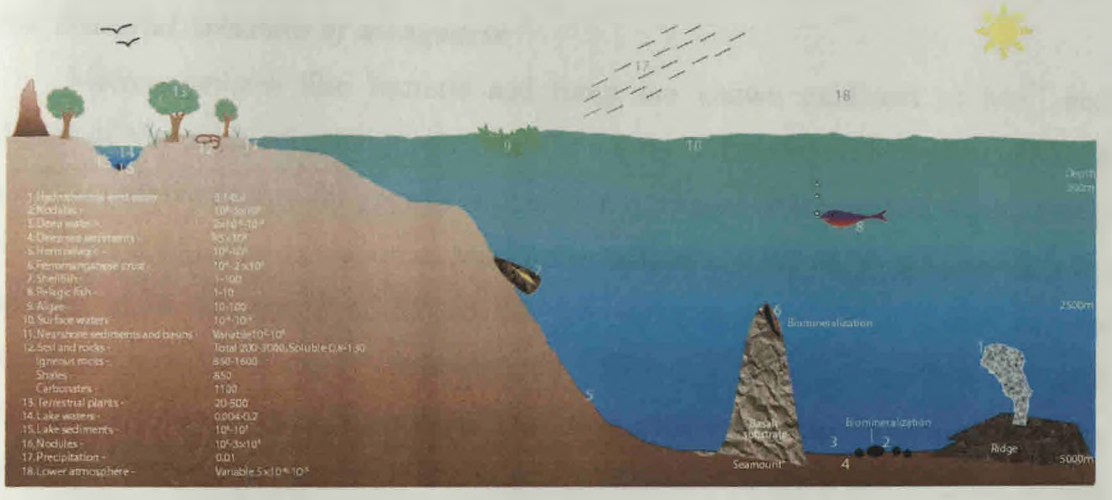

Figure 2.2. Parts per million concentrations of manganese in different environments (Sujith and Loka Bharathi, 2011).

2.8.3. Bacterial requirement of manganese

Manganese is a critical trace nutrient required for the growth and survival of many living organisms. It is essential for oxygenic photosynthesis in cyanobacteria (Yocum and Pecoraro, 1999; Keren *et al.*, 2002; Ogawa *et al.*, 2002), redox reactions, protection from toxic metals, UV light, predation or, viruses, scavenging of micronutrient trace metals, breakdown of natural organic matter into metabolizable substrates, maintenance of an electron-acceptor reservoir for use in anaerobic

respiration, oxygen production and protection against oxidative stress in bacteria (Christianson, 1997; Spiro *et al.,* 2010). It is important for general metabolism, carbohydrate metabolism and for both anabolic and catabolic functions in anaerobiosis and aerobiosis (Crowley *et al.,* 2000). It is a part of four metalloenzymes manganese superoxide dismutase (MnSOD), mangani-catalase, arginase and O-phosphatases (Christianson, 1997; Shi, 2004). Mn^{2+} containing O-phosphatases involved in controlling spore formation, stress-response, cell density during stationary phase, carbon and nitrogen assimilation and cell segregation (Shi, 2004). Additionally, non-enzymatic Mn^{2+} is crucial for the proper functioning of a variety of bacterial products, including secreted antibiotics (Archibald, 1986). It also contributes to the stabilization of bacterial cell walls (Doyle, 1989) and plays an important role in bacterial signal transduction (Jakubovics and Jenkinson, 2001). Indirectly, Mn functions in controlling nutrient availability in freshwater, most significantly by complexing with iron (Kirchner and Grabowski, 1972).

2.8.4. Bacterial oxidation of manganese

Microorganisms like bacteria and fungi are known oxidizers of Mn^{2+} and reducers of Mn-oxide containing minerals. They carry out oxidation/reduction of Mn as a way to conserve energy for growth or oxidation of carbon (Nealson and Myers, 1992; Tebo *et al.,* 2005). The oxidation of Mn^{2+} under natural conditions is catalyzed only by microbes under pH range of 5.5 to 8.0, Eh value above +200 mV and oxygen concentration of 3 to 5 mg l^{-1} (Schweisfurth, 1978). Studies on Mn nodules indicated that bacteria enhances the adsorption of Mn^{2+} from seawater in the presence of peptone and play a crucial role in nodule development (Ehrlich, 1963). The oxidation of Mn was also mediated by enzyme activity in a Mn nodule bacterium *Arthrobacter* 37. The rate of oxidation of soluble Mn by the enzyme depended on the concentration of the cell-free extract (Ehrlich, 1968). Study on the effect of temperature and pressure on *Arthrobacter* 37 demonstrated that at 5°C, temperature optimum for Mn^{2+} oxidation increases with pressure and the effect of pressure on cells can be counteracted by an appropriate increase in temperature (Ehrlich, 1971). The involvement of cytochrome in Mn oxidation by two marine bacteria stated the use of conventional electron transport chain in deriving useful energy from Mn oxidation by oxidative phosphorylation (Arcuri and Ehrlich, 1979). They observed that addition of periplasmic/intracellular fraction of proteins to membrane fraction was essential for Mn oxidation. Mn oxidation

has been postulated to be catalyzed by two groups of Mn(II) oxidizing bacteria one that acts on free Mn and the other that acts only on Mn(II) bound to Mn(IV) oxide and derive energy from the reaction (Ehrlich, 1980).

Another interesting observation on Mn(II) oxidation demonstrated the coupling of ATP synthesis with that of Mn(II) oxidation by a marine bacterial strain SSW22 (Ehrlich and Salerno, 1990). They proposed chemiosmosis (diffusion of ions across a selectively-permeable membrane) as the probable mechanism for energy coupling by intact cells, membrane vesicles or cell extracts. It has been observed that live/killed mature spores of *Bacillus* sp. strain SG-1 could oxidize Mn(II) once bound but not when free in solution (Rosson and Nealson, 1982). It was also identified that spores rather than vegetative cells are responsible for Mn^{2+} oxidation by *Bacillus* sp. strain SG-1 (Kepkay and Nealson, 1982). On the other hand, de Vrind *et al.* (1986) demonstrated that vegetative cells of the same organism could reduce the Mn oxide. The reduction of Mn by the vegetative cells was thought to make Mn^{2+} available for sporulation in a manganese-limited environment. Using radiotracers, Tebo *et al.* (1984) provided evidence for Mn(II) oxidation with oxygen as the terminal electron acceptor in Saanich Inlet and Framvaren Fjord. The oxidation of Mn by *Aurantimonas* sp. Strain SI85-9A1 has been shown to contain genes for organoheterotrophy, methylotrophy, oxidation of sulfur and carbon monoxide, the ability to grow over a wide range of oxygen concentrations and the complete Calvin cycle for carbon fixation (Dick *et al.*, 2008).

Based on a kinetic model of the oxidative pathway Webb *et al.* (2005) stated that Mn(III) is a transient intermediate and the rate-limiting step in the oxidation of Mn(II). They suggested that oxidation of Mn(II) could involve a unique multicopper oxidases (MCOs) system capable of two-electron oxidation of its substrate. MCOs are a class of enzymes that have metallocentre assembly containing four Cu atoms (Brouwers *et al.*, 2000). They couple the four-electron reduction of dioxygen to water with the oxidation of substrate. Observation on microbially mediated Mn^{2+} oxidation in bacterial isolates belonging to *Halomonas* sp from Carlsberg Ridge (Fernandes *et al.*, 2005) showed that Mn is precipitated externally by the bacterial cells. Same isolates when exposed to Ni and Co in the absence of Mn accumulated these metals both intra- and extracellularly (Sujith *et al.*, 2010; Antony *et al.*, 2011). Another study on the redox transformation of Mn in Antarctic lakes (Krishnan *et al.*, 2009) suggested that Co could

have a more profound role in Mn(II) oxidation and Ni on Mn(IV) reduction. Further, study from the mangrove sediments Krishnan *et al.* (2007) offered experimental evidence that both autochthonous autotrophs and heterotrophs work in tandem in reducing Mn and other related metal ions in sediments. These processes may indirectly promote more metal oxidation by removing end product inhibition. Further details on the oxidative cycle of Mn can be found in Sujith and Loka Bharathi (2011).

2.8.5. Bacterial reduction of manganese

Microorganisms are, either directly or indirectly, the major catalysts of Mn cycling in the natural environment. As Mn-oxide is energetically a more favourable electron acceptor than Fe-oxide or sulphate, Mn reducing microorganisms can outcompete Fe and -sulphate reducers in the utilization of common substrates and the mineralization of carbon. The Fe-Mn oxides could undergo reduction by microbial action, photochemical reactions or hydrothermal processes (Myers and Nealson, 1988b; Sunda and Huntsman, 1988; Von Damm *et al.*, 1985; Johnson *et al.*, 1992). The microbially mediated Mn-oxide reduction can occur directly through contact between the cell surface and the Mn-oxide or indirectly through microbially mediated changes in reducing conditions in the cells environment through different mechanisms like redoxolysis, acidolysis, and complexolysis (Sand *et al.*, 2001; Baglin *et al.*, 1992; Brandl and Faramarzi, 2006). On the other hand, the abiotic reduction of Mn and -Fe-oxides could occur through the involvement of inorganic and organic reductants like H_2S, Fe(II), catechol, ascorbate and humic substances (Thamdrup, 2000). The metal reducing bacteria that participate in Mn-oxide reduction could be an obligate aerobe, obligate anaerobe or a facultative anaerobe (Madgwick, 1987) and could be strictly autotrophic-heterotrophic-mixotrophic (Enrich-Prast *et al.*, 2009). Nevertheless, the metal reducing microorganisms depend on suitable reductant like glucose, lactate, succinate, acetate or hydrogen for carrying out Mn-oxide reduction (Ehrlich, 1988). The reduction of Fe and Mn-oxides coupled with hydrocarbon oxidation helps in the completion of energy-producing metabolic pathways in the absence of more favorable electron acceptors such as O_2 and nitrate (Thamdrup, 2000; Martin, 2003).

2.9. References

Adriano DC. 2001. Trace Elements in Terrestrial Environments. Springer, New York.

Ahrland S. 1975. Metal complexes in seawater. In: Dahlem workshop on the nature of seawater. Goldberg ED (ed) Dahlem Konferenzen, Abakon Verlagsgesellschaft, Berlin, pp. 219-244.

Aiking H, Stijnman A, Garderen CV, Heerikhuizen HV, Riet JV. 1984. Inorganic phosphate accumulation and cadmium detoxification in *Klebsiella aerogenes* NCTC 418 growing in continuous culture. Appl Environ Microbiol 47: 374-377.

Allain V, Kerandel J-A, Andrefouet S, Magron F, Clark M, Kirby DS, Muller-Karger FE. 2008. Enhanced seamount location database for the western and central Pacific Ocean: Screening and cross-checking of 20 existing datasets. Deep-Sea Res I 55: 1035-1047.

Antony R, Sujith PP, Fernandes SO, Verma P, Khedekar VD, Loka Bharathi PA. 2011. Cobalt immobilization by manganese oxidizing bacteria from Indian Ridge System. Curr Microbiol 62: 840-849.

Archibald F. 1986. Manganese: its acquisition by and function in the lactic acid bacteria. Crit Rev Microbiol 13: 63-109.

Arcuri EJ, Ehrlich HL. 1979. Cytochrome involvement in Mn(II) oxidation by two marine bacteria. Appl Environ Microbiol 37: 916-923.

Baglin EG, Noble EG, Lampshire DL, Eisele JA. 1992. Solubilization of manganese from ores by heterotrophic micro-organisms. Hydrometallurgy 29: 131-144.

Baker ET, Massoth GJ, Feely RA. 1987. Cataclysmic hydrothermal venting on the Juan de Fuca Ridge. Nature 329: 149-151.

Banakar VK, Hein JR, Rajani RP, Chodankar AR. 2007. Platinum group elements and gold in ferromanganese crusts from Afanasiy–Nikitin seamount, equatorial Indian Ocean: Sources and fractionation. J Earth Syst Sci 116: 3-13.

Banakar VK, Pattan JN, Mudholkar AV. 1997. Palaeoceanographic conditions during the formation of ferromanganese crust from the Afanasiy Nikitin seamount, north central Indian Ocean-geochemical evidence. Mar Geol 136: 299-315.

Banakar VK, Tarkian M. 1991. Genesis and growth of internal microstructures of manganese nodule. Indian J Mar Sci 20: 20-24.

Banakar VK. 2010. Deep-sea ferromanganese deposits and their resource potential for India. J Indian Inst Sci 90: 535-541.

Banerjee R, Iyer SD. 1991. Biogenic influence on the growth of ferromanganese micronodules in the Central Indian Basin. Mar Geol 97: 413-421.

Barceloux DG. 1999. Cobalt. Clin Toxicol 37: 201-216.

Basnakova G, Finlay JA, Macaskie LE. 1998. Nickel accumulation by immobilized biofilm of *Citrobacter* sp. containing cell-bound polycrystalline hydrogen uranyl phosphate. Biotechnol Lett 20: 949-952.

Baumgartner J, Faivre D. 2011. Magnetite biomineralization in bacteria. Prog Mol Subcell Biol 52: 3-27.

Bazylinski DA, Frankel RB. 2003. Biologically controlled mineralization in Prokaryotes. Rev Mineral Geochem 54: 217-247.

Benzerara K, Menguy N, Guyot F, Skouri F, de Luca G, Barakat M, Heulin T. 2004. Biologically controlled precipitation of calcium phosphate by *Ramlibacter tataouinensis*. Earth Planet Sci Lett 228:439-449.

Beveridge TJ, Hughes MN, Lee H, Leung KT, Poole RK, Savvaidis I, Silver S, Trevors JT. 1997. Metal-microbe interactions: contemporary approaches. Adv Microb Physiol 38: 198-243.

Blessing TC, Wielinga BW, Morra MJ, Fendorf S. 2001. $Co^{III}EDTA^-$ reduction by *Desulfovibrio vulgaris* and propagation of reactions involving dissolved sulfide and polysulfides. Environ Sci Technol 35:1599-1603.

Blust R. 2012. Cobalt. In: Fish Physiology: Homeostasis and toxicology of essential metals. Wood CM, Farrell AP, Brauner CJ (eds) Elsevier Inc, pp. 291-326.

Bogorov VG, Bezrukov PL. 1961. Vityaz in the Indian Ocean. Prioda 10:12-35 (in Russian).

Bowen HJM. 1979. Environmental chemistry of the elements. Academic Press, London.

Brandl H, Faramarzi MA. 2006. Microbe-metal interactions for the biotechnological treatment of metal-containing solid waste. China Particuology 4: 93-97.

Brewin PE, Stocks KI, Haidvogel DB, Condit C, Gupta A. 2009. Effects of oceanographic retention on decapod and gastropod community diversity on seamounts. Mar Ecol Prog Ser 383: 225-237.

Brouwers G-J, Vijgenboom E, Corstjens PLAM, de Vrind JPM, de Vrind-de Jong EW. 2000. Bacterial Mn^{2+} oxidizing systems and multicopper oxidases: An overview of mechanisms and functions. Geomicrobiol J 17: 1-24.

Burns RG. 1976. The uptake of cobalt into Fe-Mn nodules, soils, and synthetic manganese (IV) oxides. Geochim et Cosmochim Acta 40: 95-102.

Caccavo F, Lonergan DJ, Lovley DR, Davis M, Stolz JF, McInerney MJ. 1994. *Geobacter sulfurreducens* sp.-nov., a hydrogen and acetate-oxidizing dissimilatory metal-reducing microorganism. Appl Environ Microbiol 60: 3752-3759.

Cahyani VR, Murase J, Ishibashi E, Asakawa S, Kimura M. 2007. Bacterial communities in manganese nodules in rice field subsoils: Estimation using PCR-DGGE and sequencing analyses. Soil Sci Plant Nutr 53: 575-584.

Callender E, Bowser CJ. 1976. Freshwater ferromanganese deposits. In: Handbook of Strata-Bound and Stratiform ore deposits. Wolf KH (ed) Amsterdam, Elsevier, pp. 341-394.

Calvert SE, Cronan DS. 1978. Geochemistry of oceanic ferromanganese deposits [and discussion]. Phil Trans R Soc Lond 290: 43-73.

Calvert SE, Pedersen TF. 1996. Sedimentary geochemistry of manganese: Implications for the environment of formation of manganiferous black shales. Econ Geol 91: 36-47.

Cann J, Strens R. 1987. Venting events in hot water. Nature 329: 104.

Cellier M. 2002. Bacterial genes controlling manganese accumulation. In: Microbial Transport Systems, Winkelmann G (ed) Wiley-VCH Verlag GmbH & Co. KGaA, pp. 325-345.

Chau YK, Kulikovsky-Cordeiro OTR. 1995. Occurrence of nickel in the Canadian environment. Environ Rev 3: 95-120.

Christianson DW. 1997. Structural chemistry and biology of manganese metalloenzymes. Prog Biophys Mol Biol 67: 217–252.

Chu J, Stabnikov V, Ivanov V. 2012. Microbially induced calcium carbonate precipitation on surface or in the bulk of soil. Geomicrobiol J 29: 544-549.

Clark MR, Rowden AA, Schlacher T, Williams A, Consalvey M, Stocks KI, Rogers AD, O'Hara TD, White M, Shank TM, Hall-Spencer JM. 2010. The ecology of seamounts: structure, function, and human impacts. Ann Rev Mar Sci 2: 375-400.

Connell L, Barrett A, Templeton A, Staudigel H. 2009. Fungal diversity associated with an active deep sea volcano: Vailulu'u Seamount, Samoa. Geomicrobiol J 26: 597-605.

Coughtrey PJ, Thorne MC. 1983. Radionuclide distribution and transport in terrestrial and aquatic ecosystems: a critical review of data. AA Balkema, Rotterdam, pp. 191-217.

Cowen JP, de Carlo EH, McGee DL. 1993. Calcareous nannofossil biostratigraphic dating of a Fe-Mn crust from Schumann Seamount. Mar Geol 115: 289-306.

Crearar DA, Knox GW, Means JL. 1979. Biogeochemistry of bog iron in the New Jersey Pine Barrens. Chem Geol 24: 111-135.

Cronan DS. 1975. Manganese nodules and other Fe-Mn oxide deposits from the Atlantic Ocean. J Geophys Res 80: 3831-3837.

Crowley JD, Traynor DA, Weatherburn DC. 2000. Enzymes and proteins containing manganese: an overview. Met Ions Biol Syst 37: 209-278.

Cwalina B, Fischer H, Ledakowicz S. 2000. Bacterial leaching of nickel and cobalt from pentlandite. Physicochem Probl Miner Process 34: 17-24.

Das AP, Sukla LB, Pradhan N, Nayak S. 2011. Manganese biomining: A review. Bioresour Technol 102: 7381-7387.

Daughney CJ, Rioux J-P, Fortin D, Pichler T. 2004. Laboratory investigation of the role of bacteria in the weathering of basalt near deep sea hydrothermal vents. Geomicrobiol J 21: 21-31.

de Forges BR, Koslow JA, Poore GCB. 2000. Diversity and endemism of the benthic seamount fauna in the southwest Pacific. Nature 405: 944-947.

de Vrind JPM, Boogerd FC, de Vrind-de Jong EW. 1986. Manganese reduction by a marine *Bacillus* species. J Bacteriol 167: 30-34.

Dean WE, Ghosh SK. 1981. Geochemistry of freshwater ferromanganese deposits in North America. In: Geology and Geochemistry of Manganese. Varentsov IM, Grasselly GY (eds) Hungarian Academy of Sciences, Budapest, pp. 256-277.

Dick GJ, Podell S, Johnson HA, Rivera-Espinoza Y, Bernier-Latmani R, McCarthy JK, Torpey JW, Clement BG, Gaasterland T, Tebo BM. 2008. Genomic Insights into Mn(II) Oxidation by the Marine Alphaproteobacterium *Aurantimonas* sp.Strain SI85-9A1 Appl Environ Microbiol 74: 2646-2658.

Doig LE, Liber K. 2007. Nickel speciation in the presence of different sources and fractions of dissolved organic matter. Ecotoxicol Environ Saf 66: 169-177.

Donat JR, Lao KA, Bruland KW. 1994. Speciation of dissolved copper and nickel in South San Francisco Bay: a multi-method approach. Anal Chim Acta 284: 547-571.

Dong H. 2010. Mineral-microbe interactions: a review. Front Earth Sci China 4: 127-147.

Dorn RI, Oberlander TM. 1981. Microbial Origin of Desert Varnish. Science 213: 1245-1247.

Doyle RJ. 1989. How cell walls of gram-positive bacteria interact with metal ions. In: Metal Ions and Bacteria. Beveridge TJ, Doyle RJ (eds) Wiley, New York, pp. 275-293.

Dugan PR, Macmillan CB, Pfister RM. 1970. Aerobic heterotrophic bacteria indigenous to pH 2.8 acid mine water: predominant slime-producing bacteria in acid streamers. J Bacteriol 101: 982-988.

Eckhardt JD, Glasby GP, Puchelt H, Berner Z. 1997. Hydrothermal manganese crusts from Enareta and Palinuro seamounts in the Tyrrhenian Sea. Mar Georesour Geotechnol 15: 175-209.

Edwards KJ, Bach W, McCollom TM. 2005. Geomicrobiology in oceanography: microbe-mineral interactions at and below the seafloor. Trends Microbiol 13: 449-456.

Edwards KJ, Bazylinski DA. 2008. Intracellular minerals and metal deposits in prokaryotes. Geobiology 6: 309-317.

Ehrlich HL, Newman DK. 2009. Geomicrobiology. Taylor and Francis Group, CRC Press, Boca Raton, USA.

Ehrlich HL, Salerno JC. 1990. Energy coupling in Mn^{2+} oxidation by a marine bacterium. Arch Microbiol 154: 12-17.

Ehrlich HL. 1963. Bacteriology of manganese nodules. I. Bacterial action on manganese in nodule enrichments. Appl Microbiol 11: 15-19.

Ehrlich HL. 1968. Bacteriology of manganese nodules. II. Manganese oxidation by cell-free extract from a manganese nodule bacterium. Appl Microbiol 16: 197-202.

Ehrlich HL. 1971. Bacteriology of manganese nodules. V. Effect of hydrostatic pressure on bacterial oxidation of Mn(II) and reduction of MnO_2. Appl Microbiol 21: 306-310.

Ehrlich HL. 1975. The formation of ores in the sedimentary environment of the deep-sea with microbial participation: the case for ferromanganese concretions. Soil Sci 119: 36-41.

Ehrlich HL. 1976. Manganese as an energy source for bacteria. In: Environmental biogeochemistry. Nriagu JO (ed) Ann Arbor Science, Michigan, pp. 633-644.

Ehrlich HL. 1978. Inorganic energy sources for chemolithotrophic and mixotrophic bacteria. Geomicrobiol J 1: 65-83.

Ehrlich HL. 1980. Bacterial leaching of manganese ores. In: Biogeochemistry of Ancient and Modern Environments. Trudinger PA, Walter WR, Ralph BJ (eds) Australian Academy of Science, Canberra and Springer-Verlag, Berlin, pp. 609-614.

Ehrlich HL. 1988. Bioleaching of manganese by marine bacteria. In: Proceedings 8th international biotechnology symposium. Durand G, Bobichon L, Florent J (eds) Paris, pp. 1094-1105.

Ehrlich HL. 2002. Geomicrobiology. Marcel Dekker Inc, New York. p. 429-528.

Eitinger T, Suhr J, Moore L, Smith JAC. 2005. Secondary transporters for nickel and cobalt ions: Theme and variations. BioMetals 18: 399-405.

Eitinger T. 2013a. Cobalt transporters. In: Encyclopedia of Metalloproteins. Uversky VN, Kretsinger RH, Permyakov EA (eds) Springer, pp. 678-682.

Eitinger T. 2013b. Nickel transporters. In: Encyclopedia of Metalloproteins. Uversky VN, Kretsinger RH, Permyakov EA (eds) Springer, pp. 1515-1519.

Emerson D, Moyer CL. 2002. Neutrophilic Fe-oxidizing bacteria are abundant at the Loihi Seamount hydrothermal vents and play a major role in Fe oxide deposition. Appl Environ Microbiol 68: 3085-3093.

Emerson D, Moyer CL. 2010. Microbiology of seamounts: Common patterns observed in community structure. Oceanography 23: 148-163.

Emerson D. 2009. Potential for iron-reduction and iron-cycling in iron oxyhydroxide-rich microbial mats at Loihi Seamount. Geomicrobiol J 26: 639-647.

Emerson S, Kalhorn S, Jacobs L, Tebo BM, Nealson KH, Rosson RA. 1982. Environmental oxidation rate of manganese(II): bacterial catalysis. Geochim Cosmochim Acta 46: 1073-1079.

Enrich-Prast A, Bastviken D, Crill P. 2009. Chemosynthesis. In: Encyclopedia of Inland waters. Likens GE (ed) Elsevier, pp. 211-225.

Etnoyer PJ, Wood J, Shirley TC. 2010. How large is the seamount biome. Oceanography 23: 206-209.

Fernandes SO, Krishnan KP, Khedekar VD, Loka Bharathi PA. 2005. Manganese oxidation by bacterial isolates from the Indian Ridge System. Biometals 18: 483-492.

Ferris FG. 1989. Metallic ion interactions with the outer membrane of gram-negative bacteria. In: Metal Ions and Bacteria. Beveridge TJ, Doyle RJ (eds) Wiley, New York, pp. 295-323.

Ford T, Ryan D. 1995. Toxic metals in aquatic ecosystems: A microbiological perspective. Environ Health Persp 103: 25-28.

Frankel RB, Bazylinski DA. 2003. Biologically induced mineralization by bacteria. Rev Mineral Geochem 54: 95-114.

Ghiorse WC, Hirsch P. 1982. Isolation and properties of Fe-Mn depositing budding bacteria from Baltic Sea Fe-Mn concretions. Appl Environ Microbiol 43: 1464-1472.

Ghiorse WC. 1984. Biology of iron- and manganese-depositing bacteria. Ann Rev Microbiol 38: 515-550.

Gilbert PUPA, Abrecht M, Frazer BH. 2005. The organic–mineral interface in biominerals. Rev Mineral Geochem 59: 157-85.

Glasauer S, Langley S, Beveridge TJ. 2004. Intracellular manganese granules formed by a subsurface bacterium. Environ Microbiol 6: 1042-1048.

Glasby GP, Mountain B, Vineesh TC, Banakar VK, Rajani R, Ren X. 2010. Role of hydrology in the formation of Co-rich Mn crusts from the Equatorial N Pacific, Equatorial S Indian Ocean and the NE Atlantic Ocean. Resour Geol 60: 165-177.

Glasby GP. 2006. Manganese: predominant role of nodules and crusts. In: Marine Geochemistry. Schulz HD, Zabel M (eds) Springer, Berlin-Heidelberg, pp. 371-427.

Glazer BT, Rouxel OJ. 2009. Redox speciation and distribution within diverse iron dominated microbial habitats at Loihi Seamount. Geomicrobiol J 26: 606-622.

Goddard DA, Thompson G, Jones EJW, Okada H. 1987. The chemistry and mineralogy of ferromanganese encrustations on rocks from the Sierra Leone Rise, Equatorial Mid-Atlantic Ridge and New England Seamount Chain. Mar Geol 77: 87-98.

González FJ, Somoza L, Maldonado A, Lunar R, Martínezfrías J, Martín-Rubí JA, Carrión MC. 2010. "High Technology Elements" in Co-Rich Ferromanganese

Crusts from the Scotia Sea. Revista de la sociedad española de mineralogía, pp. 113-114.

Gonzalez H, Jensen TE. 1998. Nickel sequestering by polyphosphate bodies in *Staphylococcus aureus*. Microbios 93: 179-85.

Gorby Y, Caccavo FJR, Bolton HJR. 1998. Microbial Reduction of Cobalt^{III}EDTA- in the Presence and Absence of Manganese(IV) Oxide. Environ Sci Technol 32: 244-250.

Green-Pedersen H, Jensen BT, Pind N. 1997. Nickel adsorption on MnO_2, $Fe(OH)_3$, montmorillonite, humic acid and calcite: a comparative study. Environ Technol 18: 807-815.

Gregory E, Staley JT. 1982. Widespread distribution of ability to oxidize manganese among freshwater bacteria. Appl Environ Microbiol 44: 509-11.

Haferburg G, Kothe E. 2007. Microbes and metals: interactions in the environment. J Basic Microbiol 47: 453-467.

Halbach P, Schwarz-Schampera U, Marbler H. 2008. Platinum and some other trace metals in ferromanganese crusts- geochemical models to explain contradictions. In: Marine Minerals: Technological Solutions and Environmental Challenges. University of Mississippi, Oxford, USA, p. 1-6.

Halbach P, Segl M, Puteanus D, Mangini A. 1983. Co-fluxes and growth rates in Fe-Mn deposits from central Pacific seamount areas. Nature 304: 716-719.

Hamilton EI. 1994. The geobiochemistry of cobalt. Sci Total Environ 150: 7-39.

Harris RD, Troup AG. 1970. Chemistry and origin of freshwater Fe-Mn concretions. Limnol Oceanogr 15: 702-712.

Hausinger RP. 1987. Nickel utilization by microorganisms. Microbiol Rev 51:22-42.

He J, Zhang L, Jin S, Zhu Y, Liu F. 2008. Bacterial communities inside and surrounding soil iron-manganese nodules. Geomicrobiol J 25:14-24.

Hein JR, Conrad TA, Staudigel H. 2010. Seamount mineral deposits: a source of rare metals for high-technology industries. Oceanography 23:184-189.

Hein JR, Gibbs AE, Clague DA, Torresan M. 1996. Hydrothermal mineralization along submarine rift zones, Hawaii. Mar Georesour Geotechnol 14: 177-203.

Hein JR, Koschinsky A, Bau M, Manheim FT, Kang JK, Roberts L. 2000. Cobalt-rich ferromanganese crusts in the Pacific. In: Handbook of marine mineral deposits. Cronan DS (ed) CRC Press, New York, pp. 239–280.

Hein JR, Koschinsky A, Halbach P, Manheim FT, Bau M, Kang JK, Lubick N. 1997. Iron and manganese oxide mineralization in the Pacific. Geol Soc London Spl Pub 119: 123-138.

Hein JR, Schulz MS, Gein LM. 1992. Central Pacific cobalt rich Fe-Mn crusts: historical perspective and regional variability. In: Geology and Offshore Mineral Resources of the Central Pacific Basin, Circum-Pacific Council for Energy and Mineral Resources. Keating BH, Bolton BR (eds) Springer, New York, pp. 261-283.

Hem JD, Roberson CE, Lind CJ. 1985. Thermodynamic stability of CoOOH and its coprecipitation with manganese. Geochim Cosmochim Acta 49: 801-810.

Henneken L, Nötemann B, Hempel DC. 1995. Influence of Physiological Conditions on EDTA Degradation. Appl Microbiol Biotechnol 44: 190-197.

Hitchcock AP, Dynes JJ, Lawrence JR, Obst M, Swerhone GD, Korber DR, Leppard GG. 2009. Soft X-ray spectromicroscopy of nickel sorption in a natural river biofilm. Geobiology 7: 432-453.

Holden JF, Adams MWW. 2003. Microbe–metal interactions in marine hydrothermal environments. Curr Opin Chem Biol 7: 160-165.

Horsburgh MJ, Wharton SJ, Karavolos M, Foster SJ. 2002. Manganese: elemental defence for a life with oxygen? Trend Microbiol 10: 496-501.

Huber JA, Cantin HV, Huse SM, Welch DBM, Sogin ML, Butterfield DA. 2010. Isolated communities of Epsilonproteobacteria in hydrothermal vent fluids of the Mariana Arc seamounts. FEMS Microbiol Ecol 73: 538-549.

Intwala A, Patey TD, Polet DM, Twiss MR. 2008. Nutritive Substitution of Zinc by Cadmium and Cobalt in Phytoplankton Isolated from the Lower Great Lakes. J Great Lakes Res 34:1-11.

Iyaka YA. 2011. Nickel in soils: A review of its distribution and impacts. Sci Res Essays 6: 6774-6777.

Iyer SD, Das P, Kalangutkar NG, Mehta CM. 2012a. Seamounts- windows of opportunities and the Indian scenario. Curr Sci 102: 382-1391.

Iyer SD, Mehta CM, Das P, Kalangutkar NG. 2012b. Seamounts-characteristics, formation, mineral deposits and biodiversity. Geol Acta 10: 295-308.

Iyer SD. 1991. Comparison of internal features and microchemistry of ferromanganese crusts from the Central Indian Basin. Geo-Mar Lett 11: 44-50.

Iyer SD. 2009. Seamounts-their formation, mineral deposits, biodiversity and atmospheric oxygen. Geo-Spectrum Interface 4: 33-36.

Jakubovics NS, Jenkinson HF. 2001. Out of the Iron Age: new insights into the critical role of manganese homeostasis in bacteria. Microbiology 147: 1709–1718.

Johnson KS, Berelson WM, Coale KH, Coley TL, Elrod VA, Fairey WR, Lams HD, Kilgore TE, Nowicki JL. 1992. Manganese flux from continental margin sediments in a transect through the oxygen minimum. Science 257: 1242-1245.

Johnson KS. 2006. Manganese redox chemistry revisited. Science 313: 1896-1897.

Jones TS. 1985. Manganese. In: Mineral facts and problems. Bureau of Mines Bull 675, US Department of the Interior, Washington, DC, pp. 483-497.

Juniper SK, Tebo BM. 1995. Microbe-metal interactions and mineral deposition at hydrothermal vents. In: The Microbiology of Deep-Sea Hydrothermal Vents. Karl DM (ed) CRC Press, New York, p. 219–253.

Kaltwasser H, Frings W. 1980. Transport and metabolism of nickel in microorganisms. In: Nickel in the Environment. Nriagu JO (ed) Wiley, New York, p. 463-491.

Kamesh Raju KA, Ray D, Mudholkar A, Murty GPS, Gahalaut VK, Samudrala K, Paropkari AL, Ramachandran R, Surya Prakash L. 2012.Tectonic and volcanic implications of a cratered seamount off Nicobar Island, Andaman Sea. J Asian Earth Sci 56: 42-53.

Ke J, Li H. 2006. Bacterial leaching of nickel-bearing pyrrhotite. Hydrometallurgy 82: 172-175.

Keasling JD. 1997. Regulation of intracellular toxic metals and other cations by hydrolysis of polyphosphate. Ann NY Acad Sci 829: 242-249.

Kepkay PE, Nealson KH. 1982. Surface Enhancement of Sporulation and Manganese Oxidation by a Marine *Bacillus*. J Bacteriol 151: 1022-1026.

Keren N, Kidd MJ, Penner-Hahn JE, Pakrasi HB. 2002. A light-dependent mechanism for massive accumulation of manganese in the photosynthetic bacterium *Synechocystis* sp. PCC 6803. Biochemistry 41: 15085–15092.

Kim JH, Gibb HJ, Howe PD. 2006. Cobalt and inorganic cobalt compounds. In: Concise International Chemical Assessment Document 69. The International Labour Organization and the World Health Organization. 94 p.

Kirchner WB, Grabowski S. 1972. Manganese in lacustrine ecosystems: A review. Am Water Resour Assoc 8: 1259-1264.

Knauer GA, Martin JH, Gordon RM. 1982. Cobalt in north-east Pacific waters. Nature 297: 49-51.

Kobayashi M, Shimizu S. 1999. Cobalt proteins. Eur J Biochem 261: 1-9.

Komeda H, Kobayashi M, Shimizu S. 1997. A novel transporter involved in cobalt uptake. Proc Natl Acad Sci USA 94: 36-41.

Konhauser K. 2007. Biomineralization. In: Introduction to geomicrobiology. Blackwell Science Ltd, USA, pp. 139-191.

Konhauser KO. 1998. Diversity of bacterial iron mineralization. Earth-Sci Rev 43: 91-121.

Koschinsky A, Hein JR. 2003. Uptake of elements from seawater by Fe-Mn crusts: solid-phase associations and seawater speciation. Mar Geol 198: 331-351.

Kretzschmar R, Schäfer T. 2005. Metal retention and transport on particles in the environment. Elements 1: 205-210.

Krishna KS, Scrutton RA, Bull JM, Jai Shankar S, Banakar VK. 2009. Growth of the Afanasy Nikitin Seamount, Central Indian Ocean-the product of short-lived hotspots. Geophys Res Abstracts 11: EGU2009-2144-2.

Krishna KS. 2003. Structure and evolution of the Afanasy Nikitin seamount,buried hills and 85°E Ridge in the northeastern Indian Ocean. Earth Planet Sci Lett 209: 379-394.

Krishnan KP, Fernandes CEG, Fernandes SO, Loka Bharathi PA. 2006. Tolerance and Immobilization of Cobalt by Some Bacteria from Ferromanganese Crusts of the Afanasiy Nikitin Seamounts. Geomicrobiol J 23: 31-36.

Krishnan KP, Fernandes SO, Chandan GS, Loka Bharathi PA. 2007. Bacterial contribution to mitigation of iron and manganese in mangrove sediments. Mar Pollut Bull 54: 1427–1433.

Krishnan KP, Sinha RK, Krishna K, Nair S, Singh SM. 2009. Microbially mediated redox transformations of manganese (II) along with some other trace elements: a study from Antarctic lakes. Polar Biol 32: 1765-1778.

Krishnaswami S, Mangini A, Thomas JH, Sharma P, Cochran JK, Turekian KK, Parker PD. 1982. ^{10}Be and Th isotopes in manganese nodules and adjacent sediments: nodule growth histories and nuclide behaviour. Earth Planet Sci Lett 59: 217-234.

Kurek E, Francis AJ, Bollag J-M. 1991. Immobilization of cadmium by microbial extracellular products. Arch Environ Contam Toxicol 20: 106-111.

Lauff JJ, Steele DB, Coogan LA, Breitfeller JM. 1990. Degradation of the Ferric Chelate of EDTA by a Pure Culture of an *Agrobacterium* sp. Appl Environ Microbiol 56: 3346-3353.

Lee B-G, Fisher NS. 1993. Microbially mediated cobalt oxidation in seawater revealed by radiotracer experiments. Limnol Oceanogr 38:1593-1602.

Lee Y, Tebo BM. 1994. Cobalt(II) oxidation by the marine manganese(II)-oxidizing *Bacillus* sp. strain SG-1. Appl Environ Microbiol 60: 2949-2957.

Li Y-H. 1981. Ultimate removal mechanisms of elements from the ocean. Geochim Cosmochim Acta 45: 1659-1664.

Liao L, Xu X, Jiang X, Wang C, Zhang D, Ni J, Wu M. 2011. Microbial diversity in deep-sea sediment from the cobalt-rich crust deposit region in the Pacific Ocean. FEMS Microbiol Ecol 78: 565-585.

Lindsay D, Kerr W. 2011. Cobalt close-up. Nature Chem 3: 494.

Liu C, Gorby YA, Zachara JM, Fredrickson JK, Brown CF. 2002. Reduction kinetics of Fe(III), Co(III), U(VI), Cr(VI), and Tc(VII) in cultures of dissimilatory metal-reducing bacteria. Biotechnol Bioeng 80: 637-649.

Lowe RH, Evans HJ. 1962. Cobalt requirement for the growth of *Rhizobia.* J Bacteriol 83: 210-212.

Lowenstam HA, Weiner S. 1989. On Biomineralization. Oxford University Press, New York.

Macomber L, Hausinger RP. 2011. Mechanisms of nickel toxicity in microorganisms. Metallomics 3: 1153-1162.

Madgwick JC. 1987. Microbial processing of manganese. Aust J Biotechnol 1: 41-43.

Manheim FT, Lane-Bostwick CM. 1988. Cobalt in ferromanganese crusts as a monitor of hydrothermal discharge on the Pacific sea floor. Nature 335: 59-62.

Manheim FT. 1986. Marine cobalt resources. Science 232: 600-608.

Maret W, Vallee BL. 1993. Cobalt as probe and label of proteins. Methods Enzymol 226:52-71.

McDowell LR. 2000. Vitamin B12. In: Vitamins in Animal and Human Nutrition. Iowa State Press, Ames, pp. 523-563.

Mendonca A, Arıstegui J, Vilas JC, Montero MF, Ojeda A, Espino M, Martins A. 2012. Is There a Seamount Effect on Microbial Community Structure and Biomass? The Case Study of Seine and Sedlo Seamounts (Northeast Atlantic). Plos One **7:** e29526.

Mero JL. 1960. Minerals on the ocean floor. Sci Am 203: 64-72.

Moffett JW, Ho J. 1996. Oxidation of cobalt and manganese in seawater via a common microbially catalyzed pathway. Geochim Cosmochim Acta 60: 3415-3424.

Mohandass C, Rajasabapathy R, Ravindran C, Colaco A, Santos RS, Meena RM. 2012. Bacterial diversity and their adaptations in the shallow water hydrothermal vent at D. Joao de Castro Seamount (DJCS) Azores, Portugal. Cah Biol Mar 53: 65-76.

Mottl MJ. 1983. Metabasalts, axial hot springs, and the structure of hydrothermal systems at mid-ocean ridges. Geol Soc Am Bull 94: 161-180.

Moyer CL, Dobbs FC, Karl DM. 1995. Phylogenetic diversity of the bacterial community from a microbial mat at an active, hydrothermal vent system, Loihi Seamount, Hawaii. Appl Environ Microbiol 61: 1555-1562.

Mukherjee AB. 1998. Nickel: a review of occurrence, uses, emissions, and concentration in the environment in Finland. Environ Rev 6: 1-15.

Murray JW and Dillard JG. 1979. The oxidation of cobalt(II) adsorbed on manganese dioxide. Geochim Cosmochim Acta 43: 781-787.

Murray KJ, Webb SM, Bargar JR, Tebo BM. 2007. Indirect oxidation of Co(II) in the presence of the marine Mn(II)-oxidizing bacterium *Bacillus* sp. strain SG-1. Appl Environ Microbiol 73: 6905-6909.

Murton BJ, Baker ET, Sands CM, German CR. 2006. Detection of an unusually large hydrothermal event plume above the slow-spreading Carlsberg Ridge: NW Indian Ocean. Geophys Res Lett 33: 1-5.

Myers CR, Nealson KH. 1988. Bacterial manganese reduction and growth with manganese oxide as the sole electron acceptor. Science 240: 1319-1321.

Nakagawa S, Takai K, Inagaki F, Hirayama H, Nunoura T, Horikoshi K, Sako Y. 2005. Distribution, phylogenetic diversity and physiological characteristics of epsilon-*Proteobacteria* in a deep-sea hydrothermal field. Environ Microbiol 7: 1619-1632.

Nath BN. 2007. Processes of formation of Fe-Mn manganese nodules and crusts. In: Refresher course on marine geology and geophysics. 22nd October to 2nd November 2007, lecture notes. pp. 63-69.

Nayak B, Das SK, Munda P. 2013. Biogenic signature and ultra microfossils in ferromanganese nodules of the Central Indian Ocean Basin. J Asian Earth Sci 73: 296-305.

Nealson KH, Myers CR. 1992. Microbial reduction of manganese and iron: new approaches to carbon cycling. Appl Environ Microbiol 58: 439-443.

Nealson KH. 1983. The microbial manganese cycle. In: Microbial geochemistry. Krumbein WE (ed) Blackwell scientific publications, pp. 191-221.

Nicholas DJD, Kobayashi M, Wilson PW. 1962. Cobalt requirement for inorganic nitrogen metabolism in microorganisms. Proc Natl Acd Sci 48: 1537-1542.

Nieminen TM, Ukonmaanaho L, Rausch N, Shotyk W. 2007. Biogeochemistry of nickel and its release into the environment. Met Ions Life Sci 2: 1-30.

Nies DH. 1999. Microbial heavy-metal resistance. Appl Microbiol Biotechnol 51: 730-750.

Nimmo M, Van Den Berg CMG, Brown J. 1989. The chemical speciation of dissolved nickel, copper, vanadium, and iron in Liverpool Bay, Irish Sea. Estuar Coast Shelf Sci 29: 57-74.

Nitahara S, Kato S, Urabe T, Usui A, Yamagishi A. 2011. Molecular characterization of the microbial community in hydrogenetic ferromanganese crusts of the Takuyo-Daigo Seamount, northwest Pacific. FEMS Microbiol Lett 321: 121-129.

Nörtemann B. 1992. Total degradation of EDTA by mixed cultures and a bacterial isolate. Appl Environ Microbiol 58: 671-676.

Nriagu JO, Pacyna JM. 1988. Quantitative assessment of worldwide contamination of air, water and soils by trace metals. Nature 333: 134-139.

Ogawa T, Bao DH, Katoh H, Shibata M, Pakrasi HB, Bhattacharyya-Pakrasi M. 2002. A Two-component Signal Transduction Pathway Regulates Manganese Homeostasis in *Synechocystis* 6803, a Photosynthetic Organism. J Biol Chem 277: 28981-28986.

Okamoto S, Eltis LD. 2011. The biological occurrence and trafficking of cobalt. Metallomics 3: 963-970.

Pak K-R, Lim O-Y, Lee H-K, Choi S-C. 2002. Aerobic reduction of manganese oxide by Salmonella sp. strain MR4. Biotechnol Lett 24: 1181-1184.

Parthiban G, Banakar VK. 1999. Chemistry and possible resource potential of cobalt-rich ferromanganese crusts from Afanasiy-Nikitin Seamount in the Indian Ocean. Indian Mineralogist 33: 125-132.

Pearson GF, Greenway GM. 2005. Recent developments in manganese speciation. Trends in Analytical Chemistry 24: 803-809.

Persson AE, Schoeman BJ, Sterte J, Otterstedt J-E. 1995. Synthesis of stable suspensions of discrete colloidal zeolite (Na, TPA) ZSM-5 crystals. Zeolites 15: 611-619.

Price NM, Morel FMM. 1990. Cadmium and cobalt substitution for zinc in a marine diatom. Nature 344: 658-660.

Pulyaeva IA, Hein JR. 2010. Paleoceanographic conditions during the formation of Fe-Mn crusts from the Pacific Ocean: Biostratigraphic and compositional evidence. In: Toward the Sustainable Development of Marine Minerals: Geological, Technological, and Economic Aspects. 39th Underwater Mining Institute, Gelendzhik, Russia, pp. 1-11.

Pyle G and Couture P. 2012. Nickel. In: Fish Physiology: Homeostasis and Toxicology of Essential Metals. Wood CM, Farrell AP, Brauner CJ (eds) Elsevier Inc, pp. 253-289.

Rassa AC, McAllister SM, Safran SA, Moyer CL. 2009. Zeta-Proteobacteria dominate the colonization and formation of microbial mats in low-temperature hydrothermal vents at Loihi Seamount, Hawaii. Geomicrobiol J 26: 623-638.

Rathsack K, Stackebrandt E, Reitner J, Schumann G. 2009. Microorganisms isolated from deep sea low-temperature influenced oceanic crust basalts and sediment samples collected along the Mid-Atlantic Ridge. Geomicrobiol J 26: 264-274.

Reck BK, Muller DB, Rostkowski K, Graedel TE. 2008. Anthropogenic nickel cycle: insights into use, trade, and recycling. Environ Sci Technol 42: 3394-3400.

Reyss JL, Marchig V, Ku TL. 1982. Rapid growth of a deep-sea manganese nodule. Nature 295: 401- 403.

Richter RO, Theis TL. 1980. Nickel speciation in a soil/water system. In: Nickel in the Environment. Nriagu JO (ed) John Wiley and Sons, New York, pp. 189–202.

Ridgway HF, Olson BH. 1981. Scanning electron microscope evidence for bacterial colonization of a drinking-water distribution system. Appl Environ Microbiol 41: 274-287.

Riemann F. 1983. Biological aspects of deep-sea manganese nodule formation. Oceanol Acta 6: 303-311.

Robertson DE, Silker WB, Langford JC, Petersen MR, Perkins RW. 1973. Transport and depletion of radionuclides in the Columbia River. In: Radioactive contamination of the marine environment. IAEA, Vienna, pp.141-158.

Roh Y, Liu SV, Li G, Huang H, Phelps TJ, Zhou J. 2002. Isolation and characterization of metal-reducing *Thermoanaerobacter* strains from deep subsurface environments of the Piceance Basin, Colorado. Appl Environ Microbiol 68: 6013-6020.

Roitz JS, Flegal AR, Bruland KW. 2002. The biogeochemical cycling of manganese in San Francisco Bay: Temporal and spatial variations in surface water concentrations. Estuar Coast Shelf Sci 54: 227-239.

Rosson RA, Nealson KH. 1982. Manganese Binding and Oxidation by Spores of a Marine *Bacillus*. J Bacteriol 151: 1027-1034.

Rosswall T. 1973. Modern methods in the study of microbial ecology. Ecological Bulletin 17. 511p.

Saager PM, De Baar HJW, Burkill PH. 1989. Manganese and iron in Indian Ocean waters. Geochim Cosmochim Acta 53: 2259-2267.

Sand W, Gehrke T, Jozsa P, Schippers A. 2001. (Bio)chemistry of bacterial leaching-direct vs. indirect bioleaching. Hydrometallurgy 59: 159-175.

Santander PJ, Roessner CA, Stolowich NJ, Holderman MT, Scott AI. 1997. How corrinoids are synthesized without oxygen: nature's first pathway to vitamin B12. Chem Biol 4: 659-666.

Sar P, Kazy SK, Singh SP. 2001. Intracellular nickel accumulation by *Pseudomonas aeruginosa* and its chemical nature. Lett Appl Microbiol 32: 257-261.

Sardessai S, Shetye S, Maya MV, Mangala KR, Prasanna Kumar S. 2010. Nutrient characteristics of the water masses and their seasonal variability in the eastern equatorial Indian Ocean. Mar Environ Res 70: 272-282.

Satroutdinov AD, Dedyukhina EG, Chistyakova TI, Minkevich IG, Eroshin VK, Egli T. 2003. Bacterial degradation of EDTA. Microbiology 72: 8-11.

Sautya S, Ingole BS, Ray D, Stohr S, Samudrala K, Kamesh Raju KA, Mudholkar AV. 2011. Megafaunal community structure of Andaman seamounts including the back-arc basin – a quantitative exploration from the Indian Ocean. PLoS One 6: 1-15.

Sawers RG. 2013. Nickel in Bacteria and Archaea. In: Encyclopedia of Metalloproteins. Uversky VN, Kretsinger RH, Permyakov EA (eds) Springer,pp. 1490-1496.

Schaumloffel D. 2012. Nickel species: analysis and toxic effects. J Trace Elem Med Biol 26: 1–6.

Schultze-Lam S, Fortin D, Davis BS, Beveridge TJ. 1996. Mineralization of bacterial surfaces. Chem Geol 132:171-181.

Schweisfurth R, Eleftheriadis D,Gundlach H, Jacobs M, Jung W. 1978. Microbiology of the precipitation of manganese. In: Environmental biogeochemistry and geomicrobiology. Krumbein WE (ed) Ann Arbor Science, pp. 923-928.

Shi L. 2004. Manganese-dependent protein o-phosphatases in prokaryotes and their biological functions. Front Biosci 9: 1382-1397.

Shterenberg LE, Aleksandrova VA, Gablina IF, Lelikov EP, Sivtsov AV, Stepanetx MI. 1990. Composition and structure of manganese crusts from the Sea of Japan. Geol Pac Ocean 5: 232-237.

Smith IC, Carson BL. 1981. Trace metals in the environment. Ann Arbor, MI, Ann Arbor Science Publishers.

Spiro TG, Bargar JR, Sposito G, Tebo BM. 2010. Bacteriogenic manganese oxides. Accounts Chem Res 43: 2-9.

Staudigel H, Clague DA. 2010. The geological history of deep-sea volcanoes: Biosphere, hydrosphere, and lithosphere interactions. Oceanography 23: 58-71.

Staudigel H, Koppers AAP, Lavelle JW, Pitcher TJ, Shank TM. 2010. Defining the word seamount. Oceanography 23: 20-21.

Stokes PM. 1981. Nickel in aquatic systems. In: Effects of nickel in the Canadian environment. National Research Council of Canada, Ottawa, pp. 77-117.

Sudek LA, Templeton AS, Tebo BM, Staudigel H. 2009. Microbial ecology of Fe (hydr)oxide mats and basaltic rock from Vailulu'u Seamount, American Samoa. Geomicrobiol J 26: 581-596.

Sujith PP, Das A, Mourya BS, Loka Bharathi PA. 2011. Immobilisation of manganese, cobalt and nickel by deep-sea-sediment microbial communities. Chem Ecol 27: 189-206.

Sujith PP, Khedekar VD, Girish AP, Loka Bharathi PA. 2010. Immobilization of nickel by bacterial isolates from the Indian Ridge System and the chemical nature of the accumulated metal. Geomicrobiol J 27: 424-434.

Sujith PP, Loka Bharathi PA. 2011. Manganese oxidation by bacteria: biogeochemical aspects. Prog Mol Subcell Biol 52: 49-76.

Sukla LB, Panchanadikar V. 1993. Bioleaching of lateritic nickel ore using a heterotrophic micro-organism. Hydrometallurgy 32: 373-379.

Sunamura M, Higashi Y, Miyako C, Ishibashi J, Maruyama A. 2004. Two bacteria phylotypes are predominant in the Suiyo seamount hydrothermal plume. Appl Environ Microbiol 70: 1190-1198.

Sunda WG, Huntsman SA. 1988. Effect of sunlight on redox cycles of manganese in the south western Sargasso Sea. Deep Sea Res 35: 1297-1317.

Sunda WG, Huntsman SA. 1990. Diel cycles in microbial manganese oxidation and manganese redox speciation in coastal waters of the Bahama Islands. Limnol Oceanogr 35: 325-338.

Taillefert M, MacGregor BJ, Gaillard JF, Lienemann CP, Perret D, Stahl DA. 2002. Evidence for a dynamic cycle between Mn and Co in the water column of a stratified lake. Environ Sci Technol 36: 468-476.

Takai K, Campbell BJ, Cary SC, Suzuki M, Oida H, Nunoura T Hirayama, H, Nakagawa S, Suzuki Y, Inagaki F, Horikoshi K. 2005. Enzymatic and genetic characterization of carbon and energy metabolisms by deep-sea hydrothermal chemolithoautotrophic isolates of *Epsilonproteobacteria.* Appl Environ Microbiol 71: 7310-7320.

Takai K, Nakagawa S, Reysenbach AL, Hoek J. 2006. Microbial ecology of Mid-Ocean Ridges and Back-Arc Basins. In: Back-Arc spreading systems: geological, biological, chemical and physical interactions. Christie DM, Fisher CR, Lee SM, Givens S (eds) Geophysical Monograph Series, American Geophysical Union, pp.185-213.

Taylor GT, Sullivan CW. 2008. Vitamin B12 and cobalt cycling among diatoms and bacteria in Antarctic sea ice microbial communities. Limnol Oceanogr 53: 1862-1877.

Tebo BM, Bargar JR, Clement BG, Dick GJ, Murray KJ, Parker D, Verity R, Webb SM. 2004. Biogenic manganese oxides: Properties and mechanisms of formation. Annu Rev Earth Planet Sci 32: 287–328.

Tebo BM, Clement BG, Dick GJ. 2007. Biotransformations of manganese. In: Manual of environmental microbiology. Hurst CJ, Crawford RL, Garland JL, Lipson DA, Mills AL, Stetzenbach LD (eds) ASM Press, Washington, pp. 1223-1238.

Tebo BM, Geszvain K, Lee S-W. 2010. The molecular geomicrobiology of bacterial Manganese(II) oxidation. In: Geomicrobiology: Molecular and Environmental Perspective. Barton LL et al. (eds), Springer, pp. 285-308.

Tebo BM, Ghiorse WC, van Waasbergen LG, Siering PL, Caspi R. 1997. Bacterially mediated mineral formation: insights into manganese(II) oxidation from molecular genetic and biochemical studies. In: Geomicrobiology: Interactions Between Microbes and Minerals. Banfield JF, Nealson KH (eds) Mineral Soc Am, Washington, pp. 225-266.

Tebo BM, Johnson HA, McCarthy JK, Templeton AS. 2005. Geomicrobiology of manganese(II) oxidation. Trend Microbiol 13: 421-428.

Tebo BM, Lee Y. 1993. Microbial oxidation of cobalt. In: Biohydrometallurgical Technologies. Torma AE, Wey JE, Lakshmanan VL (eds) The Minerals, Metals and Materials Society, Warrendale, Pennsylvania, pp. 695-704.

Tebo BM, Nealson KH, Emerson S, Jacobs L. 1984. Microbial mediation of Mn(II) and Co(II) precipitation at the O2/H2S interfaces in two anoxic fjords. Limnol Oceanogr 29:1247-1258.

Templeton AS, Staudigel H, Tebo BM. 2005. Diverse Mn(II)-Oxidizing Bacteria Isolated from Submarine basalts at Loihi seamount. Geomicrobiol J 22: 127-139.

Thamdrup B. 2000. Microbial manganese and iron reduction in aquatic sediments. Adv Microb Ecol 16: 41-84.

Thijssen T, Glasby GP, Friedrich G, Stoffers P, Sioulas A. 1985. Manganese nodules in the Central Peru Basin. Chemie der Erde 44: 1-12.

Thomas RAP, Lawlor K, Bailey M, Macaskie LE. 1998. Biodegradation of metal-EDTA complexes by an enriched microbial population. Appl Environ Microbiol 64: 1319-1322.

Thorseth IH, Furnes H, Tumyr O. 1995. Textural and chemical effects of bacterial activity on basaltic glass: an experimental approach. Chem Geol 119: 139-160.

Tripathi P, Srivastava S. 2007. Mechanism to combat cobalt toxicity in cobalt resistant mutants of *Aspergillus nidulans*. Indian J Microbiol 47: 336-344.

Trouwborst RE, Clement BG, Tebo BM, Glazer BT, Luther GW.2006. Soluble Mn(III) in Suboxic Zones. Science 313: 1955-1957.

Tully BJ, Heidelberg JF. 2013. Microbial communities associated with ferromanganese nodules and the surrounding sediments. Frontiers in Microbiology 4: doi: 10.3389/fmicb.2013.00161.

Turekian KK, Wedepohl KH. 1961. Distribution of the elements in some major units of the Earth's Crust. Geol Soc Am Bull 72: 175-192.

Twining BS, Baines SB, Vogt S, Nelson DM. 2012. Role of diatoms in nickel biogeochemistry in the ocean. Global Biogeochem Cy 26: GB4001.

Urrutia MM, Beveridge TJ. 1994. Formation of fine-grained metal and silicate precipitates on a bacterial surface (*Bacillus subtilis*). Chem Geol 116: 261-280.

Usui A, Mellin TA, Nohara M, Yuasa M. 1989. Structural stability of marine 10Å manganates from the Ogasawara (Bonin) Arc: implication for low-temperature hydrothermal activity. Mar Geol 86: 41-56.

Usui A, Someya M. 1997. Distribution and composition of marine hydrogenetic and hydrothermal manganese deposits in the northwest Pacific. Geol Soc London Spl Pub 119: 177-198.

Verlaan PA. 1992. Benthic recruitment and manganese crust formation on seamounts. Mar Biol 113: 171-174.

Von Damm KL, Edmond JM, Grant B, Measures CI, Walden B, Weiss RF. 1985. Chemistry of submarine hydrothermal solutions at 21°N, East Pacific Rise. Geochim Cosmochim Acta 49: 2197-2220.

Wang C-S, Liao L, Xu H-X, Xu X-W, Wu M, Zhu L-Z. 2010. Bacterial Diversity in the Sediment from Polymetallic Nodule Fields of the Clarion-Clipperton Fracture Zone. J Microbiol 48: 573-585.

Wang X, Muller WEG. 2009. Marine biominerals: perspectives and challenges for polymetallic nodules and crusts. Trends Biotechnol 27: 375–383.

Wang X, Muller WEG. 2010. Are Polymetallic Nodules, Crusts and Vents Biominerals? J Sci Hal Aquat 2: 5-20.

Wang X, Schloßmacher U, Natalio F, Schroder HC, Wolf SE, Tremel W, Muller WEG. 2009. Evidence for biogenic processes during formation of ferromanganese crusts from the Pacific Ocean: Implications of biologically induced mineralization. Micron 40: 526-535.

Webb SM, Dick GJ, Bargar JR, Tebo BM. 2005. Evidence for the presence of Mn(III) intermediates in the bacterial oxidation of Mn(II). Proc Natl Acad Sci USA 102: 5558-5563.

Welch SA, Barker WW, Banfield JF. 1999. Microbial extracellular polysaccharides and plagioclase dissolution. Geochim Cosmochim Acta 63: 1405-1419.

Welch SA, Vandevivere P. 1994. Effect of microbial and other naturally occurring polymers on mineral dissolution. Geomicrobiol J 12: 227-238.

Wen X, DeCarlo EH, Li YH. 1997. Inter element relationship in Fe-Mn crusts from the central Pacific Ocean: Their implications for crust genesis. Mar Geol 136: 277-297.

Wessel P, Sandwell DT, Kim S-S. 2010. The global seamount census. Oceanography 23: 24-33.

Wilson RR, Kaufmann RS. 1987. Seamount biota and biogeography. Geophys Monogr 43: 355-377.

Wilson TRS, Thomson J, Hydes DJ, Colley S, Culkin F, Sørensen J. 1986. Oxidation fronts in pelagic sediments: diagenetic formation of metal-rich layers. Science 232: 972-975.

Wiseman JDH. 1936. The petrography and significance of a rock dredged from a depth of 744 fathoms, near to providence reef, Indian Ocean. Linn Soc Lond Trans 19: 437-443.

Witschel M, Egli T, Zehnder AJB, Wehrli E, Spycher M. 1999. Transport of EDTA into cells of the EDTA degrading bacterial strain DSM 9103. Microbiology 145: 973-983.

Witschel M, Nagel S, Egli T. 1997. Identification and characterization of the two-enzyme system catalyzing the oxidation of EDTA in the EDTA-degrading bacterial strain DSM 9103. J Bacteriol 179: 6937-6943.

Woodward S. 2003. Biomes of earth, terrestrial, aquatic and human-dominated. Greenwood Publishing Group. 165 p.

Yocum CF, Pecoraro V. 1999. Recent advances in the understanding of the biological chemistry of manganese. Curr Opin Chem Biol 3: 182-187.

Young RS. 1957. The geochemistry of Cobalt. Geochim Cosmochim Acta 13: 28-41

Zajic JE. 1969. Microbes and cobalt. In: Microbial biogeochemistry. Academic press, New York, pp. 169-178.

Zhan G, Li D, Zhang L. 2012. Aerobic bioreduction of nickel(II) to elemental nickel with concomitant biomineralization. Appl Microbiol Biotechnol 96: 273-281.

CHAPTER 3

Distribution and diversity of culturable bacteria associated with hydrogenetic ferromanganese crusts of the Afanasiy-Nikitin seamount

3.1. Abstract

The distribution of bacteria and their interactions with Mn and Fe influences a number of biogeochemical processes. It is therefore of ecological importance to study the bacteria dwelling in Fe-Mn mineral rich deep-sea habitats as they can show activities for metal immobilization, mobilization, detoxification, mineralization and recycling of organic matter. Ecological interactions can affect the distribution and abundance of metal tolerant bacteria associated with hydrogenetic crusts of the ANS. The culturability of bacteria tolerant to 100 μM concentrations of Mn^{2+}, Co^{2+} and Ni^{2+} were carried out by plate diffusion method. Antibiotic resistance, hydrolytic enzyme activity and expression of metal binding proteins in these bacteria were assessed by standard methods and phylogenetic identification by 16S rDNA analyses. On an average, the distribution of culturable bacteria showed that the specific niche dictated the dominance of bacteria tolerant to the metals. The culturability of Mn and Co tolerant bacteria was most abundant of 1.10×10^5 and 2.75×10^4 CFU g^{-1} respectively in the ANS crusts, Mn and Ni tolerant bacteria of 1.41×10^5 and 1.08×10^5 CFU g^{-1} respectively in CIOB sediments and Mn tolerant bacteria of 1.88×10^4 CFU g^{-1} in CR crusts. Among the antibiotics, ampicillin (35.71%), followed by lincomycin (32.14%), penicillin G (32.14%) and vancomycin (32.14%) resistance was more predominant in the test isolates. Hydrolytic enzyme activity was positive in 96.6% of the isolates tested with maximum numbers positive for lipase, phosphatase, DNAse and amylase. Expression of Mn binding proteins was mostly localized in the periplasmic fraction of the bacterial cells. Expression of proteins in the presence of Mn showed the upregulation of periplasmic proteins in 83.3% of the isolates and downregulation of the cytoplasmic and membrane proteins in 66.7 and 50% of the isolates respectively. The results suggest that bacteria up-regulate genes to initiate metal resistance by enzymatic detoxification when exposed to a single metal whereas bacteria expresses fewer proteins in the

presence of multiple metals like Fe, Mn, Co and Ni suggesting "tradeoff". The molecular weight of the metal binding proteins varied from 31 to 52 KDa. Phylogenetic analyses of bacterial isolates showed taxonomic affiliations to 4 lineages: *Actinobacteria*, *Firmicutes*, α- and γ-*Proteobacteria* of which γ-*Proteobacteria* represented the dominant group. TEM observation of vertical and horizontal cross sections of bacterial cells grown in the presence of Co, Ni and Mn showed intra and-extracellular electron dense precipitates. Co precipitated mostly at the cell surface and in the cytoplasm, Ni in the cytoplasm and Mn at the cell surface and in association with the exopolysaccharides. The distribution and diversity of bacteria with the high frequency of metal and antibiotic resistance in the mineral rich deep-sea environments suggest the selective pressure imposed by multiple metals present in their immediate environment. The results thus reflect the important ecological role that these bacteria could play in the biogeochemical cycling of metal ions and cycling of organic matter in the Fe-Mn mineral rich deep-sea environments.

3.2. Introduction

Bacteria are ubiquitous in near-surface geological systems and are known to play an important role in different biogeochemical processes. Understanding the bacterial ecology would therefore help in identifying the group of bacteria that are responsible for the overall health of the region and the factors that govern the activity or inactivity of microbial populations in the natural environment (Bernard *et al.*, 2000; Simu *et al.*, 2005). The natural bacterial communities generally consist of various taxa, which use different strategies to generate energy and survive (Muller, 2010). A typical example could be of the microorganisms associated with metal enriched mineral deposits of the deep-sea which may differ in their metabolic requirements. It is known that culturable fraction represents only 0.01 to 0.1% of the total bacterial counts (Kogure *et al.*, 1979; Ellis *et al.*, 2003). However, the culturable methods provide useful insights about the ecology of different bacterial species, physiology and activity of different processes that they likely mediate in the environment (Lu *et al.*, 2006). These could perform important functions based on the activity they mediate in the resident environments, which could affect the prokaryotic processes on current and geological time scale in different water depths/sediment interfaces (Gonsalves *et al.*, 2011; Parkes *et al.*, 2005; Das *et al.*, 2011). Yet, there exists a lacuna of information on

the phylogenetic diversity of cultured bacteria and their associated activity in the hydrogenetic Fe-Mn crusts.

The majority of prokaryotes in natural environments do not grow on standard laboratory media since the complex conditions of the natural habitat are difficult to reproduce (Amann *et al.,* 1995; Kaeberlein *et al.,* 2002). Many microorganisms may need oligotrophic or other fastidious conditions to be successfully cultured (Connon and Giovannoni, 2002). Further, the routine practice of determining total cell numbers in microbiology cannot substitute the cultivability of bacteria, as they do not give information about the community composition or diversity (Batzke *et al.,* 2007). Ecosystems provide many functions and therefore from molecular analysis one cannot rule out species (or diversity) relationship to various functions (Jones and Bradford, 2001). Given that, the culture-independent approach can only tell us about the existence and probable functions of microorganisms, improved culture-based approaches efficiently compliment the limitations encountered in molecular methods to delineate the diversity and functions of uncultured organisms (Goltekar *et al.,* 2006). Therefore it is of utmost importance to understand the distribution of bacteria and be able to retrieve, cultivate and maintain the ecologically diverse uncultured forms.

3.3. Materials and methods

3.3.1. Sample collection and processing

Fe-Mn crusts were collected from the flanks of the Afansiy-Nikitin Seamount (ANS) during A.A. Sidorenko cruise CC2 (2003), onboard Akademic Boris Petrov (ABP) cruise 37 (2009) and basalts bearing Mn oxide coatings from the Carlsberg Ridge during cruise ABP36 (2009). Box core sediments BC26 and BC36 and the manganese nodules from the Central Indian Ocean region during cruise onboard ABP26 (2006) (Figure 1.1; Table 1.1). The deep-sea sampling for Fe-Mn crust was done using a chain bag dredge and sediments using a 50 × 50 × 50 cm box corer. Fe-Mn crust and nodule samples were rinsed with sterile seawater soon after collection and were stored at 4°C in sterile containers for microbiological analysis and at -20°C for molecular analysis. The sediment cores of 6.3 cm diameter were sub-sectioned at 2 cm intervals down to a depth of 10 cm and thereafter at 5 cm intervals to a depth of 35 cm. They were collected in sterile polyethylene bags and stored at 4°C till analysis.

The dilutions for the total bacterial counts (TBC) and enumeration of bacteria from sediments were prepared by suspending ~1 g of homogenized sediment in 9 ml of sterile seawater and for crusts and nodules, fragments in the size range of 1.7 ± 0.62 × 1.25 ± 0.52 mm were suspended aseptically in 9 ml of sterile seawater. The resulting mixture was dispersed by sonication (Sujith *et al.,* 2014). A Vibra Cell™ generator Model VC50 (Sonics and Materials Inc., Danbury, C.T. USA) with a high power level ultrasonic probe (Model ASI) with a standard 3.2 mm diameter titanium tip was used for ultrasonication. The volumes of media containing crust fragments were kept constant at 5 ml in sterile glass vials, and the probe tip was kept 1 cm above the bottom of the tube. These tubes were pre-cooled at 4±1°C and then packed in crushed ice during sonication to dissipate heat. Sonication was carried out at 15 Hz for 15 s in bursts of 5 s with intermittent cooling for 10 s in crushed ice, allowed to settle and then used for the respective analyses.

3.3.2. Total bacterial counts

For TBC small portion of the above dilution was fixed with buffered formalin to a final concentration of 2% and was stored at 4°C until analysis (Hobbie *et al.,* 1977). Samples volume of 1 ml was filtered through a 0.22 μm black Millipore polycarbonate filter. The filter holding the samples were stained in dark with 0.01% acridine orange for 3 min prior to microscopic observation. Approximately, 10-15 microscopic fields were counted for each sample at ×1500 magnification using a Nikon epifluorescence microscope (Nikon 50i, Japan). Counts were normalized per gram of dry sediment.

3.3.3. Plate counts of bacteria

The metal tolerant heterotrophic bacteria were enumerated by standard spread plate method in 20% nutrient agar medium containing 0.26g of nutrient broth and 1.5g of bacteriological agar (Himedia, Mumbai, India) in 100ml of seawater. On the other hand, bacteria tolerant to Mn, Co and Ni were enumerated in 20% nutrient agar medium as above amended with 100μM final concentration of individual metals Mn^{2+}, Co^{2+} and Ni^{2+} in their chloride forms ($MnCl_2 \cdot 4H_2O$, $CoCl_2 \cdot 6H_2O$ and $NiCl_2 \cdot 6H_2O$, Merck, Germany) respectively. Each medium was inoculated with 0.1 ml of the above aliquots directly or were inoculated from dilutions 10^3 to 10^4 prepared in sterile seawater which ever was appropriate. The plates were incubated at 28±2°C for 7-10 d.

The CFU of Mn-oxidizing bacteria were recognized by the brown colour of the colony due to the formation of Mn-oxides. The number of CFU in each plate were counted and then normalized per gram dry weight of the sediment/rock fragment. Correlation analysis to test the strength of association between variables namely the culturable bacteria and total bacterial abundance were carried out using data analysis tool pack, Microsoft Excel 2007.

3.3.4. Antibiotic susceptibility testing

Antibiotic susceptibility screening of 28 bacterial isolates for possible resistance against a selection of 19 antibiotics was tested using a slightly modified version of the agar disc diffusion method (Kirby *et al.*, 1966). The antibiotics tested include the types listed in Table 3.1. Hexa G plus and -minus filter paper disks obtained from Himedia laboratories Pvt. Ltd., impregnated with known concentration of the above antimicrobial compounds was placed on Mueller-Hinton (MH) agar plate inoculated with test strains. Following incubation at 28±2°C for 24 to 48 h, inhibition zones around the discs were measured. Results were interpreted according to the cut-off levels proposed by Charteris *et al.* (1998) and from breakpoint tables given by European committee on antimicrobial susceptibility testing (Leclercq *et al.* 2011).

3.3.5. Phenotypic characterization

Cultures were gram-stained and tested for motility, catalase, oxidase and DNase activity according to Gerhardt *et al.* (1981). The MOF (Marine oxidation fermentation medium) test was done with 1% glucose as carbon source. Results from the MOF test were interpreted based on the colour change of the pH indicator bromothymol blue after incubation at 28±2°C for 72 h (Hugh and Leifson, 1953). The screening of bacterial isolates for amylase and lipase enzymes was performed on plates of nutrient agar supplemented with 1% starch and 1% tributyrin respectively (Bairagi *et al.*, 2002). The plates were flooded with Lugol's iodine (1%) after growth for detecting amylase activity. The hydrolysis of starch and tributyrin was observed as clear halos surrounding the colony. Similarly, screening for cellulase producers was carried out on carboxymethylcellulose (CMC) agar (0.2% $NaNO_3$, 0.1% K_2HPO_4, 0.05% $MgSO_4$, 0.05% KCl, 0.02% peptone and 1.7% agar) with 1% CMC sodium salt as substrate. Cellulase activity was detected by use of Gram's iodine reagent (Kasana *et al.*, 2008).

Table 3.1. Multiple antibiotic resistance patterns of the marine bacterial isolates resistant to heavy metals.

Sl. No	Antibiotics	Conc (mcg/U)	Strains resistant to antibiotics			Isolates resistant
			No of resistant strains	% resistant	% sensitive	
1	**Aminoglycosides**					
	Amikacin	30	0	0	100	none
	Gentamycin	10	5	17.85	82.14	ANS-08Co, ANS-10Mn, ANS-18NA, ANS-22Co, ANS-37Co
2	**β-Lactams**					
	Ampicillin	10	10	35.71	64.29	ANS-04Ni, ANS-05Co, ANS-16Co, ANS-22Co, ANS-35Ni, ANS-36Co,CIOB-12Mn, CR-42Mn, CR-44Mn, CR-45Mn
	Aztreonam	30	0	0	100	none
	Imipenam	10	0	0	100	none
	Penicillin G	10	9	32.14	67.86	ANS-04Ni, ANS-05Co, ANS-17Co, ANS-22Co, ANS-35Ni, ANS-37Co, CIOB-12Mn, CR-20Co, CR-42Mn
	Piperacillin	100	0	0	100	none
3	**Cephalosporins**					
	Cefalexin	30	8	28.57	71.43	ANS-04Ni, ANS-05Co, ANS-16Co, ANS-22Co, ANS-35Ni, CIOB-12Mn, CR-42Mn, CR-44Mn
	Ceftazidime	30	0	0	100	none
4	**Chloramphenicol**					
	Chloramphenicol	30	0	0	100	none
5	**Fluoroquinolone**					
	Ciprofloxacin	5	0	0	100	none
6	**Fusidanes**					
	Fusidic acid	30	1	3.57	96.43	CR-45Mn
7	**Glycopeptides**					
	Vancomycin	30	9	32.14	67.86	ANS-01Co, ANS-04Ni, ANS-05Co,ANS-09Ni, ANS-24Co, ANS-34Co,ANS-35Ni, CR-42Mn, CR-45Mn
8	**Lincosamides**					
	Lincomycin	15	9	32.14	67.86	ANS-01Co, ANS-04Ni, ANS-05Co, ANS-16Co, ANS-22Co, ANS-35Ni,CIOB-12Mn, CR-42Mn, CR-45Mn
	Rifampicin	5	2	7.14	92.86	ANS-04Ni, CR-45Mn
9	**Macrolides**					
	Erythromycin	15	3	10.71	89.28	ANS-04Ni, ANS-05Co, CR-43Mn
10	**Oxazolidinones**					
	Linezolid	30	1	3.57	96.43	CR-45Mn
11	**Sulfonamides**					
	Co-Trimoxazole	25	5	17.85	82.14	ANS-08Co, ANS-27Ni, ANS-32Mn, CIOB-03Mn, CIOB-12Mn
12	**Tetracycline**					
	Tetracycline	30	0	0	100	none

Total number of isolates (28)

For the extracellular caseinase production, bacterial isolates were spot inoculated on soybean-casein digest agar medium (Himedia, Mumbai, India). Regions of enzyme activity were detected as clear halos after the addition of 0.1% amido black in methanol-acetic acid-water mixture in the ratio 30:10:60 (Vermelho *et al.,* 1996). The phosphatase enzyme activity was tested by supplementing 1% final concentration of filter sterilized solution of phenolphthalein diphosphate in the nutrient agar medium. Colonies liberating free phenolphthalein by phosphatase activity turned pink on exposing to concentrated ammonia fumes. Christiansen's urea agar base amended with 2% final concentration of urea as a filter sterilized solution was used for determining urease activity. Colour change of the medium surrounding the colony to deep pink indicated the test positive for the enzyme. The hydrolysis of DNA was observed as clear halos surrounding the colony after incubation in DNase test agar medium containing DNA as the substrate (Gerhardt *et al.,* 1981). The presumptive identification of the isolates was made according to the Bergeys Manual of Determinative Bacteriology (Holt *et al.,* 1994) and as per the taxonomic key outlined for marine bacteria (Oliver, 1982).

3.3.6. Genotypic characterization

3.3.6.1. Extraction of genomic DNA

The genomic DNA was extracted from actively growing bacterial cultures after growth in 20 % nutrient broth at 28±2°C for 24-36 h following the method of Zeng *et al.* (2008). Prior to growth, the bacterial biomass was concentrated by centrifugation at 6708 × g for 10 min at 4°C (Sigma 3-K). The bacterial cell pellets were washed thrice with phosphate buffered saline (300 mM NaCl, 2.7 mM KCl, 10 mM Na_2HPO_4 and 1.7 mM NaH_2PO_4, pH 7.5) and was then resuspended in 0.5 ml of DNA extraction buffer in eppendoff tubes. The buffer was prepared by mixing individual solutions of 50 ml of 0.5 M EDTA (pH 8.0); 5 ml of 5 M NaCl; 25 ml of 20% SDS and 20 ml of 1% Cetyl trimethylammonium bromide (CTAB) making up the total volume to 100 ml. The contents present in the tubes were incubated at 100°C in a water bath with horizontal shaking (225 rpm) for 6 min with gentle inversions every 3 min. This was followed by incubation for 30 min at 60°C with gentle inversion every 10 min and then at 72°C for 30 min with gentle inversions every 10 min. After which, the pellets were extracted with equal volume of phenol/chloroform/iso-amyl alcohol mixture (25:24:1) with

gentle inversion for 1 min. The mixture was centrifuged for 5 min at 4°C and the aqueous phase was transferred to a new and sterile 2 ml eppendoff tube. The DNA was precipitated by adding 2.5 ml volumes of ice-cold absolute alcohol and the mixture was incubated at -20°C for 1 h. The DNA was concentrated by centrifugation at 11269 × g for 10 min at 4°C. The resulting pellet was washed thrice with 500 µl of ice-cold 70% ethanol to remove the associated salt precipitate. They were air dried, dissolved in 30 µl of TE buffer (pH 8.0) and was stored at -20°C. The concentration and purity of DNA was checked using NanoDrop ND-1000 Spectrophotometer (NanoDrop Technologies, Wilmington DE).

3.3.6.2. PCR Amplification

The highly conserved regions of the 16S rRNA gene were amplified using universal primers 27F (5'-AGAGTTTGATCCTGGCTCAG-3') and 1492R (3'-TTCAGCATTGTTCC ATYGGCAT-5'). The universal bacterial primers used for sequencing were 27F (5'-AGAGTTTGATCCTGGCTCAG 3'), 685R (3'-CATCGCCACTTTACGCATCT-5'), 1100R (3'-GTTGCTCGCGTTGGG-5'), and 1492R (3'- TTCAGCATTGTTCCATYGGCAT-5'). The amplification of 16S rRNA gene was carried out with PCR master mix (Genie, Bangalore) in a final reaction mixture of 50 µl consisting of 0.5 µM of each primer, 1.5 mM $MgCl_2$, 200 µM dNTPs, 1U Taq DNA polymerase and 0.05 to 1 µg of DNA template. The amplification was done for 25 cycles in a thermal cycler (Eppendroff, Germany) with temperature profiles of 5 min at 95°C, 1 min at 95°C, 60 s at 50°C, 2 min at 72°C and final extension for 10 min at 72°C (Marchesi *et al.*, 1998).

3.3.6.3. Agarose gel electrophoresis

The PCR amplified products were analyzed by electrophoresis in 1% agarose gel (Plate 3.1). The agarose was prepared in autoclaved 1X TAE buffer (pH 8.5) and dissolved by heating in microwave oven for 1.5 min. The molten agarose on cooling was poured in a gel-casting tray without air bubbles. The comb was inserted carefully and was left undisturbed for 20 min at room temperature followed by 5 min at 4°C for proper setting. The comb was removed taking care not to disturb the gel. Followed by the casting of the gel, the tray holding the gel was placed inside the horizontal electrophoresis unit. The tank was filled with 1X TAE buffer to cover the gel surface. A

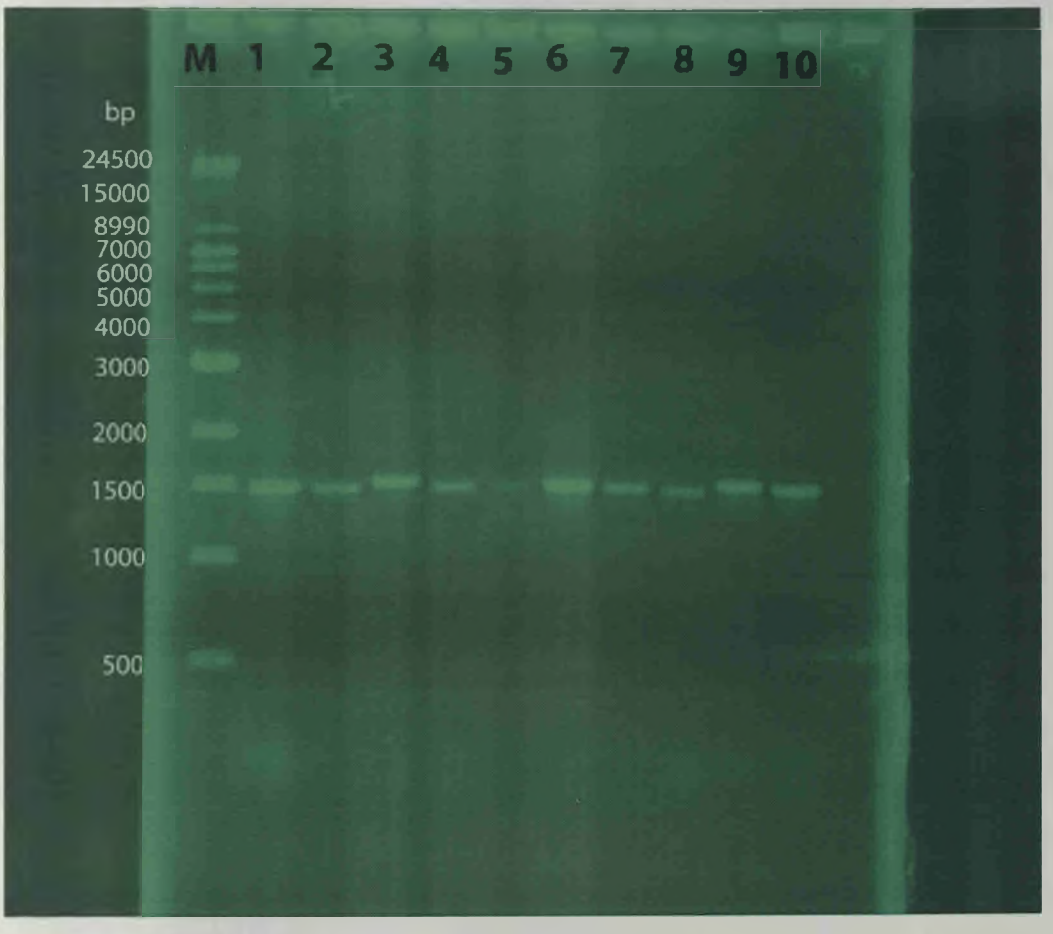

Plate 3.1. PCR amplification of 16S rDNA shows bands corresponding to different bacterial isolates named 1-10. Lane M= marker DNA.

sample volume of 10 µl for individual wells were prepared by mixing 8 µl of the template with 2 µl of the gel loading dye (Genie) in a piece of parafilm. For marker, 2 µl of the DNA ladder (supermix DNA ladder, Genie) was diluted with 6 µl of TE buffer (pH 8.0) and 2 µl of the gel loading dye. Using the micropipette, samples were carefully transferred into each well with interchange of tips in between samples to avoid cross contamination. After loading the samples, the electrodes were connected to the positive and negative terminal of the power pack unit with red terminal acting as cathode and black terminal as anode. The power was regulated at 230V AC supply with an output of 80V DC supply. The power was turned off as and when the bromophenol blue front reached three forth of the total gel length. The tray holding the gel was removed and stained with 10 µg ml^{-1} concentration of ethidium bromide for 15 min in the dark. The DNA bands were visualized under UV and the images were captured using the gel documentation and analysis system (Ingenius, USA).

3.3.6.4. Sequencing and phylogenetic analysis

The amplified PCR products were purified prior to sequencing as per the manufacturers guidelines using the QIAquick PCR Purification Kit (Qiagen, Germany). The purified PCR product was sequenced using the ABI 3130 genetic analyser (Chromous biotech PVT. Ltd., India). The 16S rRNA gene sequence of the strains was used as a query to search for homologous sequences in the EzTaxon-e database (EzBioCloud). The sequences were downloaded and aligned with 16S rRNA gene sequences of all the related species with validly published names using the CLUSTAL X software (Thompson *et al.,* 1997). Then the alignment was edited manually. Gaps at the 5′ and 3′ ends of the alignment were omitted from further analysis. The 16S rRNA gene sequence similarities were calculated from the alignment. Evolutionary distance matrices were calculated by using the algorithm of Jukes and Cantor (1969) with the DNADIST program. A phylogenetic tree was constructed using the neighbour-joining method (Saitou and Nei, 1987) available within the MEGA 4.1 software package (Kumar *et al.,* 2004). Bootstrap analysis was performed to assess the confidence limits of the branching. The partial 16S rRNA gene sequences have been deposited in the European Molecular Biology Laboratory (EMBL) data library under accession numbers given in Table 3.2.

Table 3.2. Homology comparisons of 16S rDNA sequences of culturable bacteria from Afansaiy-Nikitin Seamount of the Indian Ocean region.

Strain	Accession number	Closest match	Accession number	% similarity	% Complete -ness	Phylum
ANS-01Co	HG008709	*Salinicola zeshunii*	EU056581	99.57	95.4	γ- Proteobacteria
ANS-04Ni	HG008711	*Halomonas cupida*	L42615	98.07	70.3	γ- Proteobacteria
ANS-05Co	HG008712	*Halomonas cupida*	L42615	99.50	70.7	γ- Proteobacteria
ANS-08Co	HG008713	*Brevibacterium epidermidis*	X76565	98.61	94.5	Actinobacteria
ANS-09Ni	HG008714	*Salinicola halophilus*	AJ427626	98.66	70.9	γ- Proteobacteria
ANS-10Mn	HG008715	*Paracoccus saliphilus*	DQ923133	97.08	70.2	α- Proteobacteria
ANS-16Co	HG008718	*Bacillus subtilis subsp. inaquosorum*	EU138467	99.68	71.2	Firmicutes
ANS-17Co	HG008719	*Bacillus subtilis subsp. inaquosorum*	EU138467	99.78	71.3	Firmicutes
ANS-18NA	HG008720	*Brachybacterium paraconglomeratum*	AJ415377	99.49	94.6	Actinobacteria
ANS-21NA	HG008722	*Bacillus subtilis subsp. inaquosorum*	EU138467	99.89	70.8	Firmicutes
ANS-22Co	HG008723	*Bacillus subtilis subsp. inaquosorum*	EU138467	99.79	71.6	Firmicutes
ANS-24Co	HG008724	*Oceanobacillus iheyensis*	BA000028	99.37	95.5	Firmicutes
ANS-27Ni	HG008725	*Brevibacterium epidermidis*	X76565	96.59	70.2	Actinobacteria
ANS-28Ni	HG008726	*Corynebacterium variabile*	AJ222815	98.31	70.3	Actinobacteria
ANS-32Mn	HG008727	*Oceanobacillus kimchii*	GU784860	99.79	95.5	Firmicutes
ANS-34Co	HG008728	*Pseudomonas xanthomarina*	AB176954	98.99	94.8	γ- Proteobacteria
ANS-35Ni	HG008729	*Halomonas cupida*	L42615	99.49	95.8	γ- Proteobacteria
ANS-36Co	HG008730	*Paracoccus alcaliphilus*	D32238	99.70	95.5	α- Proteobacteria
ANS-37Co	HG008731	*Paracoccus marcusii*	Y12703	99.62	94.2	α- Proteobacteria
ANS-41Co	HG008732	*Pseudonocardia nantongensis*	JQ819252	98.26	95.4	Actinobacteria
ANS-51Co	HG008737	*Brachybacterium paraconglomeratum*	AJ415377	99.85	95.6	Actinobacteria
ANS-52Co	HG008738	*Salinicola halophilus*	AJ427626	98.64	95.7	γ- Proteobacteria

3.3.7. Bacterial growth in minimal media

3.3.7.1. Isolation of metal binding proteins

For the isolation of metal binding proteins, Tris mineral media of the following composition [6.06 g of Tris, 4.68 g of NaCl, 1.49 g of KCl, 1.07 g of NH_4Cl, 0.43 g of Na_2SO_4, 0.2 g of $MgCl_2.6H_2O$, 0.03 g of $CaCl_2.2H_2O$, 0.23 g of $Na_2HPO_4.12H_2O$, 0.005 g of Fe(III)(NH_4) and 1 ml of trace element solution (SL 7)] per liter of sea water was used (Mergeay *et al.*, 1985). Individual bacterial isolates in their pure form were inoculated in the above medium with 0.2% gluconate, 0.2% acetate or 0.2% succinate as the carbon source amended with and without the metals. Mn was used at 100 μM

final concentrations with selected isolates of metal tolerant bacteria and Co, Ni, Mn and Fe in combination at a final concentration of 100 μM in their chloride form. The media with cultures were incubated at 28±2°C for 24 to 48 h. The bacterial cells in the near exponential phase of growth (OD_{600}) were harvested by centrifugation at 5009 × g for 10 min at 4°C, washed with physiological saline (0.85%) and was suspended in 0.5 ml of buffer containing 0.5 M sucrose, 4 mM Na_2EDTA and 40 mM Tris-HCl, pH 8.0. Lysis of the bacterial cells was initiated by the addition of lysozyme at a final concentration of 10 mg ml^{-1}. After a two minute wait, 10 mM final concentration of $MgCl_2$ was added to the above mixture and was incubated at 30°C for 30 min. The supernatant containing periplasmic protein was separated by centrifugation at 11269 × g for 15 min at 4°C and was stored at -20°C. The retained cell pellet was suspended in 500 μl of TE buffer (10 mM Tris-HCl and 2 mM Na_2EDTA, pH 8). Incubation was continued for 15 min at 20°C. $MgCl_2$ was added at a 4 mM final concentration. After about 5-10 mins wait, the supernatant containing cytoplasmic protein was harvested by centrifugation as above and was stored immediately at -20°C. To the remaining pellet of lysed membranes, 200 μl of 10 mM Tris-HCl (pH 8) was added and was stored directly at -20°C until use (Wood, 1978). The concentration of protein in different cell fractions was quantified using a Quant-iT™ quantitation assay kit for proteins in a Qubit Fluorometer (Invitrogen, USA).

3.3.7.2. Polyacrylamide gel electrophoresis

The electrophoretic separation of proteins by SDS PAGE was carried out according to Laemmli (1970). Mini gels of 10 cm were prepared with a total length of 15 cm and an inner diameter of 6 mm. The preparation of gel involved several steps. First, the regular and notched glass plates were washed grease free and dried completely before use. Second, the glass plates were coupled by applying vaccum grease separated by the spacers. Third, the fixed glass plates were attached to the gel caster. And fourth, the set up was assured leak free by adding ~1 ml of sterile water. Gels containing 3% stacking gel and 10% separating gel were prepared from a stock solution of 30% by weight of acrylamide and 0.8% by weight of N,N'-bis-methylene acrylamide. The final concentration of Tris-HCl (pH 8.8) and SDS in the separating gel were fixed at 0.375 M and 0.1% respectively. The gels were polymerized chemically by the addition of 0.025% by volume of tetramethylethylenediamine (TEMED) and

ammonium persulphate. Immediately, ~2 ml of water-saturated butanol was layered on top of the gel to obtain a uniform surface. The setup was left undisturbed for 15 min for polymerization. This was followed by butanol layer removal from the gel surface and was then rinsed with sterile Milli-Q water to remove the traces of butanol. The stacking gels composed of 3% acrylamide contained 0.125 M Tris-HCl (pH 6.8) and 0.1% SDS. The comb was carefully inserted taking care not to trap any air bubbles. The gel was allowed to polymerize for 30 min and the comb was gently removed without disturbing the set up. The wells were rinsed gently through the sides with sterile Milli-Q water and excess moisture was wiped out. Each sample (15 µl) was mixed with 5 µl of sample buffer containing 0.0625 M Tris-HCl (pH 6.8), 2% SDS, 10% glycerol, 5% 2-mercaptoethanol and 0.001% bromophenol blue. The proteins were completely dissociated by immersing the samples for 1.5 min in boiling water. The gel casts were fixed tightly to the electrophoresis apparatus (Hoefer Pvt Ltd). The electrode buffer (pH 8.3) containing 0.025 M Tris, 0.192 M glycine and 0.1% SDS was prepared. The upper and lower chambers were filled with the buffer. Samples of 15 µl were loaded in each well. Mixture of individually colour coded Amersham full-range rainbow molecular weight marker proteins (GE Healthcare) of defined size (12 to 225 KDa) was used as a reference. Electrophoresis was carried out with an output of 80V DC supply until the bromophenol blue marker reached the bottom of the gel.

3.3.7.3. Silver nitrate staining

The silver nitrate staining of the proteins in gel was performed using the PlusOne Silver Staining Kit for proteins as per the protocol and procedure described therein (GE Healthcare). After electrophoresis the gel was transferred to the fixing solution (Appendix I) and was placed on the rocker for 30 min. The gel was then soaked in the sensitizing solution and left in the rocker for half an hour. The gel was washed with distilled water twice to remove excess of ethanol. Subsequently, the gel was transferred to a tray containing silver nitrate solution. The gel was incubated for 20 min and was washed with distilled water to remove the excess of silver ions. Soon after, the gel was soaked in developing solution for 2 to 5 mins. As and when the bands appeared, the developing solution was decanted and the reaction was stopped by soaking the gel in stop solution for 5 min. The gels were visualized under white light

and the images were captured using the gel documentation and analysis system (Ingenius, USA) (Plate 3.2).

3.3.7.4. Detection of metal binding proteins

The periplasmic, cytoplasmic and membrane fractions obtained were analyzed for metal binding proteins on a microgram scale using the high throughput microtitre plate assay described by Hogbom *et al.* (2005). The procedure involved the addition of 4 µl of 8.0 M urea solution and 2 µl of protein sample in each well. This was followed by addition of 10 µl of Luminal and 1 µl of 4-(2) pyridylazo resorcinol to the above mixture and were incubated at 28±2°C for 2 h. Positive controls included wells with added Mn^{2+} instead of the protein samples. Results were scored positive based on colour change of the wells from yellow to pink (Plate 3.2).

3.3.8. Transmission electron microscopy

Bacterial isolates ANS-05Co, ANS-28Ni and CR48 that were tolerant to Co, Ni and Mn were grown in 500 ml of 20% nutrient broth (2.6 g l^{-1}) amended with 100 µM concentrations of the respective metal salts individually at 25±2°C. Soon after growth, the bacterial biomass was harvested by centrifugation and subsequently washed with 0.85% saline to remove the cell debris and sea salts. This was followed by repeated washing with 10 mM HEPES buffer (pH 8.0) and then fixed with 2.5% final concentration of glutaraldehyde in 1 ml of 10 mM HEPES buffer. Samples were then dehydrated in increasing concentrations of acetone, embedded in Epon-Araldite resin, ultramicrotomed into 70-100 nm sections and mounted on formvar-coated copper grids (Hayat, 1972). Analysis was carried out on a FEI Morgagni 268D TEM at an accelerating voltage of 100 kv. EDX analysis on selected cell sectors and on metal precipitates was performed at an accelerating voltage of 15 keV.

3.4. Results

3.4.1. Total bacterial abundance and culturability of bacteria

The total abundance of bacteria averaged 1.01×10^{9} cells g^{-1} in the ANS crusts, 1.31×10^{8} cells g^{-1} in CR, 3.05×10^{8} cells g^{-1} in CIOB nodule and 1.20×10^{9} cells g^{-1} in CIOB sediments (Table 3.3).

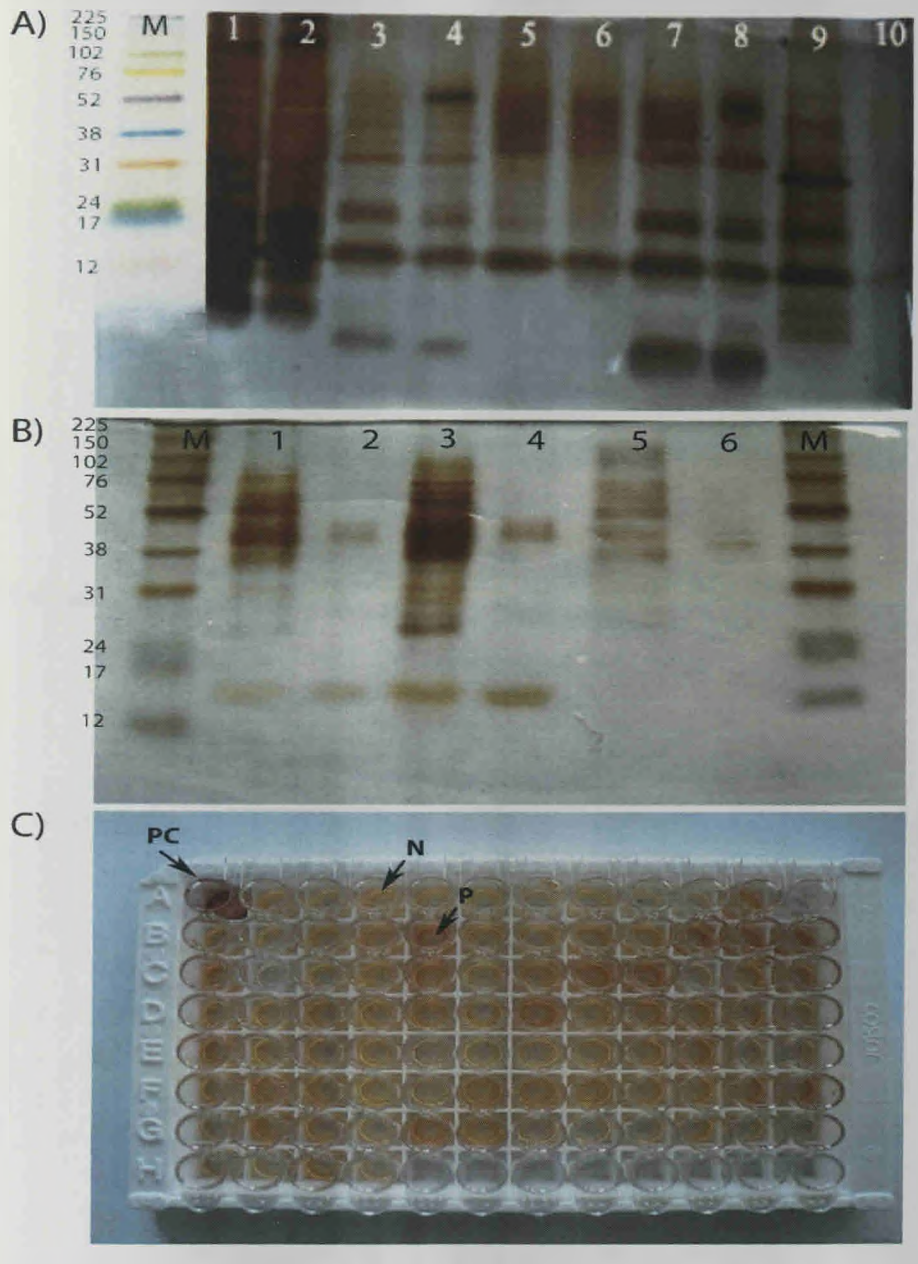

Plate 3.2.

A) metal binding proteins upregulated/downregulated in the presence of a single metal (Mn). Lanes 1,3,5,7 and 9 refers to controls without added metal and lanes 2,4, 6, 8 and 10 refers to experiment with 100µM of metal added. Lane M= marker weight in KDa.

B) metal binding protein expression suggesting "tradeoff" in the presence of multiple metals (Fe, Mn, Co and Ni). Lanes 1, 3 and 5 refers to controls without added metal and lanes 2, 4 and 6 refers to experiment with 25µM of each metal added.

C) highthroughput microtitre plate assay shows protein fractions positive for Mn (P), negative for Mn (N) and positive control with added Mn (PC) .

Table 3.3. Abundance and distribution of bacteria associated with crusts and nodules of the Indian Ocean region.

Area	Sample code	Colony forming units (CFU g^{-1})				Total counts (cells g^{-1})
		Heterotrophs	NTB	CTB	MTB	
ANS	ABP37/DRG04	$5.86\pm0.6\times10^{4}$	$1.20\pm0.4\times10^{4}$	$7.49\pm0.8\times10^{3}$	$2.18\pm0.6\times10^{5}$	$2.5\pm0.6\times10^{8}$
	ABP37/DRG07	$5.12\pm0.2\times10^{4}$	$1.62\pm0.1\times10^{3}$	$1.98\pm0.1\times10^{4}$	$1.96\pm0.2\times10^{3}$	$1.5\pm0.3\times10^{8}$
	ABP37/DRG10	$1.71\pm0.1\times10^{5}$	$3.08\pm0.1\times10^{3}$	$9.50\pm0.2\times10^{3}$	$1.10\pm0.7\times10^{5}$	$6.0\pm0.3\times10^{8}$
	ABP37/DRG10A	$5.72\pm0.1\times10^{5}$	$1.03\pm0.3\times10^{4}$	$1.86\pm0.2\times10^{4}$	$3.90\pm0.7\times10^{4}$	$4.1\pm0.4\times10^{7}$
	ABP37/DRG11A	$1.92\pm0.3\times10^{5}$	$1.70\pm0.2\times10^{4}$	$7.03\pm0.2\times10^{2}$	$4.30\pm0.5\times10^{4}$	$3.8\pm0.2\times10^{9}$
	ABP37/DRG14	$3.13\pm0.2\times10^{4}$	$4.10\pm0.1\times10^{4}$	$3.69\pm0.3\times10^{3}$	$2.14\pm0.3\times10^{5}$	$3.9\pm0.5\times10^{8}$
	CC2/ADR04	$6.13\pm0.7\times10^{5}$	$1.77\pm0.5\times10^{5}$	$1.90\pm0.4\times10^{5}$	$7.30\pm0.2\times10^{4}$	$3.9\pm0.6\times10^{9}$
	CC2/ADR11	$6.70\pm0.5\times10^{5}$	$6.60\pm0.4\times10^{3}$	$1.49\pm0.5\times10^{4}$	$1.30\pm0.4\times10^{5}$	$1.8\pm0.6\times10^{7}$
	CC2/ADR12	$9.41\pm0.2\times10^{4}$	$1.55\pm0.5\times10^{4}$	$6.47\pm0.2\times10^{3}$	$1.74\pm0.3\times10^{5}$	$4.3\pm0.3\times10^{8}$
	CC2/ADR18	$6.55\pm0.2\times10^{5}$	$1.20\pm0.3\times10^{4}$	$2.75\pm0.1\times10^{4}$	$1.64\pm0.4\times10^{5}$	$3.3\pm0.4\times10^{7}$
	CC2/ADR24	$7.30\pm0.1\times10^{5}$	$1.61\pm0.3\times10^{4}$	$2.70\pm0.1\times10^{4}$	$1.54\pm0.2\times10^{5}$	$2.4\pm0.5\times10^{9}$
	CC2/ADR27	$3.49\pm0.2\times10^{5}$	$1.80\pm0.4\times10^{5}$	$3.90\pm0.1\times10^{3}$	BDL	$1.3\pm0.4\times10^{8}$
CR	ABP36/DRG22	$2.89\pm0.5\times10^{2}$	$2.03\pm0.1\times10^{2}$	BDL	$3.73\pm0.3\times10^{4}$	$2.4\pm0.3\times10^{8}$
	ABP36/DRG23	$6.92\pm0.3\times10^{3}$	$8.00\pm0.5\times10^{3}$	$3.33\pm0.1\times10^{2}$	$2.33\pm0.4\times10^{2}$	$2.1\pm0.5\times10^{7}$
CIOB	ABP26/Nod1	$3.41\pm0.5\times10^{2}$	$1.46\pm0.3\times10^{2}$	$1.50\pm0.2\times10^{1}$	$6.50\pm0.4\times10^{1}$	$3.6\pm0.1\times10^{8}$
	ABP26/Nod2	$2.32\pm0.2\times10^{4}$	$6.80\pm0.1\times10^{2}$	$6.51\pm0.2\times10^{2}$	$2.11\pm0.2\times10^{2}$	$2.5\pm0.3\times10^{8}$

Note- NTB: nickel tolerant bacteria, CTB: cobalt tolerant bacteria and MTB: manganese tolerant bacteria,

BDL: below detection level.

The distribution of culturable bacteria indicated that the specific niche dictated the dominance of bacteria tolerant to the metals. The heterotrophic and Co tolerant bacteria recorded their maximum abundance in the cobalt rich-Fe-Mn crusts of the ANS (Table 3.3). The counts of heterotrophic bacteria varied from $9.41 \times 10^4 - 7.30 \times 10^5$ CFU g^{-1} in the crusts of the ANS and from below detectable level (BDL) -2.4×10^5 CFU g^{-1} in sediments of the CIOB. On the other hand, Co tolerant bacteria registered $7.03 \times 10^2 - 1.90 \times 10^5$ CFU g^{-1} in the Fe-Mn crust of the ANS and varied from BDL – 2.8×10^5 CFU g^{-1} in CIOB sediments. The culturable abundance of Ni tolerant bacteria was more in the CIOB sediments varying from BDL – 2.4×10^5 CFU g^{-1}. However, the culturability of Mn oxidizing bacteria was more in CIOB sediments followed by crusts of the ANS. Their numbers ranged from BDL to 3.9×10^5 CFU g^{-1} in CIOB sediments and from BDL to 2.18×10^5 CFU g^{-1} in the ANS (Table 3.4). Correlation analysis to test the strength of association between variables showed positive relationship between Co tolerant and Ni tolerant bacteria at an r-value of 0.599 ($p < 0.05$) in the ANS crusts (Table 3AT1, Appendix III). Also, the total abundance of bacteria correlated positively with the cultured fraction of Co tolerant bacteria at an r-value of 0.584 ($p < 0.05$) in the ANS.

Table 3.4. Plate counts of Ni, Co and Mn tolerant bacteria in box core BC26 and BC36 from the Central Indian Ocean Basin. The media contained 100 μM concentrations of the respective metals and 1.5 % bacteriological agar in seawater. The data represent mean colony forming units (CFU) of bacteria per gram of sediment (±SD, n=3).

Depth	BC26			BC36		
(cm)	Ni	Co	Mn	Ni	Co	Mn
2	BDL*	$4.3\pm0.3\times10^4$	$2.5\pm0.2\times10^4$	$1.6\pm0.1\times10^5$	$2.6\pm0.2\times10^5$	$1.8\pm0.1\times10^5$
4	BDL	$2.7\pm0.1\times10^4$	$1.5\pm0.2\times10^4$	$2.4\pm0.3\times10^5$	$1.7\pm0.1\times10^5$	$3.9\pm0.1\times10^5$
6	BDL	$1.5\pm0.1\times10^3$	$6.0\pm0.1\times10^2$	$9.1\pm0.4\times10^4$	$1.3\pm0.3\times10^5$	$3.3\pm0.2\times10^5$
8	BDL	$1.7\pm0.3\times10^4$	$4.1\pm0.6\times10^4$	$2.1\pm0.1\times10^5$	$1.5\pm0.2\times10^5$	$2.4\pm0.1\times10^5$
10	$9.0\pm0.1\times10^2$	$6.6\pm0.6\times10^3$	$3.8\pm0.7\times10^4$	$1.6\pm0.1\times10^5$	$2.8\pm0.1\times10^5$	$1.3\pm0.1\times10^5$
15	BDL	$1.7\pm0.1\times10^4$	$3.9\pm0.2\times10^4$	$3.9\pm0.1\times10^4$	$1.4\pm0.1\times10^5$	$1.2\pm0.2\times10^5$
20	BDL	$1.2\pm0.2\times10^4$	$4.3\pm0.4\times10^4$	$5.1\pm0.3\times10^4$	$6.6\pm0.1\times10^4$	$1.7\pm0.1\times10^5$
25	BDL	BDL	BDL	$4.2\pm0.2\times10^4$	$2.0\pm0.1\times10^4$	$1.7\pm 0.1\times10^5$
30	BDL	BDL	BDL	$9.9\pm0.1\times10^4$	$1.0\pm0.1\times10^5$	$2.2\pm0.1\times10^5$
35	BDL	BDL	BDL	$9.5\pm0.2\times10^4$	$4.8\pm0.2\times10^4$	$2.4\pm0.2\times10^5$

*BDL: below detection level

3.4.2. Antibiotic susceptibility testing

Antibiotic susceptibility of 28 metal tolerant bacterial isolates showed no growth with some isolates and total resistance with others for some of the antibiotics tested. Resistance was detected for 6 of the 19 different antibiotics tested in 2 of the test strains namely ANS-04Ni and ANS-05Co and 5 of the antibiotics in other 5 test strains (Figure 3.1). Of the different antibiotics tested, higher resistance was observed against ampicillin (35.71%), lincomycin (32.14%), penicillin G (32.14%) and vancomycin (32.14%) followed by cefalexin (28.57%), gentamycin (17.85%) and co-trimoxazole (17.85%). Isolates were sensitive to amikacin, aztreonam, ciprofloxacin, chloramphenicol, ceftazidime, imipenam, piperacillin and tetracycline (Table 3.1). But, none of the antibiotics tested were able to inhibit growth of all the isolates in any of the phylogenetic groups.

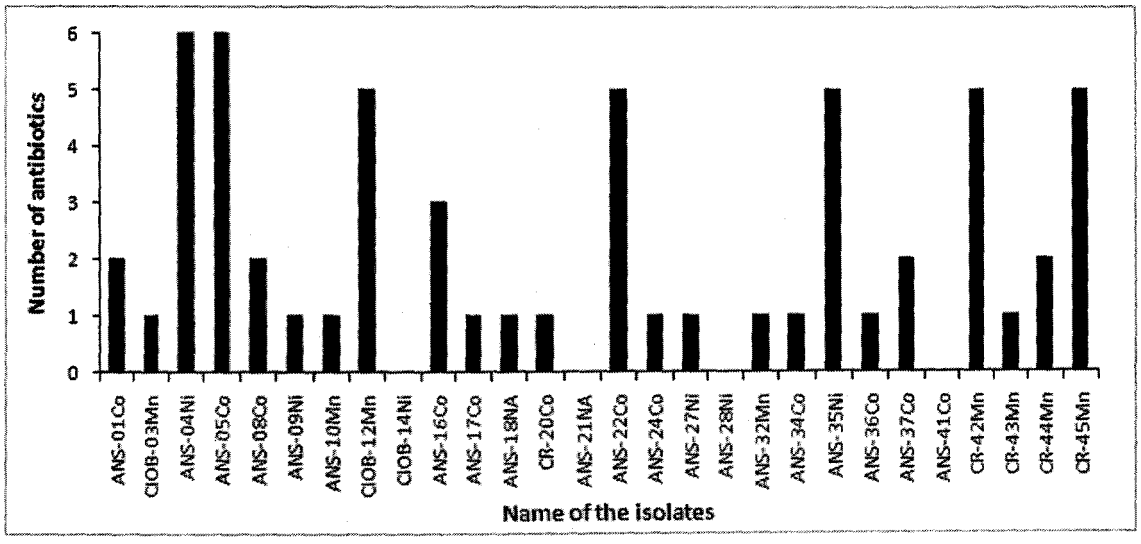

Figure 3.1. Multiple antibiotic resistance patterns of the marine bacterial isolates resistant to heavy metals.

3.4.3. Phenotypic characterization

The characterization of 30 bacterial isolates showed 53.33% of them as gram-positive and 46.67% of them as gram-negative. Wet mount observation showed 76.67% of the isolates to be motile and 23.33% as non-motile. Tests for enzyme activity showed 93.33% of the isolates to be positive for catalase, 46.67% for oxidase, 50% for amylase, 16.67% for caseinase, 40% for cellulase, 50% for DNAse, 36.67% for urease, 50% for phosphatase and 56.67% for lipase. Tests for oxidative fermentative reaction

of glucose showed 20% of the isolates as fermentative, 60% as oxidative and 20% as non-reactive. Among the isolates ANS-17Co was positive for 7/9 different enzymes and the isolates ANS-21NA, ANS-10Mn, and CR-45Mn were positive for 6/9 enzymes that were screened (Table 3.5).

3.4.4. Genotypic characterization

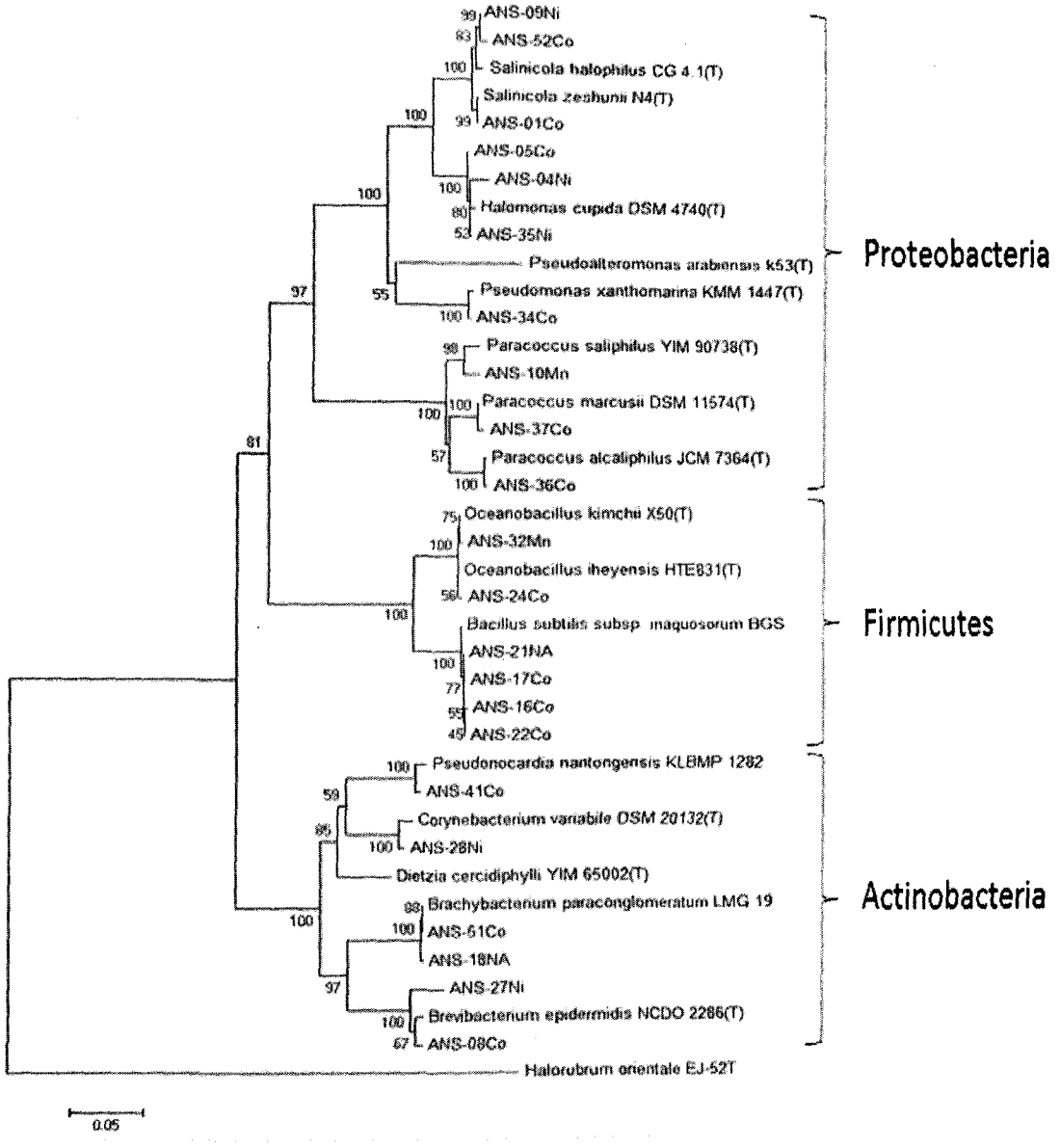

Figure 3.2. Neighbor-Joining phylogenetic tree of bacterial isolates tolerant to heavy metals constructed using MEGA4. The bootstrap values were calculated as percentage of 1000 replicate. The evolutionary distances were computed using the maximum composite likelihood method and are in the units of the number of base substitutions per site.

Table 3.5. Characterization and possible identification of bacterial isolates tolerant to heavy metals

Isolate	Gram ±	Motility	OF test	Catalase	Oxidase	Amylase	Caseinase	Cellulase	DNAse	Urease	Phosphatase	Lipase	Morphology
ANS-01Co	−	+	O	+	−	−	−	−	−	+	+	−	Rod
CIOB-03Mn	+	+	O	+	+	−	−	−	+	+	+	−	Rod
ANS-04Ni	−	+	O	+	−	−	−	−	−	+	+	−	Rod
ANS-05Co	−	−	O	+	−	+	−	−	−	+	+	+	Rod
ANS-08Co	+	+	NR	+	+	−	−	−	+	+	−	+	Rod
ANS-09Ni	−	−	O	+	+	−	−	−	−	+	+	+	Rod
ANS-10Mn	−	−	NR	+	+	+	−	−	+	−	+	+	Coccobacili
CIOB-12Mn	−	+	NR	+	+	−	−	−	+	−	+	−	Coccobacilli
CIOB-14Ni	+	+	NR	+	−	−	−	−	−	+	+	−	Cocci
ANS-16Co	+	+	F	+	−	+	−	+	+	−	−	+	Rod
ANS-17Co	+	+	F	+	+	+	+	+	+	−	−	+	Rod
ANS-18NA	+	−	O	+	−	+	−	+	+	−	+	−	Cocci
CR-20Co	+	+	F	+	−	+	+	+	+	−	−	−	Rod
ANS-21NA	+	+	F	+	+	+	+	+	−	−	−	+	Rod
ANS-22Co	+	+	F	+	−	+	−	+	−	−	−	+	Rod
ANS-24Co	+	+	O	+	−	−	−	−	−	−	+	−	Rod
ANS-27Ni	+	+	O	+	−	−	−	−	−	+	−	+	Rod
ANS-28Ni	+	−	O	+	−	+	−	+	+	−	−	+	Rod
ANS-32Mn	+	+	O	+	+	−	−	−	−	−	−	+	Rod
ANS-34Co	−	+	O	+	+	−	−	+	+	−	−	+	Rod
ANS-35Ni	−	+	O	+	−	−	−	−	+	+	+	+	Rod
ANS-36Co	−	+	NR	+	+	−	−	−	−	−	−	−	Coccobacilli
ANS-37Co	−	+	O	+	−	+	−	+	−	−	−	−	Coccobacilli
ANS-41Co	+	+	NR	−	−	−	+	−	−	−	−	+	Rod
CR42-Mn	−	+	O	+	−	+	−	−	+	+	+	−	Rod
CR43-Mn	−	+	O	+	+	+	−	+	+	−	−	−	Rod
CR44-Mn	−	+	O	−	+	+	−	−	+	−	+	+	Rod
CR45-Mn	+	+	F	+	+	+	+	+	−	−	−	+	Rod
ANS-51Co	+	−	O	+	−	+	−	+	+	−	+	−	Cocci
ANS-52Co	−	−	O	+	+	−	−	−	−	+	+	+	Rod

Note- O: oxidative, F: fermentative, NR: no reaction

Phylogenetic analysis of 22 bacterial isolates of the ANS revealed that the isolates fell into three major phyla: *Proteobacteria* (45.46%), *Firmicutes* (27.27%) and *Actinobacteria* (27.27%). Phylum *Proteobacteria* was represented by γ- and α-*Proteobacteria* constituting 70% and 30% of the 45.46% abundance of the former respectively. Of the total culturable fraction, the dominant genera were represented by the *Bacillus* (22.73%), *Halomonas* (13.64%), *Paracoccus* (13.64%) and *Salinicola* (13.64%) (Figure 3.2). The other genera represented by *Brevibacterium, Brachybacterium*, *Corynebacterium*, *Oceanobacillus*, *Pseudonocardia* and *Pseudomonas* constituted 36.35% of the total culturable fraction. Dominant genus among the phylum *Firmicutes* was represented by *Bacillus*, phylum *Actinobacteria* by *Brevibacterium* and *Brachybacterium* and phylum *Proteobacteria* by *Halomonas*, *Salinicola* and *Paracoccus*. The accession numbers of the test strains and the % similarity with that of the type strains is listed in Table 3.2.

3.4.5. Metal binding proteins

The quantification of proteins from different cellular fractions of 30 bacterial isolates grown in the absence of the metals showed the concentration of periplasmic proteins to vary from 1.63 to 14.6 μg ml^{-1} (average: 7.95 μg ml^{-1}), cytoplasmic proteins from 1.78 to 18.3 μg ml^{-1} (average: 7.10 μg ml^{-1}) and membrane proteins from 10.4 to 15.3 μg ml^{-1} (average: 12.76). In the presence of 100 μM metal the cells varied in periplasmic protein concentration from 4.91 to 26 μg ml^{-1} (average: 14.48), cytoplasmic from 1.52 to 12.7 μg ml^{-1} (average: 6.04) and membranes from 6.16 to 15.1 μg ml^{-1} (average: 12.32) (Table 3.6). The concentration of the protein in the experiment relative to controls showed downregulation of periplasmic proteins in 16.7% of the isolates, cytoplasmic proteins in 66.7% of the isolates and membrane proteins in 50% of the isolates. Further, upregulation of the proteins was observed in 83.3%, 33.3% and 40% of the isolates for periplasmic, cytoplasmic and membrane fractions respectively. But, membrane proteins in 10% of the isolates showed no change in concentration after incubation. Examination of different cellular fractions also indicated that in 30% of the isolates the metal binding proteins are localized in the periplasmic fraction, 16.7% in the membrane fraction, 26.7% in the periplasmic-cytoplasmic fraction, 20% in the periplasmic- membrane fraction, 3.3% in the periplasmic-cytoplasmic-membrane fraction and absence in 3.3% of any of the cellular fractions. In the presence of multiple

metals "tradeoff" character was observed with selected isolates of bacteria. SDS-PAGE analysis of the proteins showed the molecular weight of the metal binding proteins to vary from 31 to 52KDa (Plate 3.3). Confirmation of metal ions in the protein fractions indicated the presence of Mn in protein fractions as indicated by the change in colour of the wells from yellow to pink (Plate 3.3).

Table 3.6. Protein concentrations in different cellular fractions of the bacterial cells exposed and unexposed to heavy metals.

Isolate	Periplasmic (μg ml^{-1})		Cytoplasmic (μg ml^{-1})		Membrane (μg ml^{-1})	
	Control	Experiment	Control	Experiment	Control	Experiment
ANS-01Co	2.00	13.4*	12.7	7.20#	13.3	14.7
CIOB-03Mn	1.69	9.53	11.9	7.15	14.3	12.2
ANS-04Ni	1.94	13.6	11.7	6.62	13.9	13.2
ANS-05Co	1.83	11.7	11.7	7.10	12.6	12.6
ANS-08Co	1.77	11.5	11.4	6.97	11.2	13.4
ANS-09Ni	1.87	20.4	18.3	12.7	15.3	15.1
ANS-10Mn	12.7	14.4	7.86	7.50	13.1	11.2
CIOB-12Mn	1.63	8.12	5.09	4.11	11.3	14.2
CIOB-14Ni	9.09	5.50	3.01	2.39	12.9	12.9
ANS-16Co	7.07	6.72	3.74	2.12	11.6	13.0
ANS-17Co	12.6	7.54	2.97	2.10	12.4	14.1
ANS-18NA	13.1	4.91	8.25	5.28	11.9	12.7
CR-20Co	8.38	9.37	3.30	3.31	13.8	13.3
ANS-21NA	12.0	21.2	3.08	1.58	10.4	14.6
ANS-22Co	8.22	21.7	4.40	1.52	13.7	11.5
ANS-24Co	10.7	11.2	7.86	7.50	11.1	11.1
ANS-27Ni	2.49	10.4	6.57	12.0	13.0	14.7
ANS-28Ni	9.53	10.7	8.63	9.66	12.6	11.2
ANS-32Mn	10.8	11.2	5.82	9.41	13.3	11.7
ANS-34Co	11.5	8.13	13.3	3.70	12.3	14.2
ANS-35Ni	14.6	15.6	9.85	8.51	12.1	14.8
ANS-36Co	9.87	10.8	11.8	8.86	13.5	14.1
ANS-37Co	13.5	21.9	10.1	7.50	13.3	10.6
ANS-41Co	6.61	20.6	3.78	2.79	13.2	11.3
CR-42Mn	13.8	26.0	1.99	5.89	14.4	9.65
CR-43Mn	9.74	24.6	1.78	5.04	14.8	7.88
CR-44Mn	1.67	12.0	3.56	6.59	11.4	14.0
CR-45Mn	13.4	23.9	1.95	6.20	11.1	6.16
ANS-51Co	5.05	23.5	4.72	5.60	11.8	8.29
ANS-52Co	9.30	24.3	2.03	4.22	13.3	11.2

Note the symbol * represents the upregulation and # represents the downregulation of proteins

3.4.6. Metal precipitation by the bacterial isolates

TEM observation of horizontal and vertical cross section of the bacterial cells grown with metal showed the accumulation of metal ions as electron dense precipitates in and around the bacterial cells. The EDX analysis confirmed the sequestration of Mn, Co and Ni by the bacterial cells (Figure 3.3). The analysis of control cells grown in the absence of the metal showed no relevant peaks for the respective metals. The interactions of bacteria with the metal differed from one isolate to the other and from metal to metal depending on the toxicity level and their metabolic requirement. Several strategies in bacteria were encountered to avoid the lethal effect of metal ions on the bacterial cells. Metal precipitation along the walls of the bacterial cell and in association with the exopolysaccharides was observed with isolate ANS-05Co (Figure 3.4). Ni got precipitated internally in the bacterial isolate ANS-028Ni and Co and Mn precipitated externally in isolates ANS-05Co and CR48 respectively. Also, altered cell morphology, intense accumulation of metal, loss in cell wall rigidity and extensive cell rupture leaving behind empty ghost cells was noticed in bacteria grown in higher concentrations of the metals with respect to that of the controls.

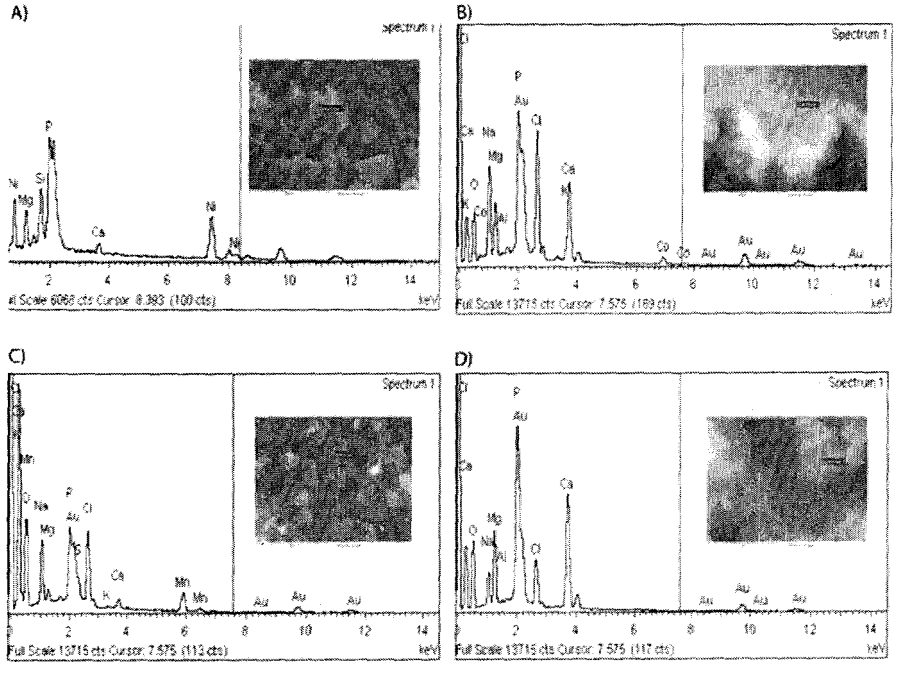

Figure 3.3. Energy dispersive x-ray analysis of bacterial cells grown with 100μM added metal A) Ni, B) Co, C) Mn and D) control without added metal.

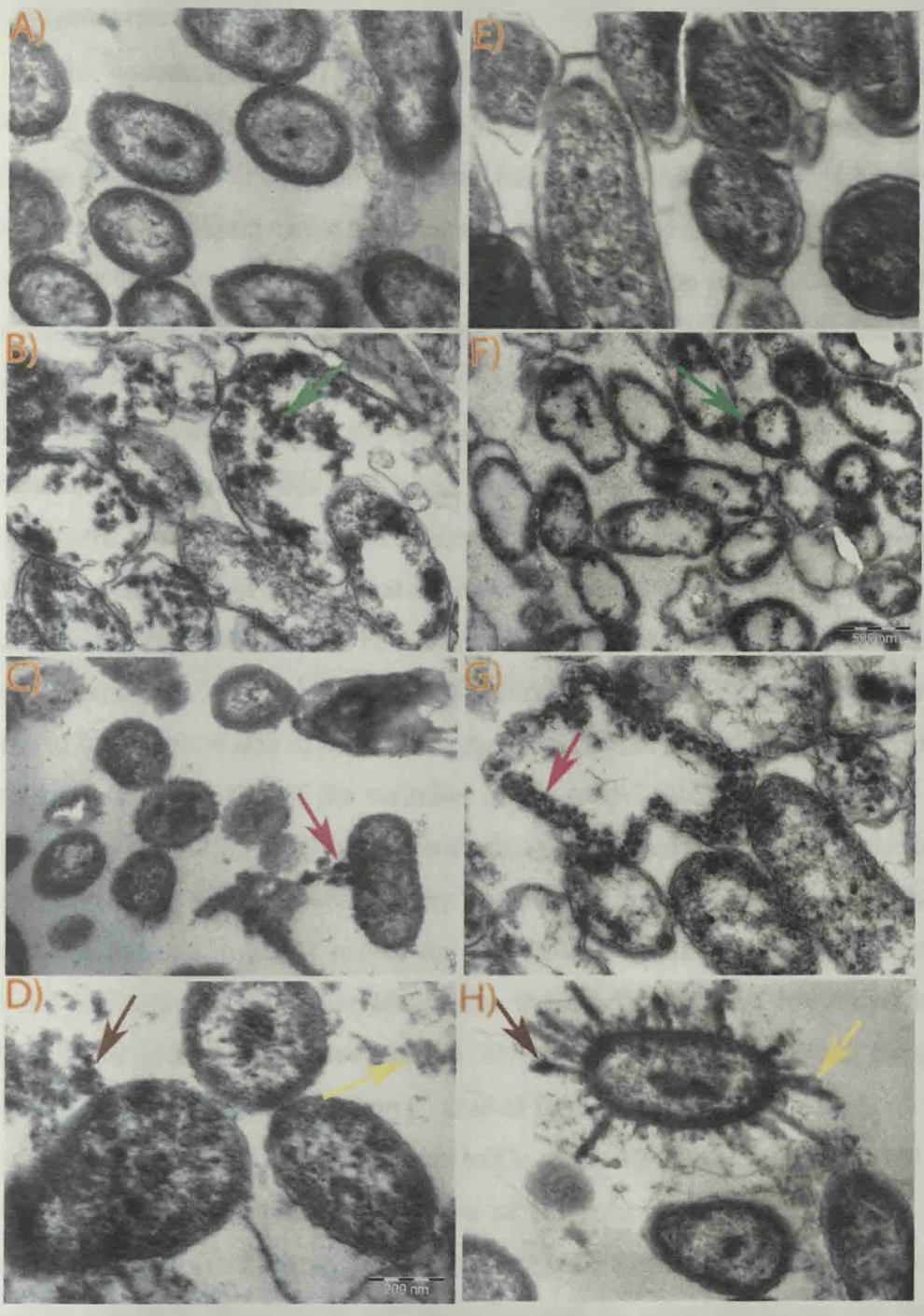

Figure 3.4. Cross sections of the bacterial cells show intracellular (B, F and G) and extracellular (C, D and H) accumulation of metals as electron dense precipitates. Images A and E refers to cross section of control cells without added metal. Arrows in pink denotes the precipitation of Co, green Ni, brown Mn and yellow the cell appendages and exopolysaccharide like materials.

3.5. Discussion

The understanding of the distribution, diversity and function of bacteria associated with the Fe-Mn crusts are important to understand their potential for the formation of metal rich mineral deposits. Besides, the interactions of bacteria with metals help in the upkeep of the environments health by reducing the aqueous solubility of metals by oxidation. The present study on the distribution of metal tolerant bacteria from Fe-Mn crusts, nodules and sediments of the Indian Ocean region showed niche specific adaptation. The distribution of Co tolerant bacteria was mostly associated with the hydrogenetic cobalt-rich Fe-Mn crusts. These bacteria could play a vital role in the enrichment of trace metals on basalt surfaces through metabolism-independent (biosorption) and/or metabolism dependent (bioaccumulation) processes. The retrievable abundance of Co tolerant bacteria in the present study fell within the order of culturability reported for the Fe-Mn crusts (Krishnan *et al.*, 2006). The culturable bacteria tolerant to Co correlated with the cultured fraction of Ni tolerant bacteria at an r-value of 0.599 ($p < 0.05$) in the ANS suggesting that the variation in the former could be responsible for 35.8% of the variation in the latter. This relation suggests that Ni immobilization could be catalyzed by bacteria tolerant to either of the metals Ni or Co. Such a relationship was also observed by Stoppel and Schlegel (1995) where they have shown that bacteria tolerant to Ni are also tolerant to Co in nickel-polluted and naturally nickel-percolated ecosystems. On the other hand, the total abundance of bacteria of the hydrogenetic crusts of the ANS positively correlated with the cultured fraction of Co tolerant bacteria at an r-value of 0.584 ($p < 0.05$). This suggests that the distribution of culturable bacteria tolerant to Co showed 34% variation with that of total bacteria. However, the retrievable counts of Mn tolerant bacteria and other general heterotrophs showed no significant correlation with that of total bacterial abundance indicating that their distribution may be influenced by other environmental variables. Similar relationship was also observed between the abundance of culturable and total bacteria for Shenzhen coastal waters (Li et al., 2011).

Since Fe-Mn minerals are enriched with multiple elements, the associated bacteria tolerant to one metal may also confer resistance to others. Such interactions are related to the maintenance of various biological functions in bacteria or may not be necessarily due to any metabolic necessity (Gomes *et al.*, 1998; Tebo *et al.*, 2005). In

the present study, the culturability of Ni tolerant bacteria showed higher abundance in the CIB sediments. This relates to the enrichment of higher concentration of Ni in the polymetallic nodules wherein bacterial precipitation of Ni from sediment porewater contributes to the immobilization of Ni on Fe-Mn oxide surfaces. The precipitation of Ni could have also been mediated by Mn oxidizing or other heterotrophic bacteria tolerant to Ni. This has been observed with two of the Mn(II)-oxidizing bacterial isolates belonging to the genus *Halomonas* isolated from the bottom waters of the Carlsberg Ridge. These isolates apart from oxidizing Mn, immobilized Co and Ni individually in the absence of Mn (Sujith *et al.,* 2010; Antony *et al.,* 2011).

On the other hand, the culturability of Mn oxidizing bacteria was higher in crust samples recovered from the CR compared to that of hydrogenetic crusts, Fe-Mn nodules and sediments. The current results agree with Sujith *et al.* (2014) on the order of culturability of Mn(II)-oxidizing bacteria from oxide bearing basalt surfaces of the CR and are lower than that reported for water samples from the same region (Fernandes *et al.,* 2005). The results suggest the differences in the distribution of Mn-oxidizing bacteria in the water column versus the rock surfaces that catalyze Mn(II)-oxidation where the complex conditions of the natural habitat for bacteria dwelling on the rock surfaces are difficult to reproduce (Amann *et al.,* 1995; Kaeberlein *et al.,* 2002). It thus permits bacteria attached to the basalt surfaces to compete effectively with the abiotic precipitation of the metals and become encrusted in Mn oxides. In addition, cross resistance to multiple antibiotics also occurs in heavy metal tolerant bacteria which may or may not be linked to any plasmid genes. In the present study, the culturable bacteria apart from exhibiting heavy metal tolerance showed resistance to several antibiotics in culture. The coating of bacteria in metal oxides and their resistance to antibiotics indicate the adaptive strategy of bacteria to protect from environmental stresses such as predation, viral attack or heavy metal toxicity (Tebo *et al.,* 2005; Spiro *et al.,* 2010).

Bacteria producing extracellular enzymes help in the degradation of refractory and structurally complex organic matter into sizes sufficiently small to be assimilated by bacteria and thus play an important role in nutrient cycling (Arnosti, 2011). The expression of multiple enzymes against different substrates by the bacterial isolates in

the present study suggests the relative processes like breakdown of starch, urea hydrolysis, phosphate solubilization, cellulose degradation, proteolysis, lipolysis and nuclease activity to occur at the crust and in the associated sediments. Among the different enzymes catalase and cytochrome oxidase activity was observed among 93.3 and 46.67% of the isolates retrieved from different geological niches of the Indian Ocean respectively. Since the ANS recline at water depth that provides oxidizing conditions suitable for Fe-Mn deposition the bacteria associated with the crusts could be adaptive to different oxygen levels because of the consumption of oxygen in Fe-Mn oxidation. The aerobic bacteria produce oxidase enzyme for the regeneration of NAD in respiration. Further, the NADH oxidases belonging to peroxiredoxin oxidoreductases involve in regeneration of NAD and in the scavenging of peroxides (Poole *et al.,* 2000). Thus, oxidases and its allied enzymes help anaerobes and facultative anaerobes to avoid oxygen related toxicity under aerobic conditions. On the other hand, the production of catalases help anaerobic bacteria in the detoxification of free radicals generated as byproducts of aerobic respiration.

Of the different enzymes 56.67% of the isolates were positive for lipases which aid in the transformation and modification of lipid compounds. Since deep-sea bacteria could derive nutritional benefit from the metabolism of lipid molecules (Boetius and Lochte, 2000) they get rapidly consumed during their sedimentation. As of that, bacteria in the deep-sea produce a suit of enzymes that helps in the scavenging and oxidation of lipid molecules which can be stored and then utilized under starvation. It thus reflects the high lipase activity to occur in sediments and on rock surfaces enriched with Fe-Mn minerals. Followed by lipase, 50% of the isolates expressed phosphatase, DNAse and amylase enzymes. Since, the remineralization of phosphorus could occur in tandem with the redox coupling of iron, precipitation or uptake of phosphorous by bacteria could occur. These results are consistent with the reports of Hirschler *et al.* (1990) and Benzerara *et al.* (2004) on the biologically induced and controlled process of phosphorous uptake and precipitation of iron oxyhydroxides. Further, DNAse activity also provides a source of phosphorous by degrading the extracellular DNA in the sediment (Divya *et al.,* 2010). Apart from phosphorous the DNA preserved in sediments could also act as a sink for carbon and nitrogen (Dell'Anno and Danovaro, 2003). Thus DNAse activity plays a crucial role in the cycling of phosphorous, carbon

and nitrogen which are considered to be very essential for bacterial growth. ANS being a potential site for Fe-Mn deposition also traps the fall of vertically migrating organisms and sinking particles from water column above due to their topographic feature. Hence, the production of enzymes like amylase and cellulase could aid bacteria dwelling on rock surfaces in metabolizing complex molecules that escaped the heterotrophic degradation processes. Such results have been encountered with culturable bacteria from the Arabian Sea sediments (Divya *et al.* (2010). The production of caseinase helps bacteria in the breakdown of proteins into immediate precursors essential for protein synthesis and other microbial cell metabolism.

Also bacteria express low molecular weight metal-binding proteins (metallothioneins) to control cellular metal ion homeostasis through chromosomal gene related mechanism of resistance (Kojima, 1991). The growth of bacteria on media containing Mn, Fe, Co and Ni resulted in the occurrence of fewer protein bands compared to that of controls lacking any metals, whereas the expression of proteins involved in the acquisition and oxidation of the metals were greatly induced suggesting a "tradeoff". The present results agree with De Souza *et al.* (2007) on multiple metal resistances of bacteria associated with fewer enzyme expressions. The second group of proteins comprised those upregulated by growth on Mn. Here the number of protein bands expressed in the presence of Mn remained similar with respect to controls lacking metal but the intensity of the protein band for Mn acquisition and oxidation was upregulated. Similar results were observed by Ramirez *et al.* (2004) in a study with iron as the metal of interest. Their study showed the upregulation of Fe oxidizing proteins on exposure to different concentrations of the metal. The third group of proteins comprised those downregulated with its level of synthesis upon growth in the presence of Mn. Similarly, repression of proteins of the sulfur oxidation pathway also occured during the growth of *Acidthiobacillus ferrooxidans* on sulfur compounds (Ramirez *et al.,* 2004). It thus suggests gene regulation/protein expression as an adaptive or homeostatic mechanism to counter the change in metabolic state or environmental stresses.

Unlike the deep-sea sediment from the cobalt-rich crust deposit region in the Pacific Ocean where the dominant bacterial groups were represented by *Proteobacteria*

and *Acidobacteria* (Liao *et al.,* 2011) the Fe-Mn crusts of the ANS were dominated by *Proteobacteria, Actinobacteria* and *Firmicutes*. This difference in the types of bacteria between the two ecosystems dictates their adaptation to specific niches depending on the availability of nutrients and key environmental conditions including the concentration of heavy metals. The common occurrence of *Proteobacteria* in samples from the Indian and Pacific oceans irrespective of the prevailing environmental conditions reiterates their importance in the cycling of Fe, Mn and the associated elements. They are also found to occur in heavy metal rich sediments and marine basalts (Mason *et al.,* 2009; Margesin *et al.,* 2011). Among the *Proteobacteria, Halomonas sp* representing the γ-Proteobacterial group was observed commonly in the Fe-Mn crusts from the ANS and basalts from the CR. This genus has also been detected by several researchers in elevated concentrations of Fe^{2+} and Mn^{2+} (Kaye and Baross, 2000; Templeton *et al.,* 2005) and has been found to produce self-assembling amphiphilic siderophores (Edwards *et al.,* 2004). Thus they may also utilize the seawater derived energy sources, such as dissolved and particulate Fe(II), Mn(II) and organic matter for growth and colonization of the seafloor rocks. They may also have the potential to proliferate under heavy metal stress and participate in the cycling of nutrients as they occur in metal rich deep-sea mineral deposits. In the Fe-Mn nodules and sediments of the CIB the isolates belonging to the genus *Bacillus* was more common. Since, the sediments are complex mixtures of Fe and Mn oxide mineral phases, detrital organic matter and several other organic and inorganic phases (Sujith *et al.,* 2011), the genus *Bacillus* could eventually proliferate because of their potential to act on dead and decaying organic matter and tolerate heavy metal stress by producing spores that could act as a permanent barrier. Due to their widespread ability to oxidize and reduce metals they have also been isolated from Fe and Mn-oxide minerals precipitating at deep subsurface oxic-anoxic interface (Mayhew *et al.,* 2008).

Further, microscopic imaging and EDS analyses of representative bacterial isolates from the ANS showed the accumulation of the metals at the cell surface and in different cellular compartments. Also the precipitation of Mn was found associated with the extracellular polymeric substances suggesting the active participation of bacteria in the enrichment of these metals in the Fe-Mn crust. Since metals and metalloids serve as cofactors in the polysaccharide synthesis, immobilization of metals

may be enhanced by the formation of water soluble complexes with Al, Fe, Si etc (Geesey *et al.,* 1988) depending on the key environmental conditions. Further, the co-oxidation of Co by marine Mn(II)-oxidizing bacteria via a common microbially catalyzed pathway (Lee and Tebo, 1994; Moffett and Ho, 1996) elaborates the widespread ability of bacteria to cope up with different metals. Thus the present results strongly suggest that microbial processes play a significant role in mineral precipitation in the ANS and other allied systems by adapting to heavy metal stress and deriving energy from the geochemical cycling of nutrients.

3.6. References

Amann RI, Ludwig W, Schleifer KH. 1995. Phylogenetic identification and *in situ* detection of individual microbial cells without cultivation. Microbiol Rev 59:143-169.

Antony R, Sujith PP, Fernandes SO, Verma P, Khedekar VD, Loka Bharathi PA. 2011. Cobalt immobilization by manganese oxidizing bacteria from the Indian Ridge system. Curr Microbiol 62: 840-849.

Arnosti C. 2011. Microbial extracellular enzymes and the marine carbon cycle. Annu Rev Mar Sci 3: 15.1-15.25.

Bairagi A, Ghosh K, Sen SK, Ray AK. 2002. Enzyme producing bacterial flora isolated from fish digestive tracts. Aquacult Int 10: 109-121.

Batzke A, Engelen B, Sass H, Cypionka H. 2007. Phylogenetic and physiological diversity of cultured deep-biosphere bacteria from Equatorial Pacific Ocean and Peru margin sediments. Geomicrobiol J 24: 261-273.

Benzerara K, Menguy N, Guyot F, Skouri F, de Luca G, Barakat M, Heulin T. 2004. Biologically controlled precipitation of calcium phosphate by *Ramlibacter tataouinensis*. Earth Planet Sci Lett 228: 439-449.

Bernard L, Schäfer H, Joux F, Courties C, Muyzer G, Lebaron P. 2000. Genetic diversity of total, active and culturable marine bacteria in coastal seawater. Aquat Microb Ecol 23: 1-11.

Boetius A, Lochte K. 2000. Regional variation of total microbial biomass in sediments of the deep Arabian Sea. Deep Sea Res II 7: 149-168.

Charteris WP, Kelly PM, Morelli L, Collins JK. 1998. Antibiotic susceptibility of potentially probiotic *Lactobacillus* species. J Food Prot 61: 1636-1643.

Connon SA, Giovannoni SJ. 2002. High-throughput methods for culturing microorganisms in very-low-nutrient media yield diverse new marine isolates. Appl Environ Microbiol 68: 3878-3885.

Das A, Fernandes CEG, Naik SS, Nath BN, Suresh I, Mascarenhas-Pereira MBL, Gupta SM, Khadge NH, Prakash Babu C, Borole DV, Sujith PP, Valsangkar AB, Mourya BS, Biche SU, Sharma R, Loka Bharathi PA. 2011. Bacterial response to contrasting sediment geochemistry in the Central Indian Basin. Sedimentology 58: 756-784.

De Souza MJ, Loka Bharathi PA, Nair S, Chandramohan D. 2007. "Trade-off" in Antarctic bacteria: limnetic psychrotrophs concede multiple enzyme expressions for multiple metal resistance. BioMetals 20: 821-828.

Dell'Anno A, Danovaro R. 2003. Extracellular DNA plays a key role in deep-sea ecosystem functioning. Science 309: 2179.

Divya B, Soumya KV, Nair S. 2010. 16SrRNA and enzymatic diversity of culturable bacteria from the sediments of oxygen minimum zone in the Arabian Sea. Antonie van Leeuwenhoek 98: 9-18.

Edwards KJ, Bach W, McCollom TM. 2004. Neutrophilic iron oxidizing bacteria in the Ocean: their habitats, diversity, and roles in mineral deposition, rock alteration, and biomass production in the deep-sea. Geomicrobiol J 21: 393-404.

Ellis RJ, Morgan P, Weightman AJ, Fry JC. 2003. Cultivation-dependent and -independent approaches for determining bacterial diversity in heavy-metal-contaminated soil. Appl Environ Microbiol 69: 3223-3230.

Fernandes SO, Krishnan KP, Khedekar VD, Loka Bharathi PA. 2005. Manganese oxidation by bacterial isolates from the Indian Ridge System. BioMetals 18: 483-492.

Geesey GG, Jang J, Jolley JG, Hankins MR, Iwaoka T, Griffiths PR. 1988. Binding of metal ions by extracellular polymers of biofilm bacteria. Water Sci Technol 20: 161-165.

Gerhardt P, Murray RGE, Costilow RN, Nester EW, Wood WA, Krieg NR, Phillips GB. 1981. Manual of Methods for General Bacteriology, American Society for Microbiology, Washington DC.

Goltekar RC, Krishnan KP, De Souza MJBD, Paropkari AL, Loka Bharathi PA. 2006. Effect of carbon source concentration and culture duration on retrievability of

bacteria from certain estuarine, coastal and offshore areas around peninsular India. Curr Sci 90:103-106.

Gomes NCM, Mendonca-Hagler LCS, Savvaidis I. 1998. Metal bioremediation by microorganisms. Revista de Microbiologia 29: 85-92.

Gonsalves M-J, Paropkari AL, Fernandes CEG, LokaBharathi PA, Krishnakumari L, Fernando V, Nampoothiri GE. 2011. Predominance of anaerobic bacterial community over aerobic community contribute to intensify 'oxygen minimum zone' in the eastern Arabian Sea. Cont Shelf Res 31: 1224-1235.

Hayat MA. 1972. Basic electron microscopy techniques. Van Nostrand Reinhold Company, New York.

Hirschler A, Lucas J, Hubert J-C. 1990. Bacterial involvement in apatite genesis. FEMS Microbiol Ecol 73: 211-220.

Hobbie JE, Daley RJ, Jasper S. 1977. Use of nucleopore filters for counting bacteria by fluorescent microscopy. Appl Environ Microbiol 3: 1225-1228.

Hogbom M, Ericsson UB, Lam R, Bakali HM, Kuznetsova E, Nordlund P, Zamble DB. 2005. A high throughput method for the detection of metalloproteins on a microgram scale. Mol Cell Proteomics 4: 827-834.

Holt JG, Krieg NR, Sneath PHA, Staley JT, Williams ST. 1994. Bergeys Manual of Determinative Bacteriology. Ninth edition. Lippincott Williams, Wilkins, Philadelphia, USA. pp. 787.

Hugh R, Leifson E. 1953. The taxonomic significance of fermentative versus oxidative metabolism of carbohydrates by various Gram-negative bacteria. J Bacteriol 66: 24-26.

Jones TH, Bradford MA. 2001. Assessing the functional implications of soil biodiversity in ecosystems. Ecol Res16: 845-858.

Jukes TH, Cantor CR. 1969. Evolution of protein molecules. In: Mammalian protein metabolism. Munro HN (ed) Academic Press, New York, pp. 21-132.

Kaeberlein T, Lewis K, Epstein SS. 2002. Isolating "uncultivable" microorganisms in pure culture in a simulated natural environment. Science 296:1127-1129.

Kasana RC, Salwan R, Dhar H, Dutt S, Gulati A. 2008. A rapid and easy method for the detection of microbial cellulases on agar plates using Gram's iodine. Curr Microbiol 57: 503-507.

Kaye JZ, Baross JA. 2000. High incidence of halotolerant bacteria in Pacific hydrothermal-vent and pelagic environments. FEMS Microbiol Ecol 32: 249-260.

Kirby WMM, Bauer AW, Sherris JC, Turck M. 1966. Antibiotic susceptibility testing by a standardized single disc method. Am J Clin Pathol 45: 493-496.

Kogure K, Simidu U, Taga N. 1979. A tentative direct microscopic method for counting living marine bacteria. Can J Microbiol 25: 415-420.

Kojima Y. 1991. Definitions and nomenclature of metallothioneins. In: Methods in enzymology: Metallobiochemistry part b metallothionein and related molecules. Riordan JF, Valee BL (eds) Academic press, London, pp. 8-10.

Krishnan KP, Fernandes CEG, Fernandes SO, Loka Bharathi PA. 2006. Tolerance and immobilization of cobalt by some bacteria from ferromanganese crusts of the Afanasiy Nikitin Seamounts. Geomicrobiol J 23: 31-36.

Kumar S, Tamura K, Nei M. 2004. MEGA3: integrated software for molecular evolutionary genetics analysis and sequence alignment. Brief Bioinform 5: 150-163.

Laemmli UK. 1970. Cleavage of structural proteins during the assembly of the head of bacteriophage T4. Nature 227: 680-685.

Leclercq R, Canton R, Brown DFJ, Giske CG, Heisig P, MacGowan AP, Mouton JW, Nordmann P, Rodloff AC, Rossolini GM, Soussy C-J, Steinbakk M, Winstanley TG, Kahlmeter G. 2011. EUCAST expert rules in antimicrobial susceptibility testing. Clin Microbiol Infect doi: 10.1111/j.1469–0691.2011.03703.x.

Lee Y, Tebo BM. 1994. Cobalt(II) oxidation by the marine manganese(II)-oxidizing *Bacillus* sp. strain SG-1. Appl Environ Microbiol 60: 2949-2957.

Li H-Y, Chen M-X, Li G, Zheng T-L, Zheng S-L, Chen B. 2011. Occurrence of total and culturable bacteria in Shenzhen coastal waters and their application in the environment assessment. Mar Environ Sci 4: 112-118.

Liao L, Xu X, Jiang X, Wang C, Zhang D, Ni J, Wu M. 2011. Microbial diversity in deep-sea sediment from the cobalt-rich crust deposit region in the Pacific Ocean. FEMS Microbiol Ecol 78: 565-585.

Lu S, Park M, Ro H-S, Lee DS, Park W, Jeon CO. 2006. Analysis of microbial communities using culture-dependent and culture-independent approaches in an anaerobic/aerobic SRB reactor. J Microbiol 44: 155-161.

Marchesi JR, Sato T, Weightman AJ, Martin TA, Fry JC, Hiom SJ, Wade WG. 1998. Design and evaluation of useful bacterium-specific PCR primers that amplify genes coding for bacterial 16S rRNA. Appl Environ Microbiol 64: 795-799.

Margesin R, Płaza GA, Kasenbacher S. 2011. Characterization of bacterial communities at heavy-metal-contaminated sites. Chemosphere 82: 1583-1588.

Mason OU, Di Meo-Savoie CA, Van Nostrand JD, Zhou J, Fisk MR, Giovannoni SJ. 2009. Prokaryotic diversity, distribution, and insights into their role in biogeochemical cycling in marine basalts. ISME J 3: 231-242.

Mayhew LE, Swanner ED, Martin AP, Templeton AS. 2008. Phylogenetic relationships and functional genes: distribution of a gene (mnxG) encoding a putative manganese-oxidizing enzyme in *Bacillus* species. Appl Environ Microbiol 74: 7265-7271.

Mergeay M, Nies D, Schlegel HG, Gerits J, Charles P, Van Gijsegem F. 1985. *Alcaligenes eutrophus* CH34 is a facultative chemolithotroph with plasmid-bound resistance to heavy metals. J Bacteriol 162: 328-334.

Moffett JW, Ho J. 1996. Oxidation of cobalt and manganese in seawater via a common microbially catalyzed pathway. Geochim Cosmochim Acta 60: 3415-3424.

Muller S. 2010. Functional flow cytometry in environmental microbiology. In: Handbook of hydrocarbon and lipid microbiology. Timmis KN (ed) Springer-Verlag, Berlin Heidelberg, pp. 4103-4112.

Oliver JD.1982. Taxonomic scheme for the identification of marine bacteria. Deep Sea Res 29: 795-798.

Parkes RJ, Webster G, Cragg BA, Weightman AJ, Newberry CJ, Ferdelman TG, Kallmeyer J, Jorgensen BB, Aiello IW, Fry JC. 2005. Deep sub-seafloor prokaryotes stimulated at interfaces over geological time. Nature 436: 390-394.

Poole LB, Reynolds CM, Wood ZA, Karplus PA, Ellis HR, Calzi ML. 2000. AhpF and other NADH: peroxiredoxin oxidoreductases, homologues of low Mrthioredoxin reductase. Eur J Biochem 267: 6126-6133.

Ramírez P, Guiliani N, Valenzuela L, Beard S, Jerez CA. 2004. Differential protein expression during growth of *Acidithiobacillus ferrooxidans* on ferrous iron, sulfur compounds, or metal sulfides. Appl Environ Microbiol 70: 4491-4498.

Saitou N, Nei M. 1987. The neighbour-joining method: a new method for reconstructing phylogenetic trees. Mol Biol Evol 4: 406-425.

Simu K, Holmfeldt K, Zweifel UL, Hagstrom Å. 2005. Culturability and coexistence of colony-forming and single-cell marine bacterioplankton. Appl Environ Microbiol 71: 4793-4800.

Spiro TG, Bargar JR, Sposito G, Tebo BM. 2010. Bacteriogenic manganese oxides. Acc Chem Res 43:2-9.

Stoppel RD, Schlegel HG. 1995. Nickel-resistant bacteria from anthropogenically nickel-polluted and naturally nickel-percolated ecosystems. Appl Environ Microbiol 61: 2276-2285.

Sujith PP, Khedekar VD, Girish AP, Loka Bharathi PA. 2010. Immobilization of nickel by bacterial isolates from the Indian ridge system and the chemical nature of the accumulated metal. Geomicrobiol J 27: 424-434.

Sujith PP, Mourya BS, Krishnamurthi S, Meena RM, Loka Bharathi PA. 2014. Mobilization of manganese by basalt associated Mn(II) oxidizing bacteria from the Indian Ridge System. Chemosphere 95: 486-495.

Sujith PP, Das A, Mourya BS, Loka Bharathi PA. 2011. Immobilisation of manganese, cobalt and nickel by deep-sea-sediment microbial communities. Chem Ecol 27:189-206.

Tebo BM, Johnson HA, McCarthy JK, Templeton AS. 2005. Geomicrobiology of manganese(II) oxidation. Trends Microbiol 13: 421-428.

Templeton, AS, Staudigel H, Tebo BM. 2005. Diverse Mn(II)-Oxidizing Bacteria Isolated from Submarine basalts at Loihi seamount. Geomicrobiol J 22: 127-139.

Thompson JD, Gibson TJ, Plewniak F, Jeanmougin F, Higgins DG. 1997. The Clustal X windows interface: Flexible strategies for multiple sequence alignment aided by quality analysis tools. Nucleic Acids Res 25: 4876-4882.

Vermelho AB, Meirelles MNL, Lopes A, Petinate SDG, Chaia AA, Branquinha MH. 1996. Detection of extracellular proteases from microorganisms on agar plates. Mem Inst Oswaldo Cruz. Rio de Janeiro 91: 755-760.

Wood PM. 1978. Periplasmic location of the terminal reductase in nitrite respiration. FEBS Lett 92: 214-218.

Zeng L, Huang J, Zhang Y, Qiu G, Tong J, Chen D, Zhou J, Luo X. 2008. An effective method of DNA extraction for bioleaching bacteria from acid mine drainage. Appl Microbiol Biotechnol 79: 881-888.

CHAPTER 4

Activity of ferromanganese crusts associated bacteria contribute to hydrogenetic metal accretion in the Afanasiy-Nikitin Seamount

4.1. Abstract

The Afanasiy-Nikitin Seamount (ANS) in the Equatorial Indian Ocean harbours hydrogenetic Fe-Mn crusts enriched with trace metals and supports significant microbial life. Microbial processes within these crusts are significant in controlling the rates of chemical reactions and thereby affecting chemical exchange between the ocean crust and the waters above. Hence, it was hypothesised that the bacterial associates catalyses the precipitation of metal hydroxides in sea water more than abiotic dissolution, thus contributing to hydrogenetic accretion of metal on the seamount. To test the above hypothesis, Fe-Mn crust samples were collected from the flanks of the ANS at a water depth of 1987 m using a chain bag dredge. Geochemical properties of water samples collected were analyzed and simulatory laboratory experiments were conducted to quantify bacterial accretion rates. Pyrosequencing was used to delineate the community associated with Fe-Mn crust. The environmental parameters of the water column indicated significant differences ($p < 0.001$) between a seamount and a non-seamount site. Experiments on Fe-Mn crust under simulated near in situ temperature (4±2°C) and pressure (20 MPa) conditions showed that biotic immobilization of metal ions were significantly higher ($p < 0.001$) than abiotic immobilization for Fe and Co. The sequence of immobilization in mg g^{-1} in the presence (0.01%) and absence of added glucose were Fe (9.34; 9.09) >Mn (0.63; 0.87) > Ni (0.003; 0.0043) > Co (0.002; 0.0008) respectively. Unlike the hydrothermal vent sites of the Pacific where ε- and ζ-*Proteobacteria* were reported to be dominant, the hydrogenetic Fe-Mn crusts of the ANS revealed a dominance of sequences related to known Fe, Mn and S oxidizing bacteria of the γ- and α-Proteobacterial groups. This difference may be attributed to the relative fractions of inorganic and organic carbon that is present at the two sites. Our results, suggest that, ambient nutrient levels trigger the γ-and α-Proteobacterial community of the ANS to sequester and release metal ions in pulses, leading to the precipitation of Fe-Mn rich minerals.

4.2. Introduction

Unlike other oceanic realms, seamounts are active sites for ferromanganese (Fe-Mn) deposition and are locations for current-topographic interactions and biophysical coupling (Clark *et al.*, 2010). They support a high concentration of planktonic and consumer biomass than the surrounding seawater which is mostly oligotrophic. This occurs because 1) the summit and flanks of the seamount trap the fall of vertically migrating planktonic organisms and 2) the flow of water collides with seamount topographies and the resulting accelerated currents sequentially intensify the horizontal food supply to seamount communities (Clark *et al.*, 2010). The ANS, in the Equatorial Indian Ocean (EIO) is a low productive environment (Fernandes *et al.*, 2008) characterized by seasonal thermohaline alteration, voluminous precipitation and fresh water inflow (Sardessai *et al.*, 2010). The circulatory pattern of the different water masses (Schott and McCreary, 2001; Matthias and Godfrey, 2003) in conjunction with the topographic setting of the ANS would influence the physicochemical parameters and the related biological variables. Subsequently, this could influence the metal enrichment processes occurring on the seamount by chemical and biological mediated mechanisms.

Precipitation of metal cations in an environment could be microbially induced, mediating both active and passive processes of metal precipitation (Luptakova *et al.*, 2007; Ehrlich and Newman, 2009). One of the processes being, the bacterial interaction with metal ions that gives rise to oxides and hydroxides of low crystallinity like the δMnO_2 (Hein *et al.*, 2000). Some of these organisms take up metals, some sequester for their own use, some transform/bind them in a nontoxic form, some chelate while others prevent their loss from chelators, some reduce and the others oxidize metals (Morel and Price, 2003). This gains significance as the prokaryotic organisms constitute 360×10^{26} cells in the photic zone, 650×10^{26} cells in the disphotic/aphotic zones and 170×10^{26} cells in the marine surface sediments (0-10 cm) of the open ocean (Whitman *et al.*, 1998) and partake in important biogeochemical processes. Moreover, the microbial involvement in the accretion or dissolution promotes the element exchange between oceanic crust and seawater (Thorseth *et al.*, 1995).

On the ANS, the hydrogenetic mineral deposits are formed in topographic heights especially on the summit and flanks of the seamount (Banakar *et al.*, 2007; Glasby *et al.*, 2010). Mostly they are confined to hard surfaces where the supply of terrigenous, volcanogenic and biogenic components is very low and where currents have kept the rocks clean for several million years (Usui and Someya, 1997; Koschinsky and Hein, 2003). The hydrogenetic precipitation is basically an inorganic colloidal-chemical and surface-chemical process (Halbach *et al.*, 2008). Microbial participation in such a process could be significant as it meets two most important properties of colloids (i.e.) surface area and surface charge. The higher surface area-to-volume ratio and the presence of specific cell wall functional groups with high affinities for dissolved metals, allow bacteria to scavenge and oxidize Mn several orders of magnitude higher than abiotic oxidation (Tebo *et al.*, 2005; Ledin, 2000). Further, bacteria bind and deposit preformed colloidal manganese oxide in association with extracellular acidic exopolysaccharide (Sly *et al.*, 1990) and encrust metal ions on the cells (Rae and Celo, 1975; Kappler *et al.*, 2005). Therefore, the associated bacteria play a significant role in colloid-facilitated adsorption of metals. These bacteria associated with hydrogenetic environments differ from that of low-temperature hydrothermally originated Mn-rich layers due to several reasons. The major differences being higher porosity (60%), extremely high specific surface area (300 $m^2 g^{-1}$), very slow growth rate of 1-6 mm/Ma, high content of trace metals and high Mn/Fe ratio of 0.7 to 1.2 reported for the hydrogenetic crusts (Hein *et al.*, 1997; Nath *et al.*, 1997; Hein *et al.*, 2003) as compared to that of hydrothermal crust. The deposits on the ANS not only contain Mn and Fe concentrations typical to that of hydrogenetic crusts but are also enriched with Co (maximum: 0.9%, average: ~0.5%), Ce (maximum: 0.37%, average: ~0.22%) and Pt (maximum: 1ppm, average: ~0.5 ppm) (Banakar *et al.*, 2007; Banakar, 2010).

Substantial studies determined the bacterial diversity in environments such as hydrothermal seamounts of Pacific and Atlantic Oceans (Emerson and Moyer, 2010; Clark *et al.*, 2010), but very little evidence exists for the microbial ecology of hydrogenetic seamount Fe-Mn crusts and their associated sediments (Kato and Yamagishi, 2011). Likewise, many experimental studies with bacteria have demonstrated their ability to participate in Fe and Mn oxidation (Konhauser, 1998; Sujith and Loka Bharathi, 2011) and also in weathering of rock substrates (Fein *et al.*,

1999; Daughney *et al.*, 2004). But to the best of our knowledge, no evidences exist for the plausible contribution by the indigenous microbial community from hydrogenetic ecosystems to the crust genesis under simulated *in situ* conditions of temperature and pressure in microcosms. This is the first study from the Indian Ocean and the Equatorial region to assess the bacterial diversity of the hydrogenetic Fe-Mn crusts and to measure the rates of crust accretion in vitro. Herein, we describe the 1) abundance, 2) diversity and their possible functions, and 3) *in vitro* metal immobilizing activity of hydrogenetic cobalt rich Fe-Mn crusts associated microbial communities. The culture-independent 454 sequencing approach has been used to probe the bacterial diversity of the Fe-Mn crust. The results obtained through this study are compared with those from other similar and related Fe-Mn crust rich ecosystems. Experimental evidence is presented to demonstrate the contribution of crust associated microbial community to ore formation.

4.3. Materials and methods

4.3.1. Study area and sampling

The ANS is located in the north central Indian Ocean and differs from seamounts of other geographical locations in summit depth, hydrogenetic metal accretion rate, physical and hydrographic characteristics (Mahoney *et al.*, 1996; Banakar *et al.*, 1997). It extends ~300 km in the north south direction and ~200 km in the east west direction (Parthiban and Banakar, 1999). The Fe-Mn crust sample for the present study was collected from the flanks of the ANS at 03°01.484'S latitude and 83°03.726'E longitude from a water depth of 1987 m. The samples were collected on board Akademic Boris Petrov (2009) using a chain bag dredge. Water samples from predetermined depths one close to the seamount and one away from the seamount (reference station) were collected using a conductivity temperature depth (CTD) sensor coupled to a Niskin bottle rosette system (Figure 4.1).

4.3.2. Collection and processing of samples

The Fe-Mn crusts samples were collected in sterile containers and were preserved at -20°C for the extraction of total DNA (tDNA). Water samples for the analysis of nutrients and chemical parameters were collected in acid cleaned bottles after rinsing with the samples. The water samples for nitrate (NO_3^-), nitrite (NO_2^-) and phosphate (PO_4^{3-}) were filtered using 0.8 μm Nucleopore filter and were then frozen at -20°C,

while for silicate (SiO_3^{2-}) water samples were preserved at 4±2°C in the dark to avoid polymerization. All freezing was done in 125 ml HDPE bottles. The bottles were filled to three fourth of its volume and were stored upright to prevent seawater from freezing around the screw-caps.

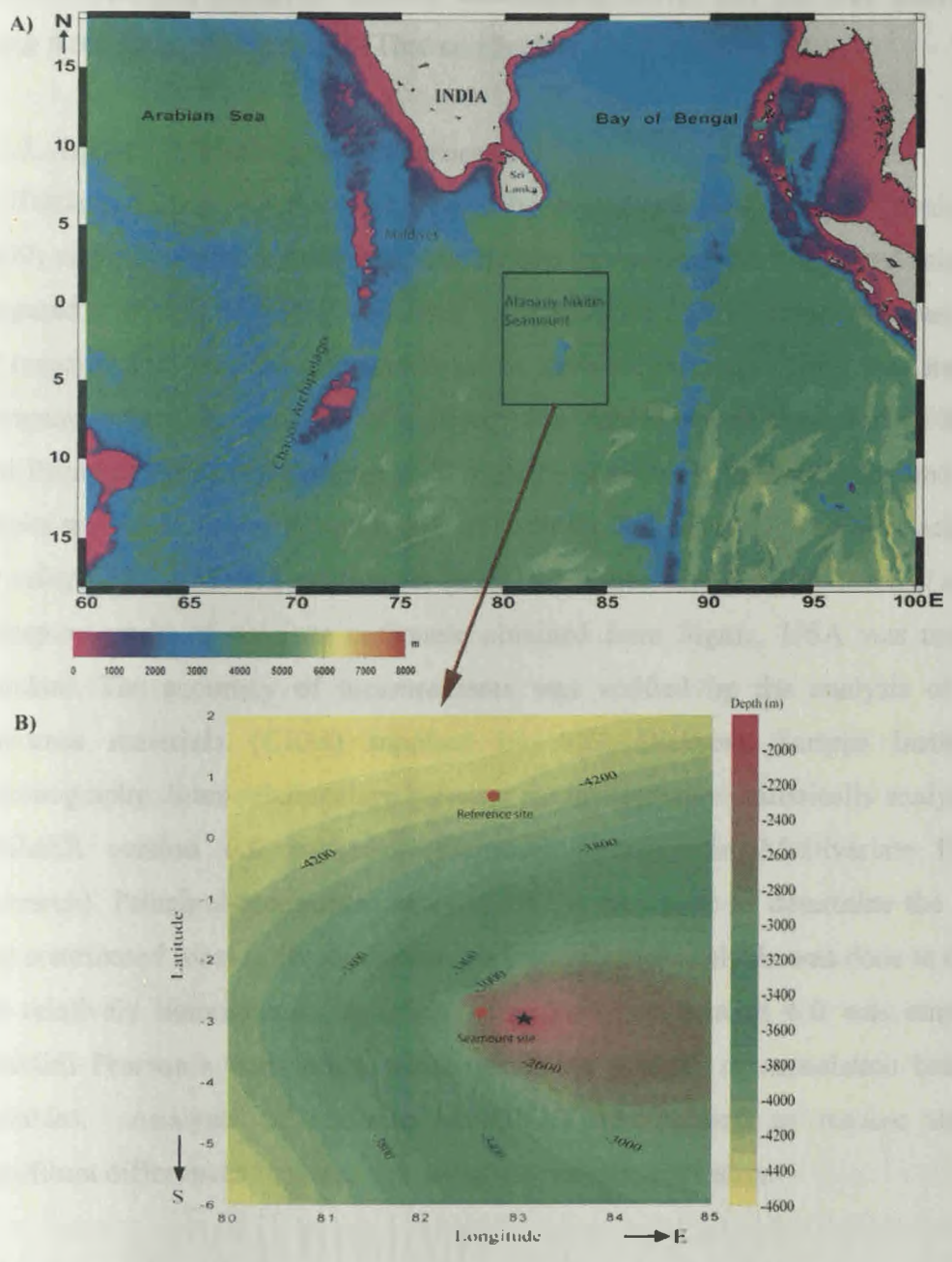

Figure 4.1. A) Location of the Afanasiy-Nikitin seamount and B) the sampling sites. The point of sampling for ferromanganese crust is denoted by a star and water samples as red circles.

For total inorganic carbon (TIC), the water samples on collection were spiked with 200 µl of saturated mercuric chloride to arrest further biological activity. The bottles were sealed and stored in the dark at -20°C. On reaching the shore laboratory, the analyses were carried out after thawing the samples at room temperature. Dissolved oxygen (DO) was analyzed onboard immediately after collection using calibrated galvanic dissolved oxygen electrode (Eutech Instruments, USA) and pH was determined by using a refillable pH electrode (Thermo Electron Corporation, USA).

4.3.3. Analysis of environmental parameters

Nutrients in sea water were analyzed by segmented flow analysis (Aminot *et al.*, 2009) using Technicon Auto-Analyzer II. The instrument was calibrated using freshly prepared standards of NO_3^-, NO_2^-, PO_4^{3-} and SiO_3^{2-} in 18.3 Ω ultrapure water. Dilution of reagents and baseline adjustment to the zero concentration level was made using ultrapure water. The analysis of nutrients was carried out as described by Strickland and Parsons (1968) and Aminot *et al.* (2009). Seawater refractive index and turbidity blanks were used to correct each type of analysis. TIC was analyzed after acidification by using a UIC CM5014 coulometer (UIC Inc., Joliet, IL, USA) (Johnson *et al.*, 1985). Ultrapure grade of calcium carbonate obtained from Sigma, USA was used as the standard. The accuracy of measurements was verified by the analysis of certified reference materials (CRM) supplied by A.G. Dickson, Scripps Institution of Oceanography. Inter-relationships between parameters were statistically analyzed using PRIMER version 6.0 packages (Plymouth Routines in Multivariate Ecological Research). Principal-component analysis (PCA) was used to determine the variables that contributed most to the ordination diagram. Cluster analysis was done to determine the relatively homogenous sampling sites. Statistica version 6.0 was employed to establish Pearson's correlation, which gives the strength of association between the variables. Analysis of variance (ANOVA) was applied to resolve statistically significant differences between the seamount and reference site.

4.3.4. Non-culturable fraction and their genotypic characterization

4.3.4.1. DNA extraction and quantification

Total DNA (tDNA) was extracted from Fe-Mn crusts by minor modification of the method by Zhou *et al.* (1996). The sample was thoroughly rinsed in sterile seawater to

remove the impurities. It was aseptically crushed using a mortar and a pestle and was lyophilized in oak ridge tubes (Heto LL1500 freeze dryer). To about 0.1 g of freeze-dried sample in pre-weighed 1.5 ml eppendorf tubes 1 ml of DNA extraction buffer (0.1 M Tris HCl, 0.1 M EDTA (pH 8.0), 0.1 M NaH_2PO_4, 1.5 M NaCl and 1% cetyltrimethylammonium bromide) and 2 µl of proteinase-K (10 mg ml^{-1}) were added. The contents were incubated at 37 °C in a water bath with horizontal shaking (225 rpm) for 2 h, followed by 100 µl of 20% sodium dodecyl sulfate. Incubation was continued for another 2 h at 65°C with gentle inversion every 5-10 min. The samples were centrifuged at 10,000 rpm for 10 min at 4°C. To the supernatant, equal volume of chloroform isoamyl alcohol mixture in the ratio 24:1 was added. Centrifugation was repeated at 14000 rpm. To the top aqueous layer, 0.6 volume of isopropanol was added. The incubation was repeated at room temperature for 1 h. The DNA was concentrated by centrifugation and was washed twice with 500 µl of ice-cold 70% ethanol. The concentration and purity of DNA in Tris-EDTA buffer (pH 8.0) was checked using NanoDrop ND-1000 Spectrophotometer (NanoDrop Technologies, Wilmington DE). DNA from replicate samples were pooled and stored at -80°C for further analysis.

4.3.4.2. Amplification and pyrosequencing of bacterial DNA

The hypervariable V6 region of 16S rRNA gene specific to the eubacterial clade was amplified with bacterial universal primers described in Sogin *et al.* (2006) and Huber *et al.* (2007). The amplicons were pyrosequenced with a 454 Life Sciences GS-FLX sequencer at the Josephine Paul Bay Center, Marine Biological Laboratory in Woods Hole, MA, USA under the auspices of International Census of Marine Microbes (ICoMM). The protocols have been described in detail by Sogin *et al.* (2006), Huber *et al.* (2007) and Huse *et al.* (2008). The sequencing results were downloaded from the Visualization and Analysis of Microbial Population Structures (VAMPS) webpage (http://vamps.mbl.edu/). The characteristics of the sequences such as average read length and tag aggregates were estimated in a R 2.8.1 programming environment after trimming and removal of low-quality reads (R Development Core Team, 2009). Further processing of the data for multiple sequence alignment, clustering of sequences into operational taxonomic units (OTUs), rarefaction analysis and estimation of diversity indices like Shannon (H') and Simpson evenness index (J'), and abundance-based

coverage estimators Chao1 and ACE were determined using the tools available in the VAMPS website (http://vamps.mbl.edu/).

4.3.5. Simulated experiments on metal immobilization

The metal immobilization experiment with Fe-Mn crust under simulated deep-sea in situ temperature and pressure conditions was conducted following pressure bag method (Kato, 2012). The various sterile media that were used for the experimental incubations were prepared in 0.22 μm filtered aged deep-sea water unless otherwise specified. Sodium azide poisoned crusts were used as abiotic controls along with secondary controls of heat killed autoclaved crust. This precaution was taken as sodium azide may chemically interfere with some of the metals within the crust. The different combinations of media used were as follows: Media I- seawater without glucose amendment (G^-); Media II- seawater with 0.01% glucose amendment (G^+); Media III- seawater without glucose and poisoned with 15mM sodium azide (G^-) and Media IV- seawater with 0.01% glucose and poisoned with 15mM sodium azide (G^+). A 10% stock of glucose and 1M stock of sodium azide was autoclaved prior to their addition in the respective media. The crust fragments that were thoroughly rinsed in sterile seawater were used as inocula for biotic experimental setup. For the heat killed abiotic controls, the autoclaved crust fragments were used as inoculums in media I and media II separately. Uninoculated media from I to IV served as blanks. The homogeneity of the sample was maximized by using the fragments from a single large rock fragment. *In vitro* experiments were set up in sterile polyethylene bags to which 1.5 to 2.0 ml of individual media and about 0.08 ± 0.03 g dry weight of Fe-Mn crust were added. The concentration of soluble Fe, Mn, Co and Ni was measured in all sets of treatment immediately after the addition of Fe-Mn crust. The day zero measurement was used as a reference to monitor the changes in metal concentrations throughout the incubation period. The bags were sealed aseptically and trapping of any air bubbles was avoided. The different media mentioned above in sets of three were incubated for 24, 35, 53, 63 and 82 d in individual pressure vessels (Tsurumi, Japan) at 4±2°C and simulating near *in situ* pressure of 20 MPa (megapascal). After incubation, the growth was measured at 595 nm (OD_{595}) in a microplate reader (Bio-Rad, 680 XR). The exact dry weights of the crust fragments were determined after drying at 105°C. Any decrease in dissolved

metal concentration observed during the experiment was assumed to be caused by metal adsorption.

4.3.6. Metal analysis

The soluble phase concentrations of metals in the above media were analyzed after centrifugation at 8000 rpm for 10 min at 4°C (Sigma 3-k). The determination of Fe, Mn, Co and Ni was made by adsorptive stripping voltammetry in interface with 797VA computrace in the differential pulse mode (Metrohm, Switzerland) according to Aldrich and van den Berg (1998), Colombini and Fuoco (1983) and Herrera-Melian *et al.* (1997). The metal concentration was determined after UV treatment of the diluted and acidified (pH < 2) supernatant for one hour at 90°C. These samples were analysed immediately on cooling or were stored in the dark at 4±2°C for later analysis. Fe, Mn, Co and Ni were quantified with two standard additions of appropriately diluted 1000 ppm concentrations of the respective metal standards prepared in seawater. Metal standards (1000 ppm) obtained from Merck-GMBH, were used for determining the analytical accuracy. The gram dry weight concentration of metal immobilized was calculated after correcting it for the blank and normalizing it for the volume of media used. The statistically significant differences between the results from the biotic and abiotic (control) incubations were checked by two way-ANOVA at the 95% confidence level ($\alpha = 0.05$, $n = 6$).

4.4. Results

4.4.1. Water column

4.4.1.1. Environmental parameters of the water column

The influence of the seamount was reflected in the patterns of nutrients and TIC distribution in the water column . NO_2^- (5.15-13.23 nM), SiO_3^{2-} (213.27-320.29 nM) and DO (150.3-177.2 μM) increased from the surface water to the deep water, but those of TIC and pH decreased. NO_3^- and PO_4^{3-} concentrations remained persistently low, with average concentrations of 0.66 nM and 0.51nM respectively. Exceptionally high NO_2^- values with an average concentration of 8.99 nM was observed at the seamount site. SiO_3^{2-} exhibited a similar trend with a higher value of 320.29 nM in the lower water column. Oxygen concentrations increased gradually from 150.3 μM in the

surface water to 177.2 μM at 2500 m. TIC concentration marked a high value of 3733.56 μM Kg^{-1} at the summit (1500 m) in the seamount station (Figure 4.2B) and 2020.4 μM Kg^{-1} in the bottom most depth of 3000 m at the reference station (Figure 4.2A). The coefficient of correlation between environmental parameters of the water column was more significant in the seamount location in comparison to those of the reference station (Table 4.1). ANOVA showed the water column parameters of the reference site to differ significantly ($p < 0.001$) with those of the seamount site (Table 4AT1, Appendix III).

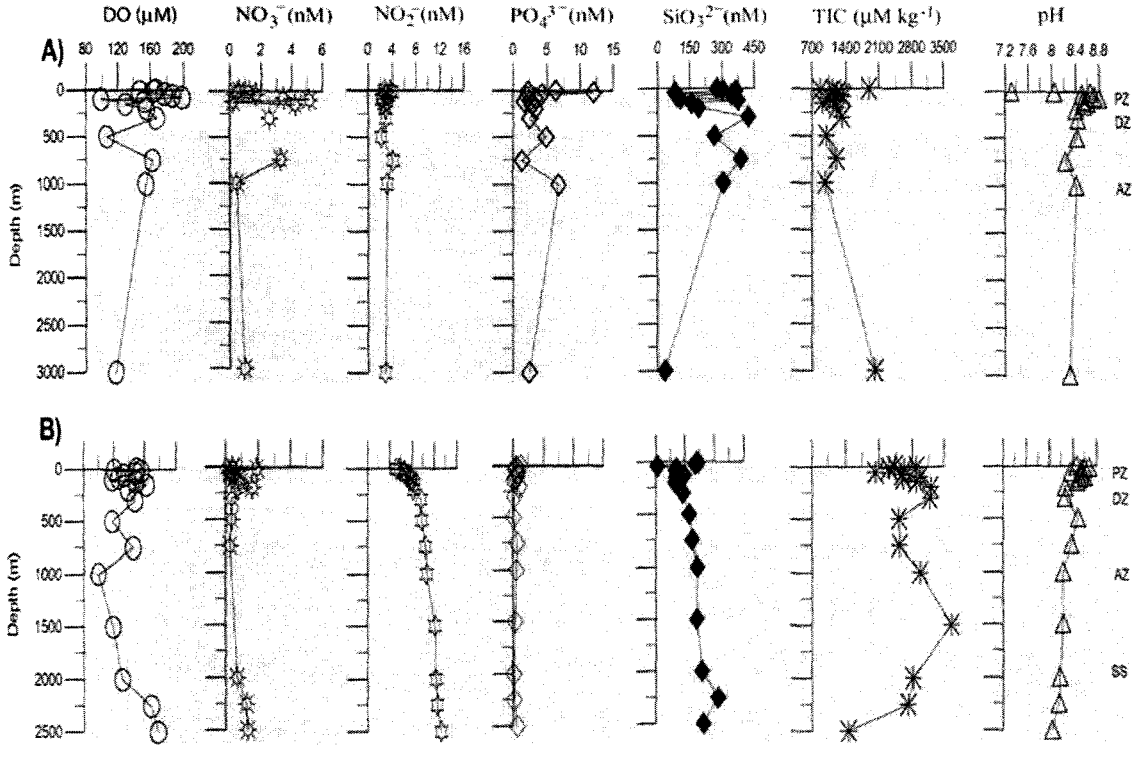

Figure 4.2. Water column profile of environmental parameters. A) Reference site and B) Seamount site. Abbreviations PZ: Photic Zone, DZ: Disphotic Zone, AZ: Aphotic Zone and SS: seamount summit.

4.4.1.2. Characteristics of water overlying the seamount summit

The water column overlying the summit of the seamount at 1500 m depth below the sea surface were characterised by negligible NO_3^- (<0.2 nM), low PO_4^{3-} (0.33 nM), average DO (119.7 μM), and high TIC (3733.56 μM kg^{-1}) (Figure 4.2B). In contrast,

NO_2^- and SiO_3^{2-} showed higher concentrations of 12.17 nM and 212.57 nM respectively at the same water depth.

Table 4.1. Correlation analysis between environmental parameters of a seamount and a non-seamount (reference) site.

Sl.No	Interrelated Parameters	Seamount site	Reference site
1	Depth/ NO_2^-	0.917***	
2	Depth/ SiO_3^{2-}	0.702**	
3	Depth/pH	-0.831***	
4	Depth/TIC	-0.139	0.531*
5	DO/ NO_3^-	0.621**	
6	DO/TIC	-0.486*	
7	NO_2^-/ PO_4^{3-}	-0.486*	
8	NO_2^-/ SiO_3^{2-}	0.543*	0.572*
9	NO_2^-/pH	-0.839***	
10	SiO_3^{2-}/pH	-0.479*	

*** significant at $p \leq 0.001$, ** significant at $p \leq 0.01$ and * significant at $p \leq 0.05$.

4.4.1.3. Principal Components analysis (PCA)

PCA analysis of the environmental parameters in the reference site using five principal components (PC1 to PC5) explained about 98.1% of the total variance (Figure 4.3A). Of those, first two components PC1 and PC2 constituted 80.6% of the variance. The variables pH, DO, NO_2^- and TIC explained ca. 64.7% of the variation in PC1. In PC2, PO_4^{3-} and NO_3^- explained ca. 15.9% of the variability. The highest variance was scored at depth of 80, 750, and 3000 m along the first component and 20 and 100 m along the second component respectively. PCA analysis of the seamount location aggregated the above abiotic variables into the first (PC1), second (PC2) and third (PC3) components (Figure 4.3B). Of those, first two components PC1 and PC2 constituted 67.4% of the variance. In PC1, variables like pH, SiO_3^{2-} and NO_2^- explained ca. 42.8% of the variation. PC2 consisted of NO_3^-, TIC, and DO, which explained ca. 24.6% of the variability and PC3 included PO_4^{3-} as the prime contributor to 11.6% of the variance. The highest variance was scored at a depth of 10, 2250 and 2500 m along the first component and 20, 1500 and 2500 m along the second component. The cluster diagram of reference site (Figure 4.4A) at 50% cut-off showed marked heterogeneity in the clustering of variables from the seamount location (Figure 4.4B). A well

differentiated clustering between variables was observed in the seamount location whereas it was least differentiated in the reference station.

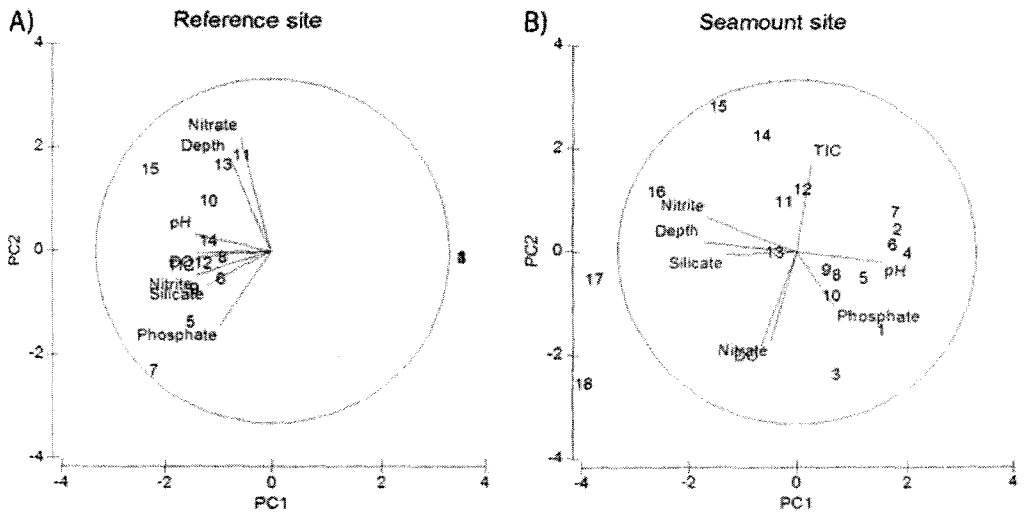

Figure 4.3. Principal Components analyses of environmental parameters. A) Reference site and B) Seamount site.

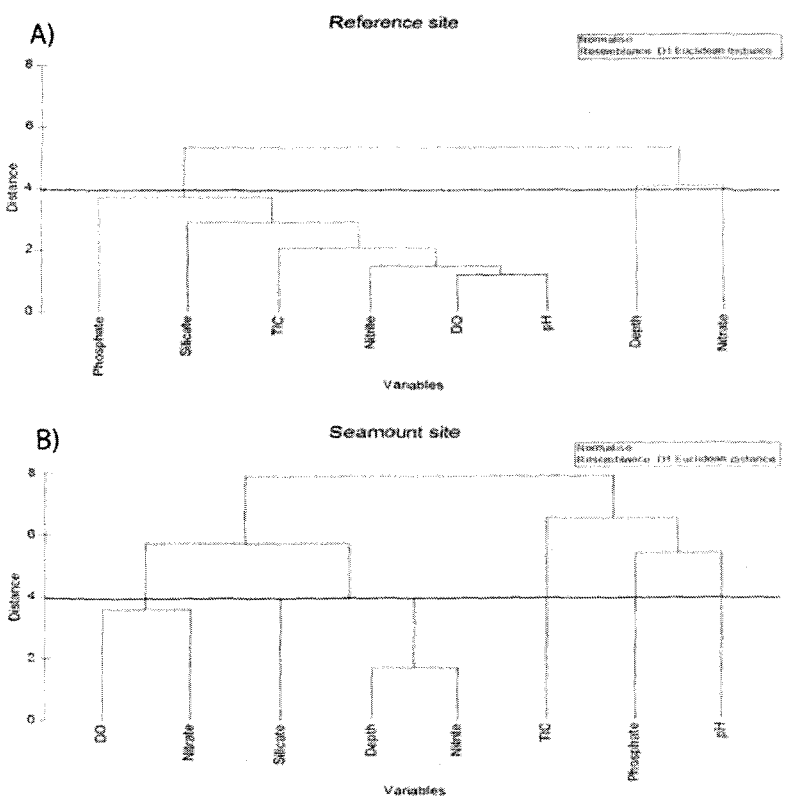

Figure 4.4. Euclidean cluster of environmental parameters. A) Reference site and B) Seamount site.

4.4.2. Fe-Mn crust

4.4.2.1. Non-culturable fraction and their genotypic characterization

The examination of 16S rRNA gene fragments (tags) of total microbial communities showed 34072 tags after the elimination of low quality reads. About 1659 ribotypes affiliated to 30 phyla were identified. The average read length of the sequences was 60.8 (± 2.45). The non-parametric richness indices such as Chao1 and ACE, calculated at 3% dissimilarity showed that bacterial communities in the Fe-Mn crusts were very heterogenous. The Chao1, and ACE richness estimates were 647 and 729 OTUs respectively. The unique OTUs represented 1657 ribotypes and 549 ribotypes at 97% similarity. The non-parametric indices H' determined at 3% divergence was 5.61 and parametric indices J' was 0.0083 (Table 4.2).

Table 4.2. Bacterial community analysis and statistics of the pyrosequencing data

Parameters	Details
Latitude/longitude	03°01.484'S, 83°03.726'E
Depth of sampling (m)	1987
Total tags	34072
Number of phyla	30
Number of genera	252
Maximum read length (bp)	81
Average read length (bp)	60.8
Number of aggregates	61
$OTU_{0.03ds}$	549
$Chao1_{0.03ds}$	647
$ACE_{0.03ds}$	729
Shannon's index	5.61
Simpsons's index	0.0083

The diversity analysis of the sample using rarefaction curve showed that curves were not saturated and that with continued deeper sampling, more organisms were yet to get identified (Figure 4.5). Among the different phyla *Proteobacteria* represented the dominant phylum. They represented 83% of the total tag abundance. The γ-*Proteobacteria* was the major sub-phylum among the *Proteobacteria* (Figure 4.6). *Halomonas* and *Thiomicrospira* constituted 21.5 and 17.2% respectively of the 68.3% tag abundance of γ-*Proteobacteria*. The other members of γ-*Proteobacteria* were *Idiomarina* (9.64%), *Methylophaga* (7.95%), *Alcanivorax* (3.97%) and *Marinobacter*

(3.91%). Besides the sequences affiliated to defined genera, 2.6% of the sequences belonged to unclassified γ-*Proteobacteria*. The second most abundant sub-phylum of *Proteobacteria* was the α-*Proteobacteria*. Among these, *Phaeobacter*, *Erythrobacter*, *Sulfitobacter*, *Aurantimonas* and an unidentified Rhodobacteraceae member represented 5.15, 4.86, 2.30, 0.64 and 0.45% of the 14.05% tag abundance of α-*Proteobacteria* respectively (Figure 4.6). In addition, an unidentified genus of Flavobacteriaceae represented 10.79% of the 13.15% tag abundance of *Bacteroidetes* group. From the results, it is clear that different groups of bacteria that are capable of oxidizing Fe and Mn inhabit the oxide surfaces over basalt. Further, to confirm their participation in the accretion process, the *in vitro* microcosm experiments with Fe-Mn oxide under near *in situ* temperature and pressure conditions were carried out.

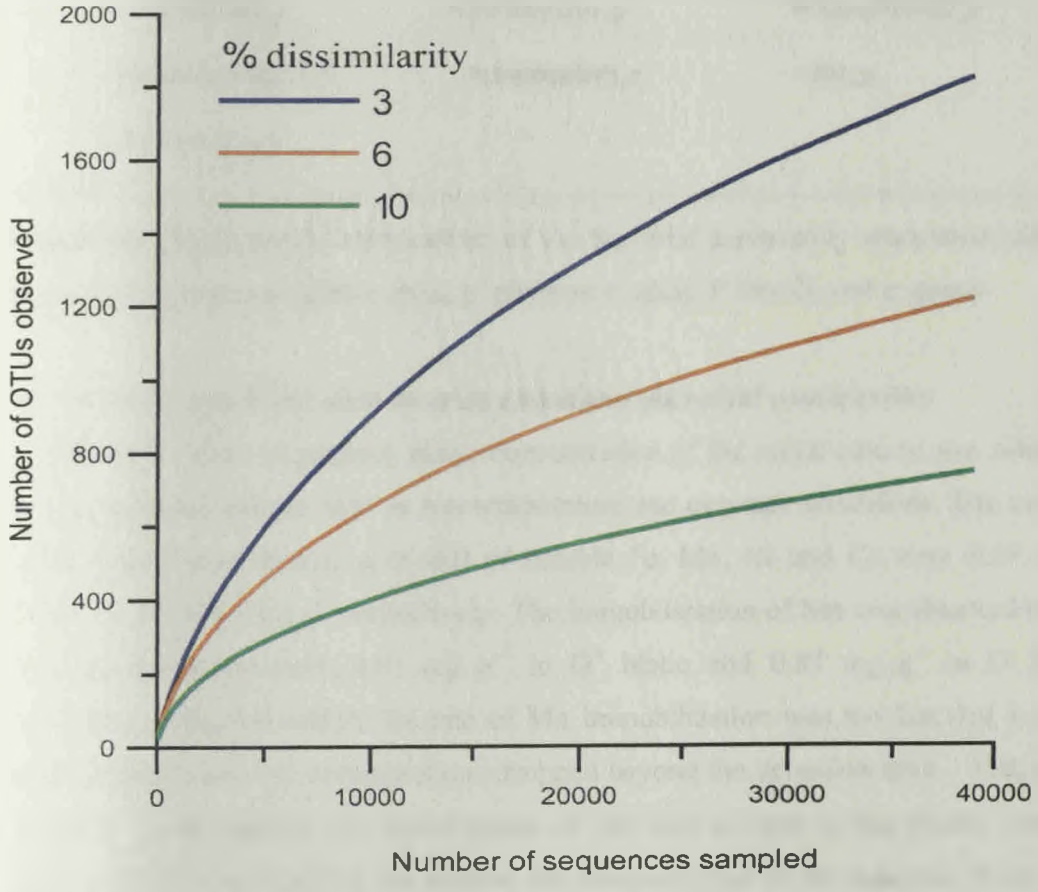

Figure 4.5. Rarefaction curves depicting the effect of percentage of dissimilarity on the number of OTUs identified.

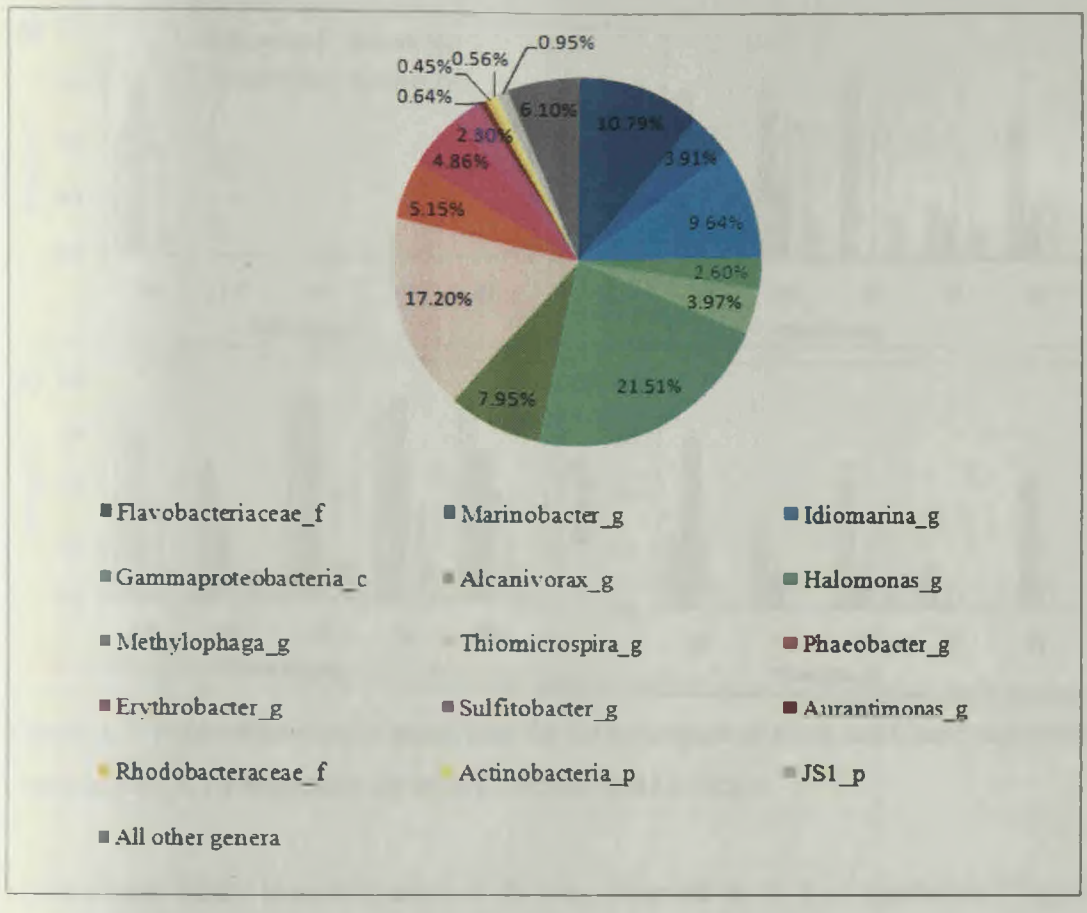

Figure 4.6. Phylogenetic composition of the bacterial community associated with the hydrogenetic ferromanganese crust; p: phylum, c: class, f: family and g: genus.

4.4.2.2. Metal immobilization by crust associated microbial communities

The fall in level of aqueous phase concentration of the metal cations was observed during incubation under near *in situ* temperature and pressure conditions. The average initial natural concentrations (n=60) of soluble Fe, Mn, Ni and Co were 9.54, 1.30, 0.0056, and 0.0021 mg g^{-1} respectively. The immobilization of Mn was observed on the 24 d of incubation with 0.63 mg g^{-1} in G^+ biotic and 0.87 mg g^{-1} in G^- biotic experiments. Beyond which, the rate of Mn immobilization was too fast that it could not be measured as the concentrations dropped beyond the detection limit. But, at the end of 82 d incubation, the mobilization of Mn was evident in the abiotic controls alone. This was evinced by the soluble Mn concentration in the aqueous phase with 0.004 mg g^{-1} in G^+ and 0.032 mg g^{-1} in G^- media (Figure 4.7A). Thus, suggesting immobilization > mobilization in the biotic treatments.

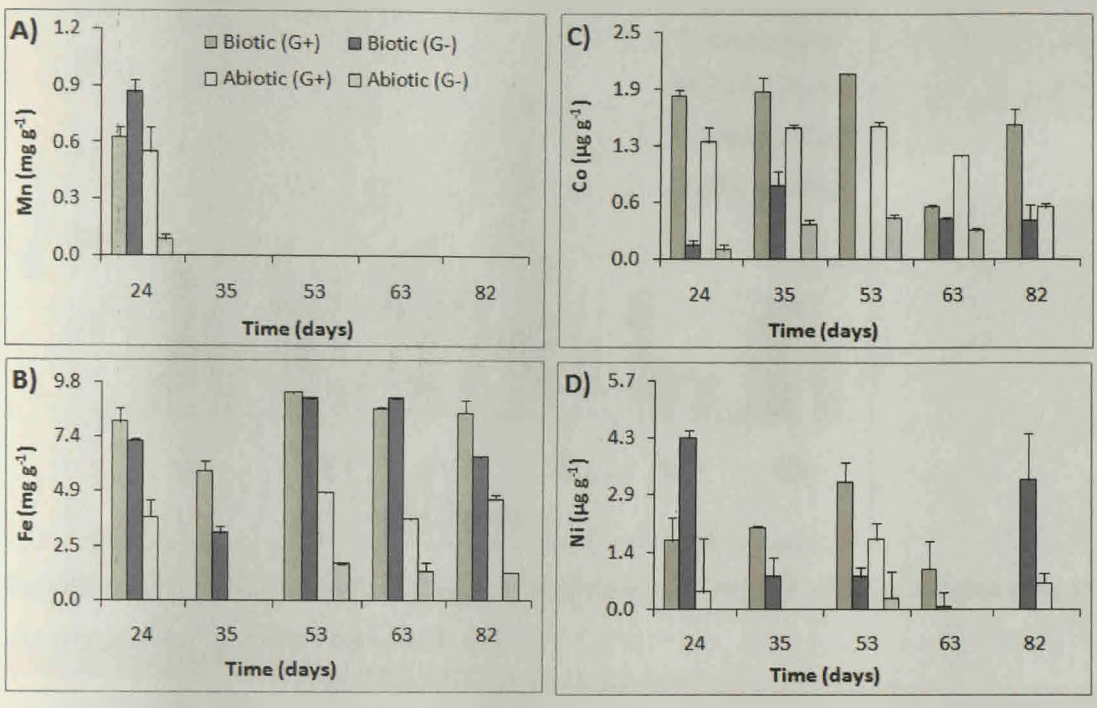

Figure 4.7. Immobilization of metal ions by ferromanganese crust associated microbial communities. A) manganese, B) iron, C) cobalt and D) nickel.

Maximum biotic immobilization of Fe was observed at 53 d of incubation (Figure 4.7B) with 9.34 mg g^{-1} in G^+ and 9.09 mg g^{-1} in G^-. On the other hand, the maximum abiotic immobilization was only 4.86 mg g^{-1} in G^+ and 1.66 mg g^{-1} in G^-. The biotic immobilization of Co was lesser than that of iron. The maximum immobilization of Co was 2.04 µg g^{-1} in G^+ at 53 d of incubation and 0.81 µg g^{-1} in G^- at 35 d of incubation (Figure 4.7C). This coincided with maximum bacterial growth recorded on 53 d of incubation in G^+ and 35 d of incubation in G^- experiments (Figure 4.8). Abiotic immobilization of 1.47 µg g^{-1} of Co in G^+ occurred after 53 d. Unlike Fe and Co, the biotic immobilization of Ni was 3.18 µg g^{-1} after 24 d and was in G^- media (Figure 4.7D). However, the abiotic immobilization of Ni was lesser than the biotic immobilization and showed a maximum of 1.77 µg g^{-1} Ni immobilization in G^+ media after 53 d. Two-way ANOVA showed significant differences ($p < 0.001$) between the biotic and the abiotic sets of incubation for Fe and Co. The gradation in the immobilization of metal ions was Fe > Mn> Ni > Co of their initial concentration. Besides immobilization rates were higher in biotic experiments than the abiotic setups. Microbial growth increased by 1.38 OD_{595} in G^+ and 0.75 OD_{595} in G^- media.

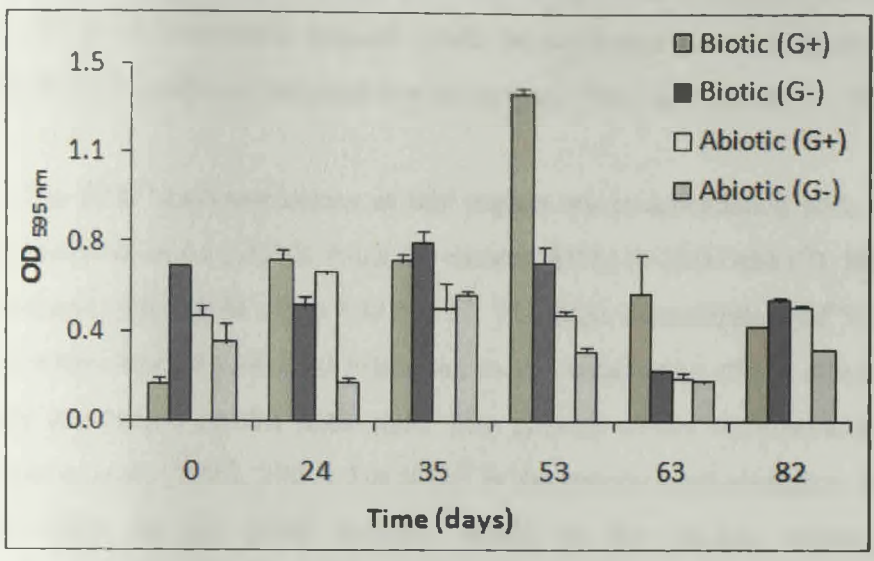

Figure 4.8. Microbial growth response to metal immobilization under simulated near in situ temperature and pressure conditions.

4.5. Discussion

The water column chemistry above the seamount could play a role on the Fe-Mn crust associated processes. The cycling of C, N, S and P within the water column not only affects the water chemistry but also the associated microbial processes occurring on basalt surfaces and vice versa. The requirement of trace metals as cofactors or intermediates in these biogeochemical cycles, couples the geochemistry of several other elements. Further, the oligotrophic nature of the water column and the presence of hydrogenetic metal accretions over the seamount summit make this ecosystem more dynamic and complex. Hence, it would be pertinent to understand the water column chemistry in order to relate it with accretion processes of economically important metals by bacteria that are associated with Fe-Mn crust of the seamount ecosystem.

4.5.1. Geochemical characteristics of the water column

The concentrations of NO_3^-, NO_2^-, and PO_4^{3-} in the surface waters of the seamount and the reference site were in the range reported by Sardessai *et al.* (2010) from the eastern EIO. The ambient NO_3^- concentration was 0.95 nM more at the reference site compared to the seamount site. Presence of a significant relationship between NO_3^- and DO ($r = 0.621$, $p < 0.01$) at the seamount and its absence at the reference station suggest the dependence of nitrification on oxygen supply (Wetzel, 2001) at the former and the

combined influence of biological and hydrodynamic factors at the latter. The depletion of DO at the seamount summit could be attributed to the oxidation of Mn^{2+} forming reactive Mn oxides at the expense of oxygen (Bach and Edwards, 2003).

The SiO_3^{2-} concentrations in this region are in accordance with the values reported by Sardessai *et al.* (2010) from the eastern EIO (10-2300 nM l^{-1}). SiO_3^{2-} concentrations increased with depth up to 600 nM l^{-1}. The high concentration of SiO_3^{2-} recorded at the seamount summit could be attributed to the weathering of the silicates and the type of rock that makes up the seamount. The present results corroborates with the report of Banakar *et al.* (2003, 2007) that SiO_3^{2-} is the second most abundant component after Fe-Mn oxide in the ANS deposit. While in the bottom waters, the high SiO_3^{2-} concentration could be attributed to the inflow of low-silica bottom water which gets enriched as it flows northward into the Northern Indian Ocean (Edmond *et al.*, 1979). The increase in SiO_3^{2-} in the deeper depths could also be an effect of the drop in pH with depth (Palmer *et al.*, 1998). This is evidenced by a negative relationship ($r = -0.479$, $p < 0.05$) between SiO_3^{2-} and pH, therefore corroborating the idea that silica may play a role as a buffering agent (Garrels, 1965). However, SiO_3^{2-} concentration in the reference site was comparatively lower and recorded maximum concentrations of 423.72 nM at 300 m water depth.

The higher concentration of TIC recorded in the surface waters of the seamount station could be attributed to the interaction of the atmosphere with the sea surface. However, in the overlying waters (1500 m) of the seamount summit, high TIC concentrations obtained well above the lysocline (3800 m) in the eastern EIO (Peterson and Prell, 1985) could be due to remobilization or diffusion of the carbonate from the summit into the surrounding sea water. Alternatively, in the reference station TIC concentration was higher at 3000 m water depth closer to the lysocline perhaps due to carbonate dissolution. This diffusion of TIC in the seamount could be influenced by the circulation patterns of different water masses that enter the region from different parts of the ocean (Schott and McCreary, 2001; Matthias and Godfrey, 2003). Similar remobilization of carbonate down the slopes of the seamount influenced by strong currents has been observed by Bostock *et al.* (2011).

4.5.2. Analysis of Fe-Mn crust associated microbial community

There is a lacuna in the studies on the non-culturable bacterial diversity of the hydrogenetic crusts (Kato and Yamagishi, 2011) except for a report from the Pacific (Nitahara *et al.*, 2011). In the Pacific, archaea formed a significant component of the prokaryotic communities in the hydrogenetic crust (Nitahara *et al.*, 2011) which may imply their contribution to Fe-Mn crust accretion. Though the studies by Liao *et al.* (2011) did not examine on crust associated bacteria, the bacterial phylotypes of the sediments around the cobalt-rich crust deposits matched with the bacterial diversity of the present study. However, in the present study the non-parametric diversity index H' of the crust determined at 3% divergence (5.61) showed that bacterial diversity is more than that of hydrogenetic Fe-Mn crust (4.06) and sediments PC-A (4.288), PC-B (4.395) and PC-C (4.294) from the Pacific Ocean (Nitahara *et al.*, 2011; Liao *et al.*, 2011). These differences in the bacterial diversity could be ascribed to the thickness of the crust and its mineral composition. It may also be due to the different techniques used in both these studies for bacterial diversity estimation. Otherwise, additionally, the Pacific crust had lower thickness (~20 mm) and lower enrichment of Mn (16%), Co (0.386%) and Ni (0.209%) as compared to that of ANS having average crust thickness of 1 to 1.5 cm and enrichment of Mn, Co, and Ni in the order of 21.3%, 0.47% and 0.31% respectively (Rajani *et al.*, 2005). However, the present diversity indices agree with the value of 5 and above reported for water samples from the North West Mediterranean Sea using the 454 approach (Pommier *et al.*, 2010). Besides, diversity analysis of the samples using rarefaction curve showed that curves are not saturated. This suggests richer diversity in the sample than that which has been identified. The present result agrees with Sogin *et al.* (2006) on the unprecedented levels of bacterial complexity for marine samples where none have reached the curvilinear or plateau phase.

However, non-parametric richness indices such as Chao1 and ACE calculated at 3% dissimilarity (Table 4.2) showed that bacterial communities in the ANS Fe-Mn crusts were very heterogenous. These results are close to the Chao1 and ACE richness estimates for deep-sea sediments around the cobalt-rich crust deposit region from the Pacific Ocean (Liao *et al.*, 2011). Their study showed Chao1 richness of 499, 548 and

223 OTUs for sediments PC-A, PC-B and PC-C respectively and ACE richness of 392 OTUs for PC-A, 439 OTUs for PC-B and 213 OTUs for PC-C.

Among the different bacterial groups, α- and γ-*Proteobacteria* dominated the hydrogenetic cobalt-rich Fe-Mn crusts of the ANS. They are known to play an ecologically important role in the biogeochemical cycles in the marine environment such as sulfur oxidation, aerobic methane oxidation, and utilization of buried organic matter or dissolved inorganic carbon (Inagaki and Nakagawa, 2008). Additionally, they represent a diverse group of chemolithoautotrophic, heterotrophic, and mixotrophic fractions of physiologically active bacteria in the heavy metal rich environments and marine basalts (Mason *et al.*, 2009; Margesin *et al.*, 2011). Therefore, the observation of α- and γ-*Proteobacteria* in the present study reiterates their tolerance to heavy metals and their ability to survive under nutrient poor conditions. Our results corroborate with a study by Nitahara *et al.* (2011) on the occurrence of γ-*Proteobacteria* in the hydrogenetic Fe-Mn crusts of Takuyo-Daigo Seamount, northwest Pacific.

4.5.2.1. γ-Proteobacteria

The members of the γ-Proteobacterial group consisted of heterotrophs like *Halomonas, Idiomarina,* and *Alcanivorax* and chemoheterotrophs like *Methylophaga, Thiomicrospira,* and *Marinobacter,* all of which are important in oceanic biogeochemical cycling. *Halomonas* was the most predominant among the γ-Proteobacterial group. This genus had been detected by several researchers using culture dependent methods in elevated concentrations of Fe(II) and Mn(II) (Kaye and Baross, 2000; Edwards *et al.*, 2003; Templeton *et al.*, 2005; Fernandes *et al.*, 2005). Additionally, this genus also showed their potential for immobilization of Mn, Ni and Co under low nutrient availability (Fernandes *et al.*, 2005; Sujith *et al.*, 2010; Antony *et al.*, 2011). Further, Martinez *et al.* (2000) and Edwards *et al.* (2004) reported them to produce self-assembling amphiphilic siderophores and partake in Fe-oxidation in the lithoautotrophic mode respectively. Thus, the above characteristics of *Halomonas* contribute to its significant role in the redox cycling of Mn and Fe in the Fe-Mn crust environment by adapting to low nutrient conditions.

Besides *Halomonas*, *Idiomarina* a heterotrophic iron oxidizing prokaryote similarly

enzyme machinery for the detoxification of heavy metals (Hou *et al.*, 2004). The siderophore production could allow them to solubilize, capture, and deliver Fe to the cells (Sandy and Butler, 2009) under nutrient depleted conditions and thus mediate the oxidative precipitation of iron (oxy)hydroxides. Also, the predominance of *Idiomarina* in the Fe-Mn crust and the low level of NO_3^- in water overlying the seamount summit make it tempting to speculate that NO_3^- may serve as a terminal electron acceptor in Fe oxidation. It coincides with the study of Straub *et al.* (1996) on the NO_3^- dependent microbial oxidation of ferrous iron. Additionally, a marine petroleum oil-degrading bacterium *Alcanivorax* known for alkane metabolism (Sabirova *et al.*, 2006) was also present in the Fe-Mn crust. The presence of *Alcanivorax* in the seamount environment may be due to their role in Mn cycling as was reported in Arctic sediments (Xuezheng *et al.*, 2008).

Apart from the heterotrophic bacteria, other groups like the chemoheterotrophs influence the biogeochemical nature of the crust. It is known from earlier studies of Bach and Edwards (2003) and Edwards *et al.* (2004) that under oligotrophic conditions chemosynthesis sustain microbial life at the expense of diverse electron donors available at redox fronts of fractures, seamounts, nodules and crusts. This could be brought about by the potential of pelagic microorganisms like methylotrophs to hydrolyze and to initiate the remineralization of high molecular weight dissolved organic carbon (Arnosti *et al.*, 2005). The predominance of methylotrophs like *Methylophaga* may suggest their role in the metabolism of C1 carbon substrates. Similar role played by these bacteria allowed Neufeld *et al.* (2007) to propose their participation in global carbon cycling. The sulfur-oxidizing chemolithoautotroph *Thiomicrospira* represented the second most dominant genera next to *Halomonas* in the ANS crusts. The occurrence of *Thiomicrospira* could be related to their active role in S cycling in the seamount crust. This S cycling could occur as the basaltic substrate that harbor hydrogenetic Fe-Mn crusts of the ANS, contain average concentration of 0.1 to 0.2% sulfur (unpublished data) and basalts from other regions contain 0.1% sulfur in the form of sulfide (Orcutt *et al.*, 2011). The composition of the microbial communities also varies with age of the seafloor basalts (Santelli *et al.*, 2009). Interestingly, the ANS crust is estimated to be relatively younger in age (5-20 Ma) than crusts from other seamounts of the Pacific (18.5 and 22.3 Ma) (Rajani *et al.*, 2005; Glasby *et al.*, 2010).

crust is estimated to be relatively younger in age (5-20 Ma) than crusts from other seamounts of the Pacific (18.5 and 22.3 Ma) (Rajani *et al.*, 2005; Glasby *et al.*, 2010). Therefore, in the present study our observation of *Thiomicrospira* could be related to the hypothesis of Thorseth *et al.* (2001) that chemolithoautotrophic microorganisms, such as S and Fe oxidizers, colonizes the younger crusts taking advantage of the reduced mineral substrates and oxygen concentrations in the surrounding seawater to fuel metabolic activity while fixing carbon.

Further, in this γ-Proteobacterial group the other major metal oxidizing genera consisted of *Marinobacter,* and an unclassified genus of *γ-Proteobacteria. Marinobacter* represents a moderately halophilic, euryhaline cosmopolitan Fe^{2+} oxidizing facultative chemoautotroph (Kaye *et al.*, 2011). Their occurrence in the Fe-Mn crust may suggest their importance in the oxidation of redox active element Fe^{2+}. Such ability to oxidize iron in *Marinobacter* has therefore been related to the use of ferrous iron as a source of energy (Edwards *et al.*, 2003). Since, the remineralization of phosphorus could occur in tandem with the redox coupling of iron, low PO_4^{3-} concentration in the present study could be attributed to the precipitation or uptake of phosphorous by bacteria. These findings agree with the results of Hirschler *et al.* (1990) and Benzerara *et al.* (2004) on the biologically induced and controlled process of PO_4^{3-} uptake and precipitation of iron oxyhydroxides. The predominance of *γ-Proteobacteria* in the ANS provides a deeper perspective of their physiological potential in rapidly exploiting bioavailable organic matter in the low productive environment and in the colonization of the hydrogenetic Fe-Mn crust.

4.5.2.2. α-Proteobacteria

In addition to γ-Proteobacteria, the predominant α-Proteobacterial members included *Phaeobacter*, *Erythrobacter*, *Sulfitobacter*, *Aurantimonas* and an unidentified genera belonging to the family Rhodobacteraceae. It has been observed by Vandecandelaere *et al.* (2009) and Collins and Nyholm (2011) that the genome of *Phaeobacter* contains the genes necessary for cobalamin synthesis. We attribute the predominance of *Phaeobacter* to their ability to rapidly exploit bioavailable Co required for cobalamin synthesis and to colonize the metal hydroxide surfaces which tend to become more enriched with metal cations over long periods. With the antagonistic mechanism,

Phaeobacter might also play an important role in controlling the distribution and diversity of other bacterial species.

Another member associated with the hydrogenetic Fe-Mn crust was *Erythrobacter* which has the ability to oxidize Mn extracellularly and to produce a Mn oxidizing protein heme peroxidase (Anderson *et al.,* 2009). The Mn oxidizer is capable of oxidizing Mn and is not restricted to one single enzyme but multiple superoxide and peroxidase like enzymes which participate in the indirect oxidation of Mn^{2+} (Learman *et al.,* 2011). Since, NO_3^- contributes to the stability of MnO_2 and also serves as a terminal electron acceptor, it is suggested that, in the ANS crust, Mn oxidation may be closely coupled to the nitrogen cycle. Although highly speculative, the decreased level of NO_3^- in the waters overlying the seamount summit could also be attributed to Mn oxidation. This is in agreement with the results of Vandenabeele *et al.* (1995) on the higher rate of Mn removal by the microbial consortia in the presence of NO_3^- and subsequent accumulation of NO_2^-. Another heterotrophic Mn(II) oxidizing genus *Sulfitobacter* (Eberhard *et al.,* 1995) was also associated with the Fe-Mn crust. These organisms are ubiquitously associated with weathered basalts but are incapable of oxidizing Mn in liquid media (Templeton *et al.,* 2005). This suggests that these organisms are very much confined to hard surfaces wherein they could contribute to the initiation of the primary layer of Mn oxide on basaltic rocks and the subsequent oxidation by other microbes. Similar reasoning may apply for the presence of *Aurantimonas* whose growth is stimulated by Mn (Anderson *et al.,* 2009). They are also known to be important contributors in the cycling of Mn in many environments. These findings may provide indications of a more significant role of bacterial populations belonging to *α-Proteobacteria* in the cycling of Mn in the hydrogenetic Fe-Mn crust.

4.5.2.3. Bacteroidetes

Besides, the next dominant group was *Bacteroidetes* which contained an unidentified genus belonging to the family Flavobacteriaceae. Significant numbers of these bacteria have also been detected in oligotrophic marine surface waters (Gomez-Pereira *et al.,* 2010) and are known to oxidize Mn in caves and acid mine drainage water (Santelli *et al.,* 2010; Carmichael *et al.,* 2013). Earlier study with Flavobacterial

strains CC10a and CC23b isolated from Fe-Mn crusts of the present study site have shown their capacity to tolerate high concentrations of cobalt (Krishnan *et al.*, 2006). Having identified the potential of this bacterial family in tolerating high concentration of Co, it is suggested that they could be candidate organisms for metal accretion in the Fe-Mn crust.

4.5.3. Immobilization of metals by the Fe-Mn crust associated microbial community

Many experimental studies with bacterial isolates have demonstrated their capability of Fe and Mn oxidation (Konhauser, 1998; Sujith and Loka Bharathi, 2011) as well as the weathering of rock baring minerals (Fein *et al.*, 1999; Daughney *et al.*, 2004). Nonetheless, till date no evidence exists on the contribution of indigenous microbial community to the crust genesis that simulates the *in situ* conditions of temperature and pressure. In the present study, the microbial community of the crust, immobilized metal ions at a greater rate than abiotic immobilization in the order of Fe > Mn > Ni > Co. This sequence of metal immobilization suggests the vacancy of surface binding sites available for adsorption of the soluble metal ions at the mineral/bacterial surface (Kennedy *et al.*, 2003). By virtue of its composition the bacterial wall carries a net negative charge that makes the bacterial surface anionic and helps them bind several metal cations with higher affinity. The binding of one such metal cation, for example iron, by bacteria couples the reduction of Fe(III) to the oxidation of organic carbon. The reduced Fe could further oxidize leading to the formation of different mineral types that vary in their composition (Zegeye *et al.*, 2010). Therefore, microbial participation in the redox cycling of metal ions controls the fate of several other associated elements. The present results showed both a increase and a decrease in soluble metal concentration during the periods of incubation. This suggests that metal oxidation and reduction could be closely coupled, occurring concomitantly in meeting the energy requirement for catalysing cells, other metabolic functions and as a process of active efflux to avoid metal toxicity. Metal adsorption by Fe-Mn crust in the biotic experiments was always greater than that of the abiotic control. This difference could be ascribed to the ability of bacteria to bind metals and participate in the biogeochemical cycling of different elements under nutrient poor conditions. The widespread distribution of bacteria and their ability to adapt with change in environmental conditions makes them the most successful life-forms to have ever

inhabited the earth (Ferris and Beveridge, 1985). The difference in the immobilization of one metal with that of the other suggests that bacterial uptake and sequestration not only depends on the availability of energy but also on the soluble metal concentration, toxicity of the metal, ionic radius of the metal and the microorganisms that are involved. The energy can be in the form of organic carbon for the heterotrophic and inorganic for the autotrophic microorganisms.

The results of the present study emphasize the significance of microbial activity in hydrogenetic Fe-Mn crust accretion. This has been shown by significant differences ($p < 0.001$) between the biotic and abiotic immobilization and in the physico-chemical parameters between the seamount and the reference site. The low primary productivity, higher bacterial production (Fernandes *et al.*, 2008) and the predominance of γ- and α-Proteobacteria in the hydrogenetic Fe-Mn crusts suggests that heterotrophic metabolism is the most dominant process occurring in the ANS. The present results agree with Duarte *et al.* (2013) where they have elaborated, based on *in vitro* and *in situ* studies, that oligotrophic deep-sea environments like ANS are net heterotrophic with a higher bacterial respiration rate and are a source for CO_2.

In the nutrient poor environments like the EIO heterotrophic activity could be subsidized by organic carbon inputs from mixotrophic metabolic pathways by *Methylophaga* and *Thiomicrospira,* or other similar organisms, which are associated with the Fe-Mn crust of the ANS. Comparison of the current results with earlier reports on hydrothermal sites suggests a typical shift in bacterial diversity between the two environments. The γ- and α-*Proteobacteria* are more dominant in hydrogenetic crusts while ε-and ζ-*Proteobacteria* dominate the hydrothermal Fe-Mn crusts. The greater abundance and diversity of metal oxidizing bacterial forms of the γ- and α-Proteobacterial groups suggests their versatility in scavenging and oxidizing multiple elements from the seawater and their probable participation in Fe and Mn cycling. This could fuel the microbial energy flow and the elemental cycling occurring over the ANS crust. Thus, it is inferred that the activity of the bacterial community of the Fe-Mn crusts contributes to its accretion with different bacterial groups mediating different degrees of metal immobilization during periods of oligotrophy when organic rains from water column above is minimal.

4.6. References

Aldrich AP, van den Berg CMG. 1998. Determination of Fe and its redox speciation in seawater using catalytic cathodic stripping voltammetry. Electroanalysis 10: 369-373.

Aminot A, Kerouel R, Coverly SC. 2009. Nutrients in seawater using segmented flow analysis. In: Practical guidelines for the analysis of seawater. Wurl O (ed) CRC Press, New York, pp.143-178.

Anderson CR, Johnson HA, Caputo N, Davis RE, Torpey JW, Tebo BM. 2009. Mn(II) Oxidation is Catalyzed by Heme Peroxidases in "*Aurantimonas manganoxydans*" Strain SI85-9A1 and *Erythrobacter* sp. Strain SD-21. Appl Environ Microbiol 75: 4130-4138.

Antony R, Sujith PP, Fernandes SO, Verma P, Khedekar VD, Loka Bharathi PA. 2011. Cobalt immobilization by manganese oxidizing bacteria from the Indian Ridge System. Curr Microbiol 62: 840-849.

Arnosti C, Durkin S, Jeffrey WH. 2005. Patterns of extracellular enzyme activities among pelagic marine microbial communities: implications for cycling of dissolved organic carbon. Aquat Microb Ecol 38: 135-145.

Bach W, Edwards K. 2003. Iron and sulphide oxidation within the basaltic ocean crust: implications for chemolithoautotrophic microbial biomass production. Geochim Cosmochim Acta 67: 3871-3887.

Banakar VK, Galy A, Sukumaran NP, Parthiban G, Volvaiker AY. 2003. Himalayan sedimentary pulses recorded by silicate detritus within a ferromanganese crust from the Central Indian Ocean. Earth Planet Sci Lett 205: 337-348.

Banakar VK, Hein JR, Rajani RP, Chodankar AR. 2007. Platinum group elements and gold in ferromanganese crusts from Afanasiy–Nikitin seamount, equatorial Indian Ocean: Sources and fractionation. J Earth Syst Sci 116: 3-13.

Banakar VK, Pattan JN, Mudholkar AV. 1997. Palaeoceanographic conditions during the formation of ferromanganese crust from the Afanasiy Nikitin seamount, north central Indian Ocean-geochemical evidence. Mar Geol 136: 299-315.

Banakar VK. 2010. Deep-sea ferromanganese deposits and their resource potential for India. J Indian Inst Sci 90: 535-541.

Benzerara K, Menguy N, Guyot F, Skouri F, de Luca G, Barakat M, Heulin T. 2004. Biologically controlled precipitation of calcium phosphate by *Ramlibacter tataouinensis*. Earth Planet Sci Lett 228: 439-449.

Bostock HC, Hayward BW, Neil HL, Currie K, Dunbar GB. 2011. Deep-water carbonate concentrations in the southwest Pacific. Deep-Sea Res 58: 72-85.

Carmichael MJ, Carmichael SK, Santelli CM, Strom A, Brauer SL. 2013. Mn(II)-oxidizing bacteria are abundant and environmentally relevant members of ferromanganese deposits in caves of the upper Tennessee River Basin. Geomicrobiol J DOI:10.1080/01490451.2013.769651.

Clark MR, Rowden AA, Schlacher T, Williams A, Consalvey M, Stocks KI, Rogers AD, O'Hara TD, White M, Shank TM, Hall-Spencer JM. 2010.The Ecology of Seamounts: Structure, Function, and Human Impacts. Ann Rev Mar Sci 2: 375-400.

Collins AJ, Nyholm SV. 2011. Draft Genome of *Phaeobacter gallaeciensis* ANG1, a Dominant Member of the Accessory Nidamental Gland of *Euprymna scolopes.* J Bacteriol 193: 3397-3398.

Colombini MP, Fuoco R. 1983. Determination of manganese at ng/ml levels in natural waters by differential pulse polarography. Talanta 30: 901-905.

Daughney CJ, Rioux J-P, Fortin D, Pichler T. 2004. Laboratory Investigation of the Role of Bacteria in the Weathering of Basalt Near Deep Sea Hydrothermal Vents. Geomicrobiol J 21: 21-31.

Duarte CM, Regaudie-de-Gioux A, Arrieta JM, Delgado-Huertas A, Agusti S. 2013. The Oligotrophic Ocean Is Heterotrophic. Ann Rev Mar Sci 5: 18.1-18.19.

Eberhard C, Wirsen CO, Jannasch HW. 1995. Oxidation of polymetal sulfides by chemolithoautotrophic bacteria from deep-sea hydrothermal vents. Geomicrobiol J 13: 145-164.

Edmond JM, Jacobs SS, Gordon AL, Mantyla AW, Weiss RF. 1979. Water column anomalies in dissolved silica over opaline pelagic sediments and the origin of the deep silica maximum. J Geophys Res 84: 7809-7826.

Edwards KJ, Bach W, McCollom TM. 2004. Neutrophilic iron oxidizing bacteria in the Ocean: their habitats, diversity, and roles in mineral deposition, rock alteration, and biomass production in the deep-sea. Geomicrobiol J 21: 393-404.

Edwards KJ, Bach W, Rogers DR. 2003. Geomicrobiology of the Ocean Crust: A Role for Chemoautotrophic Fe-Bacteria. Biol Bull 204: 180-185.

Ehrlich HL, Newman DK. 2009. Geomicrobiology. Taylor and Francis Group, CRC Press, Boca Raton.

Emerson D, Moyer CL. 2010. Microbiology of seamounts: Common patterns observed in community structure. Oceanography 23: 148-163.

Fein JB, Brady PV, Jain JC, Dorn RI, Lee J-U. 1999. Bacterial effects on the mobilization of cations from a weathered Pb-contaminated andesite. Chem Geol 158: 189-202.

Fernandes SO, Krishnan KP, Khedekar VD, Loka Bharathi PA. 2005. Manganese oxidation by bacterial isolates from the Indian Ridge System. Biometals 18 : 483-492.

Fernandes V, Rodrigues V, Ramaiah N, Paul JT. 2008. Relevance of bacterioplankton abundance and production in the oligotrophic equatorial Indian Ocean. Aquatic Ecology 42: 511-519.

Ferris FG, Beveridge TJ. 1985. Functions of Bacterial Cell Surface Structures. BioSci 35: 172-177.

Garrels RM. 1965. Silica: Role in the Buffering of Natural waters. Science 148: 69.

Glasby GP, Mountain B, Vineesh TC, Banakar VK, Rajani R, Ren X. 2010. Role of Hydrology in the Formation of Co-rich Mn Crusts from the Equatorial N Pacific, Equatorial S Indian Ocean and the NE Atlantic Ocean. Resour Geol 60: 165-177.

Gomez-Pereira PR, Fuchs BM, Alonso C, Oliver MJ, van Beusekom JEE, Amann R. 2010. Distinct *Flavobacterial* communities in contrasting water masses of the North Atlantic Ocean. ISME J 4: 472-487.

Halbach P, Schwarz-Schampera U, Marbler H. 2008. Platinum and some other trace metals in ferromanganese crusts - Geochemical models to explain contradictions. In: Marine Minerals: Technological Solutions and Environmental Challenges. Mississippi, USA.

Hein JR, Koschinsky A, Bau M, Manheim FT, Kang JK, Roberts L. 2000. Cobalt rich ferromanganese crusts in the Pacific. In: Handbook of Mineral Deposits. Cronan DS (ed) CRC, Boca Raton, pp. 239-279.

Hein JR, Koschinsky A, Halbach P, Manheim FT, Bau M, Kang JK, Lubick N. 1997. Iron and manganese oxide mineralization in the Pacific. Geol Soc London Spl Publ 119, 123-138.

Hein JR, Koschinsky A, Halliday AN. 2003. Global occurrence of tellurium-rich ferromanganese crusts and a model for the enrichment of tellurium. Geochim Cosmochim Acta 67: 1117-1127.

Herrera-Melian JA, Dona-Rodriguez JM, Hernandez-Brito J, Pena JP. 1997. Voltammetric determination of Ni and Co in water samples. J Chem Educ 74: 1444-1445.

Hirschler A, Lucas J, Hubert J-C. 1990. Bacterial involvement in apatite genesis. FEMS Microbiol Ecol 73: 211-220.

Hou S, Saw JH, Lee KS, Freitas TA, Belisle C, Kawarabayasi Y, Donachie SP, Pikina A, Galperin MY, Koonin EV, Makarova KS, Omelchenko MV, Sorokin A, Wolf YI, Li QX, Keum YS, Campbell S, Denery J, Aizawa S, Shibata S, Malahoff A, Alam M. 2004. Genome sequence of the deep-sea γ-*proteobacterium Idiomarina loihiensis* reveals amino acid fermentation as a source of carbon and energy. Proc Natl Acad Sci USA 101: 18036-18041.

Huber JA, Mark-Welch DB, Morrison H, Huse SM, Neal PR, Butterfield DA, Sogin ML. 2007. Microbial population structures in the deep marine biosphere. Science 318: 97-100.

Huse SM, Dethlefsen L, Huber JA, Welch DM, Relman DA, Sogin ML. 2007. Exploring Microbial Diversity and Taxonomy Using SSU rRNA Hypervariable Tag Sequencing. PLoS Genetics 4: e1000255.

Inagaki F, Nakagawa S. 2008. Spatial distribution of the subseafloor life: diversity and biogeography. In: Links between geological processes, microbial activities and evolution of life. Dilek Y, Furnes H, Muehlenbachs K (eds) Springer Publications, UK, pp. 135-158.

Johnson KM, King AE, Sieburth JM. 1985. Coulometric TCO_2 analyses for marine studies; an introduction. Mar Chem 16: 61-82.

Kappler A, Schink B, Newman DK. 2005. Fe(III) mineral formation and cell encrustation by the nitrate-dependent Fe(II)-oxidizer strain BoFeN1.Geobiology 3: 235-245.

Kato C. 2012. Microbiology of piezophiles in deep-sea environments. In: Extremophiles: Microbiology and Biotechnology. Anitori RP (ed) Caister Academic Press, UK, pp. 53-75.

Kato S, Yamagishi A. 2011. Microbial Biodiversity and Biogeography on the Deep Seafloor. In: Changing Diversity in Changing Environment. Grillo O, Venora G (eds) InTech, pp. 357-374.

Kaye JZ, Baross JA. 2000. High incidence of halotolerant bacteria in Pacific hydrothermal-vent and pelagic environments. FEMS Microbiol Ecol 32: 249-260.

Kaye JZ, Sylvan JB, Edwards KJ, Baross JA. 2011. *Halomonas* and *Marinobacter* ecotypes from hydrothermal vent, subseafloor and deep-sea environments. FEMS Microbiol Ecol 75: 123-133.

Kennedy CB, Martinez RE, Scott SD, Ferris FG. 2003. Surface chemistry and reactivity of bacteriogenic iron oxides from Axial Volcano, Juan de Fuca Ridge, north-east Pacific Ocean. Geobiology 1: 59-69.

Konhauser KO. 1998. Diversity of bacterial iron mineralization. Earth-Sci Rev 43: 91-121.

Koschinsky A, Hein JR. 2003. Uptake of elements from seawater by ferromanganese crusts: solid-phase associations and seawater speciation. Mar Geol 198: 331-351.

Krishnan KP, Fernandes CEG, Fernandes SO, Loka Bharathi PA. 2006. Tolerance and immobilization of cobalt by some bacteria from ferromanganese crusts of the Afanasiy Nikitin Seamounts. Geomicrobiol J 23: 31-36.

Learman DR, Voelker BM, Vazquez-Rodriguez AI, Hansel CM. 2011. Formation of manganese oxides by bacterially generated superoxide. Nature Geosci 4: 95-98.

Ledin M. 2000. Accumulation of metals by microorganisms-processes and importance for soil systems. Earth-Sci Rev 51: 1-31.

Liao L, Xu X, Jiang X, Wang C, Zhang D, Ni J, Wu M. 2011. Microbial diversity in deep-sea sediment from the cobalt-rich crust deposit region in the Pacific Ocean. FEMS Microbiol Ecol 78: 565-585.

Luptakova A, Macingova E, Slesarova A, Ubaldini S, Abbruzzese C. 2007. Solubilization and immobilization of toxic metals by bacteria. In: IMWA

Symposium: Water in Mining Environments. Cidu R, Frau F (eds) Cagliari, Italy, pp. 1-3.

Mahoney JJ, White WM, Upton BGJ, Neal CR, Scrutton RA. 1996. Beyond EM-1: Lavas from Afanasy-Nikitin Rise and the Crozet Archipelago, Indian Ocean. Geology 24: 615-618.

Margesin R, Płaza GA, Kasenbacher S. 2011. Characterization of bacterial communities at heavy-metal-contaminated sites. Chemosphere 82: 1583-1588.

Martinez JS, Zhang GP, Holt PD, Jung HT, Carrano CJ, Haygood MG, Butler A. 2000. Self-assembling amphiphilic siderophores from marine bacteria. Science 287: 1245-1247.

Mason OU, Di Meo-Savoie CA, Van Nostrand JD, Zhou J, Fisk MR, Giovannoni SJ. 2009. Prokaryotic diversity, distribution, and insights into their role in biogeochemical cycling in marine basalts. ISME J 3: 231-242.

Matthias T, Godfrey JS. 2003. Hydrology of the Indian Ocean. In: Regional Oceanography: An Introduction. Daya Publishing House, New Delhi, pp. 199-213.

Morel FMM, Price NM. 2003. The biogeochemical cycles of trace metals in the oceans. Science 300: 944-947.

Nath BN, Pluger WL, Roelandts I. 1997. Geochemical constraints on the hydrothermal origin of ferromanganese encrustations from the Rodriguez Triple Junction, Indian Ocean. Geol Soc London Spl Publ 119: 199-211.

Neufeld JD, Schafer H, Cox MJ, Boden R, McDonald IR, Murrell JC. 2007. Stable-isotope probing implicates *Methylophaga* spp and novel Gammaproteobacteria in marine methanol and methylamine metabolism. ISME J 1: 480-491.

Nitahara S, Kato S, Urabe T, Usui A, Yamagishi A. 2011. Molecular characterization of the microbial community in hydrogenetic ferromanganese crusts of the Takuyo-Daigo Seamount, northwest Pacific. FEMS Microbiol Lett 321: 121-129.

Orcutt BN, Sylvan JB, Knab NJ, Edwards KJ. 2011. Microbial Ecology of the Dark Ocean above, at, and below the Seafloor. Microbiol Mol Biol Rev 75: 361-422.

Palmer MR, Pearson PN, Cobb SJ. 1998. Reconstructing Past Ocean pH-Depth Profiles. Science 282: 1468-1471.

Parthiban G, Banakar VK. 1999. Chemistry and possible resource potential of cobalt-rich ferromanganese crusts from Afanasiy-Nikitin Seamount in the Indian Ocean. Indian Mineralogist 33: 125-132.

Peterson LC, Prell WL. 1985. Carbonate dissolution in recent sediments of the Eastern Equatorial Indian Ocean: preservation patterns and carbonate loss above the lysocline. Mar Geol 64: 259-290.

Pommier T, Neal PR, Gasol JM, Coll M, Acinas SG, Pedrós-Alió C. 2010. Spatial patterns of bacterial richness and evenness in the NW Mediterranean Sea explored by pyrosequencing of the 16S rRNA. Aquat Microb Ecol 61: 221-233.

R Development Core Team. 2009. R: A language and environment for statistical computing. In: R Foundation for Statistical Computing, Vienna, Austria. ISBN 3-900051-07-0: (http://www.R-project.org/).

Rae ICM, Celo JS. 1975. Influence of colloidal iron on the respiration of a species of the genus *Acinetobacter*. Appl Microbiol 29: 837-840.

Rajani RP, Banakar VK, Parthiban G, Mudholkar AV, Chodankar AR. 2005. Compositional variation and genesis of ferromanganese crusts of the Afanasiy-Nikitin Seamount, Equatorial Indian Ocean. J Earth Syst Sci 114: 51-61.

Sabirova JS, Ferrer M, Regenhardt D, Timmis KN, Golyshin PN. 2006. Proteomic Insights into Metabolic Adaptations in *Alcanivorax borkumensis* Induced by Alkane Utilization. J Bacteriol 188: 3763-3773.

Sandy M, Butler A. 2009. Microbial Iron Acquisition: Marine and Terrestrial Siderophores. Chem Rev 109: 4580-4595.

Santelli CM, Edgcomb VP, Bach W, Edwards KJ. 2009. The diversity and abundance of bacteria inhabiting seafloor lavas positively correlate with rock alteration. Environ Microbiol 11: 86-98.

Santelli CM, Pfister DH, Lazarus D, Sun L, Burgos WD, Hansel CM. 2010. Promotion of Mn (II) oxidation and remediation of coal mine drainage in passive treatment systems by diverse fungal and bacterial communities. Appl Environ Microbiol 76: 4871-4875.

Sardessai S, Shetye S, Maya MV, Mangala KR, Prasanna Kumar S. 2010. Nutrient characteristics of the water masses and their seasonal variability in the eastern equatorial Indian Ocean. Mar Environ Res 70: 272-282.

Schott FA, McCreary Jr JP. 2001. The monsoon circulation of the Indian Ocean. Prog Oceanogr 51: 1-123.

Sly LI, Arunpairojana V, Dixon DR. 1990. Binding of Colloidal MnO_2 by Extracellular Polysaccharides of *Pedomicrobium manganicum*. Appl Environ Microbiol 56: 2791-2794.

Sogin ML, Morrison HG, Huber JA, Welch DM, Huse SM, Neal PR, Arrieta JM, Herndl GJ. 2006. Microbial diversity in the deep sea and the underexplored "rare biosphere". Proc Natl Acad Sci USA 103: 12115-12120.

Straub KL, Benz M, Schink B, Widdel F. 1996. Anaerobic, nitrate-dependent microbial oxidation of ferrous iron. Appl Environ Microbiol 62: 1458-1460.

Strickland JDH, Parsons TR. 1968. A Practical Handbook of Sea Water Analysis. Fisheries Research Board of Canada, Bulletin No. 167, pp. 71–80.

Sujith PP, Khedekar VD, Girish AP, Loka Bharathi PA. 2010. Immobilization of Nickel by Bacterial Isolates from the Indian Ridge System and the Chemical Nature of the Accumulated Metal. Geomicrobiol J 27: 424-434.

Sujith PP, Loka Bharathi PA. 2011. Manganese oxidation by bacteria: biogeochemical aspects. Prog Mol Subcell Biol 52: 49-76.

Tebo BM, Johnson HA, McCarthy JK, Templeton AS. 2005. Geomicrobiology of manganese(II) oxidation. Trends Microbiol 13: 421-428.

Templeton AS, Staudigel H, Tebo BM. 2005. Diverse Mn(II)-Oxidizing Bacteria Isolated from Submarine basalts at Loihi seamount. Geomicrobiol J 22: 127-139.

Thorseth IH, Torsvik T, Furnes H, Muehlenbachs K. 1995. Microbes play an important role in the alteration of oceanic crust. Chem Geol 126: 137-146.

Thorseth IH, Torsvik T, Torsvik V, Daae FL, Pedersen RB, Party K-S. 2001. Diversity of life in ocean floor basalt. Earth Planet Sci Lett 194: 31-37.

Usui A, Someya M. 1997. Distribution and composition of marine hydrogenetic and hydrothermal manganese deposits in the northwest Pacific. Geol Soc London Spl Publ 119: 177-198.

Vandecandelaere I, Segaert E, Mollica A, Faimali M, Vandamme P. 2009. *Phaeobacter caeruleus* sp. nov., a blue-coloured, colony-forming bacterium isolated from a marine electroactive biofilm. Int J Syst Evol Microbiol 59: 1209-1214.

Vandenabeele J, De Beer D, Germonpre R, Van de Sande R, Verstraete W. 1995. Influence of nitrate on manganese removing microbial consortia from sand filters. Water Res 29: 579-587.

Wetzel RG. 2001. Limnology: lake and river ecosystems. San Diego: Academic Press.

Whitman WB, Coleman DC, Wiebe WJ. 1998. Prokaryotes: The unseen majority. Proc Natl Acad Sci USA 95: 6578-6583.

Xuezheng L, Aiguo G, Haowen C. 2008. Isolation and phylogenetic analysis of cultivable manganese bacteria in sediments from the Arctic Ocean. Acta Ecol Sin 28: 6364-6370.

Zegeye A, Mustin C, Jorand F. 2010. Bacterial and iron oxide aggregates mediate secondary iron mineral formation: green rust versus magnetite. Geobiology 8: 209-222.

Zhou J, Bruns MA, Tiedje JM. 1996. DNA recovery from soils of diverse composition. Appl Environ Microbiol 62: 316-322.

CHAPTER 5

Bacterial cycling of cobalt and nickel in Fe-Mn crust: influence of EDTA and Ascorbate

5.1. Abstract

The reason for the presence of particular organisms in a specific environment is an important ecological issue. Since an organisms environment has both abiotic and biotic components this chapter addresses the process that affects the biotic and the abiotic constituents of the crust. Organic and inorganic complexing agents derived from natural and/or anthropogenic activities influence the bioavailability/speciation of trace metals in the marine environment. The complexation of trace metals could have a beneficial or harmful effect on the metal immobilizing/mobilizing activity of bacteria. In the present study, the effect of model compounds like ascorbate (1mM), EDTA (1mM) and glucose (0.1%) on the biogenic cycling of Co and Ni in the hydrogenetic Fe-Mn crust was studied. Results of the study with EDTA and Fe-Mn crust isolates showed mobilization for Co and immobilization for Ni depending on the reactivity of EDTA for the corresponding metals. However, in the presence of the bacterial isolate ANS-05Co, the EDTA related mobilization of Co was lesser than that by EDTA alone suggesting immobilization. The maximum immobilization of Co in the absence and Ni in the presence of added glucose (0.1%) was 4.5±0.98 and 9.5±0.01 $\mu g\ g^{-1}$ respectively with isolate ANS-05Co. The result suggests that metal chelation by EDTA lead to the reduction in toxicity of Co and Ni to bacteria and also toxicity exerted by EDTA on bacteria. On the other hand, ascorbate an organic reductant of metal oxides promoted the chemical mobilization of Co and Ni from the Fe-Mn crusts. However, the ascorbate related maximum mobilization of Co of 5.24±0.01 $\mu g\ g^{-1}$ with isolate ANS-05Co was enhanced in the absence of added glucose. With isolate ANS-05Co, the mobilization of Ni was lesser than that of ascorbate suggesting immobilization. With isolate ANS-28Ni the net process was immobilization with a maximum of 1.72±0.03 $\mu g\ g^{-1}$ in the absence of added glucose. The ability of ascorbate to discriminate the bound form of metal from their oxidized forms could be attributed to the difference in the chemical cycling of Co versus Ni. On the other hand, the difference in the bacterial cycling of the metals could be due to the difference in the form of association of Co and Ni with the Fe-Mn oxide

phase of the crust where the former is usually bound in the +III oxidation state compared to that of the latter in the +II oxidation state. Besides, the immobilization of Co by Fe-Mn crust associated microbial communities was maximum at 165.96 μg g^{-1} in the absence of added glucose at 4±1°C and 479.75 μg g^{-1} in the presence (0.1%) of added glucose at 28±2°C. With Ni, immobilization occurred in the absence of added glucose whereas mobilization dominated in the presence of added glucose at both the temperatures with maximum immobilization of 1.89 μg g^{-1} and mobilization of 51.28 μg g^{-1} at 4±1°C. The results indicated that bacteria accelerate the immobilization of Co and Ni in the Fe-Mn crust at 4±1°C. Though Ni is influenced more by organic carbon and closely related to Co in its chemical and biochemical properties Ni differed in its affinity for organic carbon and consequently affected its interactions with Fe-Mn crust associated bacteria.

5.2. Introduction

Several trace metals are essential for bacteria and phytoplankton growth like Fe, Mn, Co, Ni, Cu, and Zn in the marine environment. However, studies are mostly concerned on the role of Fe and Mn in nature because of their global importance in biogeochemical cycling. Cobalt an essential element in prokaryotes are generally required in higher concentrations by anaerobes than by aerobes (Santander *et al.*, 1997) and could substitute for zinc in enzymes required for phytoplankton productivity (Price and Morel, 1990; Intwala *et al.*, 2008). On the other hand, Ni is closely related to Co in its chemical and biochemical properties and forms strong complexes with organic matter and iron oxyhydroxides (Nimmo *et al.*, 1989; Donat *et al.*, 1994; Nieminen *et al.*, 2007; Doig and Liber, 2007). The concentrations of these metals vary widely in different ecological niches, with low nanomolar to low micromolar levels. But they are highly enriched in the Fe-Mn crusts with average concentrations of 0.25 and 0.5% respectively (Rajani *et al.*, 2005). Since these metals are precipitated in the adsorbed state with authigenic mineral phases of Fe and Mn, the bacteria associated are more likely to participate in the cycling of Co and Ni.

The bacterial distribution across different geological horizons that hold Fe-Mn mineral deposits shows activities for metal immobilization, mobilization, detoxification and recycling of organic matter. In addition, the oxidation of organic matter by Mn-

oxides represents an important degradative pathway in some environments (Stone and Morgan, 1984). Therefore, interactions between bacteria and Fe-Mn oxides have greater significance in the geochemical cycling of several associated elements in the oceanic realms (Stockdale *et al.,* 2010). Besides, Mn and Fe oxide mineral particles formed by biological or chemical processes may be reduced and dissolved by organic and/or inorganic ligands that are microbially or chemically derived. In bacteria, the functional moieties on their surfaces and other extracellular materials released during growth could act as ligands and/or chelating agents and thereby help them in attaching to the surfaces, alleviating the toxic effect of metals and in the precipitation or dissolution of minerals (Geesey and Jang, 1989; Nealson *et al.,* 1989; Vandevivere and Kirchman, 1993; Gadd, 2009). Therefore, interactions of bacteria and their metabolites with the oxides of Fe and Mn could either increase or decrease their mobility and subsequently their availability and toxicity to other organisms.

The ligands vary widely in their structures and therefore considerably differ in their ability to reduce and dissolve the oxides of Fe and Mn (Stone and Morgan, 1984). On the other hand, the abiotic dissolution of Mn and Fe oxides occur in the presence of inorganic and organic reductants like H_2S, Fe^{2+}, catechol, ascorbate and humic substances (Thamdrup, 2000). It is therefore pertinent to understand the reactivities of organic-inorganic ligands on bacteria and their activity in Fe-Mn mineral rich environments and deduce their effect on the growth and/or dissolution of the mineral oxides. Here, in the present study, EDTA is used as a model compound for a chelating agent/ligand because of its parallel properties to that of naturally occurring organic complexes like EPS (Loaec *et al.,* 1998). Also Fe-Mn crusts have charged surfaces that encompass vital anionic and cationic species of metals, inorganic and organic particles including bacteria and their metabolites, detrital materials, EPS etc., which exhibit properties similar to EDTA. Due to the ability to form strong and stable water soluble complexes with multivalent metals, EDTA improves the solubility of metal ions, maintains the stability of the valence states of the metals through chelation and consequently reduces the toxicity of metals to microorganisms (Brooks *et al.,* 1996). On the other hand, the toxicity of EDTA to bacteria is reduced by the chelation of metals (Bergan *et al.,* 2001; Oviedo and Rodriguez, 2003). Thus, chelation of metals by EDTA leads to reduction in metal toxicity to bacteria and also reduces the toxicity of

EDTA to bacteria. It also affects the environmental mobility of the metals and minimizes their adsorption to soils and sediments (Delegard and Barney, 1983).

In contrast, ascorbate has been used as a model compound for an organic reductant of Fe-Mn oxides. The biological value of ascorbate rests in its ability to serve as a reductant, i.e. to donate electrons (Jacob, 1996). It was used in the present study mainly because of its ability to discriminate the bound form of metals from their oxidized forms by reacting specifically with the oxidized forms (Sunda and Huntsman, 1987; Stone and Morgan, 1984; Moffett, 1994; Lee and Tebo, 1994). It is a non-chelator of metal ions and therefore its presence does not alter or bring about any change in pH and as of that does not affect the adsorption/desorption of soluble or particulate phase of reduced metals. Since, ascorbate is a ubiquitous oligonutrient essential for biological function it is non-toxic to living cells even at very high concentrations (Anderson and Morel, 1982; Hapette and Poulet, 1990). Because, Mn-oxidation demands organic carbon utilization, the environment where Fe-Mn deposits are formed may become oligotrophic. To prove this point glucose was used as a model compound for organic carbon in the present study. Given that glucose could serve as a carbon and energy source for bacteria and at times a reducing agent of Fe and Mn oxides, attention has been paid on their importance in the cycling of Co and Ni. In the marine ecosystems, monomers of carbohydrate like glucose are produced by marine algae (Mopper and Larson, 1978; Mopper *et al.*, 1980) and from in-situ microbial reaction with insoluble organic detritus (Barcelona, 1980).

Therefore, the present study aims to understand the influence of EDTA, ascorbate and glucose on the bacterial cycling of Co and Ni in the Fe-Mn crust. The work examines the efficiencies of two bacterial isolates one that is tolerant to Co (ANS-05Co) and the other that is tolerant to Ni (ANS-28Ni) in immobilizing/mobilizing of Co and Ni in the presence and absence of added glucose amended with EDTA or ascorbate. In the mean while, the study also examines the participation of microbial community associated with the crust in immobilizing/mobilizing of Co and Ni at ambient and above ambient temperatures in the presence and absence of added glucose.

5.3. Materials and methods

5.3.1. Sample characterization

The texture and element composition of the natural oxide coatings on basalt was characterized by SEM and EDS. For SEM analyses, several small rock fragments bearing oxidized coatings having dimensions 0.62-1.7 × 0.52-1.25 mm (n=15) were removed using a sterile scalpel and were firmly fixed on metal stubs using a conductive adhesive. The mounted samples were sputter-coated with Au using a SPI-Module sputter coater. Samples were examined using a JEOL JSM-5800 scanning electron microscope.

The mineralogy of the Fe-Mn oxide was characterized by XRD (Villalobos *et al.*, 2003). For this, oxide coatings were removed from a single larger rock fragment using a scalpel and then powdered using an agate mortar and pestle. The XRD pattern of the oxide was recorded in a Rigaku X-ray powder diffractometer using a monochromatic Cu $K\alpha_1$ radiation (operating at 40 kV and 20 mA) and a scintillation detector. All samples were run in scan mode over a 2θ range of 0-80° with a scanning rate of 1.2° min^{-1}. The interpretation of the peaks was done according to Burns and Burns (1977).

The solid phase concentration of Co, Ni, Mn and Fe in the hydrogenetic Fe-Mn crust was measured from 50mg of the powdered rock fragments after acid digestion (Roy *et al.*, 2007). The determination of the metals was carried out by adsorptive stripping voltammetry in interface with 797 VA computrace (Metrohm, Switzerland) in a differential pulse mode. The procedures followed were as described by Herrera-Melian *et al.* (1997) for Co and Ni, Colombini and Fuoco (1983) for Mn and Aldrich and van den Berg (1998) for Fe.

5.3.2. In vitro experiment with bacterial isolates and EDTA

To examine the hypothesis that EDTA improves bacterial immobilization rates by decreasing the toxicities of heavy metals through chelation the study was carried out in the presence and absence of added EDTA (1mM). Sodium azide poisoned media or heat killed samples served as abiotic controls. Different media used for the experimental incubations (Table 5.1) were prepared in 0.22 μm filtered and autoclaved

deep-sea water unless otherwise specified. To meet the hypothesis, the study was conducted in 100 ml capacity conical flasks containing rock fragments of dimensions 9.068 ± 0.866 × 5.906 ± 0.848 mm (n=13) and 50 ml of sterile medium (Plate 5.1) inoculated with one of the two bacterial isolates, one a cobalt tolerant (ANS-05Co) and other a nickel tolerant (ANS-28Ni). The homogeneity of the sample was maximized by using the fragments from a single large rock fragment. The concentration of soluble Co and Ni was measured in all sets of treatment including controls immediately after the addition of Fe-Mn crust. The day zero measurement was used as a reference to monitor the change in metal concentration. Flasks were incubated at 4±1°C and shaken at 50 rpm. After incubation for 50 d, flasks from experiment and control setups were sacrificed for analyses.

5.3.3. In vitro experiment with bacterial isolates and ascorbate

The *in vitro* experiment to demonstrate the mobilization/immobilization of Co and Ni by bacterial isolates ANS-05Co and ANS-28Ni was conducted in the presence of ascorbate (1mM) as the reductant. Ascorbate was used to discriminate bound form of metals from their oxidized form by reacting specifically with the oxidized forms. Further, it was used because of its abundance in living cells, oxygen scavenging activity and the ability to promote the growth and activity of facultative anaerobes. The experimental setup and the procedures followed were same like that of EDTA and are given in Table 5.2.

5.3.4. In-vitro experiment on Fe-Mn crust with microbial community

The experiment to demonstrate the immobilization of Co and Ni from Fe-Mn crust by bacteria resident on it was conducted in 15 ml screw-capped tubes containing rock fragments of dimensions 0.86-9.07 × 0.85-5.91 mm and 10 ml of liquid medium as given in Table 5.3. The experiment was incubated in triplicate at 4±2°C in the dark for 30 and 50 d. Tubes from experiment and respective controls were sacrificed at the end of incubation for the analyses. The dry weights of the rock fragments were determined after drying to constant weight at 105°C.

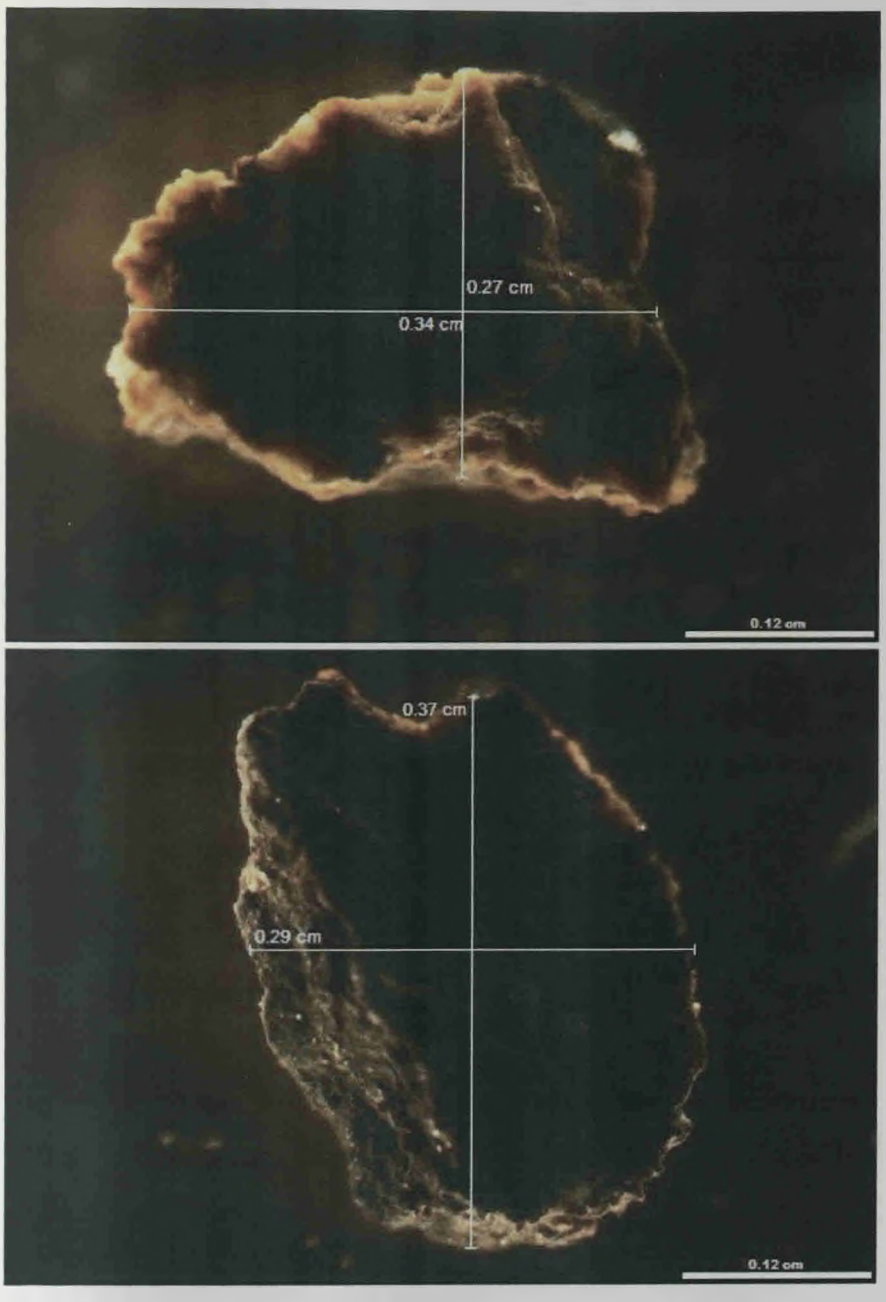

Plate 5.1. Dark field stereo zoom microscope images of Fe-Mn crust fragments used for conducting *in vitro* laboratory experiments.

Table 5.1. Experimental set up on the immobilization/mobilization of Co and Ni from ferromanganese (Fe-Mn) crust with bacterial isolates and EDTA at 4±1°C.

	Blanks*								Chemical*		Abiotic*				Biotic*			
	B1	**B2**	**B3**	**B4**	**B5**	**B6**	**B7**	**B8**	**C1**	**C2**	**A1**	**A2**	**A3**	**A4**	**E1**	**E2**	**E3**	**E4**
Glucose 10% (ml) (final 0.1%)	-	0.5	-	-	0.5	0.5	-	0.5	-	0.5	-	0.5	-	0.5	-	0.5	-	0.5
Azide 1M (ml) (final 15 mM)	-	-	0.75	-	0.75	-	0.75	0.75	-	-	0.75	0.75	0.75	0.75	-	-	-	-
EDTA 1M (ml) (final 1mM)	-	-	-	0.05	-	0.05	0.05	0.05	0.05	0.05	0.05	0.05	0.05	0.05	0.05	0.05	0.05	0.05
Isolate ANS-05Co (ml)	-	-	-	-	-	-	-	-	-	-	0.1	0.1	-	-	0.1	0.1	-	-
Isolate ANS-28Ni (ml)	-	-	-	-	-	-	-	-	-	-	-	-	0.1	0.1	-	-	0.1	0.1
Heat killed crust (g)	-	-	-	-	-	-	-	-	~1	~1	~1	~1	~1	~1	~1	~1	~1	~1
Sterile seawater (ml)	50.0	49.5	49.25	49.95	48.75	49.45	49.2	48.7	49.95	49.45	49.1	48.6	49.1	48.6	49.85	49.35	49.85	49.35
Total volume without crust (ml)	50	50	50	50	50	50	50	50	50	50	50	50	50	50	50	50	50	50

*Tubes incubated in triplicate. Heat killed refers to rock fragments that were steam-sterilized at 15 lbs per in^2 and 121°C for 15 min.

Table 5.2. Experimental set up on the immobilization/mobilization of Co and Ni from ferromanganese (Fe-Mn) crust with bacterial isolates and ascorbate at 4±1°C

	Blanks*								Chemical*		Abiotic*				Biotic*			
	B1	**B2**	**B3**	**B4**	**B5**	**B6**	**B7**	**B8**	**C1**	**C2**	**A1**	**A2**	**A3**	**A4**	**E1**	**E2**	**E3**	**E4**
Glucose 10% (ml) (final 0.1%)	-	0.5	-	-	0.5	0.5	-	0.5	-	0.5	-	0.5	-	0.5	-	0.5	-	0.5
Azide 1M (ml) (final 15 mM)	-	-	0.75	-	0.75	-	0.75	0.75	-	-	0.75	0.75	0.75	0.75	-	-	-	-
Ascorbate 1M (ml) (final 1mM)	-	-	-	0.05	-	0.05	0.05	0.05	0.05	0.05	0.05	0.05	0.05	0.05	0.05	0.05	0.05	0.05
Isolate ANS-05Co (ml)	-	-	-	-	-	-	-	-	-	-	0.1	0.1	-	-	0.1	0.1	-	-
Isolate ANS-28Ni (ml)	-	-	-	-	-	-	-	-	-	-	-	-	0.1	0.1	-	-	0.1	0.1
Heat killed crust (g)	-	-	-	-	-	-	-	-	~1	~1	~1	~1	~1	~1	~1	~1	~1	~1
Sterile seawater (ml)	50.0	49.5	49.25	49.95	48.75	49.45	49.2	48.7	49.95	49.45	49.1	48.6	49.1	48.6	49.85	49.35	49.85	49.35
Total volume without crust (ml)	50	50	50	50	50	50	50	50	50	50	50	50	50	50	50	50	50	50

*Tubes incubated in triplicate. Heat killed refers to rock fragments that were steam-sterilized at 15 lbs per in^2 and 121°C for 15 min.

Table 5.3. Experimental set up on the immobilization/mobilization of Co and Ni from ferromanganese (Fe-Mn) crust with indigenous microbial communities on crust at 4±1°C and 28±2°C.

	Blank*				Controls*		Experiments*	
	B1	**B2**	**B3**	**B4**	**Az1**	**Az2**	**E1**	**E2**
Glucose 10% (ml) (final 0.1%)	-	0.1	-	0.1	-	0.1	-	0.1
Azide 1M (ml) (final 15 mM)	-	-	0.15	0.15	0.15	0.15	-	-
Crust (g)	-	-	-	-	~1	~1	~1	~1
Sterile seawater (ml)	10	9.9	9.85	9.75	9.85	9.75	10	9.9
Total volume without crust (ml)	10	10	10	10	10	10	10	10

*Tubes incubated in triplicate.

5.3.5. Bacterial growth on basalt surfaces

TC for each sample was determined on sonication both before and after incubation (Sujith *et al.,* 2014). A Vibra Cell™ generator Model VC50 (Sonics and Materials Inc., Danbury, C.T. USA) with a high power level ultrasonic probe (Model ASI) having a standard 3.2 mm diameter titanium tip was used for the ultrasonication of the samples. The volumes of the media containing basalt fragments were kept constant at 5 ml in sterile glass vials, and the probe tip was kept 1 cm above from the bottom of the tube. The sample tubes were precooled at 4±1 °C and then packed in crushed ice during sonication to dissipate heat. Sonication was carried out at 15 Hz for 15 s in bursts of 5 s with intermittent cooling for 10 s in crushed ice. The cells were counted from 20 µl aliquots of the sonicated samples immediately using the Neubauer counting chamber or were preserved with 2% final concentration of buffered formalin prior to counting. For every sample, 50 small squares at 400X magnification were counted using a Nikon 50i bright field microscope (Tokyo, Japan) for determining the average number of cells.

5.3.6. pH and Eh

The pH measurements were carried out using Thermo Orion Triode 3-in-1 pH electrode and Eh (mV) using Thermo Orion Epoxy body sure flow, combination redox/ORP electrode (Sujith *et al.,* 2014). The above electrodes were calibrated using

reference solutions prior to measurements to ensure accurate readings. The calibration of the pH meter (Thermo Orion 3-star benchtop pH/mV/Temp. Meter) was as per the protocol given in user's guide, Thermo Electron Corporation (2005). The calibration for pH was done using buffer solutions of known pH 4, 7 and 10. For Eh, the potential of the platinum (Pt) electrode versus the Ag/AgCl reference electrode with KCl electrolyte in ZoBell's solution was measured as a function of temperature. The mV readings of the samples were made for 60 s followed by pH in triplicates. Eh values were calculated as described in standard methods APHA AWWA WEF (2005).

5.3.7. Electron microscopy

The microbial cells adhering to the surface fragments of the rock bearing Mn oxide coatings were observed by SEM both before and after 50 d of incubation for the community experiment. Rock fragments of dimensions 0.54-3.93 × 0.61-3.9 mm prepared as above were aseptically picked using sterile forceps and were rinsed with phosphate buffered saline (300 mM NaCl, 2.7 mM KCl, 10 mM Na_2HPO_4 and 1.7 mM NaH_2PO_4, pH 7.0). They were air-dried, mounted on metal stubs using conductive adhesive tape and the edges were coated with conductive silver to eliminate any possible charging. The cell morphology and other details of the sample like the presence of EPS and cell aggregates were visualized at different magnifications using JEOL JSM-5800 SEM.

5.3.8. Determination of Co and Ni

The Co and Ni in supernatant were analyzed after centrifugation of samples at 5009 × g for 10 min at 4°C (Sigma 3-k). The determination of the metals was performed by adsorptive stripping voltammetry in interface with 797 VA computrace (Metrohm, Switzerland) in a differential pulse mode according to Herrera-Melian *et al.* (1997) and as modified and described by Sujith *et al.* (2011). To deduce the change in metal concentration 1ml supernatant from each tube was diluted with 9 ml of Milli-Q water (18.2 Ω resistance) and then acidified to pH < 2 with 30% Suprapur HCl (Merck). The acidified samples were UV digested using high-pressure mercury lamp (705 UV Digester, Metrohm) in quartz cuvettes at 90°C for one hour. The UV irradiated samples were analyzed immediately after cooling or was stored in dark at 4°C for later analysis.

5.4. Results

5.4.1. Characterization of the Fe-Mn oxide

Physical characteristics of the Fe-Mn oxide surfaces on basalt showed black coloured coatings with rough to smooth surfaces with numerous pits, fissures and fractures. The thickness of the coatings varied from >1-4 mm with greater thickness on irregular surfaces and vice versa on regular surfaces. The solid phase concentration of Co, Ni, Mn and Fe in the oxide coatings were 0.48%, 0.30%, 21.8% and 22.3% respectively. Mineralogical investigations showed vernadite as the major and todorokite as the minor Mn mineral (Figure 5.1).

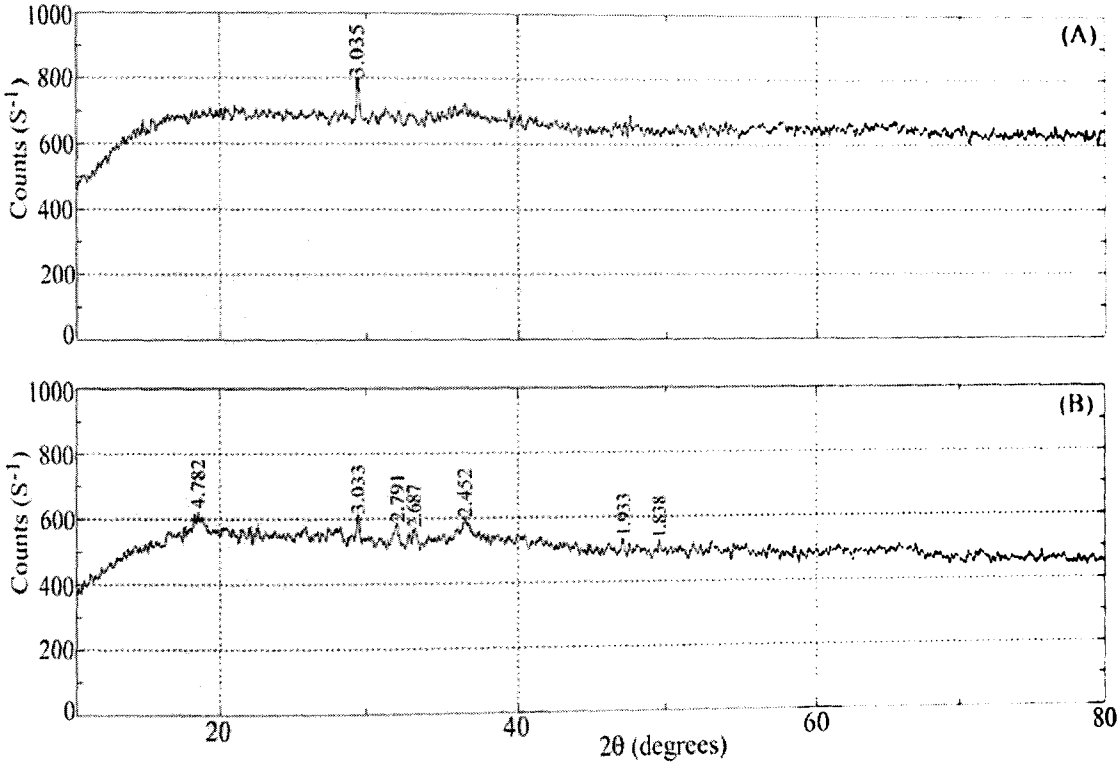

Figure 5.1. X-ray diffraction spectra A) Substrate rock and B) Fe-Mn crust. Peaks with d-values in figure-B correspond to the mineral vernadite and todorokite.

5.4.2. *In vitro* experiment with bacterial isolates and EDTA

5.4.2.1. Effect of EDTA on the cycling of Co and Ni in the Fe-Mn crust

Results of the experiment with EDTA and Fe-Mn crust showed mobilization for Co and immobilization for Ni (Figure 5.2). The chemical mobilization of Co in the presence of EDTA was greater in medium without added glucose compared to medium

with added glucose. The EDTA related mobilization was 24.9±1.4 μg g^{-1} in 'G^-' and 20±1.2 μg g^{-1} in 'G^+' after 50 d (Figure 5.2A). On the other hand, the immobilization of Ni was witnessed from the fall in level of initial concentration of soluble Ni in the presence of EDTA (Figure 5.2B). The rate of Ni immobilization remained high in the absence of added glucose (12.2±1.2 μg g^{-1}) compared to medium with added glucose (10.6±1.1 μg g^{-1}).

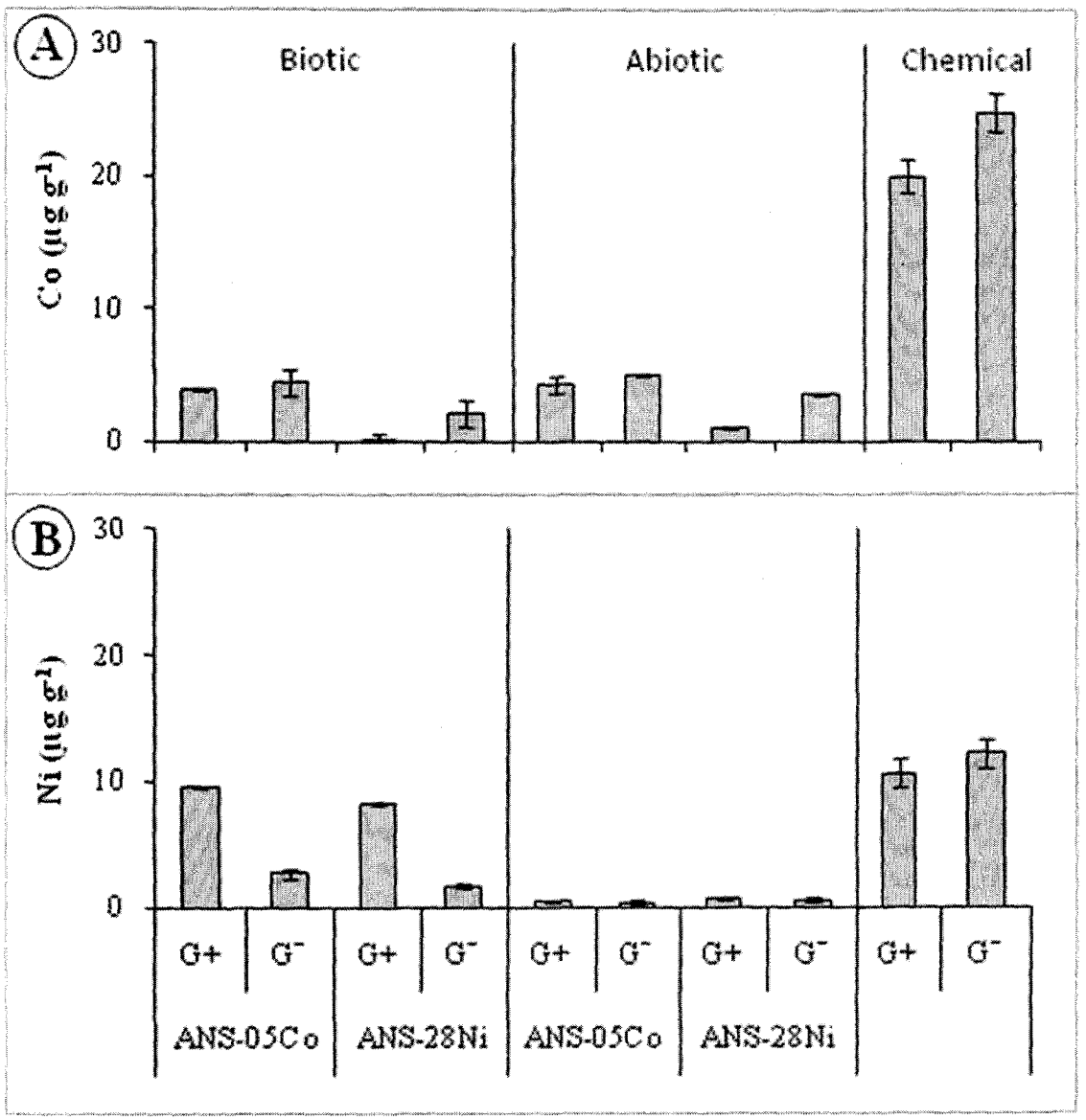

Figure 5.2. Biotic/abiotic cycling of Co and Ni by bacterial isolates in the presence of EDTA. A) Mobilization of Co and B) Immobilization of Ni.

5.4.2.2. Effect of EDTA and azide on the bacterial cycling of cobalt and nickel in the Fe-Mn crust

The parallel inhibition of bacterial growth by sodium azide and the effect of EDTA on the cycling of Co and Ni in the Fe-Mn crust showed similar trend in the cycling of metals like that of EDTA alone. It was mobilization with Co and immobilization with Ni (Figure 5.2). The abiotic mobilization of Co was greater in medium without added glucose compared to the medium with added glucose. The mobilization of Co by isolate ANS-05Co was 4.94±0.01 μg g^{-1} in 'G^-' and 4.24±0.61 μg g^{-1} in 'G^+' media. On the other hand, with isolate ANS-28Ni the mobilization of Co was 3.58±0.1 μg g^{-1} in 'G^-' and 1.04±0.07 μg g^{-1} in 'G^+' media (Figure 5.2A). However, with Ni, immobilization was observed. The immobilization of the metal with isolate ANS-05Co was 0.39±0.14 μg g^{-1} in 'G^-' and 0.49±0.12 μg g^{-1} in 'G^+' media. Nevertheless, the immobilization of Ni by isolate ANS-28Ni was 0.56±0.2 μg g^{-1} in 'G^-' and 0.63±0.08 μg g^{-1} in 'G^+' media (Figure 5.2B).

5.4.2.3. Effect of EDTA on the bacterial cycling of cobalt and nickel in the Fe-Mn crust

The bacterial (biotic) mobilization of Co in the presence of EDTA was comparably lesser than that of EDTA alone suggesting immobilization (Figure 5.2). The bacterial immobilization was greater in medium without added glucose compared to medium with added glucose. Of the two bacterial strains, the isolate ANS-05Co tolerant to Co showed greater immobilization of Co compared to that of the isolate ANS-28Ni which was tolerant to Ni. The immobilization of Co by ANS-05Co was 4.5±0.98 μg g^{-1} in 'G^-' and 4.0±0.1 μg g^{-1} in 'G^+' media. On the other hand, bacterial isolate ANS-28Ni immobilized 2.1±0.9 μg g^{-1} of Co in 'G^-' and 0.4±0.2 μg g^{-1} in 'G^+' media (Figure 5.2A). However, in the presence of EDTA and bacteria, the immobilization of Ni was comparatively lesser than that by EDTA alone. Of the two bacterial isolates, immobilization of Ni by isolate ANS-05Co was greater than isolate ANS-28Ni. The immobilization rate of Ni by isolate ANS-05Co with EDTA was 2.69±0.38 μg g^{-1} in 'G^-' and 9.5±0.01 μg g^{-1} in 'G^+' media. Nevertheless, the immobilization of Ni by isolate ANS-28Ni with EDTA was 1.71±0.26 μg g^{-1} in 'G^-' and 8.19±0.1 μg g^{-1} in 'G^+' media (Figure 5.2B).

5.4.2.4. Variation in pH and Eh

Notable difference in pH and Eh was observed in the experiment with heat killed crust and EDTA after 50 d (Figure 5.3). The pH increased from 5.4 to 7.02 in 'G^-' experiment and 5.53 to 7.28 in 'G^+' experiment with isolate ANS-05Co. Whereas, with isolate ANS-28Ni in 'G^-' experiment pH varied from 5.63 to 7.33 and in 'G^+' experiment from 5.50 to 7.54. However, in the controls containing only EDTA and heat killed crust the variation in pH was 5.31 to 7.09 in 'G^-' and 5.32 to 6.74 in 'G^+' media (Figure 5.3A). The Eh on the other hand shifted more towards positive redox potentials toward the end of incubation (50 d). The Eh increased from -43.11 to 38 mV in 'G^-' experiment and -19.7 to 29.03 mV in 'G^+' experiment with isolate ANS-05Co. The Eh varied in 'G^-' experiment with isolate ANS-28Ni from -32.61 to 22.43mV and in 'G^+' experiment from -22.89 to 3.37mV. On the other hand, in the controls the Eh varied from -71.27 to 44mV in 'G^-' and -45.08 to -40.67mV in 'G^+' media (Figure 5.3B).

5.4.2.5. Bacterial growth upon incubation

TC in the presence of EDTA increased by more than an order of magnitude in the absence and presence of added glucose (Figure 5.3C). With isolate ANS-05Co, the counts ranged from 4.0×10^5 to 1.47×10^7 cells ml^{-1} in 'G^-' and 1.55×10^6 to 1.7×10^7 cells ml^{-1} in 'G^+'. On the other hand, with isolate ANS-28Ni the counts varied from 5.33×10^5 to 1.13×10^7 cells ml^{-1} in 'G^-' and 6.13×10^5 to 2.07×10^7 cells ml^{-1} in 'G^+'. In the azide poisoned controls, the TC of isolate ANS-05Co varied from 9.07×10^5 to 3.25×10^6 cells ml^{-1} in 'G^-' and from 1.41×10^6 to 6.45×10^6 cells ml^{-1} in 'G^+' media. Moreover, with isolate ANS-28Ni the counts varied from 6.93×10^5 to 2.16×10^6 cells ml^{-1} in 'G^-' and 7.73×10^5 to 2.85×10^6 cells ml^{-1} in 'G^+' media.

5.4.3. In vitro experiment with bacterial isolates and ascorbate

5.4.3.1. Effect of ascorbate on the cycling of cobalt and nickel in the Fe-Mn crust

Ascorbate, a strong reducing agent of Mn-oxide promoted the release of Co and Ni from the hydrogenetic Fe-Mn crust (Figure 5.4). The chemical mobilization of Co by ascorbate was greater in medium without added glucose (2.11 ± 0.02 $\mu g\ g^{-1}$) as compared to medium with added glucose (1.01 ± 0.47 $\mu g\ g^{-1}$) (Figure 5.4A). On the other hand, the mobilization of Ni by ascorbate was greater than that of Co. It was 1.52 ± 0.01 $\mu g\ g^{-1}$ in 'G^-' and 4.03 ± 0.31 $\mu g\ g^{-1}$ in 'G^+' media (Figure 5.4B).

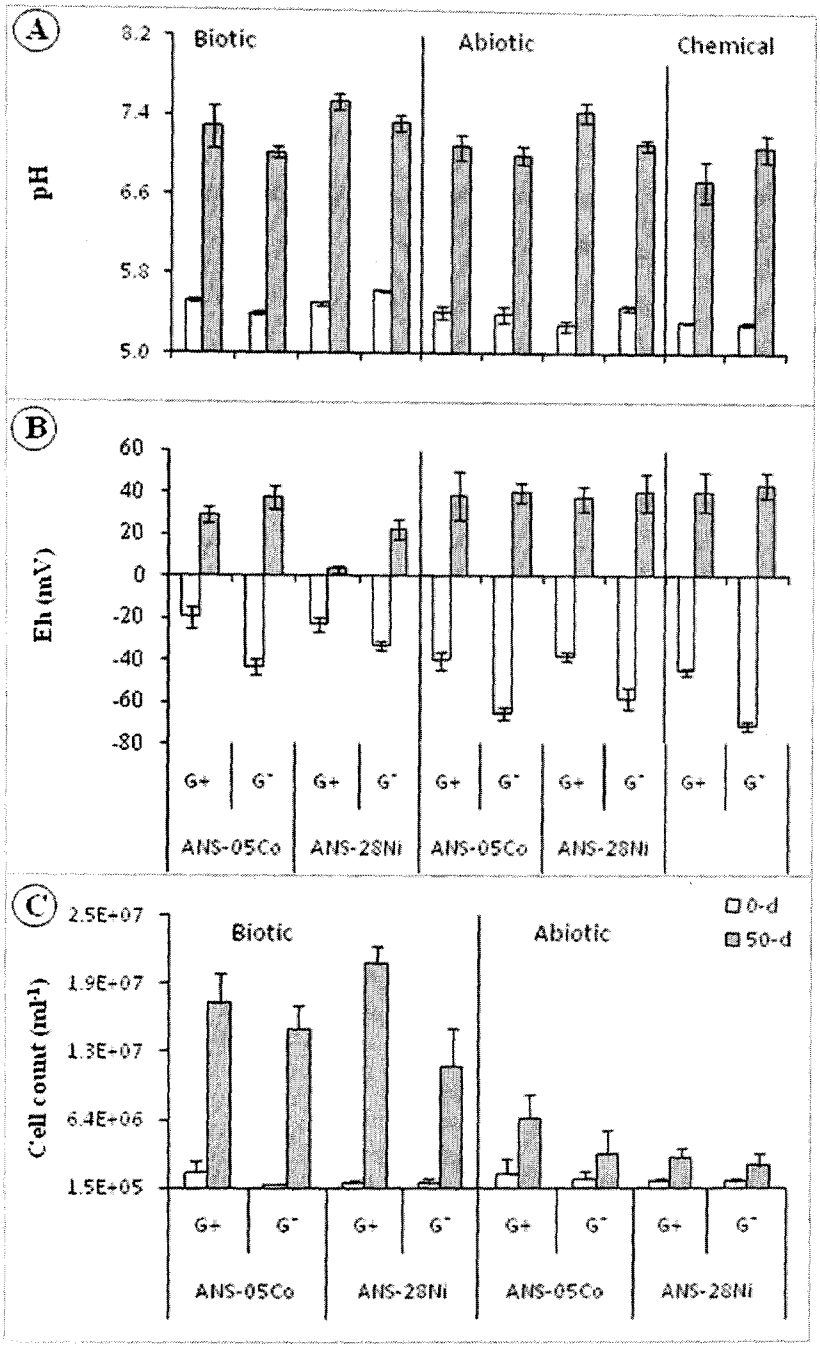

Figure 5.3. Variation in pH, Eh (mV) and cell numbers in relation to the immobilization/ mobilization of Co and Ni in the presence of EDTA.

5.4.3.2. Effect of ascorbate and azide on the cycling of cobalt and nickel in the Fe-Mn crust

The parallel inhibition of bacterial growth by sodium azide and ascorbate effect on the cycling of Co and Ni in the Fe-Mn crust showed similar trend in the cycling of metals

like that of ascorbate alone (Figure 5.4). The mobilization of Co by isolate ANS-05Co was 1.94±0.01 μg g^{-1} in medium without added glucose and 0.61±0.21 μg g^{-1} in medium with added glucose. Whilst, the mobilization of Co by isolate ANS-28Ni was 1.58±0.4 μg g^{-1} in 'G^-' and 1.04±0.17 μg g^{-1} in 'G^+' media (Figure 5.4A). On the other hand, the mobilization of Ni in the azide poisoned control was lesser than that of Co. With isolate ANS-05Co, mobilization and with isolate ANS-28Ni immobilization of Ni was evident. The mobilization of Ni by isolate ANS-05Co was 2.59±0.14 μg g^{-1} in 'G^-' and 2.89±0.12 μg g^{-1} in 'G^+' media. Nevertheless, the immobilization of Ni with isolate ANS-28Ni was 0.55±0.2 μg g^{-1} in 'G^-' and 0.28±0.08 μg g^{-1} in 'G^+' media (Figure 5.4B).

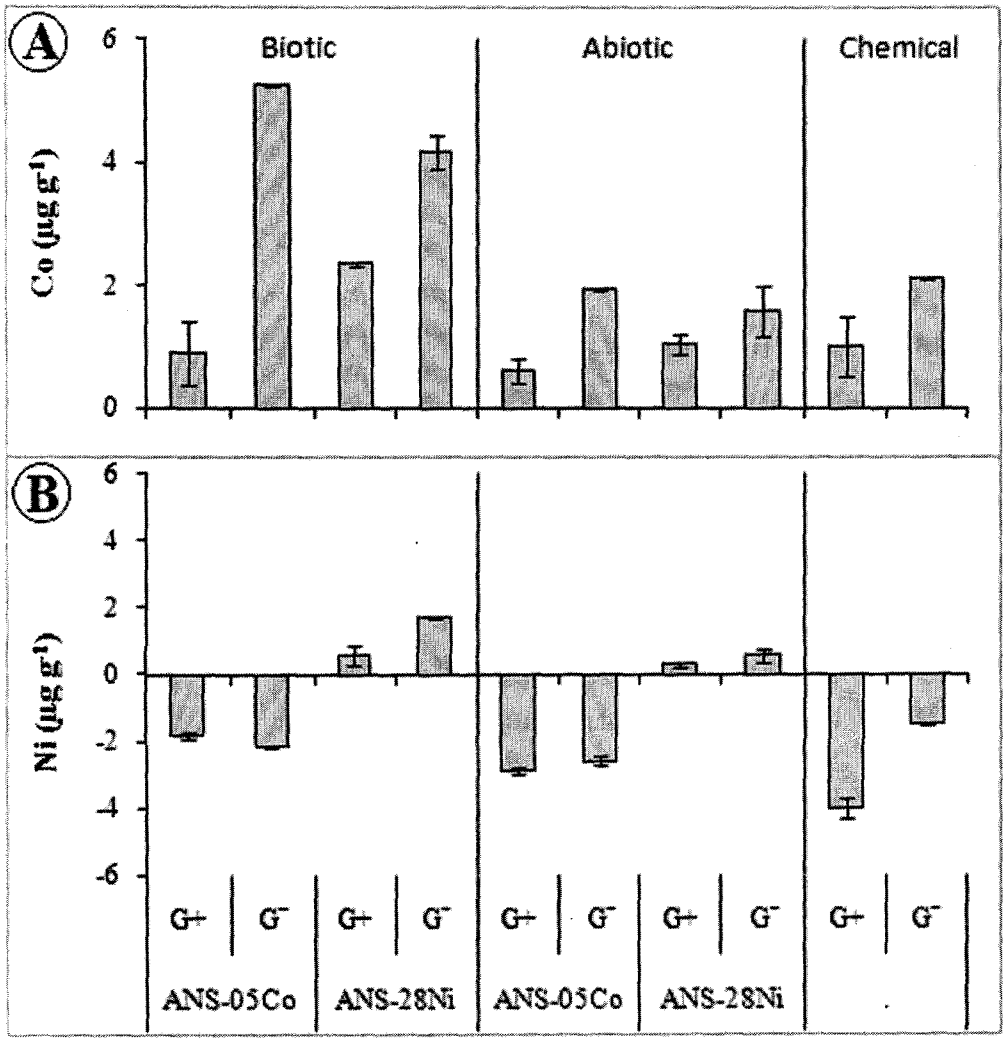

Figure 5.4. Biotic/abiotic cycling of Co and Ni by bacterial isolates in the presence of ascorbate A) mobilization of Co and B) mobilization/immobilization of Ni.

5.4.3.3. Effect of ascorbate on the bacterial cycling of cobalt and nickel in the Fe-Mn crust

In the presence of bacteria the mobilization of Co from the Fe-Mn crust was greater than that mobilized by ascorbate alone (Figure 5.4). The mobilization of Co by isolate ANS-05Co was 5.24±0.01 μg g^{-1} in medium without added glucose and 0.91±0.52 μg g^{-1} in medium with added glucose. However, the mobilization of Co by isolates ANS-28Ni was 4.17±0.28 μg g^{-1} in 'G^-' and 2.36±0.03 μg g^{-1} in 'G^+' media (Figure 5.4A). On the other hand, the bacterial mobilization of Ni in the presence of ascorbate was lesser than that by ascorbate alone. With isolate ANS-05Co, mobilization and with isolate ANS-28Ni immobilization of Ni was evident. The mobilization of Ni by isolate ANS-05Co was 2.18±0.02 μg g^{-1} in 'G^-' and 1.84±0.08 μg g^{-1} in 'G^+' media (Figure 5.4B). Nevertheless, the immobilization of Ni with isolates ANS-28Ni was 1.72±0.03 μg g^{-1} in 'G^-' and 0.48±0.31 μg g^{-1} in 'G^+' media.

5.4.3.4. Variation in pH and Eh

Notable difference in pH and Eh was not apparent between the experiment and the corresponding controls (Figure 5.5). The pH decreased from 7.63 to 7.65 in 'G^-' experiment and 7.46 to 6.58 in 'G^+' experiment with isolate ANS-05Co after 50 d. With isolate ANS-28Ni, pH varied from 7.6 to 7.46 in 'G^-' experiment and 7.48 to 7.5 in 'G^+' experiment. Whilst, in the corresponding azide poisoned controls the pH varied from 7.63 to 7.54 in 'G^-' and 7.51 to 7.40 in 'G^+' (Figure 5.5A). The Eh on the other hand, shifted more towards positive redox potentials at the end of 50 d incubation. The Eh increased from -141.23 to -68.63 mV in 'G^-' experiment and -165.41 to -114.97 mV in 'G^+' experiment with isolate ANS-05Co. With isolate ANS-28Ni, Eh varied from -151.01 to -71.93mV in 'G^-' experiment and -163.09 to -113.3 mV in 'G^+' experiment (Figure 5.5B). In the corresponding controls, the Eh varied from -130.2 to -45.17 mV in 'G^-' and -146.33 to -80.77mV in 'G^+' after 50 d.

5.4.3.5. Bacterial growth upon incubation

TC increased by more than an order of magnitude in the presence of added glucose and was less than an order of magnitude in the absence of added glucose (Figure 5.5C). It ranged from 1.01 × 10^6 to 1.52 × 10^6 cells g^{-1} in 'G^-' experiment and from 8.00 × 10^5 cells g^{-1} to 1.07 × 10^6 cells g^{-1} in 'G^+' experiment in the presence of isolate ANS-05Co

and ascorbate. On the other hand, with isolate ANS-28Ni the cell counts varied from 1.09×10^6 to 1.76×10^6 cells g^{-1} in 'G^-' experiment and from 2.56×10^6 to 1.10×10^7 cells g^{-1} in 'G^+' experiment. In the azide poisoned controls, the TC varied from 9.07×10^5 to 3.25×10^6 cells g^{-1} in 'G^-' and 1.41×10^6 to 6.45×10^6 cells g^{-1} in 'G^+' with isolate ANS-05Co. Moreover, the counts of isolate ANS-28Ni varied from 6.93×10^5 to 2.16×10^6 cells g^{-1} in 'G^-' and between 7.73×10^5 to 2.85×10^6 cells g^{-1} in 'G^+' media.

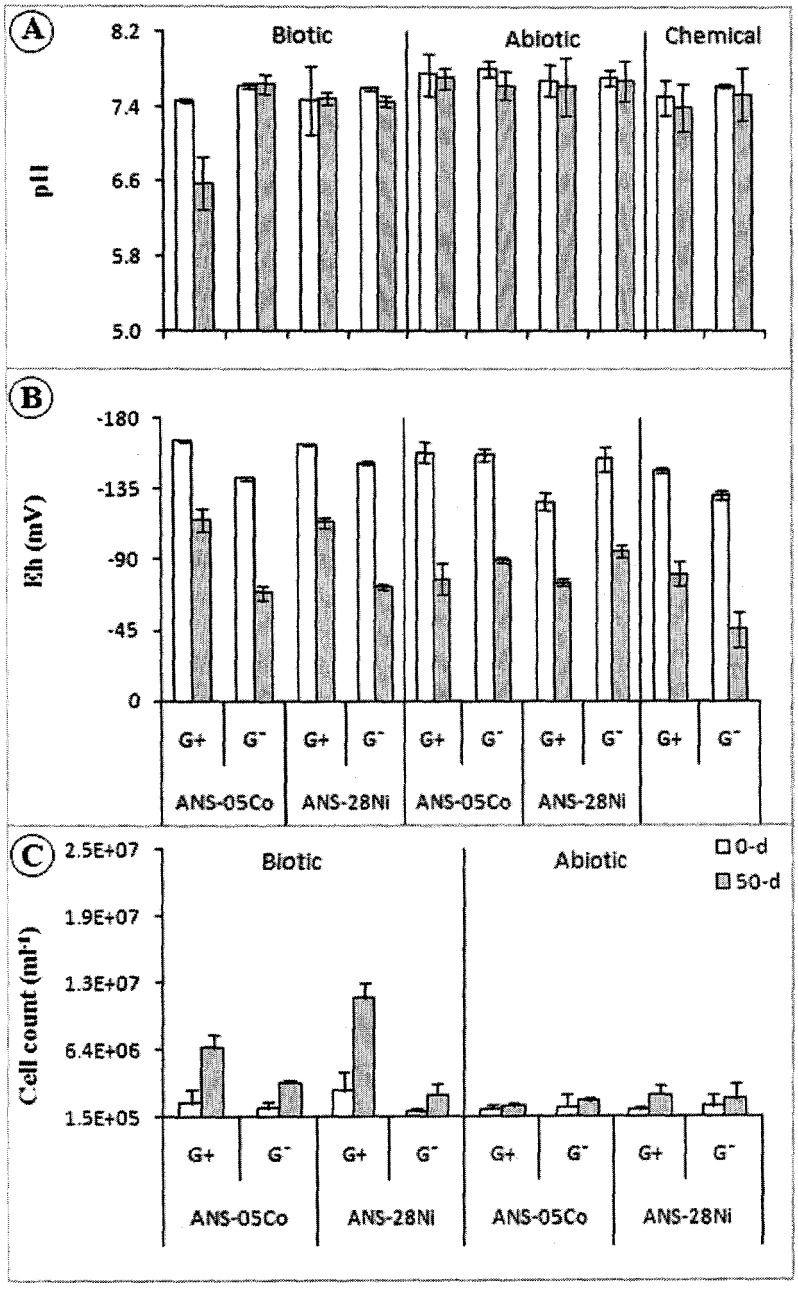

Figure 5.5. Variation in pH, Eh (mV) and cell numbers in relation to the immobilization/ mobilization of Co and Ni in the presence of ascorbate.

5.4.4. In vitro experiment with microbial community associated with the Fe-Mn crust

5.4.4.1. Microbial activity on the cycling of Co and Ni in the Fe-Mn crust

Microbial community associated with the Fe-Mn crust mobilized Co at ambient temperature of 4±1°C and above ambient temperature of 28±2°C at the beginning of the experiment (Figure 5.6A). Thereafter, with time the concentration of Co decreased in the soluble phase suggesting immobilization. The immobilization of the metal at 4±1°C was 165.96 μg g^{-1} in the absence of added glucose and 97.11 μg g^{-1} in the presence of added glucose. However, at 28±2°C the immobilization of Co was more in the presence of added glucose. It was 479.75 μg g^{-1} in the presence and 28.67 μg g^{-1} in the absence of added glucose. On the other hand, with the abiotic controls, the mobilization of Co was prominent. Maximum mobilization was registered in the presence of added glucose at both the temperatures. It was 151.47 μg g^{-1} at 4±1°C and 70.34 μg g^{-1} at 28±2°C after 50d. On the other hand, with Ni, under ambient concentration of organic carbon only immobilization was observed (Figure 5.6B). The concentration of Ni either showed a gradual decrease or else remained constant throughout the incubation period. The immobilization of Ni was 1.89 μg g^{-1} at 4±1°C and 0.64 μg g^{-1} at 28±2°C at the end of 50 d. In the presence of 0.1% added glucose the mobilization of Ni was obvious. The mobilization of Ni was 51.28 μg g^{-1} at 4±1°C and 19.45 μg g^{-1} at 28±2°C. While, in the corresponding abiotic controls the mobilization of Ni was evident both in the presence and absence of added glucose. The maximum mobilization of 24.22 μg g^{-1} was in the absence of added glucose at 4±1°C and 14.39 μg g^{-1} at 28±2°C in the presence of added glucose.

5.4.4.2. Variation in pH and Eh

Notable difference in pH and Eh was not apparent between the biotic and the abiotic sets of incubations (Figure 5.7). The pH decreased from 8.06 to 7.49 in the 'G^+' biotic and from 7.99 to 7.54 in the 'G^-' biotic after 50 days at 28±2°C. In the corresponding abiotic controls, the pH varied from 7.95 to 7.72 in the 'G^+' and from 7.58 to 7.44 in the 'G^-' after 50 d. On the other hand, at 4±1°C pH varied from 8.03 to 7.61 in the 'G^+' biotic and from 8.07 to 7.73 in the 'G^-' biotic after 50d. In the corresponding abiotic controls, the pH varied from 7.92 to 7.86 in medium amended with glucose and from 7.69 to 7.57 in medium without added glucose after 50d of

incubation (Figure 5.7A). The Eh on the other hand shifted more towards negative redox potentials toward the end of 50 d of incubation (Figure 5.7B). It varied from -31.9mV to -121.78mV in the 'G^{+}' biotic and -33.92 to -117.59 mV in the 'G^{-}' biotic at 28±2°C. In the corresponding abiotic controls, Eh showed variation from -29.92 to -113.21 mV in the 'G^{+}' and from -55.23 to -116.5mV in the 'G^{-}'. On the other hand, at 4±1°C Eh varied from -27.13 to -116.27mV in the 'G^{+}' biotic and from -47.19 to -99.6mV in the 'G^{-}' biotic after 50d. The corresponding abiotic control showed Eh variation from -29.28 to -111.4mV in 'G^{+}' and from -57.19 to -112.17mV in the 'G^{+}' media after 50d.

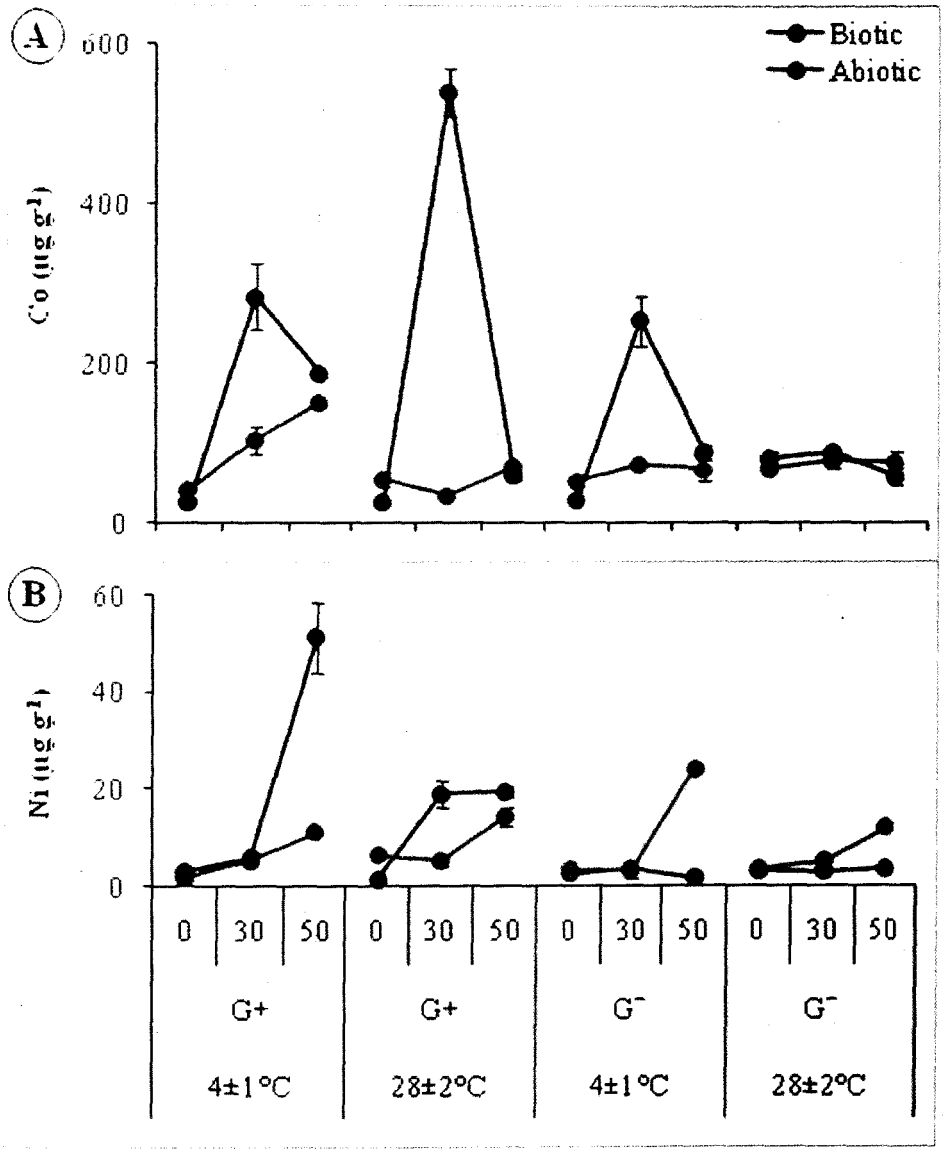

Figure 5.6. Time dependent variation in immobilization/ mobilization of Co and Ni by indigenous microbial communities associated with the ferromanganese crust.

5.4.4.3. Bacterial growth upon incubation

Total counts (TC) in the community experiment increased by more than an order of magnitude in the presence of added glucose and less than an order of magnitude in the absence of added glucose (Figure 5.7C). The maximum cell counts occurred on the 30 d of incubation. It ranged from 4.65×10^6 to 1.02×10^7 cells g^{-1} in 'G^+' biotic and 8.11×10^6 cells g^{-1} to 8.37×10^6 cells g^{-1} in 'G^-' biotic at 4±1°C. In the corresponding abiotic controls the counts ranged from 1.23×10^6 to 1.89×10^6 cells g^{-1} in the presence of added glucose and between 3.25×10^6 cells g^{-1} to 2.48×10^6 cells g^{-1} in the absence of added glucose at 4±1°C. On the other hand, at 28±2°C in the presence of added glucose TC increased from 3.60×10^6 to 1.67×10^7 cells g^{-1} and from 1.63×10^6 to 7.73×10^6 cells g^{-1} in the absence of added glucose after 30 d. In the corresponding azide poisoned abiotic control, the counts ranged from 3.63×10^6 to 3.01×10^6 cells g^{-1} in the presence of added glucose and from 1.91×10^6 to 3.09×10^6 in the absence of added glucose after 30 d.

5.4.4.4. Microscopy

SEM examination showed numerous bacterial cells adhering to the Fe-Mn crust surfaces. Their numbers increased following incubation and showed EPS like materials and secondary minerals. The oxide surfaces showed mineral morphology resembling amorphous oxides of Mn (Figure 5.8). Similar precipitates of Mn were also observed surrounding the bacterial cells suggesting their active participation in the precipitation of the Mn and the associated elements.

5.5. Discussion

The solid phase concentration of Co, Ni, Mn and Fe determined in the present study agree with those reported from the ANS (Rajani *et al.,* 2005). The mineralogy of the Mn-oxide coatings on basalt showed characteristic peaks for Mn minerals vernadite and todorokite. It agrees with the reported mineralogy of Mn-oxides from the Atlantic Ocean (Cronan, 1975). Besides, the crusts at ANS harbor metal immobilizing/mobilizing microorganisms. The functional moieties on their surfaces and other extracellular materials produced during their growth could act as ligands and/or chelating agents and thereby help them in attaching to the surfaces, alleviating the toxic effect of metals and in the precipitation or dissolution of minerals. However, the metal

binding ligands and chelating agents differ in their binding strength with metals when present together in nature (Hughes and Poole, 1989).

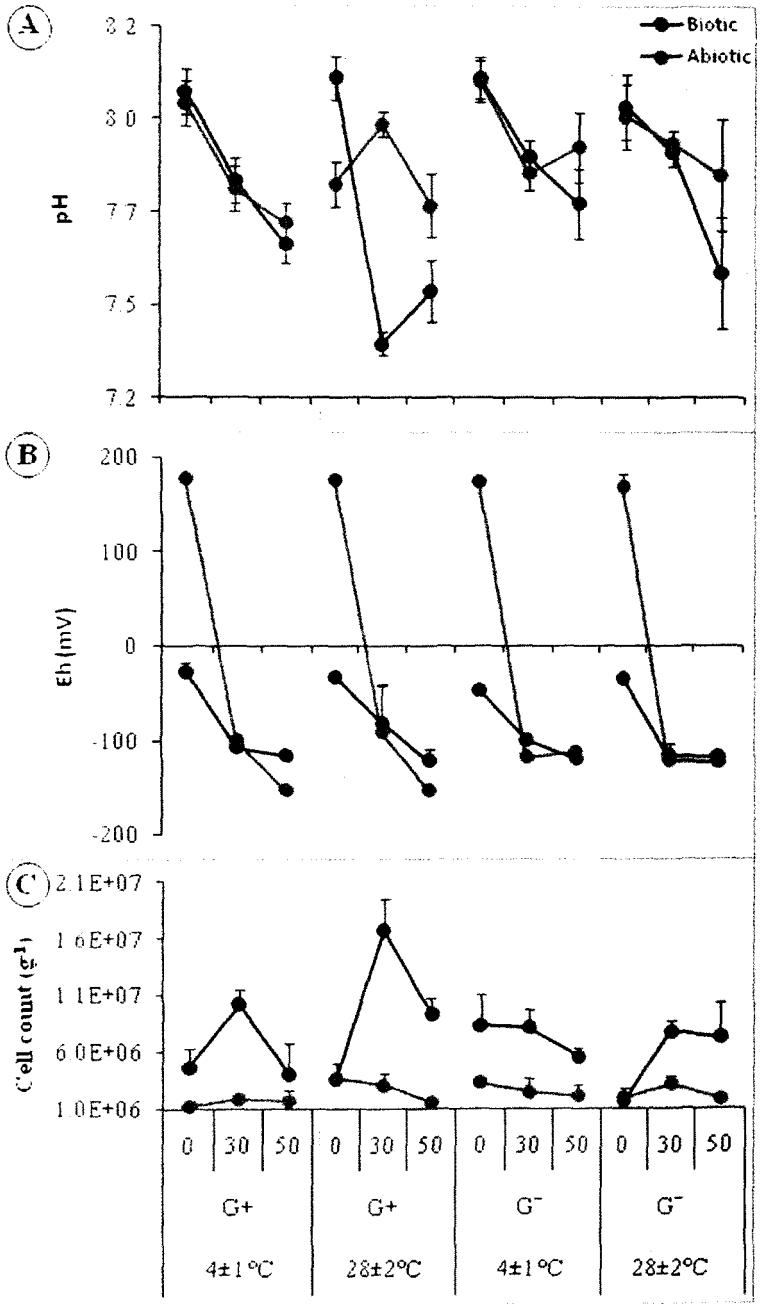

Figure 5.7. Time dependent variation in pH, Eh (mV) and cell numbers in relation to the immobilization/ mobilization of Co and Ni by indigenous microbial communities associated with the ferromanganese crust.

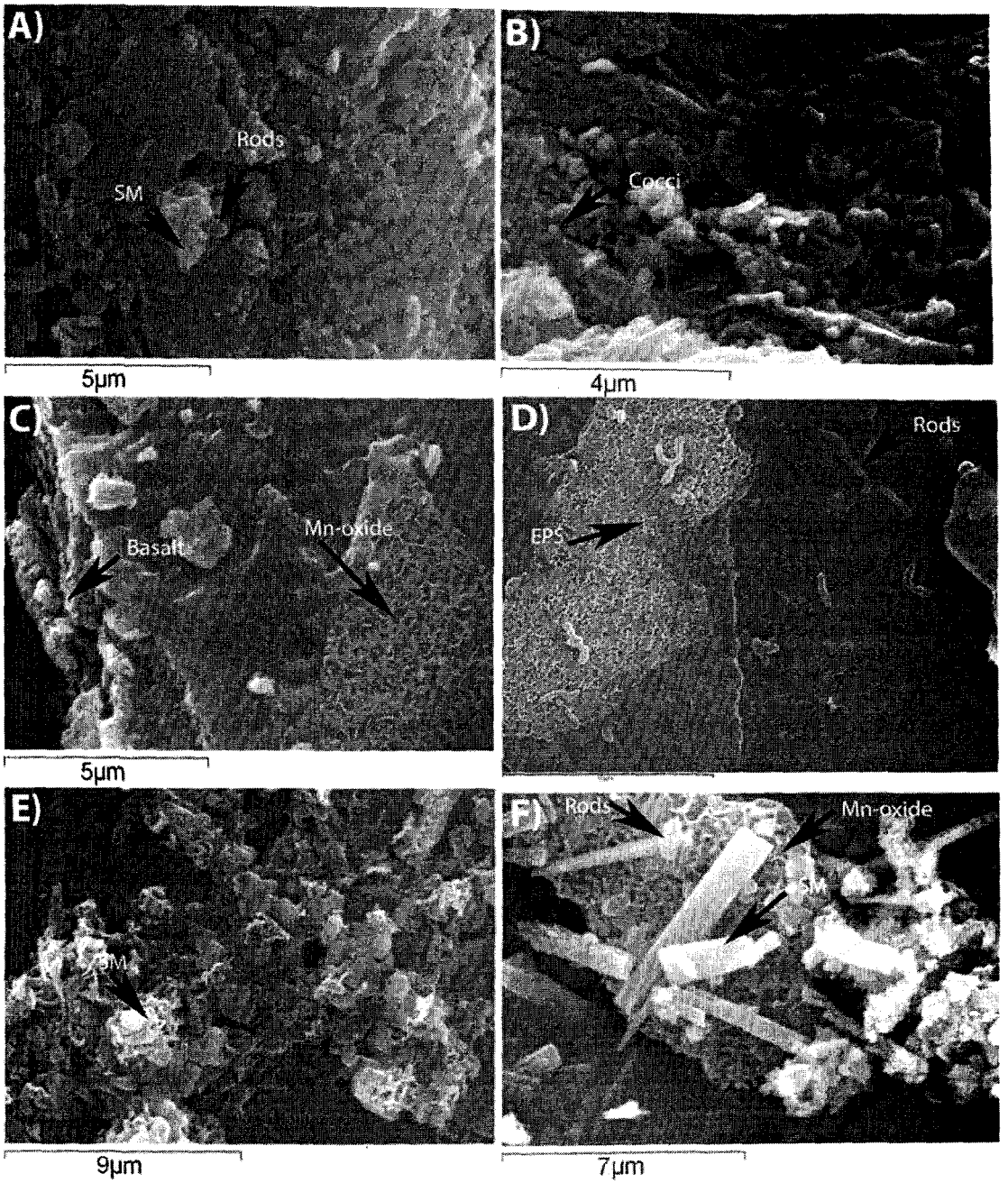

Figure 5.8. Electron microscope images show bacterial cells, exopolysaccharide (EPS) like materials, secondary minerals (SM) and mineral morphology resembling amorphous oxides of Mn on ferromanganese crust surfaces. A) image captured for sample on zero day and B, C, D, E and F are images captured for samples after 50 d of incubation.

In the present study on Fe-Mn crust and EDTA, immobilization was observed for Ni and mobilization for Co thus indicating the higher reactivity of EDTA for the former compared to that of the latter. The reactivity of EDTA with Ni and with Co depended on their stability constant of 18.56 and 16.21 respectively (Flora and Pachauri, 2010). Further reasoning that may also apply for the difference in interaction of EDTA with Ni and Co could be because of 1) the lesser enrichment of Ni than that of Co in the Fe-Mn crusts and 2) the inert nature of Ni compared to Co. The concentration of Ni and Co in the hydrogenetic Fe-Mn crusts of the ANS averaged ~0.25 and ~0.6% respectively (Rajani *et al.,* 2005). Moreover, the inertness of Ni prevents its speciation in nature and as a result remains bound to the Mn oxide phase of the crust as $Ni(II)EDTA^{2-}$. On the other hand, Co undergoes valence speciation by chemical and biological mediated mechanisms (Murray and Dillard, 1979; Tebo and Lee, 1993; Moffett and Ho, 1996). The Co species in the presence of EDTA complexes to form $Co(II)EDTA^{2-}$ and $Co(III)EDTA^{-}$. Being strongly reactive with the Mn oxide surfaces, $Co(II)EDTA^{2-}$ undergoes sorption on the oxide surface whereas $Co(III)EDTA^{-}$ which is weakly reactive remains highly stable in solution.

Apart from the above factors, pH plays an important role in the chelation of metal ions by EDTA because with decrease in pH, Co and EDTA dissociate but with increase in pH, Co and EDTA form a strong association. It is evident from Brooks *et al.* (1996) that $CoIIEDTA^{2-}$dominate the aqueous speciation of Co(II) at pH values greater than 6. Following incubation, pH of the medium containing EDTA and Fe-Mn crust increased with increase in concentration of Co and decrease in concentration of Ni in the aqueous phase. The present results agree with that of Flora and Pachauri (2010) on the formation of strong metal complexes by EDTA with greater stability under neutral-alkaline pH. Because of the general relationship between pH and Eh (Pareuil *et al.,* 2008) the redox cycling of Mn on to which the Co and Ni are usually bound could also be affected. The decrease in H^+ activity (rise in pH) leads to an Eh increase and consequently to the decreased mobilization of metallic elements and vice versa with increase in H^+ and a decrease in Eh (DeLaune and Reddy, 2005; Pareuil *et al.,* 2008).

Other than EDTA forming complexes with the metals, organic molecules/bacterial surfaces also bind to the metals forming strong complexes

(Vaughan *et al.*, 1993; Cox *et al.*, 1999). In the present study, the reactivity of EDTA towards Co and Ni was drastically reduced in the presence of bacteria and glucose. This could probably be due to the reactivity of electronegative sites on bacterial surfaces with the metals apart from chemical complexation by EDTA. The several electronegative sites on bacterial surfaces which provide the anionic character to the bacterial cells are the carboxyl, phosphoryl and amine groups (Beveridge, 1989; Cox *et al.*, 1999). Besides, surface complexation or biosorption, the bacterial cells also uptake metals by an energy requiting process leading to bioaccumulation. Therefore, the immobilization of Ni could also be due to one of the processes above. The ability of EDTA to promote the assimilation of glucose and other growth substrates by bacteria (Dedyukhina *et al.*, 2008) complement the bacterial interaction with metal ions. Additionally, by forming stable complexes with metal ions EDTA affects the toxicity of metals to bacteria by protecting the target sites of metal binding. As a result bacteria proliferate in a metal containing milieu when chelating agents like EDTA are present. Equally, the toxicity of Fe^{3+} decreased in the presence of an iron chelating agent desferrioxamine (Tilbrook and Hider, 1998).

The ability of bacteria to utilize EDTA as sole source of carbon and nitrogen (Nortemann, 1992) further emphasize their importance in the biotic-abiotic cycling of metallic elements. In the present study, the immobilization/mobilization of Ni and Co by the bacterial isolates was stimulated by the addition of glucose in an EDTA amended medium however the bacterial immobilization/mobilization was comparatively lesser than that by EDTA alone. Nevertheless, the bacterial immobilization/mobilization of the metals was greater in the presence than in the absence of EDTA. Thus EDTA increases the aqueous solubility of metal ions and through strong chelating property decreases the toxic effect of metal ions on bacterial cells. It thereby promotes the bacterial participation in the cycling of metal ions and thus controls the related biogeochemical processes.

Ascorbate being a strong reducing agent of Mn oxides (Tebo and Lee, 1993; Moffett, 1997) promoted the mobilization of Ni and Co from the hydrogenetic Fe-Mn crust. However, the mobilization rate of Ni and Co by ascorbate differed from each another mainly because of its property to react only with the higher oxidation states of

the metals present in the crust. The greater release of Ni compared to Co suggest that Ni is mostly present in the bound state as Ni(II) and Co in the oxidized state as Co(III). The release of Ni could have been mainly from the solubilization of Mn(III,IV)-oxide to which it is usually bound and Co from the solubilization of Co(III) oxide (Stone and Morgan, 1984; Lee and Tebo, 1994). On the other hand, the mobilization of Ni was greater in the presence of glucose and Co in the absence of glucose. Since glucose also serves as a suitable reductant of metal hydroxides (Ehrlich, 1988) it is not surprising to notice the greater mobilization of Ni by ascorbate in the presence of glucose. However, the lesser mobilization of Co by ascorbate with added glucose suggests the rapid binding of reduced Co to Fe-Mn crust surfaces that are being partially solubilized. The present results corroborates with Tebo and Lee (1993) on the occurrence of Co as hydroxides or oxyhydroxide phases in the Fe-Mn crusts and the ability of charged surfaces to bind metals passively. Nevertheless, the pH of the media containing ascorbate and Fe-Mn crust remained unaltered during incubations which probably suggest the inability of ascorbate to chelate metal ions (Sunda and Huntsman, 1987). Mobilization was followed by a negligible decrease in pH and very little increase in Eh suggesting the general relationship between pH and Eh where a decrease in H^+ activity leads to an increase in Eh (Pareuil *et al.*, 2008).

Contrary to the chemical controls, the mobilization of Ni by bacteria in the presence of ascorbate was more in the absence of glucose. It suggests ascorbate inhibition of oxygen uptake (Richter *et al.*, 1988) and stimulation of fermentative growth of facultative anaerobes in the absence of glucose by ascorbate due to its structural similarity to hexose sugars (Kendall and Chinn, 1938; Eddy and Ingram, 1953; Mehmeti *et al.*, 2013). In the Fe-Mn crusts more of such conditions could exist in pits, fissures and fractures due to oxygen utilization by aerobic organisms favoring the growth of anaerobes or facultative anaerobes. The only exception to this was isolate ANS-28Ni that immobilized Ni in the presence of ascorbate. The results suggest the efficiency of this organism to tolerate high concentrations of the metals released from the reduction of Fe-Mn oxides by ascorbate. Bacterial immobilization could occur in the presence of ascorbate due to adsorption or complexation of reduced metals onto bacterial and other charged surfaces as these processes are unaffected by ascorbate (Lee and Tebo, 1994). Further, the immobilization of Ni was bacterially mediated as it

was inhibited by azide in the poisoned control. Nevertheless, the mobilization of Co by bacteria increased considerably in the presence of ascorbate. This indeed occurs as bacteria mobilize Co from Fe-Mn crust apart from chemical reduction of the oxide by ascorbate. However, the addition of glucose suppressed the mobilization of Co by bacteria in the presence of ascorbate. This could occur because stimulation of bacterial growth and biofilm formation by glucose hinder the movement of ascorbic acid to the oxide surface thus decreasing the surface reactivity. Such an effect was also observed by Toner and Sposito (2005) where they obtained similar results with acid-birnessite in a liquid medium by *Psudomonas putida*. The reductive dissolution of metal oxides by ascorbate in the presence of bacteria also depends on the concentration of ascorbate, concentrations of dissolved metals like Cu and Mn, dissolved oxygen and ascorbate oxidation by cellular exudates (Davies *et al.*, 1991; Toner and Sposito, 2005).

Aside from the influence of EDTA and ascorbate on the cycling of Co and Ni by individual bacterial isolates, the study also looked into the response of crust associated bacterial community on the cycling of Co and Ni in the Fe-Mn crust. The results of the study showed the immobilization of Ni to occur at ambient concentrations of organic carbon and mobilization in the presence of added glucose. The rates were better at near ambient temperature of 4±1°C than at 28±2°C. The immobilization of Ni under ambient concentration of organic carbon could result from sorption or accumulation of Ni ions by bacteria residing on Fe-Mn crust surfaces as the *in vitro* experimental conditions simulate the near *in situ* levels of carbon and temperature. The sorption of Ni could also occur depending on the number of vacancy of surface binding sites available at the mineral/bacterial surface for the soluble metal ions to get adsorbed (Kennedy *et al.*, 2003). However, in the presence of added glucose, mobilization took the lead over immobilization. It suggests that some of the bacteria resident on Fe-Mn crust surfaces may respond reversibly to pulses of fresh organic carbon. Similar effect of organic carbon on bacterial mobilization of metals was observed by Brannon *et al.* (1984), Hunt and Kelly (1988) and Sujith *et al.* (2014). The effect of organic carbon (glucose) was prominently observed for Ni because it is usually bound to Mn-oxide phase of the crust in the +II oxidation state. Moreover, the Mn-oxides on basalt surfaces that are resilient to reduction could have Mn(III) an ideal chemical species of Mn that can act either as an oxidant or a reductant (Trouwborst *et al.*, 2006) depending on the

key environmental conditions. Thus it is possible that Ni bound to the Mn-oxide phase of the crust get mobilized on exposure to pulses of fresh organic carbon. Also Ni(II) seem to complex more often with organic carbon or ligands in the natural environment (Lawrence *et al.,* 2004; Doig and Liber, 2007) which further explains the alternate cause for its lesser enrichment in the crust.

On the other hand, with Co the net process was immobilization in both the presence and absence of added glucose. The results suggest that bacteria inhabiting the basalt surface contribute mostly to the enrichment of Co under ambient concentration of organic carbon and may conserve energy from oxidation of the reduced metal. Even under such oxidizing conditions of the crust the possibility of metals getting reduced cannot be ruled out because growth of aerobic bacteria in microniches create conducive environment for anaerobiosis. This is in agreement with the report of Orcutt *et al.* (2011) that microniches on basalts may become anoxic depending on the metabolic rate and fluid flow allowing anaerobic reactions to occur in pits and fissures. During anaerobic growth, bacteria may utilize Mn and Fe oxides as terminal electron acceptor (Myers and Nealson, 1987; Vandieken *et al.,* 2012). Additionally, biofilm formation aid in anaerobic condition by inhibiting the diffusion of oxygen on surfaces that are avoided of pits and cracks (Costerton *et al.,* 1994). Therefore, bacteria inhabiting the Fe-Mn crust surface are regularly exposed to pulses of reduced metals either from the water column above or from anaerobic reactions occurring within the crust leading to heavy metal tolerance.

Also it was observed that addition of glucose stimulates the growth and immobilization of Co by crust associated bacteria. This indeed occurs because with increase in bacterial biomass the number of electronegative sites available for metal binding on bacterial surfaces also increases. Hallberg and Martinell (1976) and Ehrenreich and Widdel (1994) also presented evidence for such an increase in the immobilization of metals by bacterial biomass at the expense of glucose. The immobilization of Co was however more at 28±2°C. Since enzyme activity is a function of temperature it is most likely that immobilization by the direct process occurs at higher temperatures. It has been shown by Wenk and Fernandis (2007) and Wallenstein and Weintraub (2008) that enzyme activity increases with increase in temperature. The

results show the participation of bacteria in the cycling of Co and Ni with respect to the accretion and dissolution of the crust depending on the levels of organic carbon and the metal.

5.6. References

Aldrich AP, van den Berg CMG. 1998. Determination of Fe and its redox speciation in seawater using catalytic cathodic stripping voltammetry. Electroanalysis 10: 369-373.

Anderson MA, Morel FMM. 1982. The influence of aqueous iron chemistry on the uptake of iron by the coastal diatom *Thalassiosira weissflogii*. Limnol Oceanogr 27: 789-813.

APHA, AWWA, WEF. 2005. Oxidation-Reduction Potential (ORP). In: Standard Methods for the Examination of Water and Wastewater. Eaton AD, Clesceri LS, Rice EW, Greenberg AE (eds) Washington, DC, pp. 2-75 to 2-79.

Barcelona MJ.1980. Dissolved organic carbon and volatile fatty acids in marine sediment pore waters. Geochim Cosmochim Acta 44: 1977-1984.

Bergan T, Klaveness J, Aasen AJ. 2001. Chelating agents. Chemotherapy 47: 10-14.

Beveridge TJ (1989) Interactions of metal ions with components of bacterial cell wall and their biomineralization. In: Metal-microbe interactions. Poole RK, Gadd GM (eds) IRL Press, Oxford, pp. 65-83.

Brannon JM, Gunnison D, Smart RM, Chen RL. 1984. Effects of added organic matter on iron and manganese redox systems in sediment. Geomicrobiol J 3: 319-341.

Brooks SC, Taylor DL, Jardine PM. 1996. Reactive transport of EDTA-complexes cobalt in the presence of ferrihydrite. Geochim Cosmochim Acta 60: 1899-1908.

Burns RG, Burns VM. 1977. Mineralogy. In: Marine Manganese Deposits. Glasby GP (ed) Elsevier, Amsterdam, pp. 185-248.

Colombini MP, Fuoco R. 1983. Determination of manganese at ng/ml levels in natural waters by differential pulse polarography. Talanta 30: 901-905.

Costerton JW, Lewandoski Z, De Beer D, Caldwell D, Korber D. 1994. Biofilms, the customized microniche. J Bacteriol 176: 2137-2142.

Cox JS, Smith DS, Warren LA, Ferris FG. 1999. Characterizing heterogeneous bacterial surface functional groups using discrete affinity spectra for proton binding. Environ Sci Technol 33: 4514-4521.

Cronan DS. 1975. Manganese nodules and other Fe-Mn oxide deposits from the Atlantic Ocean. J Geophys Res 80: 3831-3837.

Davies MB, Austin J, Partridge DA. 1991. Vitamin C: its Chemistry and Biochemistry. The Royal Society of Chemistry, Cambridge, England, p. 159.

Dedyukhina EG, Chistyakova TI, Badrutdinova DN, Yudina EI, Minkevich IG, Vainshtein M B. 2008. EDTA-dependent assimilation of glucose and organic acids by an EDTA-degrading bacterium. Appl Microbiol Biotechnol 77: 1367-1370.

DeLaune, R.D., Reddy, K.R., 2005. Redox potential. In: Encyclopedia of Soils in the Environment. Hillel D, Rosenzweig C, Powlson D, Scow K, Singer M, Sparks D (eds) Academic Press, pp. 366-371.

Delegard CH, Barney GS. 1983. Effects of Hanford High-Level Waste Components on Sorption of Cobalt, Strontium, Neptunium, Plutonium, and Americium of Hanford Sediments. RHO-RE-ST-1 P, Rockwell Hanford Operations, Richland, Washington.

Doig LE, Liber K. 2007. Nickel speciation in the presence of different sources and fractions of dissolved organic matter. Ecotoxicol Environ Safe 66: 169-177.

Donat JR, Lao KA, Bruland KW. 1994. Speciation of dissolved copper and nickel in South San Francisco Bay: a multi-method approach. Anal Chim Acta 284: 547-571.

Eddy BP, Ingram M. 1953. Interactions between ascorbic acid and bacteria. Bacteriol Rev 17: 93-107.

Ehrenreich A, Widdel F. 1994. Anaerobic oxidation of ferrous iron by purple bacteria, a new type of phototrophic metabolism. Appl Environ Microbiol 60: 4517-4526.

Ehrlich HL. 1988. Bioleaching of manganese by marine bacteria. In: Proceedings 8th International Biotechnology Symposium. Durand G, Bobichon L, Florent J (eds) Paris, France, pp. 1094-1105.

Flora SJS, Pachauri V. 2010. Chelation in metal intoxication. Int J Environ Res Public Health 7: 2745-2788.

Gadd GM. 2009. Heavy metal pollutants: environmental and biotechnological aspects. In: Encyclopedia of Microbiology. Schaechter M (ed.) Elsevier, Oxford, pp. 321-334.

Geesey GG, Jang L. 1989. Interactions between metal ions and capsular polymers. In: Metal Ions and Bacteria. Beveridge TJ, Doyle RJ (eds) Wiley, New York, pp. 325-358.

Hallberg RO. Martinell R. 1976. Vyredox-In situ purification of ground water. Ground Water 14: 88-93.

Hapette AM, Poulet SA. 1990. Variation of vitamin C in some common species of marine plankton. Mar Ecol Prog Ser 64: 69-79.

Herrera-Melian JA, Dona-Rodriguez JM, Hernandez-Brito J, Pena JP. 1997. Voltammetric determination of Ni and Co in water samples. J Chem Educ 74: 1444-1445.

Hughes MN, Poole RK. 1989. Metal mimicry and metal limitation in studies of metal-microbe interactions. In: Metal-Microbe interactions. Poole RK, Gadd GM (eds) Oxford University Press, New York, pp. 1-18.

Hunt CD, Kelly JR. 1988. Manganese cycling in coastal regions: Response to eutrophication. Estu Coast Shelf Sci 26: 527-558.

Intwala A, Patey TD, Polet DM, Twiss MR. 2008. Nutritive Substitution of Zinc by Cadmium and Cobalt in Phytoplankton Isolated from the Lower Great Lakes. J Great Lakes Res 34:1-11.

Jacob (1996) Subcellular Biochemistry 25: Ascorbic Acid: Biochemistry and Biomedical Cell Biology, Harris JR (Ed.), Plenum Press, NY.

Kendall AI, Chinn H. 1938. The decomposition of ascorbic acid by certain bacteria. Studies in bacterial metabolism. CIX. J Infect Dis 62: 330-336.

Kennedy CB, Martinez RE, Scott SD, Ferris FG. 2003. Surface chemistry and reactivity of bacteriogenic iron oxides from Axial Volcano, Juan de Fuca Ridge, North-East Pacific Ocean. Geobiology 1: 59-69.

Lawrence JR, Chenier MR, Roy R, Beaumier D, Fortin N, Swerhone GDW, Neu TR, Greer CW. 2004. Microscale and molecular assessment of impacts of nickel, nutrients, and oxygen level on structure and function of river biofilm communities. Appl Environ Microbiol 70: 4326-4339.

Lee Y, Tebo BM. 1994. Cobalt(II) oxidation by the marine manganese(II)-oxidizing *Bacillus* sp. Strain SG-1. Appl Environ Microbiol 60: 2949-2957.

Loaec M, Olier R, Guezennec J. 1998. Chelating properties of bacterial exopolysaccharides from deep-sea hydrothermal vents. Carbohydr Polym 35: 65-70.

Mehmeti I, Solheim M, Nes IF, Holo H. 2013. *Enterococcus faecalis* grows on ascorbic acid. Appl Environ Microbiol doi: 10.1128/AEM.00228-13.

Moffett JW, Ho J. 1996. Oxidation of cobalt and manganese in seawater via a common microbially catalyzed pathway. Geochim Cosmochim Acta 60: 3415-3424.

Moffett JW. 1994. A radiotracer study of cerium and manganese uptake onto suspended particles in Chesapeake Bay. Geochim Cosmochim Acta 58: 695-703.

Moffett JW. 1997. The importance of microbial Mn oxidation in the upper ocean- a comparison of the Sargasso Sea and equatorial Pacific. Deep-Sea Res I 44:1277-1291.

Mopper K, Dawson R, Leibezelt G, Ittekkot V. 1980. The monosaccharide spectra of natural waters. Mar Chem 10: 55-66.

Mopper K, Larsson K. 1978. Uronic and other organic acids in Baltic Sea and Black Sea sediments. Geochim Cosmochim Acta 42: 153-163.

Murray JW, Dillard JG. 1979. The oxidation of cobalt(II) adsorbed on manganese dioxide. Geochim Cosmochim Acta 43: 781-787.

Myers CR. Nealson KH. 1988. Bacterial manganese reduction and growth with manganese oxide as the sole electron acceptor. Science 240: 1319-1321.

Nealson KH, Rosson RA, Myers CR. 1989. Mechanisms of oxidation and reduction of manganese. In: Metal ions and bacteria. Beveridge TJ, Doyle R (eds) John Wiley and Sons, NY, pp. 383-411.

Nieminen TM, Ukonmaanaho L, Rausch N, Shotyk W. 2007. Biogeochemistry of nickel and its release into the environment. Met Ions Life Sci 2: 1-30.

Nimmo M, Van Den Berg CMG, Brown J. 1989. The chemical speciation of dissolved nickel, copper, vanadium, and iron in Liverpool Bay, Irish Sea. Estuar Coast Shelf Sci 29: 57-74.

Nortemann B. 1992. Total degradation of EDTA by mixed cultures and a bacterial isolate. Appl Environ Microbiol 58: 671-676.

Orcutt BN, Sylvan JB, Knab NJ, Edwards KJ. 2011. Microbial Ecology of the Dark Ocean above, at, and below the Seafloor. Microbiol Mol Biol Rev 75: 361-422.

Oviedo C, Rodriguez J. 2003. EDTA: the chelating agent under environmental scrutiny. Quim Nova 26: 901-905.

Pareuil P, Penilla S, Ozkan N, Bordas F, Bollinger J-C. 2008. Influence of reducing conditions on metallic elements released from various contaminated soil samples. Environ Sci Technol 42: 7615-7621.

Price NM, Morel FMM. 1990. Cadmium and cobalt substitution for zinc in a marine diatom. Nature 344: 658-660.

Rajani RP, Banakar VK, Parthiban G, Mudholkar AV, Chodankar AR. 2005. Compositional variation and genesis of ferromanganese crusts of the Afanasiy-Nikitin Seamount, Equatorial Indian Ocean. J Earth Syst Sci 114: 51-61.

Richter HE, Switala J, Loewen PC. 1988. Effect of ascorbate on oxygen uptake and growth of *Escherichia coli B.* Can. J. Microbiol. 34: 822-825.

Roy P, Balaram V, Kumar A, Satyanarayanan M, Rao TG. 2007. New REE and trace element data on two kimberlitic reference materials by ICP-MS. Geostand Geoanal Res 31: 261-273.

Santander PJ, Roessner CA, Stolowich NJ, Holderman MT, Scott AI. 1997. How corrinoids are synthesized without oxygen: nature's first pathway to vitamin B12. Chem Biol 4: 659-666.

Stockdale A, Davison W, Zhang H, Hamilton-Taylor J. 2010. The association of cobalt with iron and manganese (oxyhydr)oxides in marine sediment. Aquat Geochem 16: 575-585.

Stone AT, Morgan JJ. 1984. Reduction and dissolution of manganese(III) and manganese(IV) oxides by organics: 2. Survey of the reactivity of organics. Environ Sci Technol 18: 617-624.

Sujith PP, Mourya BS, Krishnamurthi S, Meena RM, Loka Bharathi PA. 2014. Mobilization of manganese by basalt associated Mn(II)-oxidizing bacteria from the Indian Ridge System. Chemosphere 95: 486-495.

Sujith PP, Das A, Mourya BS, Loka Bharathi PA. 2011. Immobilisation of manganese, cobalt and nickel by deep-sea-sediment microbial communities. Chem Ecol 27: 189-206.

Sunda WG, Huntsman SA. 1987. Microbial oxidation of manganese in a North Carolina estuary. Limnol Oceanogr 32: 552-564.

Tebo BM, Lee Y. 1993. Microbial oxidation of cobalt. In: Biohydrometallurgical technologies. Torma AE, Wey JE, Lakshmanan VL (eds) The minerals, metals and materials society, pp. 695-704.

Thamdrup B. 2000. Microbial manganese and iron reduction in aquatic sediments. Adv Microb Ecol 16: 41-84.

Tilbrook GS, Hider RC. 1998. Iron chelators for clinical use metal ions. Biol Syst 35: 691-730.

Toner B, Sposito G. 2005. Reductive dissolution of biogenic manganese oxides in the presence of a hydrated biofilm. Geomicrobiol J 22: 171-180.

Trouwborst RE, Clement BG, Tebo BM, Glazer BT, Luther GW. 2006. Soluble Mn(III) in Suboxic Zones. Science 313: 1955-1957.

Vandevivere P, Kirchman DL. 1993. Attachment stimulates exo-polysaccharide synthesis by a bacterium. Appl Environ Microbiol 59: 3280-3286.

Vandieken V, Pester M, Finke N, Hyun J-H, Friedrich MW, Loy A, Thamdrup B. 2012. Three manganese oxide-rich marine sediments harbor similar communities of acetate-oxidizing manganese-reducing bacteria. ISME J 6: 2078-2090.

Vaughan D, Lumsdon DG, Linehan DJ. 1993. Influence of dissolved organic matter on the bio-availability and toxicity of metals in soils and aquatic systems. Chem Ecol 8: 185-201.

Villalobos M, Toner B, Bargar J, Sposito G. 2003. Characterization of the manganese oxide produced by *Pseudomonas putida* strain MnB1. Geochim Cosmochim Acta 67: 2649-2662.

Wallenstein MD, Weintraub MN. 2008. Emerging tools for measuring and modeling the *in situ* activity of soil extracellular enzymes. Soil Biol Biochem 40: 2098-2106.

Wenk MR, Fernandis AZ. 2007. Assays. In: A manual for biochemistry protocols. Schantz J-T (ed) World Scientific Publishing, Singapore, pp. 81-99.

CHAPTER 6

Immobilization of nickel by bacterial isolates from the Indian Ridge System and the chemical nature of the accumulated metal

6.1. Abstract

Two bacterial isolates, CR35 and CR48 retrieved from bottom waters of the CR were tested for immobilization of 10 μM to 10000 μM Ni. Bacterial cells challenged with 100 μM Ni for 60 d resulted in maximum of 89.8% and 6.95% decrease in the soluble phase of metal at 28±2°C and 14.75% and 6.38% at 3±1°C with CR35 and CR48 respectively. SEM observation of CR35 grown with 10000 μM Ni showed an average cell size of 4.37±0.47 × 3.01±0.34 μm compared to the cell size of 1.72±0.2 × 1.20 ±0.14 μm in the control. With CR48, the cell size increased from 1.16±0.28 × 0.96 ±0.17 μm in control to 6.89±0.34 × 2.08±0.13 μm at the above test concentration. XRD analysis of cells showed prominent peaks for NiS in CR35 and NiS and NiP2 in CR48 suggesting cation sequestration as sulfides and phosphides. The data contributes to the knowledge of bacterial interaction with Ni in ridge and other metal percolated ecosystems.

6.2. Introduction

Marine bacteria are indigenous to an environment characterized by a small amount of organic matter and a large amount of inorganic salts (Gonye and Jones, 1973). Like any complex system, the marine environment also serves as a unique niche for many specialized life forms and supports a diverse array of microorganisms (Prescott *et al.,* 1999). The hydrothermal vent fields and the nearby water columns are a source for reduced inorganic ions. Some of the microorganisms in these habitats may oxidize certain reduced form of metals (Jannasch and Wirsen, 1979; Jannasch, 1984; Mandernack and Tebo, 1993) and are able to derive energy in oxidizing relatively large amounts of these reduced metal species to fulfil their metabolic needs (Ehrlich, 1976; 1978). The tectonically active Carlsberg Ridge in the Arabian Sea is such a habitat known to support chemosynthesis and can serve as sink for various metal ions (Mn, Fe,

Co, Ni etc). Besides the ridge sources, mining and metallurgical activities also contribute to an increase in the level of trace metals in the sediment and aquatic environments (Gonzalez *et al.,* 1997). The average global concentration of Ni in the oceans is 0.6 ppb (μg/kg) in soils 16 ppm (μg/g), in lakes and in rivers 1.0 ppb (Nriagu, 1980) and is 21-251 ppm in sediments from southwest Carlsberg Ridge (Pattan and Higgs, 1995).

Metal ion homeostasis is very crucial for optimum growth and survival of microorganisms. In order to meet the physiological needs for these nutritionally required trace elements, microorganisms have special uptake mechanisms for some of them. Once in the cell, the elements may be sequestered. Excess concentrations of these elements in ionic form in cells may, however, be toxic (Schmidt and Schlegel, 1989). The mechanisms such as intracellular sequestration of metals by proteins and polyphosphate granules may be a means of metal storage or detoxification (Keasling, 1997). However, intracellular toxicity of metals is mainly overcome by metal efflux. Excess metal uptake may also be controlled in some organisms by binding of metal ions to slime consisting of exopolysaccharide (Helmann *et al.,* 2007). This in turn limits the direct effect of metal ion on cells. As a result, the cells survive and continue to perform their normal metabolic activities in the presence of excess metal concentration. The present work attempts to understand the nature of interaction between bacteria and Ni and their ability to immobilize the metal. Our observation is applicable to sediments and other organically depleted natural ecosystems where the metal concentrations vary from a few ppm to ppb levels. This is the first study to show that, bacterial isolates from a ridge system capable of immobilizing Mn can also immobilize Ni. The oxides of Mn are otherwise generally known to stimulate the immobilization of other metals including Ni. The study demonstrates how immobilization of Ni can be effected even in the absence of manganese.

6.3. Materials and methods

6.3.1. Organism and growth

The Mn oxidizing bacterial isolates CR35 and CR48 employed in the present study were retrieved from Carlsberg Ridge waters (Fernandes *et al.,* 2005). The isolate CR35 was obtained from a water depth of 3040 m at 3°35'N latitude and 64°07'E

longitude and CR48 from a water depth of 3510 m at 4°31'N latitude and 62°33'E longitude. The isolate CR35 was capable of growing in media prepared in distilled water with 0.5% NaCl, whereas, seawater was mandatory for the growth of CR48. The isolates when grown in the presence of Ni in seawater showed no additional growth requirement. Therefore, the incubation experiment for Ni immobilization was done only with metal salt ($NiCl_2$. $6H_2O$, Merck) in aged seawater (pH 7.8). Inocula of the bacterial isolates were grown in 0.01% nutrient broth (Merck) containing 15 g peptone, 3 g yeast extract, 6 g NaCl and 1 g D(+) glucose in a litre of seawater at 3±1°C. They were harvested by centrifugation at 8000 rpm for 10 min at 4°C when the cell density reached an OD_{600} of 1.5. Cell pellets were washed twice with sterile saline, resuspended and used for the inoculation of experiment tubes. The stock cultures were maintained on 25% nutrient agar slants at 4°C.

6.3.2. Immobilization of nickel

To quantify immobilization of Ni by whole cells, the experiment was carried out in 15 ml screw capped test tubes with Ni amendments of 10, 100, 1000 and 10000 µM in seawater containing triphenyl tetrazolium chloride at a final concentration of 0.025%. Controls for each concentration of Ni, but without bacterial cells were included to correct for chemical oxidation and loss of metal due to adsorption on glassware. The experimental tubes containing 11 ml media were inoculated in triplicate to give an initial cell count of 2.97×10^7 cells ml^{-1} for CR35 and 3.52×10^7 cells ml^{-1} for CR48. The tubes were incubated at 28±2°C and 3±1°C in the dark. Samples (1 ml) were removed immediately after inoculation and after 60 d of incubation for determining the total count, respiring cell count and Ni concentration in the liquid phase. The total count and the number of respiring cells (pink) were determined after segregation of cell aggregates by sonication at 15 Hz for 3 s. The cells were counted in a Neubauer counting chamber at 400-x magnification with a bright field microscope (Nikon 80i). The formazan in experimental tubes was determined and the values were corrected for the 0 d absorbance at the end of the experiment (Fernandes *et al.*, 2005). The OD values for formazan in culture were converted to mg ml^{-1} formazan using the equation for the line of best fit derived from a standard curve of formazan (Himedia) prepared in methanol. Ni was estimated from the supernatant by a spectrophotometric method (Chester and Hughes, 1968) at 460 nm after centrifugation at 8000 rpm for 10 min. For

higher concentration of >10 μM Ni, supernatant was suitably diluted with distilled water. The experimental readings were corrected for control to estimate the rate of Ni immobilization.

6.3.3. Effect of added Ni on bacterial growth rate

The isolates CR35 and CR48 were grown at 100 μM concentration of Ni in seawater together with controls lacking added Ni to study the effect of added Ni on growth of strains CR35 and CR48. The inoculum for the experiment was prepared as above and 0.5 ml of the culture was inoculated in triplicate and was incubated at 28±2°C for 6 d. Daily 20 μl of samples from individual tubes were withdrawn and loaded on to Neubauer counting chamber for bright field microscopic (Nikon 80i) count. The cells were examined under 400-x magnification and the counts were expressed as numbers per ml of sample.

6.3.4. Microscopy

The bacterial cells grown in the presence and absence of Ni were harvested by centrifugation at 8000 rpm for 10 min at 4°C after 60 d of incubation. The cell pellet was suspended in sterile 0.85% saline and a drop was placed on small pieces of cover slip and air-dried. The cells were dehydrated by passing the cover slips carrying the cells through 10, 30, 50, 70, 90 and 100% acetone. The cover slips containing the dehydrated sample smears were mounted on an electron microscope stub, sputter coated with Au/Pd. The cells were then examined under a JEOL JSM-5800 SEM. For light microscopy, wet mounts of bacterial cells were made using acid cleaned glass slides and cover slips. Bacterial morphology and cell aggregation were observed at 400-x magnification and photographed with a digital camera and the images processed using software image pro 6.2.

6.3.5. X-ray diffraction and Energy dispersive x-ray analysis

The bacterial isolates CR35 and CR48 were grown at 28±2°C for 7 d in seawater with and without added 1000 μM $NiCl_2$. $6H_2O$. The respective cultures were then harvested and washed three times with sterile 0.85% saline and once with acetone by centrifugation at 8000 rpm for 15 min at 4°C and air-dried. The samples were powdered with a micro pestle in 2 ml eppendoff tubes. The XRD pattern (Deplanche

and Macaskie, 2008) were recorded in a Rigaku x-ray powder diffractometer using monochromatic Cu $K\alpha_1$ radiation (λ = 1.54050 A°). The diffraction spectra were recorded over the range of 10° to 100° (2θ) with a step length of 0.02° (2θ). The identification of Ni salts was based on comparison with the joint committee on powder diffraction standards file (1981). An EDX analysis was done on a small portion of intact cells from the above cultures on JEOL JSM-5800 at an accelerating voltage of 15 kV.

6.3.6. Infrared (IR) analysis

The CR35 and CR48 bacterial isolates grown at room temperature (28±2°C) for 2 d in seawater in the presence of 1) 100 µM added Ni and 2) in its absence were separated by centrifugation at 8000 rpm for 15 min at 4°C (Sigma 3-18K), washed three times with sterile 0.85% saline and once with distilled water and then lyophilized (Heto LL1500 freeze dryer). A known quantity of lyophilized bacterial sample (0.8 mg) and dry potassium bromide (1.75 mg) was placed in a smooth agate mortar and mixed thoroughly. The powder was filled in a micro-cup of 2 mm internal diameter (Naumann *et al.*, 1991). The diffuse reflectance infrared spectrum of the samples was recorded in a Shimadzu FTIR-8201PC spectrophotometer with 60 scans at a resolution of 4 cm^{-1} in the transmission mode (mid infrared region 4000-400 cm^{-1}).

6.3.7. Plasmid screening

The isolates CR35 and CR48 were grown in 0.1% nutrient broth in tubes with and without Ni (100 µM) amendment and were incubated at 28±2°C. The cells of the early exponential phase (OD_{600} of 1.2) were harvested by centrifugation at 8000 rpm for 10 min at 4°C. The cell pellets were washed twice with physiological saline (0.85%) and were immediately used for the preparation of cell lysates (Kado and Liu, 1981). The bacterial lysates were analyzed by agarose gel electrophoresis with agarose concentration of 0.6 and 1% according to the procedure of Meyers *et al.* (1976). Supermix DNA ladder (0.5 to 33.5/24.5 kb) obtained from Bangalore Genie was used as the reference marker. The gel was stained with ethidium bromide (0.5 µg ml^{-1}) for 30 min and photographed after destaining using the gel documentation and analysis system (Biorad).

6.4. Results

6.4.1. Nickel immobilization

Ni immobilization by both the isolates was enhanced with increasing Ni concentration (Figure 6.1). CR35 showed a maximum Ni immobilization of 120.7 µM at 28±2°C (Figure 6.1A) and 20.3 µM at 3±1°C (Figure 6.1B) with 1000 µM test Ni concentration. In parallel, CR48 showed maximum Ni immobilization of 309.5 µM at 28±2°C and 38.53 µM at 3±1°C with 10,000 µM test Ni concentration. Nevertheless, at 100 µM added Ni concentration, CR35 immobilized 89.8% of the Ni, at 28±2°C and 14.75% at 3±1°C, which was the maximum removal observed with this strain. With CR48, a similar trend was not observed, rather immobilization was maximum at 19.27% at 28±2°C at 1000 µM added Ni concentration and 11.9% at 3±1°C at 10 µM added Ni concentration. The study showed that temperature has an effect on Ni immobilization and was faster at 28±2°C with both of the test isolates.

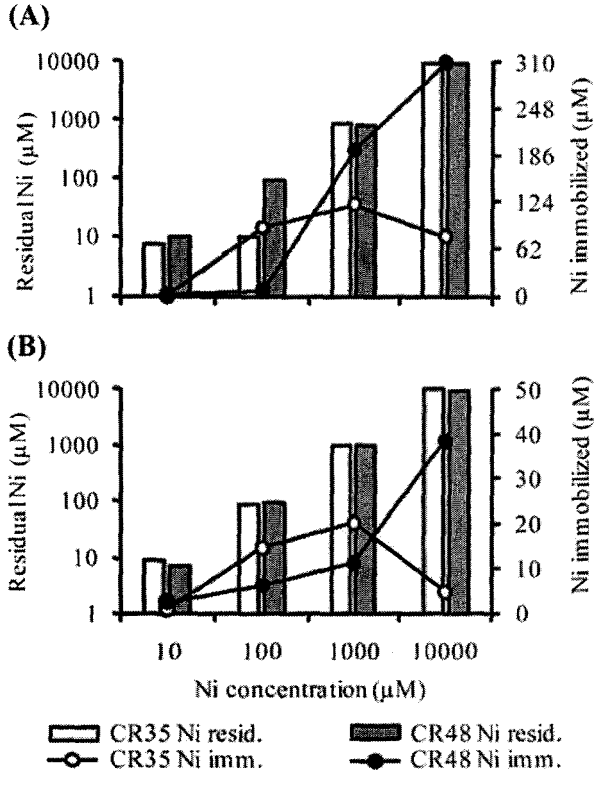

Figure 6.1. Effect of temperature on Ni immobilization by bacterial isolates CR35 and CR48. A) Immobilization at 28±2°C and B) Immobilization at 3±1°C. The legend "Ni imm" represents Ni immobilization and "Ni resid" represents Ni residual. The values are ± mean, n=3.

6.4.2. Bacterial growth

The bacterial growth was monitored with Ni to determine the effect of the metal cation on bacterial cells. The bacterial number decreased with increase in Ni concentration. The maximum cell number was 6.63 ± 4.89×10^7 cells ml^{-1} with CR35 at 28±2°C (Figure 6.2A) and 6.19 ± 5.09×10^7 cells ml^{-1} at 3±1°C (Figure 6.2B) in the presence of 10 µM added Ni. However, with CR48, the cell number was maximum at 100 µM and it was 9.32 ± 2.97×10^7 cells ml^{-1} at 28±2°C (Figure 6.2C) and 3.27 ± 9.63×10^7 cells ml^{-1} at 3±1°C (Figure 6.2D). The difference in cell number between 28±2°C and 3±1°C was 74.7% with CR35, and 85% with CR48. Beyond 100 µM Ni concentration, no increase in cell number was observed, either at 28±2°C or at 3±1°C, with both the isolates. The cell counts were comparatively smaller at 3±1°C than at 28±2°C. The formazan estimation of respiration was maximum (0.18 ± 0.01 mg ml^{-1}) at 10 µM Ni with CR35 and 0.15 ± 0.016 mg ml^{-1} with CR48 at 100 µM Ni concentration at 28±2°C (Figure 6.2).

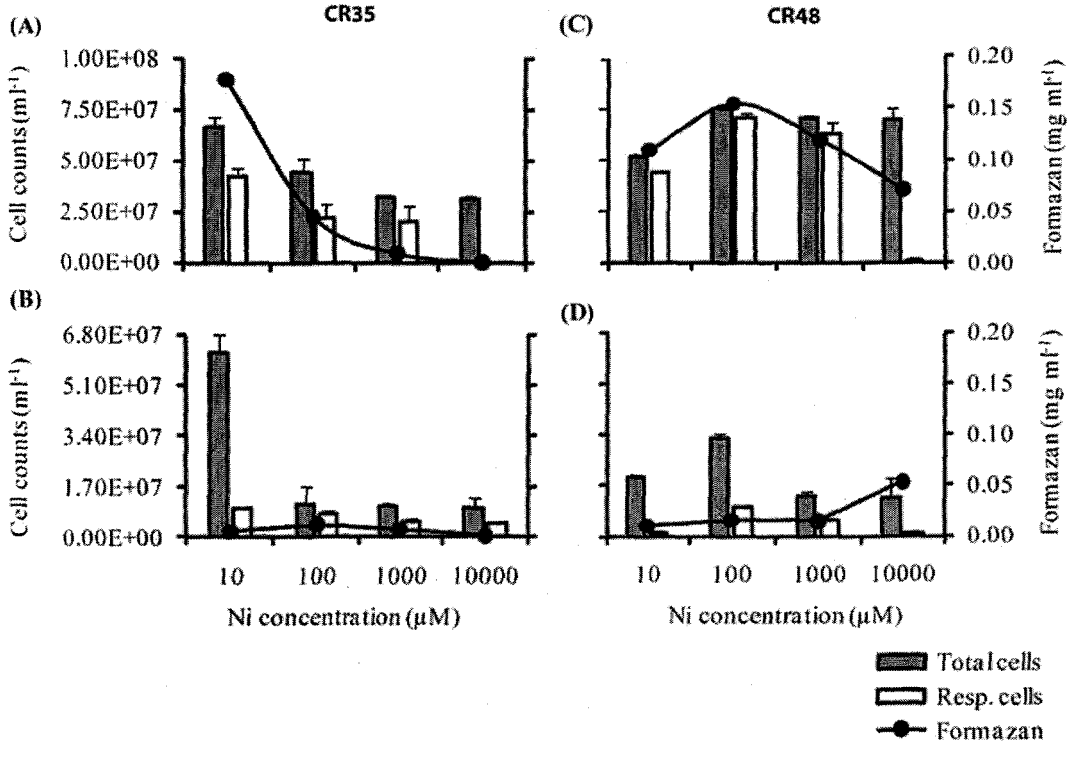

Figure 6.2. Total cell count, respiring cell count (resp.count) and formazan concentration in Ni amended seawater medium. A) CR35 (28±2°C), B) CR35 (3±1°C), C) CR48 (28±2°C) and D) CR48 (3±1°C). Note that the scale for figures 'A' and 'C' is different from 'B' and'D'.

These results suggest that 100 μM Ni is the threshold concentration for tolerance in both the isolates. The number of respiring cells at 100 μM Ni concentration was 4.26 ± 4.33×10^7 cells ml^{-1} at 28±2°C (Figure 6.2A) and 9.89 ± 3.33×10^6 cells ml^{-1} (Figure 6.2B) at 3±1°C for CR35 and 8.80 ± 2.56 $\times10^7$ cells ml^{-1} at 28±2°C (Figure 6.2C) and 9.63 ± 2.77×10^6 cells ml^{-1} at 3±1°C (Figure 6.2D) for CR48.

6.4.3. Stimulatory effect of nickel on bacteria

The growth rate of bacteria in the presence and absence of Ni is shown in Figure 6.3. The bacterial count increased with Ni (100 μM) and decreased in its absence with time. The cell count for CR35 showed a marginal increase with Ni from 2.28 ±9.8×10^8 to 5.34 ± 1.28×10^8 cells ml^{-1} at the end of 6 d incubation. With CR48, the cell count attained a maximum of 6.3 ± 6.56×10^8 cells ml^{-1} on 5 d of incubation and thereafter showed a marginal decrease on the 6 d.

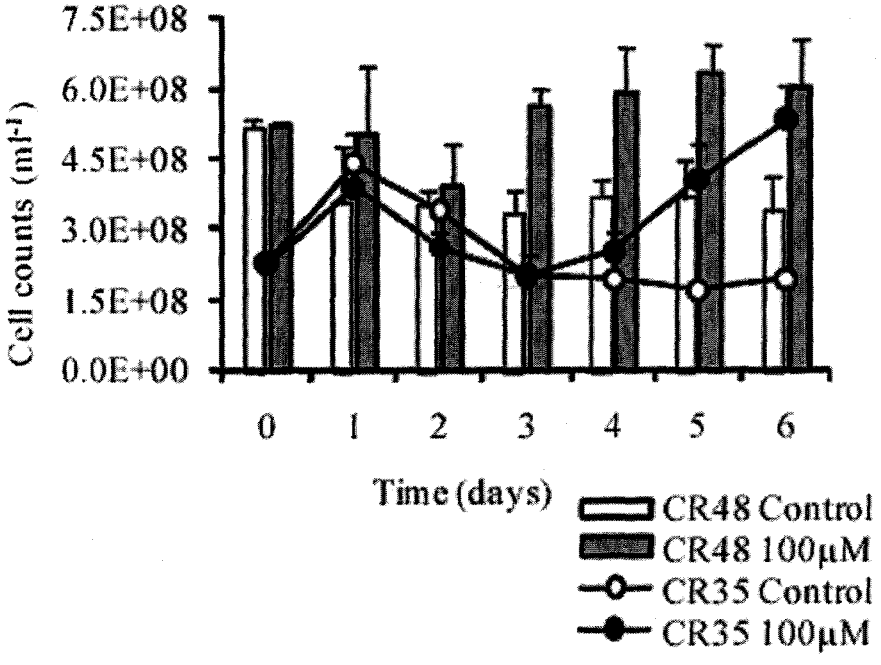

Figure 6.3. Growth rate of CR35 and CR48 in the presence (100μM) and absence of $NiCl_2$ at 28±2°C.

6.4.4. Microscopy and EDX analysis

The Ni-exposed and -unexposed bacterial cells were observed under SEM to investigate morphological changes induced by the metal after 60 d of incubation.

Control cells grown in seawater without any nutrient or Ni amendment did not show any morphological variation and appeared normal (Figure 6.4A, D).

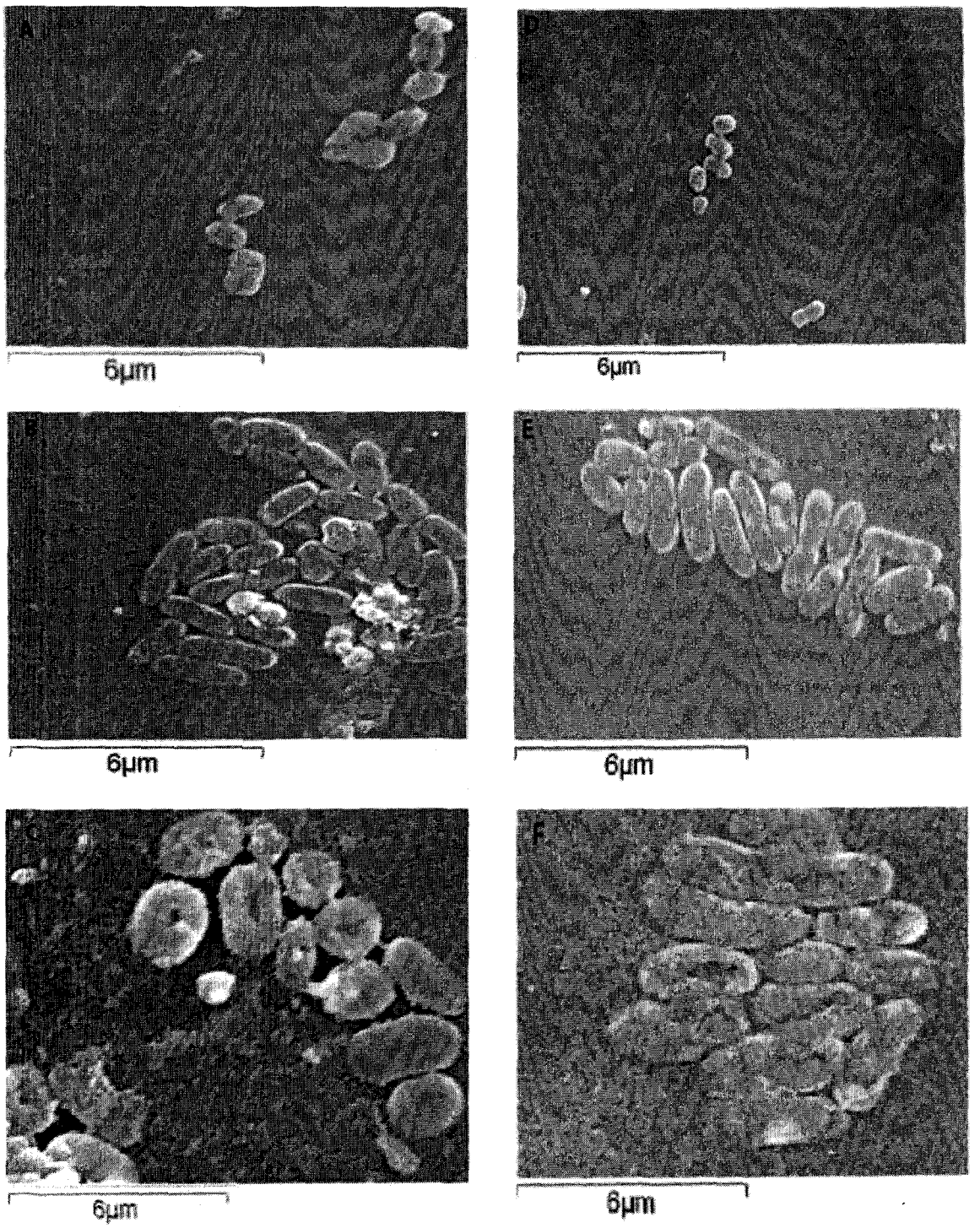

Figure 6.4. Scanning electron microscope images showing morphological changes of CR35 cells grown in seawater medium A) with no Ni added, B) 100µM and C) 1000µM added $NiCl_2$. CR48 cells grown in seawater medium D) with no Ni added, E) 100µM and F) 1000µM added $NiCl_2$.

The average cell size (L×W) of CR35 was from 1.72 ± 0.2 × 1.20 ± 0.14 μm and that of CR48 was 1.16 ± 0.28 × 0.96 ± 0.17 μm. Bacterial cells exposed to 100 μM Ni showed healthy dividing cells (Figure 6.4B, E). The average size of CR35 ranged from 4.02 ± 0.38 × 1.58 ± 0.12 μm and CR48 from 5.2 ± 0.77 × 1.83 ± 0.33 μm. At 10,000 μM Ni concentration, increase in cell size and subsequent rupture was observed (Figure 6.4C, F). The average size of CR35 ranged from 4.37 ± 0.47 × 3.01 ± 0.34 μm and CR48 from 6.89 ± 0.34 ×2.08 ± 0.13 μm. Overall, the cell size increased to 2.65 × 1.81 μm with CR35 and to 5.73 × 1.12 μm with CR48 at 10,000 μM Ni concentration. EDX analysis of CR35 and CR48 isolates grown in the absence of Ni showed peaks for phosphorus, potassium, magnesium, calcium, silicon and oxygen (Figure 6.5a, c). The bacterial cells exposed to the metal showed peaks for Ni with decrease in intensity of the peak for Mg in both the isolates and loss of K peak in CR35 indicating cation efflux (Figure 6.5b, d).

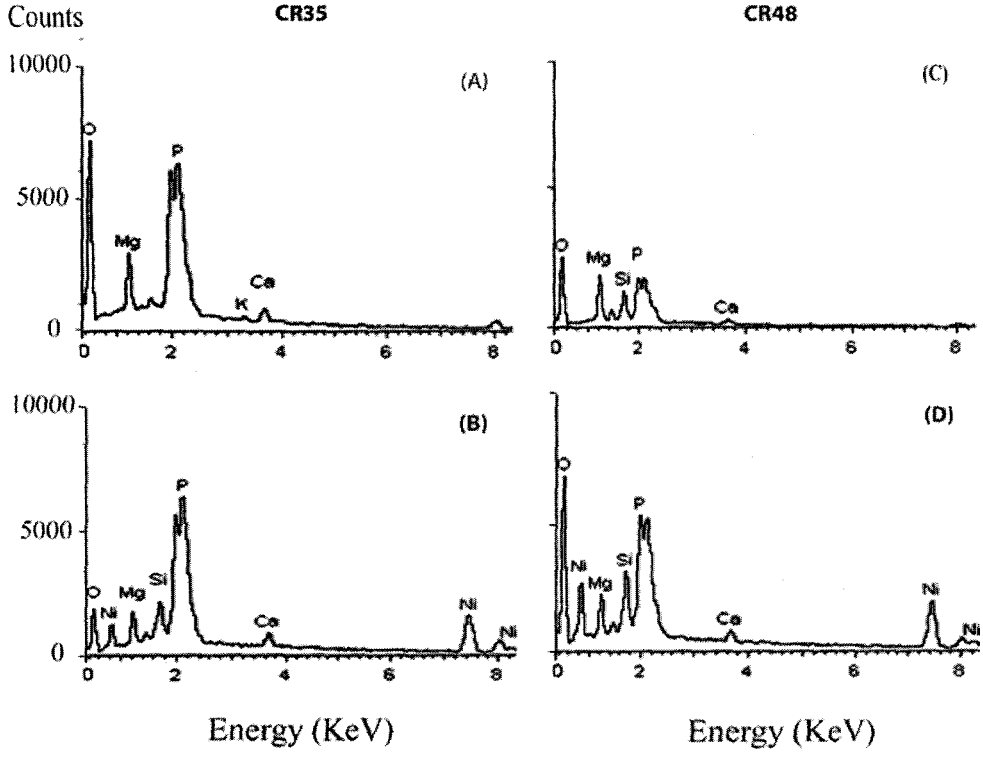

Figure 6.5. Energy dispersive x-ray spectra of bacterial cells (a) CR35 in the absence of Ni, (b) CR35 exposed to 1000 μM Ni, (c) CR48 in the absence of Ni, (d) CR48 exposed to 1000 μM Ni.

The wet mount observation under bright field microscope showed the occurrence of cell aggregates. The size of the aggregates increased and their number decreased with higher concentration of Ni. It was vice versa with lower test concentrations. Cells grown in the absence of Ni showed discrete cells (Figure 6.6).

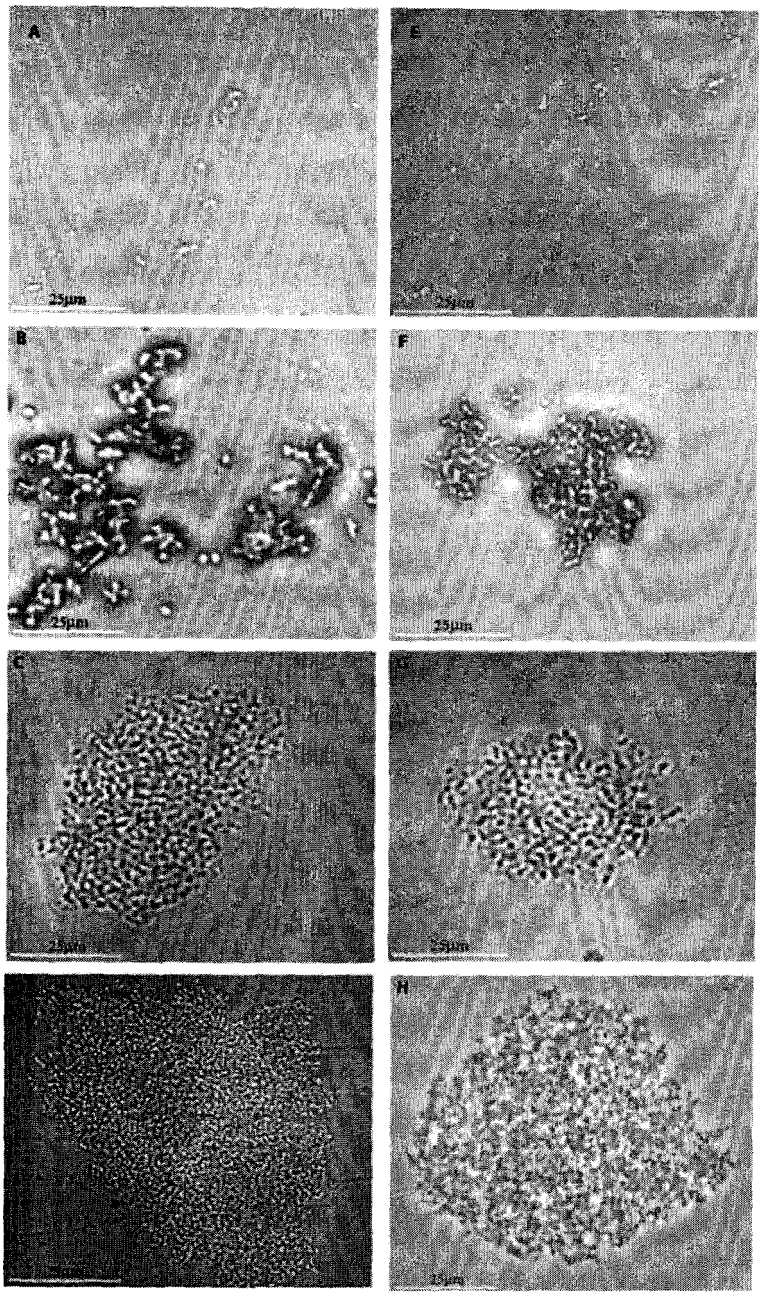

Figure 6.6. Bright field images show bacterial cell aggregate formation and difference in aggregate size following incubation in the absence and presence of added nickel as Ni^{2+}. A) CR35 isolate in the absence of Ni, B) 10μM, C) 100μM and D) 1000μM Ni. E) CR48 isolate in the absence of Ni, F) 10μM, G) 100μM and H) 1000μM Ni.

6.4.5. X-ray diffraction analysis

The XRD analysis of bacterial cells showed that Ni was sequestered as both a diphosphide and a sulfide mineral in the bacterial cells. Diffractograms of control cells CR35 (Figure 6.7a) and CR48 (Figure 6.7c), lacked any distinct peak, and showed the characteristic amorphous nature of the samples, while distinct peaks for Ni loaded biomass from the experimental flasks indicated the deposition of crystallized Ni compounds. Based on the d-values (1.42, 1.300, 1.140 and 1.01), peaks for the Ni-loaded CR35 cells (Figure 6.7b) at 2θ = 65.96, 72.68, 85 and 99.56° could be assigned to the existence of Ni sulfides. In contrast, for CR48 isolate (Figure 6.7d) most of the peaks were at 2θ =28.2, 34.66 and 59.96 with d- values of 3.162, 2.586 and 1.541 which correspond to Ni diphosphides. However, peaks at 2θ = 64.7 and 98.08 with d-values 1.44 and 1.09 could be related to Ni sulfides. Though EDX confirmed the presence of phosphorus in the cells, the interpretation of some XRD peaks were not possible which could correspond to phosphide mineral in CR35. The present study suggests that both CR35 and CR48 could accommodate Ni as both phosphide and sulfide minerals.

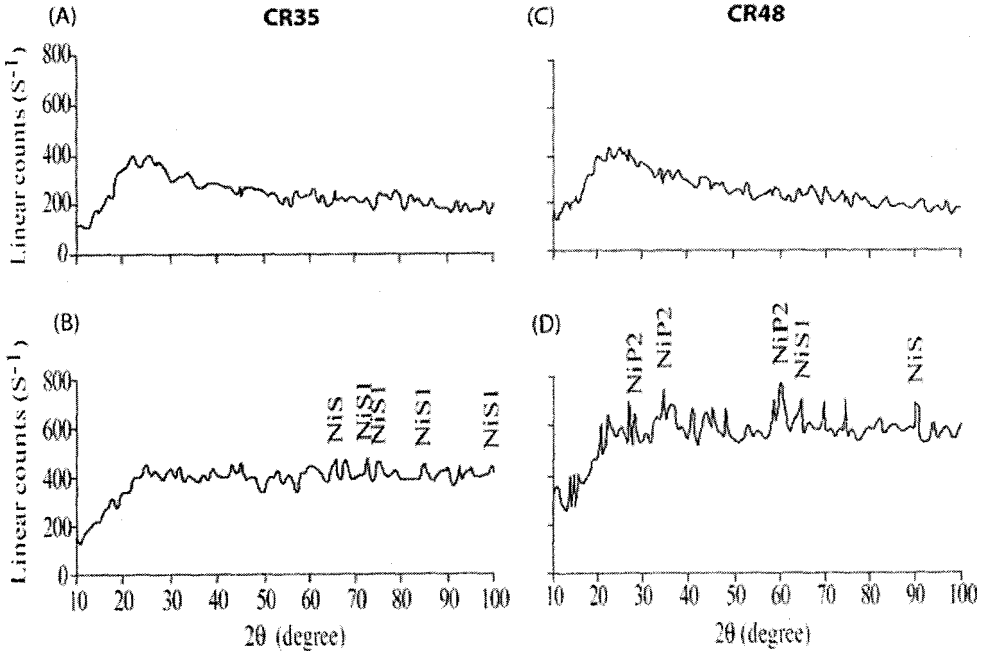

Figure 6.7. X-ray diffraction spectra of dried and powdered bacterial biomass (a) CR35 in the absence of Ni, (b) CR35 exposed to 1000μM Ni, (c) CR48 in the absence of Ni, (d) CR48 exposed to 1000μM Ni.

6.4.6. IR spectral analysis

The IR analysis of bacterial isolates CR35 and CR48 were examined in the presence and absence of Ni to understand the Ni induced changes in bonding characteristics of the functional moieties in the bacteria. The characteristic bands of CR35 biomass were at 435.9, 1064.6, 1238.2, 1647.1 and 2925.8 cm^{-1} (Figure 6.8A) and CR48 biomass were at 420.5, 1068.5, 1240.1, 1645.2 and 2923.9 cm^{-1} (Figure 6.8C). The biomass exposed to Ni indicated discernable changes in the intensities of the bands. The band at frequency 435.9 cm^{-1} in CR35 increased in intensity on Ni exposure to 451.3 cm^{-1} (Figure 6.8B).

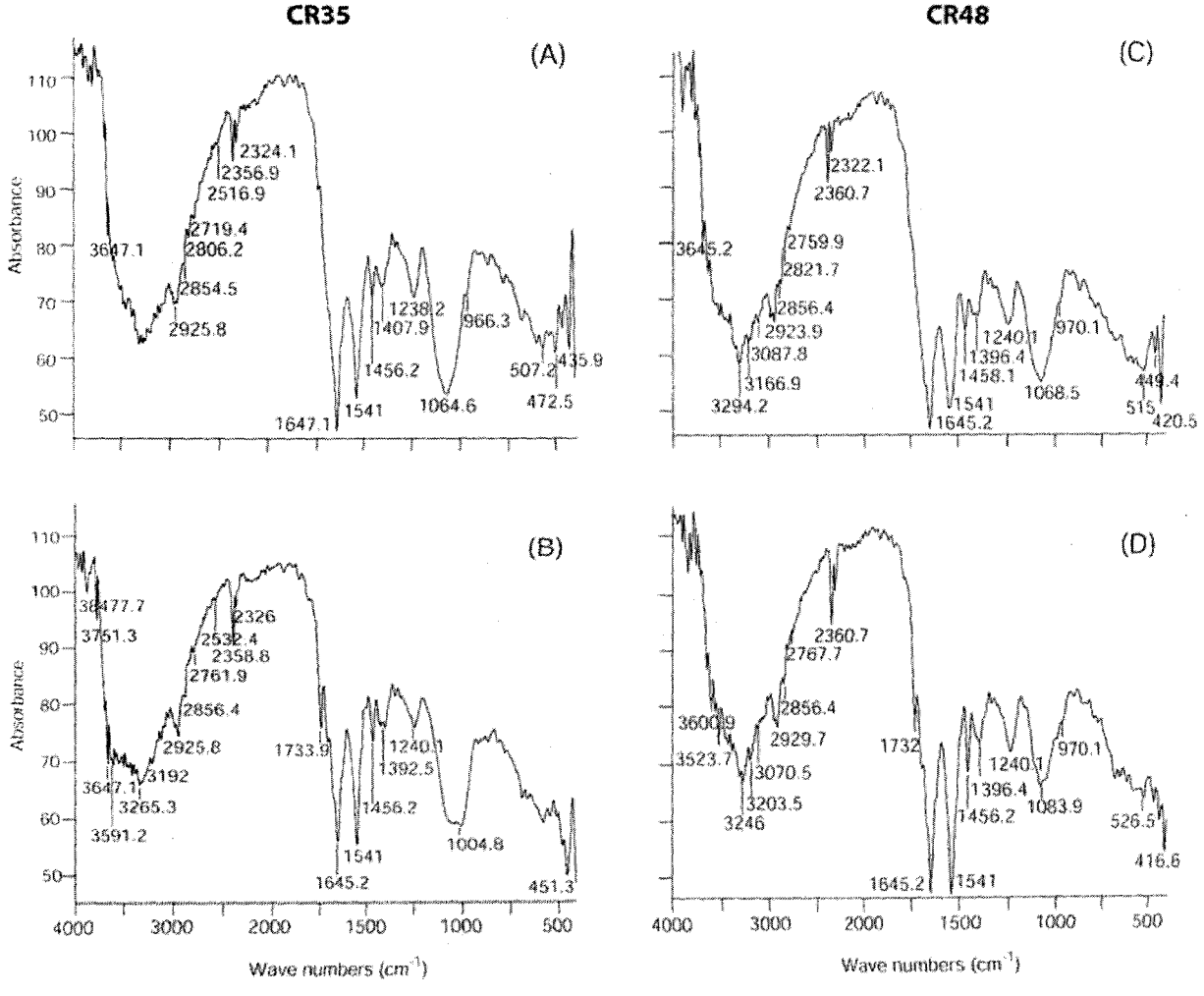

Figure 6.8. Fourier transform infrared (FTIR) spectra of bacterial biomass. (A) CR35 in the absence of Ni, (B) CR35 exposed to 100μM Ni, (C) CR48 in the absence of Ni, (D) CR48 exposed to100μM Ni.

In contrast, with CR48 the frequency at 420.5 cm^{-1} decreased in intensity to 416.6 cm^{-1} (Figure 6.8D). This shows that δ(O-H) group could participate in Ni chelation. The stretching vibration at frequency 1064.6 cm^{-1} in CR35 decreased in intensity on Ni exposure to 1004.8 cm^{-1} while in CR48 the frequency at 1068.5 cm^{-1} increased to 1083.9 cm^{-1}. This shows that (C-O), (C-C), (C-O-C), (C-O-P) of cell wall polysaccharides participate in Ni chelation. But, stretching vibration at 1645.2 cm^{-1} showed no change in intensity on Ni exposure with CR48 while the frequency at 1647.1 cm^{-1} decreased to 1645.2 cm^{-1} after Ni exposure in CR35 indicating the change in peptide bond characteristic of (C=O) group. Similar changes in frequency intensities were observed for (P=O) group in CR35 on Ni exposure and authenticate the binding of Ni to hydroxyl, carbonyl and phosphoryl functionalities.

6.4.7. Plasmid

Lysates of bacterial cells grown in the presence and absence of Ni examined by agarose gel electrophoresis showed no plasmids.

6.5. Discussion

The present study shows the Ni immobilizing ability of Mn oxidizing bacterial isolates CR35 and CR48 retrieved from Carlsberg Ridge bottom waters under ambient (28±2°C) and cold temperature (3±1°C) (Fernandes *et al.,* 2005). The sequestration of Ni as NiS, NiS1 and NiP2 was revealed by XRD. Though the cells showed active division at 100 μM Ni concentration, the cells grew larger and even formed aggregates at increasing Ni concentrations. The study highlights the stimulatory effect of Ni (Figure 6.3) at lower concentration and accumulation of the metal as either sulphides or diphosphides at higher concentration. This is the first report that gives an insight into the cellular changes and Ni accumulation within bacteria of the Indian ridge ecosystem.

Spectroscopic analysis of Ni showed a decrease of dissolved Ni in the aqueous phase in the experimental tubes. The decrease in the concentration of dissolved Ni was highest at the lower Ni concentrations and smallest at the higher Ni concentration at both 28±2°C and 3±1°C. However, the extent of Ni immobilization at 3±1°C was comparatively smaller than at 28±2°C. The lower immobilization at 3±1°C corresponds to the slower growth rate at low temperature (Figure 6.1B). The results of the study

showed an increase in bacterial number at 10 and 100 μM Ni, which suggests that the 10 and 100 μM Ni concentrations were stimulatory for bacterial growth. The studies of Bartha and Ordal (1965) on *Hydrogenomonas* strains, Partidge and Yates (1982) on *Azotobacter chroococcum* and Stults *et al.* (1987) on *Bradyrizhobium japonicum* support the previously presented evidence of growth stimulation by Ni. However, excessive concentration of Ni was found to inevitably disorder cell metabolism followed by decrease in cell count. The results agree with those of Sigee and Al-Rabaee (1986), who reported cell wall damage and subsequent reduction in growth and cell metabolism of *Pseudomonas tabaci* in excess concentration of Ni in the growth medium. In this study, the amount of formazan produced was maximum at 28±2°C and occurred below 100 μM Ni concentration with both the isolates (Figure 6.2). The present findings suggest that the strains suffered stress above a threshold concentration of Ni, some cells surviving and others perishing.

The SEM observation of bacterial morphology showed a loss in cell wall rigidity above the minimum Ni threshold concentration. Nonetheless, microscopic observation and EDX analysis suggested that Ni was sequestered by the bacterial cells (Figure 6.4 and 6.5). The decrease in the level of Mg and K in cells exposed to Ni indicated that Ni immobilization involved ion exchange. The acquisition of Ni and the cell rupture are consistent with the observed microscopic cell counts. The results are in agreement with Sigee and Al-Rabaee (1986) with respect to exchange of Ni ions in cells and consequent inhibition of cell division in excess concentration of Ni. The present findings are in agreement with a report by Nies (1999) with respect to a need for heavy metal uptake to cause any physiological or toxic effects. The observation by Cobet *et al.* (1970) of a morphological change of *Arthrobacter marinus* grown in the presence of an excess of Ni, lends support to the present findings (Cobet *et al.,* 1970). The rate of Ni uptake by strains CR35 and CR48 was slower comparatively than the rate of Mn oxidation by these two strains (Fernandes *et al.,* 2005). The Mn oxidizing activity, which was monitored maximum at 100,000 μM concentration, was ten times higher than at 10,000 μM Ni concentration. Although the cultures failed to oxidize Mn at 100,000 μM, the inhibitory effect of Ni occurred at a lower Ni concentration of 10,000 μM. Ni appeared to have been sequestered within the cells in the strains CR35 and CR48, whereas oxidized Mn was deposited on the exterior of the cells.

The precipitation of Ni as NiS (Millerite) has been suggested as the crystalline phase of biogenic nickel sulfides (Waybrant *et al.,* 1998; Southam, 2005). The degradative metabolism of assimilated sulfur-containing amino acids by bacteria could lead to Ni precipitation as NiS (Freeman *et al., 1975*). Microbial conversion of sulfate ($SO4^{2-}$) to sulfide (S^{2-}) in waters with reducing conditions could also lead to NiS formation (Babich and Stotzky, 1983). XRD analysis of Ni grown strains CR35 and CR48 showed the immobilized Ni as NiS and NiP2. The current result agrees with the report of Kazy *et al.* (1999) on accumulation of copper as CuS and Sar *et al.* (2001) on Ni as NiP2 by *Pseudomonas aeruginosa.* The reports of Aickin *et al.* (1979) and Macaskie *et al.* (1987) on sequestration of lead and cadmium as phosphate in *Citrobacter* sp also support the present findings.

IR analysis of bacterial cells showed a band at frequency 1064.6 cm^{-1} with a shoulder at 966.3 cm^{-1} for CR35 (Figure 6.8A) and 1068.5 cm^{-1} with a shoulder at 970.1cm^{-1} for CR48 (Figure 6.8B). This was interpreted as a stretching vibration of C-O, C-C, C-O-C and C-O-P groups (Wolkers *et al.,* 2004; Yee *et al.,* 2004). The intensity of the band in the presence of Ni decreased with CR35 and increased with CR48 (Figure 6.8C and 6.8D) suggesting that Ni immobilization was accompanied by a decrease/increase in polysaccharide and phosphate. Parikh and Chorover (2005) also observed a similar stretching vibration in relation to Mn oxidation. The stretching vibration characteristic of C=O of peptides was observed at 1647.1 cm^{-1} in CR35 and 1645.2 cm^{-1} in CR48. The intensity of the band decreased to 1645.2 cm^{-1} with CR35 and remained unchanged with CR48 in Ni exposed cells, which could indicate an interaction of Ni with peptide bonds of protein in CR35. Backmann *et al.* (1996) explained a similar stretching vibrations of C=O specific for peptide bond in the 1700 – 1600 cm^{-1} region. The other stretching vibration specific for P=O decreased in intensity from 1407.9 cm^{-1} to 1392.5 cm^{-1} in Ni treated cells of CR35 indicating a role of phosphate in binding of Ni. A report by Fiona *et al.* (2003) is consistent with the present results that suggested a crucial role of sugar phosphate esters in metal chelation. The bands in the lower frequencies <700 cm^{-1} are an indication of stretching vibration of the δ(O-H) group (Kamnev *et al.,* 1997). In the present study stretching vibration of δ(O-H) group and an increase in intensity at the lower frequencies of bands in Ni-exposed cells of CR35 and CR48 was observed. This could indicate an intense

formation of γ(M-O) complex (M=metal ion). The study of Kamnev *et al.* (1997) on Cu-loaded *Azospirillum brasilense* biomass suggested that a relatively higher absorption at lower frequencies could be assigned to the formation of γ(M-O) and δ(O-M-O) bands.

Bacterial resistance to Ni in heavy-metal contaminated ecosystems and in natural systems through which Ni percolates is inducible (Stoppel and Schlegel, 1995). Screening for plasmids in CR35 and CR48 isolates from the metal rich ridge ecosystem showed no plasmids. However, an uptake of Ni was evident in these isolates, which could be through the activation of dormant genes for metal uptake. However, further study is required to prove the existence of chromosome mediated genes in these isolates. The genes for Ni resistance in *Alcaligenes denitrificans* 4a-2 (Kaur *et al.*, 1990) and *Klebsiella oxytoca* CCUG 15788 (Stoppel and Schlegel, 1995) were found to reside on chromosomal DNA.

This study provides evidence of Ni sequestration and of bacterial resistance to excess dissolved Ni under conditions of nutrient starvation frequently encountered in natural seawater. Ni immobilization was faster at 28±2°C than at 3±1°C. The present observations help infer that the two bacterial isolates differ in the mechanism that permits tolerance of high concentrations of Ni and that they respond differently with respect to induction of growth to different Ni concentrations. This is the first report to show Ni immobilization as NiP2, NiS, and NiS1 by bacterial isolates from the Indian ridge system as determined by XRD analysis. The IR analysis also showed the involvement of phosphate group in addition to carboxyl and hydroxyl group as probable-binding sites occupied by Ni in CR35 and CR48 biomass. The study suggests the plausible role of the isolates in the ridge ecosystem. Because these ridge isolates are capable of tolerating and immobilizing high concentration of Ni, they could be candidate organisms for scavenging Ni ions from Carlsberg Ridge waters or other Ni rich environments.

6.6. References

Aickin RM, Dean ACR, Cheetham AK, Skarnulis AJ. 1979. Electron microscope studies on the uptake of lead by a *Citrobacter* species. Microbios Lett 9: 7-15.

Babich H, Stotzky G. 1983. Influence of chemical speciation on the toxicity of heavy metals to the microbiota. In: Aquatic toxicology. Nriagu JO (ed) Wiley interscience, pp. 1-46.

Backmann J, Schultz C, Fabian H, Hahn U, Saenger W, Naumann D. 1996. Thermally induced hydrogen exchange processes in small proteins as seen by FTIR spectroscopy. Proteins: Structure, Function and Genetics 24: 379–87.

Bartha R, Ordal J. 1965. Nickel-dependent chemolithotrophic growth of two *Hydrogenomonas* strains. J Bacteriol 89:1015-1019.

Chester R, Hughes MJ. 1968. Scheme for the spectrophotometric determination of Cu, Pb, Ni, V and Co in marine sediments: Applied earth Science. Trans Inst Min and Metallurgy 77: 37-41.

Cobet AB, Wirsen C, Jun, Jones GE. 1970. The effect of nickel on a marine bacterium *Arthrobacter marinus* sp. nov. J Gen Microbiol 62: 159-169.

Deplanche K, Macaskie LE. 2008. Biorecovery of gold by *Escherichia coli* and *Desulfovibrio desulfuricans*. Biotechnol Bioeng 99: 1055-1064.

Ehrlich HL. 1976. Manganese as an energy source for bacteria. In: Environmental biogeochemistry. Nriagu JO (ed) Ann Arbor Science, Michigan, pp.633-644.

Ehrlich HL. 1978. Inorganic energy sources for chemolithotrophic and mixotrophic bacteria. Geomicrobiol J 1: 65-83.

Fernandes SO, Krishnan KP, Khedekar VD, Loka Bharathi PA. 2005. Manganese oxidation by bacterial isolates from the Indian ridge system. Biometals 18: 483-492.

Fiona HF, Jensen P, Kepert CM, Spiccia L. 2003. Macrocyclic copper (II) and Zinc (II) complexes incorporating phosphate esters. Inorg Chem 42: 5637–44.

Freeman LR, Angelini P, Silverman GJ, Merritt C, Jr. 1975. Production of hydrogen cyanide by *Pseudomonas fluorescens*. Appl Environ Microbiol 29: 560-561.

Gonye ER, Jones GE. 1973. An ecological survey of open ocean and estuarine microbial populations. II. The oligodynamic effect of nickel on marine bacteria. In: Estuarine microbial ecology. Stevenson LH, Colwell RR (eds) University of South Carolina Press, pp. 243-257.

Gonzalez H, Ramirez M, Torres I. 1997. Impact of nickel mining and metallurgical activities on the distribution of heavy metals in sediments of Levisa, Cabonico and Nipe Bays, Cuba. Environ Geochem Hlth 19: 57-62.

Helmann JD, Soonsanga S, Gabriel S. 2007. Metalloregulators: Arbiters of metal sufficiency. In: Molecular microbiology of heavy metals. Nies DH, Silver S (eds) Springer-Verlag, Berlin, pp. 37-71.

Jannasch HW, Wirsen CO. 1979. Chemosynthetic primary production at east Pacific sea floor spreading centers. Bioscience 29: 592-598.

Jannasch HW. 1984. Microbial processes at deep sea hydrothermal vents. In: Hydrothermal processes at seafloor spreading centers. Rona PA, Bostrom K, Laubier L, Smith KL, Jr (eds) Plenum, New York, pp. 677-709.

Kado CI, Liu ST. 1981. Rapid procedure for detection and isolation of large and small plasmids. J Bacteriol 145: 1365- 1373.

Kamnev AA, Ristic M, Antonyuk LP, Chernyshev AV, Ignatov VV. 1997. Fourier transform infrared spectroscopic study of intact cells of the nitrogen-fixing bacterium *Azospirillum brasilense*. J Mol Struct 408/409: 201-205.

Kaur P, Rob K, Siddiqui RA, Schlegel HG. 1990. Nickel resistance of *Alcaligenes denitrificans* strain 4a-2 is chromosomally coded. Arch Microbiol 154: 133-138.

Kazy SK, Sar P, Asthana RK, Singh SP. 1999. Copper uptake and its compartmentalization in *Pseudomonas aeruginosa* strains: Chemical nature of cellular metal. World J Microbiol Biotechnol 15: 599-605.

Keasling, JD. 1997. Regulation of intracellular toxic metals and other cations by hydrolysis of polyphosphate. Ann NY Acad Sci 829: 242-249.

Macaskie LE, Dean ACR, Cheetham AK, Jakeman RJB, Skamulis AJ. 1987. Cadmium accumulation by a *Citrobacter* sp: The chemical nature of the accumulated metal precipitate and its location on the bacterial cells. J Gen Microbiol 133: 539-544.

Mandernack KW, Tebo BM. 1993. Manganese scavenging and oxidation at hydrothermal vents and in vent plumes. Geochim Cosmochim Acta 57: 3907-3923.

Meyers JA, Sanchez D, Elwell LP, Falkow S. 1976. Simple agarose gel electrophoretic method for the identification and characterization of plasmid deoxyribonucleic acid. J Bacteriol 127: 1529-1537.

Naumann D, Helm D, Labischinski H,Giesbrecht P. 1991. The characterisation of microorganisms by Fourier-transform infrared spectroscopy (FT-IR). In:

Modern techniques for rapid microbiological analysis. Nelson WH (ed) VCH Publishers, New York, pp.43–96.

Nies DH. 1999. Microbial heavy-metal resistance. Appl Microbiol Biotechnol 51: 730-750.

Nriagu JO. 1980. Nickel in the environment. New York: Wiley. 833 p.

Parikh SJ, Chorover J. 2005. FTIR spectroscopic study of biogenic manganese-oxide formation by *Pseudomonas putida* GB-1. Geomicrobiol J 22: 207-218.

Partridge CDP, Yates MG. 1982. Effect of chelating agents on hydrogenase in *Azotobacter chroococcum*. Evidence that nickel is required for hydrogenase synthesis. Biochem J 204: 339-344.

Pattan JN, Higgs NC. 1995. Rare earth element studies of surfacial sediments from the south western Carlsberg Ridge, Indian Ocean. Proc Ind Acad Sci 104: 569-578.

Prescott LM, Harley JP, Klein DA. 1999. Microbiology. WCB/McGraw-Hill. 962 p.

Sar P, Kazy SK, Singh SP. 2001. Intracellular nickel accumulation by *Pseudomonas aeruginosa* and its chemical nature. Lett Appl Microbiol 32: 257-261.

Schmidt T, Schlegel HG. 1989. Nickel and cobalt resistance of various bacteria isolated from soil and highly polluted domestic and industrial wastes. FEMS Microbiol Ecol 62:315–328.

Sigee DC, Al-Rabaee RH. 1986. Nickel toxicity in *Psudomonas tabaci*: Single cell and bulk sample analysis of bacteria cultured at high cation levels. Protoplasma 130: 171-185.

Southam G. 2000. Bacterial surface-mediated mineral formation. In: Environmental microbe-metal interactions. Lovley DR (ed) American Society for Microbiology Press, Washington DC, pp. 257-276.

Stoppel RD, Schlegel HG. 1995. Nickel-resistant bacteria from anthropogenically nickel-polluted and naturally nickel-percolated ecosystems. Appl Environ Microbiol 61: 2276-2285.

Stults LW, Mallick S, Maier RJ. 1987. Nickel uptake in *Bradyrhizobium japonicum*. J Bacteriol 169: 1398-1402.

Waybrandt KR, Blowes DW, Ptacek CP. 1998. Selection of reactive mixtures for use in permeable reactive walls for treatment of mine drainage. Environ Sci Technol 32: 1972-1979.

Wolkers WF, Oliver AE, Tablin F, Crowe JH. 2004. A fourier transform infrared spectroscopy study of sugar glasses. Carb Res 339:1077–85.

Yee N, Benning LG, Phoenix VR, Ferris FG. 2004. Characterization of metal-cyanobacteria sorption reactions: A combined macroscopic and infrared spectroscopic investigation. Environ Sci Technol 38: 775-782.

CHAPTER 7

Immobilization of manganese, cobalt and nickel by deep-sea-sediment-microbial communities

7.1. Abstract

Box core samples BC26 and BC36 from geologically different settings were examined to test the hypothesis that autochthonous microbial communities from polymetallic-nodule-rich Central Indian Basin sediments actively participate in immobilizing metal ions. The bottom water dissolved oxygen concentration was reported to be 4.2-4.3 ml l^{-1} in the northern siliceous ooze (BC26) and 4.1-4.2 ml l^{-1} in the southern pelagic red clay (BC36); the sedimentation rates for these regions were 0.834 and 0.041 cm kyr^{-1}, respectively. An onboard experiment, conducted under oxic and sub-oxic conditions with 100 μM of Mn, Co and Ni, showed that microbial immobilization under sub-oxic conditions was higher than in azide-treated controls in BC26 for Mn, Co and Ni at 30, 2 and 4 cm below sea floor (bsf), respectively, after 45 d. The trend in microbial community immobilization was at BC26 > BC36, Co > Mn > Ni under oxic conditions and Mn > Co > Ni under sub-oxic conditions. The depth of maximum immobilization for Co in BC26 under sub-oxic conditions coincided with the yield of cultured Co-tolerant bacteria and Ni only with organic carbon at 4 cm bsf. This study demonstrates that the organic carbon content and bioavailable metal concentrations in sediments regulate microbial participation in metal immobilization.

7.2. Introduction

Sediments are complex mixtures of Fe- and Mn-oxide mineral phases, detrital organic matter and several other organic and inorganic phases. Sediments support different groups of metal-oxidizing and -reducing microorganisms (Forstner, 1990). Microbes in sediments can interact with dilute metal ions in solution, including sequestration and aid in concentrating these ions in the sediment. The ions either remain in sediments as bio-metal complexes or undergo a series of microbial or chemical transformations. This might lead to the recycling of metals into the overlying water column or to their immobilization in sediments as authigenic mineral phases (Beveridge *et al.,* 1983). The microbial immobilization of metals can be catalytic or

non-catalytic; it proceeds via four different mechanisms, namely biosorption, bioaccumulation, redox reaction and complex formation (Brandl and Faramarzi, 2006). Immobilization may be through cellular sequestration and accumulation, or through extracellular precipitation (Ehrlich, 1997; Sujith *et al.,* 2010). Marine bacteria produce large amounts of organic surface material that interacts with metal ions. The exopolysaccharides are subsequently involved in the precipitation of soluble metal cations and the formation of oxide species on bacterial walls, which chemically react with the residual metals in solution (Corpe, 1975; Ferris *et al.,* 1987; Fortin *et al.,* 1995).

A significant portion of the metals and their various organic derivatives in nature are contained within the living biomass. For example, Razzell and Trussell (1963) addressed the interaction of *Thiobacillus* spp. with sulfide-bearing ores and their role in the dissolution of oxides and the release of valuable metals. Likewise, Fortin *et al.* (1994) and Basnakova and Macaskie (1996) highlighted the contribution of bacteria to the formation of sulfide and phosphide minerals by chemical complexing with available constituent sulfide and phosphide groups. A few studies also explain the intracellular sequestration (Glasauer *et al.,* 2004; Shao and Sun, 2007) and extracellular precipitation (Fernandes *et al.,* 2005; Mandernack *et al.,* 1995) of metals by a group of metal-resistant bacteria, each affecting metal mobility in the environment.

The deposition of organic carbon and the availability of oxygen from bottom waters are primary factors that affect the geochemical and biological processes in the sediment–water system (Schaanning *et al.,* 1996). The availability of nutrients and oxygen therefore determines the sensitivity and adaptation of an organism to metals. Sediments are the ultimate repositories for environmental particles, and microbial processes within the sediment and can also control chemical changes as a response to metal exposure. Previous studies have shown the immobilization of metals in sterile sediments by individual isolates (Ehrlich, 1978; 1982). This study aimed to investigate the immobilization of metals by autochthonous microbial communities.

The study area covers two regions of the CIOB. The region for Box Core (BC) 26 is located at 10°S latitude and 75.5°E longitude in the northern region of the ocean (Figure 7.1). The sampling site has a water depth of 5339 m, the environment is

relatively less oxidizing (Nath *et al.*, 1992) and receives more clay from rivers (Banakar *et al.*, 1998; Das *et al.*, 2011). BC36 is located at the southern region of the basin at 16°S latitude and 75.5°E longitude. The region has a water depth of 5042 m, the environment is more oxidizing (Nath *et al.*, 1992) and is known for the slower rate of sediment deposition (Das *et al.*, 2011). The formation and dissolution of authigenic (oxyhydr)oxides of Fe and Mn influence the cycling of trace metals in oxic/sub-oxic surface sediments (Stockdale *et al.*, 2010). In view of that, the experiment was performed under oxic and sub-oxic incubation conditions to test the hypothesis that autochthonous microbial communities from CIB sediments actively participate in metal immobilization. This study assesses the influence of redox conditions, microbial abundance and activity to the immobilization of Mn, Co and Ni.

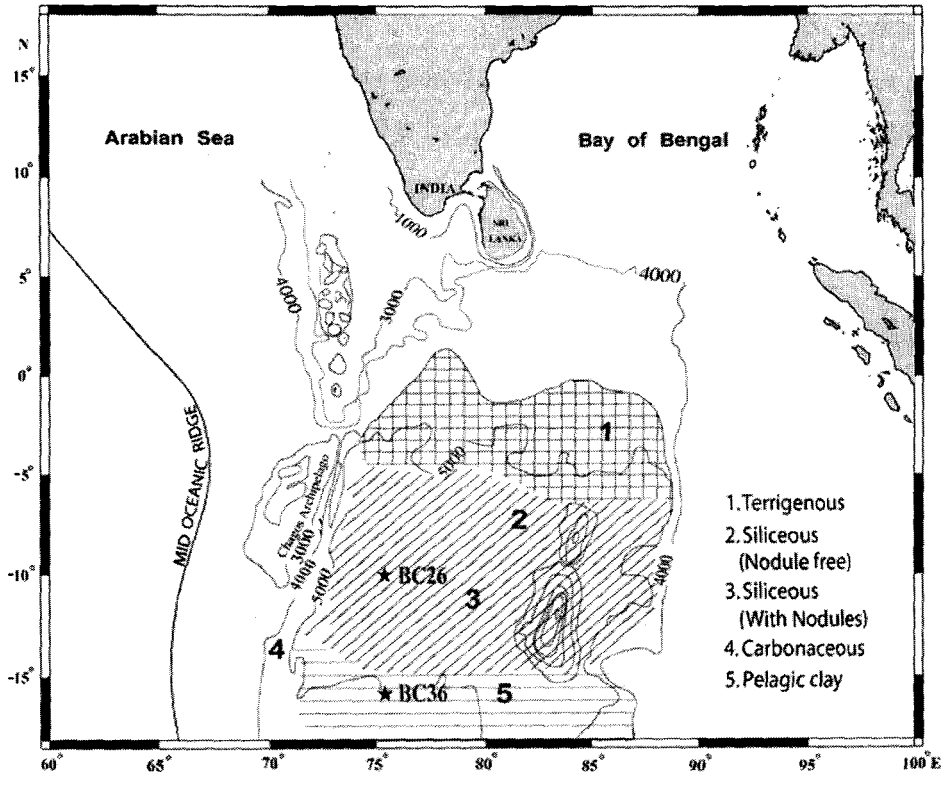

Figure 7.1. Area map shows sediment types and sampling locations for BC26 and BC36. It is modified from Mascarenhas-Pereira *et al.* (2006).

7.3. Materials and methods

7.3.1. Onboard sampling

The samples were collected and processed on-board Akademik Boris Petrov cruise number 26. Sediment cores were retrieved using a United States Naval

Electronics Laboratory (USNEL) box corer of dimensions 50 × 50 × 50 cm. BC26 was collected from a siliceous ooze area and BC36 from a pelagic red clay region. The box cores were subsampled by inserting acrylic core liners of 6.3 cm diameter into the sediment. The sediment cores were further subsectioned at 2 cm intervals up to a depth of 10 cm and thereafter at 5 cm intervals up to a depth of 35 cm. Sediment samples were collected in sterile polyethylene bags and stored at 4°C until further investigations.

7.3.2. Total bacterial counts

The sediment dilution for total bacterial counts (TBC) was prepared by suspending approximately 2 g of homogenized sediment in 9 ml of sterile seawater. A small portion of the above dilution was fixed with buffered formalin to a final concentration of 2% and was stored at 4°C until analysis (Hobbie *et al.*, 1977). The samples were sonicated at 15 Hz for 15 s, the slurry was allowed to settle for 30 s and 1 ml of the supernatant was filtered through a 0.22 μm black Millipore polycarbonate filter. Samples were then stained with 0.01% acridine orange for 3 min prior to microscopic observation. Approximately 10-15 microscopic fields were counted for each sample at ×1500 magnification using a Nikon 80i epifluorescence microscope (Nikon, Tokyo, Japan). Counts were normalized per gram of dry sediment.

7.3.3. Plate counts

Bacteria resistant to Mn, Co, Ni and heterotrophic bacteria were enumerated in triplicate using the spread plate method from the above dilution. The heterotrophs were grown on 20% ZoBell marine agar (ZMA). Metal-resistant bacteria were cultured on seawater agar (SWA) (1.5% bactoagar in natural seawater with no other additional nutrients) amended with 100 μM of metal salts $MnCl_2 \cdot 4H_2O$, $CoCl_2 \cdot 6H_2O$ and $NiCl_2 \cdot 6H_2O$ (Sd. fine Chem. Ltd). To isolate bacteria resistant to more than one metal, 100 μM of each metal was added to SWA medium of the above composition. The inoculated plates were incubated at 3±1°C for 4-10 d and the colony forming units (CFU) were counted and normalized for gram dry weight of sediment.

7.3.4. Eh measurements

Eh measurements were made at the beginning and end of the experiments. Before the measurements, the Eh electrode was rinsed with distilled water and

calibrated with oxidation reduction potential (ORP) standard solution to ensure accurate readings. For measurements, the electrode was dipped slowly into the sediment slurry in tubes and allowed to stabilize for 60 s. The direct reading obtained by mV meter was taken in triplicate and the mean values were determined. Eh was measured following the user's guide (Redox/ORP Electrodes, Thermo Electron Corporation, 2005).

7.3.5. Determination of total organic carbon

TIC was analyzed using a UIC CM 5014 Coulometer with CaCO3 as the standard and total carbon (TC) with NCS 2500 elemental analyzer (Patience *et al.*, 1990), cross-checked with a UIC CM5014 Coulometer. TOC was determined indirectly by subtracting the values of TIC from TC (Gupta and Jauhari, 1994).

7.3.6. Solid-phase concentration of metal ions in sediments

The concentration of metal ions in the sediment was determined by voltammetry after total decomposition of 50 mg of lyophilized sediments using the closed vessel digestion method (Roy *et al.*, 2007). The Mn concentration in aqueous samples was determined following the method of Colombini and Fuocco (1983) with two standard additions of $MnCl_2 \cdot 4H_2O$ (4mg l^{-1}). The concentration of Ni and Co in samples was determined using the modified method of Herrera-Melian *et al.* (1997). Analysis of the metals was carried out using a voltammeter in interface with 797VA computrace (Metrohm, Switzerland). The potential was measured against an Ag/AgCl reference electrode and a platinum rod as a counter electrode. Ni and Co determination was carried out with a hanging mercury drop electrode (HMDE) in the differential pulse mode. The determination was carried out at pH 9 in a measuring cell containing 10 ml of supporting electrolyte (ammonia buffer, pH 9.5) and 100 µl of dimethylglyoxime (0.1 M) in ethanol. A sample volume (1 ml), depending on the concentration, was appropriately diluted with Milli-Q water (18.2 Ω resistance) prior to analysis. The sample was added directly to the measuring vessel containing the electrolyte and was degassed with 99.9995% nitrogen (Medgas and Equipments) for 300 s prior to deposition. The analysis was carried out with a deposition time of 30 s, an equilibration time of 5 s and a voltage step time of 0.3 s. The potential was scanned in replications of 3 from -0.699 to -1.2V with sweep rate of 6 mV s^{-1}. The analysis was quantified with two standard stock additions of Ni(II) ($NiCl_2 \cdot 6H_2O$, 1mg l^{-1}) and Co(II) ($CoCl_2 \cdot 6H_2O$, 1mg l^{-1}).

7.3.7. Demonstration of metal immobilization

Box core sediments collected from two distinct regions of CIB were used to set up the laboratory experiments onboard. Portions of sediments from each subsection of the cores were inoculated using sterile spatula into 15 ml screw-capped tubes containing 100 μM of metal chloride salts dissolved in sterile seawater. Suitable azide (10 mM) poisoned controls to check for metal adsorption and autoclaved natural seawater amended with metal salts without any inocula (sterile controls) for abiotic precipitation were maintained. The incubation was carried out in triplicate at 3±1°C (to simulate *in situ* temperatures) under oxic and sub-oxic conditions. The oxic incubation was assured by directly inoculating 1.5 ± 0.5 g wet sediment in half-filled tubes and sub-oxic in completely filled tubes.

7.3.7.1. Metal analysis

The supernatant (1 ml) from inoculated and uninoculated tubes after centrifugation at 8000 rpm for 10 min at 4°C were analysed on day 0 and at the end of 45 d to determine the change in metal concentration. The residual concentration of metals in each tube was analyzed using a spectrophotometric (Multiskan Thermo Spectrum) method. Any samples that were delayed in analysis were acidified with 1N HCl and stored at 4°C. The Mn concentration in the sample was determined using the 1-(2-pyridylazo)-2-naphthol method at 560 nm (Chin *et al.*, 1992). Determination of Ni with dimethylglyoxime and Co with nitroso-R-salt was carried out according to the scheme of Chester and Hughes (1968) at 460 and 500 nm, respectively. Mean and SD were calculated for microbially (biotic) and non-microbially (abiotic) promoted metal immobilization. Values were corrected for chemical precipitation in both the experimental setups. One-way analysis of variance (ANOVA) and correlation analysis including the levels of significance were done for data points $n = 10$ using Statistica.

7.3.7.2. Determination of sediment dry weight

The sediment slurry from each tube was mixed and poured onto a preweighed filter positioned in a filtration set-up at the end of analysis. The filter with sediment was dried at 105°C and reweighed until constant. The filter weight was subtracted from the sediment weight to derive the actual dry weight of the sediment. The concentration of the immobilized metal was deduced and normalized for gram dry weight sediment after correcting for corresponding controls.

7.4. Results and discussion

7.4.1. Characteristics of the two sampling stations

Two sediment cores BC26 and BC36 were collected along the north–south transect of the CIB and were analyzed for immobilization of Mn, Co and Ni by the sediment microbial communities. The sediment slurry supported the growth of both heterotrophic and metal-tolerant bacteria. The yield of cultured heterotrophic bacteria varied from below detectable levels (BDL) to 5.4±0.73 × 10^3 CFU g^{-1} dry sediment in BC26 (Table 7.1) and 8.0±0.18 × 10^4 to 2.4±0.37 × 10^5 CFU g^{-1} sediment in BC36 with maximum culturability at 8 cm depth (Table 7.2). The metal-resistant bacteria count ranged from BDL to 9.0 ± 0.11 × 10^2 for Ni at 10 cm depth, 4.3±0.31 × 10^4 for Co and Mn at 2 and 20 cm depth, respectively. In mixtures of Mn, Co and Ni (100 µM each), the culturability of bacteria was 1.4±0.33 × 10^3 CFU g^{-1} at 10 cm depth in BC26 (Table 7.1). With BC36 it was 2.0±0.1 × 10^4 to 2.8±0.04 × 10^5 CFU g^{-1} for Co, with maximum culturability at 10 cm depth, 3.9±0.06 × 10^4 to 2.4±0.31 × 10^5 for Ni, 1.2±0.24 to 3.9±0.02 × 10^5 for Mn and 5.0±0.02 × 10^4 to 2.2±0.18 × 10^5 CFU g^{-1} for metals in combination with maximum culturability at 4 cm depth (Table 7.2).

Although the total bacterial abundance did not show a definite trend with the depth of the cores (Figure 7.2a, b), the distribution of organic carbon did show a trend. The organic carbon in sediments varied from 0.175 to 0.485% in BC26 (Figure 7.2c) and 0.09 to 0.19% sediment dry weights in BC36 (Figure 7.2d) with maximum carbon concentration at 4 and 2 cm depth, respectively. The TOC content in seawater was 21.78 mg C l^{-1} in BC26 and 9.18 mg C l^{-1} in BC36. The abiotic precipitation of metal ions in uninoculated sterile controls was negligible. Eh as a measure of oxidizing and reducing conditions showed that BC26 could support sub-oxic and BC36 the oxic processes better (Figure 7.2e, f). The Eh in BC26 experimental tubes decreased from +80.2 to +11.98 mV (± 2.6, n = 3) in the oxic and +6.24 mV (± 3.2, n = 3) in the sub-oxic incubations at 35 and 30 cm bsf, respectively. The Eh in BC36 decreased from +79.96 to +28.36 mV (± 2.6, n = 3) in the oxic and +25.52 mV (± 3.2, n = 3) in the sub-oxic incubations at 2 and 10 cm, respectively, for Mn (Table 7.3).

The maximum solid-phase concentration of Mn (14.93 µM g^{-1}) and Ni (4.55 µM g^{-1}) in BC26 was observed at 8 cm depth and Co (6.24 µM g^{-1}) at 30 cm depth. The

concentration of Mn in BC36 sediment core was maximum (265.8 μM g^{-1}) at 10 cm depth and Co (12.29 μM g^{-1}) and Ni (17.52 μM g^{-1}) at 35 cm depth (Figure 7.3). The concentration of the above metal ions was found to be unevenly distributed in the sediment cores. The maximum concentration for all the three metals was observed towards the surface, decreased with depth and showed a secondary maximum towards the subsurface in both the sediment cores. The present results agree with the report of Zhang *et al.* (2002) on the double maxima for solute profiles.

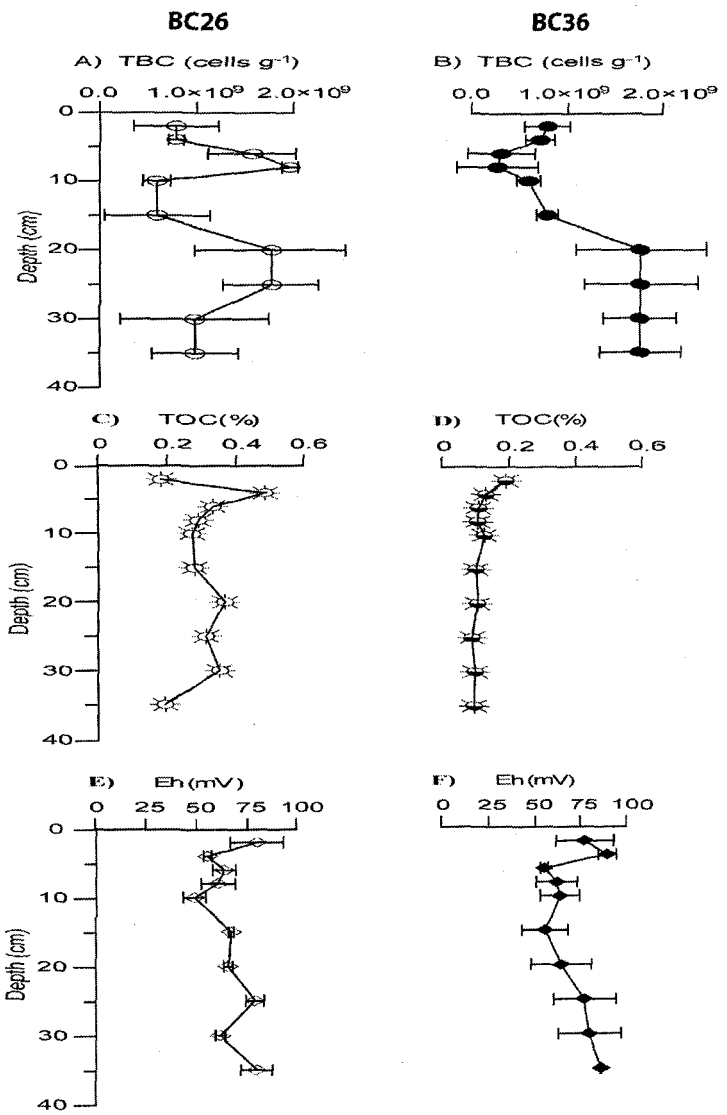

Figure 7.2. Depth profile of Total Bacterial Count (TBC), Total Organic Carbon (TOC) and Eh in sediment cores BC26 and BC36 (mean ± SD, n =10 for TBC and n = 3 for Eh).

Table 7.1. Plate counts of heterotrophic and metal resistant bacteria in 1.5 % bacto agar amended seawater with and without metal chlorides (100 μM) in BC26. All the values in the table represent CFU (Colony Forming Unit) per gram dry weight of sediment. The data represent mean values ± SD, n=3. *ZMA= ZoBell Marine Agar, SWA = Sea Water Agar, bsf= below sea floor and BDL=Below Detection Level. For details, see text (section 2.3).

Depth bsf (cm)	ZMA*	SWA*				
		No metal	Ni	Co	Mn	Ni-Co-Mn
2	$1.5\pm0.18\times10^{2}$	BDL	BDL	$4.3\pm0.31\times10^{4}$	$2.5\pm0.22\times10^{4}$	BDL
4	$2.0\pm0.40\times10^{2}$	BDL	BDL	$2.7\pm0.15\times10^{4}$	$1.5\pm0.25\times10^{4}$	BDL
6	BDL	BDL	BDL	$1.5\pm0.10\times10^{3}$	$6.0\pm0.05\times10^{2}$	BDL
8	$5.4\pm0.73\times10^{3}$	BDL	BDL	$1.7\pm0.32\times10^{4}$	$4.1\pm0.61\times10^{4}$	BDL
10	$5.0\pm0.28\times10^{1}$	$1.5\pm0.57\times10^{2}$	$9.0\pm0.11\times10^{2}$	$6.6\pm0.60\times10^{3}$	$3.8\pm0.72\times10^{4}$	$1.4\pm0.33\times10^{3}$
15	BDL	BDL	BDL	$1.7\pm0.13\times10^{4}$	$3.9\pm0.23\times10^{4}$	BDL
20	BDL	BDL	BDL	$1.2\pm0.24\times10^{4}$	$4.3\pm0.45\times10^{4}$	BDL
25	$1.4\pm0.11\times10^{3}$	BDL	BDL	BDL	BDL	BDL
30	$5.0\pm0.02\times10^{1}$	BDL	BDL	BDL	BDL	BDL
35	BDL	BDL	BDL	BDL	BDL	BDL

Table 7.2. Plate counts of heterotrophic and metal resistant bacteria in 1.5 % bacto agar amended seawater with and without metal chlorides (100 μM) in BC36. All the values in the table represent CFU (Colony Forming Unit) per gram dry weight of sediment. The data represent mean values ± SD, n=3. *ZMA= ZoBell Marine Agar, SWA = Sea Water Agar and bsf= below sea floor. For details, see text (section 2.3).

Depth bsf (cm)	ZMA*	SWA*				
		No metal	Ni	Co	Mn	Ni-Co-Mn
2	$8.0\pm0.18\times10^4$	$6.8\pm0.70\times10^4$	$1.6\pm0.02\times10^5$	$2.6\pm0.23\times10^5$	$1.8\pm0.10\times10^5$	$1.9\pm0.13\times10^5$
4	$1.0\pm0.11\times10^5$	$6.1\pm0.06\times10^4$	$2.4\pm0.31\times10^5$	$1.7\pm0.07\times10^5$	$3.9\pm0.02\times10^5$	$2.2\pm0.18\times10^5$
6	$8.8\pm0.09\times10^4$	$5.4\pm0.42\times10^4$	$9.1\pm0.46\times10^4$	$1.3\pm0.35\times10^5$	$3.3\pm0.21\times10^5$	$1.6\pm0.09\times10^5$
8	$2.4\pm0.37\times10^5$	$3.5\pm0.51\times10^4$	$2.1\pm0.10\times10^5$	$1.5\pm0.16\times10^5$	$2.4\pm0.03\times10^5$	$6.8\pm0.42\times10^4$
10	$1.6\pm0.24\times10^5$	$5.0\pm0.02\times10^4$	$1.6\pm0.05\times10^5$	$2.8\pm0.04\times10^5$	$1.3\pm0.09\times10^5$	$5.0\pm0.02\times10^4$
15	$1.2\pm0.08\times10^5$	$1.2\pm0.07\times10^4$	$3.9\pm0.06\times10^4$	$1.4\pm0.05\times10^5$	$1.2\pm0.24\times10^5$	$6.2\pm0.18\times10^4$
20	$1.4\pm0.15\times10^5$	$7.1\pm0.15\times10^4$	$5.1\pm0.31\times10^4$	$6.6\pm0.02\times10^4$	$1.7\pm0.11\times10^5$	$1.6\pm0.31\times10^5$
25	$1.6\pm0.26\times10^5$	$2.5\pm0.11\times10^4$	$4.2\pm0.17\times10^4$	$2.0\pm0.10\times10^4$	$1.7\pm0.07\times10^5$	$7.9\pm0.01\times10^4$
30	$2.0\pm0.24\times10^5$	$3.1\pm0.32\times10^4$	$9.9\pm0.06\times10^4$	$1.0\pm0.08\times10^5$	$2.2\pm0.05\times10^5$	$1.5\pm0.11\times10^5$
35	$1.7\pm0.09\times10^5$	$3.0\pm0.13\times10^4$	$9.5\pm0.22\times10^4$	$4.8\pm0.15\times10^4$	$2.4\pm0.21\times10^5$	$7.2\pm0.45\times10^4$

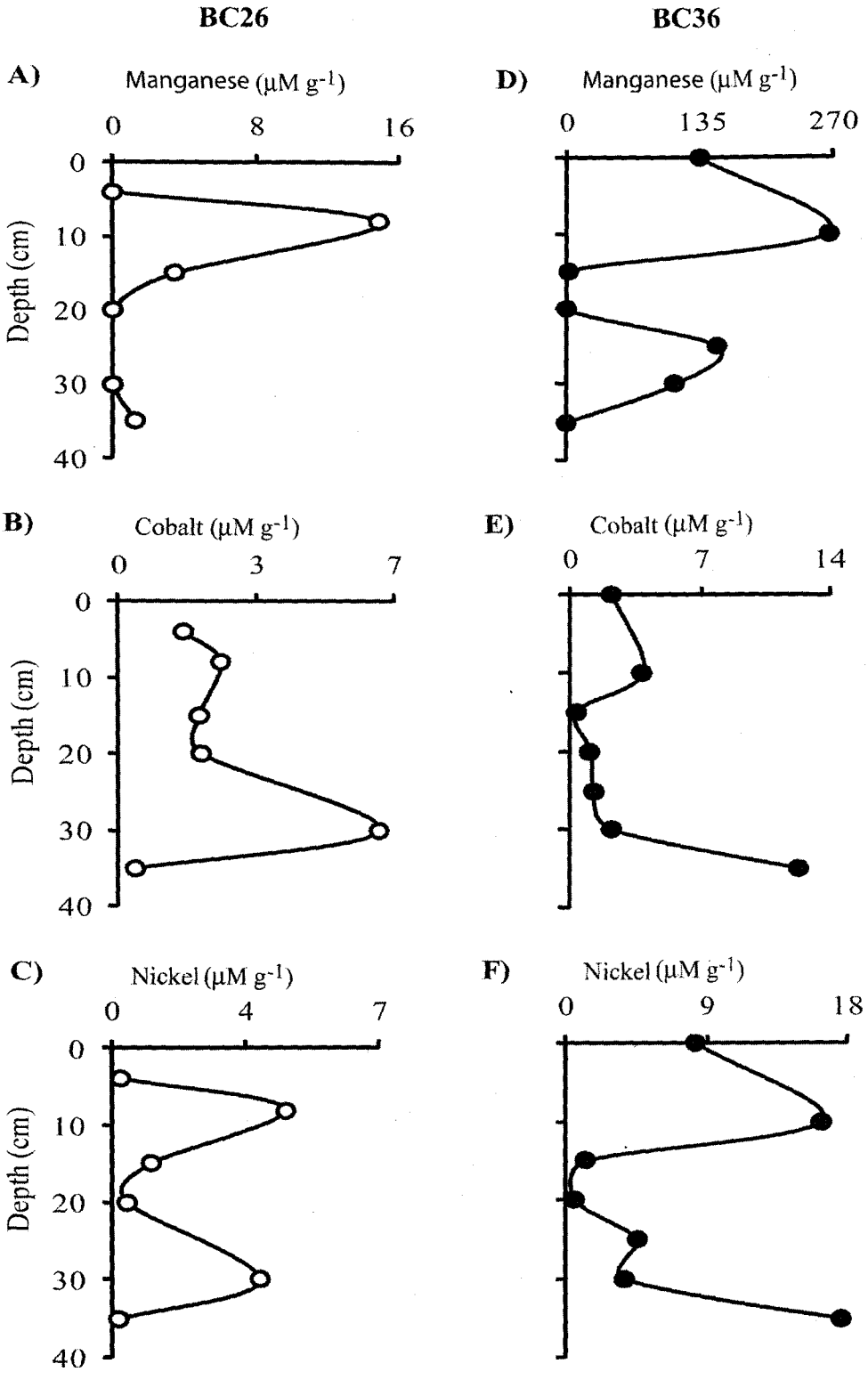

Figure 7.3. Solid phase concentrations (single measurements) of Mn, Co and Ni in sediment cores collected from Central Indian Basin. Figures A-C represents metal concentrations in BC26 and D-F in BC36.

7.4.2. Immobilization under oxic condition in BC26

7.4.2.1. Biotic immobilization

The results showed higher Mn immobilization in the subsurface sediment (Figure 7.4a). The immobilization of the metal was 34.4±0.053 μM g^{-1} dry sediment at 35 cm bsf. Mn immobilization increased with depth ($r = 0.852, p < 0.001$). The yield of cultured heterotrophic bacteria co-varied with TBC at an *r*-value of 0.602 ($p < 0.05$) suggesting that the variation in the former is responsible for 36% of the variation in the latter. The maximum immobilization observed at the deeper depth suggests that oxidized Mn is stable at this depth and is less prone to dissolution. The subsurface manganese maximum observed at 30–35 cm depth (Pattan and Mudholkar, 1990; Banakar *et al.*, 1991; Mudholkar *et al.*, 1993) in 13 different sediment cores collected from CIOB substantiates the present finding. By contrast to Mn, higher Co immobilization (35±0.328 μM g^{-1}) was recorded at the sediment surface (Figure 7.4b). Interestingly, although the immobilization of this metal was maximum at the surface and coincided with the maximum yield of cultured Co tolerant bacteria (Table 7.3), this process showed a negative relationship with the yield of cultured Co tolerant bacteria by an *r*-value of 0.745 ($p < 0.01$). This probably suggests that immobilization of Co is mediated by other metal-immobilizing bacteria in the sediments. The association of Co with Mn in the surface sediment is one process in which Mn-oxidizing bacteria participate indirectly in Co immobilization. The results agree with the observations of Sundby *et al.* (1986) and Glasby (2006) on Co enrichment in the surface sediments. The present observations also support the earlier findings (Lee and Tebo, 1994; Moffett and Ho, 1996) on the co-oxidation of Co with Mn in the aquatic systems. Likewise, immobilization of Co is known to co-occur with iron reduction in bacteria (McInerney, 1993).

Like Mn, higher immobilization of Ni (6.3±0.055 μM g^{-1}) was observed at the deeper 25 cm layer. The immobilization of Ni negatively related with the yield of Mn tolerant bacteria by *r*-value of 0.643 ($p < 0.05$). This relation suggests that Ni immobilization may not be catalyzed by Mn-oxidizing bacteria but more by bacteria resistant to Ni or Co. Further, it is also suggested that in certain microorganisms, the resistance to one metal can also confer resistance to the other metals depending on the bioavailability and combination of metals. Interestingly, a study by Stoppel and

Schlegel (1995) has shown that bacteria tolerant to Ni are also tolerant to Co and posses determinants that resemble each other.

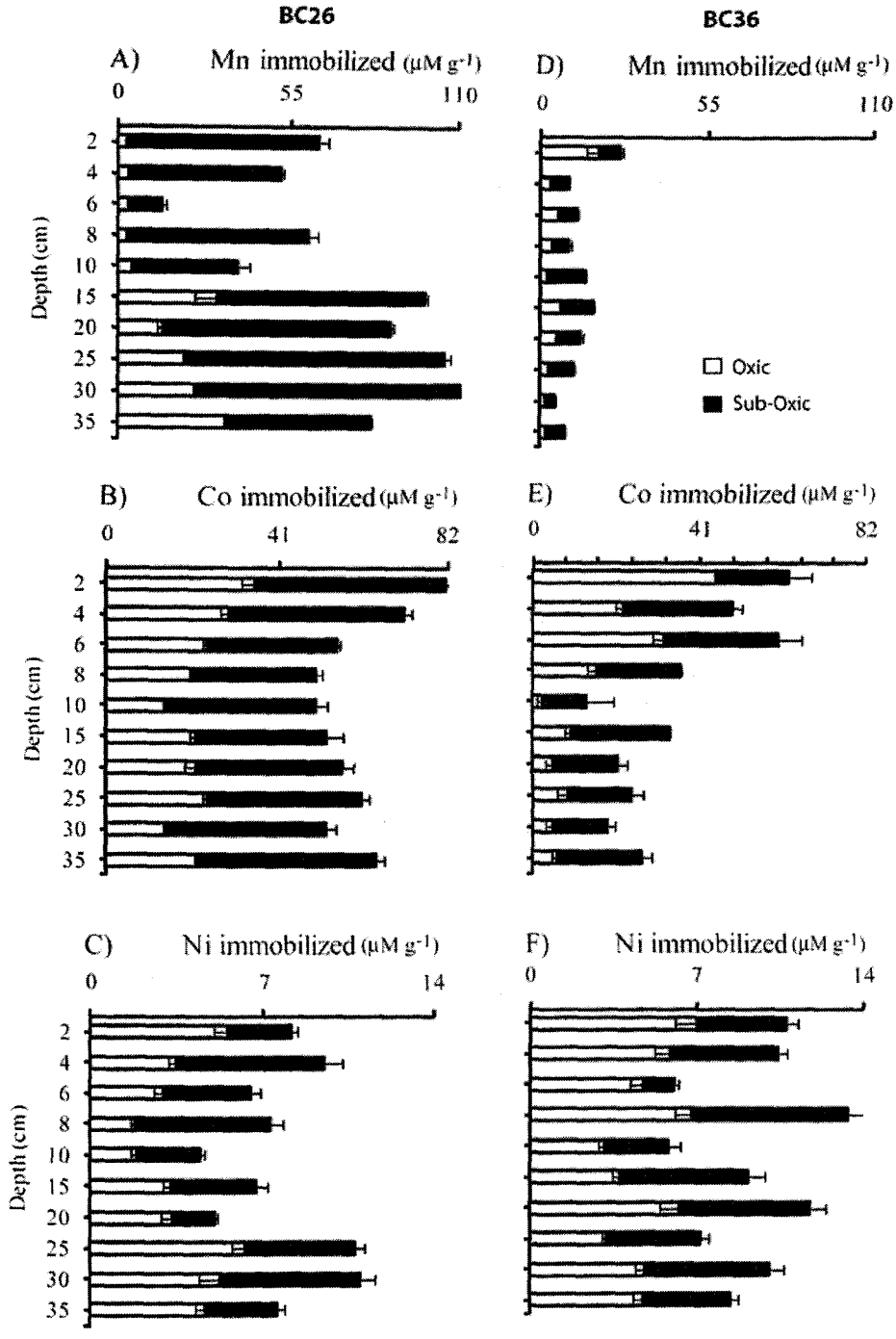

Figure 7.4. Microbially promoted immobilization of metals (μM g^{-1} dry weight, mean ± SD, n = 3) in experiments as a function of depth. Figures A-C represents the immobilization of metals in BC26 and figures D-F in BC36. The error bars are shown on the left hand side for oxic and on the right hand side for suboxic incubation.

Table 7.3. *Maximum immobilization of metals at various depths below sea floor (bsf) compared with maximum in plate counts CFU (Colony Forming Unit). All the values in the table correspond to gram dry weight of sediment. The data in the table are mean values ± SD, n=3. For details, see text (sections 2 and 3).*

Metal	Parameters	Core BC26								Core BC36								Inference
		Biotic				Abiotic				Biotic				Abiotic				
		Oxic [a]		Sub-oxic [b]		Oxic [c]		Sub-oxic [d]		Oxic [e]		Sub-oxic [f]		Oxic [g]		Sub-oxic [h]		
		Value	Depth (cm)	Value	Depth (cm)	Value	Depth (cm)	Value	Depth (cm)	Value	Depth (cm)	Value	Depth (cm)	Value	Depth (cm)	Value	Depth (cm)	
Mn	Immobilization (μM)	34.4±.053	35	85.6±.047	30	11.6±.011	35	22.5±.047	35	19.76±.41	2	13.44±.04	10	25.33±.04	6	22.89±.03	6	**a.** Suggests that oxidized Mn is less prone to dissolution at this depth. **b.** Suggests bacterial participation **c.** Suggests that 86% of the variation in biotic oxidation could be due to the variation in abiotic. **d.** Suggests passive immobilization on Mn-oxide phase **e.** Suggests mixotrophic mode of nutrition **f.** Suggests that high bac□ground Mn concentration along with the amended Mn could be toxic **g.** Could be regulated by concentration of the metal and the availability of particle binding sites in sediments **h.** Active process of immobilization is inhibited by azide and not the passive.
	Plate counts (CFU) i) Seawater agar	-		-		-		-		6.8×10^4		-		-		-		
Co	Immobilization (μM)	35±.33	2	46.3±.29	2	8.45±.055	35	6.97±.027	10	45±.028	2	27.5±.537	6	6.43±.011	8	7.18±.024	8	**a.** Immobilization of Co by other metal tolerant bacteria in the sediments. **b.** Suggests bacterial participation **c.** Only passive process could be involved **d.** Suggests passive immobilization on Mn oxide phase **e.** Could be by process where Ni immobilizing bacteria catalyze Co immobilization and vice versa **f.** Suggests co-oxidation of Co by Mn oxidizing microorganisms **g.** Could be regulated by concentration of the metal and the availability of particle binding sites in sediments **h.** Could be by metabolism independent process li□e cell surface adsorption/precipitation
	Plate counts (CFU) i) Seawater agar	-		-		-		-		6.8×10^4		-		-		-		
	ii) Co	4.3×10^4		4.3×10^4		-		-		-		-		-		-		
Ni	Immobilization (μM)	6.3±.055	25	6±.08	4	0.98±.008	25	0.65±.012	4	7.03±.09	2	6.6±.075	8	0.95±.009	25	0.703±.01	4	**a.** Ni immobilization may be catalyzed more by bacteria resistant to Ni or Co. **b.** Energy dependent low affinity upta□e process **c.** Complexation of Ni with organic carbon in sediments **d.** Complexation of Ni with organic carbon in sediments could contribute to its immobilization at a much lower rate **e.** Suggests that the same microbial communities are capable of immobilizing both the metals **f.** Suggests that the same microbial communities are capable of immobilizing both the metals **g.** Could be regulated by concentration of the metal and the availability of particle binding sites in sediments **h.** Could be by metabolism independent process li□e cell surface adsorption/precipitation
	Plate counts (CFU) i) Seawater agar	-		-		-		-		6.8×10^4		-		-		-		
	ii) ZoBell marine agar	-		-		-		-		-		2.4×10^5		-		-		

7.4.2.2. Abiotic immobilization

The abiotic immobilization was comparatively less than the biotic immobilization because only the passive process could be involved. The difference could be as much as three to four times in the case of Mn, four to six times in the case of Co, and six times in the case of Ni. The maximum immobilization of Mn (11.61±0.011 μM g^{-1}) and Co (8.45±0.06 μM g^{-1}) occurred at 30–35 cm bsf and Ni (0.98±0.08 μM g^{-1}) at 25 cm bsf (Figure 7.5). The Mn immobilization showed depth dependence with an *r*-value of 0.928 ($p < 0.001$) and was also related to biotic Mn oxidation with an *r*-value of 0.930 ($p < 0.001$), suggesting that 86% of the variation in biotic Mn oxidation could be due to the variation in abiotic oxidation. The BC26 sediments are composed of siliceous ooze and have low concentrations of metal ions (Figure 7.3). The results show that abiotic metal immobilization proceeds slowly and the rate depends upon the oxygen concentration, redox condition prevailing in the sediments, and the rate of the reverse activity ie dissolution. The results agree with the reports of Muller *et al.* (1988) and Glasby (2006) on surficial diagenesis and the regeneration rate of Mn in the sediments with that of accretion rate of the metal in the associated polymetallic nodules. The passive sorption of metal ions on sediment and mineral particles occurs by physical attraction and/or chemical precipitation.

7.4.3. Immobilization under sub-oxic condition in BC26

7.4.3.1. Biotic immobilization

As mentioned above, biotic immobilization is definitely greater than abiotic immobilization. Suboxic immobilization is 2.4 times greater with Mn and 1.3 times greater with Co than oxic. Under sub-oxic conditions, the microbial immobilization of Mn (85.6±0.047 μM g^{-1}) was maximum at 30 cm bsf. Maximum Co (46.3±0.29 μM g^{-1}) immobilization was at 2-4 cm bsf and is synchronized with the maximum yield of cultured Co-tolerant bacteria (4.3±0.31×10^4 CFU g^{-1}) and organic carbon (0.485%), suggesting bacterial participation. The current results agree with previous studies (Mills and Colwell, 1977; Timoney *et al.,* 1978; Houba and Remacle, 1980; Duxbury and Bic□nell, 1983; Hornor and Hilt, 1985) which reported a positive correlation between heavy metal concentrations and the percentage of bacteria resistant to metals in different soils and sediments. However, maximum Ni immobilization (6±0.08 μM g^{-1}) was evident at 4 cm depth (Figure 7.4c) and was synchronized with the organic carbon concentration (0.485%) in sediment, suggesting an energy dependent low-affinity

uptake process. The results are in agreement with Jasper and Silver (1977) and Bryson and Drake (1988) on energy-dependent Ni transport in bacteria and the chemo-organotrophic mode of nutrition in microorganisms in the presence of nutrients.

7.4.3.2. Abiotic immobilization

It is again emphasized that abiotic immobilization is less than biotic immobilization, especially under sub-oxic conditions. The immobilization profile of Mn was similar to that occurring under oxic conditions with a maximum of 22.5±0.047 μM g^{-1} at 35 cm bsf (Figure 7.5a). Peaks in Co and Ni immobilization of 6.97±0.027 and 0.65±0.012 μM g^{-1} were at 10 and 4 cm bsf, respectively (Figure 7.5b, c).The distribution of Mn and Co did not match the organic carbon content of the sediment. The immobilization detected at low levels in poisoned sediments suggests passive immobilization on the Mn oxide phase. The present results agree with earlier reports on such trapping of metal ions by manganese oxides (Froelich *et al.*, 1979; Shaw *et al.*, 1990). However, the immobilization of Ni was less than Co and corresponded with the organic carbon (0.485%) content of the sediment. Thus, organic carbon in sediments might also complex with Ni and contributes to its immobilization at a much lower rate than under biotic conditions. Such an association of Ni with organic carbon in sediments has been observed previously by Turner *et al.* (1998) and Xue *et al.* (2001).

7.4.4. Immobilization under oxic condition in BC36

7.4.4.1. Biotic immobilization

In this core, biotic immobilization is greater than abiotic immobilization, except in the case of Mn where it is the other way round. Under oxic conditions, immobilization of all three metals was maximum at the sediment surface (2 cm bsf) and was lower than in BC26. The trend in the immobilization was Co (45±0.028 μM g^{-1}) > Mn (19.8±0.41 μM g^{-1}) > Ni (7±0.09 μM g^{-1}), as shown in Figure 7.4d-f. The solid-phase concentrations of metal ions were Mn > Ni > Co. Thus, the depth at which maximum immobilization occurred did not match with the depth that showed a maximum for the solid-phase concentration of metal ions. This suggests that along a depth gradient the metal concentration at the surface was more optimal for immobilization. The organic carbon content of the core was maximum (0.19%) at the surface and is related to the immobilization of Mn with an r-value of 0.835 ($p < 0.01$), suggesting a mixotrophic mode of nutrition. The culturability of bacteria tolerant to

Mn-Co-Ni was maximum (1.9 to 2.2 × 10^5 CFU g^{-1}) within the 0-4 cm depth in multiple metal-amended plates. These observations suggest that microbially mediated immobilization of the above metals in BC36 sediments is driven by the nutritive status of the sediment and the predominance of metal-tolerant bacteria. It is consistent with the observation of Dean-Ross and Mills (1989), that groups of microbial communities that are relatively abundant in the sediment can utilize one or more aromatic compounds and are resistant to one or more heavy metals.

The microbial immobilization of Co synchronized with the maximum in Mn immobilization. The yield of cultured Co-tolerant bacteria was positively related to TOC and yield of Ni-tolerant bacteria with *r*-values of 0.766 ($p < 0.01$) and 0.606 ($p < 0.05$), respectively. These relations suggest that Ni and Co immobilization are mediated by the same microbes to a certain extent (36%) and 58% variation in both is dependent on the variation in TOC. The ability of Ni resistant bacteria to immobilize Co is evident from previous experimental records (Schmidt and Schlegel, 1989). However, Co and Ni immobilization can be independent of Mn immobilization and might occur by a process in which Ni-immobilizing bacteria catalyze Co immobilization and vice versa.

The immobilization of Ni was comparatively lower than the other metals. However, the yield of cultured Ni-tolerant bacteria might correlate with the yield of Co-tolerant bacteria ($r = 0.606$, $p < 0.05$), suggesting that the same microbial communities are capable of immobilizing both metals. These results agree with our recent reports (Sujith *et al.*, 2010; Antony *et al.*, 2011) on Ni and Co immobilization by Mn oxidizing bacterial isolates from the Indian Ridge system. TBC correlated positively ($r = 0.868$, $p < 0.001$) and TOC negatively with depth ($r = 0.666$, $p < 0.05$). These observations suggest that microbial abundance, the diversity of their metabolic activities and the number of metal resistant bacteria in the sediment direct the immobilization of Ni in BC36 sediments. Nonetheless, TOC in sediments also influenced the bioavailability of the metal in sediments. It is clear from the report of D'Hondt *et al.* (2004) that organisms that depend on electron-accepting pathways with higher standard free energies may have higher energy requirements than organisms that depend on pathways with lower standard free-energy yields.

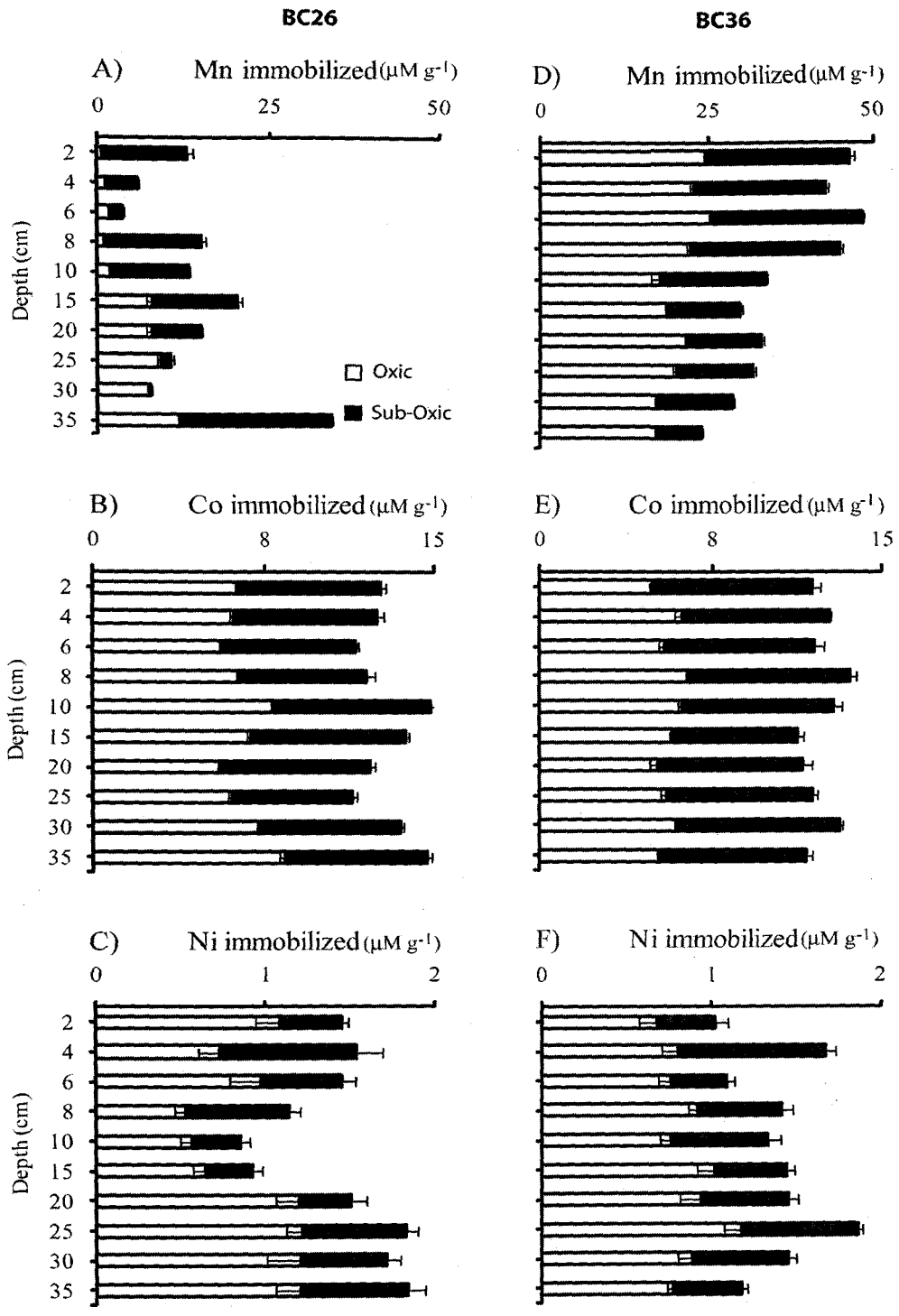

Figure 7.5. Abiotic immobilization of metals (μM g^{-1} dry weight, mean ± SD, n = 3) in azide (10 mM) treated sediments as a function of depth. Figures A-C represents the adsorption of metals in BC26 and figures D-F in BC36. The error bars are shown on the left hand side for oxic and on the right hand side for suboxic incubation.

7.4.4.2. Abiotic immobilization

Although the prevailing environmental conditions in these sediments are appropriate for microbial immobilization of Mn, abiotic immobilization of the metal was higher than biotic immobilization. It is suggested that processes that occur in these sediments could be more passive than active. The maximum immobilization of Mn (25.33±0.04 μM g^{-1}) occurred at 6 cm depth (Figure 7.5d). Co and Ni immobilization continued to remain higher under biotic conditions and showed maximum abiotic immobilization of 6.43±0.011μM g^{-1} for Co and 0.95±0.009 μM g^{-1} for Ni at 8 and 25 cm depth, respectively (Figure 7.5e, f). The immobilization of metal ions did not relate with organic carbon or the natural concentration of the metal ions in sediments. The results suggest that immobilization by abiotic processes is directed to changes with concentration of the metal and the availability of charged particle binding sites in sediments. The present results agree with a previous report (Hart, 1982) on trace metal binding to reactive sediment surfaces.

7.4.5. Immobilization under sub-oxic condition in BC36

7.4.5.1. Biotic immobilization

Unlike under oxic conditions, the immobilization of Mn was maximum (13.5±0.035 μM g^{-1}) at the greater depth of 10 cm bsf. Co and Ni continued to show maximum immobilization of 27.5±0.54 and 6.6±0.075 μM g^{-1} at shallower depths of 6 and 8 cm bsf, respectively (Figure 7.4e, f). Thereafter, a gradual decrease in immobilization was observed towards the bottom of the core. Earlier investigations (Dean-Ross and Mills, 1989) on bacterial-community composition and function along a heavy-metal gradient provide the explanation that bacteria are not exposed to the same concentrations of heavy metal *in situ* as in laboratory-prepared media. However, the present study did not use laboratory-prepared organic media. Moreover, it simulates deep-sea conditions by avoiding organic amendments and maintaining the temperature at 3±1°C. Therefore, the current results might reflect *in situ* trends to a certain extent. The maximum immobilization of Mn and Ni coincided with peak culturability of heterotrophic bacteria and the solid-phase sediment concentration of metal ions.

The immobilization of Mn showed a negative relationship with the yield of cultured Mn-tolerant bacteria ($r = 0.609$, $p < 0.05$). This suggests that the background concentration along with the amended Mn might be beyond the tolerance limit. The

toxicity of excess Mn is evident from earlier studies (Fernandes *et al.*, 2005; Cheung *et al.*, 1982). By contrast, the depth of the greatest Co immobilization was synchronized with the maximum culturability of multiple metal-tolerant bacteria and the organic carbon content of the sediments. The immobilization of Co showed correlation with the yield of cultured Mn tolerant bacteria ($r = 0.677, p < 0.05$). The association of Co with Mn and its co-oxidation by Mn-oxidizing microorganisms result in immobilization. Our results agree with those of Lienemann *et al.* (1997) on the oxidation of Co in association with Mn in aquatic systems. It is therefore inferred that the metal concentration in the sediment, its organic carbon content and the microorganisms present might govern the active immobilization of metal ions.

7.4.5.2. Abiotic immobilization

At this sampling site, abiotic immobilization of metal ions is higher than the biotic immobilization. Maximum immobilization of Mn (22.89±0.03 μM g^{-1}) occurred at 6 cm, Co (7.18±0.024 μM g^{-1}) at 8 cm and Ni (0.70±0.01 μM g^{-1}) at 4 cm bsf (Figure 7.5). The depth of maximum immobilization of Co matched that of maximum culturability of heterotrophic bacteria from the biotic samples. Also, the passive rates with the azide-treated sediments were much lower for Co and Ni than untreated samples. Similarly, depth of immobilization of Ni coincided with the yield of cultured Ni-tolerant and Mn-Co-Ni-tolerant bacterial numbers in biotic samples. Results suggest that when used as a poison, azide restricts the active process of metal immobilization by bacteria, but does not inhibit passive metal ion binding to the bacterial cell surfaces. The current results agree with the previous reports (Kuroda and Ueda, 2003) that surface adsorption is possible even in non-viable cells, albeit at low levels. Heavy metals can be immobilized by metabolism-independent process on cell-surface components and charged particles in sediment, depending upon the milieu.

7.4.6. Immobilization under oxic vs sub-oxic conditions

Microbial immobilization of metals under sub-oxic conditions was significantly higher ($p < 0.001$) in BC26 than in BC36 and was higher than in azide-treated controls. The trend in immobilization was Co (35±0.328 μM g^{-1}) > Mn (34.4±0.053 μM g^{-1}) >Ni (6.3±0.055 μM g^{-1}) under oxic conditions, and Mn (85.6±0.047 μM g^{-1}) > Co (46.3±0.29 μM g^{-1}) > Ni (6±0.08 μM g^{-1}) under sub-oxic conditions. In BC36, the metal immobilization was higher under oxic conditions. The trend in immobilization

was Co (45±0.028 μM g^{-1}) > Mn (19.8±0.41 μM g^{-1}) > Ni (7±0.09 μM g^{-1}) under oxic conditions and Co (27.5±0.54 μM g^{-1}) > Mn (13.44±0.035 μM g^{-1}) > Ni (6.6±0.075 μM g^{-1}) under sub-oxic conditions. The immobilization rates of metals in these sediments were mostly Mn > Co > Ni. Generally, the immobilizing rates of Mn and Co were greater at BC26 than at BC36, with the rates under sub-oxic conditions being higher than under oxic conditions. Such discernible differences were not seen in the case of Ni.

From this study, it is clear that the higher immobilization of metals under sub-oxic conditions in the subsurface sediment was not greatly influenced by organic carbon, but rather by the higher availability of reduced metal ions. The significant differences in metal immobilization between the experiment and poisoned controls probably indicate the involvement of both active and passive process of metal immobilization in the experiment and the latter process only in the case of control. This study demonstrates that organic carbon content and the concentration of the bioavailable metals in sediments regulate microbial participation in metal immobilization.

7.5. References

Antony R, Sujith PP, Fernandes SO, Verma P, Khedekar VD, Loka Bharathi PA. 2011. Cobalt immobilization by manganese oxidizing bacteria from the Indian Ridge system. Curr Microbiol 62: 840-849.

Banakar VK, Gupta SM, Padmavathi VK. 1991. Abyssal sediment erosion in the Central Indian Basin: evidence from radiochemical and radiolarian studies. Mar Geol 96:167-173.

Banakar VK, Parthiban G, Pattan JN, Jauhari P. 1998. Chemistry of surface sediment along a north-south transect across the equator in the Central Indian Basin: an assessment of biogenic and detrital influences on elemental burial on the seafloor. Chem Geol 147: 217-232.

Basnakova G, Macaskie LE. 1996. Bioaccumulation of nickel by microbially-enhanced chemisorption into polycrystalline hydrogen uranyl phosphate. Biotechnol Lett 18: 257-262.

Beveridge TJ, Meloche JD, Fyfe WS, Murray RGE. 1983. Diagenesis of metals chemically complexed to bacteria: laboratory formation of metal phosphates,

sulfides, and organic condensates in artificial sediments. Appl Environ Microbiol 45: 1094-1108.

Brandl H, Faramarzi MA. 2006. Microbe–metal interactions for the biotechnological treatment of metal-containing solid waste. China Particuology 4: 93-97.

Bryson MF, Drake HL. 1988. Energy-dependent transport of nickel by *Clostridium pasteurianum*. J Bacteriol 170: 234-238.

Chester R, Hughes MJ. 1968. Scheme for the spectrophotometric determination of Cu, Pb, Ni, V and Co in marine sediments. Trans Inst Min Metal B 77: 37-41.

Cheung HY, Vitkovic L, Brown MRW. 1982. Toxic effect of manganese on growth and sporulation of *Bacillus stearothermophilus*. J Gen Microbiol 128: 2345-2402.

Chin CS, Johnson KS, Coale KH. 1992. Spectrophotometric determination of dissolved manganese in natural waters with 1-(2-pyridylazo)-2-naphthol: application to analysis in situ in hydrothermal plumes. Mar Chem 37: 65-82.

Colombini MP, Fuoco R. 1983. Determination of manganese at ng/ml levels in natural waters by differential pulse polarography. Talanta 30: 901-905.

Corpe WA. 1975. Metal-binding properties of surface materials from marine bacteria. Dev Ind Microbiol 16: 249-255.

D'Hondt S, Jørgensen BB, Miller DJ, Batzke A, Blake R, Cragg BA, Cypionka H, Dickens GR, Ferdelman T, Hinrichs K, Holm NG, Mitterer R, Spivack A, Wang G, Bekins B, Engelen B, Ford K, Gettemy G, Rutherford SD, Sass H, Skilbeck CG, Aiello IW, Guerin G, House CH, Inagaki F, Meister P, Naehr T, Niitsuma S, Parkes RJ, Schippers A, Smith DC, Teske A, Wiegel J, Padilla CN, Acosta JLS. 2004. Distributions of microbial activities in deep subseafloor sediments. Science 306: 2216-2221.

Das A, Fernandes CEG, Naik SS, Nath BN, Suresh I, Mascarenhas-Pereira MBL, Gupta SM, Khadge NH, Prakash Babu C, Borole DV, Sujith PP, Valsangkar AB, Mourya BS, Biche SU, Sharma R, Loka Bharathi PA. 2011. Bacterial response to contrasting sediment geochemistry in the Central Indian Basin. Sedimentology 58: 756-784.

Dean-Ross D, Mills AL. 1989. Bacterial community structure and function along a heavy metal gradient. Appl Environ Microbiol 55: 2002-2009.

Duxbury T, Bicknell B. 1983. Metal-tolerant bacterial populations from natural and metal-polluted soils. Soil Biol Biochem 15: 243-250.

Ehrlich HL. 1978. Conditions for bacterial participation in the initiation of Mn deposition around marine sediment particles. In: Environmental Biogeochemistry and Geomicrobiology. Krumbein WE (ed) Ann Arbor Science, Michigan, USA, pp. 839-845.

Ehrlich HL. 1982. Enhanced removal of Mn^{2+} from seawater by marine sediments and clay minerals in the presence of bacteria. Can J Microbiol 28: 1389-1395.

Ehrlich HL. 1997. Microbes and metals. Appl Microbiol Biotechnol 48: 687-692.

Fernandes SO, Krishnan KP, Khedekar VD, Loka Bharathi PA. 2005. Manganese oxidation by bacterial isolates from the Indian ridge system. BioMetals 18: 483-492.

Ferris FG, Fyfe WS, Beveridge TJ. 1987. Bacteria as nucleation sites for authigenic minerals in a metal contaminated lake sediment. Chem Geol 63: 225-232.

Forstner U. 1990. Inorganic sediment chemistry and elemental speciation. In: Sediments: Chemistry and Toxicity of In-Place Pollutants. Baudo R, Giesy J, Muntau H (eds) Lewis Publishers, Boca Raton, USA, pp. 61-73.

Fortin D, Davis B, Southam G, Beveridge TJ. 1995. Biogeochemical phenomena induced by bacteria within sulfidic mine tailings. J Ind Microbiol Biotechnol 14: 178-185.

Fortin D, Southam G, Beveridge TJ. 1994. Nickel sulfide, iron–nickel sulfide and iron sulfide precipitation by a newly isolated *Desulfotomaculum* species and its relation to nickel resistance. FEMS Microbiol Ecol 14: 121-132.

Froelich PN, Klinkhammer GP, Bender ML, Heath GR, Cullin D, Dauphin P, Hammond D, Hartman B, Maynard V. 1979. Early oxidation of organic matter in pelagic sediments of the eastern equatorial Atlantic; suboxic diagenesis. Geochim Cosmochim Acta 43: 1075-1090.

Glasauer S, Langley S, Beveridge TJ. 2004. Intracellular manganese granules formed by a subsurface bacterium. Environ Microbiol 6: 1042-1048.

Glasby GP. 2006. Manganese: predominant role of nodules and crusts. In: Marine Geochemistry. Schulz HD, Zabel M (eds) Springer, Berlin, pp. 371-427.

Gupta SM, Jauhari P. 1994. Radiolarian abundance and geochemistry of the surface-sediments from the Central Indian Basin: inferences to Antarctic bottom water current. Curr Sci 66: 659-663.

Hart BT. 1982. Uptake of trace metals by sediments and suspended particulates: a review. Hydrobiologia 91: 299-313.

Herrera-Melian JA, Dona-Rodriguez JM, Hernandez-Brito J, Pena JP. 1997. Voltammetric determination of Ni and Co in water samples. J Chem Educ 74: 1444-1445.

Hobbie JE, Daley RJ, Jasper S. 1977. Use of nucleopore filters for counting bacteria by fluorescent microscopy. Appl Environ Microbiol 3: 1225-1228.

Hornor SG, Hilt BA. 1985. Distribution of zinc-tolerant bacteria in stream sediments. Hydrobiologia 128: 155-160.

Houba C, Remacle J. 1980. Composition of the saprophytic bacterial communities in freshwater systems contaminated by heavy metals. Microb Ecol 6: 55-69.

Jasper P, Silver S. 1977. Magnesium transport in microorganisms. In: Microorganisms and Minerals. Weinberg ED (ed), Marcel Dekker, NewYork, pp. 7-47.

Kuroda K, Ueda M. 2003. Bioadsorption of cadmium ion by cell surface-engineered, yeasts displaying metallothionein and hexa-His. Appl Microbiol Biotechnol 63: 182-186.

Lee Y, Tebo BM. 1994. Cobalt(II) oxidation by the marine manganese(II)-oxidizing *Bacillus* sp. strain SG-1. Appl Environ Microbiol 60: 2949-2957.

Lienemann CP, Taillefert M, Perret D, Gaillard JF. 1997. Association of cobalt and manganese in aquatic systems:chemical and microscopic evidence. Geochim Cosmochim Acta 61: 1437-1446.

Mandernack KW, Post J, Tebo BM. 1995. Manganese mineral formation by bacterial spores of the marine *Bacillus*, strain SG-1: evidence for the direct oxidation of Mn(II) to Mn(IV). Geochim Cosmochim Acta 59: 4393-4408.

Mascarenhas-Pereira MBL, Nath BN, Borole DV, Gupta SM. 2006. Nature, source and composition of volcanic ash in sediments from a fracture zone trace of Rodriguez Triple Junction in the Central Indian Basin. Mar Geol 229: 79-90.

McInerney MJ. 1993. Energetics and kinetics of anaerobic aromatic and fatty acid degradation. Report prepared for the US Department of Energy, Oklahoma.

Mills AL, Colwell RR. 1977. Microbiological effects of metal ions in Chesapeake Bay water and sediment. Bull Environ Contam Toxicol 18: 99-103.

Moffett JW, Ho J. 1996. Oxidation of cobalt and manganese in seawater via a common microbially catalyzed pathway. Geochim Cosmochim Acta 60: 3415-3424.

Mudholkar AV, Pattan JN, Parthibhan G. 1993. Geochemistry of deep sea sediment cores from the Central Indian Ocean Basin. Ind J Mar Sci 22: 241-246.

Muller PJ, Hartmann M, Suess E. 1988. The chemical environment of pelagic sediments. In: The Manganese Nodule Belt of the Pacific Ocean, Geological Environment, Nodule Formation, and Mining Aspects. Halbach P, Friedrich G, von Stackelberg U (eds) Enke Verlag, Stuttgart, pp.70-99.

Nath BN, Roelandts I, Sudhakar M, Plüger WI. 1992. Rare earth element patterns of the Central Indian Basin sediments related to their lithology. Geophys Res Lett 19: 1197-1200.

Patience RL, Clayton CJ, Kearsley AT, Rowland SJ, Bishop AN, Rees AWG, Bibby KG, Happer AC. 1990. An integrated biochemical, geochemical and sedimentological study of organic diagenesis in sediments from ODP LEG 112. Proc ODP Sci Repts.

Pattan JN, Mudholkar AV. 1990. The oxidation state of manganese in ferromanganese nodules and deep-sea sediments from the Central Indian Ocean. Chem Geol 85: 171-181.

Razzell WE, Trussell PC. 1963. Microbiological leaching of metallic sulfides. Appl Environ Microbiol 11: 105-110.

Roy P, Balaram V, Kumar A, Satyanarayanan M, Rao TG. 2007. New REE and trace element data on two kimberlitic reference materials by ICP-MS. Geostand Geoanal Res 31: 261-273.

Schaanning MT, Hylland K, Eriksen DO, Bergani TD, Gunnarson JS, Skei J. 1996. Interactions between eutrophication and contaminants. II. Mobilization and bioaccumulation of Hg and Cd from marine sediments. Mar Pollut Bull 33: 71-79.

Schmidt T, Schlegel HG (1989) Nickel and cobalt resistance of various bacteria isolated from soil and highly polluted domestic and industrial wastes. FEMS Microbiol Ecol 62: 315-328.

Shao Z, Sun F. 2007. Intracellular sequestration of manganese and phosphorus in a metal-resistant fungus *Cladosporium cladosporioides* from deep-sea sediment. Extremophiles 11: 435-443.

Shaw T, Gieskes J, Jahnke R. 1990. Early diagenesis in differing depositional environments: the response of transition metals in pore water. Geochim Cosmochim Acta 54: 1233-1246.

Stockdale A, Davison W, Zhang H, Hamilton-Taylor J. 2010. The association of cobalt with iron and manganese (oxyhydr)oxides in marine sediment. Aquat Geochem 16: 575-585.

Stoppel RD, Schlegel HG. 1995. Nickel-resistant bacteria from anthropogenically nickel-polluted and naturally nickel-percolated ecosystems. Appl Environ Microbiol 61: 2276-2285.

Sujith PP, Khedekar VD, Girish AP, Loka Bharathi PA. 2010. Immobilization of nickel by bacterial isolates from the Indian ridge system and the chemical nature of the accumulated metal. Geomicrobiol J. 27: 424-434.

Sundby B, Anderson LG, Hall POJ, Iverfeldt A. 1986. The effect of oxygen on release and uptake of cobalt, manganese, iron and phosphate at the sediment–water interface. Geochim Cosmochim Acta 50: 1281-1288.

Timoney JF, Port J, Giles J, Spanier J. 1978. Heavy metal and antibiotic resistance in the bacterial flora of sediments of New York Blight. Appl Environ Microbiol 36: 465-472.

Turner A, Nimmo M, Thuresson KA. 1998. Speciation and sorptive behaviour of nickel in an organic-rich estuary (Beaulieu, UK). *Mar Chem 63: 105-118.*

Xue HB, Jansen S, Prasch A, Sigg L. 2001. Nickel speciation and complexation kinetics in freshwater by ligand exchange and DPCSV. Environ Sci Technol 35: 539-546.

Zhang H, Davison W, Mortimer RJG, Krom MD, Hayes PJ, Davies IM. 2002. Localized remobilization of metals in a marine sediment. Sci Total Environ 296: 175-187.

CHAPTER 8

Manganese cycling and its implication on methane related processes in the Andaman continental slope sediments

8.1. Abstract

Microbial oxidation and reduction of Mn is coupled to a number of biogeochemical processes. In continental slope sediments especially where the intense recycling of organic matter occurs the microbial involvement can direct the formation of methane hydrates under optimum temperature and pressure conditions. The present study deliberates on the *in vitro* microbial cycling of Mn under oxic and suboxic incubation conditions and elucidates their plausible contribution to methane generation/oxidation. To meet this hypothesis, the study was conducted at 4±1°C with subsurface sediment samples ranging in depth from 134 to 637.5 meters below sea floor (mbsf). The experiment was conducted using 0.001% glucose as a model compound for organic carbon in the presence of 100 µM of Mn^{2+}. Biotic experiments were setup with homogenized sediments weighing ~0.05 to 0.1 g with (G^+) and without (G^-) added glucose. The corresponding abiotic controls included set-ups poisoned with 15 mM sodium azide. Results show that immobilization of Mn occurs under oxic conditions as opposed to its release from the solid phase under suboxic conditions. The biotic experimental results significantly differed from that of the abiotic controls and viz versa at $p \leq 0.001$. The immobilization of Mn was significant at 360 mbsf and coincided with the maximum abundance of methanogens (1.0×10^3 cells g^{-1}) and the peak for methane (89100 ppm-v) at 360.5 mbsf. The trend of immobilization of Mn under oxic condition was biotic > abiotic, $G^+ > G^-$ while the mobilization of Mn under suboxic condition was the opposite i.e. abiotic > biotic, $G^- > G^+$. In moderately reducing conditions of the shelf sediments, methane generation is generally attributed to the degradation of organic carbon. However, the present findings indicate that in addition to the above process, the accelerated methane production resulted from the interplay between bound and soluble Mn species that could work as microbial electron shuttles.

8.2. Introduction

Continental margins are important for intense biogeochemical processes as they are regions for high biological production and sedimentation. They are locations where accumulation rates of organic matter are very high and oxygen consumption is most rapid (Laes *et al.*, 2007). The degradation of organic carbon in these marine sediments can contribute to the formation of methane hydrates that represents the enormous source of carbon and energy (Bidle *et al.*, 1999; Briggs *et al.*, 2012). The oxidation of methane transfers terminally reduced carbon into forms readily accessible for a larger group of microorganisms in anoxic sediments. Chemosynthetic microbial communities confined to such sediments benefit from H_2S produced as a by-product of anaerobic oxidation of methane (AOM) (Orphan *et al.*, 2001). The sulfate reducing bacteria on the other hand are potent reducers of Mn oxides by virtue of their sulfide production. The presence of sulfate accelerates the Mn cycle and drive the reduction process (Nealson, 1985). The use of Fe and Mn in the oxidation of methane further reveals that AOM is coupled to a large variety of oxidants (Beal *et al.*, 2009). Further, the oxidation of hydrocarbon coupled to the reduction of Fe and Mn-oxides helps in the completion of energy-producing metabolic pathways in the absence of more favorable electron acceptors such as O_2 and nitrate (Martin, 2005). The oxidation of Mn by bacteria in the subsurface sediments consumes oxygen and thereby create conducive environment for AOM. On the other hand, the oxygen required for Mn oxidation in the subsurface sediments could be met from the relationship between Mn oxidizing bacteria and *Methoxymirabilis oxyfera* like organisms that produce oxygen (Ettwig *et al.*, 2010). Besides, acetate formed from the fermentation of glucose is known to serve as a suitable substrate for methanogenesis accounting for ~70 % of the biogenic methane (Mah *et al.*, 1977; Winter, 1980). In addition, acetate has been shown to be used as a preferential electron donor for Mn reducing bacteria (Vandieken *et al.*, 2012). Therefore, acetate utilization by Mn reducing bacteria could be coupled to methanogenesis through the utilization of common substrates in both the processes. The AOM coupled to Fe, Mn, sulfate and nitrate reduction in anaerobic methanotrophic archaea (ANME) (Joye, 2012; Haroon *et al.*, 2013) therefore could critically control the flux of methane from anoxic environments.

The enrichment of trace metals in the continental shelves occurs through riverine inputs, sediment remobilisation and hydrodynamic processes (Laes *et al.*, 2007). As the sedimentary geochemistry of Mn is controlled by its redox speciation, the behavior of Mn in such sediments varies strongly with changes in redox potential. It occurs as insoluble oxyhydroxides under well oxygenated conditions and pH above neutral, and as reduced species (Mn^{2+}) in oxygen-deficient conditions. Sedimentary anoxic conditions prevail in the continental margin and shelf sediments due to excessive burial of particulate organic matter with respect to the replenishment of dissolved oxygen (Calvert and Pedersen, 1996). The microbial involvement therefore depending upon the oxygen level show preference for nitrate, Fe and Mn oxyhydroxides as terminal electron acceptor for the oxidation of organic matter and releases H_2S as a by-product of bacterial sulfate reduction (Froelich *et al.*, 1979) leading to anoxic conditions at variable depth below the sea floor. The microbial participation in the biogeochemical cycling of Mn and their association with organic matter increases or decreases their bioavailability (Gadd, 2009). Nevertheless, Collet *et al.* (2007) has reported the presence of sub-oxic conditions which are more suitable for Mn oxidation (Sujith *et al.*, 2011). The recycling and transport of Mn via the overlying water from the shelf, out into deeper water leads to the accumulation of manganese oxides in some continental slope sediments (Jorgensen, 2006). Also, bacteria and their interaction with Mn lead to the formation of oxyhydroxide mineral phases (Sunda and Kiber, 1994). The burial of these mineral oxide into anoxic depths, promotes the mobilization of Mn through microbial respiration and abiotic reduction resulting in high Mn^{2+} concentrations in the porewaters.

The Andaman Basin has an area of 800000 km^2 separated from the Bay of Bengal by the Andaman-Nicobar Ridge. The Irrawaddy River serves as the basin's principal sediment source. Depositional rates of sediment average 15 cm/1000 year in the central trough (Rodolfo, 1969). The study site is located at 10°45.1912'N latitude, 93° 6.7365'E longitude in the Andaman Sea along the eastern coast of the Andaman Islands. The water depth is ~1344 m and the sediments of the region have <1% by weight total organic carbon (Ramaswamy *et al.*, 2008; Johnson *et al.*, 2009). The present study addresses the *in vitro* microbial cycling of Mn under oxic and sub-oxic incubation conditions and elucidates their plausible contribution to methane related processes.

8.3. Materials and methods

8.3.1. Sample collection

The methane hydrate bearing subsurface sediment samples were collected offshore of the Andaman Islands during cruise onboard JOIDES (Joint Oceanographic Institutions for Deep Earth Sampling) resolution between 28th April 2006 and 19th August 2006 under the National gas hydrate program (NGHP). Hole NGHP-01-17A was drilled on the Andaman convergent margin in Leg 4 cruise of Expedition 01. Samples were retrieved using extended core barrel (XCB) coring system. They were sub-sectioned onboard and were stored at 4 °C. From the sediment core, 25 sections between 134 to 637.5 mbsf (meters below sea floor) were sub-sampled and were used for the present study.

8.3.2. Methanotrophic bacterial enumeration

The medium used for isolation and purification of methanotrophs was the nitrate-mineral-salts (NMS) medium of Whittenbury *et al.* (1970) solidified by the addition of 1.5% (w/v) agar. The medium was dispensed into tubes. The tubes were then autoclaved at 121°C for 20 min. An appropriate dilution of samples was spread onto the NMS agar slopes in tubes. Methane was passed through a 0.2 µm pore filter syringe and injected into each tube giving about 18% methane in a head gas-phase. Control tubes without methane injection were also prepared in duplicate. The tubes were incubated at 30 °C and observed at 3-day or 1-week intervals over 3–4 weeks. The colonies formed were then enumerated and expressed per gram of sediment.

8.3.3. Methanogenic bacterial enumeration

The composition of the basal medium for the enumeration of methanogenic bacteria was according to Parkes *et al.* (2010). On preparation, the media was distributed anaerobically as described by Macy *et al.* (1972) into 60 ml serum bottles (20 ml/bottle) and into 20 ml Hungate tubes (5 ml/tube). Sterilized serum bottles and Hungate tubes were flushed with N_2/CO_2 (80/20 v/v). After sterilization, 0.01 ml of 2% $Na_2S.9H_2O$ and 0.05 ml of 10% $NaHCO_3$ were injected per ml of basal medium into the culture vessels. Three selective media were prepared by adding one of the three following substrates: formate (40 mM), methanol (40 mM) and acetate (20 mM) to the sterilized basal medium. The substrates were added from sterile and anaerobic stock

solution or from solution injected with H_2/CO_2 (80/20 v/v, 2 bar) in the gas phase. The population density of methanogens was estimated by the most probable number (MPN) method (3 tubes per dilution). Successive 10-fold serial dilutions of soil suspension were inoculated in the three selective media described above. Trophic groups of methanogens were detected, at least, on one of these media. Counts were duplicated by using two composite sediment samples. Methanogen growth was assayed by measuring CH_4 produced after 60 d of incubation at 37 °C. Inoculated tubes containing medium where no substrate was added, served as control. A tube was considered positive when CH_4 produced was at least 5% higher than in the control. Populations were expressed as MPN per g dry weight of the sediment.

8.3.4. Extraction of porewater and analysis of geochemical parameters

The porewater Mn was extracted by centrifugation of the samples in the cold (Sigma 3-18K). The determination of Mn was made by adsorptive stripping voltammetry in interface with 797VA computrace in the differential pulse mode (Metrohm, Switzerland) according to Colombini and Fuoco (1983). Mn was quantified with two standard additions of appropriately diluted 1000-ppm concentrations of the metal standards prepared in seawater. Metal standards (1000 ppm) obtained from Merck-GMBH, were used for determining the analytical accuracy. Values for methane are taken from NGHP-01-17A, Expedition 01cruise report (Collet *et al.*, 2007).

8.3.5. In vitro experiment on the cycling of Mn

The experiment with methane bearing sediment samples were conducted following the procedure described by Sujith *et al.* (2011). The various sterile media that were used for the experimental incubations were prepared in filtered and autoclaved sea water. In this experiment, glucose was used as a model compound for organic carbon. Sodium azide poisoned media were used as abiotic controls. The different combinations of media used were as follows: Media I- seawater without glucose amendment (BG^-); Media II- seawater with 0.001% glucose amendment (BG^+); Media III- seawater without glucose and poisoned with 15 mM sodium azide (AG^-) and Media IV- seawater with 0.001% glucose and poisoned with 15 mM sodium azide (AG^+). Each media received 100 μM concentration of Mn^{2+} as the metal of interest. Uninoculated media from I to IV served as sterile controls. The experiments were set up in 15 ml screw-

capped tubes under oxic and sub-oxic conditions at 4±1 °C. The oxic incubation was assured by directly inoculating ~0.05 to 0.1 g dry weight of sediment portions from each sub-section of the cores in half-filled tubes and sub-oxic in completely filled tubes of the respective media. The concentration of soluble Mn was measured in all sets of treatment immediately after the addition of sediment (0 hr) as described by Chin *et al.* (1992). The initial measurement was used as a reference to monitor the changes in metal concentrations through the incubation period of 1, 20, 32, 39, 47 and 50 d. Subsequently, after every time interval, three tubes of each media including controls were sacrificed for the determination of pH, Eh, and Mn.

8.3.5.1. Calculation of change in metal concentration

Any decrease in dissolved Mn concentration that occurred during the experiment was assumed to be caused by metal immobilization and any increase in dissolved Mn concentration was assumed to be caused by its mobilization. The concentration of the metal in solution was determined from the curve of best fit derived from different concentrations of Mn (μM) which were done in triplicates. The gram dry weight concentration of Mn was calculated after correcting for the blank as follows:-

$$Q = v(Ci-Cf)/m$$

Where:

Q = Mn immobilized/mobilized, mg g^{-1}

v = volume of media used, ml

Ci = initial concentration of Mn in solution, mg l^{-1}

Cf = equilibrium concentration of Mn in solution, mg l^{-1}

m = dry weight of sediment, mg

Two-way ANOVA and Students Newman-Keuls post hoc (SNK test) analysis were performed to find out the significant differences between depths, incubation time and biotic and abiotic sets of incubations. The analysis was carried out using Statistica 6 software package.

8.3.5.2. Eh and pH measurements

The Eh and pH electrodes were calibrated using standard reference solutions prior to measurements. For Eh, the potential of the platinum (Pt) electrode versus the Ag/AgCl reference electrode with KCl electrolyte in ZoBell's solution was measured as

a function of temperature. The calibration of the meter was as per the protocol given in user's guide, Thermo Electron Corporation (2005). The calibration for pH was done using three buffer solutions of known pH 4, 7, and 10. The Eh (mV) readings in samples were made for 60 s followed by pH in duplicates. The Eh (mV) value of the sample was calculated as described in the standard methods APHA, AWWA, WEF (2005).

8.4. Results

8.4.1. Culturability of methanotrophic and methanogenic bacteria

The yield of culturable methane oxidizing bacteria (methanotrophs) ranged from 3.0×10^{0} to 4.82 $\times10^{2}$ CFU g^{-1}. Their numbers were the maximum at the subsurface depth of 134 mbsf and decreased further gradually with depth (Figure 8.1). The colonies were mostly circular, convex and opaque with smooth edges. On the other hand, the methanogenic bacterial numbers varied from 4.0 $\times10^{1}$ to 1.0×10^{3} MPN g^{-1} of dry sediment. The maximum count of 1.0×10^{3} MPN g^{-1} was observed at 360.5 mbsf (Figure 8.1). Their numbers varied a little in most of the depths (10^{2} MPN g^{-1}) and showed a secondary maximum of 4.0×10^{2} MPN g^{-1} at 619 mbsf.

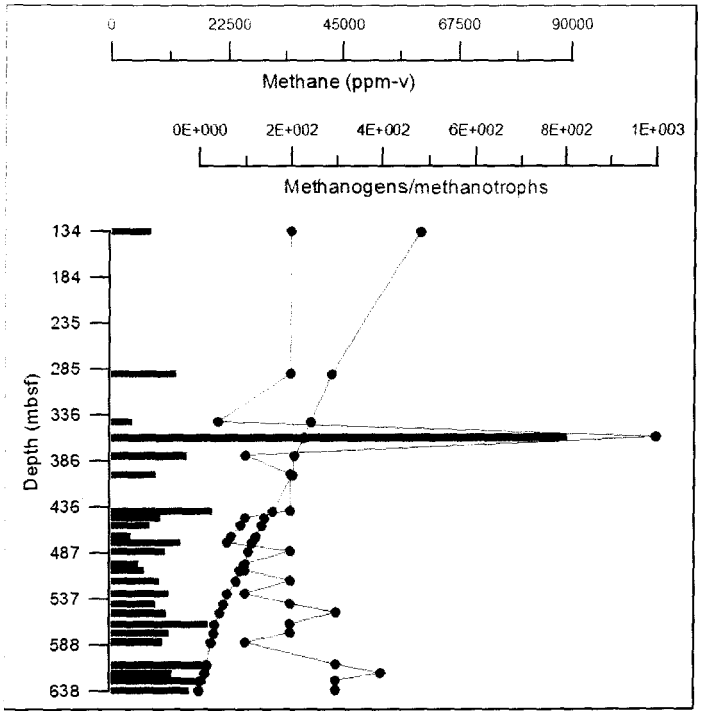

Figure 8.1. Methane profile versus the abundance of methanogens (MPN g^{-1}) and methanotrophs (CFU g^{-1}) in subsurface sediments of core 17A (MPN= most probable number and CFU= colony forming units).

8.4.2. Manganese in porewater

The lowest concentration of Mn in porewater (33.97 μM) was recorded at 134 mbsf. With deeper depths the concentration of Mn tends to increase with an initial peak of 172.65 μM recorded at 380.5 mbsf. Beyond the depth of 498.4 mbsf, the Mn concentrations oscillated between high and low values between depths. The maximum concentration of 428.99 μM Mn was recorded at the bottom most depth of 637.5 mbsf (Figure 8.2).

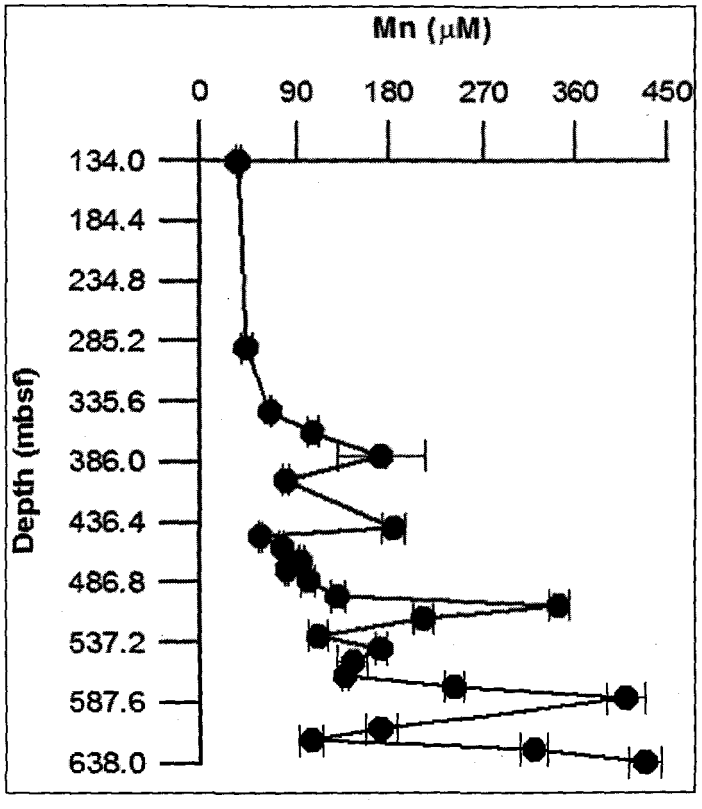

Figure 8.2. Porewater profile of manganese (Mn^{2+}) for subsurface sediments of core 17A.

8.4.3. In vitro experimental results on Mn cycling

8.4.3.1. Oxic incubation with added glucose

Under oxic incubation condition with added glucose, two way ANOVA showed significant variation ($F= 2574.1$; $p < 0.000^*$) in Mn immobilization rates between the biotic and abiotic sets of incubation (Table 8.1). Here the immobilization of Mn was biotic > abiotic. Analyses along the core showed that Mn immobilization rates tend to vary from 1.07 to 4.66 μM g^{-1} between depths in the biotic media (Figure 8.3a).

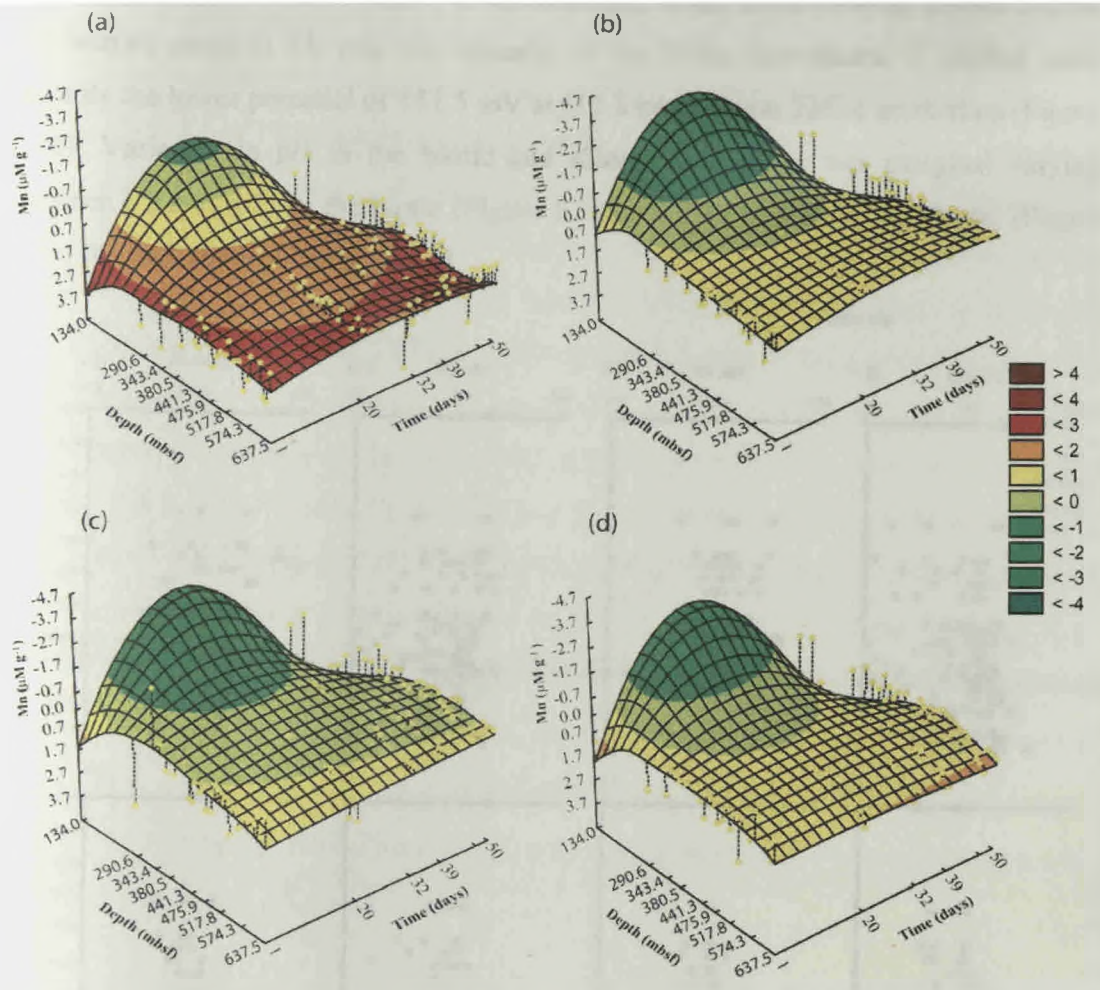

Figure 8.3. The cycling of Mn in continental shelf sediments. a) G^+ biotic oxic, b) G^+ abiotic oxic, c) G^- biotic oxic and d) G^- abiotic oxic. The coloured bar shows the rate of Mn immobilization/mobilization (μM g^{-1}) where the negative values indicate mobilization and positive values indicate immobilization (mbsf: meters below seafloor, G^+: media with added glucose and G^-: media without added glucose).

The immobilization of Mn at 360 mbsf was significantly low of 1.14 μM g^{-1} on the 20 d of incubation. Such a trend was not apparent in the corresponding abiotic controls. There the immobilization of Mn was evident at most of the depths and mobilization of Mn (-0.31 μM g^{-1}) at 360 mbsf (Figure 8.3b). The immobilization of Mn in the abiotic experiment which is used as the control was comparatively less than that of the biotic experiment with maximum values of 1.65 μM g^{-1} on the first day of incubation. In the biotic incubations, Eh showed a shift from lower redox potential of 181.9 mV to higher redox potential of 236.6 mV along the studied sections of the core. Interestingly, a well defined peak for Eh (232.9 mV) was also observed on the 32 d of

incubation at 517.8 mbsf (Figure 8.4a). Whereas, in the corresponding abiotic control the overall trend in Eh was the opposite of the biotic incubations. It shifted more towards the lower potential of 151.5 mV at 517.8 mbsf on the 32d of incubation (Figure 8.4b). Variation in pH in the biotic and abiotic incubations was marginal varying between 8.22 to 8.51 in the biotic (Figure 8.5a) and 8.19 to 8.55 in the abiotic (Figure 8.5b) through the incubation period.

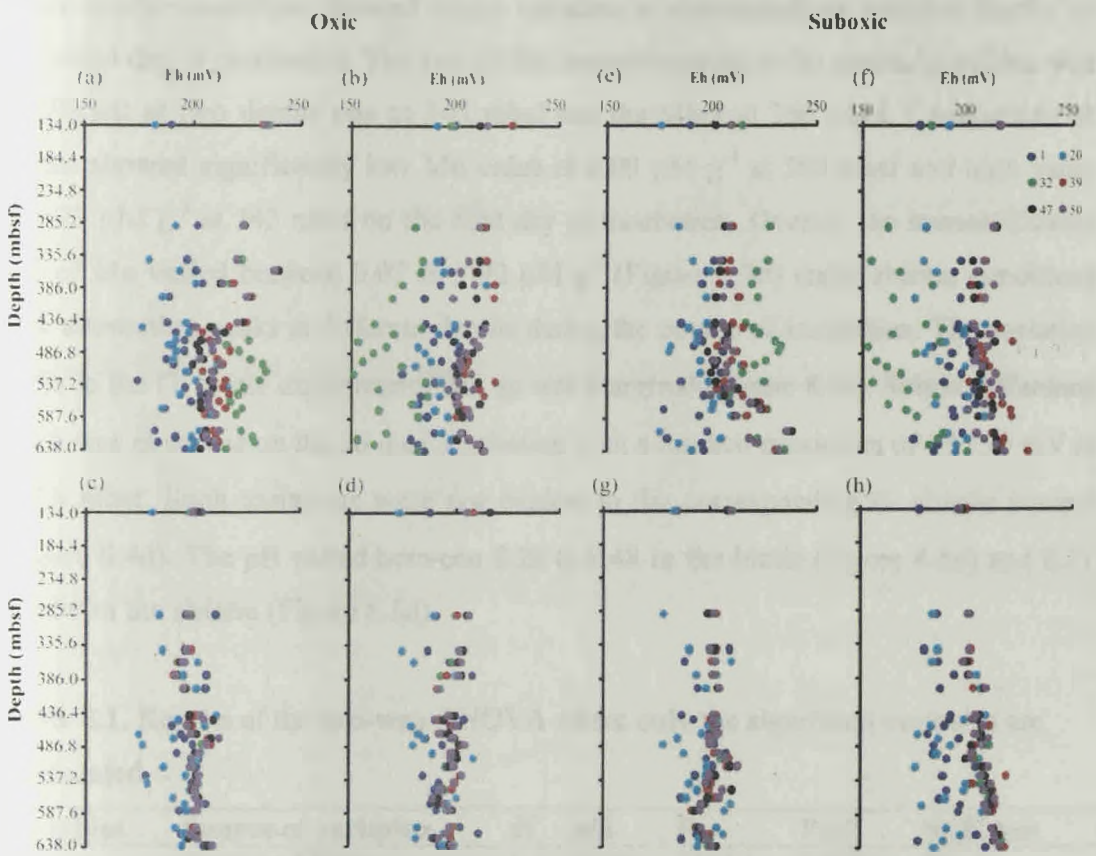

Figure 8.4. Time dependent variation of Eh (mV) in the in-vitro experiment on Mn cycling with subsurface sediments a) G^{+} biotic oxic, b) G^{+} abiotic oxic, c) G^{-} biotic oxic, d) G^{-} abiotic oxic, e) G^{+} biotic suboxic, f) G^{-} abiotic suboxic, g) G^{-} biotic suboxic, and h) G^{-} abiotic suboxic (G^{+}: media with added glucose and G^{-}: media without added glucose).

8.4.3.2. Oxic incubation without added glucose

Unlike the former, oxic incubation without added glucose showed significant variation ($F=785.2$; $p \leq 0.001$) in Mn immobilization rates between the biotic and abiotic sets of incubation on the first day of incubation (Table 8.1). Here the

immobilization of Mn was abiotic > biotic. The lower immobilization of Mn with the biotic in the absence of added glucose was not because of lesser bacterial activity but rather because of their switch over from immobilization to mobilization. Low Mn value of -0.75 μM g^{-1} at 360 mbsf and high value of -2.8 μM g^{-1} at 343 mbsf was registered on the first day of incubation. Overall, the mobilization rate of Mn varied between -0.01 to -2.8 μM g^{-1} under biotic conditions (Figure 8.3c). The abiotic immobilization of Mn under similar conditions showed major variation in concentrations between depths on the initial day of incubation. The rate of Mn immobilization in the abiotic condition was significant at two depths one at 343 mbsf and the other at 360 mbsf. Comparison of depths showed significantly low Mn value of 0.09 μM g^{-1} at 360 mbsf and high value of 1.23 μM g^{-1} at 343 mbsf on the first day of incubation. Overall, the immobilization rate of Mn varied between 0.07 to 1.92 μM g^{-1} (Figure 8.3d) under abiotic conditions with alternating peaks at different depths during the course of incubation. The variation of Eh in the G^- biotic experimental set up was marginal (Figure 8.4c). Subtle difference of Eh was observed on the 20 d of incubation with a marked maximum of 185.90 mV at 517.8 mbsf. Such variations were not evident in the corresponding G^- abiotic control (Figure 8.4d). The pH varied between 8.20 to 8.48 in the biotic (Figure 8.5c) and 8.21 to 8.56 in the abiotic (Figure 8.5d).

Table 8.1. Results of the two-way ANOVA where only the significant variables are represented.

Variables	Source of variation	df	MS	F	P (≤)	SNK test
G^+ oxic	Biotic vs Abiotic	1	669.9	2574.1	0.001*	B > A
	Depth	24	1.8	7	0.001*	360 mbsf
	Days	5	4.4	17	0.001*	20 d
G^- oxic	Biotic vs Abiotic	1	99.63	785.2	0.001*	A > B
	Depth	24	1.97	15.5	0.001*	343 & 360 mbsf
	Days	5	0.99	7.8	0.001*	01 d
G^+ suboxic	Biotic vs Abiotic	1	14.56	48.26	0.001*	B > A
	Depth	24	1.76	5.84	0.001*	447 mbsf
	Days	5	10.18	33.73	0.001*	01 d
G^- suboxic	Biotic vs Abiotic	1	45.58	110.3	0.001*	A > B
	Depth	24	7.87	19	0.001*	343 & 360 mbsf
	Days	5	37.54	90.8	0.001*	20 d

SNK test: Student-Newman-Keuls test, mbsf: meters below seafloor, G+: media with added glucose and G^-: media without added glucose.

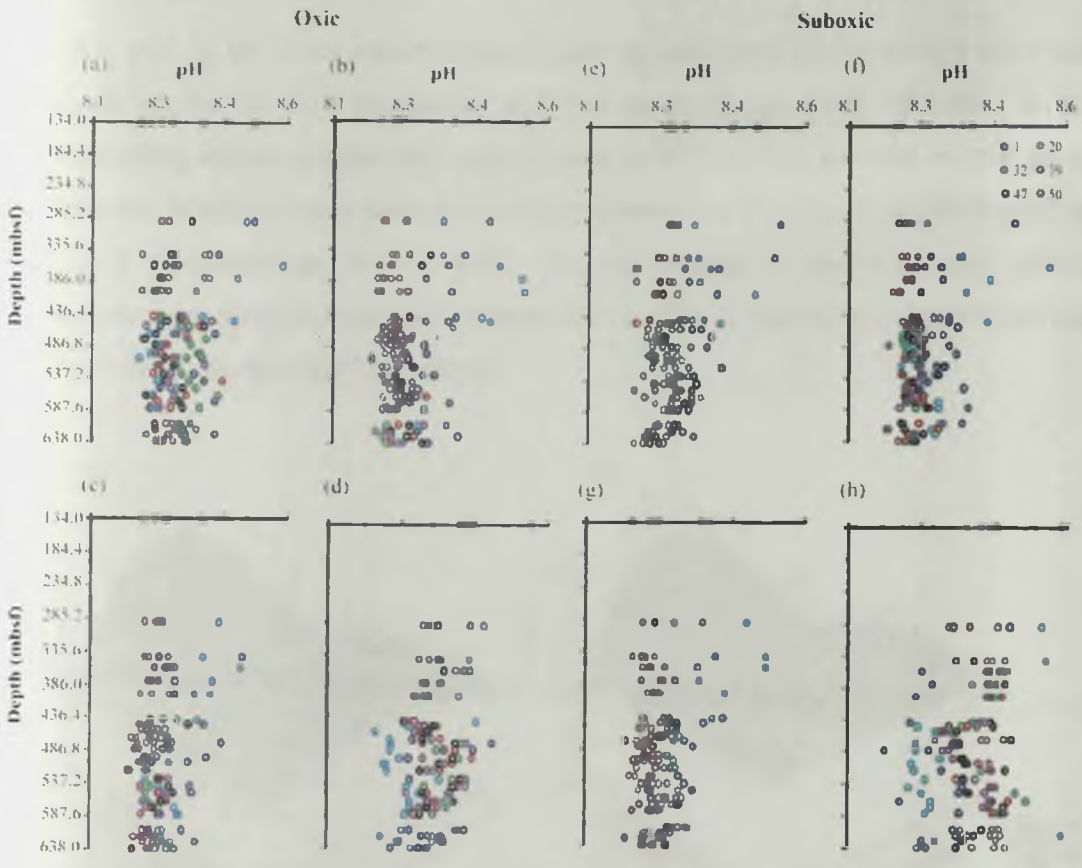

Figure 8.5. Time dependent variation of pH in the in-vitro experiment on Mn cycling with subsurface sediments a) G^{-} biotic oxic, b) G^{-} abiotic oxic, c) G^{-} biotic oxic, d) G^{-} abiotic oxic, e) G^{-} biotic suboxic, f) G^{-} abiotic suboxic, g) G^{-} biotic suboxic, and h) G^{-} abiotic suboxic (G^{-}: media with added glucose and G^{-}: media without added glucose).

8.4.3.3. Suboxic incubation with added glucose

Under suboxic incubation conditions with added glucose, the overall process was immobilization = mobilization with significant variation ($F=48.26$; $p \leq 0.001$) between the biotic and abiotic set of incubations on the first day of incubation (Table 8.1). The overall process was biotic > abiotic. The immobilization of Mn was high at 441.3 mbsf (2.95 $\mu M\ g^{-1}$) and mobilization at 531.1 mbsf (-2.98 $\mu M\ g^{-1}$). The maximum values of immobilization and mobilization were recorded on the 20 d of incubation (Figure 8.6a). This trend was not observed in the corresponding abiotic controls (Figure 8.6b) where the immobilization- mobilization of Mn was lower than that of the biotic incubations varying from 1.37 to -1.55 $\mu M\ g^{-1}$. Beyond the initial day of incubation, mobilization was prominent in the abiotic with no much difference in the rate of mobilization between the depths. Eh showed a shift from lower (177.6 mV) to higher redox potential

of 235.5 mV in the biotic incubations. A well defined peak for Eh (232.9 mV) was observed on the 32 d of incubation at 475.9 mbsf (Figure 8.4e). Whereas, in the corresponding abiotic control the overall trend in Eh was the opposite of the biotic incubations. It shifted more towards the lower potential of 152.63 mV at 475.9 mbsf on the 32 d of incubation (Figure 8.4f). The pH change in the biotic and abiotic incubations was marginal varying between 8.21 to 8.54 in the biotic (Figure 8.5e) and 8.19 to 8.56 in the abiotic (Figure 8.5f).

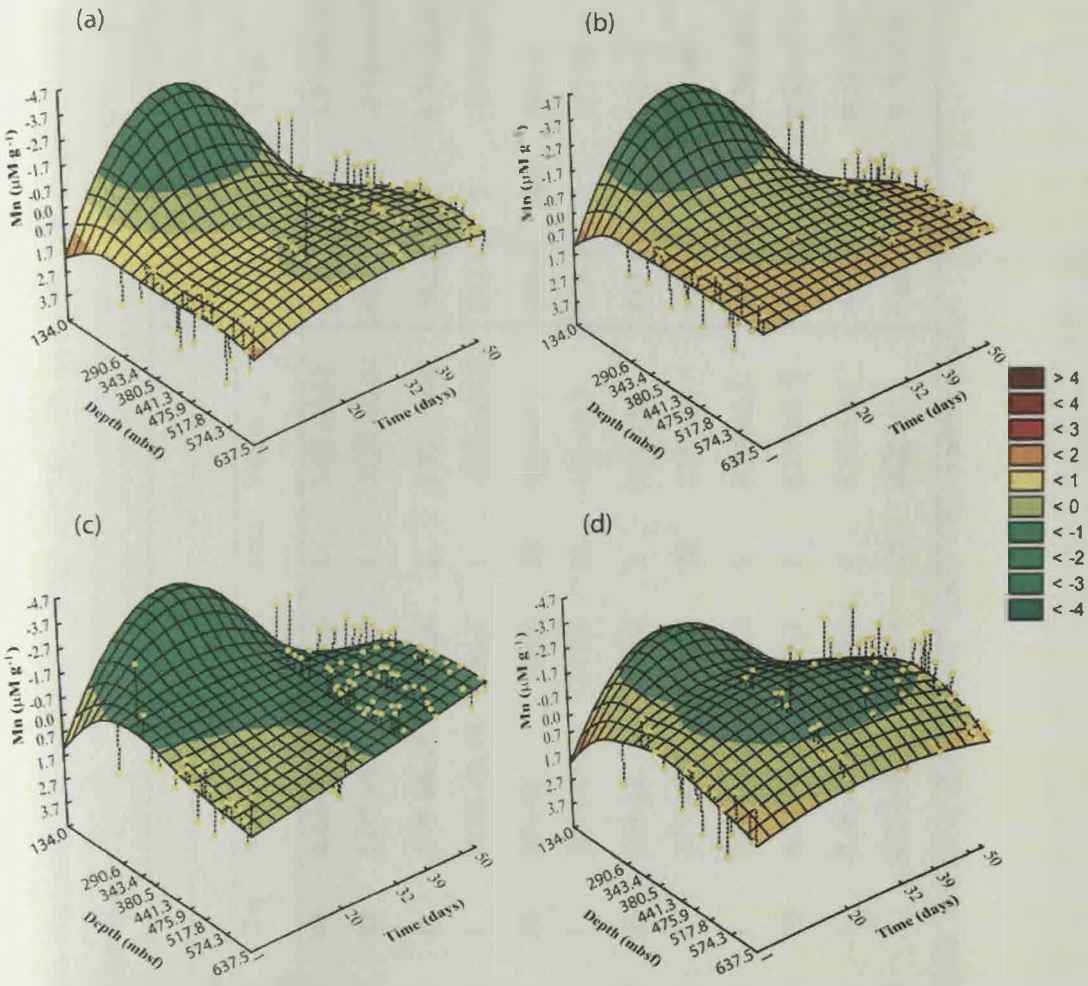

Figure 8.6. The cycling of Mn in continental shelf sediments. a) G^+ biotic suboxic, b) G^+ abiotic suboxic, c) G^- biotic suboxic and d) G^- abiotic suboxic. The coloured bar shows the rate of Mn immobilization/mobilization (μM g^{-1}) where the negative values indicate mobilization and positive values indicate immobilization (mbsf: meters below seafloor, G^+: media with added glucose and G^-: media without added glucose).

Table 8.2. Results of the in-vitro experiment on Mn cycling in the continental shelf sediments of the Andaman Sea. Values in bold represent the maximum values and the others represent the minimum values for Mn, Eh and pH. The negative values for Mn indicate mobilization and positive values indicate immobilization.

Parameters	Media	Oxic						Suboxic					
		Biotic			Abiotic			Biotic			Abiotic		
		Depth (mbsf)	Day	Value	Depth (mbsf)	Day	Value	Depth (mbsf)	Day	Value	Depth (mbsf)	Day	Value
Mn ($\mu M\ g^{-1}$)	**G^+**	**609.4**	**32**	**4.66 ±0.94**	**609.4**	**1**	**1.65 ±0.52**	**441.3**	**20**	**2.95 ±0.18**	**400.8**	**1**	**1.37 ±0.70**
		360.5	32	1.07 ±0.58	360.5	1	-0.31 ±0.04	531.1	20	-2.98 ±0.86	584.4	1	-1.55 ±0.08
Mn ($\mu M\ g^{-1}$)	**G^-**	**290.6**	**1**	**2.49 ±0.65**	**542.6**	**1**	**1.92 ±0.08**	**542.6**	**1**	**0.93 ±0.52**	**290.6**	**39**	**1.64 ±0.46**
		343.4	1	-2.80 ±0.39	584.4	1	-0.50 ±0.07	343.4	1	-3.93 ±1.73	475.9	20	-4.27 ±1.19
Eh (mV)	**G^+**	**360.5**	**50**	**236 ±1**	**134.0**	**39**	**226 ±17**	**609.4**	**50**	**235 ±1**	**637.5**	**39**	**227 ±16**
		609.4	1	181 ±6	517.8	32	151 ±4.5	574.3	1	177 ±5	475.9	32	152 ±4
Eh (mV)	**G^-**	**475.9**	**50**	**211 ±1**	**619.0**	**1**	**211 ±10**	**517.8**	**50**	**212 ±1**	**637.5**	**39**	**217 ±1**
		531.1	1	177 ±0.9	134.0	20	173 ±0.6	134.0	1	184 ±9	517.8	20	176 ±5
pH	**G^+**	**290.6**	**1**	**8.51 ±0.5**	**134.0**	**1**	**8.55 ±0.1**	**290.6**	**1**	**8.54 ±0.1**	**360.5**	**20**	**8.56 ±0.1**
		343.4	50	8.22 ±0.4	506.2	1	8.19 ±0. 5	380.5	50	8.21 ±0.2	619.0	1	8.19 ±0.5
pH	**G^-**	**343.4**	**1**	**8.48 ±0.8**	**134.0**	**1**	**8.56 ±0.1**	**441.3**	**1**	**8.41 ±0.5**	**134.0**	**1**	**8.58 ±0.2**
		517.8	1	8.20 ±0.5	456.4	20	8.21 ±0.1	626.7	1	8.19 ±0.8	485.4	1	8.18 ±0. 3

mbsf: meters below seafloor, G+: media with added glucose and G^-: media without added glucose

8.4.3.4. Suboxic incubation without added glucose

Under suboxic incubation conditions without added glucose, the overall process was mobilization with significant variation ($F=110.3$; $p \leq 0.001$) between the biotic and abiotic set of incubations on the 20 d of incubation (Table 8.1). The mobilization of Mn was abiotic > biotic. Overall the concentration of Mn in the biotic varied between 0.93 to -3.93 $\mu M\ g^{-1}$ (Figure 8.6c). On the other hand, the abiotic mobilization of Mn varied between 1.64 to -4.27 $\mu M\ g^{-1}$ with maximum immobilization on the 39 d and mobilization on the 20 d at 290.6 mbsf and 475.9 mbsf respectively. The rate of Mn mobilization in the abiotic was significant at two depths one at 134 mbsf and the other at 360 mbsf. Comparison of depths showed significantly high Mn value of 0.82 $\mu M\ g^{-1}$ at 134 mbsf and low value of -2.10 $\mu M\ g^{-1}$ at 360 mbsf (Figure 8.6d). In the biotic incubations, Eh showed a shift from lower (184.5 mV) to higher redox potential of 212.9 mV (Figure 8.4g). Whilst in the corresponding abiotic control subtle difference in Eh was observed with a minimum of 176 mV at 517.8 mbsf on the 20 d of incubation (Figure 8.4h). While, the pH change in the biotic and abiotic incubations was marginal it mainly varied between 8.19 to 8.41 in the biotic (Figure 8.5g) and 8.18 to 8.58 in the abiotic (Figure 8.5h) during the incubation period.

Results of the present study with subsurface sediments show microbial participation in Mn cycling. Under oxic and suboxic incubation conditions biotic processes dominated over abiotic in the presence of added glucose. This has been evinced by the significant variation between the biotic and abiotic incubations by two way ANOVA ($p \leq 0.001$). While in the absence of added glucose, biotic process was higher than abiotic only under oxic conditions. Whereas, under suboxic conditions the abiotic rates for Mn was significantly greater ($p \leq 0.001$) than that of the biotic rates (Figure 8.7). Under oxic condition, the lower immobilization of Mn with the biotic in the absence of added glucose was not because of lesser bacterial activity but rather because of their switch over from immobilization to mobilization. This has been evidenced by the high level of soluble Mn in the biotic incubation without added glucose (Table 8.2). It thus shows that immobilization of Mn occurs under oxic conditions (Figure 8.3) as opposed to its release under suboxic conditions (Figure 8.6). Eh, a measure of the equilibrium potential remained within the range of 151 to 236 mV (Figure 8.4). Major variation in Eh was observed only in the presence of added glucose on the 32 d of incubation under both oxic and suboxic incubations. When Eh had a propensity to increase in the biotic it

tends to decrease in the abiotic incubations. On the other hand, definite trend in pH was not apparent in the biotic or in the abiotic media (Figure 8.5). It varied from 8.18 to 8.58 between depths.

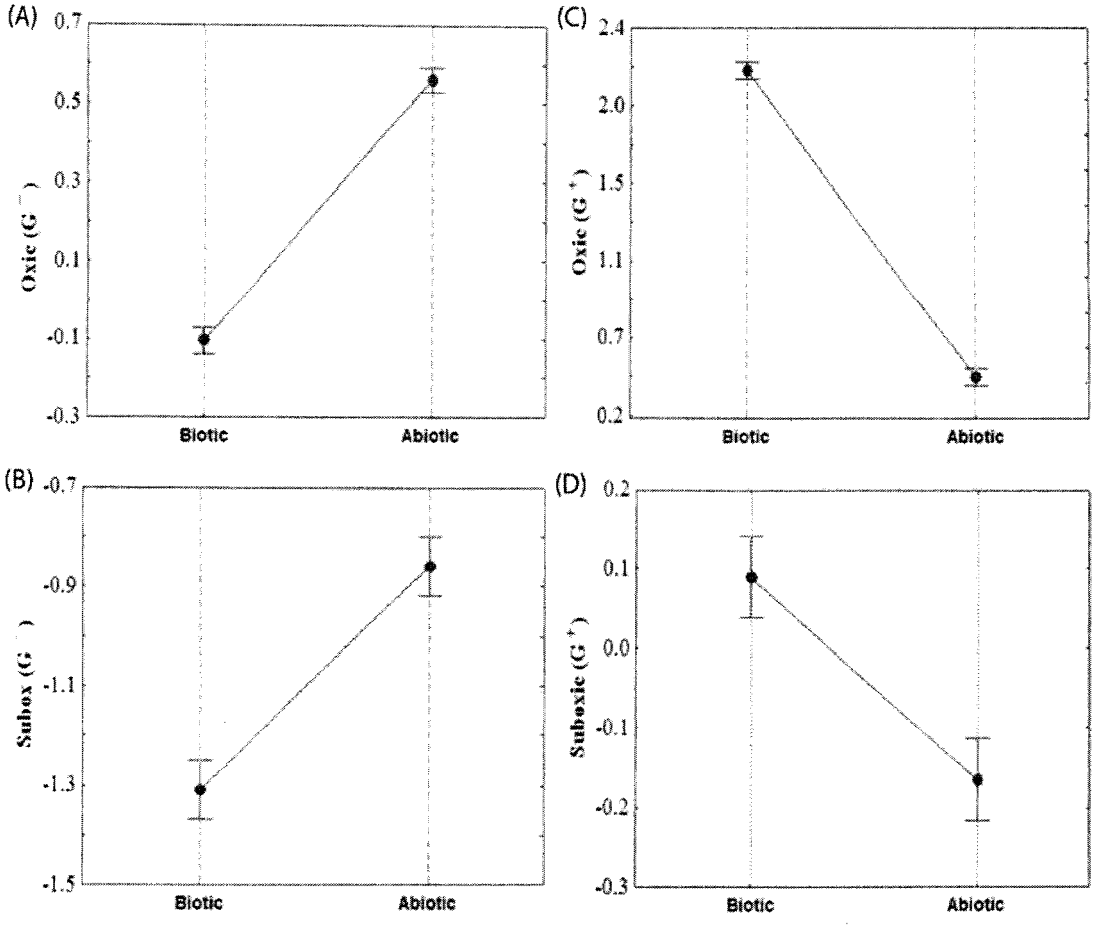

Figure 8.7. Plots show the significant difference ($p \leq 0.001$) in the biotic versus abiotic cycling of Mn in subsurface sediments of the Andaman Sea under oxic versus suboxic incubation conditions in the presence (G^+) and absence (G^-) of added glucose (0.001%). The corresponding symbol with vertical bar under each category indicates the least squares means and the standard error at 0.95 confidence intervals.

8.5. Discussion

The oxidation of organic carbon to CO_2 is balanced overall by the concomitant reduction of the inorganic electron acceptors like O_2, NO_3^-, oxides of Mn and Fe, and SO_4^{2-} (Thamdrup and Canfield, 1996). However, due to spatial heterogeneity of dynamic sediments (Davison *et al.*, 1997; Harper *et al.*, 1999) and depending on the

accessibility of electron acceptors (Beal *et al.*, 2009) the vertical separation is not very stringent and several processes may occur at the same depth in different patches. In reducing sediments like the subsurface sediments of the Andaman sections release of Mn(II) generally will occur when the oxidation rate of Mn is slower than that of its reduction rate (Yadav, 1996). In the present study, the mobilization of Mn from sediments was prominent at 360.5 mbsf irrespective of the incubation conditions and it appropriately coincided with the peak for CH_4 and maximum number of methanogenic bacteria. The reduction of MnO_2 by acetate-utilizing manganese reducers is coupled to the utilization of acetate (Vandieken *et al.*, 2012). Here, the mobilization of Mn could be related to methanogenesis because acetate utilization and CH_4 production could be tightly regulated by the cycling of Mn. This is mainly because the fermentation of glucose to acetate under anaerobic conditions could support the growth of methanogenic bacterial populations and acetate-utilizing manganese reducers. Besides, acetate is known to serve as a suitable substrate for methanogenesis accounting for ~70% of the biogenic methane (Mah *et al.*, 1977; Winter, 1980). Therefore, the possibility of both Mn-reducing microorganisms and methanogenic bacteria using common substrates is seen in these sediments thus modulating the CH_4 production rates.

On the other hand, addition of glucose as a model compound stimulated the oxidation of Mn suggesting that metabolic functions of subsurface microbial communities are regulated by organic carbon. The need for carbon in the microorganisms dwelling in the subsurface sediments may be met through methanogenesis as it contributes in the final reaction steps of the organic matter mineralization process (Megonical *et al.*, 2004). Further, the present results agrees with the study of Hallberg and Martinell (1976) that more of Mn oxidation by bacteria occurs with respect to the availability of organic carbon that supports their growth and reproduction. The useful energy derived from Mn oxidation may be used by the microorganisms in the deep subsurface for organic carbon assimilation. Such an acceleration of Mn oxidation in the presence of organic carbon gives the mixotrophs a selective advantage over other organisms that cannot oxidize Mn (Ehrlich, 1975). During a similar process Mn may be utilized concurrently with glucose or else upon the utilization of glucose. Related effect was also reported to occur with Fe oxidation in the presence of glucose and acetate (Ehrenreich and Widdel, 1994).

Further it was noticed that the rate of Mn oxidation was more under oxic condition than under suboxic condition in the presence of added glucose. This suggests that Mn oxidation reactions require molecular oxygen and so any organisms that produce oxygen might conceivably enhance the rate of Mn oxidation. This could be derived from the association between manganese oxidizers and *Methoxymirabilis oxyfera* like organisms which could make their own oxygen to fuel AOM without the aid of a metabolic partner in the subsurface sediments (Ettwig *et al.,* 2010). Consequently, the oxidation of Mn(II) by Mn oxidizing bacteria creates conducive environment for methanogenesis by consuming oxygen and making the condition more anaerobic. Also the oxidation of Mn under suboxic conditions could be either because of the higher availability of soluble Mn under sub-oxic conditions which are prevalent in hemipelagic sediments on the shelf, slope and rise of continental margins (Froelich *et al.,* 1979; Emerson *et al.,* 1980) or else owing to the fewer requirements for oxygen in certain group of organisms. Also, it has been speculated that elevated CH_4 and ammonium in plumes stimulate Mn(II) oxidation rates (Ishibashi *et al.,* 1997). The present results corroborate with the studies of Schippers *et al.* (2005) and Clement *et al.* (2009) which shows that microbial Mn(II) oxidation is oxygen-dependent at sub-micromolar levels in the sub-oxic zones of the Black Sea. Further, Tebo and Emerson (1985) stated that bacterial Mn oxidation under similar conditions could also be related to relatively high concentrations of Mn(II).

In the present study, immobilization of Mn also occurred in the abiotic controls by passive process. The passive immobilization of Mn in the presence of inhibitor sodium azide has been previously found to occur with deep-sea sediments (Sujith *et al.,* 2011). The immobilization of Mn in sediments could also be followed by its release in the presence of suitable reducing agents like H_2S, Fe(II) and humic substances which are common in the reducing slope and shelf sediments (Thamdrup, 2000). Moreover, bacterial Mn oxide reduction thought to occur mostly by enzymatic process may in situation be triumph over by non-enzymatic reduction of MnO_2 in reducing environments. During CH_4 oxidation sulphate is reduced to H_2S by the sulphate reducing bacteria wherein the H_2S produced being a potent chemical reductant of MnO_2 contribute to the solubilization of MnO_2 to Mn(II) (Burdige and Nealson, 1986). Indirectly, the microbial participation in such processes could also modify the

microenvironments suitable for abiotic adsorption/dissolution reactions. This has been observed by Gachter and Meyer (1993) wherein microbial mobilization and fixation of phosphorous was accelerated by the transfer of electron from donors to acceptors, thus providing the necessary conditions for redox and pH dependant abiotic cycling of phosphorous in sediments. Therefore, Mn that undergoes oxidation under oxic conditions may get mobilized through microbial respiration and abiotic reduction in the subsurface sediments under anaerobic conditions. The cycling of Mn could also occur by the oxidation of CH_4 by the methanotrophs during which MnO_2 could serve as the terminal electron acceptor. Such an oxidation of CH_4 coupled to Mn and Fe reduction has been reported (Beal *et al.,* 2009). Compared to iron, Mn is faster to reduce, harder to oxidize and occurs at a higher level in the oxygen gradient. Because of these reasons Mn also undergoes complete reduction within suboxic regions. This was very well evident in the abiotic control where the adsorption of Mn was followed by a drop in Eh (150mV) and it occurred on the same time period when the increase in Eh occurred with biotic incubations. This could additionally be stimulated by AOM as it contributes to the slow reductive dissolution of buried Fe/Mn layers in the sediments (Och *et al.,* 2012). Such an effect was observed in the present study wherein under suboxic conditions the mobilization of Mn was greater than the immobilization of Mn. Besides, the soluble Mn concentration in the porewater showed large variation with alternate high and low values between depths. The present results agree with the reported values for Mn^{2+} in porewater from the Pacific Ocean (D'Hondt *et al.,* 2003). However, I am unaware of any reports on Mn^{2+} concentrations beyond 450 mbsf in the marine sediments. The high soluble Mn^{2+} concentration in the deeper layers of the sediment in the present study may be ascribed to the carbonate mineral phases in the sediment. Authigenic carbonate mineral phases such as calcite and Mn-carbonate have been shown to act as sink for soluble Mn^{2+} in the subsurface sediments (Yadav, 1996). In the current study the minor increase in pH from 8.18 to 8.58 during the incubation period suggests the dissolution of metal oxides and oxyhydroxides mineral phases in the sediment. It is also well documented that in anoxic marine sediments where sediment accumulation is relatively high, mobilization of Mn occurs (Jones and Murray, 1985).

Moderately reduced sediments exhibit Eh variation between +100 and +400 mV (Jugsujinda *et al.,* 1996). Comparable variation in Eh between +151 to +236 mV was observed in the present experimental study following the biotic-abiotic cycling of Mn

by the subsurface sediment microbial communities. The immobilization of Mn in the presence of added glucose was accompanied by a discernable change in Eh and it increased on the 32 d of incubation. Since, increase in redox potentials could be associated with specific oxidation-reduction process (Black *et al.*, 2008) the shift in Eh value close to +220 mV could suggest the absolute utilization of nitrate (NO_3^-) ions in the oxidation of Mn by the sediment microbial communities. Our results agree with the typical Eh value reported (+220 mV) at which NO_3^- gets completely utilized. It corroborates with the results of Vandenabeele *et al.* (1995) on the higher rate of Mn removal by the microbial consortia in the presence of NO_3^- and Shaw *et al.* (1990) on the oxidation of Mn by NO_3^- in the southern California Borderland sediments. However, beyond the fifth week of incubation the Eh values decreased to +200mV which are suggestive of the appearance of manganous ions or that the oxides of Mn in sediments are moderately reduced. The present results agree with the report of DeLaune and Reddy (2005) that redox potential (Eh) increases with increasing activity of the oxidized component and decreases with increasing activity of the reduced component. This could most probably occur where biological process is very active as the microbial uptake of an element is always compensated by its release. Since, the redox transformation of Mn is most often microbially driven it could affect nutrient availability for greenhouse-gas emissions, net primary production and other ecosystem dynamics (Burgin *et al.*, 2011). The results therefore suggest that the accelerated methane production in the subsurface sediments could be attributed to the degradation of organic carbon under reducing conditions of the shelf sediments and the interplay between bound and soluble Mn species that could work as microbial electron shuttles.

8.6. References

APHA, AWWA, WEF. 2005. Oxidation-Reduction Potential (ORP). In: Standard methods for the examination of water and wastewater. Eaton AD, Clesceri LS, Rice EW, Greenberg AE (eds), Washington, DC, pp. 2-75 to 2-79.

Beal EJ, House CH, Orphan VJ. 2009. Manganese- and Iron-Dependent Marine Methane Oxidation. Science 325: 184-187.

Bidle KA, Kastner M, Bartlett DH. 1999. A phylogenetic analysis of microbial communities associated with methane hydrate containing marine fluids and

sediments in the Cascadia margin (ODP site 892B). FEMS Microbiol Lett 177: 101-108.

Black FJ, Gallon C, Flegal AR. 2008. Ecological Processes: Sediment Retention and Release, In: Encyclopedia of Ecology. Jorgensen SE (ed) Elsevier Press, pp. 3172-3181.

Briggs BR, Inagaki F, Morono Y, Futagami T, Huguet C, Rosell-Mele A, Lorenson TD, Colwell FS. 2012. Bacterial dominance in subseafloor sediments characterized by methane hydrates. FEMS Microbiol Ecol 81: 88-98.

Burdige DJ, Nealson KH. 1986. Chemical and microbiological studies of sulphide mediated manganese reduction. Geomicrobiol J 4: 361-387.

Burgin AJ, Yang WH, Hamilton SK, Silver WL. 2011. Beyond carbon and nitrogen: how the microbial energy economy couples elemental cycles in diverse ecosystems. Front Ecol Environ 9: 44-52.

Calvert SE, Pedersen TF. 1996. Sedimentary geochemistry of manganese: Implications for the environment of formation of manganiferous black shales. Econ Geol 91: 36-47.

Chin CS, Johnson KS, Coale KH. 1992. Spectrophotometric determination of dissolved manganese in natural waters with 1-(2-pyridylazo)-2-naphthol: application to analysis in situ in hydrothermal plumes. Mar Chem 37: 65-82.

Clement BG, Luther GW III, Tebo BM. 2009. Rapid, oxygen-dependent microbial Mn(II) oxidation kinetics at sub-micromolar oxygen concentrations in the Black Sea suboxic zone. Geochim Cosmochim Acta 73: 1878-1889.

Collett T, Riedel M, Cochran J, Boswell R, Presley J, Kumar P, Sathe A, Sethi A, Lall M, Sibal V, the NGHP Expedition 01 Scientists. 2007. Site NGHP-01-17. National Gas Hydrate Program Expedition 01 Initial Reports. pp. 1-135.

Colombini MP, Fuoco R. 1983. Determination of manganese at ng/ml levels in natural waters by differential pulse polarography. Talanta 30: 901-905.

D'Hondt SL, Jørgensen BB, Miller DJ et al., 2003. Proceedings of the Ocean Drilling Program, Initial Reports 201: 1-96.

Davison W, Fones GR, Grime GW. 1997. Dissolved metals in surface sediment and a microbial mat at 100-mu m resolution. Nature 387: 885-888.

DeLaune RD, Reddy KR. 2005. Redox potential. In: Encyclopedia of soils in the environment. Hillel D (ed) Elsevier Ltd, pp. 366-371.

Ehrenreich A, Widdel F. 1994. Anaerobic oxidation of ferrous iron by purple bacteria, a new type of phototrophic metabolism. Appl Environ Microbiol 60: 4517-4526.

Ehrlich HL. 1975. The formation of ores in the sedimentary environment of the deep sea with microbial participation: The case for ferromanganese concretions. Soil Sci 119: 36-41.

Emerson S, Jahnke R, Bender M, Froelich P, Klinkhammer G, Bowser C, Setlock G. 1980. Early diagenesis in sediments from the eastern equatorial Pacific, I. Pore water nutrient and carbonate results. Earth Planet Sci Lett 49: 57-80.

Ettwig KF, Butler MK, Le Paslier D, Pelletier E, Mangenot S, Kuypers MMM, Schreiber F, Dutilh BE, Zedelius J, de Beer D, Gloerich J, Wessels HJCT, van Alen T, Luesken F, Wu ML, van de Pas-Schoonen KT, Op den Camp HJM, Janssen-Megens EM, Francoijs K-J, Stunnenberg H, Weissenbach J, Jetten MSM, Strous M. 2010. Nitrite-driven anaerobic methane oxidation by oxygenic bacteria. Nature 464: 543-548.

Froelich PN, Klinkhammer GP, Bender ML, Luedtke NA, Heath GR, Cullen D, Dauphin P, Hammond D, Hartman B, Maynard V. 1979. Early oxidation of organic matter in pelagic sediments of the eastern equatorial Atlantic: suboxic diagenesis. Geochim Cosmochim Acta 43: 1075-1090.

Gachter R, Meyer JS. 1993. The role of microorganisms in mobilization and fixation of phosphorus in sediments. Hydrobiologia 253: 103-121.

Gadd GM. 2009. Heavy Metal Pollutants: Environmental and Biotechnological Aspects. In: Encyclopedia of Microbiology. Schaechter M (ed.) Elsevier Inc., pp. 321-334.

Hallberg RO. Martinell R. 1976. Vyredox- In situ purification of ground water. Ground Water 14: 88-93.

Haroon MF, Hu S, Shi Y, Imelfort M, Keller J, Hugenholtz P, Yuan Z, Tyson GW. 2013. Anaerobic oxidation of methane coupled to nitrate reduction in a novel archaeal lineage. Nature 500: 567-570.

Harper MP, Davison W, Tych W. 1999. One dimenional view of three dimensional sediments. Environ Sci Technol 33: 2611-2616.

Ishibashi J, Wakita H, Okamura K, Nakayama E, Feely RA, Lebon GT, Baker ET, Marumo K. 1997. Hydrothermal methane and manganese variation in the plume over the superfast-spreading southern East Pacific Rise. Geochim Cosmochim Acta 6: 485-500.

Johnson JE, Phillips SC, Miranda E, Giosan L, Rose K. 2009. Long-term variability of carbon and nitrogen in the Bay of Bengal and Arabian Sea: results from the NGHP Expedition 1. EOS Trans. AGU, 90, Abstract OS44A-01.

Jones CJ, Murray JW. 1985. The geochemistry of manganese in the northeast Pacific Ocean off Washington. Limnol Oceanogr 30: 81-92.

Jorgensen BB. 2006. Bacteria and Marine Biogeochemistry. In: Marine Geochemistry. Schulz HD, Zabel M (eds) Springer-Verlag, Berlin Heidelberg, Germany, pp. 169-200.

Joye SB. 2012. A piece of the methane puzzle. Nature 491: 538-539.

Jugsujinda A, DeLaune RD, Lindau CW, Sulaeman E, Pezeshki SR. 1996. Factors controlling carbon dioxide and methane production in acid sulfate soils. Water Air Soil Pollut 87: 345-355.

Laes A, Blain S, Laan P, Ussher SJ, Achterberg EP, Treguer P, de Baar HJW. 2007. Sources and transport of dissolved iron and manganese along the continental margin of the Bay of Biscay. Biogeosciences 4: 181-194.

Mah RA, Ward DM, Baresi L, Glass TL. 1977. Biogenesis of methane. Ann Rev Microbiol 31: 309-341.

Martin ST. 2005. Precipitation and Dissolution of Iron and Manganese Oxides. In: Environmental catalysis. Grassian VH (ed) Taylor and Francis Group, Boca Raton, FL, pp. 61-81.

McKay JL, Pedersen TF, Mucci A. 2007. Sedimentary redox conditions in continental margin sediments (N.E. Pacific)-Influence on the accumulation of redox-sensitive trace metals. Chem Geol 238: 180-196.

Megonical JP, Hines ME, Visscher PT. 2004. Anaerobic metabolism: linkages to trace gases and aerobic processes. In: Treatise on Geochemistry. Schlesinger WH, Holland HD, Turekian KK (eds), Elsevier, pp. 317-424.

Nealson KH. 1985. Possible roles of manganese redox chemistry in the sulfur cycle. NASA Technical Documents, p. 69.

Och LM, Müller B, Voegelin A, Ulrich A, Göttlicher J, Steiniger R, Mangold S, Vologina EG, Sturm M. 2012. New insights into the formation and burial of Fe/Mn accumulations in Lake Baikal sediments. Chem Geol 330-331: 244-259.

Orphan VJ, Hinrichs K-U, Ussler III W, Paull CK, Taylor LT, Sylva SP, Hayes JM, Delong EF. 2001. Comparative analysis of methane-oxidizing archaea and sulfate-

reducing bacteria in anoxic marine sediments. Appl Environ Microbiol 67: 1922-1934.

Parkes RJ, Sass H, Webster G, Watkins AJ, Weightman AJ, O'Sullivan LA, Cragg BA. 2010. Methods for studying methanogens and methanogenesis in marine sediments. In: Handbook of Hydrocarbon and Lipid Microbiology. Timmis KN (ed.) Springer-Verlag Berlin Heidelberg, pp. 3799-3826.

Ramaswamy V, Gaye B, Shirodkar PV, Rao PS, Chivas AR, Wheeler D, Thwin S. 2008. Distribution and sources of organic carbon, nitrogen and their isotopic signatures in sediments from the Ayeyarwady (Irrawaddy) continental shelf, northern Andaman Sea. Mar Chem 111: 137-150.

Rodolfo KS. 1969. Bathymetry and marine geology of the Andaman Basin, and tectonic implications for Southeast Asia. Geol Soc Am Bull 80: 1203-1230.

Schippers A, Neretin LN, Lavik G, Leipe T, Pollehne F. 2005. Manganese(II) oxidation driven by lateral oxygen intrusions in the western Black Sea. Geochim Cosmochim Acta 69: 2241-2252.

Shaw T, Jahnke R, Gieskes J. 1990. Early diagenesis in differing depositional environments: the response of transition metals in pore water. Geochim Cosmochim Acta 54: 1233-1246.

Sujith PP, Das A, Mourya BS, Loka Bharathi PA. 2011. Immobilization of manganese, cobalt and nickel by deep-sea-sediment microbial communities. Chem Ecol 27: 189-206.

Sunda WG, Kieber DJ. 1994. Oxidation of humic substances by manganese oxides yields low-molecular-weight organic substrates. Nature 367: 62-64.

Tebo BM, Emerson S. 1985. Effect of oxygen tension, Mn(II) concentration, and temperature on the microbially catalyzed Mn(II) oxidation rate in a marine fjord. Appl Environ Microbiol 50: 1268-1273.

Thamdrup B, Canfield DE. 1996. Pathways of carbon oxidation in continental margin sediments off central Chile. Limnol Oceanogr 41: 1629-1650.

Thamdrup B. 2000. Microbial manganese and iron reduction in aquatic sediments. Adv Microb Ecol 16: 41-84.

Vandenabeele J, De Beer D, Germonpre R, Van de Sande R, Verstraete W. 1995. Influence of nitrate on manganese removing microbial consortia from sand filters. Water Res 29: 579-587.

Vandieken V, Pester M, Finke N, Hyun J-H, Friedrich MW, Loy A, Thamdrup B. 2012. Three manganese oxide-rich marine sediments harbor similar communities of acetate-oxidizing manganese-reducing bacteria. ISME J 6: 2078-2090.

Whittenbury R, Phillip KC, Wilkinson JF. 1970. Enrichment, isolation and some properties of methane utilizing bacteria. J Gen Microbiol 61: 205-218.

Winter JU. 1980. Glucose fermentation to methane and CO_2, by defined mixed cultures. Zbl Bakt Hyg I Abt Orig C 1: 293-305.

Yadav DN. 1996. Manganese mobilization from the western continental margin of India. Curr Sci 71: 900-905.

CHAPTER 9

Overview of crust associated bacterial ecology in different ecosystems

9.1. Abundance and distribution of culturable bacteria tolerant to metals in different ecosystems

The present findings show that heavy metal tolerance in bacteria are widespread and are present in most of the metal rich deep-sea habitats. However, the distribution of culturable bacteria showed that the specific niche dictated the dominance of bacteria tolerant to the metals. The culturability of Mn and Co tolerant bacteria was most abundant in ANS, Mn and Ni tolerant bacteria in CIOB sediments and Mn in CR crusts. In the ANS crusts, the most abundant bacteria were Mn tolerant with an average of 1.10 $\times 10^5$ CFU g^{-1} followed by Co tolerant bacteria of 2.75×10^4 CFU g^{-1} (Table 9.1).

Table 9.1. Abundance and distribution of bacteria in samples collected from different geographical locations of the Indian Ocean region. The values are mean ± SD, n=3.

Parameters	ANS	CR	CIOB Nodule	CIOB Sediment
1) Total counts (cells g^{-1})	1.01×10^9	1.31×10^8	3.05×10^8	1.20×10^9
2) Plate counts (CFU g^{-1})				
i) NTB	4.10×10^4	4.10×10^3	7.64×10^2	1.08×10^5
ii) CTB	2.75×10^4	3.33×10^2	3.33×10^2	8.75×10^4
iii) MTB	1.10×10^5	1.88×10^4	1.38×10^2	1.41×10^5
iv) Heterotrophs	3.49×10^5	3.60×10^3	1.18×10^4	1.46×10^5

CTB: cobalt tolerant bacteria, NTB: nickel tolerant bacteria, MTB: manganese tolerant bacteria, ANS: Afanasiy-Nikitin Seamount, CR: Carlsberg Ridge; CIOB: Central Indian Ocean Basin, CFU: colony forming units.

In the CIOB sediments, the Mn tolerant bacteria was the most abundant at 1.41×10^5 CFU g^{-1} followed by Ni tolerant bacteria at1.08×10^5 CFU g^{-1} and Co tolerant bacteria at 8.75×10^4 CFU g^{-1}. Nevertheless, the culturability of metal tolerant bacteria from manganese nodules from the CIOB and crusts from the CR were comparatively lesser than that recovered from the other sites. In the CIOB nodules, Ni tolerant bacteria represented the most dominant at 7.64×10^2 CFU g^{-1} and Mn tolerant bacteria at

1.88×10^4 CFU g^{-1} dominated in the CR (Table 9.1). Thus it is inferred from the above results that the mineralogy like the hydrogenetic nature of the crust and the enrichment of trace metal content govern the distribution of metal tolerant bacteria in the Fe-Mn crusts of the ANS whereas bioavailability of the metals in the sediments and its oxidation state dictate the abundance in the CIOB sediments. The lower abundance of Co and Ni tolerant bacteria in the CR could be due to the hydrothermal nature of the crust where the enrichment of trace metals is generally low.

9.2. Effect of temperature on the in-vitro microbial immobilization/mobilization of rates of metals in different ecosystems

Experiment on the immobilization of metals by microbial communities associated with the Fe-Mn crusts at 28±2°C and at 4±1°C showed the immobilization of Co and Ni. At 4±1°C the immobilization of Co was 5.79 times more than that at 28±2°C in the absence of added glucose. On the other hand, in the presence of added glucose (0.1%) the immobilization of the metal was 4.94 times more at 28±2°C than at 4±1°C. With Ni, the immobilization was 2.95 times more at 4±1°C than at 28±2°C in the absence of added glucose (Table 9.2).

Table 9.2. Effect of temperature on the *in-vitro* microbial immobilization/mobilization rates of metals in different ecosystems.

Location	Experiment details	Cobalt		Nickel	
		4±1°C	**28±2°C**	**4±1°C**	**28±2°C**
ANS	Crust community at 4±1°C and 28±2°C with 0.1% added glucose	97.11	479.75	51.28	19.45
	Crust community at 4±1°C and 28±2°C without added glucose	165.96	28.67	1.89	0.64
CR	Bacterial isolate CR35 at 4±1°C without added glucose	-	-	20.3	120.7
	Bacterial isolate CR48 at 4±1°C without added glucose	-	-	38.53	309.5

Note: The values in table are maximum rates in $\mu M\ g^{-1}$ obtained under the conditions specified.

However, in the presence of glucose it was mobilization and the rate was 2.64 times more at 4±1°C than at 28±2°C. In another set of experiment on the immobilization of Ni by two of the Mn oxidizing bacterial isolates from the CR showed the immobilization of the metal (Table 9.2). The immobilization of Ni by bacterial isolate CR35 was 5.95 times more at 28±2°C than at 4±1°C. With CR48 isolate the immobilization of Ni was 8.03 times more at 28±2°C than at 4±1°C. The results suggest that bacteria immobilizes metals better at 4±1°C with crust associated bacterial communities and at 28±2°C with Mn oxidizing bacterial isolates of the CR ecosystem.

9.3. Effect of incubation condition oxic vs suboxic on the in-vitro microbial immobilization/mobilization rates of metals in different ecosystems

The immobilization of metals like Mn, Co and Ni by sediment associated microbial communities of the CIOB showed greater immobilization under sub-oxic than under oxic incubation conditions. The microbial immobilization of Mn was 2.49 times more under sub-oxic than under oxic conditions with BC26 and 1.47 times more under oxic than under sub-oxic conditions with BC36 (Table 9.3).

Table 9.3. Effect of incubation condition oxic vs suboxic on the *in-vitro* microbial immobilization/mobilization rates of metals in different ecosystems.

Location	Experiment details	Mn ($\mu M\ g^{-1}$)		Co ($\mu M\ g^{-1}$)		Ni ($\mu M\ g^{-1}$)	
		Oxic	Suboxic	Oxic	Suboxic	Oxic	Suboxic
CIOB	Sediment community at 4±1°C in BC26	34.4	85.6	35.0	46.3	6.3	6.0
CIOB	Sediment community at 4±1°C in BC36	19.76	13.44	45.0	27.5	7.03	6.6
Andaman	Sediment community at 4±1°C with 0.1% added glucose	4.66	2.95	-	-	-	-
Andaman	Sediment community at 4±1°C without added glucose	-2.80	-3.93	-	-	-	-

Note: The values in table are maximum rates obtained under conditions specified. Values in positive indicate immobilization and negative mobilization.

Likewise, the immobilization of Co was 1.32 times more under sub-oxic than under oxic conditions at BC26 and 1.64 times under oxic than under sub-oxic conditions at BC36. With Ni, the immobilization of the metal was 1.05 times more under oxic conditions at BC26 and 1.06 times more under oxic conditions at BC36. In another study with continental shelf sediments from the Andaman Sea, the microbial immobilization of Mn was 1.58 times more under oxic conditions than under suboxic conditions in the presence of added glucose (Table 9.3). However, in the absence of added glucose the net process was mobilization. The process was 1.4 times more under sub-oxic than under oxic conditions in the absence of added glucose. This could be mainly because under sub-oxic conditions the concentration of soluble metal available for bacterial participation in metal immobilization is more than that present under oxic conditions. This was very well observed in experiments conducted with deep-sea sediments and continental shelf sediments of the Andaman Sea.

9.4. Effect of glucose addition on the in vitro microbial immobilization/ mobilization of metals in different ecosystems

In vitro experiments conducted in the absence and in the presence of 0.001, 0.01 and 0.1% added glucose concentrations showed bacterial immobilization of metals. Addition of glucose as a model compound for organic carbon mostly stimulated bacterial growth and the subsequent immobilization of the metals. Experiments with Fe-Mn crusts from ANS at 20MPa pressure in the presence and absence of added glucose (0.01%) showed the immobilization of Mn, Co and Ni by the crust associated microbial communities. The immobilization of Co was 2.5 times more in the presence than in the absence of added glucose (Table 9.4). However, the immobilization of Mn and Ni was 1.38 and 1.43 times more in the absence of added glucose respectively. Another set of experiments conducted with Fe-Mn crust from the ANS in the absence and presence of added glucose (0.1%) showed 16.73 times more immobilization of Co in the presence than in the absence of added glucose at 28±2°C. On the other hand, under the same experimental conditions Ni was mobilized. Further studies conducted on the microbial cycling of Mn with continental shelf sediments of the Andaman Sea at 0.001% glucose concentration showed immobilization of 4.66 μM g^{-1} Mn which otherwise promoted mobilization of -2.8 μM g^{-1} Mn in the absence of added glucose. The results indicate the requirement of glucose for microbial growth and the subsequent

immobilization of Mn by the subsurface sediment microbial communities. Besides, studies conducted with deep-sea sediments from the CIOB showed microbial immobilization of Mn, Co and Ni. The immobilization of Mn was 6.37 and Co 1.68 times more in an organically richer core BC26 compared to organically poorer core BC36. The immobilization of Ni was however 1.12 times more in organically poorer core BC36 compared to that of BC26 (Table 9.4). Thus the above results suggest that organic carbon glucose enhances the immobilization of Mn and Co depending upon the nutritional status and soluble concentrations of the metals. However, mostly being a nutritive type element, the microbial immobilization of Ni was unaffected by the addition of glucose and differed from the other two elements which are considered to be of scavenged type.

Table 9.4. Effect of glucose addition on the *in vitro* microbial immobilization/ mobilization of metals in different ecosystems.

Location	Experiment details	Metals	Glucose concentration added			
			Nil	0.001%	0.01%	0.1%
ANS	Crust community at 4±1°C & 20MPa pressure	Mn	15.84	-	11.47	-
		Co	0.014	-	0.034	-
		Ni	0.073	-	0.051	-
ANS	Crust community at 4±1°C and 28±2°C	Co	165.96	-	-	479.75
		Ni	1.89	-	-	-51.28
CIOB	Sediment community at 4±1°C in BC26	Mn	85.6	-	-	-
		Co	46.3	-	-	-
		Ni	6.3	-	-	-
CIOB	Sediment community at 4±1°C in BC36	Mn	19.76	-	-	-
		Co	45	-	-	-
		Ni	7.03	-	-	-
Andaman	Sediment community at 4±1°C	Mn	-2.8	4.66	-	-

Note: The values in table are maximum rates in $\mu M\ g^{-1}$ obtained under conditions specified. Values in positive indicate immobilization and negative mobilization.

CHAPTER 10

Summary, conclusions and future scope

The Afansiy-Nikitin seamount (ANS) in the northern part of the Central Indian Ocean represents one of the potential sites for cobalt enriched ferromanganese (Fe-Mn) crusts. These crusts of hydrogenetic origin on the ANS are enriched with trace metals like Co, Ni and Mn and rare earth elements like Pt, Te and Au that are strategically important and host a great diversity of microbial life. This portion of the biogeosphere, however, remains largely unexplored. Hence, the present study aims to delineate the ecology of metal-microbe interactions in Fe-Mn crusts of the ANS. The objectives were therefore 1) to elucidate the distribution of Co and Ni tolerant bacteria in unique marine ecosystems 2) to delineate the phylogeny of culturable and non-culturable bacterial community and 3) to provide experimental evidence for the immobilization and mobilization of metal ions by bacterial communities/isolates from different marine environments. To meet these objectives the present study utilized geochemical, microscopic and molecular biological tools to gain a better understanding of the geomicrobial processes contributing to metal accretion/dissolution in Fe-Mn minerals.

This study of the seamount crust associated bacteria and their interactions with their environment gives an ecological perspective that grades the different drivers governing these geomicrobial processes. Further, the study also compares and contrasts the culturability and function of metal tolerant bacteria from metal enriched Carlsberg Ridge (CR) and the polymetalic nodule hosting Central Indian Ocean Basin (CIOB) and cobalt crust of ANS. Besides, laboratory experiments were conducted under simulated deep-sea temperature and/or pressure conditions in microcosm with intrinsic communities and/or with bacterial isolates for complementing field observations.

- The abundance and distribution of culturable bacteria tolerant to Mn, Co and Ni from different ecosystems indicated that the specific niche dictated the dominance of bacteria tolerant to metals. Maximum number of Mn and Ni tolerant forms was retrieved from CIOB, Mn from CR and Co from ANS. The Mn tolerant bacteria were most abundant at 1.41×10^5 CFU g^{-1} in the CIOB sediments and at 1.10×10^5

CFU g^{-1} in the ANS crusts. Co tolerant bacteria were maximum at 2.75×10^4 CFU g^{-1} in the ANS crusts and 8.75×10^4 CFU g^{-1} in the CIOB sediments. Ni tolerant bacteria at 1.08×10^5 CFU g^{-1} were the most abundant in the CIOB sediments. However, the culturability of Mn, Co and Ni tolerant bacteria from manganese nodules from CIOB and crusts from CR were comparatively lesser than that recovered from the other sites. These results suggest that the mineralogy of the hydrogenetic crust and the enrichment of trace metal content could govern the distribution of metal tolerant bacteria in the ANS whereas oxidation states of the metal and its bioavailability could dictate their abundance in the CIOB sediments. The low abundance of Co and Ni tolerant bacteria in the CR could be due to the hydrothermal nature of the crust where the enrichment of trace metals is relatively low.

- The expression of multiple enzymes by heavy metal tolerant bacteria against different growth substrates like starch, cellulose, urea, casein, DNA, tributyrin and phenolpthalein phosphate was observed. Hydrolytic enzyme activity showed around 57% of the isolates positive for lipase and 50% for amylase, phosphatase and DNAse. Isolate ANS-17Co was positive for 7/9 different enzymes screened. These results reflect the important ecological role that bacteria could perform in nature to sustain their growth and survival. The production of hydrolytic enzymes by one member of the community may thus feed the growth of others who are dependent on simpler forms of organic carbon like glucose for the immobilization/mobilization of metals in the Fe-Mn mineral rich deep-sea environments.

- Metal tolerance in bacteria is often linked to antibiotics resistance in polluted environments. However, bacterial isolates tested for antibiotics in the present study showed that about 36% of the isolates were resistant to ampicillin followed by 32% of them for lincomycin, penicillin and vancomycin. Resistance to 6/19 different antibiotics tested were observed with seamount based microflora ANS-04Ni and ANS-05Co. These results suggest that antibiotic resistance in heavy metal tolerant bacteria are not only prevalent in the polluted sites but are also common among bacteria of relatively pristine environments like the deep-sea.

- It is usual that environment dictates the diversity of bacteria. The 16S rDNA identification of culturable bacteria from ANS tolerant to heavy metals fell into three major phyla: *Proteobacteria* (46.66%), *Actinobacteria* (26.67%) and *Firmicutes* (26.67%). The phylum *Proteobacteria* was represented by α and γ-*Proteobacteria* with latter as the major subclass. The four major genera observed were *Bacillus*, *Halomonas*, *Paracoccus* and *Salinicola*. Pyrosequencing of non-culturable bacteria showed 30 different phyla inhabiting the hydrogenetic Fe-Mn crusts of the ANS. Among them *Proteobacteria, Actinobacteria, Bacteroidetes* and *Firmicutes* represented the four dominant phyla. The *Proteobacteria* belonging to Fe, Mn and S oxidizing bacterial groups constituted 83% of the total non-culturable fraction with γ-*Proteobacteria* as the major subclass followed by α-*Proteobacteria*. The four major genera observed were *Halomonas*, *Thiomicrospira, Idiomarina and Methylophaga*. The results suggest that ambient nutrient levels trigger the growth of α- and γ-*Proteobacterial* community in the ANS and facilitate the related processes like Fe, Mn and S oxidation to occur.

- The bacteria express low molecular weight proteins called metallothioneins to control cellular metal ion homeostasis. Screening of 30 isolates showed 30% of Mn binding proteins to be localized in the periplasmic fraction, 16.7% in the membrane fraction, 26.7% in the periplasmic-cytoplasmic fraction, 20% in the periplasmic-membrane fraction and 3.3% in the periplasmic-cytoplasmic-membrane fraction. Concentration measurements of proteins also showed the up-regulation of periplasmic proteins in 83.3% of the isolates and down-regulation of the cytoplasmic and membrane proteins in 66.7 and 50% of the isolates respectively. The molecular weight of the Mn binding proteins varied from 31 to 52 KDa. With exposure to a single metal many proteins were expressed with some proteins being expressed at higher concentration. In the presence of multiple metals fewer proteins were expressed, some in lesser concentration suggesting "tradeoff".

- The *in vitro* metal immobilizing activities of Fe-Mn crust associated microbial communities in microcosm under ambient conditions of temperature (4±2°C) and hydrostatic pressure (20MPa) showed statistically significant difference between

the biotic and abiotic sets of incubations at $p< 0.001$. The immobilization of Fe (9.34 mg g^{-1}) and Co (2 μg g^{-1}) was greater in the presence of 0.01% glucose and Mn (0.87 mg g^{-1}) and Ni (4.3 μg g^{-1}) in the absence of added glucose. Thus, it is inferred that the activity of the bacterial community of the Fe-Mn crusts contributes to its accretion with different bacterial groups mediating different degrees of metal immobilization during periods of oligotrophy and when the organic rains from water column above is minimal. The sequence of immobilization Fe > Mn> Ni > Co suggests the gradation in electronegative sites available for the adsorption of the soluble metal ions at the mineral/bacterial surfaces.

- *In vitro* experiment with bacterial isolates and EDTA as a chelating agent of metal ions, suggest that the mobilization of Co was promoted and the immobilization of Ni was stimulated from the Fe-Mn crusts of the ANS. The mobilization of Co by EDTA was maximum at 24.9 μg g^{-1} and immobilization of Ni at 12.2 μg g^{-1} in the absence of added glucose. However, in the presence of bacterial isolate ANS-05Co, the EDTA assisted immobilization of Co was more than that by EDTA alone suggesting the active participation of bacteria in the immobilization of Co. The immobilization of the metal was maximum at 4.5 μg g^{-1} with the same isolate in the absence of added glucose. On the other hand, the immobilization of Ni by bacteria was lesser than that by EDTA alone. The result suggests that metal chelation by EDTA decreases the toxicity of Co to bacteria and also toxicity exerted by EDTA on bacteria. Though Ni is closely related to Co in its chemical and biochemical properties they differed in their affinity for EDTA and consequently to the interactions with bacteria in the Fe-Mn crust.

- *In vitro* experiment with ascorbate an organic reductant of metal oxides promoted the mobilization of Co and Ni from the hydrogenetic Fe-Mn crusts of the ANS. The chemical mobilization of Co by ascorbate was maximum at 2.11 μg g^{-1} in the absence of glucose and Ni at 4.03 μg g^{-1} in the presence 0.1% of added glucose. On the other hand, in the presence of bacterial isolate ANS-05Co, the mobilization of Co by ascorbate increased considerably during the 50d incubation and was 3.2 times more in the absence than in the presence of added glucose. The results suggest the participation of bacteria in the mobilization of Co. However, the

bacteria assisted mobilization of Ni was less in the presence of ascorbate suggesting immobilization. The immobilization of Ni was maximum of 1.72 μg g^{-1} with isolate ANS-28Ni in the absence of added glucose. The above results indicate that bacteria are effective modulators of the environment where they successfully compete with reducing agents like ascorbate in balancing the level of metal concentrations which otherwise could be toxic to sensitive organisms living in the surrounding environment. The difference in the bacteria assisted cycling of Co and Ni by ascorbate could be attributed to the difference in their association with the Fe-Mn oxide phase of the crust, where the former is usually bound in the +III oxidation state compared to that of the latter in the +II oxidation state.

- *In vitro* metal immobilizing activities of Fe-Mn crust associated microbial communities in microcosm at 1atm pressure and temperatures of 4±1° C and 28±2°C indicated that bacteria participate in the immobilization of Co and Ni. The immobilization of Co in the absence of added glucose was 165.96 μg g^{-1} at 4±1°C and 28.67 μg g^{-1} at 28±2°C. On the other hand, the immobilization of Co in the presence (0.1%) of added glucose was 97.11 μg g^{-1} at 4±1°C and 479.75 μg g^{-1} at 28±2°C. With Ni, however, immobilization was observed only in the absence of added glucose whereas it was mobilization in the presence of added glucose. The immobilization of 1.89 μg Ni g^{-1} and the mobilization of 51.28 μg Ni g^{-1} of crust were greater at 4±1°C than at 28±2°C. Although Ni is closely related to Co in its chemical and biochemical properties the results indicate that the metals differ in their affinity for organic carbon and in their mode of enrichment in the crust as the former is a nutritive type of element and the latter more a scavenged type of element.

- *In vitro* experiment with two Mn oxidizing bacterial isolates CR35 and CR48 from Carlsberg Ridge waters showed immobilization of Ni even in the absence of Mn. The immobilization of the metal by isolate CR35 was 5.95 times and CR48 was 8.03 times more at 28±2°C than at 3±1°C. When challenged with different concentrations of Ni, they responded by an increase in cell size 4.37 × 3.01 μm at 10,000μM Ni and also by forming cell aggregates (ie. reducing the cell surface area). In contrast, the cell size was around 1.16 × 0.96 μm in the control without Ni.

EDS analysis of the bacterial cells showed peaks for Ni with decrease in intensity of the peak for Mg in both the isolates and loss of K in CR35 indicating cation efflux. FTIR spectroscopy of bacteria confirmed the participation of hydroxyl, carbonyl, sulfide and phosphryl groups in Ni binding. XRD analysis showed the precipitation of Ni as NiS and NiP2 by the bacterial isolates. The results confirm that immobilization of Ni by bacteria can be effected even in the absence of Mn and re-examines the accepted paradigm that Mn oxidation govern the fate of other elements in the marine environment. Further, the study also suggests the ability of bacteria to interact with different metals in the natural environment and the strategies they adopt to counter the toxicity of Ni and other related elements when in excess.

- *In vitro* experiment on the immobilization of Mn, Co and Ni by indigenous microbial communities associated with deep-sea sediments from the CIOB region showed the microbial immobilization of Mn, Co and Ni at 4±1°C. The immobilization of Mn and Co under suboxic condition was 2.4 times and 1.3 times greater than under oxic conditions respectively. It was also observed that immobilization of Mn and Co dominate organically richer (0.175 to 0.485%) core BC26 as opposed to organically poorer (0.09 to 0.19%) core BC36. Suboxic conditions are better than oxic conditions for the immobilization of Mn and Co in BC26 and oxic conditions favour over suboxic for the immobilization Co and Ni in BC36. In general, the immobilization of the metals was BC26 > BC36. These results suggest that suboxic and organically rich conditions favor Mn and Co immobilization whereas oxic and organically poor conditions favor Ni immobilization. The greater immobilization of Mn under sub-oxic than under oxic incubation conditions could account for the higher availability of Mn required for bacterial participation under sub-oxic conditions and the lower requirements for oxygen in certain group of organisms within the community. The general trend in immobilization of the metals in BC26 was Mn (85.6 $\mu M\ g^{-1}$) > Co (46.3 $\mu M\ g^{-1}$) > Ni (6 $\mu M\ g^{-1}$). These results suggest the sequence of enrichment of the respective metals in the Fe-Mn crust and nodules and the suitable conditions that favor microbial growth and enrichment of trace metals.

- In order to understand how these elements especially behave closer to the shelf, *in vitro* experiment was carried out with methane hydrate bearing sediments from the Andaman continental shelf. In the presence of glucose, (0.001%) microbial immobilization of Mn was noticed, whereas in the absence of added glucose it was mobilization that was discernible. The immobilization of Mn with added glucose was 1.58 times more under oxic than under suboxic conditions at 4±1°C. The immobilization of Mn showed statistically significant difference between the biotic and abiotic sets of incubations at $p < 0.001$. The results suggest that both active and passive processes contribute to the microbial immobilization of the metals and only passive process contributes in the abiotic process. Since microorganisms are active participants in the cycling of Mn and dictate the direction in which the reactions occur the generation of methane in moderately reducing shelf sediments could also result from the interplay between bound and soluble Mn species that could work as microbial electron shuttles.

- SEM observation of morphological features of the crust showed dense population of spherical and rod-shaped bacteria colonizing the Fe-Mn oxide surfaces in association with extracellular polymeric substances and secondary minerals. EDS composition of these oxides showed peaks for Na, Mg, K, Ca, P, Si and O apart from other major peaks for metals like Fe, Mn, Co and Ni. XRD analysis of the oxides showed poorly crystalline minerals vernadite and todorokite with background peaks for calcite and quartz. Besides, TEM observation of thin cross sections of bacterial cells and subsequent x-ray analysis showed the accumulation of metals as electron dense precipitates mainly at the cell surface and in different cell sectors. Thus, the mineralogy of the natural oxides, its composition and morphological features with resemblance to biogenic mineral precipitates which are generally amorphous and paracrystalline along with TEM and experimental evidence suggest more of biogenic involvement in the accretion process of the crust.

Conclusions

- Results show that accumulation and release of metal ions by bacteria in pulses in the microniches contribute to the immobilization of metals by bacteria at higher rates. Of the different factors, mineralogy of the crust, bioavailable concentration of the metal, relative toxicity of the metal, the availability of metal binding ligands, level of organic carbon and oxygen were found to regulate microbial participation in metal immobilization.

- It has been hitherto believed that hydrogenetic metal accretion is purely driven by chemical processes. However, this study on the ecology of metal-microbe interactions collectively shows that microorganisms intrinsic to the Fe-Mn crust surfaces have a definite role in the hydrogenetic accretion process of the crusts not only by serving as catalysts but also by directly participating in the processes of metal enrichment. It is further stated that environment dictates the dominance of microorganisms involved in the accretion process of the crust and the direction in which the reactions occur.

- Finally to conclude this study is the first to deal with the hydrogenetic mineralization by the Fe-Mn crusts associated bacteria. Though the hydrogenetic processes of metal accretion are slower, the bacterial participation accelerates the trace metal enrichment more when compared to that in hydrothermally formed crust. It furthers the understanding of the competitive nature of nutrient acquisition by heavy metal tolerant bacteria and their important role in biogeochemical processes. Further, the data contributes to the knowledge of bacterial interaction with the metals in the crust and other metal related ecosystems.

Implication

- The study elucidates how environmental variables orchestrate metal microbe interactions. Such understanding would help us in the choice of microbes for varied applications and ecological management.

Applications

- The above study would help in tapping economically important strategic metals from the Fe-Mn crust and allied sources.
- It would also help in harnessing the potential of metal tolerant bacteria in environmental cleanup through detoxification.

Future scope

- It would be relevant to examine metal microbe interactions along redox and organic carbon gradients. Throughput analysis of results from such a study would be able to enlighten when communities or isolates change from net mobilizers to immobilizers and vice versa.

Appendix I

MICROBIOLOGICAL MEDIA AND REAGENTS

Standard nutrient broth

Nutrient broth powder	13g
Agar	15g
Seawater	1000ml
pH	8.0

Trace element solution SL7 (Biebl and Pfennig, 1981)

25% HCl	1ml
$ZnCl_2$	70mg
$MnCl_2.4H_2O$	100mg
H_3BO_3	60mg
$CoCl_2.6H_2O$	200mg
$CuCl_2.2H_2O$	20mg
$NiCl_2.6H_2O$	20mg
$Na_2MoO_4.2H_2O$	40mg
Distilled water	1000ml

Artificial seawater (Kepkay and Nealson, 1987)

NaCl	0.3M
KCl	0.01M
$MgSO_4$	0.05M
$CaCl_2$	0.01M
pH	7.8

Total bacterial counts

Buffered formalin

Formaldehyde (38%)
Hexamine
Saturate formaldehyde with hexamine, filter sterilize and store at room temperature.

Acridine orange stain (0.1%)

Acridine orange	0.1g
Formaldehyde (5%)	100ml

Filter through 0.22μM polycarbonate paper. Store in amber coloured bottle at 4±2°C.

BIOCHEMICAL MEDIA AND REAGENTS

Tributyrin agar medium for lipase

Peptone	5.0g
Yeast extract	3.0g
Tributyrin	10ml
Agar	15g
Seawater	1000ml
pH	7.5

Phenolphthalein diphosphate medium for phosphatase (Gerhardt *et al.*, 1981)

Beef extract	3.0g
Peptone	5.0g
Phenolphthalein diphosphate	0.1g
Agar	15g
Seawater	1000ml
pH	7.0

Christensen urea agar for urease (Gerhardt *et al.*, 1981)

Urea	20.0g
Sodium chloride	5.0g
Potassium dihydrogen phosphate	2.0g
Peptone	1.0g
Glucose	1.0g
Phenol red	0.012g
Seawater	1000ml
pH	7.0

Starch-agar medium for amylase (Bairagi *et al.*, 2002)

Starch	10g
KH2PO4	4.0g
Na2HPO4	4.0g
Tryptone	2.0g
MgSO4.7H2O	0.2g
CaCl2	0.001g
FeSO4.7H2O	0.004g
Agar	15g
Seawater	1000ml
pH	7.5

DNase medium (Gerhardt *et al.*, 1981)

Pancreatic digest of casein	10.0g
Peptic digest of animal tissue	10.0g
L-Arabinose	10.0g
Sodium chloride	5.0g
Deoxyribonucleic acid	2.0g
Methyl green	0.09g
Phenol red	0.05g
Seawater	1000ml

Agar	15g
pH	7.5

Soybean casein agar for caseinase (Gerhardt et al. 1981)

Pancreatic digest of casein	15.0g
Pancreatic digest of soy meal	5.0g
Sodium chloride	5.0g
Seawater	1000ml
pH	7.3

Marine oxidation fermentation medium (Hugh and Leifson 1953)

Peptone	2g
NaCl	5g
K2HPO4	0.3g
Bromothymol blue	0.03g
Dextrose	10g
Agar	7.5g
Seawater	1000ml
pH	7.1

Gram's Stain Reagents

Crystal violet (Hucker's)
Solution A

Crystal violet	2.0g
Ethanol (95%)	20ml

Solution B

Ammonium oxalate	0.8g
Distilled water	80ml

Note: Mix solution A and B

Gram's iodine

Iodine	1g
Potassium iodide	2g
Distilled water	300ml

Decolourizer

Ethanol (100%)	95ml
Distilled water	05ml

Counter stain

Safranin	0.25g
Ethanol (95%)	10ml
Distilled water	100ml

CHEMICAL REAGENTS

Reagents for sediment digestion (Roy *et al.*, 2007)

Solution A

Hydrofluoric acid	70ml
Nitric acid	30ml
Hydrochloric acid	20ml

Solution B

Nitric acid	50ml
Milli Q water	50ml

Preparation of stock solution for metals

Cobalt (II) chloride hexahydrate ($CoCl_2 . 6H_2O$)

Molecular weight: 237.93
Atomic weight of Co: 58.933

Co^{2+} (1mg l^{-1}) prepared by dissolving 4.04 mg of the above salt in ultrapure water and making up the volume to 1 litre with the same water.

Nickel (II) chloride hexahydrate ($NiCl_2.6H_2O$)

Molecular weight: 237.70
Atomic weight of Ni: 58.69

Ni^{2+} (1mg l^{-1}) prepared by dissolving 4.05 mg of the above salt in ultrapure water and making up the volume to 1 litre with the same water.

Manganese (II) chloride tetrahydrate ($MnCl_2.4H_2O$)

Molecular weight: 197.92
Atomic weight of Mn: 54.938

Mn^{2+} (1mg l^{-1}) prepared by dissolving 3.603 mg of the above salt in 0.01M HCl and making up the volume to 1 litre with ultrapure water.

Ammonium iron (II) sulphate hexahydrate ($NH_4FeSO_4.6H_2O$)

Molecular weight: 392.14
Atomic weight of Fe: 55.847

Fe^{2+} (1mg l^{-1}) prepared by dissolving 7.02 mg of the above salt in 0.01M HCl and making up the volume to 1 litre with 0.01M HCl.

Ammonium iron (III) sulphate dodecahydrate ($NH_4FeSO_4.12H_2O$)

Molecular weight: 482.19
Atomic weight of Fe: 55.847

Fe^{3+} (1mg l^{-1}) prepared by dissolving 8.634 mg of the above salt in 0.01M HCl and making up the volume to 1 litre with 0.01M HCl.

GENOMIC REAGENTS

DNA Extraction from sediments (Zhou et al. 1996)

DNA Extraction Buffer (pH 8.0)

Solution I	
Tris HCl	100mM
EDTA	100mM
Sodium phosphate	100mM
Milli Q water	1000ml
Solution II	
Sodium chloride	1.5M
Cetyltrimethylammonium bromide	1%
Solution III	
Proteinase-k	1%

TE Buffer (pH 8.0)

Tris HCl	10mM
EDTA	1mM
pH	8.0

Chloroform Isoamyl alcohol mixture

Chloroform	24ml
Isoamyl alcohol	1ml

DNA extraction from bacterial isolates (Zeng *et al.*, 2008)

Phosphate buffered saline

Sodium chloride	300mM
Potassium chloride	2.7mM
Di-sodium hydrogen phosphate	10mM
Sodium di-hydrogen phosphate	1.7mM
pH	8.0

DNA extraction buffer

0.5M EDTA (pH 8.0)	50ml
5M Sodium chloride	5ml
20% SDS	25ml
1% CTAB	20ml

Phenol Chloroform Isoamyl alcohol mixture (25:24:1)

Phenol	25ml
Chloroform	24ml
Isoamyl alcohol	1ml

Plasmid extraction from bacterial isolates (DeBarro *et al.*, 1995)

Lysing solution

Tris HCl	10mM

EDTA	1mM
Lysozyme (ml)	10mg
Distilled water	1000ml
pH	8.0

Phenol-chloroform (1:1)

Phenol	1ml
Chloroform	1ml

Agarose gel electrophoresis (Palanivelu, 2001)

TAE buffer (50x)

50mM Tris	302.5g
25mM glacial acetic acid	71.4ml
1mM Disodium EDTA	18.6g
Distilled water	1000ml
pH	8.6

Agarose (1%)

1X TAE buffer (pH 8.6)	50ml
Agarose	0.5g

Sample loading dye

Glycerol	0.7ml
50X TAE buffer (pH 8.6)	0.2ml
3% bromophenol blue	0.1ml

Staining solution

Ethidium bromide	0.05mg
1X TAE buffer (pH 8.6)	100ml

PCR amplification of 16S rRNA gene

PCR master mix

dNTP mix	200µM
Primer 27F	0.5µM
Primer 1492R	0.5µM
PCR buffer-B	1X
$MgCl_2$	1.5mM
Taq polymerase	1U
Water	50µl

PROTEOMIC REAGENTS

Extraction of proteins from bacteria

Solution I

Sucrose	0.5M
Disodium EDTA	4mM
Tris HCl	40mM
Distilled water	1000m
pH	8.0

Solution II

Magnesium chloride	1M
Distilled water	1000ml

Solution III

Ammonium acetate	100mM
Acetic acid	100mM
Distilled water	1000ml
pH	6.5

Solution IV

Tris-HCl	0.01M
Distilled water	1000ml
pH	8.0

Sodium dodecyl sulphate polyacrylamide gel electrophoresis

Acrylamide-bisacrylamide solution (30%)

Acrylamide		29.2g
Bis acrylamide		0.80g
Distilled water	to	100ml

Separating gel buffer (4x) (pH 8.8)

Tris		18.15g
Distilled water	to	100ml

Stacking gel buffer (4x) (pH 6.8)

Tris		3.0g
Distilled water	to	50ml

Sodium dodecyl sulphate (10%)

SDS	10g
Distilled water	100ml

Initiator (10%)

Ammonium persulphate	0.1g
Distilled water	1.0ml

Catalyst

TEMED used as such

Separating gel overlaying solution

n-butanol	50ml
Distilled water	50ml

Bromophenol (0.1%)

Bromophenol blue	5mg
Distilled water	5ml

Sample buffer (2x)

0.5M Tris (pH 6.8)	2.5ml
10% SDS	4.0ml
100% Glycerol	2.0ml
β–mercaptoethanol	0.8ml
0.1% Bromophenol blue	300µl
Distilled water (400µl) to	10ml

Tank Buffer (pH 8.3)

Tris	6.05g
Glycine	28.8g
10% SDS	10ml
Distilled water to	1000ml

Preparation of 10% separating gel (10ml)

Distilled water	4.0ml
30% acrylamide: bisacrylamide	3.33ml
4x Tris (pH 8.8)	2.5ml
TEMED	05µl
10% SDS	100µl
10% APS	50µl

Preparation of 4% stacking gel (5ml)

Distilled water	3.0ml
30% acrylamide: bisacrylamide	0.67ml
4x Tris (pH 6.8)	1.25ml
TEMED	2.5µl
10% SDS	25µl
10% APS	50µl

Silver Nitrate Staining of Polyacrylamide Gels

Fixing solution

Ethanol	50ml
Glacial acetic acid	12.25ml
Distilled waterto	125ml

Sensitizing solution

Ethanol	37.5ml
Sodium thiosulphate	5.0ml
Sodium acetate	8.5g
Distilled water	125ml
Glutaraldehyde (before use)	0.625ml

Staining solution

Silver nitrate solution	12.5ml
Distilled waterto	125ml

Developing solution

Sodium carbonate	3.125g
Distilled water	125ml
Formaldehyde (before use)	0.1ml

Stop solution

Disodium EDTA	1.825g
Distilled waterto	125ml

Washing solution

Distilled Water as required

Preserving solution

Ethanol	37.5ml
Glycerol	5.75ml
Distilled waterto	125ml

Metalloprotein Assay Reagents (Hogbom *et al.*, 2005)

Reagent I

Luminol	11mM
Na_2CO_3	500mM
H_2O2	230mM

Reagent II

Urea	8M
Milli Q water	1000ml

Reagent III

4-(2-pyridylazo)resorcinol (PAR)	2mM
Milli Q water	1000ml

Appendix II

Estimation of Mn by spectrophotometric method (Chin *et al.*, 1992)

Borate buffer

Boric acid	0.618g
0.1N NaOH	100ml

1-(2-pyridylazo)-2-naphthol (PAN) Reagent (0.8mM)

PAN	0.05g
Triton X-100	5.0ml
Milli Q water	50.0ml

Note: after dissolving make up the volume to 250ml with distilled water/borate buffer (pH 9.7-10.0)

Desferrioxamine B solution (250 mM)

Desferrioxamine B	500mg
Milli Q water	3.05ml

PAN mixed reagent

250mM Desferrioxamine B solution	400µl
0.8mM PAN Reagent	250ml

Standard curve for manganese using $MnCl_2.4H_2O$ as standard

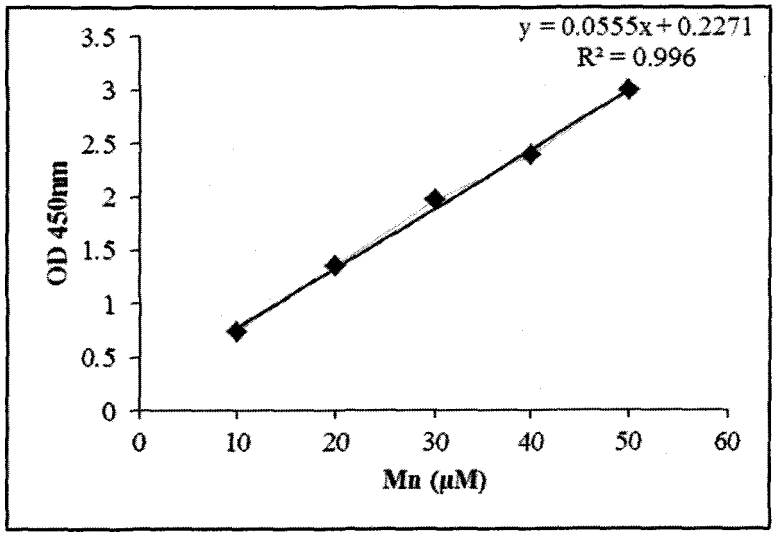

Estimation of Co by spectrophotometric method (Chester and Hughes, 1968)

0.2M Citric acid solution

Citric acid	21g
Distilled water	500ml

nitroso-R-salt solution (0.2%)

nitroso-R-salt	0.2g
Distilled water	100ml

Buffer Reagent

NaOH	10g
Na_2HPO_4	27g
Boric acid	3.0g
Distilled water	250ml

Standard curve for cobalt using $CoCl_2.6H_2O$ as standard

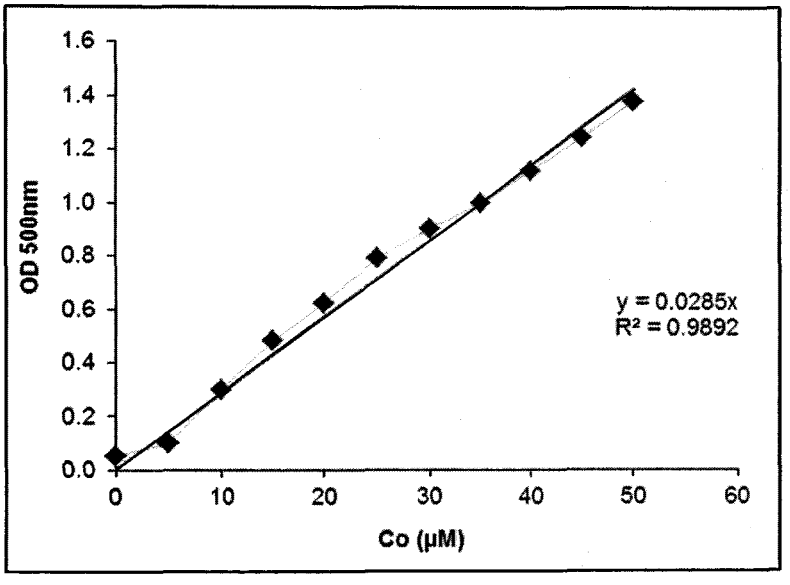

Estimation of Ni by spectrophotometric method (Chester and Hughes, 1968)

Dimethylglyoxime (1%)

Dimethylglyoxime	1g
Ethanol	100ml

Potassium persulphate (2%)

Potassium persulphate	2g
Distilled water	100ml

0.5N Ammonium hydroxide

Mixed reagent

Potassium hydroxide	5.0g
Distilled water	100ml
1% Dimethylglyoxime	25ml

Standard curve for nickel using $NiCl_2.6H_2O$ as standard

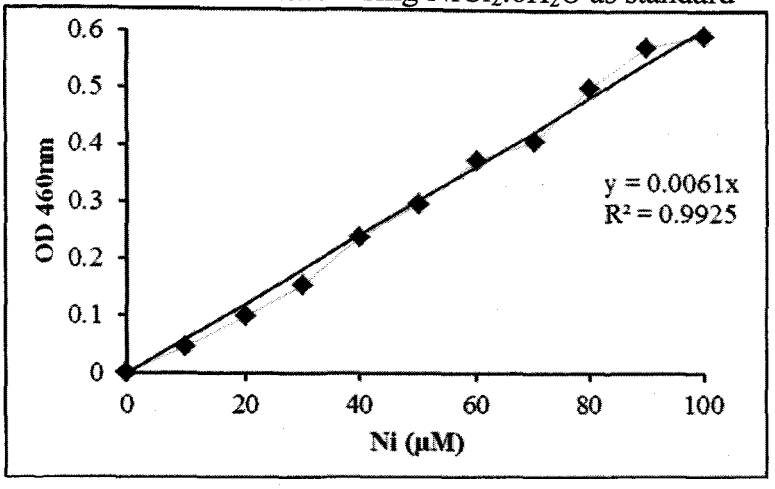

Estimation of formazon

2,3,5-Triphenyltetrazolium chloride (0.5%)

TTC	0.5g
Distilled water	100ml
pH	7.6

Triphenyl Formazon (0.025%)

Triphenyl Formazon	0.025g
Methanol	100ml

Standard curve for formazon using triphenyl formazon as standard

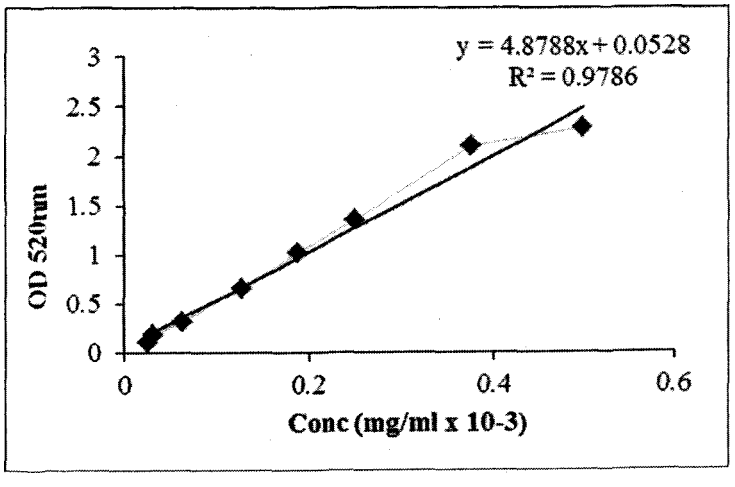

Determination of Mn by differential pulse voltammetry (Colombini and Fuoco, 1983)

Borate buffer solution	
Borax	0.5M
NaOH	0.34M
pH	9.5
Citrate solution	
Citric acid	1M
pH	9.0

Standard curve for manganese using $MnCl_2.4H_2O$ as standard

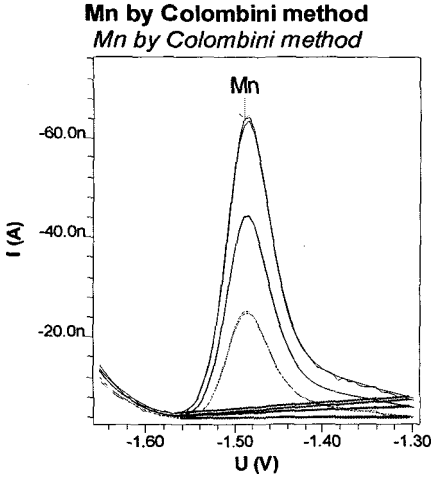

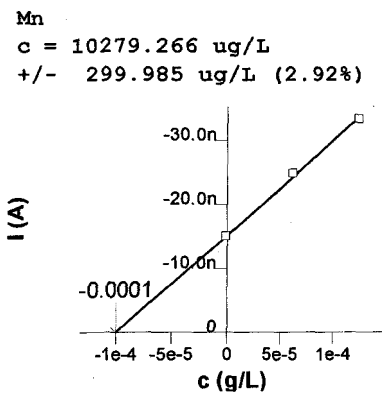

Calculations

Concentration of metal in the original sample is calculated based on the equation

$$C_o = \frac{C_s \times V_s}{V_o} \times \frac{i_o}{(i_s - i_o)}$$

Where:
C_o = concentration of metal in sample, mg/l
C_s = concentration of metal in standard solution, mg/l
i_o = stripping peak height in original sample
i_s = stripping peak height in sample with standard addition
V_o = volume of sample, ml and
V_s = volume of standard solution added, ml

Determination of cobalt and nickel by Differential Pulse Voltammetry (Herrera-Melian et al. 1997)

Ammonia Buffer

NH3	0.2M
NH4Cl	0.1M
pH	9.5

Dimethylglyoxime 0.1M in Ethanol

Standard curve for cobalt using $CoCl_2.6H_2O$ as standard

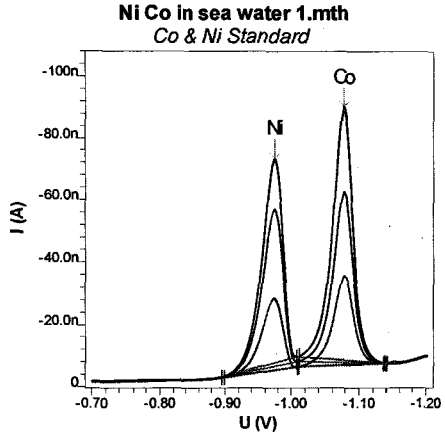

Standard curve for nickel using $NiCl_2.6H_2O$ as standard

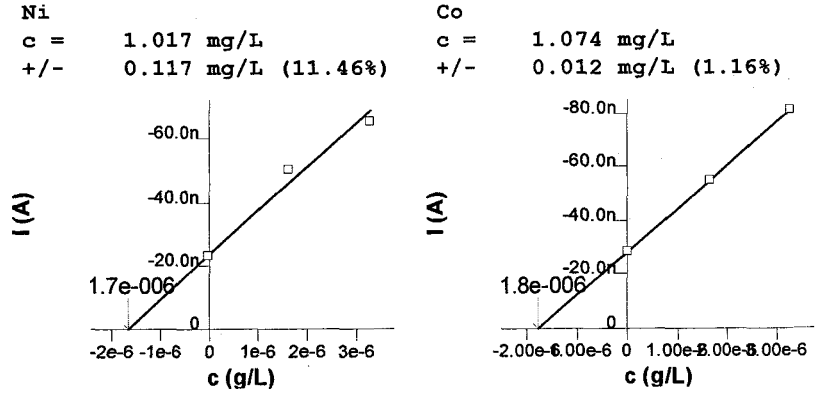

Determination of iron by differential pulse voltammetry (Kennedy,1990)

Tartarate buffer solution

Ammonium Tartarate	0.1M
HEPES	0.1M
pH	7.5

Sodium chloride solution (0.15M)

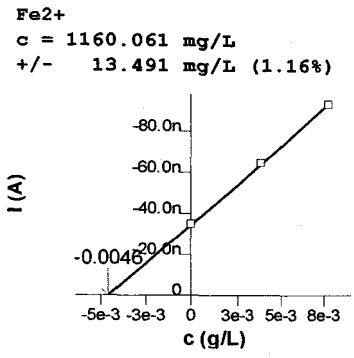

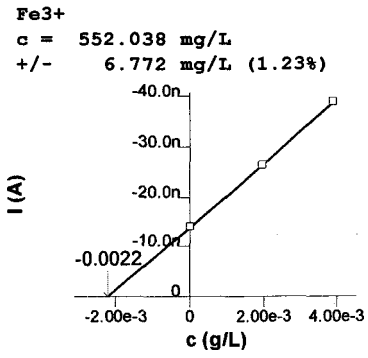

Standard curve for Fe(II) and Fe(III) were generated using ammonium Iron (II) sulphate hexahydrate and ammonium Iron (III) sulphate dodecahydrate as standard

Appendix III

Table 3AT1: Pearson's correlation analysis between culturable bacteria and total bacterial counts for ANS.

	Heterotrophs	**CTB**	**NTB**	**MTB**	**TBC**
Heterotrophs	1				
CTB	0.408	1			
NTB	0.180	0.599*	1		
MTB	-0.100	-0.144	-0.366	1	
TBC	0.202	0.583*	0.329	-0.182	1

Note- CTB: cobalt tolerant bacteria, NTB: nickel tolerant bacteria, MTB: manganese tolerant bacteria and TBC: total bacterial counts. The values that are significant at $p < 0.05$ are indicated by the symbol*

Table 4AT1: ANOVA showing significant variation in environmental parameters between the seamount and a non-seamount site.

	SS	df	MS	F	P	F crit
Seamount vs non-seamount	2.503	1	0.078	2.838	$p < 0.001$	1.504

Note: F-value greater than F-critical value indicate significant difference

LIST OF PUBLICATIONS

(Manuscripts from thesis*)

1. **Sujith PP**, Khedekar VD, Prabhu GA, Loka Bharathi PA. 2010. Immobilization of Nickel by Bacterial Isolates from the Indian Ridge System and the Chemical Nature of the Accumulated Metal. Geomicrobiology Journal 27: 424–434 (**IF: 1.830**)*.
2. **Sujith PP**, Das A, Mourya BS, Loka Bharathi PA. 2011. Immobilization of manganese, cobalt and nickel by deep-sea-sediment microbial communities. Chemistry and Ecology 27: 189-206 (**IF: 0.615**)*.
3. Runa A, **Sujith PP**, Fernandes SO, Pankaj V, Khedekar VD, Loka Bharathi PA. 2011. Cobalt immobilization by manganese oxidizing bacteria from the Indian Ridge system. Current Microbiology 62: 840-849 (**IF: 1.815**).
4. Das A, **Sujith PP,** Mourya BS, Biche SU, Loka Bharathi PA. 2011. Chemosynthetic activity prevails in deep-sea sediments of Central Indian Basin. Extremophiles 15: 177-189 (**IF: 2.941**).
5. Das A, Fernandes CEG, Naik SS, Nath BN, Suresh I, Mascarenhas-Pereira MBL, Gupta SM, Khadge NH, Prakash Babu C, Borole DV, **Sujith PP,** Valsangkar AB, Mourya BS, Biche SU, Sharma R, Loka Bharathi PA. 2011. Bacterial response to contrasting sediment geochemistry in the Central Indian Basin. Sedimentology 58: 756-784 (**IF: 2.295**).
6. **Sujith PP,** Loka Bharathi PA. 2011. Manganese oxidation by bacteria: Biogeochemical aspects. In: Molecular Biomineralization: Aquatic organisms forming extraordinary minerals. Progress in Molecular and Subcellular Biology 52: 49-76*.
7. **Sujith PP**, Mourya BS, Krishnamurthi S, Meena RM, Loka Bharathi PA. 2014. Mobilization of manganese by basalt associated Mn(II) oxidizing bacteria from the Indian Ridge System. Chemosphere 95: 486-495 (**IF 3.137**).

MANUSCRIPTS UNDER REVIEW/COMMUNICATED

1. **Sujith PP**, Gonsalves MJBD, Bhonsle S, Shaikh S, Loka Bharathi PA. Activity of ferromanganese crust-associated bacteria contributes to hydrogenetic metal accretion in the Afanasiy-Nikitin seamount*.
2. **Sujith PP**, Gonsalves MJBD, Rajkumar V, Miriam Sheba V. Manganese cycling and its implication on methane related processes in the Andaman continental shelf sediments*.
3. **Sujith PP,** Madhavu V, Gonsalves MJBD. EDTA and Ascorbate aids the sorption/release of cobalt and nickel by bacteria from cobalt-rich ferromanganese crusts*.
4. **Sujith PP,** Ramanan D, Gonsalves MJBD, Loka Bharathi PA. Microbial activity accelerates the enrichment of cobalt and nickel on hydrogenetic ferromanganese crusts*.
5. **Sujith PP,** Gonsalves MJBD, Loka Bharathi PA. Distribution and diversity of culturable bacteria associated with hydrogenetic ferromanganese crusts of the Afanasiy-Nikitin Seamount*.
6. **Sujith PP**, Gonsalves MJBD. Ferromanganese mineral deposits: geochemical and microbiological perspectives of interactions of cobalt and nickel*.
7. Fernandes CEG, **Sujith PP**, Kumar P, Naik SS, Loka Bharathi PA. Iron mineral formation and cell encrustation by Fe13 a bacterial isolate from ilmenite rich beach sediment.
8. Miriam Sheba V, **Sujith P.P**, Gonsalves MJBD. Diversity and activity of methane oxidizing bacteria in subsurface sediments of the Krishna Godavari Basin.
9. Das A, Fernandes CEG, Naik SS, Mourya BS, **Sujith PP**, Sharma R, Loka Bharathi P A. Storage of deep-sea sediments under ambient tropical condition demonstrates their fitness for metallurgical applications.
10. Fernandes CEG, Malik A, Jineesh VK, Fernandes SO, Das A, Pandey S, Kanolkar G, **Sujith PP**, Velip DM, Shaikh S, Helekar S, Gonsalves MJBD, Nair S, Loka Bharathi PA. Estuarine influence on coastal waters: comparison of systems influenced by iron released by mining and that released from ilmenite along West Coast of India.

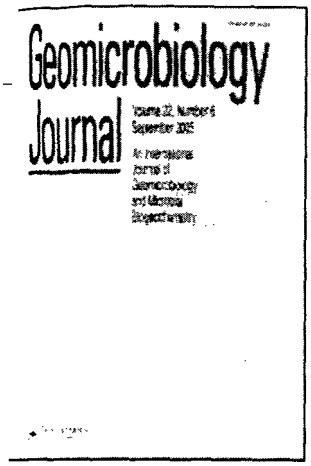

Geomicrobiology Journal
Publication details, including instructions for authors and subscription information:
http://www.informaworld.com/smpp/title~content=t713722957

Immobilization of Nickel by Bacterial Isolates from the Indian Ridge System and the Chemical Nature of the Accumulated Metal

P. P. Sujith[a]; V. D. Khedekar[a]; A. P. Girish[a]; P.A. Loka Bharathi[a]
[a] National Institute of Oceanography (CSIR), Dona Paula, Goa, India

Online publication date: 08 June 2010

To cite this Article Sujith, P. P. , Khedekar, V. D. , Girish, A. P. and Bharathi, P.A. Loka(2010) 'Immobilization of Nickel by Bacterial Isolates from the Indian Ridge System and the Chemical Nature of the Accumulated Metal', Geomicrobiology Journal, 27: 5, 424 — 434
To link to this Article: DOI: 10.1080/01490450903480285
URL: http://dx.doi.org/10.1080/01490450903480285

Geomicrobiology Journal, 27:424–434, 2010

ISSN: 0149-0451 print / 1521-0529 online
DOI: 10.1080/01490450903480285

Taylor & Francis

Immobilization of Nickel by Bacterial Isolates from the Indian Ridge System and the Chemical Nature of the Accumulated Metal

P. P. Sujith, V. D. Khedekar, A. P. Girish, and P. A. Loka Bharathi
National Institute of Oceanography (CSIR), Dona Paula, Goa, India

Bacterial isolates from Carlsberg-Ridge waters were tested for their ability to immobilize Ni. For this, test cultures were suspended for 60 d in seawater with and without added Ni at concentrations of 10 to 10,000 μM. At an initial concentration of 100 μM, isolates CR35 and CR48 caused a 89.8 and 6.95 μM decrease in dissolved Ni at 28 ± 2°C and a 14.75 and 6.38 μM at 3 ± 1°C. Analyses showed the contribution of hydroxyl, carbonyl, sulfide and phosphoryl groups in Ni binding. The study proves that Ni immobilization can occur even in the absence of Mn and suggests their plausible role in the ridge ecosystem.

Keywords Carlsberg Ridge, energy dispersive x-ray, immobilization, infrared spectroscopy, nickel, scanning electron microscope, X-ray powder diffraction

INTRODUCTION

Marine bacteria are indigenous to an environment characterized by a small amount of organic matter and a large amount of inorganic salts (Gonye and Jones 1973). Like any complex system, the marine environment also serves as a unique niche for many specialized life forms and supports a diverse array of microorganisms (Prescott et al. 1999). The hydrothermal vent fields and the nearby water columns are a source for reduced inorganic ions. Some of the microorganisms in these habitats may oxidize certain reduced form of metals (Jannasch and Wirsen 1979; Jannasch 1984; Mandernack and Tebo 1993) and are able to derive energy in oxidizing relatively large amounts of these reduced metal species to fulfil their metabolic needs (Ehrlich 1976, 1978).

The tectonically active Carlsberg Ridge in the Arabian Sea is such a habitat known to support chemosynthesis and can serve as sink for various metal ions (Mn, Fe, Co, Ni, etc). Besides the ridge sources, mining and metallurgical activities also contribute to an increase in the level of trace metals in the sediment and aquatic environments (Gonzalez et al. 1997). The average global concentration of Ni in the oceans is 0.6 ppb (μg/kg), in soils 16 ppm (μg/g), in lakes and in rivers 1.0 ppb (Nriagu 1980), and in sediments from southwest Carlsberg Ridge 21-251 ppm (Pattan and Higgs 1995).

Metal ion homeostasis is very crucial for optimum growth and survival of microorganisms. In order to meet the physiological needs for these nutritionally required trace elements, microorganisms have special uptake mechanisms for some of them. Once in the cell, the elements may be sequestered. Excess concentrations of these elements in ionic form in cells may, however, be toxic (Schmidt and Schlegel 1989). The mechanisms such as intracellular sequestration of metals by proteins and polyphosphate granules may be a means of metal storage or detoxification (Keasling 1997). However, intracellular toxicity of metals is mainly overcome by metal efflux.

Excess metal uptake may also be controlled in some organisms by binding of metal ions to slime consisting of exopolysaccharide (Helmann et al. 2007). This in turn limits the direct effect of metal ion on cells. As a result, the cells survive and continue to perform their normal metabolic activities in the presence of excess metal concentration. In the present study, we attempted to understand the nature of interaction between bacteria and nickel and their ability to immobilize the metal.

Our observation is applicable to sediments and other organically depleted natural ecosystems where the metal concentrations vary from a few ppm to ppb levels. This is the first study to show that, bacterial isolates from a ridge system capable of immobilizing Mn can also immobilize Ni. The oxides of Mn are otherwise generally known to stimulate the immobilization of other metals including Ni. The study demonstrates how immobilization of Ni can be effected even in the absence of manganese.

Received 25 February 2009; accepted 5 November 2009.
We thank the Director, NIO for providing the required facilities to conduct this research work. The work has been carried out under the project "Preliminary exploration of cobalt-rich seamount crusts in the northern Indian Ocean" funded by the Ministry of Earth Sciences (Government of India) lead by Dr. V.K. Banakar. Dr. V.P. Rao helped with XRD and Dr. Keisham Sarjit Singh and Divya Shridhar with IR analysis. Dr. M.P. Tapaswi gave us unstinting support with required literature. Dr. Maria Judith B.D. Gonsalves critically went through the manuscript. SPP acknowledges the Council of Scientific and Industrial Research, New Delhi-India, for the award of Senior Research Fellowship. We thank the two anonymous reviewers who critically reviewed the manuscript and helped us to improve the contents. This manuscript has NIO contribution No. 4644.
Address correspondence to Dr. P. A. Loka Bharathi, National Institute of Oceanography (CSIR), Dona Paula, Goa 403 004, India. E-mail: loka@nio.org.

METHODS AND MATERIALS

Organism and Growth

The Mn oxidizing bacterial isolates CR35 and CR48 employed in the present study were retrieved from Carlsberg Ridge waters (Fernandes et al. 2005). The isolate CR35 was obtained from a water depth of 3040 m at 3°35'N Lat and 64°07'E Long and CR48 from a water depth of 3510 m at 4°31'N Lat and 62°33'E Long. The isolate CR35 was capable of growing in media prepared in distilled water with 0.5% NaCl, whereas, seawater was mandatory for the growth of CR48. The isolates when grown in the presence of Ni in seawater showed no additional growth requirement. Therefore, the incubation experiment for Ni immobilization was done only with metal salt ($NiCl_2.6H_2O$, Merck) in aged seawater (pH 7.8).

Inocula of the bacterial isolates were grown in 0.01% nutrient broth (Merck) containing 15g peptone, 3g yeast extract, 6g sodium chloride and 1g D(+) glucose in a litre of seawater at 3 ± 1°C. They were harvested by centrifugation at 8000 rpm for 10 min at 4°C when the cell density reached an OD_{600} of 1.5. Cell pellets were washed twice with sterile saline, resuspended and used for the inoculation of experiment tubes. The stock cultures were maintained on 25% nutrient agar slants at 4°C.

Immobilization of Nickel

To quantify immobilization of Ni by whole cells, the experiment was carried out in 15 ml screw capped test tubes with Ni amendments of 10, 100, 1000 and 10000 μM in seawater containing triphenyl tetrazolium chloride at a final concentration of 0.025%. Controls for each Ni concentration, but without cells were included to correct for chemical oxidation and loss of metal due to adsorption on glassware. The experimental tubes containing 11 ml media were inoculated in triplicate to give an initial cell count of 2.97×10^7 cells ml^{-1} for CR35 and 3.52×10^7 cells ml^{-1} for CR48. The tubes were incubated at 28 ± 2°C and 3 ± 1°C in the dark. Samples (1 ml) were removed immediately after inoculation and after 60d of incubation for determining the total count, respiring cell count and Ni concentration in the liquid phase. The total count and the number of respiring cells (pink) were determined after segregation of cell aggregates by sonication at 15 Hz for 3s.

The cells were counted in a Neubauer counting chamber at 400-x magnification with a bright field microscope (Nikon 80i). The formazan in experimental tubes was determined and the values were corrected for the 0d absorbance at the end of the experiment (Fernandes et al. 2005). The OD values for formazan in culture were converted to mg ml^{-1} formazan using the equation for the line of best fit derived from a standard curve of formazan (Himedia) prepared in methanol. Ni was estimated from the supernatant by a spectrophotometric method (Chester and Hughes 1968) at 460 nm after centrifugation at 8000 rpm for 10 min. For higher concentration >10 μM Ni, supernatant was suitably diluted with distilled water. The experimental readings were corrected for control to estimate the rate of Ni immobilization.

Effect of Added Ni on Bacterial Growth Rate

The isolates CR35 and CR48 were grown at 100 μM concentration of Ni in seawater together with controls lacking added Ni to study the effect of added Ni on growth of strains CR35 and CR48. The inoculum for the experiment was prepared as above and 0.5 ml of the culture was inoculated in triplicate and was incubated at 28 ± 2°C for 6 d. Daily 20 μl of samples from individual tubes were withdrawn and loaded into Neubauer counting chamber for bright field microscopic (Nikon 80i) count. The cells were examined under 400-x magnification and the counts were expressed as numbers per ml of sample.

Microscopy

The bacterial cells grown in the presence and absence of Ni were harvested by centrifugation at 8000 rpm for 10 min at 4°C after 60 d of incubation. The cell pellet was suspended in sterile 0.85% saline and a drop was placed on small pieces of cover slip and air-dried. The cells were dehydrated by passing the cover slips carrying the cells through 10, 30, 50, 70, 90 and 100% acetone. The cover slips containing the dehydrated sample smears were mounted on an electron microscope stub, sputter coated with Au/Pd. The cells were then examined under a JEOL JSM-5800 scanning electron microscope (SEM). For light microscopy, wet mounts of bacterial cells were made using acid cleaned glass slides and cover slips. Bacterial morphology and cell aggregation were observed at 400-x magnification and photographed with a digital camera and the images processed using software image pro 6.2.

X-ray Diffraction (XRD) and Energy Dispersive X-ray (EDX) Analysis

The bacterial isolates CR35 and CR48 were grown at 28 ± 2°C for 7d in seawater with and without added 1000 μM $NiCl_2.6H_2O$. The respective cultures were then harvested and washed three times with sterile 0.85% saline and once with acetone by centrifugation at 8000 rpm for 15 min at 4°C and air-dried. The samples were powdered with a micro pestle in 2 ml eppendoff tubes.

The XRD pattern (Deplanche and Macaskie 2008) were recorded in a Rigaku x-ray powder diffractometer using monochromatic Cu $K\alpha_1$ radiation ($\lambda = 1.54050$ A°). The diffraction spectra were recorded over the range of 10° to 100° (2θ) with a step length of 0.02° (2θ). The identification of Ni salts was based on comparison with the joint committee on powder diffraction standards file (1981). An EDX analysis was done on a small portion of intact cells from the above cultures on JEOL JSM-5800 at an accelerating voltage of 15 kV.

Infrared (IR) Analysis

The CR35 and CR48 bacterial isolates grown at room temperature (28 ± 2°C) for 2 d in seawater in the presence of

100 μM added Ni and in its absence were separated by centrifugation at 8000 rpm for 15 min at 4°C (Sigma 3-18K), washed three times with sterile 0.85% saline and once with distilled water and then lyophilized (Heto LL1500 freeze dryer). A known quantity of lyophilized bacterial sample (0.8 mg) and dry potassium bromide (1.75 mg) was placed in a smooth agate mortar and mixed thoroughly. The powder was filled in a micro-cup of 2 mm internal diameter (Naumann et al. 1991). The diffuse reflectance infrared spectrum of the samples was recorded in a Shimadzu FTIR-8201PC spectrophotometer with 60 scans at a resolution of 4 cm^{-1} in the transmission mode (mid infrared region 4000–400 cm^{-1}).

Plasmid Screening

The isolates CR35 and CR48 were grown in 0.1% nutrient broth in tubes with and without Ni (100 μM) amendment and were incubated at 28 ± 2°C. The cells of the early exponential phase (OD_{600} of 1.2) were harvested by centrifugation at 8000 rpm for 10 min at 4°C. The cell pellets were washed twice with physiological saline (0.85%) and were immediately used for the preparation of cell lysates (Kado and Liu 1981). The bacterial lysates were analyzed by agarose gel electrophoresis with agarose concentration of 0.6 and 1% according to the procedure of Meyers et al. (1976). Supermix DNA ladder (0.5 to 33.5/24.5 kb) obtained from Bangalore Genie was used as the reference marker. The gel was stained with ethidium bromide (0.5 μg ml^{-1}) for 30 min and photographed after destaining using the gel documentation and analysis system (Biorad).

RESULTS

Nickel Immobilization

The Ni immobilization by both the isolates enhanced was with increasing Ni concentration (Figure 1). CR35 showed a maximum Ni immobilization of 120.7 μM at 28 ± 2°C (Figure 1A) and 20.3 μM at 3 ± 1°C (Figure 1B) with 1000 μM test Ni concentration. In parallel, CR48 showed maximum Ni immobilization of 309.5 μM at 28 ± 2°C and 38.53 μM at 3 ± 1°C with 10,000 μM test Ni concentration. Nevertheless, at 100 μM added Ni concentration, CR35 immobilized 89.8% of the Ni, at 28 ± 2°C and 14.75% at 3 ± 1°C, which was the maximum removal observed with this strain. With CR48, similar trend was not observed, rather immobilization was maximum of 19.27% at 28 ± 2°C at 1000 μM added Ni concentration and 11.9% at 3 ± 1°C at 10 μM added Ni concentration. The study showed that temperature has an effect on Ni immobilization and was faster at 28 ± 2°C with both of the test isolates.

Bacterial Growth

The bacterial growth was monitored with Ni to determine the effect of the metal cation on bacterial cells. The bacterial number decreased with increase in Ni concentration. The maximum cell number was $6.63 \pm 4.89 \times 10^7$ cells ml^{-1} with CR35

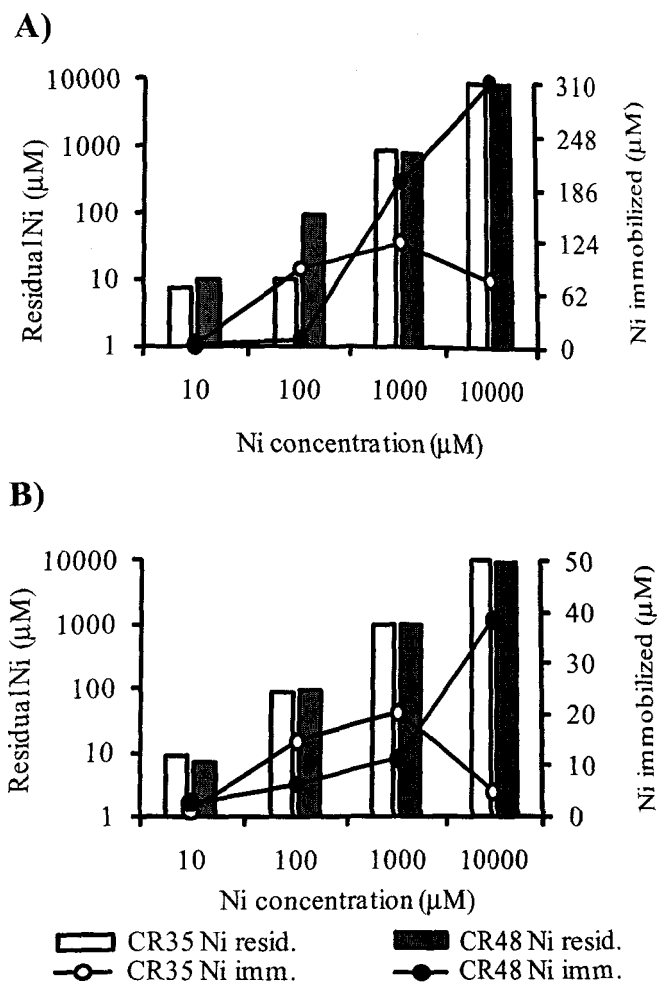

FIG. 1. Effect of temperature on Ni immobilization by bacterial isolates CR35 and CR48. A) Immobilization at 28 ± 2°C and B) Immobilization at 3 ± 1°C. The legend "Ni imm" represents Ni immobilization and "Ni resid" represents Ni residual. The values are ± mean, n = 3.

at 28 ± 2°C (Figure 2A) and $6.19 \pm 5.09 \times 10^7$ cells ml^{-1} at 3 ± 1°C (Figure 2B) in the presence of 10 μM added Ni. However, with CR48, the cell number was maximum at 100 μM and it was $9.32 \pm 2.97 \times 10^7$ cells ml^{-1} at 28 ± 2°C (Figure 2C) and $3.27 \pm 9.63 \times 10^7$ cells ml^{-1} at 3 ± 1°C (Figure 2D). The difference in cell number between 28 ± 2°C and 3 ± 1°C was 74.7% with CR35, and 85% with CR48. Beyond 100 μM Ni concentration, no increase in cell number was observed, either at 28 ± 2°C or at 3 ± 1°C, with both the isolates.

The cell counts were comparatively smaller at 3 ± 1°C than at 28 ± 2°C. The formazan estimation of respiration was maximum (0.18 ± 0.01mg ml^{-1}) at 10 μM Ni with CR35 and 0.15 ± 0.016 mg ml^{-1} with CR48 at 100 μM Ni concentration at room temperature (Figure 2). These results suggests that 100 μM Ni is the threshold concentration for tolerance in both the isolates. The number of respiring cells at 100 μM Ni concentration was $4.26 \pm 4.33 \times 10^7$ cells ml^{-1} at 28 ± 2°C (Figure 2A) and $9.89 \pm 3.33 \times 10^6$ cells ml^{-1}

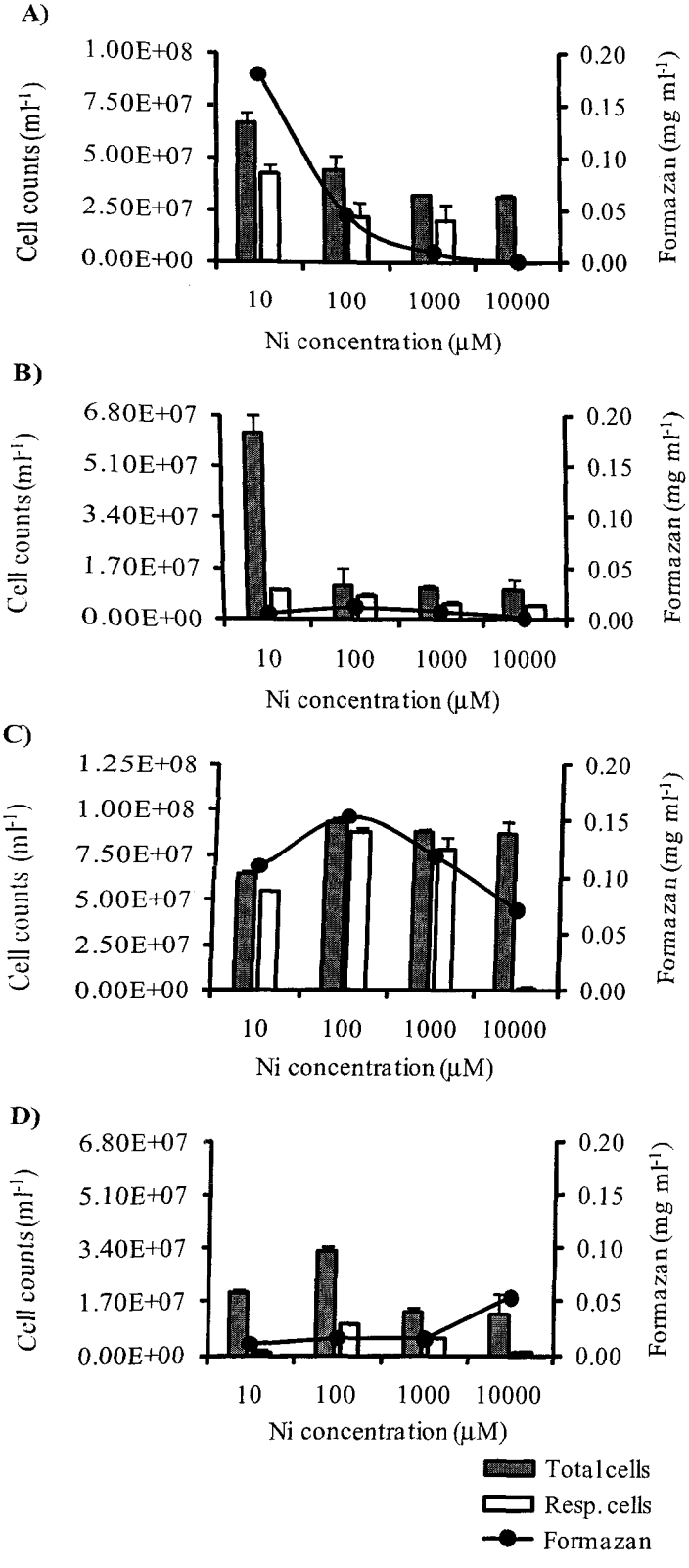

FIG. 2. Total cell count, respiring cell count (resp. count) and formazan concentration in Ni amended seawater medium. A) CR35 (28 ± 2°C), B) CR35 (3 ± 1°C), C) CR48 (28 ± 2°C) and D) CR48 (3 ± 1°C). Note that the scale for figures 'A' and 'C' is different from 'B' and 'D'.

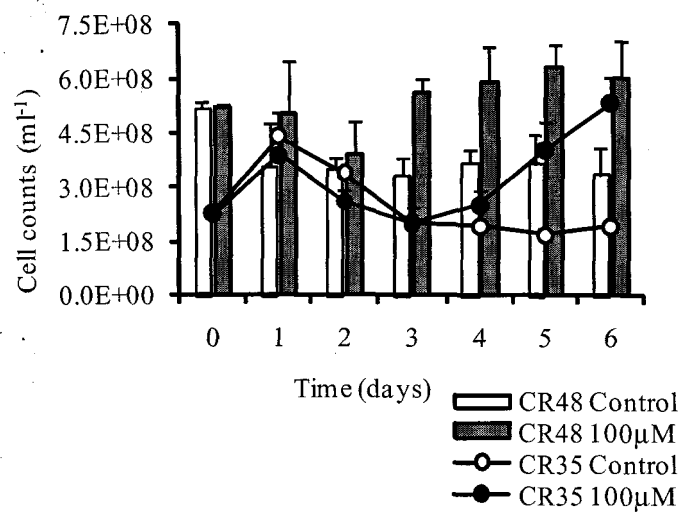

FIG. 3. Growth rate of CR35 and CR48 in the presence (100 μM) and absence of $NiCl_2$ at 28 ± 2°C.

(Figure 2B) at 3 ± 1°C for CR35 and $8.80 \pm 2.56 \times 10^7$ cells ml^{-1} at 28 ± 2°C (Figure 2C) and $9.63 \pm 2.77 \times 10^6$ cells ml^{-1} at 3 ± 1°C (Figure 2D) for CR48.

Stimulatory Effect of Nickel on Bacteria

The growth rate of bacteria in the presence and absence of Ni is shown in Figure 3. It is clear from the figure, the bacterial count increased with Ni (100 μM) and decreased in its absence with time. The cell count for CR35 showed a marginal increase with Ni from $2.28 \pm 9.8 \times 10^8$ to $5.34 \pm 1.28 \times 10^8$ cells ml^{-1} at the end of 6d incubation. With CR48, the cell count attained a maximum ($6.3 \pm 6.56 \times 10^8$ cells ml^{-1}) on 5d of incubation and thereafter showed a marginal decrease on 6d.

Microscopy and EDX Analysis

The Ni-exposed and -unexposed bacterial cells were observed under SEM to investigate morphological changes induced by the metal after 60 d of incubation. Control cells grown in seawater without any nutrient or Ni amendment did not show any morphological variation and appeared normal (Figure 4A, D). The average cell size (l × w) of CR35 was from $1.72 \pm 0.2 \times 1.20 \pm 0.14$ μm and that of CR48 was $1.16 \pm 0.28 \times 0.96 \pm 0.17$ μm. Bacterial cells exposed to 100 μM Ni showed healthy dividing cells (Figure 4B, E). The average size of CR35 ranged from $4.02 \pm 0.38 \times 1.58 \pm 0.12$ μm and CR48 from $5.2 \pm 0.77 \times 1.83 \pm 0.33$ μm. At 10,000 μM Ni concentration, increase in cell size and subsequent rupture was observed (Figure 4C&F). The average size of CR35 ranged from $4.37 \pm 0.47 \times 3.01 \pm 0.34$ μm and CR48 from $6.89 \pm 0.34 \times 2.08 \pm 0.13$ μm.

Overall, the cell size increased to 2.65×1.81 μm with CR35 and to 5.73×1.12 μm with CR48 at 10,000 μM Ni concentration. EDX analysis of CR35 and CR48 isolates grown in the absence of Ni showed peaks for phosphorus, potassium,

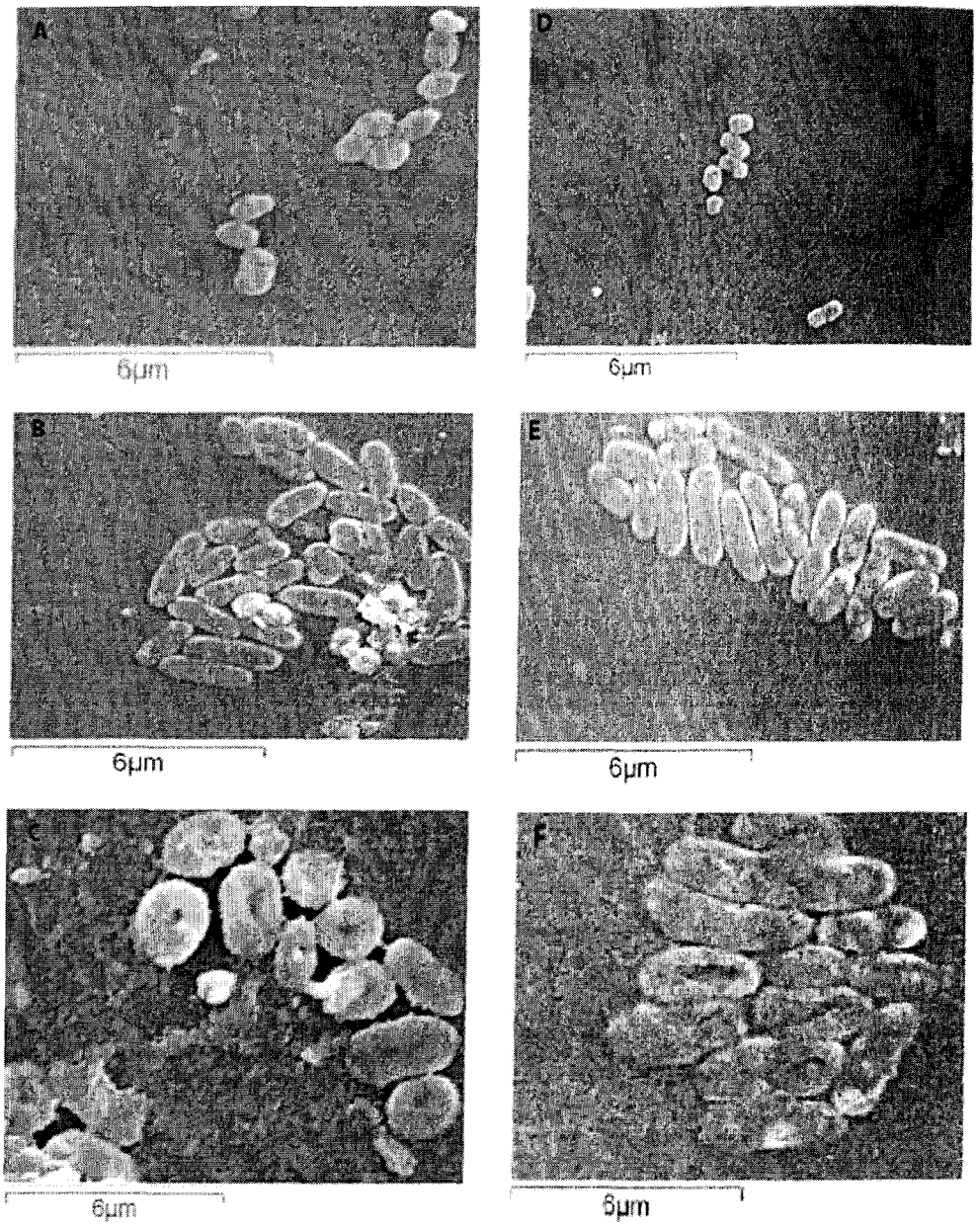

FIG. 4. Scanning electron microscope images showing morphological changes of CR35 cells grown in seawater medium A) with no Ni added, B) 100 μM and C) 1000 μM added $NiCl_2$. CR48 cells grown in seawater medium D) with no Ni added, E) 100 μM and F) 1000 μM added $NiCl_2$.

magnesium, calcium, silicon and oxygen (Figure 5a, c). The bacterial cells exposed to the metal showed peaks for Ni with decrease in intensity of the peak for Mg in both the isolates and loss of K peak in CR35 indicating cation efflux (Figure 5b, d). The wet mount observation under bright field microscope showed the occurrence of cell aggregates. The size of the aggregates increased and their number decreased with higher concentration of Ni. It was vice versa with lower test concentrations. Cells grown in the absence of Ni showed discrete cells (Figure 6). In an another attempt it was observed that, above 10,000 μM Ni concentration both cell aggregate size and their number decrease with no further increase in cell growth (data not shown).

X-ray Diffraction Analysis

The XRD analysis of bacterial cells showed that Ni was sequestered as both a diphosphide and a sulfide mineral in the bacterial cells. Diffractograms of control cells CR35 (Figure 7a) and CR48 (Figure 7c), lacked any distinct peak, and showed the characteristic amorphous nature of the samples, while distinct peaks for Ni loaded biomass from the experimental flasks indicated the deposition of crystallized Ni compounds. Based on the D values (1.42, 1.300, 1.140 and 1.01), peaks for the Ni-loaded CR35 cells (Figure 7b) at 2θ = 65.96, 72.68, 85 and 99.56° could be assigned to the existence of Ni sulfides. In contrast, for CR48 isolate (Figure 7d) most of the peaks were at 2θ = 28.2,

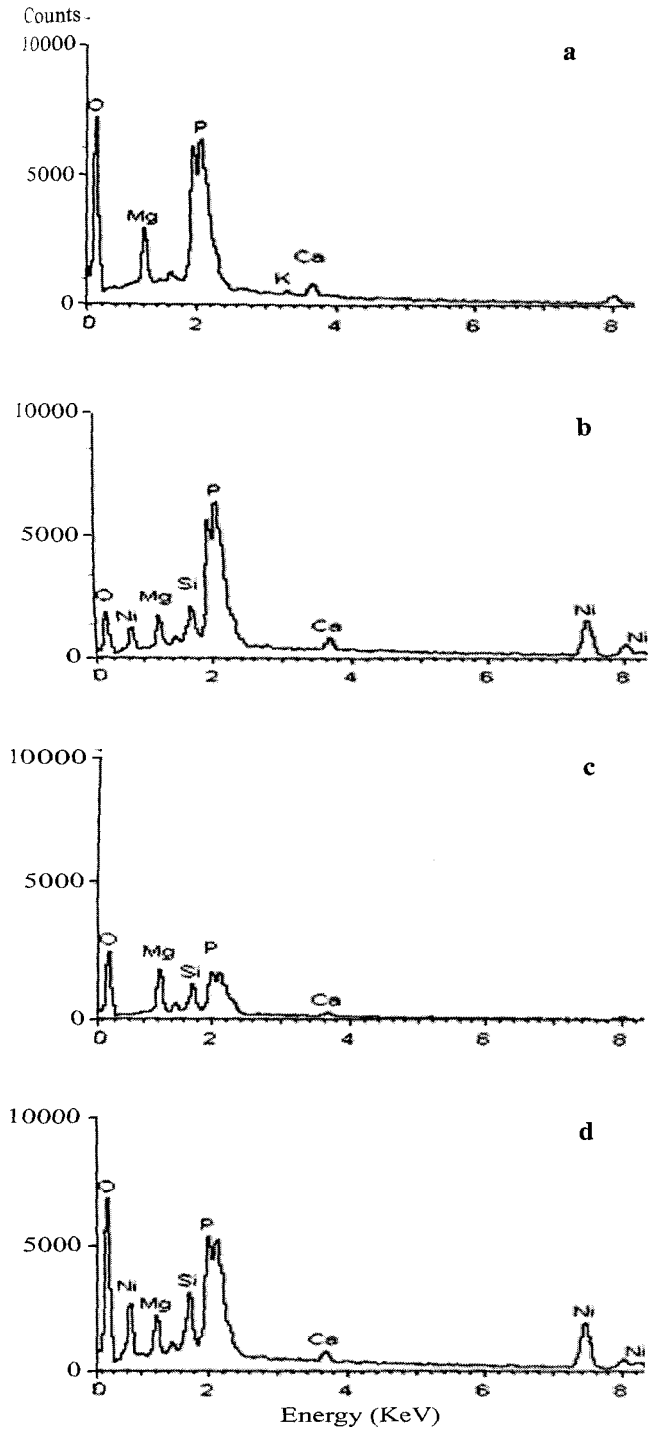

FIG. 5. Energy dispersive x-ray spectra of bacterial cells (a) CR35 in the absence of Ni, (b) CR35 exposed to 1000 μM Ni, (c) CR48 in the absence of Ni, (d) CR48 exposed to 1000 μM Ni.

34.66 and 59.96 with D values of 3.162, 2.586 and 1.541 which correspond to Ni diphosphides. However, peaks at $2\theta = 64.7$ and 98.08 with D values 1.44 and 1.09 could be related to Ni sulfides. Though EDX confirmed the presence of phosphorus in the cells, we were unable to interpret some XRD peaks, which could correspond to phosphide mineral in CR35. The present study suggests that both CR35 and CR48 could accommodate Ni as both phosphide and sulfide minerals.

IR Spectral Analysis

The IR analysis of bacterial isolates CR35 and CR48 were examined in the presence and absence of Ni to understand the Ni induced changes in bonding characteristics of the functional moieties in the bacteria. The characteristic bands of CR35 biomass were at 435.9, 1064.6, 1238.2, 1647.1 and 2925.8 cm^{-1} (Figure 8A) and CR48 biomass were at 420.5, 1068.5, 1240.1, 1645.2 and 2923.9 cm^{-1} (Figure 8C). The biomass exposed to Ni indicated discernable changes in the intensities of the bands. The band at frequency 435.9 cm^{-1} in CR35 increased in intensity on Ni exposure to 451.3 cm^{-1} (Figure 8B).

In contrast, with CR48 the frequency at 420.5 cm^{-1} decreased in intensity to 416.6 cm^{-1} (Figure 8D). This shows that δ(O-H) group could participate in Ni chelation. The stretching vibration at frequency 1064.6 cm^{-1} in CR35 decreased in intensity on Ni exposure to 1004.8 cm^{-1}, while in CR48 the frequency at 1068.5 cm^{-1} increased to 1083.9 cm^{-1}. This shows that (C-O), (C-C), (C-O-C), (C-O-P) of cell wall polysaccharides participate in Ni chelation. But, stretching vibration at 1645.2 cm^{-1} showed no change in intensity on Ni exposure with CR48 while the frequency at 1647.1 cm^{-1} decreased to 1645.2 cm^{-1} after Ni exposure in CR35 indicating the change in peptide bond characteristic of (C=O) group. Similar changes in frequency intensities were observed for (P=O) group in CR35 on Ni exposure and authenticate the binding of Ni to hydroxyl, carbonyl and phosphoryl functionalities.

Plasmid

Lysates of bacterial cells grown in the presence and absence of Ni examined by agarose gel electrophoresis showed no plasmids.

DISCUSSION

The present study shows the Ni immobilizing ability of Mn oxidizing bacterial isolates CR35 and CR48 retrieved from Carlsberg Ridge bottom waters under ambient (28 ± 2°C) and cold temperature (3 ± 1°C) (Fernandez et al. 2005). The sequestration of Ni as NiS, NiS_1 and NiP_2 was revealed by X-ray diffraction analysis. Though the cells showed active division at 100 μM Ni concentration, the cells grew larger and even formed aggregates at increasing Ni concentrations. The study highlights the stimulatory effect of Ni (Figure 3) at lower concentration and accumulation of the metal as either sulphides or diphosphides at higher concentration. This is the first report that gives an insight into the cellular changes and Ni accumulation within bacteria of the Indian ridge ecosystem.

Spectroscopic analysis of Ni showed a decrease of dissolved Ni in the aqueous phase in the experimental tubes. The decrease in the concentration of dissolved Ni was highest at the lower

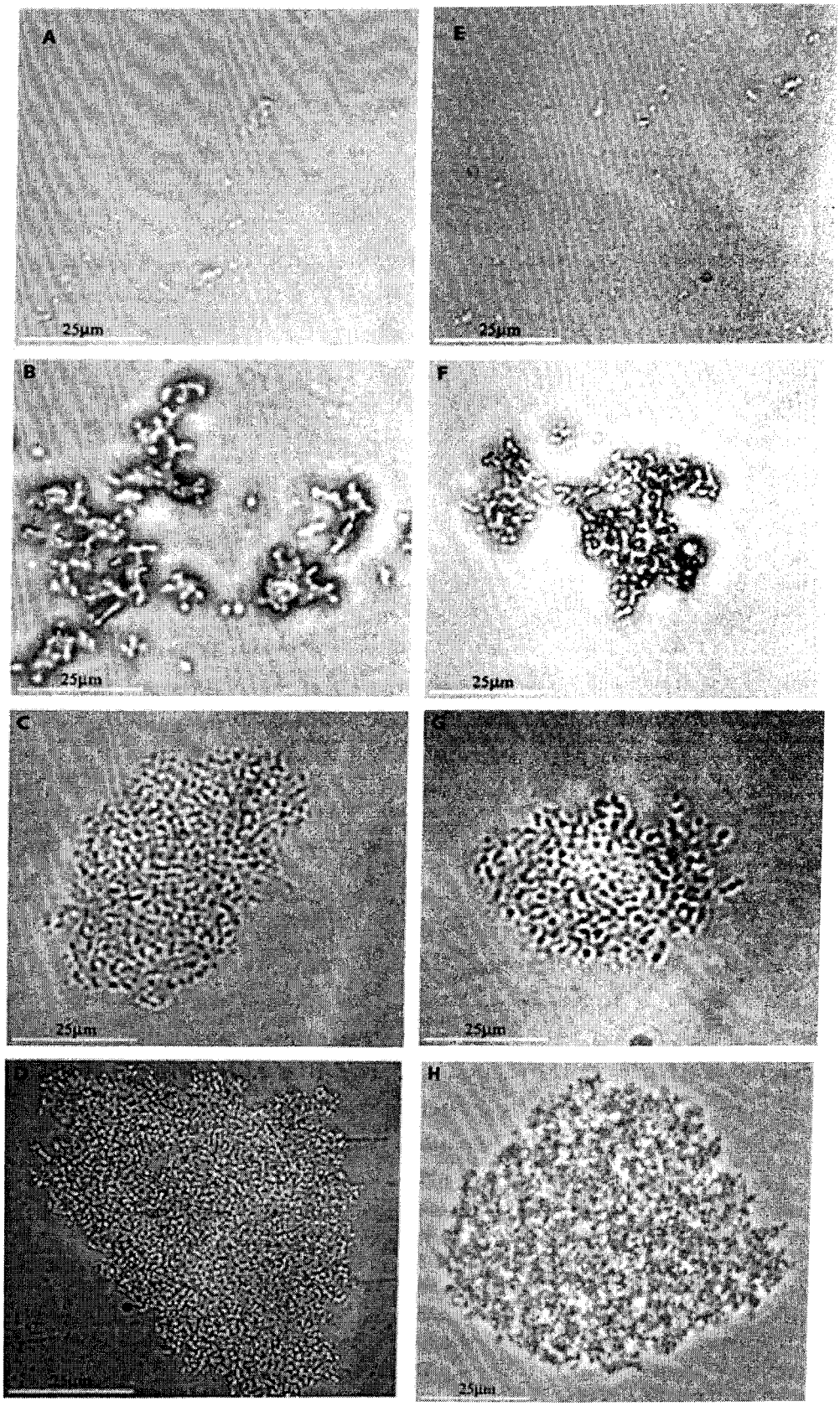

FIG. 6. Bright field images showing bacterial cell aggregates and their size difference respect to concentration of Ni in seawater medium. A) CR35 in the absence of Ni, B) 10 μM, C) 100 μM and D) 1000 μM added $NiCl_2$. E) CR48 in the absence of Ni, F) 10 μM G) 100 μM and H) 1000 μM added $NiCl_2$.

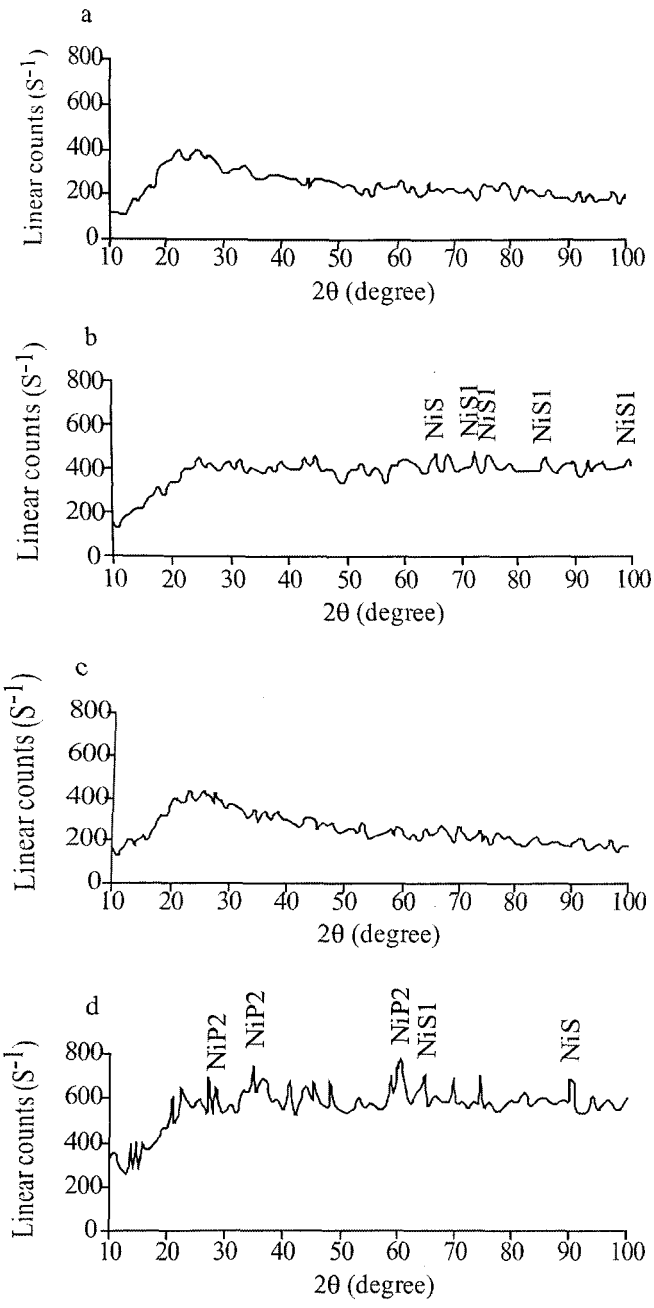

FIG. 7. X-ray diffraction spectra of dried and powdered bacterial biomass (a) CR35 in the absence of Ni, (b) CR35 exposed to 1000 μM Ni, (c) CR48 in the absence of Ni, (d) CR48 exposed to 1000 μM Ni.

Ni concentrations and smallest at the higher Ni concentration at both 28 ± 2°C and 3 ± 1°C. However, the extent of Ni immobilization at 3 ± 1°C was comparatively smaller than at 28 ± 2°C. The lower immobilization at 3 ± 1°C corresponds to the slower growth rate at low temperature (Figure 1B). The results of the study showed an increase in bacterial number at 10 and 100 μM Ni, which suggests that the 10 and 100 μM Ni concentrations were stimulatory for bacterial growth.

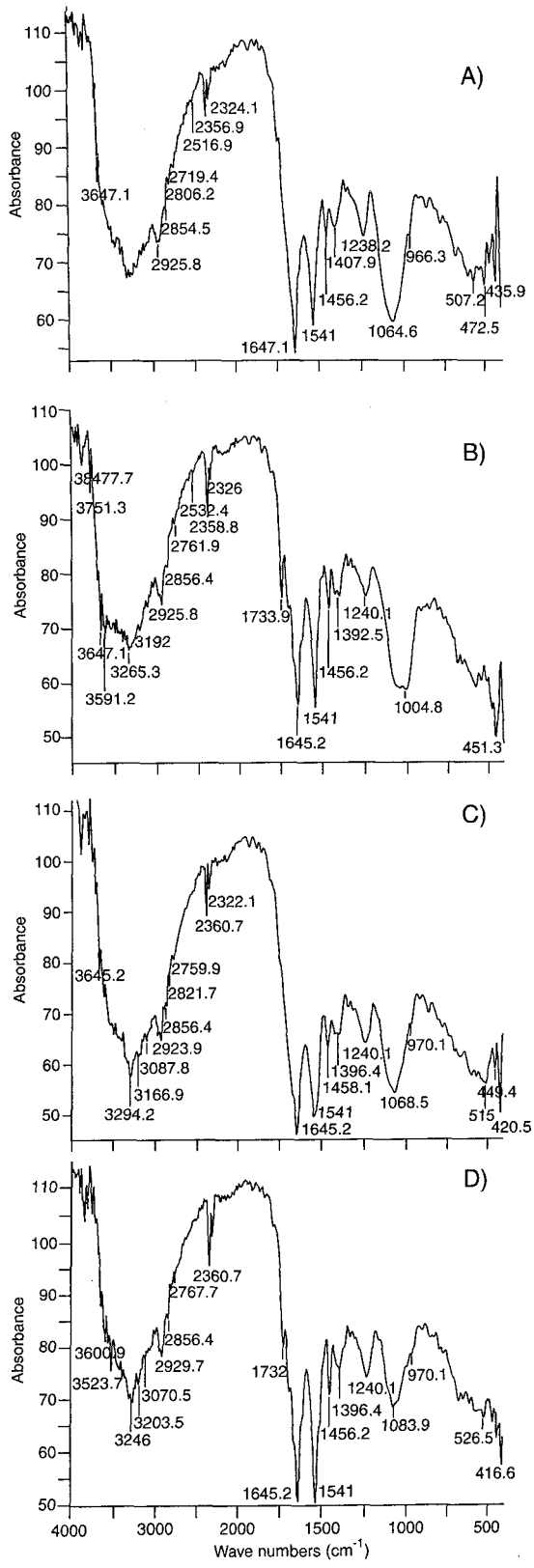

FIG. 8. Fourier transform infrared (FTIR) spectra of bacterial biomass. (A) CR35 in the absence of Ni, (B) CR35 exposed to 100 μM Ni, (C) CR48 in the absence of Ni, (D) CR48 exposed to100 μM Ni.

The studies of Bartha and Ordal (1965) on *Hydrogenomonas* strains, Partidge and Yates (1982) on *Azotobacter chroococcum* and Stults et al. (1987) on *Bradyrizhobium japonicum* support the previously presented evidence of growth stimulation by Ni. However, excessive concentration of Ni was found to inevitably disorder cell metabolism followed by decrease in cell count. The results agree with those of Sigee and Al-Rabaee (1986), who reported cell wall damage and subsequent reduction in growth and cell metabolism of *Pseudomonas tabaci* in excess concentration of Ni in the growth medium. We observed in our study that, the amount of formazan produced was maximum at $28 \pm 2°C$ and occurred below 100 μM Ni concentration with both isolates (Figure 2). Our findings suggest that our strains suffered stress above a threshold concentration of Ni, some cells surviving and others perishing.

The SEM observation of bacterial morphology showed a loss in cell wall rigidity above the minimum Ni threshold concentration. Nonetheless, microscopic observation and EDX analysis suggested that Ni was sequestered by the bacterial cells (Figure 4 and 5). The decrease in the level of Mg and K in cells exposed to Ni indicated that Ni immobilization involved ion exchange. The acquisition of Ni and the cell rupture are consistent with the observed microscopic cell counts. The results are in agreement with Sigee and Al-Rabaee (1986) with respect to exchange of Ni ions in cells and consequent inhibition of cell division in excess concentration of Ni.

Our findings are in agreement with a report by Nies (1999) with respect to a need for heavy metal uptake to cause any physiological or toxic effects. The observation by Cobet et al. (1970) of a morphological change of *Arthrobacter marinus* grown in the presence of an excess of Ni, lends support to our findings. Nickel availability in excess of that required and tolerated by an organism may impair its growth. The rate of Ni uptake by strains CR35 and CR48 was slower comparatively than the rate of Mn oxidation by these two strains (Fernandes et al. 2005). The Mn oxidizing activity, which was monitored maximum at 100,000 μM concentration, was 10 times higher than at 10,000 μM Ni concentration. Although the cultures failed to oxidize Mn at 100,000 μM, the inhibitory effect of Ni occurred at a lower Ni concentration of 10,000 μM. Ni appeared to have been sequestered within the cells in the strains CR35 and CR48, whereas oxidized Mn was deposited on the exterior of the cells.

The precipitation of Ni as NiS (Millerite) has been suggested as the crystalline phase of biogenic nickel sulfides (Waybrant et al. 1998; Southam 2005). The degradative metabolism of assimilated sulfur-containing amino acids by bacteria could lead to Ni precipitation as NiS (Freeman et al. 1975). Microbial conversion of sulfate (SO_4^{2-}) to sulfide (S^{2-}) in waters with reducing conditions could also lead to NiS formation (Babich and Stotzky 1983). Our XRD analysis of Ni grown strains CR35 and CR48 showed the immobilized Ni as NiS and NiP_2. Our result agree with the report of Kazy et al. (1999) on accumulation of copper as CuS and Sar et al. (2001) on Ni as NiP_2 by *Pseudomonas aeruginosa*. The reports of Aickin et al. (1979) and Macaskie et al. (1987) on sequestration of lead and cadmium as phosphate minerals in *Citrobacter* sp also support the present findings.

Our IR analysis of bacterial cells showed a band at frequency 1064.6 cm^{-1} with a shoulder at 966.3 cm^{-1} for CR35 (Figure 8A) and 1068.5 cm^{-1} with a shoulder at 970.1 cm^{-1} for CR48 (Figure 8B). This was interpreted as a stretching vibration of C-O, C-C, C-O-C and C-O-P groups (Wolkers et al. 2004; Yee et al. 2004). The intensity of the band in the presence of Ni decreased with CR35 and increased with CR48 (Figure 8C and 8D) suggesting that Ni immobilization was accompanied by a decrease/increase in polysaccharide and phosphate. Parikh and Chorover (2005) also observed a similar stretching vibration in relation to manganese oxidation. The stretching vibration characteristic of C=O of peptides was observed at 1647.1 cm^{-1} in CR35 and 1645.2 cm^{-1} in CR48.

The intensity of the band decreased to 1645.2 cm^{-1} with CR35 and remained unchanged with CR48 in Ni exposed cells, which could indicate an interaction of Ni with peptide bonds of protein in CR35. Backmann et al. (1996) explained a similar stretching vibrations of C=O specific for peptide bond in the 1700–1600 cm^{-1} region. The other stretching vibration specific for P=O decreased in intensity from 1407.9 cm^{-1} to 1392.5 cm^{-1} in Ni treated cells of CR35 indicating a role of phosphate in binding of Ni. A report by Fiona et al. (2003) is consistent with our results that suggested a crucial role of sugar phosphate esters in metal chelation. The bands in the lower frequencies <700 cm^{-1} are an indication of stretching vibration of the δ(O-H) group (Kamnev et al. 1997).

In the present study we observed stretching vibration of δ(O-H) group and an increase in intensity at the lower frequencies of bands in Ni-exposed cells of CR35 and CR48. This could indicate an intense formation of γ(M-O) complex (M=metal ion). The study of Kamnev et al. (1997) on Cu-loaded *Azospirillum brasilense* biomass suggested that a relatively higher absorption at lower frequencies could be assigned to the formation of γ(M-O) and δ(O-M-O) bands.

Bacterial resistance to Ni in heavy-metal contaminated ecosystems and in natural systems through which Ni percolates is inducible (Stoppel and Schlegel 1995). Screening for plasmids in CR35 and CR48 isolates from the metal rich ridge ecosystem showed no plasmids. However, an uptake of Ni was evident in these isolates, which could be through the activation of dormant genes for metal uptake. However, further study is required to prove the existence of chromosome mediated genes in these isolates. The genes for Ni resistance in *Alcaligenes denitrificans* 4a-2 (Kaur et al. 1990) and *Klebsiella oxytoca* CCUG 15788 (Stoppel and Schlegel 1995) were found to reside on chromosomal DNA.

CONCLUSIONS

This study provides evidence of Ni sequestration and of bacterial resistance to excess dissolved Ni under conditions of

nutrient starvation frequently encountered in natural seawater. Ni immobilization was faster at 28 ± 2°C than at 3 ± 1°C. The present observations help us to infer that the two bacterial isolates differ in the mechanism that permits toleration of high concentrations of Ni and that they respond differently in respect to induction of growth at different Ni concentrations. This is the first report to show Ni immobilization as NiP_2, NiS, and NiS_1 by bacterial isolates from the Indian ridge system as determined by X-ray diffraction analysis. The IR analysis also showed the involvement of phosphate group in addition to carboxyl and hydroxyl group as probable-binding sites occupied by Ni in CR35 and CR48 biomass. The study suggests the plausible role of the isolates in the ridge ecosystem. Because these ridge isolates are capable of tolerating and immobilizing high concentration of Ni, they could be candidate organisms for scavenging Ni ions from Carlsberg Ridge waters.

REFERENCES

Aickin RM, Dean ACR, Cheetham AK, Skarnulis AJ. 1979. Electron microscope studies on the uptake of lead by a *Citrobacter* species. Microbios Lett 9:7–15.

Babich H, Stotzky G. 1983. Influence of chemical speciation on the toxicity of heavy metals to the microbiota. In: Aquatic toxicology. Nriagu JO (ed), Wiley Interscience: New York; p. 1–46.

Backmann J, Schultz C, Fabian H, Hahn U, Saenger W, Naumann D. 1996. Thermally induced hydrogen exchange processes in small proteins as seen by FTIR spectroscopy. Proteins: Structure, Function and Genetics 24:379–87.

Bartha R, Ordal J. 1965. Nickel-dependent chemolithotrophic growth of two *Hydrogenomonas* strains. J Bacteriol 89:1015–1019.

Chester R, Hughes MJ. 1968. Scheme for the spectrophotometric determination of Cu, Pb, Ni, V and Co in marine sediments: Applied earth Science. Trans Inst Min Metallurgy 77:37–41.

Cobet AB, Wirsen C, Jun, Jones GE. 1970. The effect of nickel on a marine bacterium *Arthrobacter marinus* sp. nov. J Gen Microbiol 62:159–169.

Deplanche K, Macaskie LE. 2008. Biorecovery of gold by *Escherichia coli* and *Desulfovibrio desulfuricans*. Biotechnol Bioeng 99:1055–1064.

Ehrlich HL. 1976. Manganese as an energy source for bacteria. In: Environmental biogeochemistry. Nriagu JO (ed.) Ann Arbor Science, Michigan. P 633–644.

Ehrlich HL. 1978. Inorganic energy sources for chemolithotrophic and mixotrophic bacteria. Geomicrobiol J 1:65–83.

Fernandes SO, Krishnan KP, Khedekar VD, Loka Bharathi PA. 2005. Manganese oxidation by bacterial isolates from the Indian ridge system. Biometals 18:483–492.

Fiona HF, Jensen P, Kepert CM, Spiccia L. 2003. Macrocyclic copper (II) and Zinc (II) complexes incorporating phosphate esters. Inorg Chem 42:5637–5644.

Freeman LR, Angelini P, Silverman GJ, Merritt C, Jr. 1975. Production of hydrogen cyanide by *Pseudomonas fluorescens*. Appl Environ Microbiol 29:560–561.

Gonye ER, Jones GE. 1973. An ecological survey of open ocean and estuarine microbial populations. II. The oligodynamic effect of nickel on marine bacteria. In: Estuarine microbial ecology. Stevenson LH, Colwell RR (eds) University of South Carolina Press. P 243–257.

Gonzalez H, Ramirez M, Torres I. 1997. Impact of nickel mining and metallurgical activities on the distribution of heavy metals in sediments of Levisa, Cabonico and Nipe Bays, Cuba. Environ Geochem Hlth 19:57–62.

Helmann JD, Soonsanga S, Gabriel S. 2007. Metalloregulators: Arbiters of metal sufficiency. In: Molecular microbiology of heavy metals. Nies DH, Silver S (eds) Springer-Verlag, Berlin. P 37–71.

Jannasch HW, Wirsen CO. 1979. Chemosynthetic primary production at east Pacific sea floor spreading centers. Bioscience 29:592–598.

Jannasch HW. 1984. Microbial processes at deep sea hydrothermal vents. In: Hydrothermal processes at seafloor spreading centers. Rona PA, Bostrom K, Laubier L, Smith KL, Jr (eds) Plenum, New York. P 677–709.

Kado CI, Liu ST. 1981. Rapid procedure for detection and isolation of large and small plasmids. J Bacteriol 145:1365–1373.

Kamnev AA, Ristic M, Antonyuk LP, Chernyshev AV, Ignatov VV. 1997. Fourier transform infrared spectroscopic study of intact cells of the nitrogen-fixing bacterium *Azospirillum brasilense*. J Mol Struct 408/409:201–205.

Kaur P, Rob K, Siddiqui RA, Schlegel HG. 1990. Nickel resistance of *Alcaligenes denitrificans* strain 4a-2 is chromosomally coded. Arch Microbiol 154:133–138.

Kazy SK, Sar P, Asthana RK, Singh SP. 1999. Copper uptake and its compartmentalization in *Pseudomonas aeruginosa* strains: Chemical nature of cellular metal. World J Microbiol Biotechnol 15:599–605.

Keasling, JD. 1997. Regulation of intracellular toxic metals and other cations by hydrolysis of polyphosphate. Ann NY Acad Sci 829:242–249.

Macaskie LE, Dean ACR, Cheetham AK, Jakeman RJB, Skamulis AJ. 1987. Cadmium accumulation by a *Citrobacter* sp: The chemical nature of the accumulated metal precipitate and its location on the bacterial cells. J Gen Microbiol 133:539–544.

Mandernack KW, Tebo BM. 1993. Manganese scavenging and oxidation at hydrothermal vents and in vent plumes. Geochim Cosmochim Acta 57:3907–3923.

Meyers JA, Sanchez D, Elwell LP, Falkow S. 1976. Simple agarose gel electrophoretic method for the identification and characterization of plasmid deoxyribonucleic acid. J Bacteriol 127:1529–1537.

Naumann D, Helm D, Labischinski H, Giesbrecht P. 1991. The characterisation of microorganisms by Fourier-transform infrared spectroscopy (FT-IR). In: Modern Techniques for Rapid Microbiological Analysis. Nelson WH (ed.) VCH Publishers, New York, P 43–96.

Nies DH. 1999. Microbial heavy-metal resistance. Appl Microbiol Biotechnol 51:730–750.

Nriagu JO. 1980. Nickel in the Environment. New York: Wiley. 833 p.

Parikh SJ, Chorover J. 2005. FTIR spectroscopic study of biogenic manganese-oxide formation by *Pseudomonas putida* GB-1. Geomicrobiol J 22:207–218.

Partridge CDP, Yates MG. 1982. Effect of chelating agents on hydrogenase in *Azotobacter chroococcum*. Evidence that nickel is required for hydrogenase synthesis. Biochem J 204:339–344.

Pattan JN, Higgs NC. 1995. Rare earth element studies of surfacial sediments from the south western Carlsberg Ridge, Indian Ocean. Proc Ind Acad Sci 104:569–578.

Prescott LM, Harley JP, Klein DA. 1999. Microbiology. WCB/McGraw-Hill. 962 p.

Sar P, Kazy SK, Singh SP. 2001. Intracellular nickel accumulation by *Pseudomonas aeruginosa* and its chemical nature. Lett Appl Microbiol 32:257–261.

Schmidt T, Schlegel HG. 1989. Nickel and cobalt resistance of various bacteria isolated from soil and highly polluted domestic and industrial wastes. FEMS Microbiol Ecol 62:315–328.

Sigee DC, Al-Rabaee RH. 1986. Nickel toxicity in *Psudomonas tabaci*: Single cell and bulk sample analysis of bacteria cultured at high cation levels. Protoplasma 130:171–185.

Southam G. 2000. Bacterial surface-mediated mineral formation. In: Environmental microbe-metal interactions. Lovley DR (ed.) American Society for Microbiology Press, Washington, DC, p. 257–276.

Stoppel RD, Schlegel HG. 1995. Nickel-resistant bacteria from anthropogenically nickel-polluted and naturally nickel-percolated ecosystems. Appl Environ Microbiol 61:2276–2285.

Stults LW, Mallick S, Maier RJ. 1987. Nickel uptake in *Bradyrhizobium japonicum*. J Bacteriol 169:1398–1402.

Waybrandt KR, Blowes DW, Ptacek CP. 1998. Selection of reactive mixtures for use in permeable reactive walls for treatment of mine drainage. Environ Sci Technol 32:1972–1979.

Wolkers WF, Oliver AE, Tablin F, Crowe JH. 2004. A fourier transform infrared spectroscopy study of sugar glasses. Carb Res 339:1077–1085.

Yee N, Benning LG, Phoenix VR, Ferris FG. 2004. Characterization of metal-cyanobacteria sorption reactions: A combined macroscopic and infrared spectroscopic investigation. Environ Sci Technol 38:775–82.

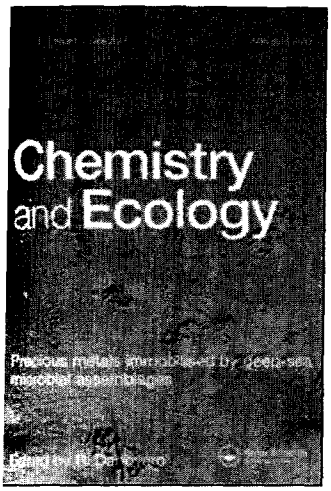

Chemistry and Ecology
Publication details, including instructions for authors and subscription information:
http://www.informaworld.com/smpp/title~content=t713455114

Immobilisation of manganese, cobalt and nickel by deep-sea-sediment microbial communities

P. P. Sujith[a]; Anindita Das[a]; Babu Shashikant Mourya[a]; P.A. Loka Bharathi[a]
[a] Microbiology Laboratory, National Institute of Oceanography, Council of Scientific and Industrial Research, Dona Paula, Goa, India

First published on: 20 April 2011

To cite this Article Sujith, P. P. , Das, Anindita , Mourya, Babu Shashikant and Loka Bharathi, P.A.(2011) 'Immobilisation of manganese, cobalt and nickel by deep-sea-sediment microbial communities', Chemistry and Ecology, 27: 3, 189 — 206, First published on: 20 April 2011 (iFirst)
To link to this Article: DOI: 10.1080/02757540.2011.565749
URL: http://dx.doi.org/10.1080/02757540.2011.565749

Chemistry and Ecology
Vol. 27, No. 3, June 2011, 189–206

Taylor & Francis
Taylor & Francis Group

Immobilisation of manganese, cobalt and nickel by deep-sea-sediment microbial communities

P.P. Sujith, Anindita Das, Babu Shashikant Mourya and P.A. Loka Bharathi*

Microbiology Laboratory, National Institute of Oceanography, Council of Scientific and Industrial Research, Dona Paula, Goa, India

(*Received 7 June 2010; final version received 14 February 2011*)

Box core samples BC26 and BC36 from geologically different settings were examined to test the hypothesis that autochthonous microbial communities from polymetallic-nodule-rich Central Indian Basin sediments actively participate in immobilising metal ions. The bottom water dissolved oxygen concentration was reported to be 4.2–4.3 $mL \cdot L^{-1}$ in the northern siliceous ooze (BC26) and 4.1–4.2 $mL \cdot L^{-1}$ in the southern pelagic red clay (BC36); the sedimentation rates for these regions were 0.834 and 0.041 $cm \cdot kyr^{-1}$, respectively. An onboard experiment, conducted under oxic and sub-oxic conditions with 100 μmol of Mn, Co and Ni, showed that microbial immobilisation under sub-oxic conditions was higher than in azide-treated controls in BC26 for Mn, Co and Ni at 30, 2 and 4 cm below sea floor (bsf), respectively, after 45 days. The trend in immobilisation was BC26 > BC36, Co > Mn > Ni under oxic conditions and Mn > Co > Ni under sub-oxic conditions. The depth of maximum immobilisation for Co in BC26 under sub-oxic conditions coincided with the yield of cultured Co-tolerant bacteria and Ni only with organic carbon at 4 cm bsf. This study demonstrates that the organic carbon content and bioavailable metal concentrations in sediments regulate microbial participation in metal immobilisation.

Keywords: metals; microbes; immobilisation; sediment; Central Indian Basin

1. Introduction

Sediments are complex mixtures of Fe- and Mn-oxide mineral phases, detrital organic matter and several other organic and inorganic phases. Sediments support different groups of metal-oxidising and -reducing microorganisms [1]. Microbes in sediments can interact with dilute metal ions in solution, including sequestration, and aid in concentrating these ions in the sediment. The ions either remain in sediments as bio-metal complexes or undergo a series of microbial or chemical transformations. This might lead to the recycling of metals into the overlying water column or to their immobilisation in sediments as authigenic mineral phases [2].

The microbial immobilisation of metals can be catalytic or non-catalytic; it proceeds via four different mechanisms, namely biosorption, bioaccumulation, redox reaction and complex formation [3]. Immobilisation may be through cellular sequestration and accumulation, or through extracellular precipitation [4,5]. Marine bacteria produce large amounts of organic surface material that interacts with metal ions. The exopolysaccharides are subsequently involved in the precipitation

*Corresponding author. Email: loka@nio.org

ISSN 0275-7540 print/ISSN 1029-0370 online

DOI: 10.1080/02757540.2011.565749
http://www.informaworld.com

of soluble metal cations and the formation of oxide species on bacterial walls, which chemically react with the residual metals in solution [6–8].

A significant portion of the metals and their various organic derivatives in nature are contained within the living biomass. For example, Razzell and Trussell [9] addressed the interaction of *Thiobacillus* spp. with sulphide-bearing ores and their role in the dissolution of oxides and the release of valuable metals. Likewise, Fortin et al. [10] and Basnakova and Macaskie [11] highlighted the contribution of bacteria to the formation of sulphide and phosphide minerals by chemical complexing with available constituent sulphide and phosphide groups. A few studies also explain the intracellular sequestration [12,13] and extracellular precipitation [14,15] of metals by a group of metal-resistant bacteria, each affecting metal mobility in the environment.

The deposition of organic carbon and the availability of oxygen from bottom waters are primary factors that affect the geochemical and biological processes in the sediment–water system [16]. The availability of nutrients and oxygen therefore determines the sensitivity and adaptation of an organism to metals. Sediments are the ultimate repositories for environmental particles, and microbial processes within the sediment can also control chemical changes as a response to metal exposure. Previous studies have shown the immobilisation of metals in sterile sediments by individual isolates [17,18]. This study aimed to investigate the immobilisation of metals by autochthonous microbial communities.

The study area covers two regions of the Central Indian Basin (CIB) (Figure 1) [19]. The region for box core (BC) 26 is located at 10°S latitude and 75.5°E longitude in the northern region of the ocean. The sampling site has a water depth of 5339 m, the environment is relatively less oxidising [20] and receives more clay from rivers [21,22]. BC36 is located at the southern region of the basin at 16°S latitude and 75.5°E longitude. The region has a water depth of 5042 m, the

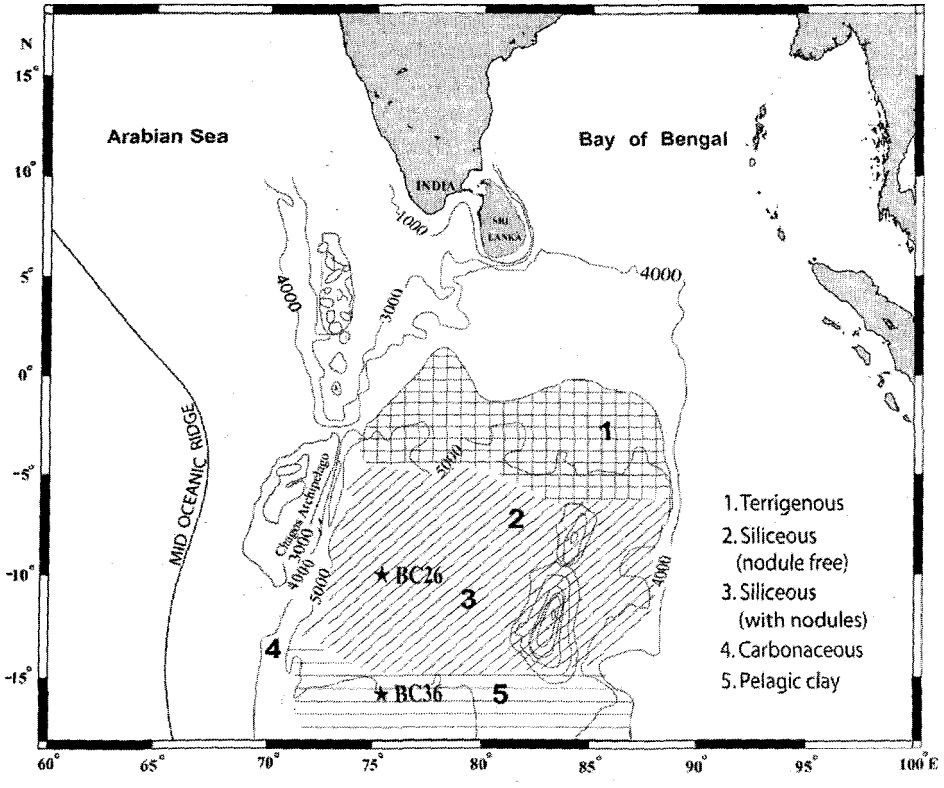

Figure 1. Area map shows sediment types and sampling locations for BC26 and BC36. Modified from Mascarenhas-Pereira et al. [19].

environment is more oxidising [20] and is known for the slower rate of sediment deposition [21]. The formation and dissolution of authigenic (oxyhydr)oxides of Fe and Mn influence the cycling of trace metals in oxic/sub-oxic surface sediments [23]. In view of that, we performed our experiment under oxic and sub-oxic incubation conditions to test the hypothesis that autochthonous microbial communities from CIB sediments actively participate in metal immobilisation. This study assesses the contribution of redox conditions, microbial abundance and activity to the immobilisation of Mn, Co and Ni.

2. Materials and methods

2.1. *Onboard sampling*

The samples were collected and processed on board Akademik Boris Petrov cruise number 26. Sediment cores were retrieved using a United States Naval Electronics Laboratory (USNEL) box corer of dimensions 50 × 50 × 50 cm. BC26 was collected from a siliceous ooze area and BC36 from a pelagic red clay region. The box cores were subsampled by inserting acrylic core liners of 6.3 cm diameter into the sediment. The sediment cores were further subsectioned at 2 cm intervals up to a depth of 10 cm and thereafter at 5 cm intervals up to a depth of 35 cm. Sediment samples were collected in sterile polyethylene bags and stored at 4 °C until further investigations.

2.2. *Total bacterial counts*

The sediment dilution for total bacterial counts (TBC) was prepared by suspending ~2 g of homogenised sediment in 9 mL of sterile seawater. A small portion of the above dilution was fixed with buffered formalin to a final concentration of 2% and was stored at 4 °C until analysis [24]. The samples were sonicated at 15 Hz for 15 s, the slurry was allowed to settle for 30 s and 1 mL of the supernatant was filtered through a 0.22 μm black Millipore polycarbonate filter. Samples were then stained with 0.01% acridine orange for 3 min prior to microscopic observation. Approximately 10–15 microscopic fields were counted for each sample at ×1500 magnification using a Nikon 80i epifluorescence microscope (Nikon, Tokyo, Japan). Counts were normalised per gram of dry sediment.

2.3. *Plate counts*

Bacteria resistant to Mn, Co, Ni and heterotrophic bacteria were enumerated in triplicate using the spread plate method from the above dilution. The heterotrophs were grown on 20% ZoBell marine agar (ZMA). Metal-resistant bacteria were cultured on seawater agar (SWA) (1.5% bacto agar in natural seawater with no other additional nutrients) amended with 100 μmol of metal salts $MnCl_2 \cdot 4H_2O$, $CoCl_2 \cdot 6H_2O$ and $NiCl_2 \cdot 6H_2O$ (Sd. Fine Chem. Ltd). To isolate bacteria resistant to more than one metal, 100 μmol of each metal was added to SWA medium of the above composition. The inoculated plates were incubated at 3 ± 1 °C for 4–10 days and the colony forming units (cfu) were counted and normalised for gram dry weight of sediment.

2.4. *Eh measurements*

Eh measurements were made at the beginning and end of the experiments. Before the measurements, the Eh electrode was rinsed with distilled water and calibrated with oxidation reduction potential (ORP) standard solution to ensure accurate readings. For measurements, the electrode

was dipped slowly into the sediment slurry in tubes and allowed to stabilise for 60 s. The direct reading obtained by mV meter was taken in triplicate and the mean values were determined. Eh was measured following the user's guide (Redox/ORP Electrodes, Thermo Electron Corporation 2005).

2.5. *Determination of total organic carbon*

Total inorganic carbon (TIC) was analysed using a UIC CM 5014 Coulometer with $CaCO_3$ as the standard and total carbon with an NCS 2500 elemental analyser [25], cross-checked with a UIC CM 5014 Coulometer. Total organic carbon (TOC) was determined indirectly by subtracting the values of TIC from total carbon [26].

2.6. *Solid-phase concentration of metal ions in sediments*

The concentration of metal ions in the sediment was determined by voltammetry after total decomposition of 50 mg of lyophilised sediments using the closed vessel digestion method [27]. The Mn concentration in aqueous samples was determined following the method of Colombini and Fuocco [28] with two standard additions of $MnCl_2 \cdot 4H_2O$ ($4\ mg \cdot L^{-1}$). The concentration of Ni and Co in samples was determined using the modified method of Herrera-Melian et al. [29]. Analysis of the metals was carried out using a voltammeter in interface with 797VA computrace (Metrohm, Switzerland). The potential was measured against an Ag/AgCl reference electrode and a platinum rod as a counter electrode. Ni and Co determination was carried out with a hanging mercury drop electrode (HMDE) in the differential pulse mode. The determination was carried out at pH 9 in a measuring cell containing 10 mL of supporting electrolyte (ammonia buffer, pH 9.5) and 100 μL of dimethylglyoxime (0.1 mol) in ethanol. A sample volume (1 mL), depending on the concentration, was appropriately diluted with Milli-Q water (18.2 Ω resistance) prior to analysis. The sample was added directly to the measuring vessel containing the electrolyte and was degassed with 99.9995% nitrogen (Medgas and Equipments) for 300 s prior to deposition. The analysis was carried out with a deposition time of 30 s, an equilibration time of 5 s and a voltage step time of 0.3 s. The potential was scanned in replications of 3 from −0.699 to −1.2 V with sweep rate of $6\ mV \cdot s^{-1}$. The analysis was quantified with two standard stock additions of Ni^{2+} ($NiCl_2 \cdot 6H_2O$, $1\ mg \cdot L^{-1}$) and Co^{2+} ($CoCl_2 \cdot 6H_2O$, $1\ mg \cdot L^{-1}$).

2.7. *Demonstration of metal immobilisation*

Box core sediments collected from two distinct regions of CIB were used to set up the laboratory experiments onboard. Portions of sediments from each subsection of the cores were inoculated using sterile spatula into 15 mL screw-capped tubes containing 100 μmol of metal chloride salts dissolved in sterile seawater. Suitable azide (10 mmol) poisoned controls to check for metal adsorption and autoclaved natural seawater amended with metal salts without any inocula (sterile controls) for abiotic precipitation were maintained. The incubation was carried out in triplicate at 3 ± 1 °C (to simulate *in situ* temperatures) under oxic and sub-oxic conditions. The oxic incubation was assured by directly inoculating 1.5 ± 0.5 g wet sediment in half-filled tubes and sub-oxic in completely filled tubes.

2.8. *Metal analysis*

The supernatant (1 mL) from inoculated and uninoculated tubes after centrifugation (8000 rpm for 10 min at 4 °C) were analysed on day 0 and at the end of 45 days to determine the change in metal concentration. The residual concentration of metals in each tube was analysed using

a spectrophotometric (Multiskan Thermo Spectrum) method. Any samples that were delayed in analysis were acidified with 1 N HCl and stored at 4 °C. The Mn concentration in the sample was determined using the 1-(2-pyridylazo)-2-naphthol method at 560 nm [30]. Determination of Ni with dimethylglyoxime and Co with nitroso-R-salt were carried out according to the scheme of Chester and Hughes [31] at 460 and 500 nm, respectively. Mean and SD were calculated for microbially (biotic) and non-microbially (abiotic) promoted metal immobilisation. Values were corrected for chemical precipitation in both the experimental setups. One-way analysis of variance (ANOVA) and correlation analysis including the levels of significance were done for data points $n = 10$ using Statistica.

2.9. *Determination of sediment dry weight*

The sediment slurry from each tube was mixed and poured onto a preweighed filter positioned in a filtration set-up at the end of analysis. The filter with sediment was dried at 105 °C and reweighed until constant. The filter weight was subtracted from the sediment weight to derive the actual dry weight of the sediment. The concentration of the immobilised metal was deduced and normalised for gram dry weight sediment after correcting for corresponding controls.

3. Results and discussion

3.1. *Characteristics of the two sampling stations*

Two sediment cores BC26 and BC36 were collected along the north–south transect of the CIB and were analysed for immobilisation of Mn, Co and Ni by the sediment microbial communities. The sediment slurry was found to support the growth of both heterotrophic and metal-resistant bacteria. The yield of cultured heterotrophic bacteria varied from below detectable levels (BDL) to $5.4 \pm 0.73 \times 10^3$ cfu·g^{-1} dry sediment in BC26 (Table 1) and $8.0 \pm 0.18 \times 10^4$ to $2.4 \pm 0.37 \times 10^5$ cfu·g^{-1} sediment in BC36 with maximum culturability at 8 cm depth (Table 2). The metal-resistant bacteria count ranged from BDL to $9.0 \pm 0.11 \times 10^2$ for Ni at 10 cm depth, $4.3 \pm 0.31 \times 10^4$ for Co and Mn at 2 and 20 cm depth, respectively. In mixtures of Mn, Co and Ni (100 µmol each), the culturability of bacteria was $1.4 \pm 0.33 \times 10^3$ cfu·g^{-1} at 10 cm depth in BC26 (Table 1). With BC36 it was $2.0 \pm 0.1 \times 10^4$ to $2.8 \pm 0.04 \times 10^5$ cfu·g^{-1} for Co, with maximum culturability at 10 cm depth, $3.9 \pm 0.06 \times 10^4$ to $2.4 \pm 0.31 \times 10^5$ for Ni, 1.2 ± 0.24 to $3.9 \pm 0.02 \times 10^5$ for Mn and $5.0 \pm 0.02 \times 10^4$ to $2.2 \pm 0.18 \times 10^5$ cfu·g^{-1} for metals in combination with maximum culturability at 4 cm depth (Table 2).

Although the total bacterial abundance did not show a definite trend with the depth of the cores (Figure 2a,b), the distribution of organic carbon did. The organic carbon in sediments varied from 0.175 to 0.485% in BC26 (Figure 2c) and 0.09 to 0.19% sediment dry weights in BC36 (Figure 2d) with maximum carbon concentration at 4 and 2 cm depth, respectively. The TOC content in seawater was 21.78 mg C·L^{-1} in BC26 and 9.18 mg C·L^{-1} in BC36. The abiotic precipitation of metal ions in uninoculated sterile controls was negligible. Eh as a measure of oxidising and reducing conditions showed that BC26 could support sub-oxic and BC36 the oxic processes better (Figure 2e,f). The Eh in BC26 experimental tubes decreased from +80.2 mV to +11.98 mV ($\pm$ 2.6, $n = 3$) in the oxic and +6.24 mV ($\pm$ 3.2, $n = 3$) in the sub-oxic incubations at 35 and 30 cm bsf, respectively. The Eh in BC36 decreased from +79.96 mV to +28.36 mV ($\pm$ 2.6, n = 3) in the oxic and +25.52 mV ($\pm$ 3.2, n = 3) in the sub-oxic incubations at 2 and 10 cm, respectively, for Mn (Table 3).

The maximum solid-phase concentration of Mn (14.93 µmol·g^{-1}) and Ni (4.55 µmol·g^{-1}) in BC26 was observed at 8 cm depth and Co (6.24 µmol·g^{-1}) at 30 cm depth. The concentration of Mn

Table 1. Plate counts of heterotrophic and metal-resistant bacteria in 1.5% bacto agar-amended seawater with and without metal chlorides (100 μmol) in BC26.

Depth		SWA				
bsf (cm)	ZMA	No metal	Ni	Co	Mn	Ni–Co–Mn
2	$1.5 \pm 0.18 \times 10^2$	BDL	BDL	$4.3 \pm 0.31 \times 10^4$	$2.5 \pm 0.22 \times 10^4$	BDL
4	$2.0 \pm 0.40 \times 10^2$	BDL	BDL	$2.7 \pm 0.15 \times 10^4$	$1.5 \pm 0.25 \times 10^4$	BDL
6	BDL	BDL	BDL	$1.5 \pm 0.10 \times 10^3$	$6.0 \pm 0.05 \times 10^2$	BDL
8	$5.4 \pm 0.73 \times 10^3$	BDL	BDL	$1.7 \pm 0.32 \times 10^4$	$4.1 \pm 0.61 \times 10^4$	BDL
10	$5.0 \pm 0.28 \times 10^1$	$1.5 \pm 0.57 \times 10^2$	$9.0 \pm 0.11 \times 10^2$	$6.6 \pm 0.60 \times 10^3$	$3.8 \pm 0.72 \times 10^4$	$1.4 \pm 0.33 \times 10^3$
15	BDL	BDL	BDL	$1.7 \pm 0.13 \times 10^4$	$3.9 \pm 0.23 \times 10^4$	BDL
20	BDL	BDL	BDL	$1.2 \pm 0.24 \times 10^4$	$4.3 \pm 0.45 \times 10^4$	BDL
25	$1.4 \pm 0.11 \times 10^3$	BDL	BDL	BDL	BDL	BDL
30	$5.0 \pm 0.02 \times 10^1$	BDL	BDL	BDL	BDL	BDL
35	BDL	BDL	BDL	BDL	BDL	BDL

Note: All the values in the table represent colony forming units (cfu)·g^{-1} dry weight of sediment. The data are given as mean ± SD, $n = 3$. ZMA, ZoBell marine agar; SWA, seawater agar; bsf, below sea floor; BDL, below detection level. For details, see text (Section 2.3).

Table 2. Plate counts of heterotrophic and metal-resistant bacteria in 1.5% bacto agar-amended seawater with and without metal chlorides (100 μmol) in BC36.

Depth		SWA				
bsf (cm)	ZMA	No metal	Ni	Co	Mn	Ni–Co–Mn
2	$8.0 \pm 0.18 \times 10^4$	$6.8 \pm 0.70 \times 10^4$	$1.6 \pm 0.02 \times 10^5$	$2.6 \pm 0.23 \times 10^5$	$1.8 \pm 0.10 \times 10^5$	$1.9 \pm 0.13 \times 10^5$
4	$1.0 \pm 0.11 \times 10^5$	$6.1 \pm 0.06 \times 10^4$	$2.4 \pm 0.31 \times 10^5$	$1.7 \pm 0.07 \times 10^5$	$3.9 \pm 0.02 \times 10^5$	$2.2 \pm 0.18 \times 10^5$
6	$8.8 \pm 0.09 \times 10^4$	$5.4 \pm 0.42 \times 10^4$	$9.1 \pm 0.46 \times 10^4$	$1.3 \pm 0.35 \times 10^5$	$3.3 \pm 0.21 \times 10^5$	$1.6 \pm 0.09 \times 10^5$
8	$2.4 \pm 0.37 \times 10^5$	$3.5 \pm 0.51 \times 10^4$	$2.1 \pm 0.10 \times 10^5$	$1.5 \pm 0.16 \times 10^5$	$2.4 \pm 0.03 \times 10^5$	$6.8 \pm 0.42 \times 10^4$
10	$1.6 \pm 0.24 \times 10^5$	$5.0 \pm 0.02 \times 10^4$	$1.6 \pm 0.05 \times 10^5$	$2.8 \pm 0.04 \times 10^5$	$1.3 \pm 0.09 \times 10^5$	$5.0 \pm 0.02 \times 10^4$
15	$1.2 \pm 0.08 \times 10^5$	$1.2 \pm 0.07 \times 10^4$	$3.9 \pm 0.06 \times 10^4$	$1.4 \pm 0.05 \times 10^5$	$1.2 \pm 0.24 \times 10^5$	$6.2 \pm 0.18 \times 10^4$
20	$1.4 \pm 0.15 \times 10^5$	$7.1 \pm 0.15 \times 10^4$	$5.1 \pm 0.31 \times 10^4$	$6.6 \pm 0.02 \times 10^4$	$1.7 \pm 0.11 \times 10^5$	$1.6 \pm 0.31 \times 10^5$
25	$1.6 \pm 0.26 \times 10^5$	$2.5 \pm 0.11 \times 10^4$	$4.2 \pm 0.17 \times 10^4$	$2.0 \pm 0.10 \times 10^4$	$1.7 \pm 0.07 \times 10^5$	$7.9 \pm 0.01 \times 10^4$
30	$2.0 \pm 0.24 \times 10^5$	$3.1 \pm 0.32 \times 10^4$	$9.9 \pm 0.06 \times 10^4$	$1.0 \pm 0.08 \times 10^5$	$2.2 \pm 0.05 \times 10^5$	$1.5 \pm 0.11 \times 10^5$
35	$1.7 \pm 0.09 \times 10^5$	$3.0 \pm 0.13 \times 10^4$	$9.5 \pm 0.22 \times 10^4$	$4.8 \pm 0.15 \times 10^4$	$2.4 \pm 0.21 \times 10^5$	$7.2 \pm 0.45 \times 10^4$

Note: All the values in the table represent colony forming units (cfu)·g^{-1} dry weight of sediment. The data are given as mean ± SD, $n = 3$. ZMA, ZoBell marine agar; SWA, seawater agar; bsf, below sea floor; BDL, below detection level. For details, see text (Section 2.3).

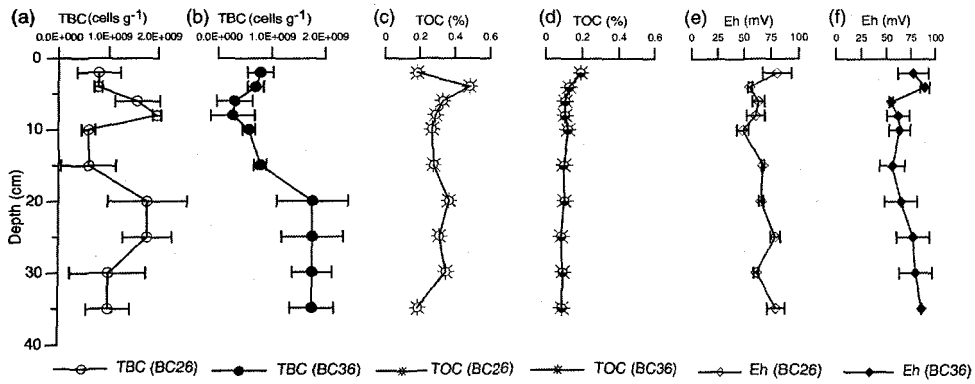

Figure 2. Depth profile of total bacterial count (TBC), total organic carbon (TOC) and Eh in sediment cores BC26 and BC36 (mean ± SD, $n = 10$ for TBC and $n = 3$ for Eh).

Table 3. Maximum immobilisation of metals at various depths below sea floor (bsf) compared with maximum in plate counts (colony forming units; cfu).

		Core BC26								
		Biotic				Abiotic				
		Oxic[a]		Sub-oxic[b]		Oxic[c]		Sub-oxic[d]		
Metal	Parameters	Value	Depth (cm)	Value	Depth (cm)	Value	Depth (cm)	Value	Depth (cm)	Inference
Mn	Immobilisation (μmol)	34.4 ± 0.053	35	85.6 ± 0.047	30	11.6 ± 0.011	35	22.5 ± 0.047	35	a. Suggests that oxidised Mn is less prone to dissolution at this depth
	Plate counts (cfu)									b. Suggests bacterial participation
	i) Seawater agar	–		–		–		–		c. Suggests that 86% of the variation in biotic oxidation could be due to the variation in abiotic
										d. Suggests passive immobilisation on Mn-oxide phase
Co	Immobilisation (μmol)	35 ± 0.33	2	46.3 ± 0.29	2	8.45 ± 0.055	35	6.97 ± 0.027	10	a. Immobilisation of Co by other metal-tolerant bacteria in the sediments
	Plate counts (cfu)									b. Suggests bacterial participation
	i) Seawater agar	–		–		–		–		c. Only passive process could be involved
	ii) Co	4.3×10^4		4.3×10^4		–		–		d. Suggests passive immobilisation on Mn oxide phase
Ni	Immobilisation (μmol)	6.3 ± 0.055	25	6 ± 0.08	4	0.98 ± 0.008	25	0.65 ± 0.012	4	a. Ni immobilisation may be catalysed more by bacteria resistant to Ni or Co
	Plate counts (cfu)									b. Energy-dependent low-affinity uptake process
	i) Seawater agar	–		–		–		–		c. Complexation of Ni with organic carbon in sediments
	ii) ZoBell marine agar	–		–		–		–		d. Complexation of Ni with organic carbon in sediments could contribute to its immobilisation at a much lower rate

(*Continued*)

Table 3. Continued.

		Core BC36								
		Biotic				Abiotic				
		Oxic[e]		Sub-oxic[f]		Oxic[g]		Sub-oxic[h]		
Metal	Parameters	Value	Depth (cm)	Value	Depth (cm)	Value	Depth (cm)	Value	Depth (cm)	Inference
Mn	Immobilisation (μmol)	19.76 ± 0.41	2	13.44 ± 0.04	10	25.33 ± 0.04	6	22.89 ± 0.03	6	e. Suggests mixotrophic mode of nutrition f. Suggests that high background Mn concentration along with the amended Mn could be toxic g. Could be regulated by concentration of the metal and the availability of particle-binding sites in sediments h. Active process of immobilisation is inhibited by azide and not the passive
	Plate counts (cfu)									
	i) Seawater agar	6.8×10^4		–		–		–		
Co	Immobilisation (μmol)	45 ± 0.028	2	27.5 ± 0.537	6	6.43 ± 0.011	8	7.18 ± 0.024	8	e. Could be by process in which Ni-immobilising bacteria catalyse Co immobilisation and vice versa f. Suggests co-oxidation of Co by Mn-oxidising microorganisms g. Could be regulated by concentration of the metal and the availability of particle-binding sites in sediments h. Could be by a metabolism-independent process like cell surface adsorption/precipitation
	Plate counts (cfu)									
	i) Seawater agar	6.8×10^4		–		–		–		
	ii) Co	–		–		–		–		
Ni	Immobilisation (μmol)	7.03 ± 0.09	2	6.6 ± 0.075	8	0.95 ± 0.009	25	0.703 ± 0.01	4	e. Suggests that the same microbial communities are capable of immobilising both the metals f. Suggests that the same microbial communities are capable of immobilising both the metals g. Could be regulated by concentration of the metal and the availability of particle-binding sites in sediments h. Could be by a metabolism-independent process like cell-surface adsorption/precipitation
	Plate counts (cfu)									
	i) Seawater agar	6.8×10^4		–		–		–		
	ii) ZoBell marine agar	–		2.4×10^5		–		–		

Note: All the values in the table correspond to gram dry weight of sediment. The data in the table are given as mean ± SD, $n = 3$. For details, see text (Sections 2 and 3).

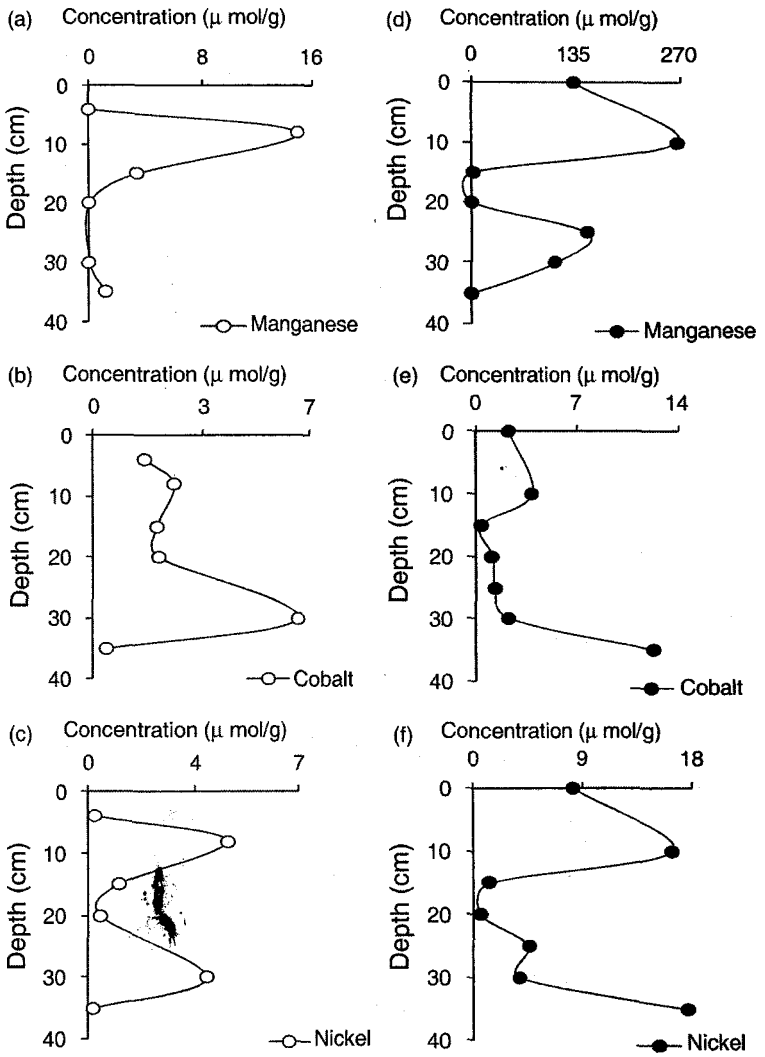

Figure 3. Solid-phase concentrations (single measurements) of Mn, Co and Ni in sediment cores collected from the Central Indian Basin. (a–c) Metal concentrations in BC26, (d–f) metal concentrations in BC36.

in BC36 sediment core was maximum (265.8 $\mu mol \cdot g^{-1}$) at 10 cm depth and Co (12.29 $\mu mol \cdot g^{-1}$) and Ni (17.52 $\mu mol \cdot g^{-1}$) at 35 cm depth (Figure 3). The concentration of the above metal ions was found to be unevenly distributed in the sediment cores. The maximum concentration for all the three metals was observed towards the surface, decreased with depth and showed a secondary maximum towards the subsurface in both the sediment cores. Our results agree with the report of Zhang et al. [32] on the double maxima for solute profiles.

3.2. *Immobilisation under oxic condition in BC26*

3.2.1. *Biotic immobilisation*

The results showed higher Mn immobilisation in the subsurface sediment (Figure 4a). The immobilisation of the metal was 34.4 ± 0.053 $\mu mol \cdot g^{-1}$ dry sediment at 35 cm bsf. Manganese

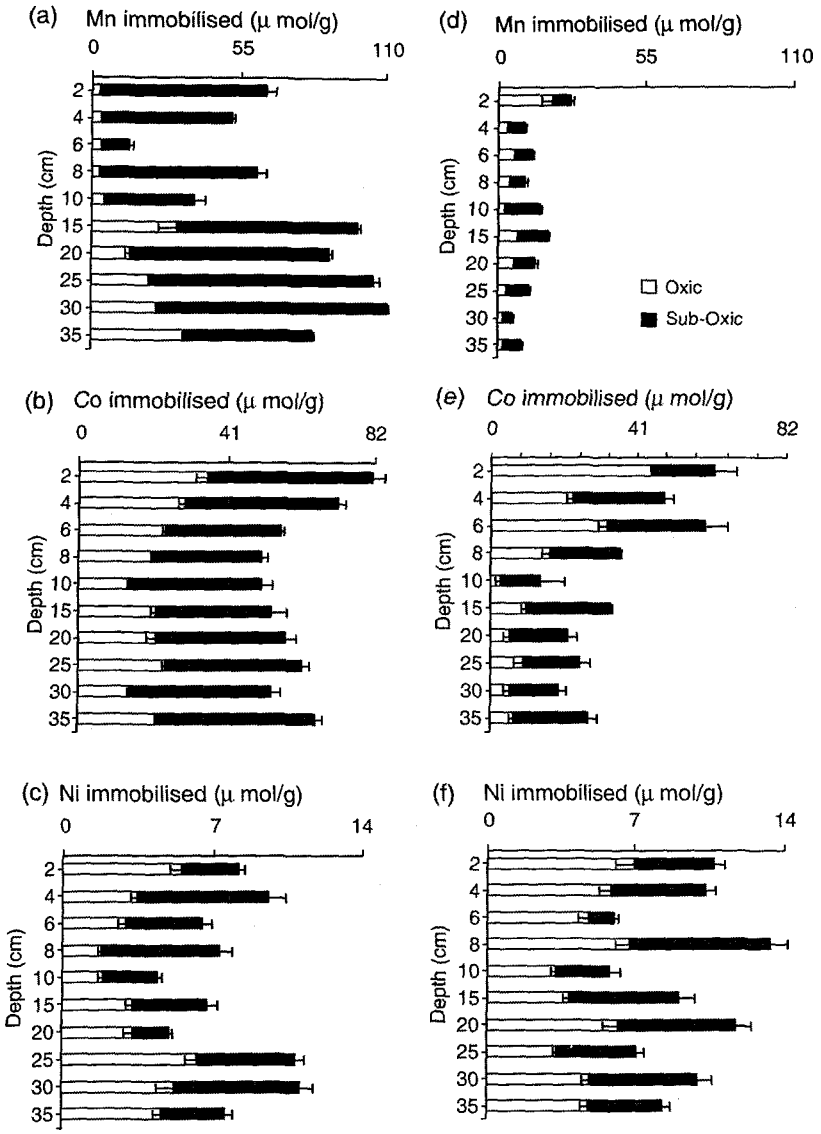

Figure 4. Microbially promoted immobilisation of metals ($\mu mol \cdot g^{-1}$ dry weight, mean ± SD, $n = 3$) in experiments as a function of depth. (a–c) The immobilisation of metals in BC26, (d–f) the immobilisation of metals in BC36. The error bars are shown on the left-hand side for oxic incubation and on the right-hand side for sub-oxic incubation.

immobilisation increased with depth ($r = 0.852$, $p < 0.001$). The yield of cultured heterotrophic bacteria co-varied with TBC at an r-value of 0.602 ($p < 0.05$) suggesting that the variation in the former is responsible for 36% of the variation in the latter. The immobilisation maximum observed at the deeper depth suggests that oxidised Mn is stable at this depth and is less prone to dissolution. The subsurface manganese maximum observed at 30–35 cm depth [33–35] in 13 different sediment cores collected from CIB substantiates the present finding.

By contrast to Mn, higher Co immobilisation (35 ± 0.328 $\mu mol \cdot g^{-1}$) was recorded at the sediment surface (Figure 4b). Interestingly, although the immobilisation of this metal was maximum at the surface and coincided with the maximum yield of cultured Co tolerant bacteria (Table 3), this process showed a negative relationship with the yield of cultured Co tolerant bacteria by an

r-value of 0.745 ($p < 0.01$). This probably suggests that immobilisation of Co is mediated by other metal-immobilising bacteria in the sediments. The association of Co with Mn in the surface sediment is one process in which Mn-oxidising bacteria participate indirectly in Co immobilisation. The results agree with the observations of Sundby et al. [36] and Glasby [37] on Co enrichment in the surface sediments. Our observations also support the earlier findings [38,39] on the co-oxidation of Co with Mn in the aquatic systems. Likewise, immobilisation of Co is known to co-occur with iron reduction in bacteria [40].

Like Mn, higher immobilisation of Ni ($6.3 \pm 0.055\,\mu mol \cdot g^{-1}$) was observed at the deeper 25 cm layer. The immobilisation of Ni negatively related with the yield of Mn tolerant bacteria by r-value of 0.643 ($p < 0.05$). This relation suggests that Ni immobilisation may not be catalysed by Mn-oxidising bacteria but more by bacteria resistant to Ni or Co. Further it is also suggested that in certain microorganisms, the resistance to one metal can also confer resistance to the other metals depending on the bioavailability and combination of metals. Interestingly, a study by Stoppel and Schlegel [41] has shown that bacteria tolerant to Ni are also tolerant to Co and posses determinants that resemble each other.

3.2.2. *Abiotic immobilisation*

The abiotic immobilisation was comparatively less than the biotic immobilisation because only the passive process could be involved. The difference could be as much as three to four times in the case of Mn, four to six times in the case of Co, and six times in the case of Ni. The maximum immobilisation of Mn (11.61 ± 0.011) and Co ($8.45 \pm 0.06\,\mu mol \cdot g^{-1}$) occurred at 30–35 cm bsf and Ni ($0.98 \pm 0.08\,\mu mol \cdot g^{-1}$) at 25 cm bsf (Figure 5). The Mn immobilisation showed depth dependence with an r-value of 0.928 ($p < 0.001$) and was also related to biotic Mn oxidation with an r-value of 0.930 ($p < 0.001$), suggesting that 86% of the variation in biotic Mn oxidation could be due to the variation in abiotic oxidation. The BC26 sediments are composed of siliceous ooze and have low concentrations of metal ions (Figure 3). Our results shows that abiotic metal immobilisation proceeds slowly and the rate depends upon the oxygen concentration, redox condition prevailing in the sediments, and the rate of the reverse activity ie dissolution. The results agree with the reports of Muller et al. [42] and Glasby [37] on surficial diagenesis and the regeneration rate of Mn in the sediments with that of accretion rate of the metal in the associated polymetallic nodules. The passive sorption of metal ions on sediment and mineral particles occurs by physical attraction and/or chemical precipitation.

3.3. *Immobilisation under sub-oxic condition in BC26*

3.3.1. *Biotic immobilisation*

As mentioned above, biotic immobilisation is definitely greater than abiotic immobilisation. Sub-oxic immobilisation is 2.4 times greater with Mn and 1.3 times greater with Co than oxic.

Under sub-oxic conditions, the microbial immobilisation of Mn ($85.6 \pm 0.047\,\mu mol \cdot g^{-1}$) was maximum at 30 cm bsf. Maximum Co ($46.3 \pm 0.29\,\mu mol \cdot g^{-1}$) immobilisation was at 2–4 cm bsf and is synchronised with the maximum yield of cultured Co-tolerant bacteria ($4.3 \pm 0.31 \times 10^4\,cfu \cdot g^{-1}$) and organic carbon (0.485%), suggesting bacterial participation. Our results agree with previous studies [43–47] which reported a positive correlation between heavy metal concentrations and the percentage of bacteria resistant to metals in different soils and sediments. However, maximum Ni immobilisation ($6 \pm 0.08\,\mu mol \cdot g^{-1}$) was evident at 4 cm depth (Figure 4c) and was synchronised with the organic carbon concentration (0.485%) in sediment, suggesting an energy-dependent low-affinity uptake process. The results are in agreement with Jasper and Silver [48] and

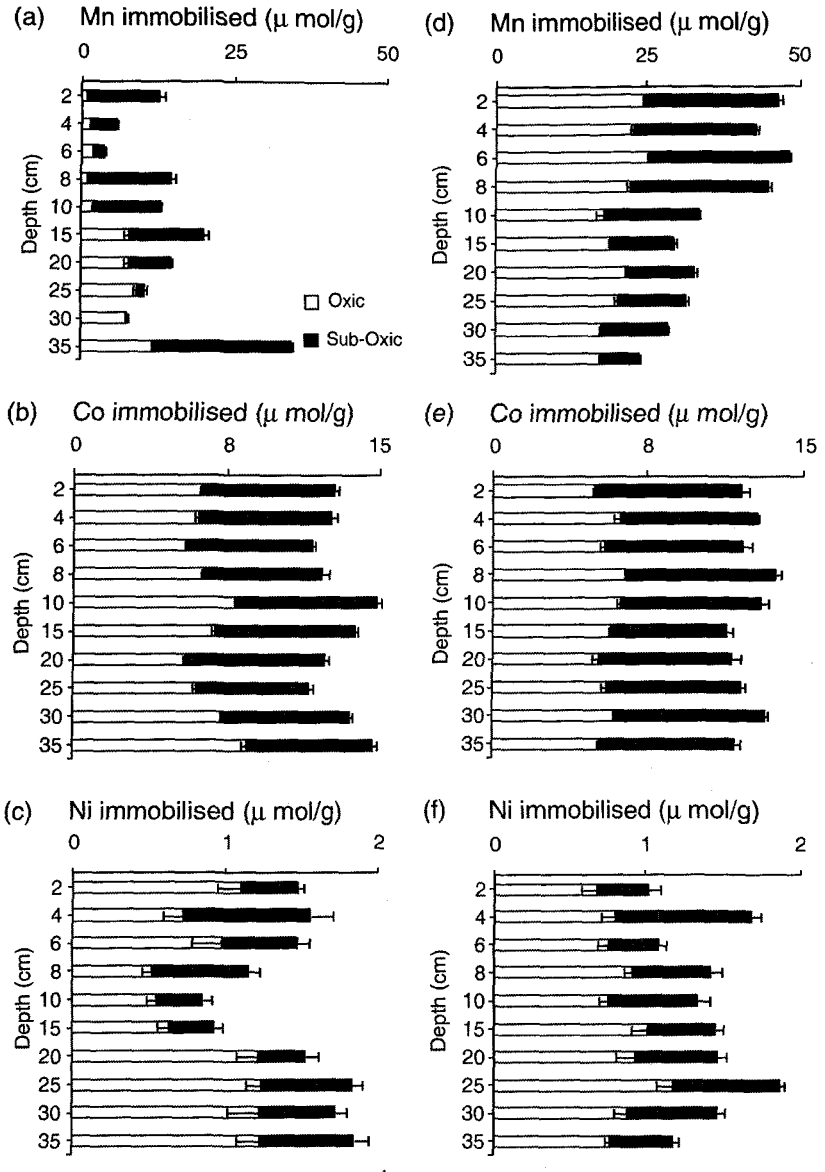

Figure 5. *Abiotic immobilisation* of metals ($\mu mol \cdot g^{-1}$ dry weight, mean ± SD, $n = 3$) in azide (10 mmol)-treated sediments as a function of depth. (a–c) The adsorption of metals in BC26, (d–f) the adsorption of metals in BC36. Error bars are shown on the left-hand side for oxic incubation and on the right-hand side for sub-oxic incubation.

Bryson and Drake [49] on energy-dependent Ni transport in bacteria and the chemo-organotrophic mode of nutrition in microorganisms in the presence of nutrients.

3.3.2. *Abiotic immobilisation*

It is again emphasised that abiotic immobilisation is less than biotic immobilisation, especially under sub-oxic conditions. The immobilisation profile of Mn was similar to that occurring under oxic conditions with a maximum of 22.5 ± 0.047 $\mu mol \cdot g^{-1}$ at 35 cm bsf (Figure 5a). Peaks in Co and Ni immobilisation of 6.97 ± 0.027 and 0.65 ± 0.012 $\mu mol \cdot g^{-1}$ were at 10 and 4 cm bsf,

respectively (Figure 5b,c). The distribution of Mn and Co did not match the organic carbon content of the sediment. The immobilisation detected at low levels in poisoned sediments suggests passive immobilisation on the Mn oxide phase. Our results agree with earlier reports on such trapping of metal ions by manganese oxides [50,51]. However, the immobilisation of Ni was less than Co and corresponded with the organic carbon (0.485%) content of the sediment. Thus, organic carbon in sediments might also complex with Ni and contribute to its immobilisation at a much lower rate than under biotic conditions. Such an association of Ni with organic carbon in sediments has been observed previously by Turner et al. [52] and Xue et al. [53].

3.4. *Immobilisation under oxic condition in BC36*

3.4.1. *Biotic immobilisation*

In this core, biotic immobilisation is greater than abiotic immobilisation, except in the case of Mn where it is the other way round. Under oxic conditions, immobilisation of all three metals was maximum at the sediment surface (2 cm bsf) and was lower than in BC26. The trend in the immobilisation was Co ($45 \pm 0.028\ \mu mol \cdot g^{-1}$) > Mn ($19.8 \pm 0.41\ \mu mol \cdot g^{-1}$) > Ni ($7 \pm 0.09\ \mu mol \cdot g^{-1}$), as shown in Figure 4d–f. The solid-phase concentrations of metal ions were Mn > Ni > Co. Thus, the depth at which maximum immobilisation occurred did not match with the depth that showed a maximum for the solid-phase concentration of metal ions. This suggests that the gradient of the metal concentration was more optimal for immobilisation at the surface than at the subsurface. The organic carbon content of the core was maximum (0.19%) at the surface and is related to the immobilisation of Mn with an r-value of 0.835 ($p < 0.01$), suggesting a mixotrophic mode of nutrition. The culturability of bacteria tolerant to Mn–Co–Ni was maximum (1.9 to $2.2 \times 10^5\ cfu \cdot g^{-1}$) within the 0–4 cm depth in multiple metal-amended plates. These observations suggest that microbially mediated immobilisation of the above metals in BC36 sediments is driven by the nutritive status of the sediment and the predominance of metal-tolerant bacteria. It is consistent with the observation of Dean-Ross and Mills [54], that groups of microbial communities that are relatively abundant in the sediment can utilise one or more aromatic compounds and are resistant to one or more heavy metals.

The microbial immobilisation of Co was synchronised with the maximum in Mn immobilisation. The yield of cultured Co-tolerant bacteria was positively related to TOC and yield of Ni-tolerant bacteria with r-values of 0.766 ($p < 0.01$) and 0.606 ($p < 0.05$), respectively. These relations suggest that Ni and Co immobilisation are mediated by the same microbes to a certain extent (36%) and 58% variation in both is dependent on the variation in TOC. The ability of Ni-resistant bacteria to immobilise Co is evident from previous experimental records [55]. However, Co and Ni immobilisation can be independent of Mn immobilisation and might occur by a process in which Ni-immobilising bacteria catalyse Co immobilisation and vice versa.

The immobilisation of Ni was comparatively lower than the other metals. However, the yield of cultured Ni-tolerant bacteria might correlate with the yield of Co-tolerant bacteria ($r = 0.606$, $p < 0.05$), suggesting that the same microbial communities are capable of immobilising both metals. These results agree with our recent reports [4,56] on Ni and Co immobilisation by Mn-oxidising bacterial isolates from the Indian Ridge system. TBC correlated positively ($r = 0.868$, $p < 0.001$) and TOC negatively with depth ($r = 0.666$, $p < 0.05$). These observations suggest that microbial abundance, the diversity of their metabolic activities and the number of metal-resistant bacteria in the sediment direct the immobilisation of Ni in BC36 sediments. Nonetheless, TOC in sediments were also found to influence the bioavailability of the metal in sediments. It is clear from the report of D'Hondt et al. [57] that organisms that depend on electron-accepting

pathways with higher standard free energies may have higher energy requirements than organisms that depend on pathways with lower standard free-energy yields.

3.4.2. *Abiotic immobilisation*

Although the prevailing environmental conditions in these sediments are appropriate for microbial immobilisation of Mn, abiotic immobilisation of the metal was higher than biotic immobilisation. It is suggested that processes that occur in these sediments could be more passive than active. The maximum immobilisation of Mn ($25.33 \pm 0.04\ \mu mol \cdot g^{-1}$) occurred at 6 cm depth (Figure 5d). Co and Ni immobilisation continued to remain higher under biotic conditions and showed maximum abiotic immobilisation of $6.43 \pm 0.011\ \mu mol \cdot g^{-1}$ for Co and $0.95 \pm 0.009\ \mu mol \cdot g^{-1}$ for Ni at 8 and 25 cm depth, respectively (Figure 5e,f). The immobilisation of metal ions did not relate with organic carbon or the natural concentration of the metal ions in sediments. The results suggest that immobilisation by abiotic processes is directed to changes with concentration of the metal and the availability of charged particle binding sites in sediments. Our results agree with a previous report [58] on trace metal binding to reactive sediment surfaces.

3.5. *Immobilisation under sub-oxic condition in BC36*

3.5.1. *Biotic immobilisation*

Unlike under oxic conditions, the immobilisation of Mn was maximum ($13.5 \pm 0.035\ \mu mol \cdot g^{-1}$) at the greater depth of 10 cm bsf. Co and Ni continued to show maximum immobilisation of 27.5 ± 0.54 and $6.6 \pm 0.075\ \mu mol \cdot g^{-1}$ at shallower depths of 6 and 8 cm bsf, respectively (Figure 4e,f). Thereafter, a gradual decrease in immobilisation was observed towards the bottom of the core. Earlier investigations [54] on bacterial-community composition and function along a heavy-metal gradient provide the explanation that bacteria are not exposed to the same concentrations of heavy metal *in situ* as in laboratory-prepared media. However, our study did not use laboratory-prepared organic media. Moreover, it simulates deep-sea conditions by avoiding any organic amendments and maintaining the temperature at $3 \pm 1\ °C$. Therefore, it is suggested that our results might reflect *in situ* trends to a certain extent. The maximum immobilisation of Mn and Ni coincided with peak culturability of heterotrophic bacteria and the solid-phase sediment concentration of metal ions.

The immobilisation of Mn showed a negative relationship with the yield of cultured Mn-tolerant bacteria ($r = 0.609$, $p < 0.05$). This suggests that the background concentration along with the amended Mn might be beyond the tolerance limit. The toxicity of excess Mn is evident from earlier studies [14, 59]. By contrast, the depth of the greatest Co immobilisation was synchronised with the maximum culturability of multiple metal-tolerant bacteria and the organic carbon content of the sediments. The immobilisation of Co showed correlation with the yield of cultured Mn-tolerant bacteria ($r = 0.677$, $p < 0.05$). The association of Co with Mn and its co-oxidation by Mn-oxidising microorganisms result in immobilisation. Our results agree with those of Lienemann et al. [60] on the oxidation of Co in association with Mn in aquatic systems. It is therefore inferred that the metal concentration in the sediment, its organic carbon content and the microorganisms present might govern the active immobilisation of metal ions.

3.5.2. *Abiotic immobilisation*

At this sampling site, abiotic immobilisation of metal ions is higher than the biotic immobilisation. Maximum immobilisation of Mn ($22.89 \pm 0.03\ \mu mol \cdot g^{-1}$) occurred at 6 cm, Co

($7.18 \pm 0.024\,\mu mol \cdot g^{-1}$) at 8 cm and Ni ($0.70 \pm 0.01\,\mu mol \cdot g^{-1}$) at 4 cm bsf (Figure 5). The depth of maximum immobilisation of Co matched that of maximum culturability of heterotrophic bacteria from the biotic samples. Also, the passive rates with the azide-treated sediments were much lower for Co and Ni than untreated samples. Similarly, depth of immobilisation of Ni coincided with the yield of cultured Ni-tolerant and Mn–Co–Ni-tolerant bacterial numbers in biotic samples. Results suggest that when used as a poison, azide restricts the active process of metal immobilisation by bacteria, but does not inhibit passive metal ion binding to the bacterial cell surfaces. Our results agree previous reports [61] that surface adsorption is possible even in non-viable cells, albeit at low levels. Heavy metals can be immobilised by metabolism-independent process on cell-surface components and charged particles in sediment, depending upon the milieu.

3.6. *Immobilisation under oxic vs. sub-oxic conditions*

Microbial immobilisation of metals under sub-oxic conditions was significantly higher ($p < 0.001$) in BC26 than in BC36 and was higher than in azide-treated controls. The trend in immobilisation was Co ($35 \pm 0.328\,\mu mol \cdot g^{-1}$) > Mn ($34.4 \pm 0.053\,\mu mol \cdot g^{-1}$) > Ni ($6.3 \pm 0.055\,\mu mol \cdot g^{-1}$) under oxic conditions, and Mn ($85.6 \pm 0.047\,\mu mol \cdot g^{-1}$) > Co ($46.3 \pm 0.29\,\mu mol \cdot g^{-1}$) > Ni ($6 \pm 0.08\,\mu mol \cdot g^{-1}$) under sub-oxic conditions. In BC36, the metal immobilisation was higher under oxic conditions. The trend in immobilisation was Co ($45 \pm 0.028\,\mu mol \cdot g^{-1}$) > Mn ($19.8 \pm 0.41\,\mu mol \cdot g^{-1}$) > Ni ($7 \pm 0.09\,\mu mol \cdot g^{-1}$) under oxic conditions and Co ($27.5 \pm 0.54\,\mu mol \cdot g^{-1}$) > Mn ($13.44 \pm 0.035\,\mu mol \cdot g^{-1}$) > Ni ($6.6 \pm 0.075\,\mu mol \cdot g^{-1}$) under sub-oxic conditions. The immobilisation rates of metals in these sediments were mostly Mn > Co > Ni. Generally, the immobilising rates of Mn and Co were greater at BC26 than at BC36, with the rates under sub-oxic conditions being higher than under oxic conditions. Such discernible differences were not seen in the case of Ni.

4. Summary and conclusions

From this study it is clear that the higher immobilisation of metals under sub-oxic conditions in the subsurface sediment was not greatly influenced by organic carbon, but rather by the higher availability of reduced metal ions. The significant differences in metal immobilisation between the experiment and poisoned controls probably indicate the involvement of both active and passive process of metal immobilisation in the experiment and the latter process only in the case of control. This study demonstrates that organic carbon content and the concentration of the bioavailable metals in sediments regulate microbial participation in metal immobilisation.

Acknowledgements

We are grateful to the Director, National Institute of Oceanography, Goa, for his encouragement. Dr. V.K. Banakar, Project Leader of the programme "Preliminary exploration of cobalt-rich seamount crusts in the northern Indian Ocean" funded by the Ministry of Earth Sciences, Government of India, kindly permitted SPP to participate and execute this work on board. The Project Leader, Dr R. Sharma and team members of the Polymetallic Nodules Environmental Impact Assessment Programme of the Ministry of Earth Sciences, Government of India are also thanked for the support of this work. The Chief Scientist, Dr N.H. Khadge, Captain, and Crew onboard *Akademic Boris Petrov* cruise no. 26 were extremely cooperative. Dr N.T. Manoj and M.P. Pawaskar helped in generating the map and Dr B.N. Nath and M.B.L. Mascarenhas-Pereira gave valuable suggestions. SPP and AD are indebted to all labmates for their positive support. The authors thank Ministry of Earth Sciences (Government of India), for funding. AD and SPP acknowledge the Council of Scientific and Industrial Research, New Delhi, India, for the award of Senior Research Fellowships. Comments from anonymous reviewers greatly improved the contents. This manuscript has NIO contribution number 4920.

References

[1] U. Forstner, *Inorganic sediment chemistry and elemental speciation*, in *Sediments: Chemistry and Toxicity of In-Place Pollutants*, R. Baudo, J. Giesy, and H. Muntau, eds., Lewis Publishers, Boca Raton, USA, 1990, pp. 61–73.

[2] T.J. Beveridge, J.D. Meloche, W.S. Fyfe, and R.G.E. Murray, *Diagenesis of metals chemically complexed to bacteria: laboratory formation of metal phosphates, sulfides, and organic condensates in artificial sediments*, Appl. Environ. Microbiol. 45 (1983), pp. 1094–1108.

[3] H. Brandl and M.A. Faramarzi, *Microbe–metal interactions for the biotechnological treatment of metal-containing solid waste*, China Particuology 4 (2006), pp. 93–97.

[4] P.P. Sujith, V.D. Khedekar, A.P. Girish, and P.A. Loka Bharathi, *Immobilization of nickel by bacterial isolates from the Indian ridge system and the chemical nature of the accumulated metal*, Geomicrobiol J. 27 (2010), pp. 424–434.

[5] H.L. Ehrlich, *Microbes and metals*, Appl. Microbiol. Biotechnol. 48 (1997), pp. 687–692.

[6] W.A. Corpe, *Metal-binding properties of surface materials from marine bacteria*, Dev. Ind. Microbiol. 16 (1975), pp. 249–255.

[7] F.G. Ferris, W.S. Fyfe, and T.J. Beveridge, *Bacteria as nucleation sites for authigenic minerals in a metal-contaminated lake sediment*, Chem. Geol. 63 (1987), pp. 225–232.

[8] D. Fortin, B. Davis, G. Southam, and T.J. Beveridge, *Biogeochemical phenomena induced by bacteria within sulfidic mine tailings*, J. Ind. Microbiol. Biotechnol. 14 (1995), pp. 178–185.

[9] W.E. Razzell and P.C. Trussell, *Microbiological leaching of metallic sulfides*, Appl. Environ. Microbiol. 11 (1963), pp. 105–110.

[10] D. Fortin, G. Southam, and T.J. Beveridge, *Nickel sulfide, iron–nickel sulfide and iron sulfide precipitation by a newly isolated* Desulfotomaculum *species and its relation to nickel resistance*, FEMS Microbiol. Ecol. 14 (1994), pp. 121–132.

[11] G. Basnakova and L.E. Macaskie, *Bioaccumulation of nickel by microbially-enhanced chemisorption into polycrystalline hydrogen uranyl phosphate*, Biotechnol. Lett. 18 (1996), pp. 257–262.

[12] S. Glasauer, S. Langley, and T.J. Beveridge, *Intracellular manganese granules formed by a subsurface bacterium*, Environ. Microbiol. 6 (2004), pp. 1042–1048.

[13] Z. Shao and F. Sun, *Intracellular sequestration of manganese and phosphorus in a metal-resistant fungus* Cladosporium cladosporioides *from deep-sea sediment*, Extremophiles. 11 (2007), pp. 435–443.

[14] S.O. Fernandes, K.P. Krishnan, V.D. Khedekar, and P.A. Loka Bharathi, *Manganese oxidation by bacterial isolates from the Indian ridge system*, Biometals. 18 (2005), pp. 483–492.

[15] K.W. Mandernack, J. Post, and B.M. Tebo, *Manganese mineral formation by bacterial spores of the marine* Bacillus, *strain SG-1: evidence for the direct oxidation of Mn(II) to Mn(IV)*, Geochim. Cosmochim. Acta 59 (1995), pp. 4393–4408.

[16] M.T. Schaanning, K. Hylland, D.O. Eriksen, T.D. Bergani, J.S. Gunnarson, and J. Skei, *Interactions between eutrophication and contaminants. II. Mobilization and bioaccumulation of Hg and Cd from marine sediments*, Mar. Pollut. Bull. 33 (1996), pp. 71–79.

[17] H.L. Ehrlich, *Conditions for bacterial participation in the initiation of Mn deposition around marine sediment particles*, in *Environmental Biogeochemistry and Geomicrobiology*, W.E. Krumbein, ed., Ann Arbor Science, Michigan, USA, 1978, pp. 839–845.

[18] H.L. Ehrlich, *Enhanced removal of Mn^{2+} from seawater by marine sediments and clay minerals in the presence of bacteria*, Can. J. Microbiol. 28 (1982), pp. 1389–1395.

[19] M.B.L. Mascarenhas-Pereira, B.N. Nath, D.V. Borole, and S.M. Gupta, *Nature, source and composition of volcanic ash in sediments from a fracture zone trace of Rodriguez Triple Junction in the Central Indian Basin*, Mar. Geol. 229 (2006), pp. 79–90.

[20] B.N. Nath, I. Roelandts, M. Sudhakar, and W.I. Plüger, *Rare earth element patterns of the Central Indian Basin sediments related to their lithology*, Geophys. Res. Lett. 19 (1992), pp. 1197–1200.

[21] Das A, C.E.G. Fernandes, S.S. Naik, B.N. Nath, I. Suresh, M.B.L. Mascarenhas-Pereira, S.M. Gupta, N.H. Khadge, C. Prakash Babu, D.V. Borole, P.P. Sujith, A.B. Valsangkar, B.S. Mourya, S.U. Biche, R. Sharma, and P.A. Loka Bharathi, *Bacterial response to contrasting sediment geochemistry in the Central Indian Basin*, Sedimentology 58 (2011), pp. 756–784.

[22] V.K. Banakar, G. Parthiban, J.N. Pattan, and P. Jauhari, *Chemistry of surface sediment along a north-south transect across the equator in the Central Indian Basin: an assessment of biogenic and detrital influences on elemental burial on the seafloor*, Chem. Geol. 147 (1998), pp. 217–232.

[23] A. Stockdale, W. Davison, H. Zhang, and J. Hamilton-Taylor, *The association of cobalt with iron and manganese (oxyhydr)oxides in marine sediment*, Aquat. Geochem. 16 (2010), pp. 575–585.

[24] J.E. Hobbie, R.J. Daley, and S. Jasper, *Use of nucleopore filters for counting bacteria by fluorescent microscopy*, Appl. Environ. Microbiol. 3 (1977), pp. 1225–1228.

[25] R.L. Patience, C.J. Clayton, A.T. Kearsley, S.J. Rowland, A.N. Bishop, A.W.G. Rees, K.G. Bibby, and A.C. Happer, *An integrated biochemical, geochemical and sedimentological study of organic diagenesis in sediments from ODP LEG 112*, Proc. ODP Sci. Repts, 1990.

[26] S.M. Gupta and P. Jauhari, *Radiolarian abundance and geochemistry of the surface-sediments from the Central Indian Basin: inferences to Antarctic bottom water current*, Curr. Sci. 66 (1994), pp. 659–663.

[27] P. Roy, V. Balaram, A. Kumar, M. Satyanarayanan, and T.G. Rao, *New REE and trace element data on two kimberlitic reference materials by ICP-MS*, Geostand. Geoanal. Res. 31 (2007), pp. 261–273.
[28] M. P. Colombini and R. Fuoco, *Determination of manganese at ng/ml levels in natural waters by differential pulse polarography*, Talanta 30 (1983), pp. 901–905.
[29] J.A. Herrera-Melian, J.M. Dona-Rodriguez, J. Hernandez-Brito, and J.P. Pena, *Voltammetric determination of Ni and Co in water samples*, J. Chem. Educ. 74 (1997), pp. 1444–1445.
[30] C.S. Chin, K.S. Johnson, and K.H. Coale, *Spectrophotometric determination of dissolved manganese in natural waters with 1-(2-pyridylazo)-2-naphthol: application to analysis in situ in hydrothermal plumes*, Mar. Chem. 37 (1992), pp. 65–82.
[31] R. Chester and M.J. Hughes, *Scheme for the spectrophotometric determination of Cu, Pb, Ni, V and Co in marine sediments*, Trans. I. Min. Metal. B 77 (1968), pp. 37–41.
[32] H. Zhang, W. Davison, R.J.G. Mortimer, M.D. Krom, P.J. Hayes, and I.M. Davies, *Localised remobilization of metals in a marine sediment*, Sci. Total. Environ. 296 (2002), pp. 175–187.
[33] J.N. Pattan and A.V. Mudholkar, *The oxidation state of manganese in ferromanganese nodules and deep-sea sediments from the Central Indian Ocean*, Chem. Geol. 85 (1990), pp. 171–181.
[34] V.K. Banakar, S.M. Gupta, and V.K. Padmavathi, *Abyssal sediment erosion in the Central Indian Basin: evidence from radiochemical and radiolarian studies*, Mar. Geol. 96 (1991), pp. 167–173.
[35] A.V. Mudholkar, J.N. Pattan, and G. Parthibhan, *Geochemistry of deep sea sediment cores from the Central Indian Ocean Basin*, Ind. J. Mar. Sci. 22 (1993), pp. 241–246.
[36] B. Sundby, L.G. Anderson, P.O.J. Hall, and A. Iverfeldt, *The effect of oxygen on release and uptake of cobalt, manganese, iron and phosphate at the sediment–water interface*, Geochim. Cosmochim. Acta 50 (1986), pp. 1281–1288.
[37] G.P. Glasby, *Manganese: predominant role of nodules and crusts*, in *Marine Geochemistry*, H.D. Schulz and M. Zabel, eds., Springer, Berlin, 2006, pp. 371–427.
[38] Y. Lee and B.M. Tebo, *Cobalt(II) oxidation by the marine manganese(II)-oxidizing* Bacillus *sp. strain SG-1*, Appl. Environ. Microbiol. 60 (1994), pp. 2949–2957.
[39] J.W. Moffett and J. Ho, *Oxidation of cobalt and manganese in seawater via a common microbially catalyzed pathway*, Geochim. Cosmochim. Acta 60 (1996), pp. 3415–3424.
[40] M.J. McInerney, *Energetics and kinetics of anaerobic aromatic and fatty acid degradation*, Report prepared for the US Department of Energy, Oklahoma, 1993.
[41] R.D. Stoppel and H.G. Schlegel, *Nickel-resistant bacteria from anthropogenically nickel-polluted and naturally nickel-percolated ecosystems*, Appl. Environ. Microbiol. 61 (1995), pp. 2276–2285.
[42] P.J. Muller, M. Hartmann, and E. Suess, *The chemical environment of pelagic sediments*, in *The Manganese Nodule Belt of the Pacific Ocean, Geological Environment, Nodule Formation, and Mining Aspects*, P. Halbach, G. Friedrich, and U. von Stackelberg, eds., Enke Verlag, Stuttgart, 1988, pp. 70–99.
[43] A.L. Mills and R.R. Colwell, *Microbiological effects of metal ions in Chesapeake Bay water and sediment*, Bull. Environ. Contam. Toxicol. 18 (1977), pp. 99–103.
[44] J.F. Timoney, J. Port, J. Giles, and J. Spanier, *Heavy metal and antibiotic resistance in the bacterial flora of sediments of New York Blight*, Appl. Environ. Microbiol. 36 (1978), pp. 465–472.
[45] C. Houba and J. Remacle, *Composition of the saprophytic bacterial communities in freshwater systems contaminated by heavy metals*, Microb. Ecol. 6 (1980), 55–69.
[46] T. Duxbury, and B. Bicknell, *Metal-tolerant bacterial populations from natural and metal-polluted soils*, Soil Biol. Biochem. 15 (1983), pp. 243–250.
[47] S.G. Hornor and B.A. Hilt, *Distribution of zinc-tolerant bacteria in stream sediments*, Hydrobiologia 128 (1985), pp. 155–160.
[48] P. Jasper and S. Silver, *Magnesium transport in microorganisms*, in *Microorganisms and Minerals*, E.D. Weinberg, ed., Marcel Dekker, New York, 1977, pp. 7–47.
[49] M.F. Bryson and H.L. Drake, *Energy-dependent transport of nickel by* Clostridium pasteurianum, J. Bacteriol. 170 (1988), pp. 234–238.
[50] P.N. Froelich, G.P. Klinkhammer, M.L. Bender, G.R. Heath, D. Cullin, P. Dauphin, D. Hammond, B. Hartman, and V. Maynard, *Early oxidation of organic matter in pelagic sediments of the eastern equatorial Atlantic; suboxic diagenesis*, Geochim. Cosmochim. Acta 43 (1979), pp. 1075–1090.
[51] T. Shaw, J. Gieskes, and R. Jahnke, *Early diagenesis in differing depositional environments: the response of transition metals in pore water*, Geochim. Cosmochim. Acta 54 (1990), pp. 1233–1246.
[52] A. Turner, M. Nimmo, and K.A. Thuresson, *Speciation and sorptive behaviour of nickel in an organic-rich estuary (Beaulieu, UK)*, Mar. Chem. 63 (1998), pp. 105–118.
[53] H.B. Xue, S. Jansen, A. Prasch, and L. Sigg, *Nickel speciation and complexation kinetics in freshwater by ligand exchange and DPCSV*, Environ. Sci. Technol. 35 (2001), pp. 539–546.
[54] D. Dean-Ross and A.L. Mills, *Bacterial community structure and function along a heavy metal gradient*, Appl. Environ. Microbiol. 55 (1989), pp. 2002–2009.
[55] T. Schmidt and H.G. Schlegel, *Nickel and cobalt resistance of various bacteria isolated from soil and highly polluted domestic and industrial wastes*, FEMS Microbiol. Ecol. 62 (1989), pp. 315–328.
[56] R. Antony, P.P. Sujith, S.O. Fernandes, P. Verma, V.D. Khedekar, and P.A. Loka Bharathi, *Cobalt immobilization by manganese oxidizing bacteria from the Indian Ridge system*, Curr. Microbiol. 62 (2011), pp. 840–849.
[57] S. D'Hondt, B.B. Jørgensen, D.J. Miller, A. Batzke, R. Blake, B.A. Cragg, H. Cypionka, G.R. Dickens, T. Ferdelman, K. Hinrichs, N.G. Holm, R. Mitterer, A. Spivack, G. Wang, B. Bekins, B. Engelen, K. Ford, G. Gettemy,

S.D. Rutherford, H. Sass, C.G. Skilbeck, I.W. Aiello, G. Guerin, C.H. House, F. Inagaki, P. Meister, T. Naehr, S. Niitsuma, R.J. Parkes, A. Schippers, D.C. Smith, A. Teske, J. Wiegel, C.N. Padilla, and J.L.S. Acosta, *Distributions of microbial activities in deep subseafloor sediments*, Science 306 (2004), pp. 2216–2221.

[58] B.T. Hart, *Uptake of trace metals by sediments and suspended particulates: a review*, Hydrobiologia 91 (1982), pp. 299–313.

[59] H.Y. Cheung, L. Vitkovic, and M.R.W. Brown, *Toxic effect of manganese on growth and sporulation of* Bacillus stearothermophilus, J. Gen. Microbiol. 128 (1982), pp. 2345–2402.

[60] C.P. Lienemann, M. Taillefert, D. Perret, and J.F. Gaillard, *Association of cobalt and manganese in aquatic systems: chemical and microscopic evidence*, Geochim. Cosmochim. Acta 61 (1997), pp. 1437–1446.

[61] K. Kuroda, and M. Ueda, *Bioadsorption of cadmium ion by cell surface-engineered, yeasts displaying metallothionein and hexa-His*, Appl. Microbiol. Biotechnol. 63 (2003), pp. 182–186.

Progress in Molecular and Subcellular Biology
Marine Molecular Biotechnology

Werner E. G. Müller *Editor*

Molecular Biomineralization

Aquatic Organisms Forming Extraordinary Materials

Springer

Chapter 3
Manganese Oxidation by Bacteria: Biogeochemical Aspects

P.P. Sujith and P.A. Loka Bharathi

Contents

Abstract Manganese is an essential trace metal that is not as readily oxidizable like iron. Several bacterial groups posses the ability to oxidize Mn effectively competing with chemical oxidation. The oxides of Mn are the strongest of the oxidants, next to oxygen in the aquatic environment and therefore control the fate of several elements. Mn oxidizing bacteria have a suit of enzymes that not only help to scavenge Mn but also other associated elements, thus playing a crucial role in biogeochemical cycles. This article reviews the importance of manganese and its interaction with microorganisms in the oxidative Mn cycle in aquatic realms.

P.A. Loka Bharathi (✉)
National Institute of Oceanography (Council of Scientific and Industrial Research), Dona Paula, Goa 403 004, India
e-mail: loka@nio.org

W.E.G. Müller (ed.), *Molecular Biomineralization*, Progress in Molecular and Subcellular Biology 52, DOI 10.1007/978-3-642-21230-7_3,

3.1 Introduction

Manganese comprises about 0.1% of the total mass of the Earth (Nealson 1983) and occurs as $MnAl_2O_4$ (Zajic 1969). It is the fifth most abundant transition metal in the Earth's crust (Tebo et al. 2007) and is the second most common trace metal after iron (Tebo et al. 1997). The name manganese is derived from the Greek word mangania, meaning magic (Horsburgh et al. 2002). It occupies the 25th position in the periodic table and belongs to group VII transition elements (Cellier 2002). Mn exist in seven different oxidation states ranging from 0 to +7 and in nature it occurs in +II, +III, and +IV oxidation states (Tebo et al. 1997, 2004). Mn^{2+} has an ionic radius of 0.80 A° and has Gibbs standard energy of −54.5 $\Delta G°$ in aqueous solutions (Hem 1978). It occurs at a concentration of 100–1000 ppm in river, 1–10 ppm in ground water (Nealson 1983), and averages 8 μg kg^{-1} in freshwater and 0.2 μg kg^{-1} in seawater (Bowen 1979 and Ehrlich 2002a). The concentration of dissolved Mn (Mn^{2+}) in the open ocean ranges from 0.2–3 nmol kg^{-1} of seawater (Glasby 2006). Further details about its distribution and abundance are shown in Fig. 3.1. As Mn exists at a higher redox potential than iron, following comparisons can be made on Mn–Fe relationships. (1) Mn reduces more easily than iron, (2) Mn is harder to oxidize than iron, and (3) Soluble Mn (Mn^{2+}) occurs at a somewhat higher level in the oxygen gradient than iron (Kirchner and Grabowski 1972). Mn enrichment occurs as a result of both artificial and natural processes. The sources of Mn in the ocean are atmospheric input, intense scavenging at mid-depth, and fluxes from reducing shelf and slope sediments and emanations from submarine hydrothermal vents (Saager et al. 1989). This study focuses on the bacterial groups that participate in Mn oxidation and the recent advancements made in the field of metal–microbe interaction. It also delves into genomic and proteomic aspects covering both freshwater and marine systems. Lastly, the review addresses the bacterial contribution to mineral formation and their potential use in biotechnological applications.

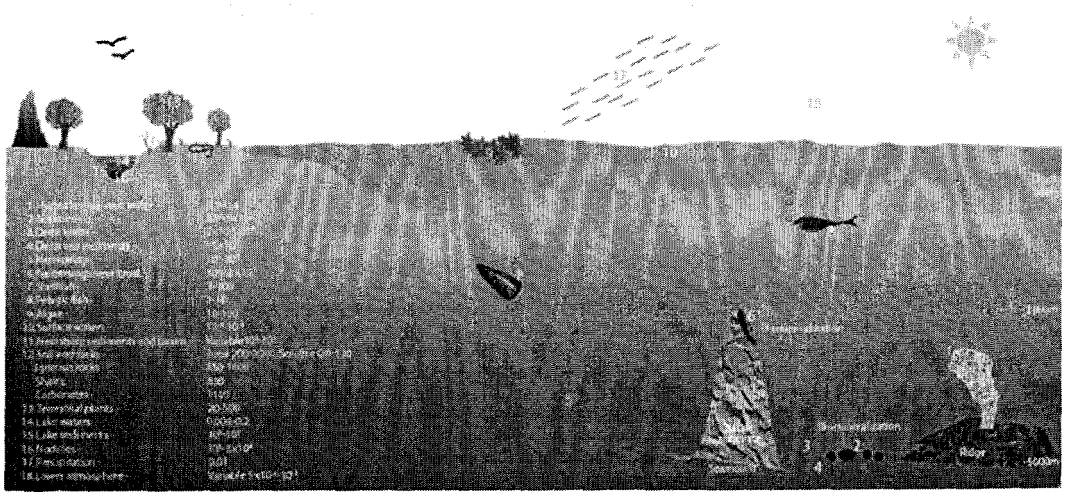

Fig. 3.1 Concentrations of manganese in different environments in ppm (*modified from Nealson* 1983)

3.2 Importance of Manganese

Manganese is a critical trace nutrient required for the growth and survival of many living organisms. It is essential for oxygenic photosynthesis in cyanobacteria (Yocum and Pecoraro 1999; Keren et al. 2002; Ogawa et al. 2002), redox reactions, protection from toxic metals, UV light, predation or, viruses, scavenging of micronutrient trace metals, breakdown of natural organic matter into metabolizable substrates, maintenance of an electron-acceptor reservoir for use in anaerobic respiration, oxygen production, and protection against oxidative stress in bacteria (Christianson 1997; Spiro et al. 2010). It is important for general metabolism, carbohydrate metabolism, and for both anabolic and catabolic functions in anaerobiosis and aerobiosis (Crowley et al. 2000). It is a part of four metalloenzymes manganese superoxide dismutase (MnSOD), mangani-catalase, arginase, and O-phosphatases (Christianson 1997; Shi 2004). Mn^{2+} containing O-phosphatases are involved in controlling spore formation, stress-response, cell density during stationary phase, carbon and nitrogen assimilation, vegetative growth, development of fruiting bodies, and cell segregation (Shi 2004). Additionally, nonenzymatic Mn^{2+} is crucial for the proper functioning of a variety of bacterial products, including secreted antibiotics (Archibald 1986). It also contributes to the stabilization of bacterial cell walls (Doyle 1989) and plays an important role in bacterial signal transduction (Jakubovics and Jenkinson 2001). Mn^{2+} is required for the stimulation of poly-β-hydroxybutyrate oxidation in *Sphaerotilus discophorous* (Stokes and Powers 1967) and exopolysaccharides (EPS) production in *Rhizobium meliloti* JJ-1 (Appanna 1988). Being a part of an enzyme in glycolysis, Mn^{2+} is required for the activity of 3-phosphoglycerate mutase in several endospore-forming gram-positive bacteria (Chander et al. 1998). Indirectly, Mn functions in controlling nutrient availability in freshwater, most significantly by complexing with iron (Kirchner and Grabowski 1972).

3.3 Biogeochemistry of Manganese

The geochemistry of Mn is a complex pattern of mutually exclusive chemical reactions of oxidation and reduction (Kirchner and Grabowski 1972). The geochemical behavior of Mn differs in environment which shows gradation in oxygen profile (Roitz et al. 2002). Mn occurs as highly soluble Mn^{2+} in oxygen-deficient settings and as insoluble oxyhydroxides under well-oxygenated conditions (Calvert and Pedersen 1996). The concentration of soluble Mn in the environments varies with change in redox condition and the group of microorganisms present. The oxidation of Mn by microorganisms results in decrease in the dissolved Mn^{2+} concentration of metal and increase in the particulate/higher oxidation states (Mn^{3+} and Mn^{4+}) of Mn (Ehrlich 1976, 1978). Redox transitions between soluble Mn^{2+} ions and insoluble Mn^{3+} and Mn^{4+} oxides form the backbone of aquatic

biogeochemistry of Mn (Sunda and Huntsman 1990). Mn^{3+} being a strong oxidant and a reductant, it has been largely ignored due to its property to disproportionate to Mn^{2+} and MnO_2 (Johnson 2006). However, recent improvements in the understanding of Mn chemistry indicate that dissolved Mn exist mostly as Mn^{3+} in sub-oxic regions (Trouwborst et al. 2006). Mn being one of the strongest oxidant in the natural environment, eventually participates in redox reactions and due to its sorptive characteristics controls the distributions and bioavailability of several toxic and essential trace elements (Tebo et al. 2004). Microorganisms like bacteria and fungi are known oxidizers of Mn^{2+} and reducers of Mn oxide-containing minerals. They carry out oxidation/reduction of Mn as a way to conserve energy for growth or oxidation of carbon (Nealson and Myers 1992; Tebo et al. 2005). The oxidation of Mn^{2+} under natural conditions is catalyzed only by microbes under pH range of 5.5–8.0, Eh value above +200 mV and oxygen concentration of 3–5 mg L^{-1} (Schweisfurth et al. 1978).

The three representative stoichiometric relationships that typically follow the oxidation of Mn^{2+} depending on the oxide product formed according to Nealson et al. (1988) are

$$Mn^{2+} + \frac{1}{2}O_2 + H_2O \rightarrow MnO_2 + 2H^+$$

$$Mn^{2+} + \frac{1}{4}O_2 + \frac{3}{2}H_2O \rightarrow MnOOH + 2H^+$$

$$3Mn^{2+} + \frac{1}{2}O_2 + 3H_2O \rightarrow Mn_3O_4 + 6H^+$$

A number of bacteria capable of mixotrophic and autotrophic growth could derive useful energy from Mn^{2+} oxidation. The oxidation of Mn^{2+} by bacteria could yield ΔF_r of +2.79 and $\Delta F'_r$ of −16.31 kcal (Ehrlich 1976, 1978) in the reaction

$$Mn^{2+} + \frac{1}{2}O_2 + H_2O \rightarrow MnO_2 + 2H^+$$

and yield ΔG −18.5 kcal in the reverse reaction

$$MnO_2 + 4H^+ + 2e \rightarrow Mn^{2+} + 2H_2O$$

when allowance for physiological pH of 7.0 is made (Ehrlich 1987).

The key steps in the reduction of Mn^{4+} to Mn^{2+} involve the reactions of strongly bound Mn^{3+} $\{\{Mn^{3+}\}\}$ and weakly bound Mn^{2+} $\{Mn^{2+}\}$ on the surface of MnO_2 (Ehrlich 2002b). The following steps explain the process

$$\{Mn^{2+}\} + MnO_2 + 2H_2O \rightarrow 2\{\{Mn^{3+}\}\} + 4OH^-$$

$$2\{\{Mn^{3+}\}\} + 2e^- \rightarrow \{Mn^{2+}\} + Mn^{2+}$$

The reduction of Mn oxide is predicted based on standard redox potential of +1.29 mV (Rusin and Ehrlich 1995) based on the equation

$$\frac{1}{2}MnO_2 + 2H^+ + e^- \rightarrow \frac{1}{2}Mn^{2+} + H_2O$$

In environment where Mn and iron oxides coexist such as in ferromanganese nodules, bacteria preferentially attack manganese oxides. The possible explanation suggested for the preference of Mn over Fe by bacteria was the lower midpoint potential for the Fe(III)/Fe(II) couple relative to the Mn(IV)/Mn(II) couple (Ehrlich 1987). However, the exact reason is yet to be determined.

3.4 Effect of Salinity on Manganese Oxidation

The solubility of Mn is more in freshwater compared to salt water. However, the oxidation rate of Mn^{2+} decreased sixfold in creek water of an English estuary when the salinity of water increased from 1 to 5 (Vojak et al. 1985). Likewise, Spratt et al. (1994b) also demonstrated a fourfold decrease in the rates of manganese oxide production in high marsh sediments than in creek bank sediments. In another study, Spratt et al. (1994a) showed decrease in rate of Mn oxidation in high marsh sediments experimentally exposed to hypersaline (102) conditions. They demonstrated that Mn oxidation in creek bank sediments exhibit much higher rates of oxidation than high marsh sites (2.31 $\pm$ 0.28 and 0.45 $\pm$ 0.14 nmol mg dwt^{-1} h^{-1}). In mangrove swamp estuary, highest rates of microbial Mn oxide production was encountered in sediments with salinities between 0 and 8 (50–119 pmol mg dwt^{-1} h^{-1}, respectively) compared with sediments from the mouth of the estuary with salinities of 24 and 34 (3–16 pmol mg dwt^{-1} h^{-1}, respectively). Nevertheless, the overall rates of microbial Mn oxide production in salt-marsh sediments were much higher than in mangrove sediments.

3.5 Toxicity of Manganese in the Presence of Other Metals

In an undisturbed marine environment, metal ions are more likely to occur in combinations than in single (Yang and Ehrlich 1976). The microbial response to individual metals may differ from the response to stress from multiple metals. When interactions of one metal have a protective effect on the toxicity of other metal, the resulting effect is referred as antagonistic and the reverse effect where toxicity of one metal is enhanced in the presence of the other metal is synergistic. Third, interactions where the final toxicity is simply a sum of the individual toxicities of the metal ions is called additive (Babich and Stotzky 1983). The effect of Mn, Ni, Cu, and Co in combinations of 10 μg mL^{-1} in seawater enriched with 1% glucose and 0.05%

peptone at 18°C showed different toxic effects (Yang and Ehrlich 1976). Mn and Co when tested alone had no effect on growth but their combination did. The combination of Co and Ni was more toxic than Co alone but less toxic than Ni alone. Cu was comparatively more toxic than other metals. Its toxicity was slightly relieved by Co or by the combination of Co and Mn, or Co, Mn, and Ni, but by no other metal combinations tried. The mixtures of Mn and Ni and of Mn, Co, and Ni were more toxic than their individual components. Likewise, Appanna et al. (1996) demonstrated the influence of Mn, Co, Cs, and Ni on the ability of *Pseudomonas fluorescens* to adapt to and to decontaminate the multiple-metal environment. There the toxicity of metals was comparatively lower in multiple-metal combinations than when individual metals were tested. Mn was the least toxic followed by Cs, Co, and Ni. Cs and Mn did not alter the cellular yield significantly; however, Ni and Co showed marked inhibitory effect on bacterial growth.

A study on redox transformation of Mn in Antarctic lakes (Krishnan et al. 2009) showed maximum stimulation of Mn oxidation (81 ± 57 ppb d^{-1}) in Lister Hooded (LH) strains with Mn–Co combination rather than combinations of Fe (37 ± 16 ppb d^{-1}) and Ni (40 ± 47 ppb d^{-1}), suggesting the role of Co in Mn oxidation. Conversely, maximum stimulation of Mn reduction occurred in combinations of the metals containing Ni. The rates were >50 ppb d^{-1} with strain LH-11 and >125 ppb d^{-1} with strain LH-8 in combinations of Mn–Ni and Mn–Fe–Ni which suggest the critical role of Ni in Mn reduction.

3.6 Manganese Oxidation by Marine Bacteria

The oxidation of Mn^{2+} by marine bacteria is more versatile. Dick et al. (2008a) have shown that *Aurantimonas* sp. Strain SI85-9A1, a marine α-proteobacterium, contain genes for organoheterotrophy, methylotrophy, oxidation of sulfur and carbon monoxide, the ability to grow over a wide range of oxygen concentrations, and the complete Calvin cycle for carbon fixation. In an early study, Ehrlich (1963) observed that bacteria in Mn nodules can enhance the adsorption of Mn^{2+} from seawater in the presence of peptone. He proposed that bacteria play a crucial role in nodule development. Besides, Mn^{2+} oxidation by cell-free extract from a Mn nodule bacterium *Arthrobacter* 37 was found to be mediated by enzyme activity (Ehrlich 1968). The rate of oxidation of free Mn^{2+} by the enzyme depended on the concentration of cell-free extract used. In another study on the effect of temperature and pressure on *Arthrobacter* 37, Ehrlich (1971) demonstrated that at 5°C, temperature optimum for Mn^{2+} oxidation increases with pressure and the effect of pressure on cells can be counteracted by an appropriate increase in temperature. Further, Arcuri and Ehrlich (1979) stated the involvement of cytochrome in Mn^{2+} oxidation by two marine bacteria. With the use of conventional electron transport chain, the bacterium could derive useful energy from Mn^{2+} oxidation by oxidative phosphorylation. By a detailed observation of bacteria that catalyze Mn^{2+} oxidation, Ehrlich (1980) postulated that two groups of Mn^{2+}-oxidizing bacteria exist, one that acts on

free Mn (Mn^{2+}) and the other that acts only on Mn^{2+} bound to Mn(IV) oxide and derive energy from the reaction. At the same time, Arcuri and Ehrlich (1980) proposed that cytochromes were involved in Mn^{2+} oxidation by *Oceanospirillum* BIII 45. They could observe that addition of periplasmic/intracellular fraction to membrane fraction was essential for Mn oxidation. Yet in another study on the removal efficiency of Mn^{2+} from seawater by marine sediments and clay minerals with the same organism, Ehrlich (1982) observed that ferric chloride pretreatment of clays is essential when intact cells are used and not when cell-free extracts are used. He remarked that ferric chloride pretreatment was necessary for activating the sediment for bacterial oxidation of sorbed Mn^{2+}.

Another interesting observation on Mn^{2+} oxidation by bacterial isolates from hydrothermal area (Ehrlich 1983) showed that Mn^{2+} oxidation could occur through an inducible enzyme system and an initial fixation of Mn(II) to Mn(IV) oxide was not essential for oxidation to proceed. Our earlier observation on the bacteriology of Fe–Mn nodules from the Indian Ocean region showed that psychrotrophic heterotrophic bacteria were capable of mobilizing and immobilizing Mn. The maximum percentage of Mn oxidizers (32.2%) was restricted to nodule surface and possessed various hydrolytic enzymes (Chandramohan et al. 1987). Later on, Ehrlich and Salerno (1990) demonstrated the coupling of ATP synthesis with that of Mn^{2+} oxidation by a marine bacterial strain SSW22. They proposed chemiosmosis (diffusion of ions across a selectively permeable membrane) as the probable mechanism for energy coupling by intact cells, membrane vesicles, or cell extracts.

In a different study, Rosson and Nealson (1982) observed that live/killed mature spores of *Bacillus* Strain SG-1 could oxidize Mn^{2+} once bound but not when free in solution. They hypothesized that Mn^{2+} may form complex with exosporium or a spore coat protein. In another observation, Kepkay and Nealson (1982) identified that spores rather than vegetative cells are responsible for Mn^{2+} oxidation by SG-1. The adherence of bacterial cells to solid surfaces was found to be essential for proper sporulation and Mn^{2+} oxidation. Using radiotracers, Emerson et al. (1982) explained that Mn^{2+} oxidation in Saanich Inlet is bacterially mediated and the removal of Mn^{2+} is very fast and would occur in a matter of few days on solid surfaces. The study on the role of plasmids in Mn^{2+} oxidation (Lidstrom et al. 1983; Schuett et al. 1986) showed that in marine *Pseudomonads*, increased levels of both binding and oxidation of Mn^{2+} could occur in the presence of plasmids. Using radiotracers, Tebo et al. (1984) provided evidence for Mn^{2+} oxidation with oxygen as the terminal electron acceptor in Saanich Inlet and Framvaren Fjord. The Mn^{2+} oxidation was found to occur faster under air-saturated condition than under conditions of oxygen limitation. Interestingly, Rosson et al. (1984) using poisoned control could differentiate biological from abiotic Mn^{2+} oxidation and demonstrated that bacteria could significantly enhance the rate of Mn^{2+} removal from manganese-rich particulate layer in the water column. Further, by in situ experimental evidence on Mn^{2+} oxidation in Saanich Inlet, Tebo and Emerson (1985) showed that the rate of Mn^{2+} oxidation was limited by both oxygen and the concentration of microbial binding sites in the environment. In a study on Mn^{2+} removal from porewater, Edenborn et al. (1985) observed that Mn^{2+} removal rate is

(Ghiorse and Hirsch 1979; Sly et al. 1990). The mechanism of Mn^{2+} oxidation was found to involve a two-step process composed of rapid binding of Mn^{2+} to EPS followed by the oxidation of Mn^{2+} by an unknown factor (Ghiorse and Hirsch 1979). Incidentally, they could identify the unusual factor, perhaps a protein responsible for Mn^{2+} oxidation associated with the polymer that could not be completely inhibited by glutaraldehyde, $HgCl_2$, or heat. Further findings using inhibitors and cellular fractionation methods (Larsen et al. 1999) showed that heat treatment of cells could enhance Mn^{2+} binding but abolish Mn-oxidizing activity. They could restore the activity of the enzyme upon the addition of Cu in the medium and suggested that Cu-dependent enzyme MCOs catalyze the Mn^{2+} oxidation in *Pedomicrobium* ACM 3067.

Jaquet et al. (1982) indicated that *Metallogenium* plays a key role in Mn cycling in Lake Leman. In contrast, Maki et al. (1987) using ^{54}Mn tracer could not find any significant difference between poisoned and non-oxygen controls in the biological Mn^{2+} oxidation and the number of *Metallogenium* morphotypes in Lake Washington. They suggested that *Metallogenium* plays only a weak role in Mn^{2+} oxidation in Lake Washington. In a discussion on the retention of Mn in the Wahnbach reservoir by bacteria, Herschel and Clasen (1998) state that *Metallogenium personatum* could be a propelling force behind microbially catalyzed transformation of Mn in the reservoir. They explained that increase in dissolved oxygen level in deep water is conducive for Mn^{2+} oxidation. In some earlier observations, Tyler and Marshall (1967) and Tyler (1970) addressed the widespread occurrence of stalked, budding bacteria *Hyphomicrobium* belonging to α-proteobacteria in Mn deposits and suggested that some *Hyphomicrobia* could preferentially oxidize Mn over Fe in hydroelectric pipelines.

In an interesting observation, Uren and Leeper (1978) stated that microbial oxidation of Mn^{2+} in soil could occur at low oxygen pressures provided CO_2 supplied is adequate. With *Arthrobacter* sp from soil, Bromfield and David (1976) had also showed that oxides of Mn could rapidly adsorb manganous ions from aqueous solutions but not in the case of abiotic control. In a kinetic study with cell free extracts of two bacterial isolates *Pseudomonas* III and *Citrobacter freundii* belonging to γ-proteobacteria, Douka (1980) identified that the rate of Mn^{2+} oxidation increased with its concentration, suggesting a strong affinity between the oxidizing system and Mn. Conversely, Chapnick et al. (1982) could show that Mn^{2+} removal from water column and oxidation in Lake Oneida during summer months are mediated by metabolically active Mn-oxidizing bacteria. They also showed that particles in lake water when removed by filtration or killed by ethanol treatment inhibit the activity. Besides, Gregory and Staley (1982) suggested that plasmids may be directly involved in Mn oxidation by providing essential gene products or may act indirectly by altering the microenvironment in a way as to make the chemical oxidation of Mn^{2+} favorable. Using in situ dialysis technique, Kepkay (1985) showed that Mn precipitation in soil could be a microbially mediated process causing a fivefold enhancement of abiotic process such as adsorption. Likewise, Vojak et al. (1985) stated that biological process could be responsible for the change in oxidation state of Mn^{2+} to Mn^{4+}. The rates of Mn^{2+}

oxidation in their study differed with increase in salinity and were depressed in the presence of inhibitors. Similarly, Johnson and Kipphut (1988) showed by in situ incubation technique, the rate of Mn^{2+} oxidation is largely microbially mediated in Toolik lake and is regulated by Mn^{2+} concentration rather than temperature or oxygen concentration. With more detailed experiment on mutants that lack the ability to oxidize Mn^{2+}, Caspi et al. (1998) stated that the Mn-oxidizing ability of *Pseudomonas putida* MnB1 can be recovered by complementation of the mutation in a c-type cytochrome biogenesis-defective mutant. In the kinetic studies on Mn uptake and oxidation by Moy et al. (2003), the uptake of Mn^{2+} by *Rhizobium* sp was greater than the conversion of Mn^{2+} to Mn oxides with significant production of polysaccharides. They suggested that polysaccharides might be involved in the uptake of Mn and in minimizing Mn oxide production. The study on redox transformation of Mn in Antarctic lakes (Krishnan et al. 2009) showed that Co could have a more profound role in Mn^{2+} oxidation and Ni on Mn oxide reduction. Although several studies report the oxidation of Mn^{2+} by bacteria, the identity of Mn-oxidizing bacteria remained undisclosed. Recently, Falamin and Pinevich (2006) determined the phylogenetic position and phenotypic properties of *Pseudomonas siderocapsa* sp.nov. They suggested a mixotrophic mode of nutrition in the strain and deposition of Mn oxides in their capsules rather than in outer membrane as observed in other *Pseudomonas* species.

As an attempt to understand the Mn-oxidizing ability of *Leptothrix discophora* SS-1 Adams and Ghiorse (1986) examined the ultrastructure of the strain by electron microscopy. They could observe extracellular blebs in cells and proposed it as vehicles for Mn-oxidizing protein. Manganese oxidation by sheathless strain of *Leptothrix discophora* SS-1 belonging to β_1 subdivision of proteobacteria (Boogerd and de Vrind 1987) in buffered medium at pH 7.5 showed the release of Mn^{2+}-oxidizing factors in the spent culture medium and was found associated with MnO_2 aggregates. Meanwhile, Adams and Ghiorse (1987) isolated the Mn^{2+}-oxidizing protein from *Leptothrix discophora* SS-1 and characterized the extracellular Mn^{2+}-oxidizing activity. The same authors in 1988 identified the oxidation states of Mn in the Mn oxide produced by *Leptothrix discophora* SS-1. They could identify that the oxidation state of Mn in fresh samples exist as Mn^{3+} and on aging give rise to a mixture of Mn (III,IV) oxides in older samples. Later, study by Corstjens et al. (1997) could identify that gene *mofA* is linked to Mn oxidation. In addition, Nelson et al. (1999) showed that Mn oxides produced by SS-1 can adsorb toxic metal lead. Moreover, Brouwers et al. (2000b) stated that being the core element in putative MCOs, Cu^{2+} could stimulate the oxidation of Mn^{2+}. Investigation on kinetics of Mn^{2+} oxidation by Zhang et al. (2002) explained that at circumneutral pH, at a relatively low numbers of Mn-oxidizing bacteria (*Leptothrix discophora* SS-1), biologically mediated Mn^{2+} oxidation exceeded abiotic oxidation. Interestingly, a recent study by El Gheriany et al. (2009) remarked that Fe is essential for efficient Mn^{2+} oxidation in *Leptothrix discophora* SS-1.

faster in the oxidized surface sediment where the Mn-oxidizing bacteria are abundant.

In an attempt to describe the general mechanism of Mn^{2+} oxidation, Tebo and Emerson (1986) describe a model where they conclude that Mn oxidation rate is not dependent on Mn concentration in the water column but is rather a function of the total number of surface-binding sites available. Similarly, de Vrind et al. (1986b) showed with experimental evidence that mature spores of marine *Bacillus* SG-1 could oxidize Mn^{2+}. On the other hand, de Vrind et al. (1986a) demonstrated that vegetative cells of the same organism could reduce manganese. The reduction of Mn by the vegetative cells was thought to make Mn^{2+} available for sporulation in a manganese-limited environment. Accumulation of MnO_2 by the spore coat prevented further oxidation of bound Mn^{2+} as the active sites get masked when oxygen gets consumed and protons get liberated. In another approach, the marine *Pseudomonas* sp. Strain S-36 when grown in continuous culture was found to obtain energy for CO_2 fixation from Mn^{2+} oxidation (Kepkay and Nealson 1987).

In a different approach, Sunda and Huntsman (1987) used radiotracers to determine the kinetics of particulate Mn formation in seawater. According to them, Mn^{2+} oxidation is microbially catalyzed and the rates depend upon the increase in temperature with respect to the ratio of particulate to dissolved Mn in estuarine water. The indirect process of Mn^{2+} oxidation by *Chlorella* sp at high pH (>9.0) resulting from photosynthesis was reported by Richardson et al. (1988). They demonstrated that growth of photosynthetic organisms as aggregates or as concentrated cell suspension in pelagic waters could generate microenvironments with steep gradients of oxygen and pH conducive for Mn^{2+} oxidation. Radiotracer studies on hydrothermal vent locations showed the scavenging of Mn^{2+} at higher rates under in situ incubations compared to onboard studies (Mandernack and Tebo 1993). Their results could suggest that bacteria not only enhance the scavenging of Mn within vent waters, but also facilitated Mn deposition to the sediments. In another interesting observation by Hansel and Francis (2006), the unrecognized role of *Roseobacter* like planktonic bacteria in Mn^{2+} oxidation and cycling in coastal waters was identified suggesting an alternative means of Mn^{2+} oxidation in the photic zone. The bacterium showed the ability to oxidize Mn^{2+} in the presence of light through photooxidation pathway and by direct enzymatic action in the dark. Based on a kinetic model of the oxidative pathway, Webb et al. (2005) stated that Mn^{3+} is a transient intermediate and the rate-limiting step in the oxidation of Mn^{2+}. They suggested that oxidation of Mn^{2+} could involve a unique multicopper oxidases (MCOs) system capable of two-electron oxidation of its substrate. MCOs are a class of enzymes that have metallocentre assembly containing four Cu atoms (Brouwers et al. 2000b). They couple the four-electron reduction of dioxygen to water with the oxidation of substrate. The well-defined MCOs are laccase, ascorbate oxidase, and ceruloplasmin. The others include phenoxazinone synthase, bilirubin oxidase, dihydrogeodin oxidase, sulochrin oxidase, and FET3 (Solomon et al. 1996).

Our observation on microbially mediated Mn^{2+} oxidation in bacterial isolates belonging to *Halomonas* sp from Carlsberg Ridge (Fernandes et al. 2005) showed that Mn is precipitated extracellularly. Same isolates when grown in the presence of Ni and Co in the absence of Mn^{2+} showed the ability to accumulate these metals both intra- and extracellularly (Sujith et al. 2010; Antony et al. 2010). Further, study from the mangrove sediments Krishnan et al. (2007) offered experimental evidence to demonstrate that both autochthonous autotrophs and heterotrophs work in tandem in reducing Mn^{2+} and other related metal ions in sediments. These processes may indirectly promote more metal oxidation by removing end product inhibition.

3.7 Manganese Oxidation by Freshwater Bacteria

The Mn and Fe oxidizing/depositing bacteria in freshwater habitats belong to *Sphaerotilus*, *Gallionella*, *Leptothrix*, *Pedomicrobium*, *Metallogenium*, *Hyphomicrobium*, *Crenothrix*, *Clonothrix*, and *Cladothrix* groups (Gregory and Staley 1982; Ghiorse 1984). Based on their abundance, Pringsheim (1949) stated that their significance in biochemical processes in rivers must be great but require further investigations to know about their nutritional needs, metabolism, and enzymatic systems. Knowing the importance of Mn^{2+} oxidation by bacteria, Johnson and Stokes (1966) readily stated with experimental evidence that *Sphaerotilus discophorus* belonging to β_1 subdivision of proteobacteria could oxidize Mn^{2+} to dark-brown manganic oxide. They pointed out that cells can lose the Mn^{2+}-oxidizing activity on heating and not poisoned by treatment with $HgCl_2$ suggestive of endogenous Mn^{2+} oxidation catalyzed by an inducible enzyme(s). In continuation of the earlier study with *Sphaerotilus discophorus*, Stokes and Powers (1967) ruled out that endogenous oxidation of Mn^{2+} could be stimulated by the oxidation of poly-β-hydroxybutyrate, a storage product within the cell. Further study by Ali and Stokes (1971) could observe autotrophic growth promotion in *Sphaerotilus discophorus* with Mn^{2+} as the sole source of energy. The results were later on evaluated with evidence that in the late phase of growth, *S. discophorus* do oxidize and accumulate MnO_2 but do not serve as energy source in this organism (Hajj and Makemson 1976). Conversely, Mills and Randles (1979) using electron transport chain inhibitors in their study suggested that Mn^{2+} oxidation in *Sphaerotilus discophorus* could be cytochrome mediated.

In an another study with different Mn-oxidizing filamentous budding bacteria *Pedomicrobium* belonging to α-proteobacteria, Ghiorse and Hirsch (1978) noted that very active Mn-depositing bacterial strains are also very active iron depositors. The presence of budding bacteria in freshwater distribution systems leads to the formation of biofilms heavily encrusted with Mn oxides (Tyler and Marshall 1967; Sly et al. 1988). The depositions of Mn oxides occur in close association with an extracellular matrix of acidic polysaccharides or polymer in these bacterial strains

3.8 Manganese Oxidation: A Genomic Perspective

In the recent years, several studies were attempted by researchers to understand the genetics involved in bacterial Mn^{2+} oxidation. Marine bacteria are efficient Mn oxidizers; however, only few studies report the genetic mechanism(s) involved in Mn oxidation. The well-studied Mn-oxidizing bacteria is *Bacillus* sp. Strain SG-1, a marine gram-positive bacterium isolated from shallow marine sediment that produces Mn-oxidizing spores (van Wassbergen et al. 1993, 1996; Francis et al. 2002; Francis and Tebo 2002). This is the only organism for which the direct involvement of MCOs in Mn oxidation is established. They proposed MnxG as one of the first gene products ever shown to be associated with the exosporium possessing oxidase activity. Francis et al. (2002) demonstrated that MnxG is localized to the exosporium of wild-type spores and is absent in the nonoxidizing spores of transposon mutants within the *mnx* gene cluster. Dick et al. (2006) based on phylogenetic analysis of 16S rRNA and *mnxG* genes explained that Mn-oxidizing *Bacillus* sp isolated from Guaymas Basin resembled deep-sea isolates reported earlier from coastal sediments, with few representing novel strains and clusters. Recently, Mayhew et al. (2008) proposed that vertical inheritance and gene loss influenced the distribution of the gene *mnxG* among the *Bacillus* sp.

For the first time, van Waasbergen et al. (1993) identified the genes involved in Mn^{2+} oxidation. They demonstrated that *mnx* region encodes factors that are required for oxidation of Mn^{2+} by SG-1 spores by protoplast transformation and mutagenesis. Later, van Waasbergen et al. (1996) suggested that among the several genes (*mnxA* to *mnxG*) that were earlier proposed to be involved in Mn^{2+} oxidation, the *mnxG* gene product may function like a copper oxidase and would be directly responsible for the oxidation of Mn^{2+} by the bacterial spores. The first direct evidence for the presence of RubisCo genes in a gram-negative Mn-oxidizing bacterium strain S185-9A1 was given by Caspi et al. (1996). The genes were more related to those from non-chlorophyte algal chloroplasts than from bacteria. Dick et al. (2008b) suggested that MnxG catalyzes two sequential one-electron oxidations from Mn^{2+} to Mn^{3+} and from Mn^{3+} to Mn^{4+}, a novel type of reaction for a multicopper oxidase.

Aurantimonas manganoxydans Strain. SI85-9A1 (Dick et al. 2008a, Anderson et al. 2009a, b) and *Erythrobacter* sp Strain. SD-21 (Anderson et al. 2009b) are the two other marine Mn-oxidizing α-proteobacteria known to oxidize Mn^{2+} that have been recently studied in detail. Anderson et al. (2009b) identified five annotated MCOs in the genome sequence of the above strains but none of the MCOs were reported to have any role in Mn^{2+} oxidation. In contrast, they could illustrate the role of heme peroxidase in Mn^{2+} oxidation and tentatively suggested MopA for the putative Ca^{2+} binding heme peroxidase.

Leptothrix discophora SS-1 a freshwater bacterial species that deposits Mn oxides on its extracellular sheath was studied in detail by Corstjens et al. (1997) and Brouwers et al. (2000a) using sophisticated molecular tools. Based on the results, they proposed that MCOs like gene *mofA* (manganese-oxidizing factor) to be involved in Mn^{2+} oxidation and genes *mofB* and *mofC* to be a part of the same

mofA operon. At the same time, Siering and Ghiorse (1997b) by variable stringency hybridization analysis using digoxigenin-labelled mofA probe of *Leptothrix discophorora* SS-1 showed that Mn-oxidation genes of other *Leptothrix* spp were closely related to one another but were not homologous to the unidentified presumptive Mn oxidation genes from other genera. In the meanwhile, Siering and Ghiorse (1997a) could detect sheathed bacteria (*Leptothrix* spp) in environmental samples based on their designed 16S rRNA-targeted specific probes and proposed its applications in further research.

The other common bacterial genera known for Mn^{2+} oxidation are *Pseudomonas putida* Strains MnB1 and GB-1. There are several reports (Caspi et al. 1996; Caspi et al. 1998; Brouwers et al. 1999; de Vrind et al. 2003) that describe the Mn-oxidizing ability of these strains. But only few (Brouwers et al. 1999, 2000a) attempts have been made to understand the genetic mechanisms involved in Mn^{2+} oxidation. They could identify by molecular analysis that gene *cumA* (copper protein involved in Mn oxidation) participates with MCOs in Mn^{2+} oxidation and *cumB* for optimal growth. Later, Francis and Tebo (2001) surprisingly observed highly conserved *cumA* gene sequences in non-Mn-oxidizing *Pseudomonas* strains. Based on the results, they suggested that *cumA* gene may not be expressed or that it may not be the only gene to confer the ability to oxidize Mn^{2+}. Conversely, they could exert an alternative function in these organisms and the gene could occur in phylogenetically diverse *Pseudomonas* strains.

Pedomicrobium sp. ACM3067 another aquatic bacteria could oxidize Mn^{2+} in close association with an extracellular matrix of acidic polysaccharides or polymer (Ghiorse and Hirsch 1979). Further, understanding about the mechanism involved in Mn^{2+} oxidation (Larsen et al. 1999) showed that Mn^{2+} oxidation is catalyzed by a copper-dependent enzyme in *Pedomicrobium* sp. ACM3067. Recent study by Ridge et al. (2007) provided evidence that *moxA* gene encoding a MCO homolog is essential for both Mn^{2+} oxidation and laccase-like activity in *Pedomicrobium* sp. ACM3067.

Mn-oxidizing genus *Hypomicrobium* is less probed at genetic level. Only one study by Layton et al. (2000) recorded the abundance of *Hypomicrobium* populations in activated sludge based on 16S rRNA analysis. About 5% of 16S rRNA in activated sludge corresponded to *Hypomicrobium* sp. Gregory and Staley (1982) showed experimental evidence that Mn^{2+}-oxidizing ability in the bacterial isolates was lost when maintained in the absence of the metal in the laboratory. They hypothesized that Mn oxidation may be directly related to the presence of plasmids.

3.9 Manganese Oxidation: A Proteomic Perspective

Metal ion efflux systems are central to cellular physiology. The uptake of Mn in bacteria occurs through (1) P-type ATPase (MntA) (Hao et al. 1999), (2) metal binding protein-dependent ABC transport system: Group PsaA, (3) pH-dependent

metal ion transporter: MntH Groups A, B, C, and (4) natural resistance-associated macrophage protein (NRAMP) family (Jakubovics and Jenkinson 2001; Cellier 2002; Papp-Wallace and Maguire 2006). Metallochaperones are responsible for the incorporation of correct metal into some of the proteins; however, most metalloproteins acquire their metals directly from cellular pools. In an attempt to understand the cellular mechanisms that govern metal acquisition by most nascent proteins, Tottey et al. (2008) identified the most abundant Cu^{2+}-protein, CucA and the most abundant Mn^{2+}-protein, MncA in the periplasm of cyanobacteria *Synechocystis* PCC 6803. They showed that compartmentalization kept competitive metals out of the wrong nascent proteins during protein folding.

The only Mn-oxidizing proteins identified and characterized so far in bacteria were the MCOs (Brouwers et al. 2000b; Francis and Tebo 2000). Another class of proteins in bacteria rarely known to oxidize Mn is the heme-containing manganese peroxidases (MNPs) (Palma et al. 2000; Anderson et al. 2009b). The known Mn-oxidizing proteins include the MnxG (~138 kDa) of *Bacillus* SG-1 (van Wassbergen et al. 1996; Francis et al. 2002) and MopA of *Aurantimonas manganoxidans* Strain. SI85-9A1 and *Erythrobacter* sp Strain. SD-21[Anderson et al. (2009b)]. In marine α-Proteobacterium SD-21, manganese-oxidizing factors of ≈250 and 150 kDa was observed in the logarithmic phase of growth. However, the expression of Mn(II) oxidase was not completely dependent on Mn^{2+} rather it was required for higher growth yield (Francis et al. 2001). They claimed it as the first group of Mn-containing metalloenzyme in gram-negative marine bacteria. Francis and Tebo (2002) could identify the first active Mn-oxidizing enzymes in spores or gram-positive bacteria. Their study came across proteins of different molecular weights in Mn-oxidizing marine *Bacillus* sp isolated from coastal marine sediment. Based on the inhibition of Mn-oxidizing activity by azide a multicopper oxidase inhibitor suggested that the unidentified proteins belong to the MCO group of enzymes. The role of metalloregulatory protein MntR, a transcriptional regulator of Mn homeostasis, was determined by Lieser et al. (2003). They demonstrated that differences in metal-activated DNA binding could play a role in the mechanism of Mn(II)-selective transcription of factors and the oligomerization of MntR that was metal independent. Further, Huang and Wu (2004) revealed the identity of the genes under control of manganese response regulator ManR in the cyanobacterium, *Anabaena* sp. PCC 7120.

The known Mn-oxidizing proteins include the CumA (50.5 kDa) of *Pseudomonas putida* GB-1 (Brouwers et al. 1999), MofA (~180 kD) of *Leptothrix discophora* SS-1 (Corstjens et al. 1997; Brouwers et al. 2000a), and MoxA (52.47 kDa) of *Pedomicrobium* sp. ACM3067 (Ridge et al. 2007). Several regulatory pathways for Mn in bacteria were investigated by different authors. Que and Helmann (2000), Guedon et al. (2003), and Moore and Helmann (2005) found that MntR, Fur, TnrA, and σ^B regulons regulated Mn uptake in *Bacillus subtilis*. Platero et al. (2004) stated that Fur was involved in manganese-dependent regulation of *mntA*. Patzer and Hantke (2001) and Hohle and O'Brian (2009) provided evidence to show that *mntH* gene encoding NRAMP like Mn^{2+} transporter was repressed by Fur and MntR of the *mntH* gene. Conversely, Kehres et al. (2000) inferred that NRAMP

proteins are selective Mn transporters involved in response to reactive oxygen. Diaz-Mireles et al. (2004) affirmed that Fur-like protein Mur (manganese uptake regulator), a Mn^{2+}-responsive transcriptional regulator of *Rhizobium leguminosarum*, differs from Fur that binds Fe^{2+} in γ-proteobacteria and engage in Mn uptake. Groot et al. (2005) identified the expression of three putative Mn transport systems (*mtsCBA*, *mntH1*, *and mntH2*) besides *mntA* in *Lactobacillus plantarum*. They observed the specific derepression or induction of transport systems upon Mn^{2+} limitation, suggesting their role in Mn^{2+} homeostasis. Subsequently, Jakubovics and Valentine (2009) identified the novel Mn^{2+} efflux system MntE in *Streptococcus pneumoniae*. They stated that disruption of the *mntE* gene could lead to widespread transcriptional changes that are distinct from responses to extracellular Mn^{2+}.

The expression of 25 kDa cytoplasmic protein was identified as superoxide dismutase isoenzyme (Mn-SOD) in *Arthrobacter* sp (Ercole et al. 1999). The functioning of the protein under both aerobic and anaerobic conditions in the presence of Mn oxide was found to have additional physiological function. The higher-molecular-weight surface protein (30 kDa) showed no homology with any of the identified proteins and its function is yet to be identified. Jung and Schweisfurth (1979) observed that *Pseudomonas* sp. Strain MnB1 produced a heat labile intracellular Mn-oxidizing protein during stationary phase of growth. Mn-oxidizing protein was not induced by the presence of Mn^{2+}, rather it was particularly dependent on the age of the culture. Likewise, in a comparative study on Mn oxidation using growing and resting cells of a freshwater bacterial isolate strain FMn 1, Zapkin and Ehrlich (1983) observed enzymatic nature of Mn-oxidizing activity in the strain. The activity of the enzyme was inducible. In a review, Shi (2004) stated that protein phosphatases are metalloenzymes with active centers containing two metal ions functioning as cofactors. The Mn-dependent prokaryotic protein O-phosphatases and their function were stated to add new insight into Mn^{2+} homeostasis and protein O-phosphorylation in prokaryotic cells.

3.10 Molecular Biomineralization

Organisms are capable of forming a diverse array of minerals, some of which cannot be formed inorganically in the biosphere. Biogenic minerals may be amorphous, paracrystalline, or crystalline (Lowenstam 1981). The mineralization processes driven by biological activity involving microorganisms constitute biomineralization (Wang and Müller 2009). The microorganisms and their interaction with geologic materials result in geochemical transformations switching between soluble and insoluble phases (White et al. 1997). As a result of close interaction between mineral and bacteria, biomineralization co-occur (Fig. 3.1). It can lead to precipitation of the metal leachate and formation of metal oxide coatings on bacterial wall and other inert surfaces contributing directly as

nucleation sites for further mineral formation (Fortin et al. 1995). Microorganisms interact with minerals for creating a more hospitable surrounding by extraction of nutrients and sequestration of toxic substances. Microbes use minerals as sources and sinks of electrons, for coupled oxidation–reduction reactions. Many of these reactions enable the release and capture of energy from unstable or metastable minerals (Shock 2009). Deep-sea minerals in polymetallic nodules, Fe–Mn crusts, and hydrothermal vents are not only formed by abiogenic mineralization but also by free-living and biofilm-forming bacteria which form matrix for Mn deposition. Here the mineralization processes proceed in close association with organic molecules or matrices. It can be an either induced (biological–chemical) or a controlled (enzymatic) process and the details of the processes and the references have been described by Wang and Müller (2009). Besides, in order to understand the biogeochemical phenomena occurring in the Mn-rich marine environments, several microbiological studies have focused on hydrothermal vents and Fe–Mn encrusted seamounts in the recent years (Davis et al. 2009; Emerson 2009; Glazer and Rouxel 2009; Rassa et al. 2009; Sudek et al. 2009). Few extended their research on biologically induced mineralization (Douglas and Beveridge 1998; Wang et al. 2009a, b; Dong 2010). Wang et al. (2009b) examined the biogenic components of the crust and He et al. (2008) examined the microbial community composition of Iron–Manganese nodules using sophisticated analytical tools. They found acidobacteria and proteobacteria in nodules and associated sediments. The firmicutes were restricted to nodules and the soils had more acidobacteria and Verrucomicrobia compared to nodules. Advancement in element-specific mapping of rock surfaces revealed hot spots of Mn accumulation in microbial biofilms (Templeton and Knowles 2009).

The mineral phases produced by bacteria are mostly amorphous and sometimes poorly crystalline. The crystallization process occurs with prolonged incubation time (Tazaki 2005) and the characteristic oxides thus produced are not identical to known synthetic solids possibly, because of solid-phase incorporation of biomolecular constituents (Parikh and Chorover 2005). It is observed that surficial proteins associate with Mn oxidation during the production of a poorly crystalline Mn(IV) phase. The formation of mixed phase minerals like hausmannite (Mn_3O_4), feiknechtite (β-MnOOH), manganite (γ-MnOOH), and Na-buserite following Mn (II) oxidation by *Bacillus* SG-1 was reported by Mann et al. (1988) and Mandernack et al. (1995). Whereas, a todorokite-like mineral was found to be produced by *Leptothrix discophora* Strain SP-6 (Kim et al. 2003) and MnOx produced by *Pseudomonas putida* Strain MnB1 was most similar to "acid" birnessite (Villalobos et al. 2003). Recent understanding about the genes and proteins involved in Mn oxidation help to spread its application in biotechnology. The gene *mnxG* responsible for Mn oxidation in Bacillus SG-1 (van Wassbergen et al. 1996), *cumA* in *Pseudomonas putida* GB-1 (Brouwers et al. 1999), *mofA* in *Leptothrix discophora* SS-1 (Corstjens et al. 1997; Brouwers et al. 2000a), *moxA* in *Pedomicrobium* sp. ACM3067 (Ridge et al. 2007), and *mopA* in *Aurantimonas manganoxidans* Strain. SI85-9A1 and *Erythrobacter* sp Strain. SD-21 (Anderson et al. 2009b) could be cloned and the products expressed under laboratory condition.

3.11 Biotechnological Applications of Manganese Oxidation

Manganese, a comparatively less toxic element, can become toxic to domestic and aquatic lives when its concentration exceeds beyond the EPA permissible levels (0.05 mg L^{-1}). During summer, it is observed that Mn oxides undergo reduction when the oxygen level drops in public and private wells, municipal water supplies, etc. The solubilized Mn is quite stable in the presence of oxygen and therefore can become a health risk for public who consumes the drinking water. The Mn-oxidizing bacterial residents of the Mn^{2+}-rich environments can oxidize Mn^{2+} and reduce its solubility and thereby provide protective mechanism against toxic levels of soluble Mn (Bromfield 1978). An application of Mn oxidizers or their products to such habitats offer chemical/biological solution to the problem on a seasonal/permanent basis (Czekalla et al. 1985). Mn oxides are also excellent electron acceptors for anaerobic respiration (Nealson et al. 1989). The application of Mn-oxidizing bacteria and Mn in sedimentary environments can stimulate respiratory carbon mineralization and could offer a natural system of "Pumping" (via precipitation and sedimentation of Mn oxides) electron-acceptor equivalents into an anaerobic environment (Nealson et al. 1989). It is observed that Mn oxides are potent chelators of several other trace metals, their application has proved to be efficient in the removal of radium from water supplies (Moore and Reid 1973), in retaining heavy metals like Co, Ni, Zn, and others in soil, polymerization of organic compounds, participation in humus formation by oxidation of phenols and quinines (Vodyanitskii 2009).

The removal of Mn^{2+} is conventionally achieved by inorganic oxidation such as chlorination or permanganate oxidation, followed by sand filtration (Miyata et al. 2007). In 1986, Ghiorse proposed the exploitation of Mn-precipitating microorganisms for industrial metal recovery processes. The use of Mn-oxidizing bacteria in treating effluents can minimize the addition of chemical reagents and unwanted by-product formation. The increase in filtration rate and longer runs due to less clogging, savings on wash water, and rapid return to equilibrium following a backwash sequence reduce the operational cost in treatment and maintenance of sludge in biological effluent treatment (Mouchet 1992; Katsoyiannis and Zouboulis 2004; Stembal et al. 2005). The biological processes take advantage of active and passive process in treatment by a variety of mechanisms like adsorption, accumulation, precipitation, and oxidation. The drawback of using bacteria for treating effluent biotechnologically is the slow rate of Mn oxidation. As an early solution to the problem, Stuetz et al. (1996) proposed the usage of combined algal–bacterial Mn oxidation and optimization of bioreactor parameters for treating metal effluents effectively. When using Mn oxide (scavengers of the environment) for treatment of any effluents with unknown composition, precaution needs to be taken as it is known that sometimes interaction of Mn oxide with other elements can result in phase transformations [Se(IV) to Se(VI), Cr(III) to Cr(VI), and As(III) to As(V)], contributing to increase/decrease in metal toxicity (Vodyanitskii 2009; He et al. 2010).

Recent advancement in the understanding of microbial Mn oxidation provides insight into the mechanisms of metal oxidation and the processes involved. This oxidation proceeds at rates up to five orders of magnitude greater than abiotic oxidation (Tebo et al. 1997). The Mn oxides produced by microorganisms are abundant environmental nanoparticles, they have great importance in biotechnology for the removal of heavy metals from aqueous matrices and oxidation of organic micropollutants in wastewater treatment plants (Villalobos et al. 2005b). The higher specific surface area of negatively charged biogenic Mn oxides than synthetic d-MnO_2 and commercially available pyrolusite allow greater sorption of positively charged heavy metals in solution (Hennebel et al. 2009). The bacterial spores from a potent Mn-oxidizing bacteria *Bacillus* sp. SG-1 have found extensive capacity for actively binding and oxidizing Mn and passively binding other metals. Likewise, Mn-oxidizing protein from *Pseudomonas putida* Strains MnB1 and GB-1 as well as sheath of *Leptothrix discophora* is found to have similar function (Francis and Tebo 1999). It was observed by Nelson et al. (2002); Villalobos et al. (2005a) that Mn oxides produced by Leptothrix *discophora* SS-1 and *Pseudomonas putida* MnB1 can adsorb five times more Pb per mole of Mn than abiotic Mn(IV) (hydr) oxide and 500–5,000 times more than pyrolusite oxides, thus stimulating interest in the development of Mn oxides for use in bioremediation. Likewise, Toner et al. (2006) observed a tenfold higher capacity for biogenic Mn oxides in adsorbing Zn than chemically synthesized Mn oxides, and Murray and Tebo (2007) detected seven times higher adsorption of Cr in biogenic Mn oxides produced by *Bacillus* sp. SG-1 than synthetic d-MnO_2. The utilization of these microorganisms in concentrating metal ions from effluents will have intense application in biotechnology for treatment of wastewaters and metal-containing effluents.

It has also been observed recently that biogenic Mn oxides can oxidize 17a-Ethinylestradiol, a potent endocrine-disrupting recalcitrant, and reduce its estrogenic activity to 81.7% (de Rudder et al. 2004). In another recent observation, Forrez et al. (2010) have shown that biogenic Mn oxides can oxidize diclofenac, a nonsteroidal anti-inflammatory drug and can reduce its lethal concentration and toxicity. Similar observations made for triclosan (Zhang and Huang 2003) and ciprofloxacin (Zhang and Huang 2005) with biogenic Mn oxides suggest that biogenic manganese oxide can be a promising polishing technique for sewage treatment plant effluents.

3.12 Conclusion

The current understanding about bacterial Mn oxidation comprises the participation of MCOs, but their direct link to oxidation is emphasized only in *Bacillus* SG-1 and not in other organisms like *Pseudomonas putida* MnB1, GB1, *Leptothrix discophora* SS1, or *Pedomicrobium* sp. ACM3067. The various regulatory mechanisms and transport systems for Mn uptake in bacterial cells are studied but the role of metalloproteins in Mn oxidation or how the proteins select the right

metal when competitive metal ions are in excess is still not fully understood. What is known at present is that the compartmentalization of protein during folding regulates the binding of correct metal. Therefore, the production and utilization of biogenic Mn oxide nanoparticle in biotechnology requires further understanding about the molecular mechanism of Mn oxidation.

Acknowledgments We thank the Director, NIO for providing the required facilities to conduct this research work. The work has been carried out under the project "Preliminary exploration of cobalt-rich seamount crusts in the northern Indian Ocean" funded by the Ministry of Earth Sciences (Government of India) lead by Dr. V.K. Banakar. SPP wishes to thank Dr. M.P. Tapaswi for continuous support with required literature for reference and also acknowledges the Council of Scientific and Industrial Research, New Delhi-India, for the award of Senior Research Fellowship. This manuscript has NIO contribution No 5005.

References

Adams LF, Ghiorse WC (1986) Physiology and ultrastructure of *Leptothrix discophora* SS-1. Arch Microbiol 145:126–135

Adams LF, Ghiorse WC (1987) Characterization of an extracellular Mn^{2+}-oxidizing activity and isolation of Mn^{2+}-oxidizing protein from *Leptothrix discophora* SS-1. J Bacteriol 169: 1279–1285

Adams LF, Ghiorse WC (1988) Oxidation state of Mn in the Mn oxide produced by *Leptothrix discophora* SS-1. Geochim Cosmochim Acta 52:2073–2076

Ali SH, Stokes JL (1971) Stimulation of heterotrophic and autotrophic growth of *Sphaerotilus discophorus* by manganous ions. Anton Van Leeuwenhoek 37:519–528

Anderson CR, Dick GJ, Chu ML, Cho JC, Davis RE, Bräuer SL, Tebo BM (2009a) *Aurantimonas manganoxydans*, sp. nov. and *Aurantimonas litoralis*, sp. nov.: Mn(II) oxidizing representatives of a globally distributed clade of alpha-Proteobacteria from the order Rhizobiales. Geomicrobiol J 26:189–198

Anderson CR, Johnson HA, Caputo N, Davis RE, Torpey JW, Tebo BM (2009b) Mn(II) oxidation is catalyzed by heme peroxidases in "*Aurantimonas manganoxydans*" Strain SI85-9A1 and *Erythrobacter* sp. Strain SD-21. Appl Environ Microbiol 75:4130–4138

Antony R, Sujith PP, Fernandes SO, Verma P, Khedekar VD, Loka Bharathi PA (2010) Cobalt immobilization by manganese oxidizing bacteria from Indian Ridge System. Curr Microbiol 62:840–849

Appanna VD (1988) Stimulation of exopolysaccharide production in *Rhizobium meliloti* JJ-1 by manganese. Biotechnol Lett 10:205–206

Appanna VD, Gazso LG, St. Pierre M (1996) Multiple-metal tolerance in *Pseudomonas fluorescens* and its biotechnological significance. J Biotechnol 52:75–80

Archibald F (1986) Manganese: its acquisition by and function in the lactic acid bacteria. Crit Rev Microbiol 13:63–109

Arcuri EJ, Ehrlich HL (1979) Cytochrome involvement in Mn(II) oxidation by two marine bacteria. Appl Environ Microbiol 37:916–923

Arcuri EJ, Ehrlich HL (1980) Electron transfer coupled to Mn(II) oxidation in two deep-sea pacific ocean isolates. In: Trudinger PA, Walter MR, Ralph BJ (eds) Biogeochemistry of ancient and modern environments. Springer, New York, pp 339–344

Babich H, Stotzky G (1983) Influence of chemical speciation on the toxicity of heavy metals to the microbiota. In: Nriagu JO (ed) Aquatic toxicology. Wiley Interscience, New York, pp 1–46

Boogerd FC, de Vrind JPM (1987) Manganese oxidation by *Leptothrix discophora*. J Bacteriol 169:489–494

Bowen HJM (1979) Environmental chemistry of the elements. Academic, London

Bromfield SM (1978) The oxidation of manganous ions under acidic conditions by an acidophilous actinomycete from acid soil. Aust J Soil Res 16:91–100

Bromfield SM, David DJ (1976) Sorption and oxidation of manganous ions and reduction of manganese oxide by cell suspensions of a manganese oxidizing bacterium. Soil Biol Biochem 8:37–43

Brouwers G-J, de Vrind JPM, Corstjens PLAM, Cornelis P, Baysse C, de Vrind-de Jong EW (1999) *CumA*, a gene encoding a multicopper oxidase, is involved in Mn^{2+}-oxidation in *Pseudomonas putida* GB-1. Appl Environ Microbiol 65:1762–1768

Brouwers G-J, Corstjens PLAM, de Vrind JPM, Verkamman A, de Kuyper M, de Vrind-de Jong EW (2000a) Stimulation of Mn^{2+} oxidation in *Leptothrix discophora* SS-1 by Cu^{2+} and sequence analysis of the region flanking the gene encoding putative multicopper oxidase MofA. Geomicrobiol J 17:25–33

Brouwers G-J, Vijgenboom E, Corstjens PLAM, de Vrind JPM, de Vrind-de Jong EW (2000b) Bacterial Mn^{2+} oxidizing systems and multicopper oxidases: An overview of mechanisms and functions. Geomicrobiol J 17:1–24

Calvert SE, Pedersen TF (1996) Sedimentary geochemistry of manganese: implications for the environment of formation of manganiferous black shales. Econ Geol 91:36–47

Caspi R, Haygood MG, Tebo BM (1996) Unusual ribulose-1,5-bisphosphate carboxylase/oxygenase genes from a marine manganese-oxidizing bacterium. Microbiology 142: 2549–2559

Caspi R, Tebo BM, Haygood MG (1998) c-type cytochromes and manganese oxidation in *Pseudomonas putida* strain MnB1. Appl Environ Microbiol 64:3549–3555

Cellier M (2002) Bacterial genes controlling manganese accumulation. In: Winkelmann G (ed) Microbial Transport Systems. Wiley-VCH Verlag GmbH & Co., KGaA, pp 325–345

Chander M, Setlow B, Setlow P (1998) The enzymatic activity of phosphoglycerate mutase from gram-positive endospore-forming bacteria requires Mn^{2+} and is pH sensitive. Can J Microbiol 44:759–767

Chandramohan D, Loka Bharathi PA, Nair S, Matondkar SGP (1987) Bacteriology of ferromanganese nodules from the Indian Ocean. Geomicrobiol J 5:17–31

Chapnick SD, Mire WS, Nealson KH (1982) Microbially mediated manganese oxidation in a freshwater lake. Limnol Oceanogr 27:1004–11014

Christianson DW (1997) Structural chemistry and biology of manganese metalloenzymes. Prog Biophys Mol Biol 67:217–252

Corstjens PLAM, de Vrind JPM, Goosen T, de Vrind-de Jong EW (1997) Identification and molecular analysis of the *Leptothrix discophora* SS-1 *mofA* gene, a gene putatively encoding a manganese-oxidizing protein with copper domains. Geomicrobiol J 14:91–108

Crowley JD, Traynor DA, Weatherburn DC (2000) Enzymes and proteins containing manganese: an overview. Met Ions Biol Syst 37:209–278

Czekalla C, Mevius W, Hanert H (1985) Quantitative removal of iron and manganese by microorganisms in rapid sand filters. Wat Suppl 3:111–123

Davis RE, Stakes DS, Wheat CG, Moyer CL (2009) Bacterial variability within an iron-silica-manganese-rich hydrothermal mound located off-axis at the cleft segment, Juan de Fuca Ridge. Geomicrobiol J 26:570–580

de Rudder J, Van de Wiele T, Dhooge W, Comhaire F, Verstraete W (2004) Advanced water treatment with manganese oxide for the removal of 17 a-ethynylestradiol (EE2). Water Res 38:184–192

de Vrind JPM, Boogerd FC, de Vrind-de Jong EW (1986a) Manganese reduction by a marine *Bacillus* species. J Bacteriol 167:30–34

de Vrind JPM, de Vrind-de Jong EW, de Voogt J-WH, Westbroek P, Boogerd FC, Rosson RA (1986b) Manganese oxidation by spores and spore coats of a marine *Bacillus* species. Appl Environ Microbiol 52:1096–1100

de Vrind J, de Groot A, Brouwers GJ, Tommassen J, de Vrind-de Jong EW (2003) Identification of a novel Gsp-related pathway required for secretion of the manganese oxidizing factor of *Pseudomonas putida* strain GB-1. Mol Microbiol 47:993–1006

Diaz-Mireles E, Wexler M, Sawers G, Bellini D, Todd JD, Johnston AWB (2004) The Fur-like protein Mur of *Rhizobium leguminosarum* is a Mn^{2+}-responsive transcriptional regulator. Microbiology 150:1447–1456

Dick GJ, Lee YE, Tebo BM (2006) Manganese(II)-oxidizing *bacillus* spores in guaymas basin hydrothermal sediments and plumes. Appl Environ Microbiol 72:3184–3190

Dick GJ, Podell S, Johnson HA, Rivera-Espinoza Y, Bernier-Latmani R, McCarthy JK, Torpey JW, Clement BG, Gaasterland T, Tebo BM (2008a) Genomic insights into Mn(II) oxidation by the marine alphaproteobacterium *Aurantimonas* sp.Strain SI85-9A1. Appl Environ Microbiol 74:2646–2658

Dick GJ, Torpey JW, Beveridge TJ, Tebo BM (2008b) Direct Identification of a bacterial manganese(ii) oxidase, the multicopper oxidase MnxG, from spores of several different marine *Bacillus* species. Appl Environ Microbiol 74:1527–1534

Dong H (2010) Mineral-microbe interactions: a review. Front Earth Sci China 4:127–147

Douglas S, Beveridge TJ (1998) Mineral formation by bacteria in natural microbial communities. FEMS Microbiol Ecol 26:79–88

Douka C (1980) Kinetics of manganese oxidation by cell-free extracts of bacteria isolated from manganese concretions from soil. Appl Environ Microbiol 39:74–80

Doyle RJ (1989) How cell walls of gram-positive bacteria interact with metal ions. In: Beveridge TJ, Doyle RJ (eds) Metal Ions and Bacteria. Wiley, New York, pp 275–293

Edenborn HM, Paquin Y, Chateauneuf G (1985) Bacterial contribution to manganese oxidation in a deep coastal sediment. Estuar Coast Shelf Sci 21:801–815

Ehrlich HL (1963) Bacteriology of manganese nodules. I. Bacterial action on manganese in nodule enrichments. Appl Microbiol 11:15–19

Ehrlich HL (1968) Bacteriology of manganese nodules. II. Manganese oxidation by cell-free extract from a manganese nodule bacterium. Appl Microbiol 16:197–202

Ehrlich HL (1971) Bacteriology of manganese nodules. V. Effect of hydrostatic pressure on bacterial oxidation of Mn(II) and reduction of MnO_2. Appl Microbiol 21:306–310

Ehrlich HL (1976) Manganese as an energy source for bacteria. In: Nriagu JO (ed) Environmental biogeochemistry. Ann Arbor Science, Michigan, pp 633–644

Ehrlich HL (1978) Inorganic energy sources for chemolithotrophic and mixotrophic bacteria. Geomicrobiol J 1:65–83

Ehrlich HL (1980) Different forms of microbial manganese oxidation and reduction and their environmental significance. In: Trudinger PA, Walter MR, Ralph BJ (eds) Biogeochemistry of ancient and modern environments. Springer, New York, pp 327–332

Ehrlich HL (1982) Enhanced removal of Mn^{2+} from seawater by marine sediments and clay minerals in the presence of bacteria. Can J Microbiol 28:1389–1395

Ehrlich HL (1983) Manganese-oxidizing bacteria from a hydrothermally active area on the Galapagos. Rift Ecol Bull 35:357–366

Ehrlich HL (1987) Manganese oxide reduction as a form of anaerobic respiration. Geomicrobiol J 5:423–431

Ehrlich HL (2002a) Geomicrobiology. Marcel Dekker Inc., New York

Ehrlich HL (2002b) How microbes mobilize metals in ores: a review of current understandings and proposals for future research. Miner Metall Proc 19:220–224

Ehrlich HL, Salerno JC (1990) Energy coupling in Mn^{2+} oxidation by a marine bacterium. Arch Microbiol 154:12–17

Emerson D (2009) Potential for iron-reduction and iron-cycling in iron oxyhydroxide-rich microbial mats at Loihi Seamount. Geomicrobiol J 26:639–647

Emerson S, Kalhorn D, Jacobs L, Tebo BM, Nealson KH, Rosson RA (1982) Environmental oxidation rate of manganese (II): Bacterial catalysis. Geochim Cosmochim Acta 46: 1073–1079

Ercole C, Altieri F, Piccone C, Del Gallo M, Lepidi A (1999) Influence of manganese dioxide and manganic ions on the production of two proteins in *Arthrobacter* sp. Geomicrobiol J 16:95–103

Falamin AA, Pinevich AV (2006) Isolation and characterization of a unicellular manganese-oxidizing bacterium from a freshwater lake in Northwestern Russia. Microbiology 75:180–185

Fernandes SO, Krishnan KP, Khedekar VD, Loka Bharathi PA (2005) Manganese oxidation by bacterial isolates from the Indian Ridge System. Biometals 18:483–492

Forrez I, Carballa M, Verbeken K, Vanhaecke L, Schlusener M, Ternes T, Boon N, Verstraete W (2010) Diclofenac oxidation by biogenic manganese oxides. Environ Sci Technol 44:3449–3454

Fortin D, Davis B, Southam G, Beveridge TJ (1995) Biogeochemical phenomena induced by bacteria within sulfidic mine tailings. J Ind Microbiol Biotechnol 14:178–185

Francis CA, Tebo BM (1999) Marine *Bacillus* spores as catalysts for oxidative precipitation and sorption of metals. J Mol Microbiol Biotechnol 1:71–78

Francis CA, Tebo BM (2000) New insights into the diversity of genes and enzymes involved in bacterial Mn(II) oxidation. In: Morgan J (ed) Chemical speciation and reactivity in water chemistry and water technology: a symposium in honor of James. ILSI Press, Washington, DC, pp 488–490

Francis CA, Tebo BM (2001) cumA multicopper oxidase genes from diverse Mn(II)-oxidizing and non-Mn(II)-oxidizing *Pseudomonas* strains. Appl Environ Microbiol 67:4272–4278

Francis CA, Tebo BM (2002) Enzymatic manganese(II) oxidation by metabolically dormant spores of diverse *Bacillus* species. Appl Environ Microbiol 68:874–880

Francis CA, Co E, Tebo BM (2001) Enzymatic manganese(II) oxidation by a marine α-proteobacterium. Appl Environ Microbiol 67:4024–4029

Francis CA, Casciotti KL, Tebo BM (2002) Localization of Mn(II)-oxidizing activity and the putative multicopper oxidase, MnxG, to the exosporium of the marine *Bacillus* sp. strain SG-1. Arch Microbiol 178:450–456

El-Gheriany IA, Bocioaga D, Hay AG, Ghiorse WC, Shuler ML, Lion LW (2009) Iron requirement for Mn(II) oxidation by *Leptothrix discophora* SS-1. Appl Environ Microbiol 75:1229–1235

Ghiorse WC (1984) Biology of iron- and manganese-depositing bacteria. Annu Rev Microbiol 38:515–550

Ghiorse WC, Hirsch P (1978) Iron and manganese deposition by budding bacteria. In: Krumbein WE (ed) Environmental biogeochemistry and geomicrobiology. Ann Arbor Science, Ann Arbor, pp 897–909

Ghiorse WC, Hirsch P (1979) An ultrastructural study of iron and manganese deposition associated with extracellular polymers of *Pedomicrobium*-like budding bacteria. Arch Microbiol 123:213–226

Ghoirse WC (1986) Applications of ferromanganese-depositing microorganisms to industrial metal recovery processes. Biotech Bioeng Symp 16:141–148

Glasby GP (2006) Manganese: predominant role of nodules and crusts. In: Schulz HD, Zabel M (eds) Marine geochemistry. Springer Berlin, Heidelberg, pp 371–427

Glazer BT, Rouxel OJ (2009) Redox speciation and distribution within diverse iron-dominated microbial habitats at Loihi Seamount. Geomicrobiol J 26:606–622

Gregory E, Staley JT (1982) Widespread distribution of ability to oxidize manganese among freshwater bacteria. Appl Environ Microbiol 44:509–511

Groot MNN, Klaassens E, de Vos WM, Delcour J, Hols P, Kleerebezem M (2005) Genome-based in silico detection of putative manganese transport systems in *Lactobacillus plantarum* and their genetic analysis. Microbiology 151:1229–1238

Guedon E, Moore CM, Que Q, Wang T, Ye RW, Helmann JD (2003) The global transcriptional response of Bacillus subtilis to manganese involves the MntR, Fur, TnrA and σ^B regulons. Mol Microbiol 49:1477–1491

Hajj H, Makemson J (1976) Determination of growth of *Sphaerotilus discophorus* in the presence of manganese. Appl Environ Microbiol 32:699–702

Hansel CM, Francis CA (2006) Coupled photochemical and enzymatic Mn(II) oxidation pathways of a planktonic *Roseobacter*-like bacterium. Appl Environ Microbiol 72:3543–3549

Hao Z, Chen S, Wilson DB (1999) Cloning, expression and characterization of cadmium and manganese uptake genes from *Lactobacillus plantarum*. Appl Environ Microbiol 65: 4746–4752

He J, Zhang L, Jin S, Zhu Y, Liu F (2008) Bacterial communities inside and surrounding soil iron–manganese nodules. Geomicrobiol J 25:14–24

He J, Meng Y, Zheng Y, Zhang L (2010) Cr(III) oxidation coupled with Mn(II) bacterial oxidation in the environment. J Soil Sediment 10:767–773

Hem JD (1978) Redox processes at surfaces of manganese oxide and their effects on aqueous metal ions. Chem Geol 21:199–218

Hennebel T, Gusseme BD, Boon N, Verstraete W (2009) Biogenic metals in advanced water treatment. Trends Biotechnol 27:90–98

Herschel A, Clasen J (1998) The importance of the manganese-oxidizing microorganism *Metallogeniurn personaturn* for the retention of manganese in the Wahnbach reservoir. Internat Rev Hydrobiol 83:19–30

Hohle TH, O'Brian MR (2009) The *mntH* gene encodes the major Mn^{2+} transporter in *Bradyrhizobium japonicum* and is regulated by manganese via the Fur protein. Mol Microbiol 72:399–409

Horsburgh MJ, Wharton SJ, Karavolos M, Foster SJ (2002) Manganese: elemental defence for a life with oxygen? Trends Microbiol 10:496–501

Huang W, Wu Q (2004) Identification of genes controlled by the manganese response regulator, ManR, in the cyanobacterium, *Anabaena* sp. PCC 7120. Biotechnol Lett 26:1397–1401

Jakubovics NS, Jenkinson HF (2001) Out of the iron age: new insights into the critical role of manganese homeostasis in bacteria. Microbiology 147:1709–1718

Jakubovics NS, Valentine RA (2009) A new direction for manganese homeostasis in bacteria: identification of a novel efflux system in *Streptococcus pneumonia*. Mol Microbiol 72:1–4

Jaquet JM, Nembrim G, Garcla J, Vernet JP (1982) The manganese cycle in Lac Leman, Switzerland: the role of *Metallogenium*. Hydrobiologia 91:323–340

Johnson KS (2006) Manganese redox chemistry revisited. Science 313:1896–1897

Johnson CG, Kipphut GW (1988) Microbially mediated Mn(II) oxidation in an oligotrophic Arctic lake. Appl Environ Microbiol 54:1440–1445

Johnson AH, Stokes JL (1966) Manganese oxidation by *Sphaerotilus discophorus*. J Bacteriol 91:1543–1547

Jung WK, Schweisfurth R (1979) Manganese oxidation by an intracellular protein of a *Pseudomonas* species. Z Allg Mikrobiol 19:107–115

Katsoyiannis IA, Zouboulis AI (2004) Biological treatment of Mn(II) and Fe(II) containing groundwater: kinetic considerations and product characterization. Water Res 38:1922–1932

Kehres DG, Zaharik ML, Finlay BB, Maguire ME (2000) The NRAMP proteins of *Salmonella typhimurium* and *Escherichia coli* are selective manganese transporters involved in the response to reactive oxygen. Mol Microbiol 36:1085–1100

Kepkay PE (1985) Kinetics of microbial manganese oxidation and trace metal binding in sediments: results from an in situ dialysis technique. Limnol Oceanogr 30:713–726

Kepkay PE, Nealson KH (1982) Surface enhancement of sporulation and manganese oxidation by a marine *Bacillus*. J Bacteriol 151:1022–1026

Kepkay PE, Nealson KH (1987) Growth of a manganese oxidizing *Pseudomonas* sp. in continuous culture. Arch Microbiol 148:63–67

Keren N, Kidd MJ, Penner-Hahn JE, Pakrasi HB (2002) A light-dependent mechanism for massive accumulation of manganese in the photosynthetic bacterium *Synechocystis* sp. PCC 6803. Biochemistry 41:15085–15092

Kim HS, Pasten PA, Gaillard JF, Stair PC (2003) Nanocrystalline todorokite-like manganese oxide produced by bacterial catalysis. J Am Chem Soc 125:14284–14285

Kirchner WB, Grabowski S (1972) Manganese in lacustrine ecosystems: a review. Am Water Resour Assoc 8:1259–1264

Krishnan KP, Fernandes SO, Chandan GS, Loka Bharathi PA (2007) Bacterial contribution to mitigation of iron and manganese in mangrove sediments. Mar Pollut Bull 54:1427–1433

Krishnan KP, Sinha RK, Krishna K, Nair S, Singh SM (2009) Microbially mediated redox transformations of manganese (II) along with some other trace elements: a study from Antarctic lakes. Polar Biol 32:1765–1778

Larsen EI, Sly LI, McEwan AG (1999) Manganese(II) adsorption and oxidation by whole cells and a membrane fraction of *Pedomicrobium* sp. ACM 3067. Arch Microbiol 171:257–264

Layton AC, Karanth PN, Lajoie CA, Meyers AJ, Gregory IR, Stapleton RD, Taylor DE, Sayler GS (2000) Quantification of *Hyphomicrobium* populations in activated sludge from an industrial wastewater treatment system as determined by 16S rRNA analysis. Appl Environ Microbiol 66:1167–1174

Lidstrom ME, Engebrecht J, Nealson KH (1983) Evidence for plasmid-encoded manganese oxidation in a marine pseudomonad. FEMS Microbiol Lett 19:1–6

Lieser SA, Davis TC, Helmann JD, Cohen SM (2003) DNA-binding and oligomerization studies of the manganese(II) metalloregulatory protein MntR from *Bacillus subtilis*. Biochemistry 42:12634–12642

Lowenstam HA (1981) Minerals formed by organisms. Science 211:1126–1131

Maki JS, Tebo BM, Palmer FE, Nealson KH, Staley JT (1987) The abundance and biological activity of manganese-oxidizing bacteria and *Metallogenium-like* morphotypes in Lake Washington, USA. FEMS Microbiol Ecol 45:21–29

Mandernack KW, Tebo BM (1993) Manganese scavenging and oxidation at hydrothermal vents and in vent plumes. Geochim Cosmochim Acta 57:3907–3923

Mandernack KW, Post J, Tebo BM (1995) Manganese mineral formation by bacterial-spores of the marine *Bacillus*, SG-1: evidence for the direct oxidation of Mn(II) to Mn(IV). Geochim Cosmochim Acta 59:4393–4408

Mann S, Sparks NHC, Scott GHE, de Vrind-de Jong EW (1988) Oxidation of manganese and formation of Mn_3O_4 (Hausmannite) by spore coats of a Marine *Bacillus* sp. Appl Environ Microbiol 54:2140–2143

Mayhew LE, Swanner ED, Martin AP, Templeton AS (2008) Phylogenetic relationships and functional genes: distribution of gene (*mnxG*) encoding a putative manganese-oxidizing enzyme in *Bacillus* species. Appl Environ Microbiol 74:7265–7271

Mills VH, Randles CI (1979) Manganese oxidation in *Sphaerotilus discophorus* particles. J Gen Appl Microbiol 25:205–207

Miyata N, Tani Y, Sakata M, Iwahori K (2007) Microbial manganese oxide formation and interaction with toxic metal ions. J Biosci Bioeng 104:1–8

Moore CM, Helmann JD (2005) Metal ion homeostasis in *Bacillus subtilis*. Curr Opin Microbiol 8:188–195

Moore WS, Reid DF (1973) Extraction of radium from natural waters using manganese-impregnated acrylic fibers. J Geophys Res 78:8880–8886

Mouchet P (1992) From conventional to biological removal of iron and manganese in France. J Am Water Works Assoc 84:158–167

Moy YP, Neilan BA, Foster LJR, Madgwick JC, Rogers PL (2003) Screening, identification and kinetic characterization of a bacterium for Mn(II) uptake and oxidation. Biotechnol Lett 25:1407–1413

Murray KJ, Tebo BM (2007) Cr(III) is indirectly oxidized by the Mn(II)-oxidizing bacterium *Bacillus* sp strain SG-1. Environ Sci Technol 41:528–533

Nealson KH (1983) The microbial manganese cycle. In: Krumbein WE (ed) Microbial geochemistry. Blackwell Scientific Publications, Oxford, pp 191–221

Nealson KH, Myers CR (1992) Microbial reduction of manganese and iron: new approaches to carbon cycling. Appl Environ Microbiol 58:439–443

Nealson KH, Tebo BM, Rosson RA (1988) Occurrence and mechanisms of microbial oxidation of manganese. Adv Appl Microbiol 33:279–318

Nealson KH, Rosson RA, Myers CR (1989) Mechanisms of oxidation and reduction of manganese. In: Beveridge T, Doyle R (eds) Metal ions and bacteria. Wiley, New York, pp 383–411

Nelson YM, Lion LW, Ghiorse WC, Shuler ML (1999) Production of biogenic Mn oxides by *Leptothrix discophora* SS-1 in a chemically defined growth medium and evaluation of their Pb adsorption characteristics. Appl Environ Microbiol 65:175–180

Nelson YM, Lion LW, Shuler ML, Ghiorse WC (2002) Effect of oxide formation mechanisms on lead adsorption by biogenic manganese (hydr)oxides, iron (hydr)oxides, and their mixtures. Environ Sci Technol 36:421–425

Ogawa T, Bao DH, Katoh H, Shibata M, Pakrasi HB, Bhattacharyya-Pakrasi M (2002) A two-component signal transduction pathway regulates manganese homeostasis in *Synechocystis* 6803, a photosynthetic organism. J Biol Chem 277:28981–28986

Palma C, Martinez AT, Lema JM, Martinez MJ (2000) Different fungal manganese-oxidizing peroxidases: a comparison between *Bjerkandera* sp. and *Phanerochaete chrysosporium*. J Biotechnol 77:235–245

Papp-Wallace KM, Maguire ME (2006) Manganese transport and the role of manganese in virulence. Annu Rev Microbiol 60:187–209

Parikh SJ, Chorover J (2005) FTIR spectroscopic study of biogenic Mn-oxide formation by *Pseudomonas putida* GB-1. Geomicrobiol J 22:207–218

Patzer SI, Hantke K (2001) Dual repression by Fe^{2+}-Fur and Mn^{2+}-MntR of the *mntH* gene, encoding an NRAMP-like Mn^{2+} transporter in *Escherichia coli*. J Bacteriol 183:4806–4813

Platero R, Peixoto L, O'Brian MR, Fabiano E (2004) Fur is involved in manganese-dependent regulation of mntA (sitA) expression in *Sinorhizobium meliloti*. Appl Environ Microbiol 70:4349–4355

Pringsheim EG (1949) The filamentous bacteria *Sphaerotilus*, *Leptothrix*, *Cladothrix*, and their relation to iron and manganese. Phil Trans R Soc Lond 233:453–482

Que Q, Helmann JD (2000) Manganese homeostasis in *Bacillus subtilis* is regulated by MntR, a bifunctional regulator related to the diphtheria toxin repressor family of proteins. Mol Microbiol 35:1454–1468

Rassa AC, McAllister SM, Safran SA, Moyer CL (2009) Zeta-proteobacteria dominate the colonization and formation of microbial mats in low-temperature hydrothermal vents at Loihi Seamount, Hawaii. Geomicrobiol J 26:623–638

Richardson LL, Aguilar C, Nealson KH (1988) Manganese oxidation in pH and O_2 microenvironments produced by phytoplankton. Limnol Oceanogr 33:352–363

Ridge JP, Lin M, Larsen EI, Fegan M, McEwan AG, Sly LI (2007) A multicopper oxidase is essential for manganese oxidation and laccase-like activity in *Pedomicrobium* sp. ACM 3067. Environ Microbiol 9:944–953

Roitz JS, Flegal AR, Bruland KW (2002) The biogeochemical cycling of manganese in San Francisco Bay: temporal and spatial variations in surface water concentrations. Estuar Coast Shelf Sci 54:227–239

Rosson RA, Nealson KH (1982) Manganese binding and oxidation by spores of a marine *Bacillus*. J Bacteriol 151:1027–1034

Rosson RA, Tebo BM, Nealson KH (1984) The use of poisons in the determination of microbial manganese binding rates in seawater. Appl Environ Microbiol 47:740–745

Rusin P, Ehrlich HL (1995) Developments in microbial leaching-mechanisms of manganese solubilization. In: Fiechter A (ed) Advances in biochemical engineering/biotechnology. Springer-Verlag Berlin, Heidelberg, pp 1–26

Saager PM, De Baar HJW, Burkill PH (1989) Manganese and iron in Indian Ocean waters. Geochim Cosmochim Acta 53:2259–2267

Schuett C, Zelibor JL Jr, Colwell RR (1986) Role of bacterial plasmids in manganese oxidation: evidence for plasmid-encoded heavy metal resistance. Geomicrobiol J 4:389–406

Schweisfurth R, Eleftheriadis D, Gundlach H, Jacobs M, Jung W (1978) Microbiology of the precipitation of manganese. In: Krumbein WE (ed) Environmental biogeochemistry and geomicrobiology. Ann Arbor Science, Ann Arbor, pp 923–928

Shi L (2004) Manganese-dependent protein o-phosphatases in prokaryotes and their biological functions. Front Biosci 9:1382–1397

Shock EL (2009) Minerals as energy source for microorganisms. Econ Geol 104:1235–1248

Siering PL, Ghiorse WC (1997a) Development and application of 16S rRNA-targeted probes for detection of iron- and manganese-oxidizing sheathed bacteria in environmental samples. Appl Environ Microbiol 63:644–651

Siering PL, Ghiorse WC (1997b) PCR detection of a putative manganese oxidation gene (*mofA*) in environmental samples and assessment of *mof*A gene homology among diverse manganese-oxidizing bacteria. Geomicrobiol J 14:109–125

Sly LI, Arunpairojana V, Hodgkinson MC (1988) *Pedomicrobium manganicum* from drinking-water distribution systems with manganese-related "dirty water" problems. Syst Appl Microbiol 11:75–84

Sly LI, Arunpairojana V, Dixon DR (1990) Binding of colloidal MnO_2 by extracellular polysaccharides of *Pedomicrobium manganicum*. Appl Environ Microbiol 56:2791–2794

Solomon EI, Sundaram UM, Machonkin TE (1996) Multicopper oxidases and oxygenases. Chem Rev 96:2563–2605

Spiro TG, Bargar JR, Sposito G, Tebo BM (2010) Bacteriogenic manganese oxides. Acc Chem Res 43:2–9

Spratt HG Jr, Hodson RE (1994) The effect of changing water chemistry on rates of manganese oxidation in surface sediments of a temperate saltmarsh and a tropical mangrove estuary. Estuar Coast Shelf Sci 38:119–135

Spratt HG Jr, Siekmann EC, Hodson RE (1994) Microbial manganese oxidation in saltmarsh surface sediments using leuco crystal violet manganese oxide detection technique. Estuar Coast Shelf Sci 38:91–112

Stembal T, Marinko M, Ribicic N, Briski F, Sipos L (2005) Removal of ammonia, iron and manganese from ground waters of Northern Croatia: pilot plant studies. Process Biochem 40:327–335

Stokes JL, Powers MT (1967) Stimulation of polyhydroxybutyrate oxidation in *Sphaerotilus discophorus* by manganese and magnesium. Arch Microbiol 59:295–301

Stuetz RM, Greene AC, Madgwick JC (1996) The potential use of manganese oxidation in treating metal effluents. Miner Eng 9:1253–1261

Sudek LA, Templeton AS, Tebo BM, Staudigel H (2009) Microbial ecology of Fe (hydr)oxide mats and basaltic rock from Vailulu'u Seamount, American Samoa. Geomicrobiol J 26:581–596

Sujith PP, Khedekar VD, Girish AP, Loka Bharathi PA (2010) Immobilization of nickel by bacterial isolates from the Indian ridge system and the chemical nature of the accumulated metal. Geomicrobiol J 27:424–434

Sunda WG, Huntsman SA (1987) Microbial oxidation of manganese in a North Carolina estuary. Limnol Oceanogr 32:552–564

Sunda WG, Huntsman SA (1990) Diel cycles in microbial manganese oxidation and manganese redox speciation in coastal waters of the Bahama Islands. Limnol Oceanogr 35:325–338

Tazaki K (2005) Microbial formation of a halloysite-like mineral. Clays Clay Miner 53:224–233

Tebo BM, Emerson S (1985) The effect of oxygen tension, Mn(II) concentration and temperature on the microbially catalyzed Mn(I1) oxidation rate in a marine fjord. Appl Environ Microbiol 50:1268–1273

Tebo BM, Emerson S (1986) Microbial manganese(II) oxidation in the marine environment: a quantitative study. Biogeochemistry 2:149–161

Tebo BM, Nealson KH, Emerson S, Jacobs L (1984) Microbial mediation of Mn(II) and Co(II) precipitation at the O_2/H_2S interfaces in two anoxic fjords. Limnol Oceanogr 29:1247–1258

Tebo BM, Ghiorse WC, van Waasbergen LG, Siering PL, Caspi R (1997) Bacterially mediated mineral formation: insights into manganese(II) oxidation from molecular genetic and biochemical studies. In: Banfield JF, Nealson KH (eds) Geomicrobiology: interactions between microbes and minerals. Mineral Soc Am, Washington, DC, pp 225–266

Tebo BM, Bargar JR, Clement BG, Dick GJ, Murray KJ, Parker D, Verity R, Webb SM (2004) Biogenic manganese oxides: properties and mechanisms of formation. Annu Rev Earth Planet Sci 32:287–328

Tebo BM, Johnson HA, McCarthy JK, Templeton AS (2005) Geomicrobiology of manganese(II) oxidation. Trends Microbiol 13:421–428

Tebo BM, Clement BG, Dick GJ (2007) Biotransformations of manganese. In: Hurst CJ, Crawford RL, Garland JL, Lipson DA, Mills AL, Stetzenbach LD (eds) Manual of environmental microbiology. ASM Press, Washington, DC, pp 1223–1238

Templeton A, Knowles E (2009) Microbial transformations of minerals and metals: recent advances in geomicrobiology derived from synchrotron- based X-ray spectroscopy and X-ray microscopy. Annu Rev Earth Planet Sci 37:367–391

Toner B, Manceau A, Webb SM, Sposito G (2006) Zinc sorption to biogenic hexagonal-birnessite particles within a hydrated bacterial biofilm. Geochim Cosmochim Acta 70:27–43

Tottey S, Waldron KJ, Firbank SJ, Reale B, Bessant C, Sato K, Cheek TR, Gray J, Banfield MJ, Dennison C, Robinson NJ (2008) Protein-folding location can regulate manganese binding versus copper- or zinc-binding. Nature 455:1138–1142

Trouwborst RE, Clement BG, Tebo BM, Glazer BT, Luther GW (2006) Soluble Mn(III) in suboxic zones. Science 313:1955–1957

Tyler PA (1970) *Hyphomicrobia* and the oxidation of manganese in aquatic ecosystems. Anton Van Leeuwenhoek 36:567–578

Tyler PA, Marshall KC (1967) Microbial oxidation of manganese in hydro-electric pipelines. Anton Van Leeuwenhoek 33:171–183

Uren NC, Leeper GW (1978) Microbial oxidation of divalent manganese. Soil Biol Biochem 10:85–87

van Waasbergen LG, Hoch JA, Tebo BM (1993) Genetic analysis of the marine manganese oxidizing *Bacillus* sp. strain SG-1: protoplast transformation, Tn917 mutagenesis and identification of chromosomal loci involved in manganese oxidation. J Bacteriol 175:7594–7603

van Waasbergen LG, Hildebrand M, Tebo BM (1996) Identification and characterization of a gene cluster involved in manganese oxidation by spores of the marine *Bacillus* sp. strain SG-1. J Bacteriol 178:3517–3530

Villalobos M, Toner B, Bargar J, Sposito G (2003) Characterization of the manganese oxide produced by *Pseudomonas putida* strain MnB1. Geochim Cosmochim Acta 67:2649–2662

Villalobos M, Bargar J, Sposito G (2005a) Mechanisms of Pb(II) sorption on a biogenic manganese oxide. Environ Sci Technol 39:569–576

Villalobos M, Bargar J, Sposito G (2005b) Trace metal retention on biogenic manganese oxide nanoparticles. Elements 1:223–226

Vodyanitskii YN (2009) Mineralogy and geochemistry of manganese: a review of publications. Eurasian Soil Sci 42:1170–1178

Vojak PWL, Edwards C, Jones MV (1985) Evidence for microbial manganese oxidation in the River Tamar estuary, South West England. Estuar Coast Shelf Sci 20:661–671

Wang X, Müuller WEG (2009) Marine biominerals: perspectives and challenges for polymetallic nodules and crusts. Trends Biotechnol 27:375–383

Wang X, Schloßmacher U, Natalio F, Schröder HC, Wolf SE, Tremel W, Müller WEG (2009a) Evidence for biogenic processes during formation of ferromanganese crusts from the Pacific ocean: implications of biologically induced mineralization. Micron 40:526–535

Wang X, Schröder HC, Wiens M, Schloßmacher U, Müller WEG (2009b) Manganese/polymetallic nodules: micro-structural characterization of exolithobiontic- and endolithobiontic microbial biofilms by scanning electron microscopy. Micron 40:350–358

Webb SM, Dick GJ, Bargar JR, Tebo BM (2005) Evidence for the presence of Mn(III) intermediates in the bacterial oxidation of Mn(II). Proc Natl Acad Sci USA 102:5558–5563

White C, Sayer JA, Gadd GM (1997) Microbial solubilization and immobilization of toxic metals: key biogeochemical processes for treatment of contamination. FEMS Microbiol Rev 20: 503–516

Yang SH, Ehrlich HL (1976) Effect of four heavy metals (Mn, Ni, Cu and Co) on some bacteria from the deep sea. In: Sharpley JM, Kaplan AM (eds) Proceedings of the third international biodegradation symposium. Applied Science Publishers Ltd, London, pp 867–874

Yocum CF, Pecoraro V (1999) Recent advances in the understanding of the biological chemistry of manganese. Curr Opin Chem Biol 3:182–187

Zajic JE (1969) Microbial biogeochemistry. Academic, New York

Zapkin MA, Ehrlich HL (1983) A comparison of manganese oxidation by growing and resting cells of a freshwater bacterial isolate, strain FMn 1. Z Allg Mikrobiol 23:447–455

Zhang HC, Huang CH (2003) Oxidative transformation of triclosan and chlorophene by manganese oxides. Environ Sci Technol 37:2421–2430

Zhang HC, Huang CH (2005) Oxidative transformation of fluoroquinolone antibacterial agents and structurally related amines by manganese oxide. Environ Sci Technol 39:4474–4483

Zhang J, Lion LW, Nelson YM, Shuler ML, Ghiorse WC (2002) Kinetics of Mn(II) oxidation by *Leptothrix discophora* SS1. Geochim Cosmochim Acta 66:773–781